



FACULTEIT LANDBOUWKUNDIGE EN
TOEGEPASTE BIOLOGISCHE
WETENSCHAPPEN



Academiejaar 1999-2000

**CALIBRATION, IDENTIFIABILITY AND OPTIMAL EXPERIMENTAL
DESIGN OF ACTIVATED SLUDGE MODELS**

**CALIBRATIE, IDENTIFICEERBAARHEID EN OPTIMALE
PROEFOPZET VOOR ACTIEF-SLIB MODELLEN**

door

ir. Britta PETERSEN

*Thesis submitted in fulfillment of the requirements
for the degree of Doctor (Ph.D) in Applied Biological Sciences*

*Proefschrift voorgedragen tot het bekomen van de graad
van Doctor in de Toegepaste Biologische Wetenschappen*

op gezag van

Rector: **Prof. Dr. ir. J. WILLEMS**

Decaan:

Prof. Dr. ir. O. VAN CLEEMPUT

Promotoren:

Prof. Dr. ir. P.A. VANROLLEGHEM

Prof. M. HENZE

22/09/2000

The author and the promoters give the authorization to consult and to copy parts of this work for personal use only. Any other use is limited by the Laws of Copyright. Permission to reproduce any material contained in this work should be obtained from the author.

De auteur en de promotoren geven de toelating dit doctoraatswerk voor consultatie beschikbaar te stellen, en delen ervan te kopiëren voor persoonlijk gebruik. Elk ander gebruik valt onder de beperkingen van het auteursrecht, in het bijzonder met betrekking tot de verplichting uitdrukkelijk de bron te vermelden bij het aanhalen van de resultaten van dit werk.

De promotoren:

De auteur:

Prof. Dr. ir. Peter Vanrolleghem

Prof. Mogens Henze

ir. Britta Petersen

The research reported in this dissertation was conducted at the Department of Applied Mathematics, Biometrics and Process Control (BIOMATH) in co-operation with EPAS n.v., Gent, Belgium.

Contents

Chapter 1	Introduction and problem statement
Chapter 2	Literature review
Chapter 3	Activated sludge monitoring with combined respirometric - titrimetric measurements
Chapter 4	Improved theoretical identifiability of Monod model parameters by combined respirometric - titrimetric measurements. A generalisation of results
Chapter 5	Practical identifiability of model parameters by combined respirometric - titrimetric measurements
Appendix 5.1	Output sensitivity functions of single step nitrification model
Chapter 6	Effect of parameter scaling on the Fisher Information Matrix (FIM) and FIM based experimental designs
Chapter 7	Optimal experimental design
Appendix 7.1	Output sensitivity functions of two-step nitrification model and first order substrate degradation model
Chapter 8	Evaluation of an ASM1 model calibration procedure on a municipal-industrial wastewater treatment plant
Chapter 9	Conclusions and perspectives

References

List of abbreviations

Summary - Samenvatting

Curriculum Vitae

Chapter 1

-

Introduction and problem statement

Chapter 1

Introduction and problem statement

1. Introduction

The activated sludge process is one of the most widespread biological wastewater purification technologies. In this process, wastewater is mixed with a concentrated bacterial biomass suspension (the activated sludge) which degrades the pollutants. Originally, the concern was mainly to remove the organic carbon substances from the wastewater, which could be obtained rather easily by simple process designs. However, during the last two decades more stringent effluent standards for nutrients (nitrogen and phosphorus) have been imposed by legislation. As a consequence, the design and operation of activated sludge plants had to be modified to more advanced levels to make the treatment plants suited for biological nitrogen and phosphorus removal.

Implementation of biological nutrient removal on wastewater treatment plants (WWTP's) resulted in an increased knowledge on the biological degradation processes. This resulted in the development and use of more advanced dynamic mathematical models that may be able to describe the biological nutrient removal processes. These activated sludge models allow to study and to further increase the understanding of the influence of process modifications on treatment process efficiency. The dynamic models are for example increasingly used for scenario evaluations aiming at the optimisation of activated sludge processes (Stokes *et al.*, 1993; de la Sota *et al.*, 1994; Coen *et al.*, 1997 among many others). The Activated Sludge Model No.1 (ASM1) presented by the IAWQ Task Group on Mathematical Modelling for Design and Operation of Biological Wastewater Treatment Processes (Henze *et al.*, 1987) is generally accepted as state-of-the-art. ASM1 was primarily developed for municipal activated sludge wastewater treatment plants to describe the removal of organic carbon substances and nitrogen with simultaneous consumption of oxygen and nitrate as electron acceptors, and to yield a good description of the sludge production. ASM1 has been extended to include a description of biological phosphorus removal, resulting in ASM2 and ASM2d (Henze *et al.*, 1995, 1998). Recently, some of the model concepts behind ASM1 have been altered in ASM3 (Gujer *et al.*, 1999), a model that also focuses on the degradation of carbon and nitrogen but allows the introduction of processes describing the storage of bio-polymers under transient conditions.

2. Problem statement

Problems arise in the model calibration of the Activate Sludge Models. In this context a model calibration is understood as the adaptation of the model to fit a certain data set obtained for a full-scale WWTP with the purpose of describing the biological processes that take place in the WWTP. This task is often rather time-consuming and very often the time and resources needed for a reliable model calibration is underestimated. Although ASM1 was published more than ten years ago a consistent model calibration procedure has not been defined. One important reason for this is probably that the purpose of the model calibration will to a large extent decide how to approach the calibration, and how accurate the model must describe the full-scale observations. However, also of importance is the fact that the high complexity of the ASM with its numerous processes and parameters often gives rise to parameter identifiability problems resulting in more than one parameter set that can describe the observations equally well.

Identifiability is defined here as the ability to obtain a unique parameter set that is able to describe the behaviour of a system. One should distinguish between theoretical and practical identifiability. Theoretical identifiability is based on the model structure and deals with the question whether it is possible to obtain unique parameter values from a certain selected set of ideal noise-free measurements. On the other hand, practical identifiability includes the quality of the data. For instance, it has been shown that parameters may be unidentifiable in practice because of noise corrupted data, although these parameters are theoretically identifiable (Holmberg, 1982; Jeppsson, 1996).

The identifiability problems (either of theoretical or practical origin) of ASM mean that in most cases it will be too complicated to apply automatic mathematical calibration techniques. A model calibration is therefore most often done via a step-wise procedure, and only one or a few parameters are changed at a time. However, a model calibration procedure based on a trial and error approach, i.e. by manual modification of the parameters until a good description of the data is obtained, is obviously not very advisable due to the identifiability problems. As mentioned above, more than one parameter set may be able to describe the data equally well (Dupont and Sinkjær, 1994, Kristensen *et al.*, 1998). However, if the model is to be applied for more than a description of the data, e.g. for scenario analyses with the aim of process optimisation, it is important that the parameter set resulting from the model calibration procedure consists of realistic values, in order to obtain reliable model predictions. It therefore becomes important to gather information from different sources that can help in framing the model calibration procedure, e.g. to choose realistic parameter values.

Data from the full-scale WWTP alone are most often not sufficient for a model calibration since e.g. the sludge kinetics can not be readily obtained from such data, except for specific designs like sequencing batch reactors and alternating systems (Vanrolleghem and Coen, 1995). Therefore, for a model calibration of a full-scale WWTP the modeller is typically aiming at combining the more information rich results derived

from lab-scale experiments (carried out with activated sludge and wastewater from the full-scale installation), with data obtained from measuring campaigns on the treatment plant under study (e.g. Dupont and Sinkjær, 1994; Xu and Hultman, 1996; Coen *et al.*, 1997; Kristensen *et al.*, 1998).

In this thesis the main focus will be turned to the derivation of information from lab-scale experiments. Typically, such experiments will aim at the identification of a few model parameters or components of the full ASM and the data analysis is therefore often carried out via reduced sub-models based on ASM. However, before any model-based data interpretation takes place it is of utmost importance to address the identifiability properties of the model that is used for the data analysis, together with the conditions under which the experiments should be carried out.

The problems of parameter identifiability and experimental conditions are illustrated in Fig. 1 and will be explained below.

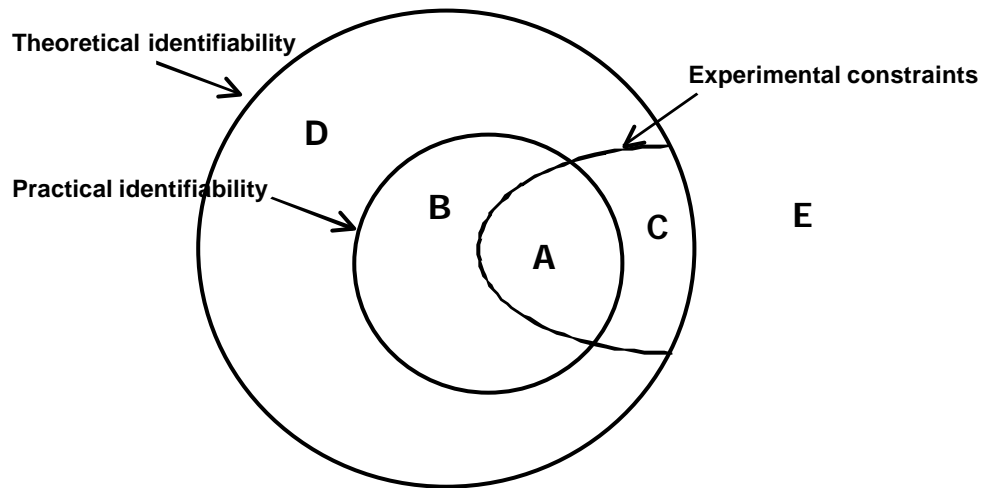


Figure 1. Conceptual idea of parameter identifiability and optimal experimental design

The space in Fig. 1 consists of ranges of different kinds of experimental conditions, i.e. each point in the figure represents a specific set of experimental conditions. The experimental conditions can both be measured and environmental variables. Examples of measured variables are oxygen concentration (S_O), oxygen uptake rate (r_O), pH etc. Environmental variables may, for instance, be origin and concentration of the activated sludge that is used in the experiment, initial substrate to biomass ratio ($S(0)/X(0)$), availability of nutrients etc.

Basically, the environmental variables will determine the response of the system, whereas the measured variables and the frequency of the measurements will determine what kind of information is obtained on the experimental response. Some examples of possible experimental responses can be nitrification, significant or neglectable biomass growth, storage of substrate etc.

It should be stressed that the experimental conditions are all user-defined and will depend on the purpose

of the actual experiment, i.e. what kind of experimental response and information content are sought to allow estimation of certain model parameters with a certain accuracy. A point located at a certain position in Fig. 1 is defined by a certain set of experimental conditions, and will thus result in a certain experimental response and related information content. If these experimental conditions comply with the purpose of the study, the experimental conditions will define a point that will lay within one of the “interesting” regions A - D. The precise location will depend on the experimental conditions and information content, as will be explained in detail below. However, if a set of experimental conditions do not comply with the purpose of the experimental study, then the experimental conditions will define a point that will lay somewhere in region E.

The outer circle in Fig.1 contains all the experimental conditions that will theoretically allow identification of the parameters that one wants to obtain from the experiment. The determination of this region is based on a theoretical identifiability analysis of the model for which parameters are sought. Thus, the region of theoretical identifiability (regions A - D in Fig. 1) will frame the experimental conditions where unique parameter values can theoretically be estimated from the available data set. This region is considered to be a hard, ultimate bound on the experimental conditions, since only the model structure and the available measurements determine the theoretical identifiability.

On the contrary, the region that frames the sets of experimental conditions that allow practical identifiability of the parameters one wants to obtain (the area within the inner circle in Fig.1 or the regions A and B) is determined by the quality of the experimental data and thereby their information content. As stated above, the available data may not be of sufficient quality to allow for a determination of all the theoretically identifiable parameters. The latter explains why this region is a sub-set of the set of experimental conditions that result from the theoretical identifiability study. In addition, it should be noted that, contrary to the theoretical identifiability region, the practical identifiability region is not fixed at a certain position in the experimental condition space. The set of experimental conditions that allow practical identifiability can be located elsewhere, for instance when the actual model parameter values are different or the collected data and their properties, e.g. noise level, change.

Finally, the half-region (A, C) is important and indicates that certain constraints can be imposed on the experimental conditions to fulfil a certain experimental purpose. The purpose could for example be to obtain kinetic parameters that can be applied in a model to describe the full-scale observations. Thus, the parameters derived from the lab-scale experiments must be representative for, and thereby transferable to, a full-scale system. In such case the experiments should be carried out under conditions that are as close as possible to the full-scale system, e.g. with respect to pH, temperature, substrate load etc. At first sight such constraints may not seem very severe. However, the transferability of results from a lab-scale to a full-scale system may not be straightforward. Note that the model may still be able to describe data that are collected under experimental conditions that are outside the region defined by these constraints. However, the

information obtained from the experiment will not be in accordance with the purpose of obtaining parameter values that are representative for the full-scale system.

The optimal experiments (region A in Fig. 1) can now be defined as the experiments for which the conditions belong to the intersection of the three regions (theoretically identifiable, practically identifiable, constraints), and within this set of possible experiments the best one has to be selected. Consequently, it is aimed to maximise the information content of the experimental data imposed by these given constraints. Such a maximisation can be obtained by applying optimal experimental design theory (OED). The Fisher Information Matrix (FIM) is central in the theory of Optimal Experimental Design for parameter estimation. The inverse of the FIM is, under certain conditions, equal to the parameter estimation error covariance matrix (COV) which is the rationale behind the central role of FIM. The core of OED is basically to reduce the COV. Different optimal experimental design criteria have been defined based on different scalar functions of the FIM (e.g. Walter and Pronzato, 1990; Munack, 1989, 1991).

The problem of achieving sufficiently informative data from the full-scale WWTP can now be illustrated by the same concept (see Fig. 2). Imagine that the purpose is to obtain information for a model calibration of e.g. ASM1 on the basis of full-scale observations. Obviously, the experimental conditions are equal to the full-scale conditions and the imposed constraints are related to obtaining parameters that are representative for the full-scale system. It is clear that a much larger range of experiments is allowed and may be able to describe the full-scale behaviour. However, most experimental data will not contain sufficient information to allow for a practical identification of the desired parameters. Thus, the region of practical identifiability is very small and may not even overlap the region of experimental constraints.

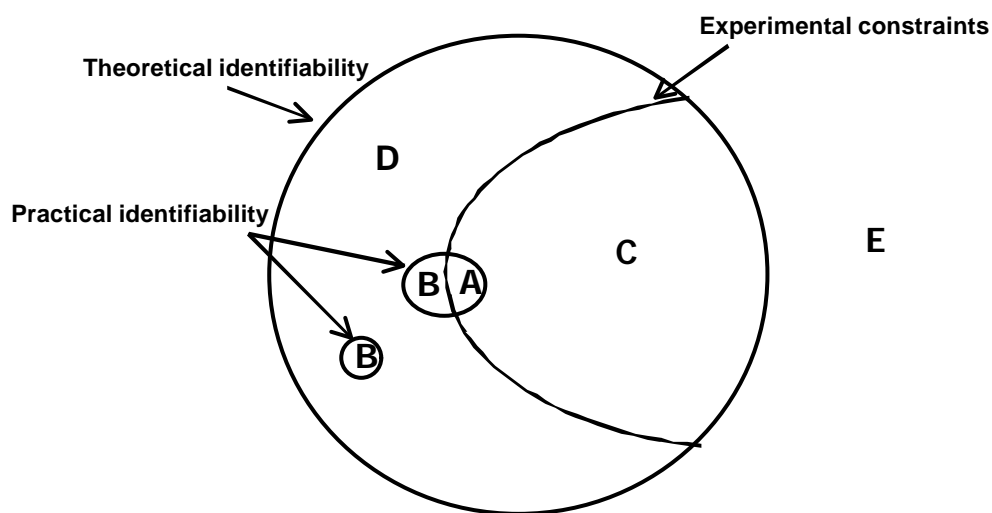


Figure 2. Conceptual idea of parameter identifiability and optimal experimental design in case information is retrieved from full-scale experiments

On the contrary, lab-scale experimental conditions may allow for a larger region of practical identifiability,

but problems may arise whether the obtained parameters are transferable to full-scale application. Thus, in this case, the region of experimental constraints, that may frame the experimental conditions for which the lab-scale results are transferable to full-scale behaviour, is very small, and one can imagine that there may be no overlap between this region and the one of the practical identifiability (see Fig. 3).

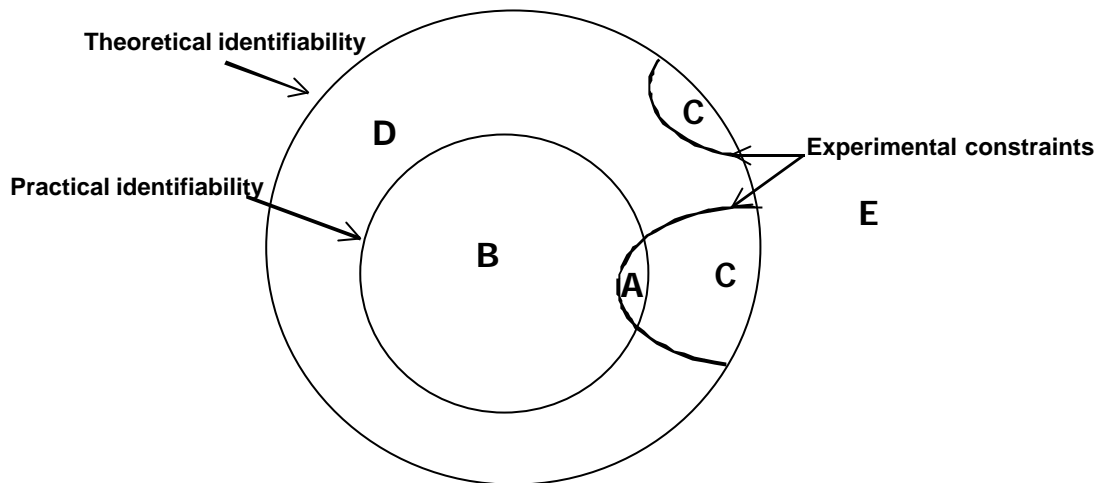


Figure 3. Conceptual idea of parameter identifiability and optimal experimental design in case information is retrieved from lab-scale experiments

3. Objective

The objectives of this thesis were to set-up a more methodological approach for model calibration with special focus to the investigation, illustration and solution of the problems encountered when deriving information from lab-scale experiments, as outlined in Fig. 1 – 3 above. The study will thus focus on the development of a general methodology to apply optimal experimental design on lab-scale experiments with activated sludge. The thesis will include a thorough study on the theoretical and practical identifiability properties of the models that are applied to interpret the experimental data obtained from lab-scale experiments, with the aim of obtaining the maximum amount of information from each experiment. The main aim of the pursued optimal experimental designs will be to obtain accurate parameter estimates. However, the transferability of the experimental results to full-scale behaviour will also be addressed and discussed.

The methodology is to be evaluated and it was chosen to do this on combined respirometric-titrimetric experiments for the characterisation of wastewater and reaction kinetics of activated sludge, in particular in the frame of a model calibration of a full-scale wastewater treatment plant model.

4. Outline of the thesis

The thesis is written such that the different chapters can be read independently. Thus, some repetitions may appear of e.g. theory or methodology. It is however aimed at minimising such repetitions as much as

possible.

First, an extensive literature review is given in chapter 2. The first part of this review focuses on how model calibration of ASM1 has been approached in other studies. It was subsequently attempted to gather and summarise the information needed to achieve a successful model calibration, and based on this a general model calibration procedure is proposed. The main part of the literature review is devoted to reviewing the different methods that have been developed and applied for the characterisation of wastewater and reaction kinetics in relation to ASM1. The methodologies are critically discussed, and it is attempted to illustrate the power of the different methods for characterisation, all within the frame of ASM1 model calibration. Finally, it is discussed which wastewater components and parameters are most relevant to be characterised via lab-scale experiments. This discussion includes the problem of transferability between lab-scale and full-scale observations, and also touches the problems related to the use of potentially different model concepts. One of the most discussed experimental factors determining the experimental response is the ratio between initial substrate and biomass concentration ($S(0)/X(0)$). A separate section is focusing upon this factor.

From the literature review (chapter 2) it becomes apparent that respirometric (and in recent years also titrimetric) methods are very popular in model calibration studies. Therefore, a short review of different respirometric methods is presented first in chapter 3, and advantages and disadvantages of different measurement principles are discussed. Based on this a new experimental lab-scale methodology of combined respirometric – titrimetric measurements is developed and evaluated. A model-based data interpretation is applied and compared to a more basic calculation method. Finally, confidence intervals of parameter estimates are calculated and the estimation accuracy based on respirometric and titrimetric alone or based on combined measurements is evaluated.

Chapter 4 focuses on the theoretical identifiability region (see Fig. 1 – 3). A thorough theoretical identifiability analysis was carried out focusing on the two-step nitrification Monod model with titrimetric (cumulative proton production) and respirometric measurements (dissolved oxygen or oxygen uptake rates) from two types of respirometer. Two model structures were considered including either presence or absence of significant biomass growth. The theoretical identifiability was studied via the Taylor series expansion and generating series methods. Finally, it is shown how the results of the theoretical identifiability study can be generalised.

The issue of practical parameter identifiability is addressed in chapter 5. Here the practical identifiability of a two step nitrification process, already introduced in chapter 3, was further investigated based on the theoretical results of chapter 4. This study was carried out via evaluation of the output sensitivity functions and the corresponding Fisher Information Matrix (FIM). In the second part of this chapter the accuracy of parameter estimates based on separate respirometric or titrimetric data as well as the combination of both

data sets is investigated thoroughly.

The focus is finally turned towards optimal experimental design in chapter 6 and 7. In chapter 6 some specific problems related to parameter rescaling and the resulting effects of parameter scaling on the optimal experimental design criteria are investigated. Parameter scaling was investigated because it showed to be an essential step to obtain a mathematically stable inversion of the matrices that are to be used in the optimal experimental design procedure.

Based on Fig. 1 above a complete procedure for optimal experimental design is proposed in chapter 7. The procedure is illustrated for two case studies. The first case study deals with a well-known example, the two step nitrification process where the aim is more specifically to identify the kinetic parameters of the second nitrification step. Secondly, a combined municipal-industrial wastewater treatment process is studied with the purpose of simultaneously determining the kinetics of heterotrophic substrate degradation and nitrification.

Finally, the ASM1 model calibration procedure defined earlier in chapter 2 is applied for a full-scale combined municipal – industrial WWTP in chapter 8. It will be illustrated how additional information from different information sources helps in framing the parameters applied in the model calibration exercise. The calibrated model is evaluated via a sensitivity analysis that helps to quantify the influence of changes of model parameters and influent component concentrations on the model output.

Chapter 9 summarises the results of this thesis. Future perspectives, research and applications of the developed methodologies are discussed.

Chapter 2

-

Literature review

Parts of this chapter were published as:

Vanrolleghem P.A., Spanjers H., Petersen B., Ginestet P. and Takacs I. (1999) Estimating (combinations of) activated sludge model No. 1 parameters and components by respirometry. *Water Science and Technology*, **39**(1), 195 – 214.

The main part of this chapter is in press as:

Petersen B., Gernaey K., Henze M. and Vanrolleghem P.A. (2000) Calibration of activated sludge models: A critical review of experimental designs. In: Agathos S. and Reineke W. (Eds.), *Biotechnology for the Environment. Focus on Biotechnology*, Vol. 3, Kluwer Academic Publishers BV.

Chapter 2

Literature review

Abstract - This review begins with an overview of literature data on methodologies that have been applied in other studies to calibrate Activated Sludge Model No. 1 (ASM1). An attempt was made to gather and summarise the information needed to achieve a successful model calibration, and based on this a general model calibration procedure is proposed. The main part of the literature review is devoted to reviewing the different methods that have been developed and applied for the characterisation of wastewater and reaction kinetics in relation to ASM1. The methodologies are critically discussed and it is attempted to illustrate the power of the different methods for characterisation, all within the frame of ASM1 calibration. Finally, it is discussed which wastewater components and parameters are most relevant to be characterised via lab-scale experiments. This discussion also includes the problem of transferability between lab-scale and full-scale observations and potentially different model concepts. One of the most discussed experimental factors determining the experimental response is the ratio between initial substrate and biomass concentration ($S(0)/X(0)$). A separate section is focusing upon this factor.

1. Introduction

One of the most widespread biological wastewater treatment techniques is the activated sludge process. In this process, a bacterial biomass suspension is responsible for the removal of pollutants. Depending on the design and the specific application, an activated sludge wastewater treatment plant can achieve biological nitrogen removal and biological phosphorus removal, besides removal of organic carbon substances. The increased knowledge about the mechanisms of different biological processes taking place in an activated sludge plant was translated into dynamic models that were developed to describe the degradation processes in the activated sludge plant. This review will focus on the Activated Sludge Model No. 1 (ASM1) (Henze *et al.*, 1987), which through the years has been the state-of-the-art model for activated sludge plants with biological nitrogen removal.

2. Description of the State-of-the-Art Activated Sludge Models

In the following the model concepts of ASM1 (Henze *et al.*, 1987) and the recent modifications leading to ASM3 (Gujer *et al.*, 1999) are described. A description of ASM2/ASM2d (Henze *et al.*, 1995, 1999) is, however, not included since phosphorus removal is not dealt with in this study.

2.1. Activated Sludge Model No.1 (ASM1)

ASM1 is presented in a matrix format in Table 1 according to Henze *et al.* (1987). Many of the basic concepts of ASM1 were adapted from the activated sludge model defined by Dold (1980). Some of the central concepts (the different model components and processes) of ASM1 are summarised below. For further details the reader is referred to the IAWQ Task group reports.

2.1.1. COD components in ASM1

COD is selected as the most suitable parameter for defining the carbon substrates as it provides a link between electron equivalents in the organic substrate, the biomass and oxygen utilised. In ASM1 the COD is subdivided based on (i) solubility, (ii) biodegradability (iii) biodegradation rate and (iv) viability (biomass):

- (i) The total COD is divided into soluble (S) and particulate (X) components.
- (ii) The COD is further subdivided into non-biodegradable organic matter and biodegradable matter. The non-biodegradable matter is biologically inert and passes through an activated sludge system in unchanged form. The inert soluble organic matter (S_I) leaves the system at the same concentration as it enters. Inert suspended organic matter in the wastewater influent (X_I) or produced via decay (X_P) becomes enmeshed in the activated sludge and is removed from the system via the sludge wastage.
- (iii) The biodegradable matter is divided into soluble readily biodegradable (S_S) and slowly biodegradable (X_S) substrate. Already here it should be stressed that some slowly biodegradable matter may actually be soluble. The readily biodegradable substrate is assumed to consist of relatively simple molecules that may be taken in directly by heterotrophic organisms and used for growth of new biomass. On the contrary, the slowly biodegradable substrate consists of relatively complex molecules that require enzymatic breakdown prior to utilisation.
- (iv) Finally, heterotrophic biomass (X_{BH}) and autotrophic biomass (X_{BA}) are generated by growth on the readily biodegradable substrate (S_S) or by growth on ammonia nitrogen (S_{NH}). The biomass is lost via the decay process where it is converted to X_P and X_S (death regeneration, see below).

Summarising, the total COD balance of ASM1 is defined by Eq. 1 and further illustrated in Fig. 1.

$$\text{COD}_{\text{tot}} = S_I + S_S + X_I + X_S + X_{BH} + X_{BA} + X_P \quad (1)$$

Table 1. The ASM1 process matrix (Henze *et al.*, 1987)

Component (i) → ↓ Process (j)	1 S _I	2 S _S	3 X _I	4 X _S	5 X _{BH}	6 X _{BA}	7 X _P	8 S _O	9 S _{NO}	10 S _{NH}	11 S _{ND}	12 X _{ND}	13 S _{ALK}	Process rate (ρ _j)
1 Aerobic growth of heterotrophic biomass		$\frac{1}{Y_H}$			1			$\frac{1-Y_H}{Y_H}$		$-i_{XB}$			$\frac{i_{XB}}{14}$	$\mu_{maxH} \frac{S_S}{K_S + S_S} \frac{S_O}{K_{OH} + S_O} X_{BH}$
2 Anoxic growth of heterotrophic biomass		$\frac{1}{Y_H}$			1					$-i_{XB}$			$\frac{1-Y_H}{14 \cdot 2.86 Y_H}$ $-\frac{i_{XB}}{14}$	$\eta_g \mu_{maxH} \frac{S_S}{K_S + S_S} \frac{K_{OH}}{K_{OH} + S_O}$ $\frac{S_{NO}}{K_{NO} + S_{NO}} X_{BH}$
3 Aerobic growth of autotrophic biomass						1		$-\frac{4.57 - Y_A}{Y_A}$	$-\frac{1}{Y_A}$	$-i_{XB} \frac{1}{Y_A}$			$\frac{2}{14 Y_A} \frac{i_{XB}}{14}$	$\mu_{maxA} \frac{S_{NH}}{K_{NH} + S_{NH}} \frac{S_O}{K_{OA} + S_O} X_{BA}$
4 Decay of heterotrophic biomass				$1-f_p$	-1		f_p					$i_{XB} - f_p i_{XB}$		$b_H X_{BH}$
5 Decay of autotrophic biomass				$1-f_p$		-1	f_p					$i_{XB} - f_p i_{XB}$		$b_A X_{BA}$
6 Ammonification of soluble organic nitrogen										1	-1		$\frac{1}{14}$	$k_a S_{ND} X_{BH}$
7 Hydrolysis of slowly biodegradable substrate		1		-1										$k_h \frac{X_S / X_{BH}}{K_X + X_S / X_{BH}} \frac{S_O}{K_{OH} + S_O}$ $+ \eta_h \frac{K_{OH}}{K_{OH} + S_O} \frac{S_{NO}}{K_{NO} + S_{NO}} X_{BH}$
8 Hydrolysis of organic nitrogen											1	-1		$p_7 (X_{ND} / X_S)$

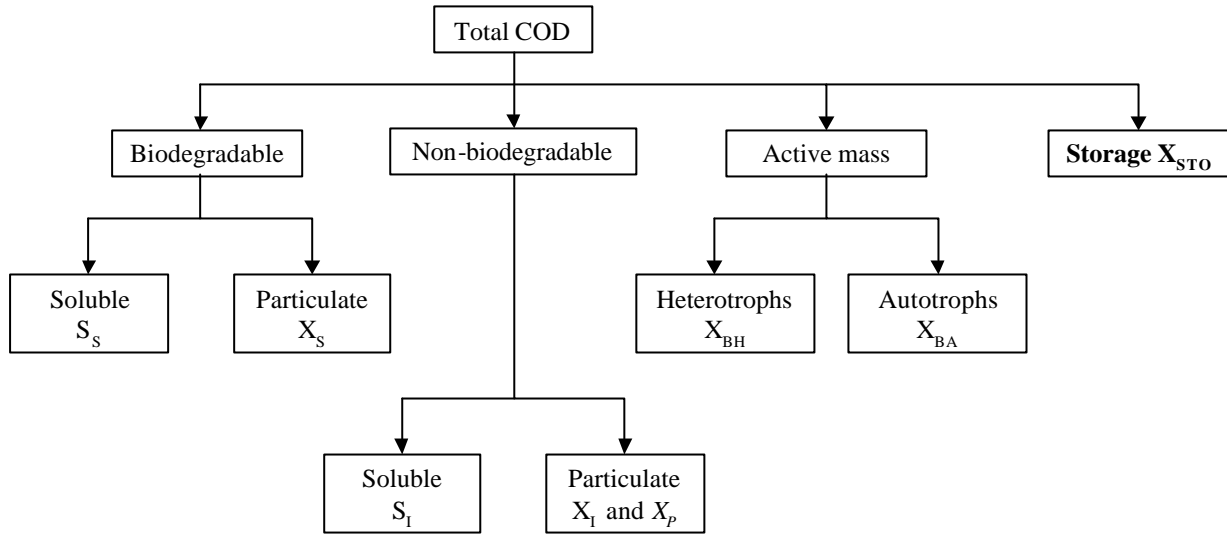


Figure 1. COD components in ASM1 and ASM3 (figure modified from Jeppsson, 1996), components specifically related to ASM3 are given in bold and the ones only related to ASM1 are given in italics

2.1.2. Nitrogen components in ASM1

Similar to the organic matter, total nitrogen can be subdivided based on (i) solubility, (ii) biodegradability and (iii) biodegradation rate:

- (i) The total nitrogen can be subdivided into soluble (S) and particulate (X) components.
- (ii) The nitrogen is divided into non-biodegradable matter and biodegradable matter. The non-biodegradable particulate organic nitrogen (X_{NI}) is associated with the non-biodegradable particulate COD (X_I or X_P), whereas the soluble non-biodegradable organic nitrogen (S_{NI}) is assumed to be negligible and therefore not incorporated into the model.
- (iii) The biodegradable nitrogen is subdivided into ammonia nitrogen (S_{NH}), nitrate + nitrite nitrogen (S_{NO}), soluble organic nitrogen (S_{ND}) and particulate organic nitrogen (X_{ND}). The particulate organic nitrogen is hydrolysed to soluble organic nitrogen in parallel with hydrolysis of the slowly biodegradable organic matter (X_S) (either present in the wastewater or produced via the decay process). The soluble organic nitrogen is converted to ammonia nitrogen via ammonification. Ammonia nitrogen serves as the nitrogen source for biomass growth (the parameter i_{XB} indicates the amount of nitrogen incorporated per COD unit). Finally, the autotrophic conversion of ammonia results in nitrate nitrogen (S_{NO}) which is considered to be a single step process in ASM1.

Summarising, the total nitrogen balance for the components in ASM1 is defined by Eq. 2 and further illustrated in Fig. 2.

$$N_{tot} = S_{NH} + S_{ND} + S_{NO} + X_{ND} + X_{NI} + i_{XB} \cdot (X_{BH} + X_{BA}) + i_{XP} \cdot X_P \quad (2)$$

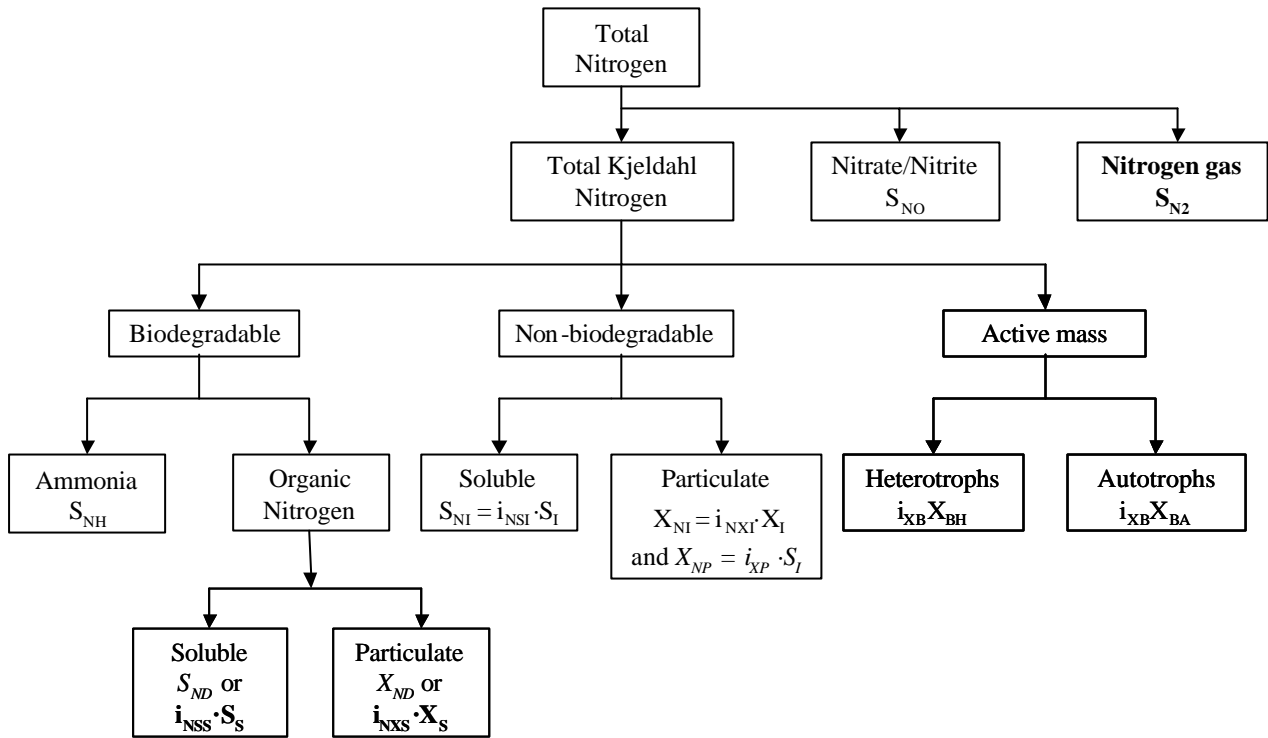


Figure 2. Nitrogen components in ASM1 (modified from Jeppsson, 1996), components specifically related to ASM3 are given in bold and the ones only related to ASM1 in italics

2.1.3. Processes in ASM1

Basically there are four different main processes defined in ASM1 (Henze *et al.*, 1987):

- 1) Growth of biomass
- 2) Decay of biomass
- 3) Ammonification of organic nitrogen
- 4) Hydrolysis of particulate organic matter

The substrate flows in ASM1 are illustrated in Fig. 3.

Aerobic growth of heterotrophic biomass

Growth takes place by degradation of soluble readily biodegradable substrate (S_S) under the consumption of oxygen (S_O). Ammonia nitrogen (S_{NH}) is incorporated into cell mass, as described above. Both the concentrations of S_S and S_O may be rate limiting for the growth process. The Monod relationship is used to describe the growth of heterotrophic and autotrophic organisms.

Anoxic growth of heterotrophic biomass (denitrification)

In the absence of oxygen the heterotrophic organisms are capable of using nitrate as the terminal electron acceptor with S_N as substrate resulting in biomass growth and nitrogen gas. The same Monod kinetics as used for aerobic growth is applied except that the kinetic rate expression is multiplied by a correction factor η_g (<1). This factor is accounting for the fact that the anoxic substrate removal rate is slower compared to aerobic conditions. This can either be caused by a lower maximum growth rate or because only a fraction of the heterotrophic biomass is able to denitrify. Furthermore, anoxic growth is inhibited when oxygen is present which is described by the switching function $K_{OH}/(K_{OH}+S_O)$. The coefficient K_{OH} has the same value as in the expression for aerobic growth. Thus, as aerobic growth declines, the capacity for anoxic growth increases.

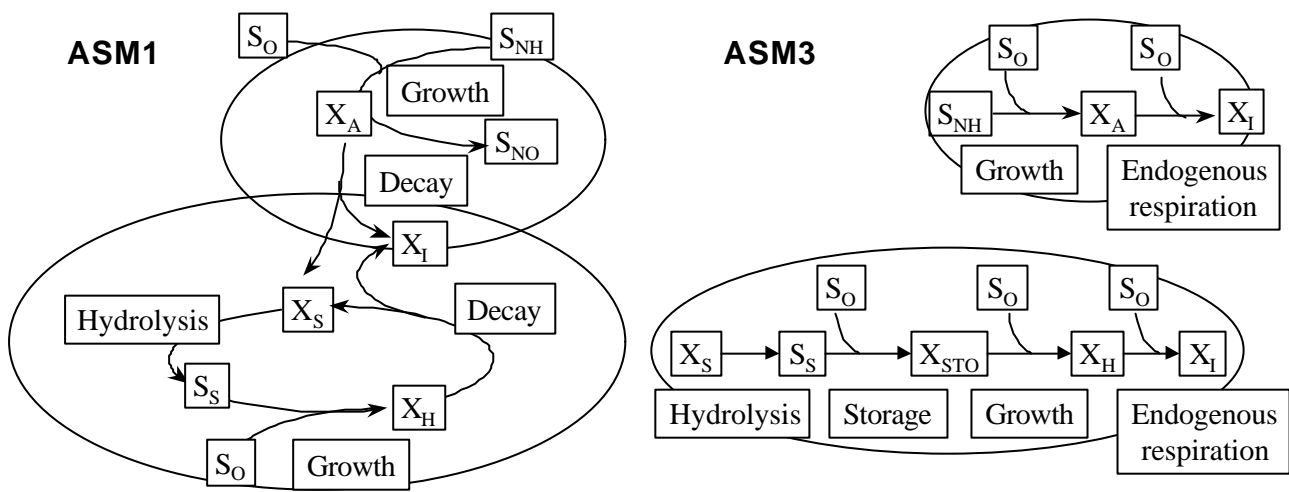


Figure 3. Substrate flows in ASM1 and ASM3 (modified from Gujer *et al.*, 1999)

Aerobic growth of autotrophic biomass (nitrification)

Ammonia nitrogen (S_{NH}) is oxidised to nitrate resulting in production of autotrophic biomass. Furthermore, a part of the S_{NH} is also incorporated in the autotrophic cell mass. As for heterotrophic growth the concentrations of S_{NH} and S_O can be rate limiting for the process. Nitrification has a considerable effect on the alkalinity (S_{ALK}).

Decay of heterotrophic biomass

The death regeneration concept of Dold (1980) is applied to describe the different reactions that take place when organisms die. The traditional endogenous respiration concept describes how a fraction of the organism mass disappears to provide energy for maintenance. However, in the death regeneration concept oxygen is not directly associated with microbial decay. Decay is assumed to result in the release of slowly biodegradable substrate that is recycled back to soluble substrate and used for more cell growth. Thus, the oxygen utilisation normally associated directly with decay is calculated as if it occurs indirectly from growth

of new biomass on released substrate. A parallel conversion of organic nitrogen to ammonia nitrogen occurs. It should be noted that the magnitude of the decay coefficient used in this approach is different from that of the endogenous respiration. In endogenous respiration the loss of one unit of biomass COD leads to the utilisation of one unit of oxygen minus the COD of the inert particulate products that are formed. However, in the death regeneration model the loss of one biomass COD unit results in the ultimate formation of one unit of COD due to the formed readily biodegradable substrate minus the formed inert particulate products. When the readily biodegradable COD is used for cell synthesis, only a fraction of a unit of oxygen (determined by the yield) will be required because of the energy incorporated into the cell mass. That cell mass undergoes in turn decay etc. before the unit of oxygen is finally removed. Summarising, to give the same amount of oxygen utilisation per time due to the decay process, the decay rate coefficient must be larger for the death regeneration concept than if a more traditional endogenous decay process was adopted. This has the effect that the cell mass turnover rate increases, resulting in a higher microbial growth rate in the death regeneration model.

Decay of autotrophic biomass

The decay of autotrophs is described similar to the heterotrophic decay process.

Ammonification of soluble organic nitrogen (S_{ND})

Biodegradable soluble organic nitrogen (S_{ND}) is converted to ammonia nitrogen (S_{NH}) in a first order process. Hydrogen ions consumed in this conversion process result in an alkalinity change.

Hydrolysis

Slowly biodegradable substrate (X_S) enmeshed in the sludge is broken down producing readily biodegradable substrate (S_S). The degradation of slowly biodegradable matter has appeared rather important to realistic modelling of activated sludge systems because it is primarily responsible for realistic electron acceptor profiles (Dold, 1980). This process is modelled on the basis of surface reaction kinetics and occurs only under aerobic and anoxic conditions. The hydrolysis rate is reduced under anoxic conditions in the same way as anoxic growth, by applying a correction factor $\eta_h (<1)$. The rate is also first order with respect to the heterotrophic biomass concentration present but saturates as the amount of entrapped substrate becomes large in proportion to the biomass.

2.1.4. Restrictions of ASM1

A number of restrictions concerning ASM1 are summarised below (Henze *et al.*, 1987):

- 1) The system must operate at constant temperature.
- 2) The pH is constant and near neutrality. It is known that the pH has an influence on many of the

parameters, however only limited knowledge is available to be able to express these possible influences. Consequently, a constant pH has been assumed. The inclusion of alkalinity in the model, however, does allow for detection of pH problems.

- 3) No considerations have been given to changes in the nature of the organic matter within any given wastewater fractions (e.g. the readily biodegradable substrate). Therefore, the parameters in the rate expressions have been assumed to have constant values. This means that only concentration changes of the wastewater components can be handled whereas changes in the wastewater character can not.
- 4) The effects of nutrient limitations (e.g. N and P) on the cell growth have not been considered. It is, however, easy to add limitation terms in the model if needed.
- 5) The correction factors for denitrification (η_g and η_h) are fixed and constant for a given wastewater, even though it is possible that their values are depending on the system configuration.
- 6) The parameters for nitrification are assumed to be constant and to incorporate any inhibitory effects that wastewater constituents may have on them.
- 7) The heterotrophic biomass is homogeneous and does not undergo changes in species diversity with time. This assumption is inherent to the assumption of constant kinetic parameters. This means that any changes in substrate concentration gradients, reactor configuration, etc. on sludge settleability are not considered.
- 8) The entrapment of particulate organic matter in the biomass is assumed to be instantaneous.
- 9) The hydrolysis of organic matter and organic nitrogen are coupled and occur simultaneously with equal rates.
- 10) The type of electron acceptor present does not affect the loss of biomass by decay.
- 11) The type of electron acceptor does not affect the heterotrophic yield coefficient.
- 12) ASM1 is developed for simulation of treatment of municipal wastewater, and it is therefore not advised to apply the model to systems where industrial contributions dominate the characteristics of the wastewater.
- 13) ASM1 does not include processes that describe behaviours under anaerobic conditions. Simulations of systems with large fractions of anaerobic reactor volume may therefore lead to errors.
- 14) ASM1 can not deal with elevated nitrite concentrations.
- 15) ASM1 is not designed to deal with activated sludge systems with very high load or small sludge

retention time (SRT) (<1 day).

2.2. Activated Sludge Model No. 3 (ASM3)

The ASM3 process rates are presented in matrix form in Table 2. For a complete description of the ASM3 stoichiometric matrix the reader is referred to Gujer *et al.* (1999).

Table 2. Process rate expressions of ASM3 (Gujer *et al.*, 1999)

j	Process	Process rate equation ρ_j , all $\rho_j \geq 0$
1	Hydrolysis	$k_H \cdot \frac{X_S / X_H}{K_X + X_S / X_H} \cdot X_H$
Heterotrophic organisms, aerobic and denitrifying activity		
2	Aerobic storage of S_S	$k_{STO} \cdot \frac{S_{O_2}}{K_{O_2} + S_{O_2}} \cdot \frac{S_S}{K_S + S_S} \cdot X_H$
3	Anoxic storage of S_S	$k_{STO} \cdot \eta_{NOX} \cdot \frac{K_{O_2}}{K_{O_2} + S_{O_2}} \cdot \frac{S_{NOX}}{K_{NOX} + S_{NOX}} \cdot \frac{S_S}{K_S + S_S} \cdot X_H$
4	Aerobic growth	$\mu_H \cdot \frac{S_{O_2}}{K_{O_2} + S_{O_2}} \cdot \frac{S_{NH_4}}{K_{NH_4} + S_{NH_4}} \cdot \frac{S_{ALK}}{K_{ALK} + S_{ALK}} \cdot \frac{X_{STO}/X_H}{K_{STO} + X_{STO}/X_H} \cdot X_H$
5	Anoxic growth (Denitrification)	$\mu_H \cdot \eta_{NOX} \cdot \frac{K_{O_2}}{K_{O_2} + S_{O_2}} \cdot \frac{S_{NOX}}{K_{NOX} + S_{NOX}} \cdot \frac{S_{NH_4}}{K_{NH_4} + S_{NH_4}} \cdot \frac{S_{ALK}}{K_{ALK} + S_{ALK}} \cdot \frac{X_{STO}/X_H}{K_{STO} + X_{STO}/X_H} \cdot X_H$
6	Aerobic endogenous respiration	$b_{H,O_2} \cdot \frac{S_{O_2}}{K_{O_2} + S_{O_2}} \cdot X_H$
7	Anoxic endogenous respiration	$b_{H,NOX} \cdot \frac{K_{O_2}}{K_{O_2} + S_{O_2}} \cdot \frac{S_{NOX}}{K_{NOX} + S_{NOX}} \cdot X_H$
8	Aerobic respiration of X_{STO}	$b_{STO,O_2} \cdot \frac{S_{O_2}}{K_{O_2} + S_{O_2}} \cdot X_{STO}$
9	Anoxic respiration of X_{STO}	$b_{STO,NOX} \cdot \frac{K_{O_2}}{K_{O_2} + S_{O_2}} \cdot \frac{S_{NOX}}{K_{NOX} + S_{NOX}} \cdot X_{STO}$
Autotrophic organisms, nitrifying activity		
10	Aerobic growth of X_A , Nitrification	$\mu_A \cdot \frac{S_{O_2}}{K_{A,O_2} + S_{O_2}} \cdot \frac{S_{NH_4}}{K_{A,NH_4} + S_{NH_4}} \cdot \frac{S_{ALK}}{K_{A,ALK} + S_{ALK}} \cdot X_A$
11	Aerobic endogenous respiration	$b_{A,O_2} \cdot \frac{S_{O_2}}{K_{A,O_2} + S_{O_2}} \cdot X_A$
12	Anoxic endogenous respiration	$b_{A,NOX} \cdot \frac{K_{A,O_2}}{K_{A,O_2} + S_{O_2}} \cdot \frac{S_{NOX}}{K_{A,NOX} + S_{NOX}} \cdot X_A$

In the development of ASM3 some limitations of ASM1 were evaluated, and combined with the experiences gained with the application of ASM1 the following list of “defects” of ASM1 was defined (Gujer *et al.*, 1999):

- 1) ASM1 does not include expressions to deal with nitrogen and alkalinity limitations.
- 2) ASM1 considers biodegradable soluble and particulate organic nitrogen as model components. These can, however, not easily be measured and may in most cases unnecessarily complicate the use of ASM1.
- 3) The ammonification kinetics can not be easily quantified, and moreover this process is typically rather fast and does therefore not affect model predictions significantly.
- 4) ASM1 differentiates between inert suspended organic matter present in the influent wastewater and produced within the activated sludge process. In reality, however, it is impossible to distinguish between these two components.
- 5) Hydrolysis has a rather dominating effect upon the predictions of the oxygen consumption and denitrification by heterotrophic organisms. In reality this process includes different coupled processes such as hydrolysis, lysis and storage of substrates. Therefore, the identification of the kinetic parameters of this combined process is difficult.
- 6) The death regeneration concept is covering lysis combined with hydrolysis of released substrate and subsequently growth on this substrate. In reality it is difficult to determine the decay coefficient related to the death regeneration concept.
- 7) Elevated concentrations of readily biodegradable organic substrates can lead to storage of polyhydroxy-alkanoates, lipids or glycogen. This process is not included in ASM1.
- 8) ASM1 does not include the possibility to differentiate between decay rates of nitrifiers under aerobic and anoxic conditions. This may lead to problems with the predictions of the maximum nitrification rates in cases of high SRT and high fractions of anoxic reactor volumes.

The main difference between ASM1 and ASM3 is the recognition of the importance of storage polymers in the heterotrophic conversions in the activated sludge processes (point 7 above). The aerobic storage process in ASM3 describes the storage of the readily biodegradable substrate (S_S) into a cell internal component (X_{STO}). This approach requires that the biomass is modelled with cell internal structure similar to ASM2. The energy required for this process is obtained via aerobic respiration. This internal component is then subsequently used for growth. In ASM3 it is assumed that all S_S is first taken up and stored prior to growth. Thus, a division of the storage and growth process, allowing growth to take place on external

substrate directly, is not considered.

Furthermore, the death regeneration concept is replaced by endogenous respiration, which is closer to the phenomena observed in reality (point 6 above, endogenous respiration can readily be obtained from a simple batch test, see below under section 4.3.1.2.). Also, ASM3 allows a differentiation between aerobic and anoxic decay.

Fig. 3 illustrates the difference in COD flows between ASM1 and ASM3. The first thing to notice is that conversion processes of the two groups of organisms (autotrophs and heterotrophs) are clearly separated in ASM3, whereas the decay regeneration cycles of the autotrophs and heterotrophs are strongly interrelated in ASM1. This change of decay concept (and introduction of the storage step) means that there are more “entry” points for oxygen utilisation resulting in, at some points, easier separation and characterisation of the processes (see also discussion under 4.3.4.). Second, there is a shift of emphasis from hydrolysis to storage of organic matters. This gives a change in how wastewater characterisation should be defined since the separation between S_S and X_S now should be based on the storage process rather than on the growth process (see also discussion in paragraph 4.1.3.). Still, the separation remains somewhat based on biodegradation rates. In ASM3 hydrolysis is obviously of a less dominating importance for the rates of oxygen consumption since only hydrolysis of X_S in the influent is considered (see point 5 above).

Below the components and processes of AMS3 are summarised focusing on the differences between ASM1 and ASM3.

2.2.1. COD components in ASM3

The COD components in ASM3 are basically defined in the same way as in ASM1. Only the separation between inert suspended organic matter in the wastewater influent (X_I) and produced via the decay process (X_P) is no longer maintained (see point 4 above), and, second, the component X_{STO} is introduced, as described above. The substrate S_S goes through the storage process but is basically still biodegradable. Thus, the total COD balance is defined by Eq. 3 and further illustrated in Fig. 1, where the components specifically related to ASM3 are given in bold and the ones only related to ASM1 are given in italics.

$$\text{COD}_{\text{tot}} = S_I + S_S + X_I + X_S + X_H + X_A + X_{STO} \quad (3)$$

2.2.2. Nitrogen components in ASM3

The nitrogen balance in ASM3 is simplified compared to ASM1, since the soluble and particulate organic nitrogen components are no longer considered (point 2 and 3 above). Furthermore, a nitrogen gas component (S_{N_2}) is included allowing for a closed nitrogen mass balance. The nitrogen incorporated in S_I , S_S , X_I , X_S , and the biomass is defined in ASM3 as a fraction of these components. This fraction is

consumed or produced when the corresponding COD fraction is formed or degraded respectively. Summarising, the total nitrogen balance for the components in ASM3 is defined by Eq. 4, and further illustrated in Fig. 2. Again, the components specifically related to ASM3 are shown in bold and the ones related to ASM1 in italics.

$$N_{tot} = S_{NH} + S_{NO} + S_{N2} + i_{NSI} \cdot S_I + i_{NSS} \cdot S_S + i_{NXS} \cdot X_S + i_{NBM} \cdot (X_B + X_A) + i_{NXI} \cdot X_I \quad (4)$$

2.2.3. Processes in ASM3

In ASM3 there are also four basic processes, however, slightly different from ASM1 (Gujer *et al.*, 1999):

- 1) Storage of readily biodegradable substrate
- 2) Growth of biomass
- 3) Decay of biomass
- 4) Hydrolysis of particulate organic matter

Aerobic storage of readily biodegradable substrate

This process describes the storage of readily biodegradable substrate (S_S) in the form of $X_{S_{TO}}$ with the consumption of oxygen. As stated above, it is assumed that all S_S first becomes stored material before use for cell growth. It is realised that this is not in accordance with reality. However, no model is currently available to predict the separation of S_S into direct growth and storage. Gujer *et al.* (1999) therefore suggested to apply a low storage yield ($Y_{S_{TO}}$) and a higher growth yield (Y_H) to approximate direct growth.

Anoxic storage of readily biodegradable substrate

This process is identical to the aerobic storage, only is nitrate used as terminal electron acceptor instead of oxygen. Furthermore, a correction factor (η_{NO}) is applied to indicate that only a fraction of the heterotrophic biomass may be capable of denitrifying.

Aerobic growth of heterotrophs

Aerobic heterotrophic growth takes place by degradation of $X_{S_{TO}}$ with the consumption of oxygen (S_O). Ammonia nitrogen (S_{NH}) is incorporated into cell mass, as described above for ASM1.

Anoxic growth of heterotrophs (denitrification)

Anoxic growth is similar to aerobic growth but respiration is based on denitrification. Again, a correction factor (η_{NO}) is applied to account for the observation of reduced anoxic respiration rates compared to aerobic respiration.

Aerobic growth of autotrophs (nitrification)

This process is described similar to ASM1.

Aerobic decay of heterotrophs

The energy requirements not associated with growth but including maintenance, lysis, etc. are described by endogenous respiration in ASM3 according to a simple first order reaction kinetics.

Anoxic decay of heterotrophs

ASM3 allows for a description of anoxic decay in a similar way as the aerobic decay process.

Aerobic and anoxic decay of autotrophs

The decay of autotrophs is described in the same way as the heterotrophic decay process.

Aerobic and anoxic respiration of storage products

These processes are analogous to endogenous respiration and ensure that the storage product X_{STO} decays together with the biomass.

Hydrolysis

Just as in ASM1 hydrolysis is responsible for the breakdown of slowly biodegradable substrate (X_S) to readily biodegradable substrate (S_S). However, in ASM3 hydrolysis is assumed to be electron donor independent, and as stressed above the hydrolysis does not play the same dominating role as in ASM1.

2.2.4. Restrictions of ASM3

The number of restrictions listed for ASM1 above basically still holds for ASM3, except for restriction 10 stating that the type of electron acceptor does not affect the biomass decay.

3. Model calibration

In this study model calibration is understood as the adaptation of the model to fit a certain set of information obtained from the full-scale WWTP under study. This task is often rather time-consuming, and typically the time needed for a model calibration is underestimated. Even though more than a decade has passed since the publication of ASM1, a fully developed model calibration procedure has not been defined yet. We have not been able to find a complete model calibration report in literature. There may be many reasons for this. Important to realise is that the purpose of a model being built is very much determining on how to approach the calibration, making it difficult to generalise (Henze *et al.*, 1995). Still, considering the wide application of the activated sludge models there are surprisingly few references that contain details on the

applied model calibration procedure. Most often it is not specified in detail how the model was calibrated but the focus is more on the applications, e.g. for process scenarios and optimisations etc. Thus, to obtain information on model calibration procedures one often has to collect bits and pieces from various sources to obtain an overview.

Before going on with a discussion on how to approach a model calibration of ASM1, it is relevant to define how parameter estimation is understood in this study and what the difference is between parameter estimation and model calibration. Furthermore, the term identifiability will be defined and the problem of identifiability with respect to ASM in general will be addressed.

Parameter estimation consists of determining the “optimal” values of the parameters of a given model with the aid of measured data. Here, the numerical techniques for estimation will not be discussed, but reference is made to the literature (Robinson, 1985; Vanrolleghem and Dochain, 1998). Only the basic idea behind parameter estimation is schematised in Fig. 4. Initially, the model structures, of which certain selected parameters need to be estimated, and the experimental data need to be defined. Moreover, first guesses of the initial conditions, i.e. concentrations, and parameters, have to be given. The parameter estimation routine then basically consists of minimising an objective function, which for example can be defined as the weighted sum of squared errors between the model output and the data. When the objective function reaches a minimum with a certain given accuracy the optimal parameter values are obtained.

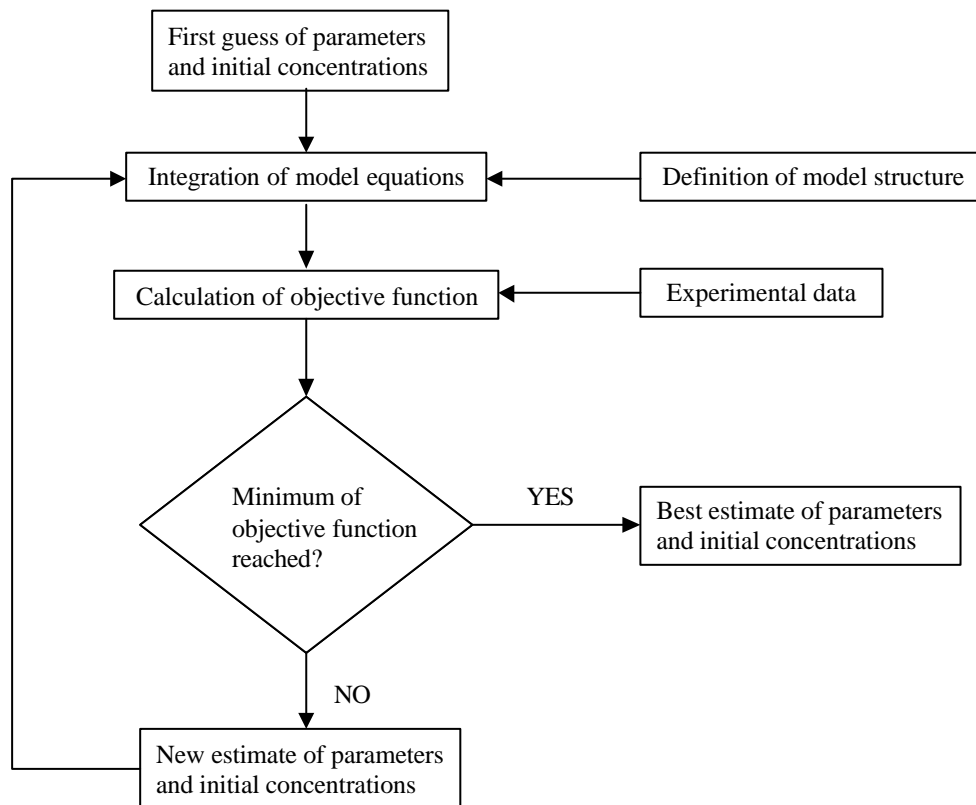


Figure 4. Illustration of parameter estimation routine (modified from Wanner *et al.*, 1992)

Thus, parameter estimation is carried out via specific mathematical search algorithms. However, due to the high complexity caused by the numerous parameters and the unidentifiable nature of the ASM models, it will be rather cumbersome to apply mathematical calibration techniques.

Indeed, a major problem encountered in calibration of ASM is the (lack of) identifiability of the model parameters. Identifiability is the ability to obtain a unique combination of parameters describing a system behaviour. A distinction should be made between theoretical and practical identifiability. Theoretical identifiability is a property of the model structure, and relates to the question whether it is at all possible to obtain unique parameter values for a given model structure considering certain selected outputs, and assuming ideal measurements. Practical identifiability, on the other hand, includes the quality of the data. Thus, theoretically identifiable parameters may be practically unidentifiable if the data are too noise corrupted (Holmberg, 1982; Jeppsson, 1996). This subject will be dealt with in much more detail in chapter 4 and 5.

For now, it should be stressed that a typical problem related to the model calibration of ASM is that more than one combination of influent characteristics and model parameters can give the same good description of the collected data (Dupont and Sinkjær, 1994; Kristensen *et al.*, 1998). Indeed, this indicates identifiability problems of either theoretical or practical origin.

The model calibration of ASM is typically based on a step-wise procedure, and by changing just a few of the many parameters instead of applying an automatic mathematical optimisation routine. Based on the above statements concerning identifiability problems it is, however, obvious that a calibration procedure where the model parameters are changed by trial and error until a good description of the measured data is reached is not advisable (Dupont and Sinkjær, 1994; Kristensen *et al.*, 1998). Thus, it becomes important to gather as much information as possible that can help the framing of realistic parameter combinations. In this review it was attempted to gather and summarise the type of information needed for successful model calibration.

3.1. Information set for model calibration

The set of information that should be collected for successful model calibration was extracted and combined from different sources (Henze *et al.*, 1987; Henze, 1992; Lesouef *et al.*, 1992; Pedersen and Sinkjær, 1992; Siegrist and Tschui, 1992; Stokes *et al.*, 1993; de la Sota *et al.*, 1994; Dupont and Sinkjær, 1994; Funamizu and Takakuwa, 1994; Weijers *et al.*, 1996; Xu and Hultman, 1996; Coen *et al.*, 1997; Mino *et al.*, 1997; Kristensen *et al.*, 1998) and is summarised below:

1. Design data: reactor volumes, pump flows and aeration capacities.
2. Operational data:
 - 2.1. Flow rates, as averages or dynamic trajectories, of influent, effluent, recycle and waste flows.

- 2.2. pH, aeration and temperatures.
3. Characterisation for the hydraulic model, e.g. the results of tracer tests.
4. Characterisation for the settler model, e.g. zone settling velocities at different mixed liquor suspended solids concentrations.
5. Characterisation for the biological model, ASM, of:
 - 5.1. Wastewater concentrations of full-scale WWTP influent and effluent (as well as some intermediate streams between the WWTP's unit processes), as averages or as dynamic trajectories: e.g. SS, COD, TKN, NH₄-N, NO₃-N, PO₄-P etc.
 - 5.2. Sludge composition: e.g. SS, VSS, COD, N and/or P content.
 - 5.3. Reaction kinetics: e.g. growth and decay rates.
 - 5.4. Reaction stoichiometry : e.g. biomass yields

The list does not discuss on how the particular information can be collected in practice, since this will be discussed more in detail in the following sections.

As mentioned above, the required quality and quantity of the information will depend very much on the purpose of the modelling. In case the model is to be used for educational purposes (e.g. to increase basic understanding of the processes), for comparison of design alternatives for non-existing plants or in other situations where qualitative comparisons are sufficient, the default parameter values defined by Henze *et al.* (1987) can be applied. A reasonably good description can most often be obtained with this default parameter set for typical municipal cases without significant industrial influences (Henze *et al.*, 1997). However, if the calibrated model is going to be used for process performance evaluation and optimisation, it may be necessary to have a more accurate description of the actual processes under study. Some processes may need a more adequate description than others depending on the purpose of the model calibration. This may especially apply for models that are supposed to describe the processes in an industrial or combined municipal and industrial treatment plant (Coen *et al.*, 1997, 1998). In such cases the wastewater characterisation, and thereby the activated sludge, may differ significantly from standard municipal wastewater. In addition, special attention often has to be paid to the characterisation of nitrification kinetics (e.g. Dupont and Sinkjær, 1994), since nitrification typically is the determining process for the process designs. Also, the availability of readily biodegradable carbon substances is important for the successful achievement of both denitrification and biological P removal, and may need to be characterised in more detail (Coen *et al.*, 1997).

In this study the focus will mainly be on the information described in point 5 above. Although not considered in detail, it should be stressed that the information listed in point 1 - 4 is also very essential and

should not be neglected for a successful model calibration. Major calibration problems can, for example, be related to rather simple errors in the recording of operational data (point 2), e.g. erroneous data of the waste sludge measurements might result in an incorrect sludge balance (Melcer, 1999). Moreover good characterisation of hydraulics and settling can be of great importance since e.g. poor or erroneous hydraulic modelling may result in hydraulic effects being lumped into the biological parameters of ASM1.

The information needed for the characterisation of the biological model, listed in point 5 above, can basically be gathered from three sources:

1. Default values from literature (e.g. Henze *et al.*, 1987).
2. Full-scale plant data
 - 2.1. Average or dynamic data from grab or time/flow proportional samples.
 - 2.2. Conventional mass balances of the full-scale data.
 - 2.3. On-line data.
 - 2.4. Measurements in reactors to characterise process dynamics (mainly relevant for SBR's and alternating systems).
3. Information obtained from different kinds of lab-scale experiments with wastewater and activated sludge from the full-scale plant under study.

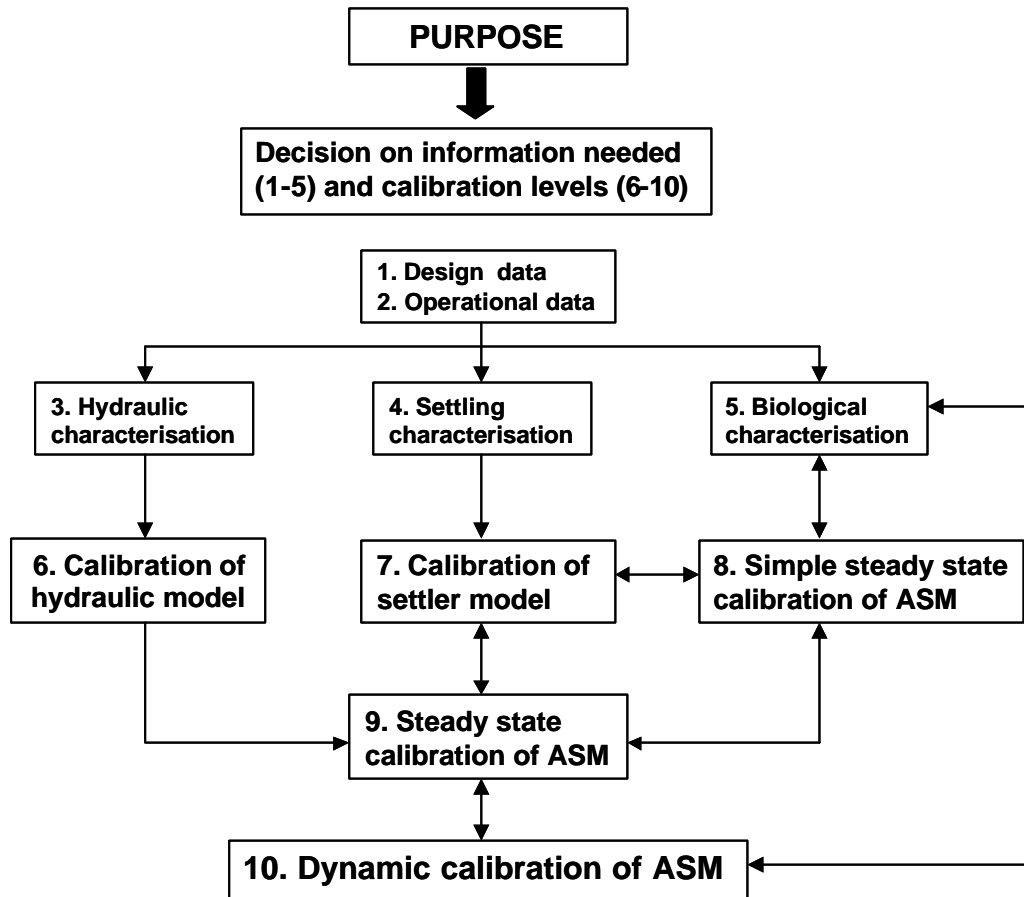


Figure 5. Schematic overview of the different general steps in an activated sludge model calibration procedure

Again, the intended use of the model will determine which information source to choose for the characterisation of the different biological processes in the model. In addition, the purpose will decide to which level the model has to be calibrated, since the quality of the desired model predictions will depend strongly on the quality of the model calibration. Fig. 5 illustrates the different general steps in a model calibration procedure. It should be stressed that not all steps may have to be taken depending on the purpose. This will be discussed further with examples below, and will be concretised for one case study carried out in the frame of this study (see chapter 8).

3.2. Model calibration levels.

Steps 1-5 in Fig. 5 indicate the collection of information. Design (1) and operational (2) data are in general always needed for a model calibration. E.g. the flow and load variations are important in the design of measuring campaigns for hydraulic, sludge settling and biological characterisation of the full-scale WWTP. The hydraulics (3) are typically characterised via tracer tests at the full-scale installation (De Clercq *et al.*, 1999). The settling properties (4) can be characterised via on-line or lab-scale settling tests (Vanderhasselt

et al., 1999a, 1999b). Finally, the biology can be characterised via different information sources (see below).

In Fig. 5 steps 6-10 illustrate different calibration levels. The calibration of the hydraulic model via tracer test results, and the settler model calibration via results from sludge settling tests are indicated in steps 6 and 7 respectively. A first ASM calibration level is typically a simple steady state model calibration (8).

3.2.1. Steady state model calibration

In this step data obtained from the full-scale WWTP are averaged, thereby assuming that this average represents a steady state, and a simple model not including hydraulic detail is calibrated to average effluent and sludge waste data. Typically, the calibrations of the ASM and the settler are linked together, since the aim is most often to describe the final effluent quality. Moreover, the recycle from the settler has an influence on the activated sludge system. Thus, at this stage, there may be an interaction between the steady state calibration and the settler model calibration, indicated in Fig. 5 with the double arrow. Finally, the characterisation of wastewater components may be adjusted according to the calibration of the full-scale model, indicated with the double arrow between (8) and (5) in Fig. 5.

The next step in the calibration procedure is a steady state model calibration that includes the hydraulic model (9). In general, with a steady state model calibration, only parameters responsible for long-term behaviour of the WWTP can be determined, i.e. Y_H , f_p , b_H and X_I in the influent (Henze *et al.*, 1998; Nowak *et al.*, 1999). These parameters are correlated to a certain degree, meaning that a modification of one parameter value can be compensated by a modification of another parameter value. In the study of Nowak *et al.* (1999) on mass balances of full-scale data, it was therefore chosen to fix Y_H and f_p , leaving X_I in the influent and b_H to be determined from the steady state data. In the study of Lesouef *et al.* (1992), two WWTP models were calibrated via steady state calibration only, and this calibrated model was applied to simulate dynamic process scenarios. However, if one relies entirely on a steady state calibration some problems may be encountered since the real input variations are usually faster than the slow process dynamics that were focused upon during the steady state calibration. In other words, the process does not operate in steady state but one still attempts to fit a steady state simplification of the model to an unsteady situation. A steady state calibration is, however, very useful for the determination of initial conditions prior to a dynamic model calibration and for the initiation of first parameter iteration (e.g. Pedersen and Sinkjær, 1992; Stokes *et al.*, 1993; Dupont and Sinkjær, 1994; Xu and Hultman, 1996; Kristensen *et al.*, 1998).

3.2.2. Dynamic model calibration

If it is the aim to describe and predict more short-term and dynamic situations, a model calibration to dynamic data will be needed since such data contain more information than steady state data, especially on fast dynamic behaviour. The important point in model calibration based on dynamic data is to obtain a

more reliable estimation of the maximum specific growth rates $\mu_{\max H}$ and $\mu_{\max A}$ (Henze *et al.*, 1998), which are the most important parameters in predicting dynamic situations.

At the WWTP data are most often collected routinely with a daily or weekly sampling frequency. This sampling frequency may, however, not be high enough, and for more accurate modelling it may therefore be required to run special measuring campaigns (e.g. Pedersen and Sinkjær 1992; Dupont and Sinkjær, 1994; de la Sota *et al.*, 1994; Xu and Hultman, 1996). The sampling frequencies should be chosen in relation to the time constants of the process and influent variations. One of the important time constants of the process is the hydraulic retention time (HRT). Ideally, one should choose to sample about five times faster than the hydraulic retention time and have a test duration of 3-4 times this key time constant (Ljung, 1987). However, since measurements on full-scale WWTP's are relatively expensive these recommendations may not always be completely fulfilled.

Furthermore, data from the full-scale installation alone may be insufficient for a dynamic model calibration since the reaction kinetics can not be readily obtained from such data, except for specific designs like SBR's and alternating systems (Vanrolleghem and Coen, 1995). For a dynamic model calibration on a full-scale WWTP the modeller is therefore typically aiming at combining more information rich results derived from lab-scale experiments (carried out with sludge and wastewater from the full-scale installation) with data obtained from measuring campaigns on the WWTP under study (Dupont and Sinkjær, 1994; Xu and Hultman, 1996; Kristensen *et al.*, 1998).

In Table 3 an attempt is made to gather and summarise the available literature examples on model calibrations where detailed information is given on the model calibration procedures. The table should not be regarded as a complete list of possibilities but can serve as a starting point. The purpose of the different model calibrations is given together with the applied calibration strategy. Furthermore, the information sources for the characterisation of (1) wastewater, (2) sludge, (3) kinetics and (4) stoichiometry, are listed. Table 3 does not indicate the kind of experiments that may have been carried out to gather the information, since this will be discussed in one of the next sections of this review. The model parameters that are not mentioned in Table 3 have either been taken from literature or their origin may not have been clearly indicated in the references. Considering wastewater characterisation it is not always specified how the wastewater information was converted into the wastewater components according to ASM1. In these cases only the type of measurement (e.g. COD, TKN etc.) is listed in the Table.

Based on Table 3, it is obvious that the choice of information needed for the model calibration is governed by the purpose. E.g. in the studies of Pedersen and Sinkjær (1992) and Dupont and Sinkjær (1994) the emphasis was to have a description of the nitrification and denitrification, and the model calibrations therefore focused on adjustment of the parameters related to these processes. In contrast, other studies aimed at a description of both COD and N removal, and as a result more parameters had to be considered

for adjustment in the model calibration (Siegrist and Tschui, 1992; de la Sota *et al.*, 1994; Xu and Hultman, 1996; Kristensen *et al.*, 1998).

The wastewater characterisation has both been carried out via full-scale data combined with mass balances and via lab-scale experiments, e.g. for the inert components S_I and X_I (Lesouef *et al.*, 1992) and the S_S component (Xu and Hultman, 1996; Kristensen *et al.*, 1998). In one study all wastewater components were determined via model calibration on the full-scale data (de la Sota *et al.*, 1994). The determination of the stoichiometric and kinetic parameters is often carried out via calibration of the model to the full-scale data only. However, some studies have also included the effort of characterising some parameters in lab-scale experiments, e.g. for the determination of the specific growth rate of the autotrophic biomass (e.g. Lesouef *et al.*, 1992; Dupont and Sinkjær, 1994) or to collect further information on the half-saturation coefficients (Kristensen *et al.*, 1998).

In addition, Table 3 indicates that if the purpose of the model calibration was more than “just” a description of the processes, more emphasis was put on the characterisation of the relevant parameters via lab-scale experiments. For example in the study of Dupont and Sinkjær (1994) the aim was to apply the model for optimisation of nitrogen removal.

Finally, Table 4 aims at summarising the most relevant parameters to adjust in the steady state and dynamic model calibration. The parameters related to the hydrolysis process are not included in Table 4. This was done on purpose since it was not clear from the literature whether the parameters of this process are most influential to short- or long-term treatment plant behaviour.

Table 3. Information sources for model calibration of ASM1

Reference	Purpose	Calibration strategy	Characterisation						
			Wastewater		Sludge	Kinetic and stoichiometric			
			Full-scale data	Model components			Lab-scale analyses	Model calibration	Lab-scale experiments
Mass balances	Lab-scale	Model calibration							
ST92	Description: Nitrification, COD removal	Steady state n.i. Dynamic	3,7,8,9	S_I	X_I			$Y_H, \mu_H, K_S, k_b,$ K_X, b_H, μ_A, K_{NH}	
L92	Optimisation: N-removal	Steady state	3,4,8,9	S_S, X_S, X_{BH}	S_I, X_I		1,2,3,7	K_X, k_b	μ_A, b_A
PS92	Description: N-removal	Steady state Dynamic	3,4,5,7,8, 9	S_S, S_I, X_I				μ_A, K_S, η_E	
DS94	Optimisation: N-removal	Steady state Dynamic	3,4,5,7,8, 9	n.i.			n.i.	K_S, η_E	$\mu_A, b_A, K_{NH}, K_{OA}$
S93	Description: Nitrification, COD removal	Steady state Dynamic	1,3,5,6,8	n.i.			1,2,3	μ_H, K_S, μ_A	
dS94	Optimisation: All processes	Steady state Dynamic	3,5,7,8,9, 10			all	1,2,3,7	$\mu_A, b_A, \mu_H, K_S, k_b,$ $K_X, K_{NO}, \eta_E, \eta_b$	
XH96	Description: COD removal, N removal	Steady state Dynamic	3,4,6,8,9	S_I, S_S	S_S, X_{BH}, X_S	X_I	1	$\mu_A, K_{OH}, K_{NH}, \eta_E$	
K98	Description: COD removal, N removal	Steady state Dynamic	1,2,3,4,7, 8,9		S_S		1,2	$k_b, K_X, b_H, \eta_E,$ K_{OH}	$b_H, \mu_H, \mu_A, K_{OA}$

- n.i. procedures not described in detail, but probably carried out.
- 1) SS : Suspended Solids
 - 2) VSS : Volatile Suspended Solids
 - 3) COD_{tot} : total COD
 - 4) COD_{sol} : soluble COD
 - 5) BOD₅ : Biological Oxygen Demand (5days)
 - 6) TN : Total Nitrogen
 - 7) TKN : Kjeldahl Nitrogen
 - 8) NH₄-N : Ammonium Nitrogen
 - 9) NO_x-N : Nitrate + Nitrite Nitrogen
 - 10) PO₄-P : Ortho-phosphate

- dS94 de la Sota *et al.*, (1994)
 DS94 Dupont and Sinkjær (1994)
 K98 Kristensen *et al.*, (1998)
 L92 Lesouef *et al.*, (1992)
 PS92 Pedersen and Sinkjær (1992)
 ST92 Siegrist and Tshui (1992)
 S93 Stokes *et al.* (1993)
 XH96 Xu and Hultman (1996)

Table 4. Most relevant parameters in steady state and dynamic model calibration.

	Steady state calibration	Dynamic calibration
Predictions	Long-term	Short-term
Main relevant parameters	$Y_H, f_P, b_H, X_{I,influent}$	$\mu_{maxH}, \mu_{maxA}, \eta_g, \eta_h, K_S, K_{NH}, K_{OH}, K_{OA}$

4. Characterisation of wastewater and sludge kinetics

Different methods may be proposed to structure the wealth of methods that have been developed and applied for the characterisation of wastewater and reaction kinetics in relation to ASM1. At this point it is assumed that the reader is familiar with the ASM1 terminology. In this review it has been chosen to focus on the methodologies, i.e. what can be achieved with different methods, their advantages and disadvantages, rather than focus on the different wastewater components and processes separately. This choice was motivated by the fact that some methods typically can yield information on more than one component or process. In the end of the review it is attempted to illustrate the power of the different methods for wastewater and sludge kinetics characterisation in the frame of ASM1. Finally, the relevance of characterising the different components and processes in the frame of ASM1 model calibration is critically evaluated.

4.1. Wastewater characterisation

Wastewater can be characterised either with physical-chemical methods or with biological methods. In practice one typically ends up with a combined approach to obtain an estimate of the concentrations of all components. In the following physical-chemical and biological methods will first be described separately to obtain an overview of what can be achieved with the different methods. Finally, an overview of what can be achieved by combining both approaches is illustrated and discussed. In ASM1 the COD_{tot} of the wastewater is considered to consist of inert soluble organic matter (S_I), readily and slowly biodegradable substrate (S_S and X_S respectively) and inert suspended organic matter (X_I), whereas biomass in the wastewater is considered to be insignificant:

$$COD_{tot} = S_I + S_S + X_I + X_S \quad (5)$$

4.1.1. Physical-chemical characterisation

A wastewater can be separated into different components in a relatively simple manner via physical-chemical separation methods.

The difference in molecular size can give an indication on biodegradability because small molecules can be taken up directly over the cell membranes whereas bigger molecules need to be broken down prior to

uptake. Enzymatic hydrolysis is primarily a surface phenomenon, which means that the hydrolysis rate is directly related to the surface area. Thus, smaller molecules are readily degraded whereas degradation of larger material can be kinetically limited.

In early studies the wastewater components were separated physically into four size-depending fractions by successive sedimentation, centrifugation, and filtration. The fractions were classified as settleable, supracolloidal, colloidal, and soluble (Rickert and Hunter, 1971), and were analysed for Chemical Oxygen Demand (COD). An important conclusion from these early studies was that particles smaller than 1.0 μm were approximated to be the true soluble fraction. Moreover, the particles smaller than 1.0 μm were observed to be more rapidly degradable than particles larger than 1.0 μm . In a more recent study Levine *et al.* (1985) studied the size distribution of the organic matter in wastewater and the relationship to different wastewater treatment processes. In this study it was concluded that a separation over a membrane with a pore size of 0.1 μm was valid for a differentiation between the true soluble and particulate organic fractions. The organic particles smaller than 0.1 μm are typically cell fragments, viruses, macromolecules and miscellaneous debris. The major groups of macromolecules in wastewater are polysaccharides, proteins, lipids and nucleic acids. The fraction measured by the standard test for suspended solids (1.2 μm) includes protozoa, algae, bacterial flocs and single cells. However some bacterial cells, cell fragments, viruses and inorganic particles have a size from 0.1 to 1.2 μm and will thus also pass through the more typically applied filter size of 0.45 μm for separation between soluble and particulate matter (Levine *et al.*, 1985). The size of colloidal matter is typically in the range 0.1-50 μm whereas material with a size larger than 50 μm usually settles (Levine *et al.*, 1985).

The ASM models do not differentiate between filtered, colloidal and settleable wastewater fractions. It is therefore necessary to convert the fractions resulting from a physical-chemical characterisation to the ASM components. The possibilities and limitations of physical-chemical methods to accomplish this task are summarised and discussed below.

Inert soluble organic matter S_i

Soluble inert organic matter S_i is present in the influent, but, importantly, is also produced during the activated sludge process (Chudoba, 1985; Orhon *et al.*, 1989; Boero *et al.*, 1991; Germirli *et al.*, 1991; Sollfrank *et al.*, 1992). Most of the evidence for the production of soluble organics by micro-organisms is collected from experiments with simple known substrates, e.g. glucose (Chudoba, 1985; Boero *et al.*, 1991). However, the production has also been proven to take place with wastewater (Orhon *et al.*, 1989; Germirli *et al.*, 1991; Sollfrank *et al.*, 1992). The S_i production seems to depend on the initial substrate concentration and on cultivation conditions (Chudoba, 1985). A model has been proposed relating the S_i formation to the hydrolysis of non-viable cellular materials in the system, thereby linking the S_i production to the initial substrate concentration and the decay of the produced biomass (Orhon *et al.*, 1989). This

model was verified in a study with different industrial wastewaters and, although the data were not of very high quality, some evidence was given that the S_I production depends very much on the wastewater type (Germirli *et al.*, 1991). The hypothesis that the S_I production originates from the decay process was, however, contradicted in a study on municipal wastewater (Sollfrank *et al.*, 1992) where it was concluded that the S_I production was related to the hydrolysis of slowly biodegradable COD of the incoming wastewater.

Thus, although the origin of the S_I production may remain unexplained, it seems clear that it does take place to various extents depending on different factors as mentioned above, resulting in a S_I concentration in the effluent that may be higher than the influent. Such S_I production is, however, not included in the ASM models, where S_I is considered a conservative component. To deal with this discrepancy between model concept and reality a simplified approach is typically applied by the definition of a fictive model influent concentration S_I which includes the produced S_I together with the real S_I influent concentration (Henze, 1992).

It is not possible to measure S_I directly and different approximations are therefore usually applied. Most often S_I is determined by the soluble effluent COD, which has appeared to be a good estimate for S_I in case of a low loaded activated sludge process (Ekama *et al.*, 1986). On the other hand Siegrist and Tschui (1992) suggested that the influent S_I could be estimated as 90% of the effluent COD. These approximations may hold in most cases, but a more correct approach would be to consider it as the soluble effluent COD minus the soluble effluent Biochemical Oxygen Demand (BOD) multiplied with a BOD/COD conversion factor (Henze, 1992). Furthermore, S_I can be determined as the soluble COD remaining after a long-term BOD test with the influent (Henze *et al.*, 1987; Lesouef *et al.*, 1992). The latter approach is in fact a combination of physical-chemical and biological methods. However, in case of significant S_I production during the test the influent S_I may be overestimated (Sollfrank *et al.*, 1992), which may lead to an underestimation of influent S_S eventually. Finally, a procedure was developed to distinguish between S_I of the influent wastewater and S_I produced during degradation (Germirli *et al.*, 1991). However, in order to achieve significant response glucose was added in these tests assuming that the wastewater under study resembled glucose, an assumption that may not hold in practice.

Summarising, it will be case depending whether it is needed to characterise the produced S_I or whether the model component can be approximated as described above.

Readily biodegradable substrate S_S

The soluble COD fraction excluding the soluble inert organic matter (S_I) is mostly considered to represent the readily biodegradable substrate S_S . The correctness of this approach does however evidently depend on the pore size of the filters used for the separation. As described above the “true” soluble fraction passes through a 0.1 μm filtration step according to Levine *et al.* (1985). However, in practice larger filter sizes

are most often used, which may result in an overestimation of the soluble readily biodegradable substrate concentration, assuming that the definition of Levine *et al.* (1985) holds.

Another study confirmed that the fraction passing a 0.1 μm filter gave a good representation of the soluble readily biodegradable substrate (Torrijos *et al.*, 1994). It was confirmed biologically (via respirometry, see below for a detailed description) that the studied wastewater did not contain any particulate readily biodegradable matter. In contrast with this, Spanjers and Vanrolleghem (1995) found, also via respirometry, that filtered wastewater (0.45 μm) had a lower biological response than unfiltered wastewater, indicating that parts of the readily biodegradable wastewater fraction was retained on the filter. Similarly, for an industrial wastewater it was found that the filtrate fraction produced via ultrafiltration (pore size $< 0.001 \mu\text{m}$) had a lower biodegradability (13% of COD_{tot}) than the fraction determined with a respirometric characterisation method (20% of COD_{tot}) (Bortone *et al.*, 1994). Further it was also found that part of the soluble COD can be slowly biodegradable (Sollfrank and Gujer, 1991).

Finally, a method based on flocculation with $\text{Zn}(\text{OH})_2$ has been developed to remove colloidal matter of 0.1-10 μm that normally passes through 0.45 μm filter membranes, and was successfully applied to a phosphorus removal activated sludge system (Mamais *et al.*, 1993). However, the flocculation has appeared to be rather sensitive to interference and appears highly depending on the pH value during the flocculation (Haider, 2000).

Inert suspended organic matter X_i

The test proposed for the determination of S_r , as the residual soluble COD remaining after a long-term BOD test, by Lesouef *et al.* (1992) can also be applied to determine X_i . The X_i concentration is then determined as the residual particulate COD, assuming that X_i is not produced during the test. This assumption may, however, be questionable since X_i will be produced due to decay during the long-term BOD test and corrections for this will have to be considered.

Slowly biodegradable substrate X_s

As mentioned earlier, a physical characterisation based on different molecular sizes can be used to distinguish between readily biodegradable substrate S_s and slowly biodegradable substrate X_s . In one study it has been proposed that X_s may be determined as the colloidal fraction defined by 0.1 – 50 μm (Torrijos *et al.*, 1994). However, this hypothesis could not be supported since the results indicated that the colloids mainly disappeared according to a physical removal mechanism without any related biological oxidation. In another study of contact stabilisation, a multiple filtration procedure was used to isolate and monitor the variation in concentration of the colloidal fraction between 0.03 – 1.5 μm (Bunch and Griffin, 1987). Here it was further confirmed that colloidal matter was removed physically, probably by adsorption. However, the subsequent increase in soluble organic matter, and corresponding oxygen uptake resulting

from breakdown of colloidal substrate, were not observed. Thus, based on these two studies it is not clear whether colloids can be considered equal to X_S . Part of the colloidal substrate may be inert, as was probably the case in the example of Bunch and Griffin (1987), but this was not considered in these studies.

In addition, parts of the soluble substrate (Sollfrank and Gujer, 1991) and the settleable matters may belong to the X_S fraction making it rather problematic to characterise X_S entirely by a physical-chemical method.

Finally, if the components S_S , S_I and X_I are known and if it is assumed that the biomass concentration is negligible, X_S can be determined via a simple mass COD balance.

Biomass X_{BH} and X_{BA}

It is not possible to distinguish biomass concentrations via a physical-chemical method.

Nitrogen components S_{NH_4} , S_{NO_2} , S_{NO_3} , X_{ND}

The nitrogen components can rather easily be detected by physical-chemical analysis via a combination of standard analyses of ammonium, nitrite and nitrate and Kjeldahl nitrogen (TKN) on filtered and non-filtered samples (Henze *et al.*, 1987).

Summary and discussion of physical-chemical wastewater characterisation

Based on the descriptions and discussions above it can be concluded that a wastewater characterisation entirely based on physical-chemical characterisation alone will not be sufficient to obtain an accurate distribution of the organic substrate over the different ASM1 components (Fig. 6A). However, physical-chemical methods alone may be adequate for the estimation of the nitrogen components (Fig. 6B). In Fig. 6 the dashed line indicates the range of uncertainty with respect to the determination of the organic components.

Summarising, the two main problems with respect to determination of the organic components entirely by physical-chemical means are:

4. The reliability of S_S determination based on soluble COD depends very much on the applied filter size but, even more, on the kind of wastewater under study since it is possible that part of the particulate substrate is also readily biodegradable.
5. Defining X_S as being the colloids can induce errors because the colloidal fraction may also contain inert matter. Moreover, parts of the soluble and settleable fractions may belong to X_S . Thus, it is not possible to separate the particulate X_S , X_I and X_{BH} components adequately.

Table 5 summarises the characterisation of wastewater components via physical-chemical methods, and the assumptions needed, as described in the literature review above. According to this table it can be seen that with some assumptions and a combination of a physical-chemical and a biological method for assessment of X_I (long-term BOD test) (Lesouef *et al.*, 1992), it is possible to determine all COD components (S_S , S_I , X_S and X_I). Knowledge of X_I allows a determination of X_S via a mass balance of particulate COD, assuming that X_{BH} is zero. However, it should be kept in mind that the determination of X_I via a long-term BOD test may not be accurate, as discussed above. Moreover the assumption that particulate COD is not readily biodegradable may be incorrect.

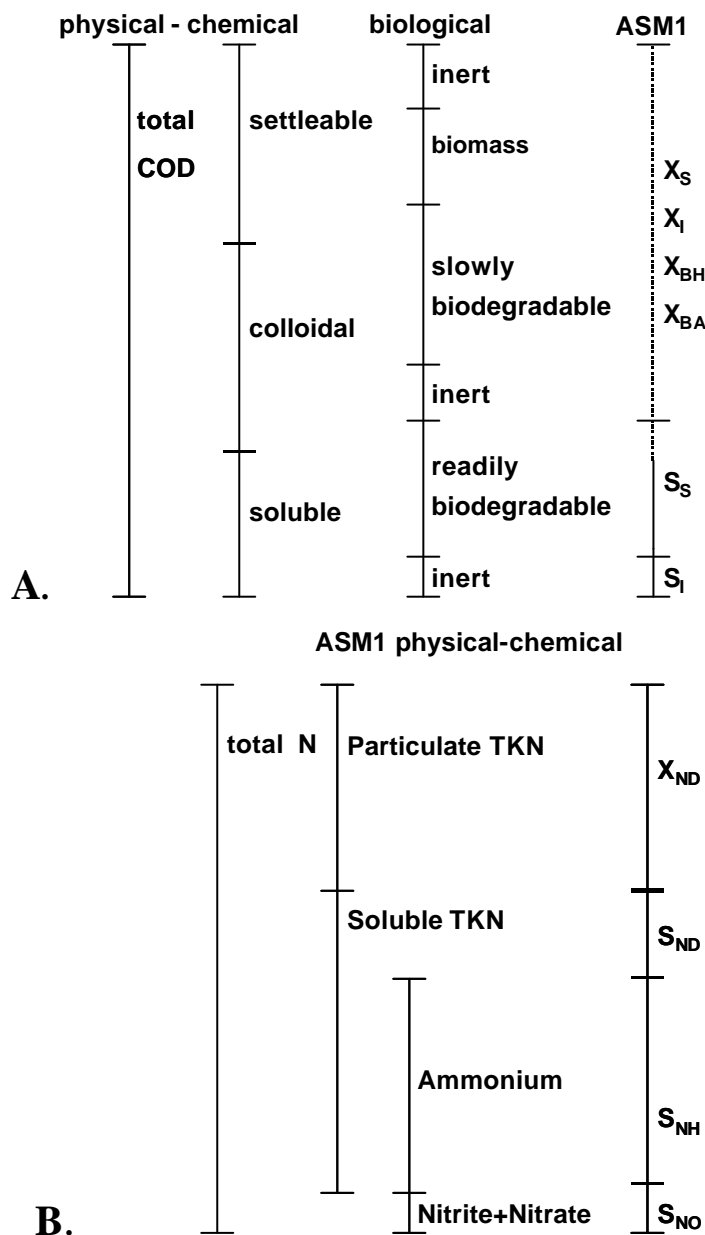


Figure 6. Characterisation of ASM1 wastewater components by physical-chemical methods (**A:** modified from STOWA (1996), and **B:** modified from Henze *et al.* (1995))

Table 5. Overview of physical-chemical methods for determination of wastewater components (Fields with grey background indicate that a physical-chemical method is not applicable)

Component	Method	Additional information.	Assumptions	References
S _I	0.45 µm filtration of effluent		low loaded system (no biodegradable substrate in effluent)	E86
	90% of effluent COD			ST92
	7-8 µm filtration after long-term aeration test		no S _I production during degradation	L92; S92
	COD profiles in batch tests		wastewater similar to glucose	G91
S _S	0.1 µm filtration	S _I	Particulates do not contain readily biodegradable matters	L85; T94
	7-8 µm filtration	S _I		L92
	Zn(OH) ₂ flocculation	S _I		M93
X _I	7-8 µm filtration after long-term aeration test		no X _I production during degradation	L92
X _S	mass balance	S _S , S _I , X _I	X _{BH} , X _{BA} negligible	H87
X _{BH}				
X _{BA}				
X _P				
S _O	Standard analysis of oxygen concentration			
S _{NO}	Standard analysis			H87
S _{NH}	Standard analysis			H87
S _{ND}	Standard analysis of soluble TKN	S _{NH}		H87
X _{ND}	Standard analysis of particulate TKN			H87
S _{ALK}	Standard analysis of alkalinity			

References:

E86	Ekama <i>et al.</i> , 1986	G91	Germirli <i>et al.</i> , 1991	H87	Henze <i>et al.</i> , 1987
L92	Lesouef <i>et al.</i> , 1992	L85	Levine <i>et al.</i> , 1985	M93	Mamais <i>et al.</i> , 1993
ST92	Siegrist and Tschui, 1992	S92	Sollfrank <i>et al.</i> , 1992	T94	Torrijos <i>et al.</i> , 1994

4.1.2. Biological characterisation

The ASM models are in general biologically defined models. Thus, it is not surprising that biological wastewater characterisation methods have found wider application and acceptance than physical-chemical characterisation tests. In the biological methods the fractionation of organic matter is based on its rate of degradation (Henze, 1992) which makes the relation to the ASM concepts more direct. It is obvious that mainly the biodegradable components and the microbial biomass in the wastewater (S_S , X_S , S_{NH} , S_{ND} , X_{ND} and X_{BH}) can be characterised directly by these methods, whereas the inert components S_I and X_I may be determined by a combination of physical-chemical and biological tests, as already mentioned above (Lesouef *et al.*, 1992). Typically, a biological characterisation is based on measurements of the biomass response during substrate degradation in either a continuous flow-through system or batch type experiment. This means that the concentration determination of the biodegradable components is indirect, since the biomass activity has to be interpreted in terms of a substrate concentration. In principle the consumption of substrate can be measured directly by measurements of e.g. COD. However, this is typically not very practical due to problems of sampling and filtration of sludge samples etc. Instead, the biomass response during substrate degradation can be monitored by recording the utilisation of electron acceptors, such as oxygen or nitrate, or the formation of products, such as protons, nitrate or carbon dioxide.

A main part of the review on biological characterisation will deal with respirometry. Respirometry is defined as the measurement and interpretation of the oxygen uptake rate of activated sludge (Spanjers *et al.*, 1998). In fact the main goal of a WWTP is to reduce the biochemical oxygen demand of the wastewater, and ASM1 was primarily developed to yield a good description of the sludge production and consumption patterns of electron acceptors, as described above. Thus, it is not surprisingly that respirometry has turned into one of the most popular biological characterisation methods, since the total respiration rate is affected by the concentration of all aerobically biodegradable components, to which the majority of wastewater components usually belong. However, nitrate utilisation rates can also be applied for characterisation of the denitrification potential of a wastewater. Finally, a titrimetric technique, especially applicable for determination of the ammonium concentration available for nitrification, will be reviewed.

Before the description and discussion on the application of respirometry, nitrate utilisation rates and titrimetry for wastewater characterisation, the methodology of each method is described in more detail. Thus, the readers already familiar with these methodologies can skip these intermediate sections and directly continue reading about their applications for wastewater characterisation.

4.1.2.1. Respirometry

Historically, the determination of the Biochemical Oxygen Demand (BOD) during an incubation period of 5 to 7 days (BOD_5 or BOD_7) has been widely applied to quantify the effects of pollutants on the oxygen demand of receiving waters, and was further applied for the characterisation of wastewater. However, due to the rather arbitrary choice of 5 or 7 days the test result represents a varying part of the ultimate BOD of different wastewaters, depending on the wastewater composition. For a more complete analysis of the ultimate oxygen demand of a wastewater the BOD test can be expanded to 20-30 days, typically 28 days. In the BOD tests the oxygen content is most often only recorded at the start and end of the test without information on the evolution of the oxygen consumption over time. This means that the test can not give any information on the different biodegradable fractions.

The test length of 5-7 days or even longer is not very suitable in the frame of wastewater treatment plant operation. As a consequence the concept of short-term biochemical oxygen demand (BOD_{st}) was introduced (Vernimmen *et al.*, 1967). The concentration of BOD_{st} can be determined via respirometry. As defined above, respirometry deals with the measurement and interpretation of the oxygen uptake rate, r_O , of activated sludge. In general, the r_O may be considered to consist of two components (Spanjers, 1993): The exogenous oxygen uptake rate ($r_{O,ex}$), which is the immediate oxygen uptake needed to degrade a substrate, and the endogenous oxygen uptake rate ($r_{O,end}$). Different definitions of $r_{O,end}$ appear in literature. The definition applied by Spanjers (1993) is that the $r_{O,end}$ is the oxygen uptake rate in absence of readily biodegradable substrate. In the context of ASM1 it is assumed that $r_{O,end}$ is associated with the oxidation of readily biodegradable matter produced by (1) hydrolysis of the slowly biodegradable matter that results from lysis of decayed biomass and, (2) the use of substrate for maintenance. The integral of the $r_{O,ex}$ profile is a measure of BOD_{st} (Spanjers *et al.*, 1998).

Contrary to the BOD_5 method, the BOD_{st} test is carried out with the same biomass as in the activated sludge plant under study and may therefore be a more representative measure of the effect of the wastewater on the particular activated sludge plant under study. Several attempts have been made to correlate BOD_5 to BOD_{st} (Vernimmen *et al.*, 1967; Farkas, 1981; Suschka and Ferreira, 1986; Vandebroek, 1986; Ciaccio, 1992; Vanrolleghem and Spanjers, 1994). However, the success of such a correlation seems to depend strongly on the type of wastewater, since the wastewater may contain varying proportions of readily and slowly biodegradable fractions.

Fig. 7 illustrates the conceptual idea of respirometry. The degradation of substrate S_1 and S_2 (Fig. 7A) results in a total exogenous uptake rate $r_{O,ex}$ (Fig. 7B). Fig. 7B illustrates a rather typical respirogram (i.e. a time course of respiration rates) with an initial peak in $r_{O,ex}$ caused by oxidation of the most readily biodegradable matter, here S_1 , followed by, in this case, one “shoulder” in the $r_{O,ex}$ profile where component S_2 continues to be degraded. Thus, in this example the contribution of S_1 and S_2 to the total

$r_{O,ex}$, and related total BOD_{st} , can easily be distinguished.

However, it will become clear from the “wheel-work” described in Table 6 (Vanrolleghem *et al.*, 1999) that most of the processes in ASM1 eventually act on the oxygen mass balance and may result in more complicated $r_{O,ex}$ profiles. The total $r_{O,ex}$ of the activated sludge in contact with wastewater is given in Eq. 6 according to ASM1.

$$r_{O,ex} = (1 - Y_H) \frac{X_{BH} \cdot m_{maxH}}{Y_H} \cdot \frac{S_S}{K_S + S_S} + (4.57 - Y_A) \frac{X_{BA} \cdot m_{maxA}}{Y_A} \cdot \frac{S_{NH}}{K_{NH} + S_{NH}} \quad (6)$$

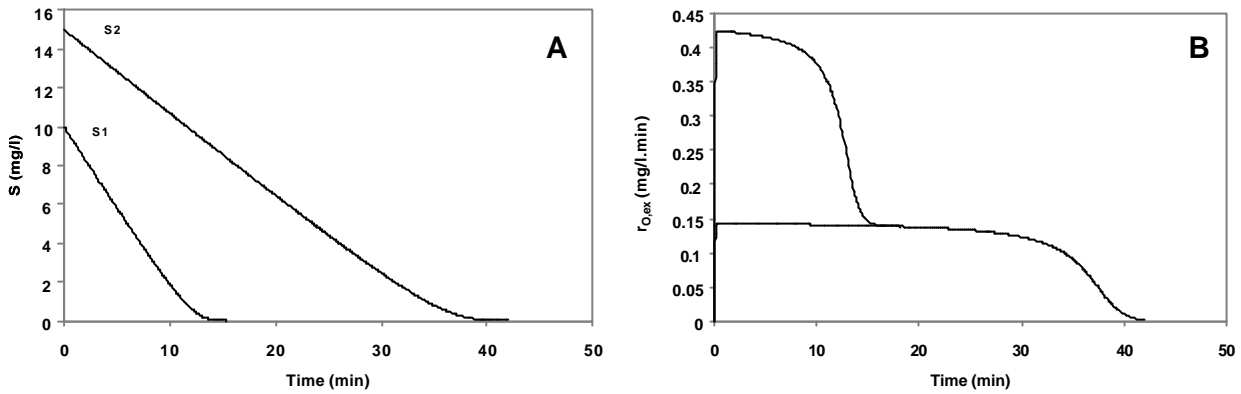


Figure 7. Conceptual respirogram resulting from degradation of substrate S_1 and S_2

The concentration of S_S and S_{NH} depend on the influent wastewater and also on the rates at which X_S , S_{ND} and X_{ND} are degraded. As an example we will follow the arrows from X_{BH} to S_O (Table 6): in the mass balance of the heterotrophic biomass X_{BH} (column, c., 5) the production of X_{BH} by aerobic growth (row, r., 1) is counteracted by the loss of X_{BH} by heterotrophic decay (r. 4). In this decay process component X_{BH} (c. 5) is converted to component X_S (c. 4). This production of X_S is counteracted by the loss of X_S by hydrolysis (r. 7), leading to production of component S_S (c. 2). S_S is subsequently used for heterotrophic growth (r. 1) where it is converted to component X_{BH} (c. 5) with concomitant consumption of oxygen S_O (c. 8), i.e. respiration. A similar reasoning can be made for the processes involving the nitrogen components (S_{NH} , S_{ND} and X_{ND}) and autotrophic (nitrifying) organisms (X_{BA}).

Fig. 8 shows different examples of respirograms collected in a batch experiment where synthetic wastewaters were added to endogenous sludge. Note that in Fig. 8 C-D only the exogenous oxygen consumption due to substrate oxidation is given, $r_{O,ex}$, whereas the total r_O is given in Fig. 8 A-B. It now becomes clear that the respirograms can differ significantly in shape depending on the substrate added and may not be as straightforward to interpret as the conceptual example given in Fig. 7. Thus, the challenge is to interpret and perhaps divide the respirogram according to the contribution of $r_{O,ex}$ by different wastewater components.

Table 6. Kinetic and stoichiometric relationships for COD removal, nitrification and denitrification (Vanrolleghem *et al.*, 1999)

Component i	1	2	3	4	5	6	7	8	9	10	11	12	13	Process rate ρ_j ML ⁻³ T ⁻¹
j Process	S_1	S_2	X_1	X_2	X_{BH}	X_{BA}	X_P	S_0	S_{NO}	S_{NH}	S_{ND}	X_{ND}	S_{ALK}	
1 Aerobic heterotrophic growth		$-\frac{1}{Y_H}$			1			$1 - \frac{1}{Y_H}$		$-i_{XB}$			$-\frac{i_{XB}}{14}$	$\mu_H X_{BH}$
2 Anoxic heterotrophic growth		$-\frac{1}{Y_H}$			1				$-\frac{1 - Y_H}{2.86 Y_H}$	$-i_{XB}$			$\frac{1 - Y_H}{2.86 \cdot 14 \cdot Y_H} - \frac{i_{XB}}{14}$	$\mu^o_H X_{BH}$
3 Aerobic autotrophic growth						1		$1 - \frac{4.57}{Y_A}$	$\frac{1}{Y_A}$	$\frac{1}{Y_A} - i_{XB}$			$-\frac{2}{14 \cdot Y_A} - \frac{i_{XB}}{14}$	$\mu_A X_{BA}$
4 Het. decay				$1 - f_p$	-1		f_p					$i_{XB} f_p i_{XP}$		$b_H X_{BH}$
5 Aut. Decay				$1 - f_p$	-1		f_p					$i_{XB} f_p i_{XP}$		$b_A X_{BA}$
6 Ammonification										1	-1		1/14	$k_A S_{ND} X_{BH}$
7 Hydrolysis		1			-1									$k'_h X_S$
8 Hydrolysis of N											1	-1		$k_u X_{ND}$
Observed conversion rates ML ⁻³ T ⁻¹	$r_i = \sum_j r_{ij} = \sum_j v_{ij} \rho_j$													
Stoichiometric parameters (see text)	Nomenclature, see text All units in ML ⁻³ (COD or N, depending on variable)													Kinetic parameters (see text)

$$\mu_H = \mu_{\max H} \left(\frac{S_S}{K_S + S_S} \right) \left(\frac{S_0}{K_{O,H} + S_0} \right) \quad \mu_H^o = \eta_g \mu_{\max H} \left(\frac{S_S}{K_S + S_S} \right) \left(\frac{K_{OH}}{K_{OH} + S_0} \right) \left(\frac{S_{NO}}{K_{NO} + S_{NO}} \right)$$

$$\mu_A = \mu_{\max A} \left(\frac{S_{NH}}{K_{NH} + S_{NH}} \right) \left(\frac{S_0}{K_{OA} + S_0} \right)$$

$$k'_h = k_h \frac{1}{K_X + (X_S/X_{BH})} \left(\frac{S_0}{K_{OH} + S_0} \right) + \eta_h \left(\frac{K_{OH}}{K_{OH} + S_0} \right) \left(\frac{S_{NO}}{K_{NO} + S_{NO}} \right)$$

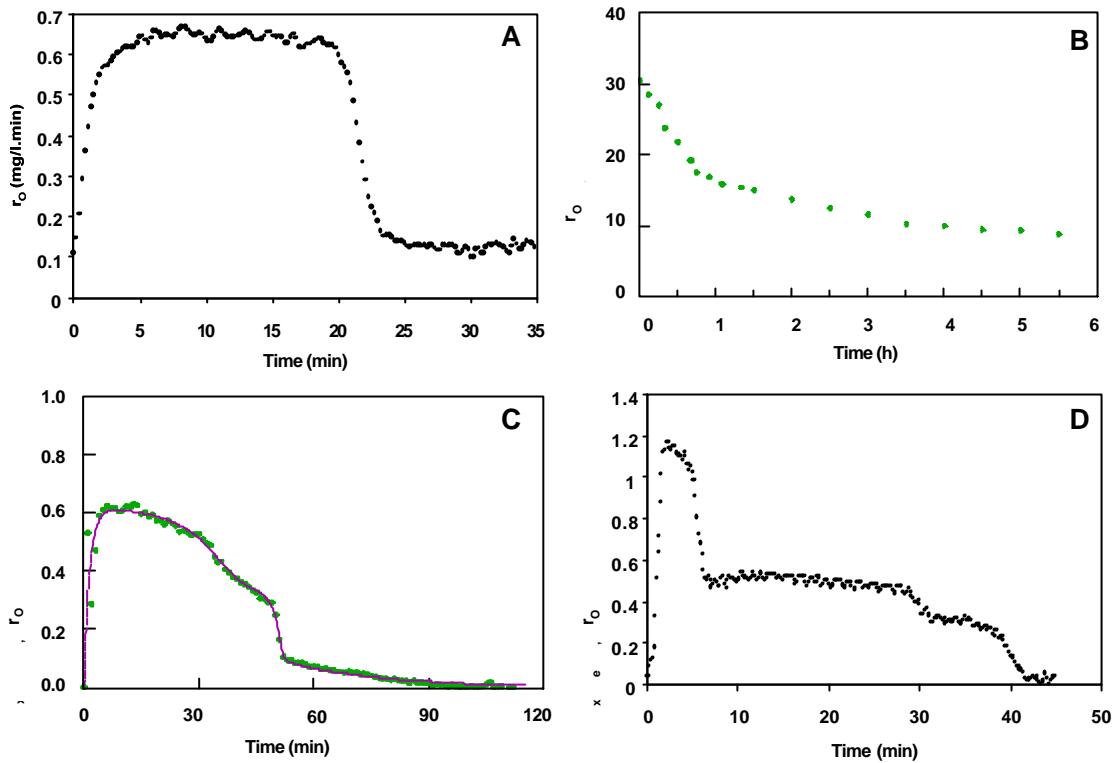


Figure 8. **A:** Typical acetate profile (reference; see also chapter 3) **B:** Municipal wastewater (Kappeler and Gujer, 1992), **C:** Municipal wastewater (Spanjers and Vanrolleghem, 1995), **D:** Industrial wastewater (Coen *et al.*, 1998)

There are two approaches for the determination of model parameters and components: *direct methods* focus on specific parameters and components which can directly be evaluated from the measured respiration rates (Ekama *et al.*, 1986; Spanjers *et al.*, 1999), whereas *optimisation methods* use a (more or less simplified) model that is fitted to the measured data (Kappeler and Gujer, 1992; Larrea *et al.*, 1992; Wanner *et al.*, 1992; Spanjers and Vanrolleghem, 1995; Brouwer *et al.*, 1998; Coen *et al.*, 1998). In the latter, numerical techniques are used to estimate parameter values that lead to the smallest deviation between model predicted and measured respiration rates (see Fig. 4).

Below, examples of respirometric experiments to assess the different wastewater components will be reviewed and important experimental factors with respect to wastewater characterisation will be discussed. The overview does not attempt to review and evaluate different respirometric principles, since a review of these is included in the introduction to chapter 3. Different methods may only be included here to illustrate points that are specifically related to wastewater characterisation.

Readily biodegradable substrate S_s

The readily biodegradable substrate is presumably composed of simple and low molecular soluble

compounds, such as volatile fatty acids, alcohols, etc. (Henze, 1992). The characteristic of these compounds is that they are degraded rapidly and hence result in a fast respirometric response, e.g. as in Fig. 8A.

The most typical batch test for determination of S_S involves the addition of a wastewater sample to endogenous sludge, and the monitoring of the respiration rate until it returns back to the endogenous level (Ekama *et al.*, 1986, among others). The examples shown in Fig. 8 are all obtained with such an approach. The respirometric methods may vary (see review in Chapter 3) from a very simple lab-scale batch test to more complex methods that may even be applied on-line. The concentration of readily biodegradable substrate initially present in the mixture of biomass and wastewater in the experiment is generally calculated according to Eq. 7.

$$S_S(0) = \frac{1}{1 - Y_H} \left(\int_0^{t_{fin}} r_{O,ex} dt \right) \quad (7)$$

The concentration of S_S in the wastewater is then easily calculated by taking the dilution into account. The end point t_{fin} of the integration interval is the time instant where S_S is completely oxidised and where the exogenous respiration rate for S_S becomes zero. The integral can directly and easily be obtained by determining the area under the $r_{O,ex}$ profile, e.g. by using a spreadsheet program. An alternative consists of solving the mass balance equations with a numerical integrator to predict the exogenous respiration rates for S_S and a given initial value $S_S(0)$. It may be a bit overdone to apply numerical integration for the profile illustrated in Fig. 8A, however for more complex profiles (Fig. 8 B-D), the approach may become necessary and more straightforward than direct calculation, as will be discussed further below.

Notice that knowledge of the heterotrophic yield coefficient Y_H is needed for the calculation of S_S from respiration rates (Eq. 7). The yield indicates the COD fraction that is converted to cell mass. The rest of the COD is used to provide the energy that is required to drive different synthesis reactions. This energy is made available by oxidative phosphorylation, which requires a terminal electron acceptor, in this case oxygen. The produced energy is proportional to the mass of electron acceptor utilised, which in turn is proportional to the COD consumed. As a consequence $(1 - Y_H) \cdot \text{COD}$ is equal to the integral under the $r_{O,ex}$ curve. Evidently, the parameter Y_H is always involved when oxygen consumption is converted to substrate equivalents.

The batch test described above is also used to assess other ASM1 components and, likewise, kinetic and stoichiometric parameters. This will be explained further in the next section on characterisation of sludge kinetics, but this indicates already the popularity of this test in assessing wastewater components and reaction kinetics.

Apart from the typical batch test as described above, other experimental designs have also been tried out

for the determination of S_S . One example consists of monitoring the respiration rate of unsettled sewage without inoculum for a relatively long period, approximately 20 hours (Wentzel *et al.*, 1995). A respirogram similar to the one depicted in Fig. 9 is obtained. The S_S concentration is calculated from the respiration rates observed between the start of the test up to the time with the precipitous drop (due to depletion of S_S), with correction for the increasing endogenous respiration due to the increase of biomass during the test. In addition to Y_H , knowledge of the maximum specific growth rate is required, information that can be obtained from the same test (see below).

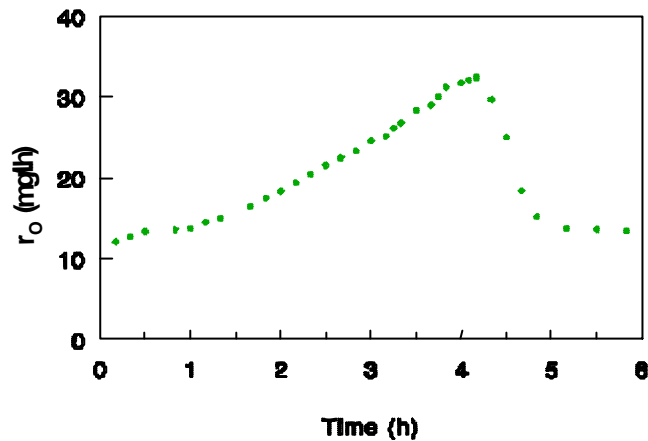


Figure 9. Respiration rates measured in a batch experiment for estimation of $\mu_{\max H}$ and K_S (after Kappeler and Gujer, 1992)

An often-referred continuous flow-through method was developed by Ekama *et al.* (1986), see Fig. 10.

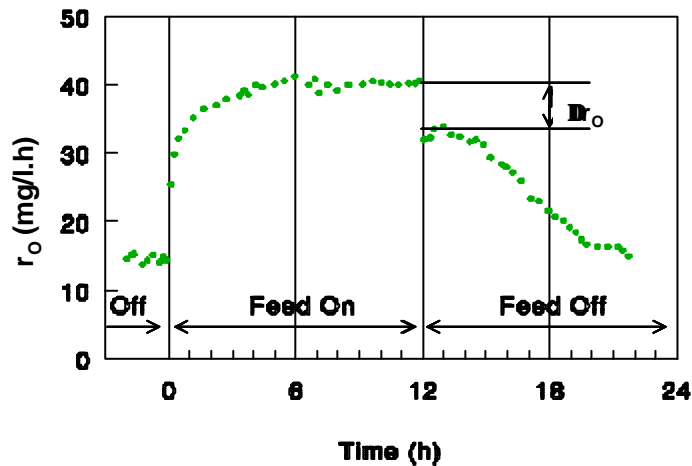


Figure 10. Respiration rates obtained with the experimental set-up of Ekama *et al.* (1986)

This method involves the monitoring of respiration rate in a completely mixed reactor operated under a daily cyclic square-wave feeding pattern. The experiment is designed in such a way that the supply of S_S from hydrolysis of X_S remains constant for a period after the feed is stopped and gives rise to a second r_o plateau. It is hypothesised that the difference in r_o plateau values corresponds uniquely to the S_S that has

entered via the influent. Hence, the concentration of readily biodegradable substrate in the wastewater can be calculated as given in Eq. 8.

$$S_S = \frac{V}{Q} \frac{\Delta r_O}{(1 - Y_H)} \quad (8)$$

An obvious disadvantage of this method is the experimental length (24 h which is not including the stabilisation of the continuous reactor used for the test), and the fact that sufficient X_S is needed in the feed to achieve a constant hydrolysis rate and to create as such the step change in r_O . In addition, the method is rather difficult to carry out in practice (Sollfrank and Gujer, 1991; Wentzel *et al.*, 1995).

A final method for the evaluation of S_S was based on the evolution of the respiration rates obtained in a continuously fed respirometer during transients between two modes of operation; a mode of endogenous respiration and wastewater addition respectively (Spanjers *et al.*, 1994). In the work of Lukasse *et al.* (1997) the estimation technique developed for the determination of S_S in the respirometer of Spanjers *et al.* (1994) was further evaluated and improved. In the work of Witteborg *et al.* (1996) the same continuously fed respirometer was used but a different estimation of S_S was proposed as now the measurement of respiration rate was performed under three different wastewater loading conditions. The wastewater S_S was calculated by numerically solving a set of mass balances pertaining to different loading conditions of the respirometer.

Slowly biodegradable substrate X_S

It is assumed that slowly biodegradable substrate X_S is composed of (high-molecular) compounds ranging from soluble to colloidal and particulate (Henze, 1992). The common feature of these compounds is that they cannot pass the cell membrane as such, but have to undergo hydrolysis to low-molecular compounds (S_S) which are subsequently assimilated and oxidised. The respirometric response on X_S is slower because the hydrolysis rate is lower than the oxidation rate of S_S .

In a batch test an exponentially decreasing “tail” can frequently be observed in respirograms (Fig. 8 B-C). In Fig. 8B, this tailing starts after approximately 0.75 hours. The wastewater concentration of X_S can be assessed in a similar way as above, Eq. 7 (Sollfrank and Gujer, 1991; Kappeler and Gujer, 1992). Simultaneously occurring oxidation processes such as nitrification might interfere and complicate the separation of the respiration rate due to hydrolysis in the total respiration rate. In that case a nitrification inhibitor may be used to facilitate the assessment of X_S (Spanjers and Vanrolleghem, 1995). Alternatively, if the data of such respirometric batch tests are used in combination with mathematical curve fitting techniques to match the response of the model to the data, the nitrification part can rather easily be extracted from the respirogram (Spanjers and Vanrolleghem, 1995).

It has also been proposed to estimate X_S based on a long-term BOD test where X_S is obtained by

subtracting S_S from $BOD/(1-Y_H)$ (STOWA, 1996). Note that the value of Y_H here should be lower than the one applied in Eq. 7, due to internal turnover of substrate from decayed biomass in long-term tests.

Heterotrophic biomass X_{BH}

In the ASM1 report the influent concentration of heterotrophic biomass, X_{BH} , is assumed to be negligible, as earlier mentioned. However, some wastewaters can contain a significant concentration of heterotrophic biomass (Henze, 1992), and there may therefore be a need to quantify this component. A batch test has been proposed where X_{BH} is assessed from the respirometric response of raw wastewater without inoculum (Kappeler and Gujer, 1992; Wentzel *et al.*, 1995). The calculation requires knowledge of Y_H together with two parameters (μ_{maxH} and b_H) that can be obtained from the same data. Respirograms look similar to the one presented in Fig. 9. The procedure basically backtracks the amount of heterotrophic biomass originally present in the wastewater by comparing the original respiration rate with the respiration rate after significant (hence, well quantifiable) growth of X_{BH} .

Autotrophic biomass X_{BA}

So far, no procedures were found by which the autotrophic biomass concentration in wastewater is determined. However, it could be imagined that a similar procedure as the one developed for X_{BH} is applicable. Thus, by evaluation of the respiration rate for nitrification, $r_{O,ex}^N$, of the autotrophs present in the wastewater and by comparison to the respiration rate of a culture with known autotrophic biomass concentration X_{BA} , e.g. after significant growth, the originally present X_{BA} could be determined.

Ammonium S_{NH}

The concentration of ammonium in wastewater can be determined by using conventional analytical techniques, as mentioned earlier. However, respirometry also offers the possibility to deduce S_{NH} from batch measurements in a similar way as S_S and X_S , provided the test is done with nitrifying activated sludge and the oxygen consumption for nitrification can be separated from the other oxygen consuming processes. As follows from Table 6, the autotrophic yield coefficient Y_A is needed to convert the oxygen consumption for nitrification to a nitrogen concentration by division by $(4.57-Y_A)$, where 4.57 indicates the amount of oxygen needed to oxidise one unit of ammonium nitrogen. The value of Y_A is typically 0.24 g COD(biomass)/g N, which means that the determination of S_{NH} is not very sensitivity to Y_A since its value is small compared to 4.57.

Notice that part of the available ammonium may be assimilated into new heterotrophic biomass, which may be a considerable fraction of the nitrogen in case a large amount of COD is biodegraded ($COD^{Degraded}$) simultaneously with the nitrification. The actual nitrified ammonium nitrogen, denoted N^{Nitr} , can be approximated by Eq. 9 in which i_{XB} is the nitrogen content of newly formed biomass:

$$N^{\text{Nitr}} = S_{\text{NH}} - i_{\text{XB}} \cdot Y_{\text{H}} \cdot \text{COD}^{\text{Degraded}} \quad (9)$$

From this equation one can easily deduce the original nitrogen concentration when $\text{COD}^{\text{Degraded}}$, and the stoichiometric parameters i_{KB} and Y_{H} are given. Note, however that fitting a model in which carbon and nitrogen oxidation are included to the respirometric data will automatically take this correction into account (Vanrolleghem and Verstraete, 1993; Spanjers and Vanrolleghem, 1995; Brouwer *et al.*, 1998).

Organic nitrogen S_{ND} and slowly biodegradable organic nitrogen X_{ND}

Probably because the ammonification and hydrolysis rates of organic nitrogen compounds are relatively fast, little attention has been devoted so far to the establishment of respirometric techniques for S_{ND} and X_{ND} quantification. In batch tests these compounds are typically converted to S_{NH} before the S_{NH} that was originally present in the wastewater is removed by nitrification. Therefore, S_{ND} and X_{ND} are not directly observable in such tests but may be lumped into the fraction of nitrified ammonium. Still, for some industrial wastewaters the ammonification and hydrolysis steps may be considerably slower and quantification of these component concentrations may be required. In such cases, one can imagine a procedure in which the nitrification respiration rate $r_{\text{O,ex}}^{\text{N}}$ is monitored and interpreted in terms of ammonification and hydrolysis, similar to the way the respiration resulting from COD degradation is interpreted in terms of the biodegradation of readily biodegradable substrate and the hydrolysis process. Subsequently, the amounts of nitrogen containing substrates could be assessed by taking the integral of $r_{\text{O,ex}}^{\text{N}}$ for the corresponding fractions and dividing these by $(4.57 - Y_{\text{A}})$. In case simultaneous COD removal is taking place, correction should again be made for nitrogen assimilated into new heterotrophic biomass (see above).

4.1.2.2. Nitrate utilisation rates

Readily or slowly biodegradable substrate S_{S} and X_{S}

The basis for wastewater characterisation via monitoring of nitrate utilisation rates (r_{NO_3}) to determine the denitrification potential is rather similar to that of respirometry (Nichols *et al.*, 1985; Ekama *et al.*, 1986; Kristensen *et al.*, 1992; Naidoo *et al.*, 1998; Spérandio, 1998; Urbain *et al.*, 1998; Kujawa and Klapwijk, 1999). The application of nitrate utilisation rates for wastewater characterisation within the frame of ASM1 is however not as widespread as respirometry.

The readily biodegradable component S_{S} (or X_{S}) is determined by Eq. 10 (similar to Eq. 7). A typical r_{NO_3} profile is given in Fig. 11, indicating two biodegradable wastewater fractions.

$$S_{\text{S}}(0) = \frac{2.86}{1 - Y_{\text{H}}} \left(\int_0^{t_{\text{fin}}} r_{\text{NO}_3, \text{ex}} dt \right) \quad (10)$$

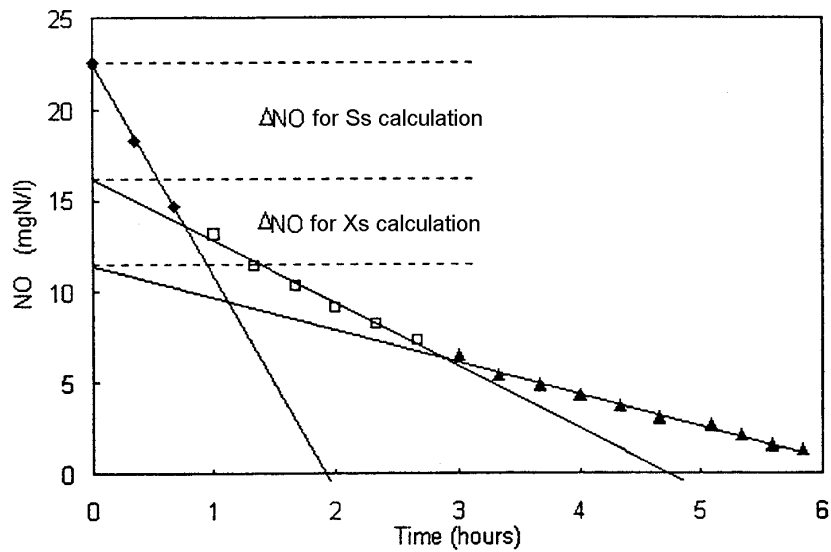


Figure 11. Typical profile of r_{NO_3} as function of time for determination of S_s and X_s (Urbain *et al.*, 1998)

The factor 2.86 g O_2 /g NO_3 -N originates from the fact that the theoretical electron acceptor capacity of nitrate (as N) is 2.86 times that of oxygen (as O), assuming that NO_3 -N is converted completely to nitrogen gas N_2 (Payne, 1981; van Haandel *et al.*, 1981). The factor has been verified experimentally by Copp and Dold (1998).

In Eq. 10 it is assumed that the Y_H of aerobic and anoxic substrate degradation is equal, as also assumed in ASM1. In a study on a pure denitrifying culture it has however been reported since long that aerobic yields are larger than anoxic yields (Koike and Hattori, 1975). It has been theoretically proven, based on the energetics of the metabolic processes, that anoxic yields indeed are consistently lower than aerobic ones (Orhon *et al.*, 1996). Indeed similar differences between aerobic and anoxic yield were obtained experimentally with activated sludge (McClintock *et al.*, 1998; Spérandio *et al.*, 1999). Thus, to apply nitrate utilisation rates for wastewater characterisation it is important to correct for this difference in aerobic and anoxic yield since application of aerobic yield values in Eq. 10 will lead to overestimation of the readily biodegradable wastewater components.

4.1.2.3. Titrimetry

The buffer capacity of water samples can be measured accurately by advanced titration techniques (Van Vooren *et al.*, 1995), and has recently been successfully applied for the determination of ammonium and phosphorus in low concentrations (0 – 100 mg/l) in effluents, surface waters and manure (Van Vooren, 2000).

Some efforts have been done to characterise VFA concentrations related to anaerobic processes based on titration procedures and pH measurements (e.g. Münch and Greenfield, 1998). These techniques may also

be applicable for wastewater characterisation in the frame of ASM2 where one component is defined as the concentration of fermentation products. This will however not be dealt with any further in this presentation.

Alternative to the classical titration methods (up and down titrations) Ramadori *et al.* (1980) proposed to monitor the acid and/or base consumption rate that was needed to keep the pH constant in an activated sludge sample where pH-affecting biological reactions occur. This titrimetric method has been successfully applied for the monitoring of nitrification, which has a clearly defined effect on the pH, and concentrations of S_{NH} (Massone *et al.*, 1995; Gernaey *et al.*, 1997a). Recently, it has also been attempted to apply the method for the determination of the total nitrifiable nitrogen concentration of a wastewater (Yuan *et al.*, 1999).

Ammonium, S_{NH}

A typical cumulative base addition curve and a pH profile collected during a titration experiment with nitrifying sludge sampled on-line from a pilot plant are shown in Fig. 12 (Gernaey *et al.*, 1998). In a first phase, the pH of the nitrifying activated sludge sample is increased to the pH setpoint, and base is added at a maximum rate. This phase took about 2 minutes for the example of Fig. 12. For the experiments described here, a pH setpoint $\pm \Delta\text{pH}$ interval value of 8.2 ± 0.03 was used. Every time the pH of the sludge sample becomes lower than 8.17 (= pH setpoint minus ΔpH interval), base is added to the sludge. Dosage of base is repeated until the pH has returned within the pH setpoint $\pm \Delta\text{pH}$ interval range.

The analyses of the data can either be via a simple manual interpretation or model-based (Gernaey *et al.*, 1998). The simple procedure is based on the detection of the two slopes (S1 and S2) in the cumulative base addition curve, followed by an extrapolation of the different lines to the Y-axis (Fig. 13). The S_{NH} concentration (mg N/l) and the nitrification rate r_N (mg N/l.min) can be calculated according to Eq. 11 and 12, where the intercepts B1 and B2 are expressed in meq/l units. The factor 0.143 meq/mg N (i.e., 2 mole H^+ per mole N), is the stoichiometric coefficient relating the amount of acid (meq) produced per mg of nitrogen nitrified. The slopes S1 and S2 are expressed in meq/l.min units.

$$S_{NH} = \frac{(B2 - B1)}{0.143} \quad (11)$$

$$r_N = \frac{(S1 - S2)}{0.143} \quad (12)$$

In the application of Gernaey *et al.* (1998) the sludge was sampled at the last compartment of an activated sludge pilot plant thereby reducing the likelihood of presence of organic substrates. In case ammonification is slower than nitrification it may be relevant to determine S_{ND} , as described above in the section on respirometry. Thus, the titrimetric method may also be applicable for S_{ND} determination. It is obvious,

however, that degradation of organic substrates may cause acid or base consumption effects that may interfere with the determination of S_{NH} according to the described methodology.

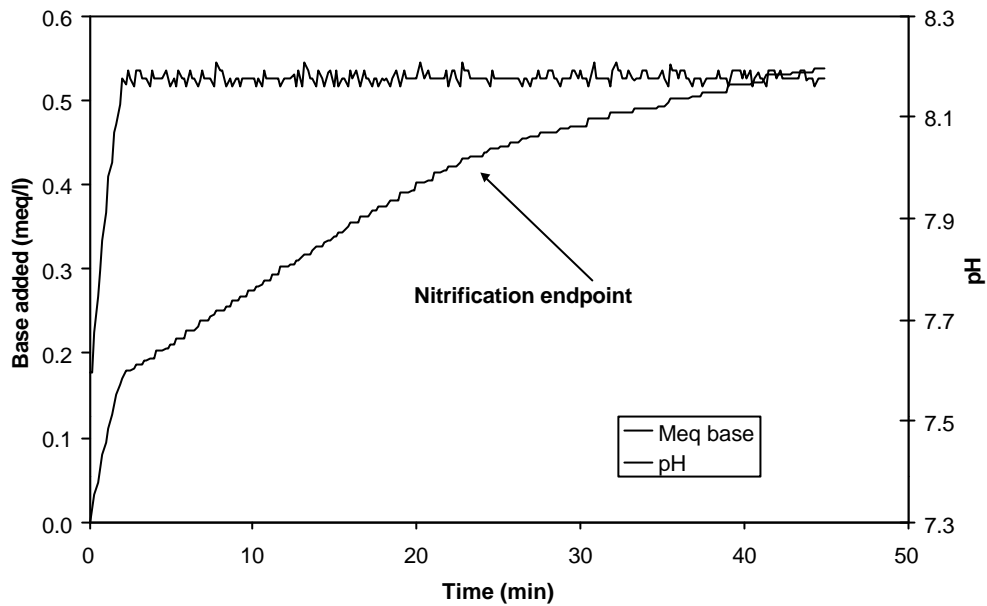


Figure 12. Typical cumulative base addition curve (expressed as amount of base dosed per liter of activated sludge sample) and pH profile obtained during an on-line titration experiment with a mixed liquor sample. For this example, the nitrification phase is finished after about 25 minutes (Gernaey *et al.*, 1998)

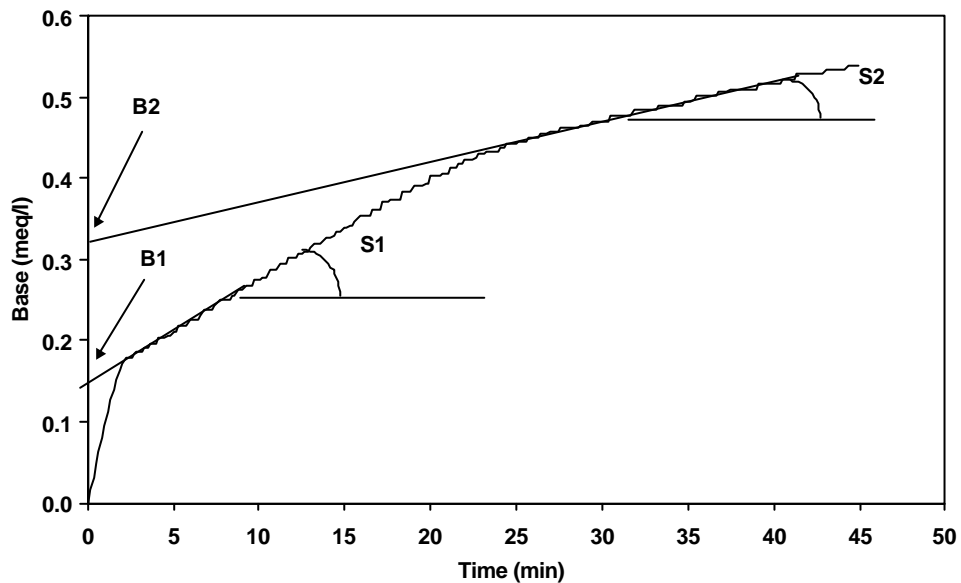


Figure 13. Simple manual interpretation of a typical cumulative base addition curve (Gernaey *et al.*, 1998)

Readily biodegradable substrate S_s

The titrimetric methodology has also been applied for the determination of readily biodegradable COD available for denitrification, and within control strategies for additional carbon dosage (Bogaert *et al.*,

1997). A complicating factor is that depending on the carbon source denitrification will either produce or consume acid (Bogaert *et al.*, 1997). However, preliminary results (Dhaene, 1996; Rozzi *et al.*, 1997) have indicated that the method may be used to evaluate the readily biodegradable substrate in concentrated wastewaters.

4.1.2.4. Summary and discussion of biological wastewater characterisation

The capabilities of the different biological methods presented above to directly determine the ASM1 wastewater components are illustrated in Fig. 14 (the dashed lines indicate areas of uncertainties) and summarised in Table 7. According to Fig. 14 it is obvious that the readily biodegradable organic wastewater components, i.e. S_S and parts of X_S (Fig. 14A), and the nitrogen components S_{NH} and parts of S_{ND} and X_{ND} (Fig. 14B), can be determined directly via the biological methods. The determination of the slower biodegradable component X_S can be carried out indirectly via a long-term BOD test and knowledge of S_S (STOWA, 1996). However, uncertainties may be introduced by long-term BOD tests since significant interference from product formation may occur during the lengthy test.

For the determination of S_{NH} it should be remembered that it is in fact the nitrifiable nitrogen that is determined via the biological methods (as indicated with dashed lines into the regions of organic nitrogen, since parts of the organic nitrogen may be hydrolysed making it readily available for nitrification). This is in contrast to the physical-chemical method where the S_{NH} component is determined via a chemical analysis of ammonia.

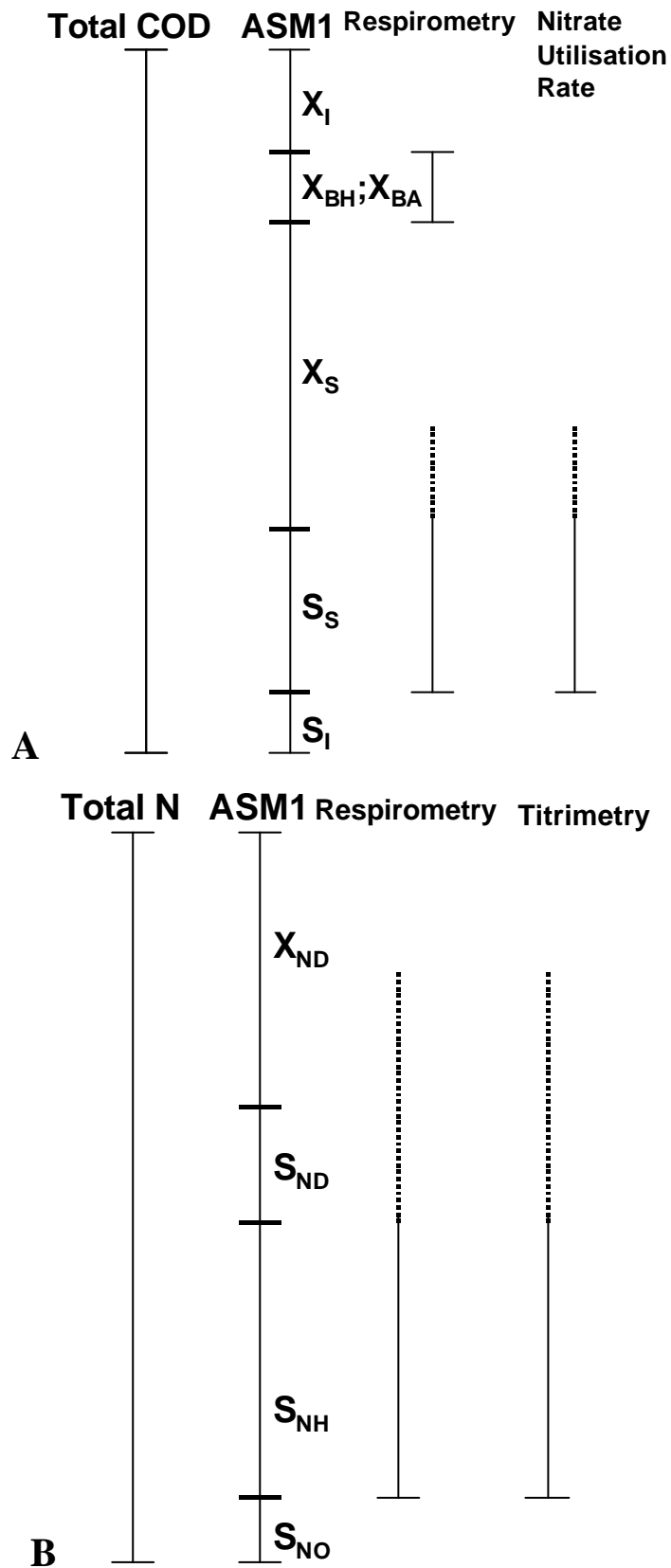


Figure 14. Characterisation of ASM1 wastewater components by different biological methods (the dashed lines indicate areas of uncertainties). **A:** COD components; **B:** Nitrogen components

Table 7. Overview of biological methods for estimation of wastewater component concentrations. (Fields with grey background indicate that a respirometric method is not applicable or relevant)

Component	Method	Type of experiment	Additional Information	Assumptions	References
S_I	R	BOD _∞ , WW	Y_H		H87; L92
S_S	R	B, WW add.	Y_H		E86
		B, WW	Y_H, μ_{maxH}, K_S		We95
		C	Y_H		Wi96
		C (on/off)	Y_H		E86; SG91; We95
	N	B, WW add.	Y_H		E86; K92; N98; U98; KK99
	T	B, WW, S	C/N	C/N constant	B97; R97; D96
X_I					
X_S	R	B, WW	Y_H		SG91;KG92; SV95
		BOD _∞ , WW			S96
		B, WW add.	Y_H		N98; U98; KK99
X_{BH}	R	B, WW	Y_H		KG92; We95; B95
X_{BA}	R	B, WW	Y_A		This review
X_P					
S_O					
S_{NO}	T	B, S	C/N	C/N constant	B97
S_{NH}	R	B, WW	$Y_A, i_{XB}, Y_H, COD^{Deg}$		VV93, SV95; B98
	T	B, WW			M95, G97; G98
S_{ND}	R	B, WW	$Y_A, i_{XB}, Y_H, COD^{Deg}$		This review
X_{ND}	R	B, WW	$Y_A, i_{XB}, Y_H, COD^{Deg}$		This review
S_{ALK}					

Explanation to Table 7

Method:

R: Respirometry N: Nitrate respiration test T: Titrimetry

Type of experiment:

Ac: acetate B: batch reactor add.: addition adds.: additions

C: continuous system WW: wastewater S: synthetic substrate

References

B95: Bjerre *et al.*, 1995 B97 Bogaert *et al.*, 1997 B94 Brands *et al.*, 1994
 B98 Brouwer *et al.*, 1998 D96 Dhaene, 1996 E86 Ekama *et al.*, 1986
 G97 Gernaey *et al.*, 1997a G98 Gernaey *et al.*, 1998 H87 Henze *et al.*, 1987
 KG92 Kappeler and Gujer, 1992 K92 Kristensen *et al.*, 1992 KK99 Kujawa and Klapwijk 1999
 L92 Lesouef *et al.*, 1992 M95 Massone *et al.*, 1995 N98 Naidoo *et al.*, 1998
 R97 Rozzi *et al.*, 1997 SG91 Sollfrank and Gujer, 1991 SV95 Spanjers and Vanrolleghem, 1995
 S96 STOWA, 1996 U98 Urbain *et al.*, 1998 VV93 Vanrolleghem and Verstraete, 1993
 We95 Wentzel *et al.*, 1995 Wi96 Witteborg *et al.*, 1996

4.1.3. Discussion on physical-chemical versus biological wastewater characterisation

By definition the total COD in ASM1 is subdivided based on (i) solubility, (ii) biodegradability, (iii) biodegradation rate and (iv) viability (biomass), as earlier described. Summarising, the COD components to consider in a wastewater are:

$$\text{COD}_{\text{tot}} = S_I + S_S + X_I + X_S + (X_{\text{BH}}) \quad (13)$$

In previous sections it has been thoroughly reviewed how to determine these components by either physical-chemical or biological methods, and different limitations of the methodologies have been underlined and discussed. Furthermore, it is obvious that the division of the wastewater into model components is to some extent artificial. For example, a division is made between soluble and readily biodegradable substrate (S_S) and particulate slowly biodegradable matter (X_S), although it is for example known that some slowly biodegradable substrate may be soluble etc.

It became clear that an application of physical-chemical methods alone is not sufficient for characterisation of the wastewater into model COD components. These methods basically only allow to distinguish between soluble and particulate COD and do not differentiate with respect to biodegradability (non-biodegradable versus biodegradable matters) and biodegradation rate (readily versus slowly biodegradable substrates). However, by application of biological characterisation methods it is possible to obtain knowledge of the biodegradability and biodegradation rate of the wastewater. Thus, it is obvious that a combination of physical-chemical and biological characterisation methods is advantageous for the translation of the wastewater characteristics into the ASM1 model components. A suggestion for such a combined approach, based on the literature review above, is presented in Fig. 15. Here it is suggested to determine the readily biodegradable substrate (S_S) directly via respiration tests (respirometry or nitrate utilisation rates). The presence of biomass in the wastewater may also be determined by respiration tests. The slowly biodegradable matter (X_S) can be determined via the results of a long-term BOD test. The same kind of test may provide information on the soluble and particulate inert (S_I and X_I) matters. Here, however, the reservation should be repeated that long-term BOD tests may not be very accurate due to possible product formation (S_I) and decay which results in X_I . Therefore, the determination of X_I via a long-term BOD test may be questionable. Indeed, it is proposed by Henze *et al.* (1987) to determine the influent X_I via the complete model during the calibration of the sludge balance. Subsequently, X_S may be determined via a COD mass balance as the difference between total COD and the other components. If it is chosen to determine S_I by a long-term BOD test, it may be advisable to combine it with analyses of the effluent, as proposed in the section about physical-chemical methods. It is again clear from Fig. 15 that the borderline especially between particulate and soluble COD, the differentiation between model components (S_S and X_S) and the results from short-term respiration and long-term BOD tests may not be completely

consistent.

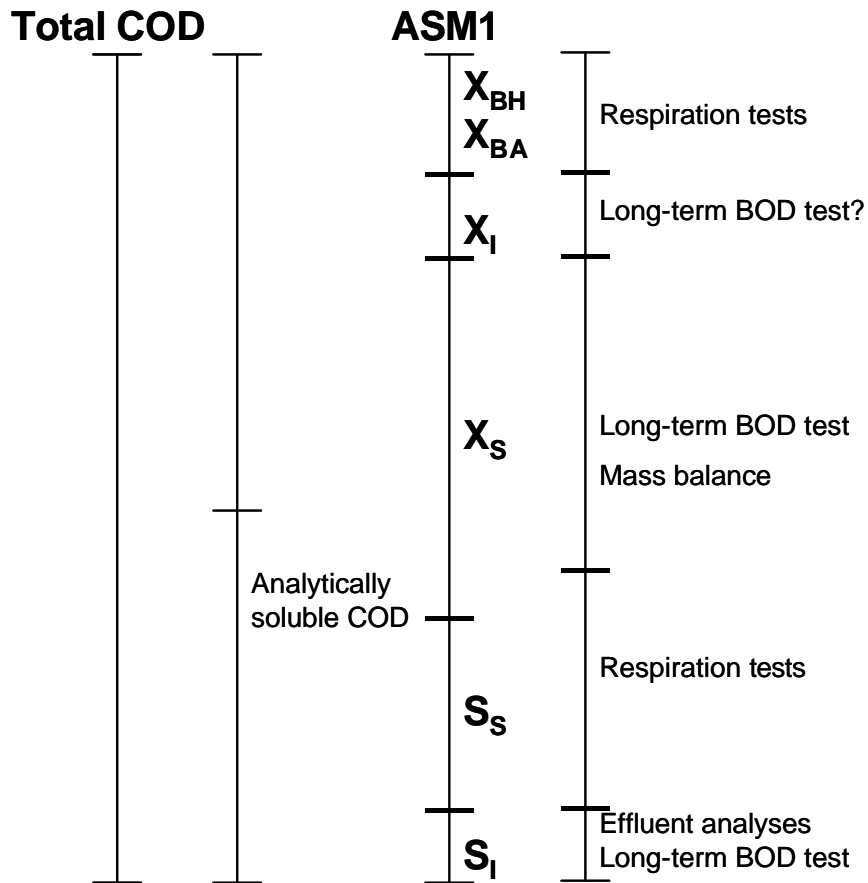


Figure 15. Suggested wastewater characterisation by combined physical-chemical and biological methods

The nitrogen ASM1 components are somewhat easier to determine since they can basically all be determined via mass balances based on standard chemical analyses of total nitrogen, Kjeldahl nitrogen, ammonium nitrogen and nitrate nitrogen (see Fig. 6). It can, however, be advantageous to combine these chemical analyses with biological methods (respirometry or titrimetry) to obtain the nitrifiable nitrogen as a measure of S_{NH} (see Fig. 14) for studies where the focus is specifically on nitrification capacities.

In a study of STOWA (STOWA, 1996) a similar, but less extensive, study of physical-chemical versus biological (only respirometric) influent wastewater characterisation was carried out. In this study guidelines for the COD components were finally defined based on a more traditional choice of physical-chemical methods combined with long-term BOD measurements to allow for an easy implementation in already existing routine analysis programs. It was concluded that respirometry is not yet at a state where it can easily be applied for routine wastewater characterisation. The STOWA guidelines for determination of the COD components are summarised in Fig. 16. Here the concentration of inert soluble matters (S_I) is determined as 90% of the effluent COD for low loaded systems, according to Siegrist and Tschui (1992).

For high loaded systems S_1 is also determined as 90% of the effluent COD but the effluent BOD (multiplied by a COD/BOD factor) is subtracted. S_s is determined as the difference between soluble COD and S_1 . Furthermore, the concentration of X_s is based on a long-term BOD test as the difference between $BOD/(1-Y_H)$ and S_s , as described above. The yield coefficient in this long-term test is set to 0.20. Finally, X_i is defined as the difference between particulate COD and the determined X_s . Obviously, in this approach the division of the wastewater into ASM1 components is based on solubility and to some extent on biodegradability according to physical-chemical methods supplemented by measurements of the ultimate BOD_∞ or BOD_5 . The problem with this approach is that the biodegradation rate of the wastewater is not really considered. This means that the division of the biodegradable substrate into readily and slowly biodegradable substrates may not be correct. It should be stressed though that the approach chosen by STOWA is simple to implement into existing standard measuring routines at full-scale WWTP's, which is a factor not to be underestimated.

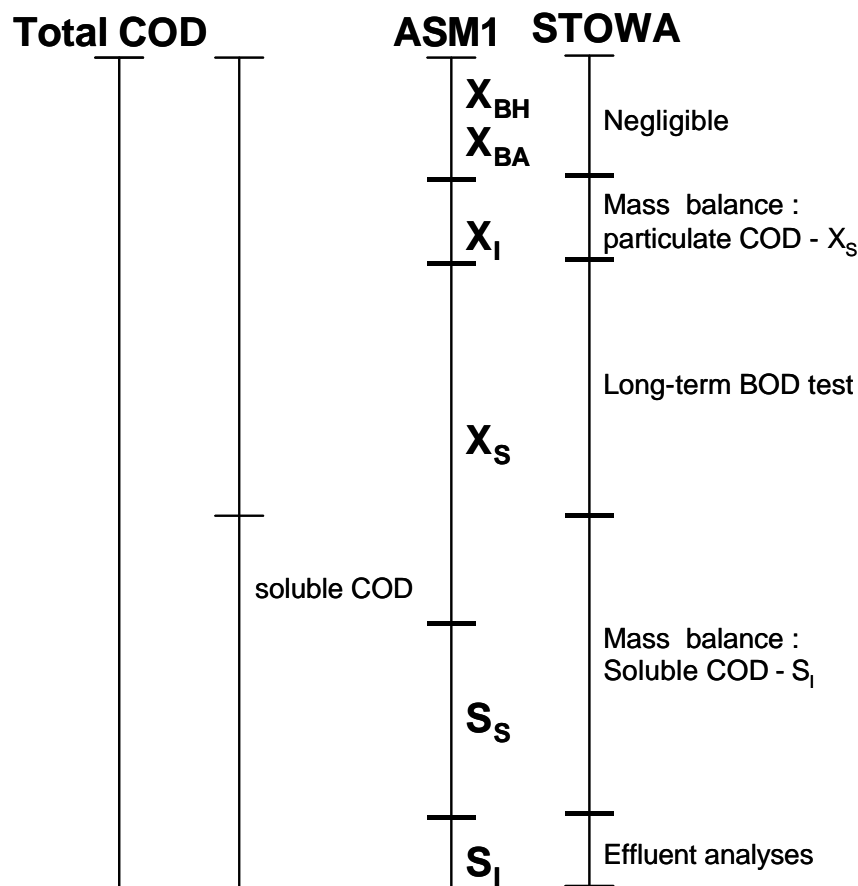


Figure 16. The STOWA guidelines for determination of COD components (STOWA, 1996)

The STOWA guidelines for nitrogen components are also rather simple and based on physical-chemical analyses. The S_{NH} component is obtained based on standard analyses of soluble ammonium nitrogen, and the determination of the organic nitrogen fractions (S_{ND} and X_{ND}) is based on certain fixed fractions of N in

organic components. It is advised that these organic nitrogen fractions are checked regularly based on measurements of total nitrogen, Kjeldahl nitrogen etc. according to Fig. 6B.

In this literature review the focus has been on characterisation of the ASM1 wastewater components. However, with the introduction of ASM3 (see Table 2), that also focuses on a description of oxygen consumption, sludge production and N removal, it is interesting to discuss whether the approaches for wastewater characterisation applied for ASM1 can hold for ASM3 as well.

As described above, there is a shift of emphasis from hydrolysis to storage of organic matter in ASM3. Furthermore, all S_S is supposed to go through the storage process (conversion to X_{STO}) before being used for growth. This means a change in how wastewater characterisation should be viewed, since the separation between S_S and X_S should now be based on the storage process rather than on the growth process. In ASM3 (Gujer *et al.*, 1999) it is supposed that the soluble (S_S) and particulate (X_S) biodegradable components can be differentiated with filtration over 0.45 μm membrane filters, whereas a significant fraction of X_S in ASM1 may be contained in the filtrate of the influent wastewater. In ASM3 the latter is assumed to be due to the conversion of soluble biodegradable COD to storage polymers in the respiration tests. Whether this may hold in any case seems yet rather unclear. In Gujer *et al.* (1999) it was recognised that the model concept of converting all S_S into a storage component is not in accordance with reality. Indeed, Krishna and van Loosdrecht (1999) illustrated that the difference between feast and famine phases could not be described accurately. This was caused by the fact that ASM3 does not allow growth on the substrate S_S alone. Therefore, a new model structure was proposed where growth on external substrate is allowed in parallel with the storage process. It remains however uncertain how to differentiate between the amount of S_S that is directed to storage and growth respectively. Furthermore, the yield coefficient (which is needed to convert respirometric responses to COD components) in ASM3 is composed of two factors: $Y_{net} = Y_{STO} \cdot Y_H$, where Y_{STO} is the storage yield and Y_H the heterotrophic yield for the growth process. Also, here it does not seem clear how to differentiate between the two yields. Basically, concerning the characterisation of COD wastewater components, more experience will be needed before a wastewater characterisation of the COD components related to the new storage concept of ASM3 can be proposed.

The characterisation of the nitrogen components in ASM3 is however simplified by the fact that organic nitrogen components are included in the model as a fraction of the corresponding COD components. Degradation of the corresponding COD component results in immediate release of the organic nitrogen as ammonium. The latter was based on the assumption that the ammonification is fast and the conversion of organic nitrogen into ammonium therefore hardly affects the model predictions (Gujer *et al.*, 1999). Thus, the nitrogen balance includes on the one hand ammonium nitrogen (S_{NH}) and nitrate nitrogen (S_{NO}), which both can be measured easily via standard chemical analyses, and on the other hand organic nitrogen components. However, typically the fractions of organic nitrogen in the COD components can be

considered to be constant.

4.2. Characterisation of sludge composition

In this section special attention is only paid to the assessment of the slower varying sludge characteristics. Knowing the initial value of the concentrations of soluble components (e.g. ammonia) is not really essential because it has little impact on typical simulation results with a calibrated model. Hence, the concentrations of the following particulate, slowly varying components must be assessed: X_{BH} , X_{BA} and $X_I (+X_P)$, assuming that the system is in balance with no accumulation of X_S . Only two concentrations must be assessed since the sum of the concentrations is equal to the particulate COD (X) of the sludge that can easily be measured by using traditional COD analysis (Eq. 14)

$$X = X_I + (X_P) + X_{BH} + X_{BA} \quad (14)$$

Below some fast and direct methods for assessing sludge components are summarised. Notice that the particulate nitrogen components are not considered here as their concentrations are assumed to be low.

Heterotrophic biomass X_{BH}

One can show that the concentration of heterotrophs in a continuous system in steady state is equal to:

$$X_{BH} = Y_H \cdot \frac{q_X}{q_H} \cdot \frac{COD^{Degraded}}{1 + b_H q_X} \quad (15)$$

where θ_X is the sludge age, θ_H is the hydraulic retention time, $COD^{Degraded}$ the total amount of COD removed (taken over a sufficiently long period, e.g. one sludge age), b_H the decay rate coefficient and Y_H the yield coefficient. Respirometric methods to determine the parameters b_H and Y_H are discussed below, while a respirometric evaluation of $COD^{Degraded}$ can be performed with the respirometric measurements of biodegradable COD fractions (S_S , X_S) that was already presented above.

As an alternative, Bjerre *et al.* (1995) used the method of Kappeler and Gujer (1992) to determine the concentration of heterotrophs in the mixed liquor. Recently, this method was thoroughly evaluated by Ubisi *et al.* (1997).

Autotrophic organisms X_{BA}

In much the same way, the concentration of nitrifying organisms in the activated sludge can be evaluated by means of a mass balance for the autotrophs (over a sufficiently long time) (Dupont and Sinkjær, 1994):

$$X_{BA} = Y_A \cdot \frac{q_X}{q_H} \cdot \frac{f^{Aerobic} \cdot N^{Nitr}}{1 + b_A q_X} \quad (16)$$

where f^{Aerobic} is the aerobic fraction of the reactor; N^{Nitr} the amount of nitrified nitrogen ; b_A the autotrophic decay rate coefficient and Y_A the autotrophic yield coefficient. The methods to determine the parameter b_A and Y_A are discussed in the next paragraph, while N^{Nitr} can be quantified using the respirometry-based nitrifiable nitrogen evaluation methods that were given above.

Produced inert suspended organic matter X_P

To determine the produced inert matters, X_P , an evaluation of the mass balance of X_P in steady state can be made. Assuming that the autotrophic biomass can be neglected, Eq. 17 is obtained:

$$X_P = f_P \cdot b_H \cdot X_{BH} \cdot q_X \quad (17)$$

The total concentration of inert matters, including the often significant contribution of suspended inert material from the influent, is given in Eq. 18.

$$X_P = \frac{q_X}{q_H} X_i + f_P \cdot b_H \cdot X_H \cdot q_X \quad (18)$$

Respirometry can be involved in calculating this fraction via f_P and b_H (see below).

4.3. Characterisation of stoichiometric and kinetic parameters

Similar to the overview of wastewater characterisation the overview on characterisation of stoichiometric and kinetic parameters will be clarified according to the applied methodology. The focus will, however, only be on different biological methods since physical-chemical characterisation is not very relevant when it comes to characterisation of reactions. As highlighted in the previous section the majority of the processes involve oxygen consumption, which means that respirometry will again be the dominating method in the review. However, also other methods such as nitrate utilisation rates, titrimetry and ammonium uptake rate are powerful to assess some of the kinetic and stoichiometric parameters.

4.3.1. Respirometry

4.3.1.1. Stoichiometric parameters

By definition, determination of stoichiometric parameters requires the measurement of two factors that are related to the substrate uptake. One of these factors may be the respiration rate. Theoretically, for ASM1 the following stoichiometric parameters can be evaluated using respirometry: Y_H , Y_A , i_{KB} and f_P , though attempts are reported only for the first two.

Heterotrophic yield coefficient Y_H

This parameter not only influences the estimation of sludge production and oxygen demand but also has an

impact on the value of other parameters whose determination requires a value for Y_H (see Table 6) An example is the determination of S_S from respirometric data as described above (Eq. 7). Hence, an accurate value for Y_H is of great importance. Y_H can be determined using respirometry by addition of an amount of wastewater COD and measurements of the substrate oxidation $r_{O,ex}$ (Sollfrank and Gujer, 1991; Brands *et al.*, 1994). Eq. 19 is then applied to evaluate Y_H .

$$Y_H = \frac{\text{COD}_{\text{degradable}} - \int_0^t r_{O,ex}(t)dt}{\text{COD}_{\text{degradable}}} \quad (19)$$

The amount of degradable COD ($\text{COD}_{\text{degradable}}$) is given by the concentration of COD in the filtered wastewater minus the inert portion (S_I). In the study of Sollfrank and Gujer (1992) S_I was determined as the soluble COD concentration in the effluent.

Brands *et al.* (1994) and Liebeskind *et al.* (1996) circumvent the problem of determining S_I by using a completely biodegradable substrate (acetate) instead of wastewater. Hence, $\text{COD}_{\text{degradable}}$ is known exactly. This approach is, however, doubtful. First, the choice of acetate is rather arbitrary and there is quite some evidence that the yield coefficient for acetate differs from influent wastewater (Dircks *et al.*, 1999). Hence, acetate is not really representative for wastewater COD. Moreover, due to the experimental conditions in the batch reactor, it can be expected that part of the acetate is stored in the cell (Majone *et al.*, 1999). In this case the observed oxygen demand only represents the needs for transport of the substrate and incorporation in storage material of the cell, and not for the complete conversion into new biomass. Conclusively, these procedures for estimation of the heterotrophic yield do not seem without problems.

Autotrophic yield coefficient Y_A

A value of 0.24 g biomass COD per g nitrified nitrogen is generally assumed to be a good theoretical value for Y_A . If required it is possible however to determine the actual Y_A from a respirometric batch experiment in which a known pulse of ammonium ($S_{NH}(0)$) is added to a nitrifying activated sludge sample (Eq. 20).

$$Y_A = \frac{4.57 \cdot S_{NH}(0) - \int_0^t r_{O,ex}(t)dt}{S_{NH}(0)} \quad (20)$$

In this approach care has to be taken that no significant net growth of heterotrophs take place as they would incorporate part of the added ammonium. In the model-based data interpretation applied by Spanjers and Vanrolleghem (1995) correction for incorporation of S_{NH} into biomass is taken into account directly via the model.

Nitrogen content of the biomass i_{XB}

Obviously, the most likely method for evaluation of i_{XB} would consist of a nitrogen analysis of the biomass. However, one can imagine (albeit maybe not very realistically) that nitrogen incorporation into biomass can be assessed using two respirometric experiments with nitrifying sludge in which different amounts of COD are degraded, the difference being denoted as $\Delta\text{COD}^{\text{Degraded}}$. The reduction in the oxygen consumption for nitrification $\Delta \int r_{\text{O,ex}}^{\text{N}}(t)dt$ that can be observed for the higher COD loading then allows a calculation of i_{XB} (development of Eq. 9).

$$i_{XB} = \frac{Y_H}{4.57 - Y_A} \cdot \frac{\Delta\text{COD}^{\text{Degraded}}}{\Delta \int r_{\text{O,ex}}^{\text{N}}(t)dt} \quad (21)$$

Inert particulate fraction of the biomass f_P

Decay of biomass results in a fraction being transformed into inert particulate products. Typically 20 % of the biomass consists of inert material (Henze *et al.*, 1987). This inert biological fraction is called f'_P . The model f_P can be calculated starting from the biological f'_P with the following implicit equation:

$$f'_P = \frac{f_P}{1 - Y_H \cdot (1 - f_P)} \quad (22)$$

If the studied activated sludge has a yield coefficient (estimated for instance by using respirometry) deviating from the one reported in literature, the f_P -value must be adapted for this. Keesman *et al.* (1998) showed theoretically that the value of f_P can be estimated directly from a batch test in which only the evolution of the respiration rate and sludge concentration are monitored over sufficiently long time.

4.3.1.2. Kinetic parameters

Basically the kinetic parameters that can be determined via respirometry are related to aerobic growth, decay and nitrification.

Heterotrophic decay coefficient b_H

The classical respirometric method for determination of b'_H described by Henze *et al.* (1987) is the protocol proposed by Marais and Ekama (1976), and is the most typical method applied for the determination of the decay coefficient (e.g. Sollfrank and Gujer, 1991; Kappeler and Gujer, 1992). Sludge is inhibited for nitrification and is aerated in a non-fed batch reactor. The (endogenous) respiration rate is measured at certain time instants over a period of several days. Since the endogenous respiration is proportional with the active biomass concentration, a plot of the logarithm of the endogenous respiration rate $r_{\text{O,end}}$ as function of time describes the exponential biomass decrease as a straight line with slope b'_H .

The death regeneration concept implies that the classical methods for determination of the decay of biomass based on endogenous decay can not be applied directly. The parameter based on the endogenous decay concept has to be translated to the death regeneration concept, similarly to f_p (Eq. 22), leading to the ASM1 decay coefficient b_H (Eq. 23).

$$b_H = \frac{b'_H}{1 - Y_H \cdot (1 - f_p)} \quad (23)$$

Hence, the stoichiometric parameters Y_H and f_p are necessary for calculation of b_H .

Vanrolleghem *et al.* (1992) described a fast method for the estimation of b'_H using only one measurement of the endogenous respiration (in absence of nitrification) in a batch reactor. By means of Eq. 24 describing endogenous respiration, b_H can be calculated on condition that f_p and X_{BH} are known.

$$r_{O,end} = (1 - f_p) \cdot b'_H \cdot X_{BH} \quad (24)$$

The estimation of b'_H can also be based on the fact that the respiration rate for substrate oxidation is proportional to the heterotrophic biomass concentration (Spanjers and Vanrolleghem, 1995). If a sufficiently high amount of oxygen S_O and substrate S_S are present, $r_{O,ex}$ is not substrate limited and will only be proportional to X_{BH} . Consequently, the decay of the heterotrophic biomass can be determined by (i) taking a sludge sample from the aerated and non-fed batch reactor at certain time instants (t_k), (ii) adding a sufficient amount of substrate and (iii) measuring the maximum respiration rate. Assuming that Y_H and μ_{maxH} remain constant during incubation, plotting the logarithm of $r_{O,ex}(t_k)$ as function of time again allows to determine b'_H as the slope of the curve obtained via linear regression. In the study of Spanjers and Vanrolleghem (1995) a model-based interpretation was applied to obtain accurate values of the maximum respiration rates. However, only two data points were used for the semilog regression, which does not make the estimated decay coefficients in this study very reliable.

In the study of Avcioglu *et al.* (1998) a similar procedure was developed, where the decay rate b'_H was assessed by monitoring the decrease in maximum respiration rate. Avcioglu *et al.* (1998) included more data points compared to the study of Spanjers and Vanrolleghem (1995). It was proposed that this method of determining the decay rate should be more reliable, since interference of slowly biodegradable substrate, especially in the initial phase of the traditional test of Marais and Ekama (1976), and inaccuracy of low endogenous respiration rate measurements were avoided. The latter will, however, evidently depend on the sensitivity of the applied respirometric method.

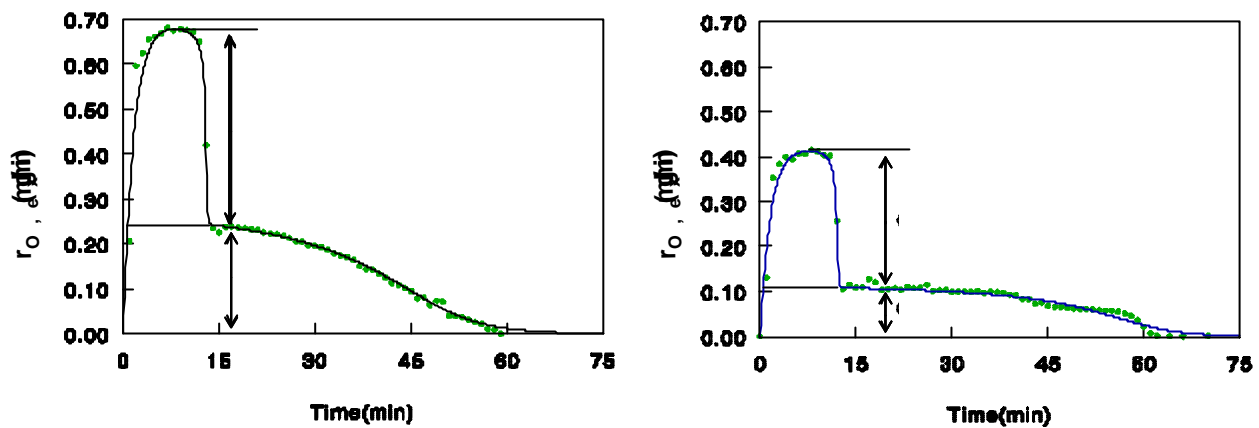


Figure 17. Respirograms obtained after injection of a C/N mixture for the simultaneous determination of b_H and b_A according to the procedure of Spanjers and Vanrolleghem (1995). Left: after 1 day incubation, Right: after 7 days

Furthermore, in the work of Avcioglu *et al.* (1998) it was experimentally verified that the anoxic heterotrophic decay rate was reduced with about 40-50% compared to aerobic conditions. Other studies confirm the observation that the heterotrophic decay is slower under anoxic conditions (McClintock *et al.*, 1988; Siegrist *et al.*, 1999).

Autotrophic decay rate coefficient b_A

The death regeneration concept is not applied for the autotrophic biomass in ASM1. However, the approach of monitoring the decrease in $r_{O,end}$ as function of time can not be applied for the determination of b_A since that would require for instance an inhibition of the heterotrophic biomass. Instead, the method based on the maximum substrate (here S_{NH}) degradation rate as function of time can be applied similar to the procedure for the heterotrophic decay coefficient. In fact, in the procedure described by Spanjers and Vanrolleghem (1995) the heterotrophic and autotrophic decay rate coefficients were determined simultaneously by addition of a mixture of acetate and ammonium. Fig. 17 shows the $r_{O,ex}$ data for the two respirometric tests performed after one and seven days of sludge incubation, clearly illustrating the decreasing activity.

Nowak *et al.* (1994) pointed to the fact that the release of nitrogen due to decay of heterotrophic biomass may result in some growth of nitrifying organisms. Hence, an underestimation of b_A would result. To correct this, they proposed the incubation of the sludge under anoxic conditions to prevent the growth of nitrifiers. Daily a sludge sample was removed from the anoxic reactor and (after aeration) the maximum respiration rate was determined. It was however observed that the reduction in maximum respiration rate was significantly smaller (about 50%) under anoxic than aerobic conditions. This was further confirmed by work on immobilised *Nitrosomonas* (Leenen *et al.*, 1997) and by the findings of Siegrist *et al.* (1999).

Maximum specific heterotrophic growth rate $\mu_{\max H}$ and half-saturation concentration K_S

The maximum heterotrophic growth rate $\mu_{\max H}$ can easily be determined from the maximum $r_{O,ex}$ (Eq. 25) (Ekama *et al.*, 1986), assuming that the substrate concentration is in excess and the yield coefficient and heterotrophic biomass concentration (see previous section) are known.

$$m_{\max H} = \frac{r_{O,ex} \cdot Y_H}{(1 - Y_H) \cdot X_{BH}} \tag{25}$$

However, the methodology proposed by Ekama *et al.* (1986) does not provide information on K_S .

The increase of the substrate uptake rate with increasing S_S concentration is depicted in Fig. 18. From such Monod type evolution the maximum specific growth rate $\mu_{\max H}$ and the half-saturation constant K_S can be determined. In Cech *et al.* (1984) a respirometric method is described in which a number of measurements are performed, each of which add one point to Fig. 18. In this procedure experiments are carried out with addition of different amounts of wastewater (substrate) to endogenous sludge, allowing to achieve various substrate uptake rates, i.e. exogenous respiration rates ($r_{O,ex}$), up to a maximum rate. The parameters $\mu_{\max H}$ and K_S can, for instance, be found by Lineweaver-Burk linearisation of Eq. 26 that describes the curve in Fig. 18 (Cech *et al.*, 1984), although the statistical quality of this procedure is not optimal (Robinson, 1985).

$$\frac{dS_S}{dt} = -\frac{\mu_{\max H} \cdot X_{BH}}{Y_H} \cdot \frac{S_S}{K_S + S_S} \tag{26}$$

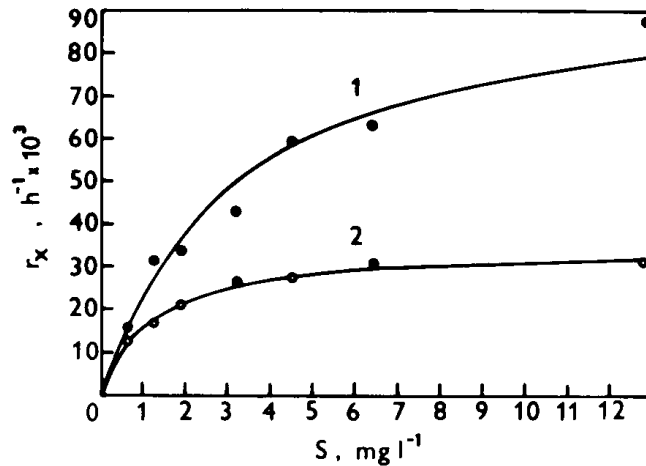


Figure 18. A plot of substrate uptake rate versus substrate concentration for estimation of the parameters for growth, example with valeric acid (Cech *et al.*, 1984)

The method of Cech *et al.* (1984), which was also applied by e.g. Volskay and Grady (1990), is rather

time consuming and the experimental effort is high. As an alternative a more efficient approach was presented, using a continuously aerated respirometer to which a single substrate pulse is added (Vanrolleghem *et al.*, 1990; Kong *et al.*, 1994). In this method $r_{O,ex}$ is recorded frequently as the experiment progresses and one experiment is sufficient for the determination of both μ_{maxH} and K_S provided that the concentration of added substrate is sufficiently high. In this approach a model (Eq. 27 - 28) is fitted to the $r_{O,ex}$ profile for the determination of μ_{maxH} and K_S . An example of an acetate addition is illustrated in Fig. 19 (obtained from Kong *et al.*, 1994) where $r_{O,ex}$ is illustrated together with the corresponding cumulative oxygen consumption and substrate concentrations as function of time.

$$\frac{dS_S}{dt} = -\frac{m_{maxH} \cdot X_{BH}}{Y_H} \cdot \frac{S_S}{K_S + S_S} \quad (27)$$

$$r_{O,ex} = (1 - Y_H) \frac{m_{maxH} \cdot X_{BH}}{Y_H} \cdot \frac{S_S}{K_S + S_S} \quad (28)$$

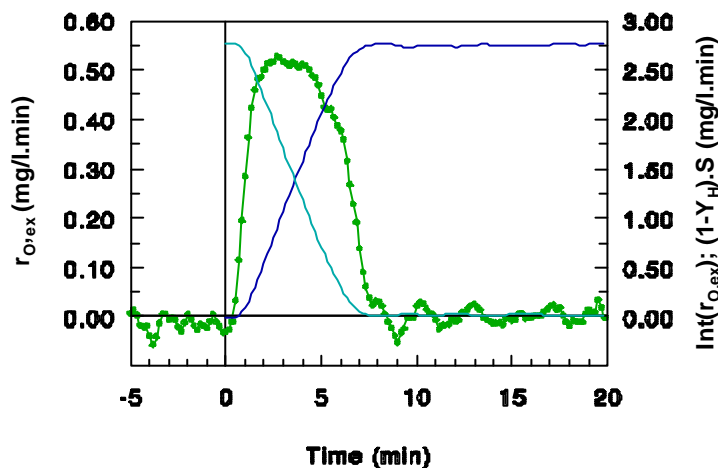


Figure 19. $r_{O,ex}$ (symbols), cumulative oxygen uptake (increasing line) and substrate concentration (decreasing line) in batch experiment (Kong *et al.*, 1994)

The heterotrophic kinetic parameters can also be determined based on the cumulative oxygen uptake profiles rather than oxygen uptake rate data. In the methodology described by Ellis *et al.* (1996) and Smets *et al.* (1996) the kinetics are determined for specific organic chemicals. However, the procedure is directly applicable for wastewaters as well.

A batch experiment with high initial substrate (wastewater) to sludge ratio (called the $S(0)/X(0)$ ratio) was proposed by Kappeler and Gujer (1992). This procedure also enables estimation of μ_{maxH} and K_S from a single experiment. An alternative to Kappeler and Gujer (1992) is to plot the oxygen uptake rate versus the cumulative oxygen uptake rate (Smets *et al.*, 1996). Fig. 9 shows a respirogram obtained with such an experiment (Kappeler and Gujer, 1992). Contrary to the procedures of e.g. Vanrolleghem and Verstraete

(1993) biomass growth is significant and $\mu_{\max H}$ can be assessed directly without knowledge of Y_H . A plot of the logarithm of the r_0 measurements versus time has the slope $(\mu_{\max H} - b_H)$. If b_H is known, a calculation of $\mu_{\max H}$ is possible (in the work presented by Kappeler and Gujer (1992), it is assumed that the decay rate is 5% of the growth rate). Attention has to be paid to the fact that the high $S(0)/X(0)$ ratio in this experimental set-up (about 4/1) gives rise to significant growth of the biomass during the experiment. This means that the observed kinetic characteristics may no longer be representative for the original sludge, due to the risk that the experimental conditions may have favoured fast growing organisms that become dominant during the experiment. Novák *et al.* (1994) gave practical evidence for this hypothesis by evaluating results from experiments with different $S(0)/X(0)$ ratios. A 2.5 times higher specific growth rate was obtained at high $S(0)/X(0)$ ratio, compared to an experiment with a low $S(0)/X(0)$ ratio.

In the work of Grady *et al.* (1996) the terminology of intrinsic and extant kinetics was introduced. Intrinsic kinetics refers to the ultimate capacity of the biomass activity whereas extant kinetics refers to the biomass activity prior to the lab-scale experiments, e.g. in the full-scale plant. This will be discussed further in section 4.4 and 5.

Maximum specific autotrophic growth rate $\mu_{\max A}$ and half-saturation concentration

K_{NH}

In the studies by Drtil *et al.* (1993) and Nowak *et al.* (1994) the above mentioned methodology of Cech *et al.* (1984) was applied to evaluate the maximum specific autotrophic growth rate and half-saturation concentration K_{NH} . To assess the r_0 for autotrophic activity only, the heterotrophic endogenous respiration was determined by a separate experiment, where ATU was added, and was subtracted from the total r_0 obtained from an ammonium addition. Here too knowledge of Y_A and X_{BA} is needed for the calculation of $\mu_{\max A}$. In the work by Nowak *et al.* (1994) the concentration of X_{BA} was determined based on full-scale data.

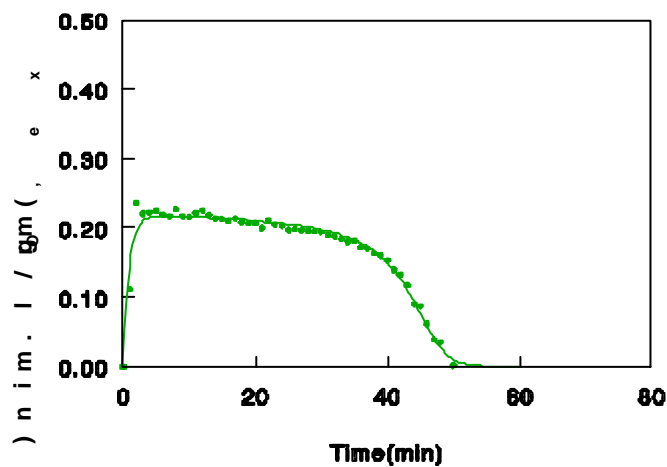


Figure 20. Respirogram obtained after injection of 3.31 mg NH_4-N in 1.4 l of activated sludge (Spanjers and Vanrolleghem, 1995)

Alternatively, $\mu_{\max A}$ and K_{NH} can be obtained directly from experimental data of a simple ammonium addition as presented in Fig. 20. In a study by Spanjers and Vanrolleghem (1995) a model-based interpretation was applied for the determination of the nitrification kinetic parameters (Eq. 29), similar to the approach described above for the kinetic parameters of heterotrophic growth.

$$r_{\text{O,ex}} = (4.57 - Y_A) \frac{m_{\max A} \cdot X_{\text{BA}}}{Y_A} \cdot \frac{S_{\text{NH}}}{K_{\text{NH}} + S_{\text{NH}}} \quad (29)$$

Hydrolysis constants k_h , K_X

As far as known the only experimental protocol that enables a determination of both parameters of the hydrolysis process is the “cyclic square wave feed” experiment proposed by Ekama *et al.* (1986). This method has already been described earlier for the determination of S_s with a typically obtained profile shown in Fig. 10. To determine the hydrolysis parameters the data obtained after the drop in respiration rate are important. If r_o remains constant on a plateau value (as is noticed in Fig. 10 between $t = 12$ and $t = 15$ h), this is related to the hydrolysis that proceeds at maximum rate and biomass is saturated with hydrolysable products ($X_s/X_{\text{BH}} \gg K_X$). As such, these data contain the information to assess the value of k_h on condition that the heterotrophic biomass concentration X_{BH} and the yield coefficient Y_H are known. With decreasing X_s also the rate of hydrolysis decreases and the respiration rate is depending on the value for K_X , allowing its estimation. Estimation of the parameters is best by means of model optimisation (Henze *et al.*, 1987).

In many cases the dependency of the rate of hydrolysis on the heterotrophic biomass concentration may be neglected and first order hydrolysis process dynamics are then obtained (Sollfrank and Gujer, 1991). This assumes that $X_s/X_{\text{BH}} \ll K_X$. Sollfrank and Gujer (1991) proposed a method to determine the first order hydrolysis constant, i.e. k_h/K_X , using respiration rates measured by dosage of wastewater to a continuous flow pilot reactor. To simplify the estimation, they suggested plotting the respiration rate as function of the residual amount of substrate. In this plot one is able to isolate a linear part from which the hydrolysis constant k_h/K_X is deduced (provided Y_H is known).

For estimation of the first order hydrolysis constant k_h/K_X Kappeler and Gujer (1992) performed a batch experiment with an initial COD based $S(0)/X(0)$ ratio which was 10 times higher than their experiment for determination of the maximum specific growth rate ($S(0)/X(0)=1/2$). Fig. 8B shows the respiration rate data of such an experiment, from which the slowly biodegradable substrate, X_s , can also be determined, as described above. Once the readily biodegradable substrate S_s is removed (in Fig. 8B after 0.75 h) the further decrease of the respiration rate is determined by hydrolysis of X_s . As a consequence, the r_o measurements enable to estimate the hydrolysis rate constant. The authors advise to do this exercise at different biomass concentrations to check for a possible dependency of the hydrolysis rate to the biomass concentration.

Parameters of “switching functions” K_{OH} , K_{OA}

Kappeler and Gujer (1992) determined the respiration rate as function of different oxygen concentrations in the respiration chamber of their respirometer. According to these authors the concentration of readily biodegradable substrate S_S needs to exceed a minimal concentration in order to have an accurate determination of K_{OH} . The same technique can be used for K_{OA} with ammonia as substrate.

Ammonification rate constant k_a

So far, no respirometric method has been reported for the determination of the ammonification rate. However, it is theoretically possible (see Table 6) to assess this parameter from the evolution of the oxygen consumption for nitrification resulting from ammonified nitrogen, provided ammonification is the rate limiting step.

4.3.1.3. Simultaneous determination of kinetic parameters for heterotrophic and autotrophic growth

In the previous sections on determination of heterotrophic and autotrophic growth kinetics the focus was put on how to determine the kinetic parameters for the heterotrophic and autotrophic processes separately. However, except for the examples of Sollfrank and Gujer (1991) and Kappeler and Gujer (1992) the presented examples mainly dealt with additions of known substrates (acetate as carbon source and ammonium). The fact is that when dealing with real wastewater and activated sludge both heterotrophic and autotrophic processes will take place simultaneously, and a detailed data interpretation of the respirograms and good experimental design will be needed to “separate” and as such determine the kinetic parameters for the different processes.

Vanrolleghem and Verstraete (1993) proposed an experimental design that enables to simultaneously measure both heterotrophic and autotrophic maximum respiration rates. In their approach a mixture of ammonium and acetate was added to endogenous sludge. The maximum respiration rate for carbon oxidation and nitrification can be derived from the respirograms on the condition that the two aerobic processes can be clearly distinguished from each other. The problem with this approach is however that the kinetic parameters are highly dependent on the nature of the substrate. Thus, use of a single compound to represent a complex substrate like wastewater is difficult to justify scientifically.

In the study on wastewater by Spanjers and Vanrolleghem (1995) experiments with municipal wastewater were presented with much lower substrate to biomass ratios ($S(0)/X(0)$) compared to Kappeler and Gujer (1992). Fig. 21 shows a typical respirogram from an experiment with a $S(0)/X(0)$ of 1/200. This respirogram is much more complicated to interpret than the ones shown so far. First, simultaneous carbon oxidation and nitrification take place. The only seven minutes lasting initial peak in $r_{O,ex}$ is assumed to be due to the oxidation of S_S . After some time only nitrification and, assumingly, oxidation of substrates

released by hydrolysis occurs. In this work the respirograms of the wastewater were interpreted with a more complex ASM1 based model including degradation of two readily biodegradable substrates S_{S1} and S_{S2} , first order hydrolysis and nitrification. Thus, kinetic parameters for all these processes were obtained simultaneously. Experiments in the presence of a nitrification inhibitor ATU were performed to check the contribution of nitrification to the respiration rate. This is shown in the insert of Fig. 21, where the $r_{O,ex}$ related to the degradation of S_S and X_S can be observed.

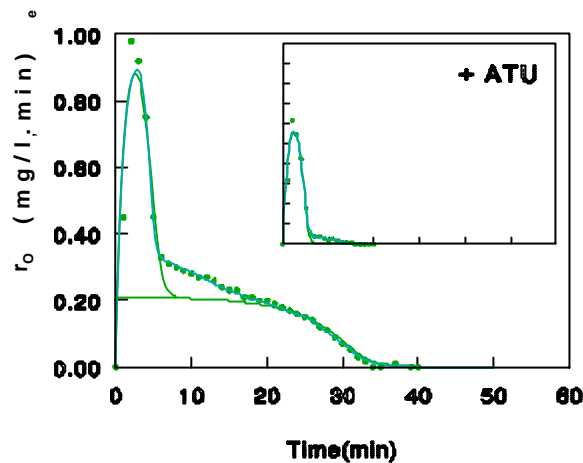


Figure 21. Respiration rate after injection of 70 ml raw wastewater to 1.5 l activated sludge. Insertion: similar experiment but after addition of ATU (Spanjers and Vanrolleghem, 1995)

An approach circumventing ATU addition, suggested by Spanjers and Vanrolleghem (1995), consisted of the following two-step procedure. First, the nitrification process is characterised separately via an experiment where only ammonium was added, as described above and illustrated in Fig. 20. In a second step, the full model is applied to fit to the data of Fig. 21. However, during this step the nitrification parameters are kept at their values obtained from the separate nitrification experiment, and are thereby used to “eliminate” the nitrification oxygen consumption in an experiment with addition of wastewater. The amount of nitrogen in the wastewater sample can be estimated simultaneously as it determines the length of the nitrification shoulder. Spanjers and Vanrolleghem (1995) demonstrated that the ATU and model-based elimination of the nitrification respiration rate lead to similar values for the kinetic parameters and wastewater characteristics.

Another example of a detailed interpretation of a respirometric test with municipal wastewater addition is given by Brouwer *et al.* (1998). Here a model including degradation of two readily biodegradable substrates, hydrolysis and two step nitrification is applied to interpret wastewater respirograms. The problem encountered in this study was, however, that not all processes were clearly identifiable from the respirograms. It was thus suggested that the number of unknown model parameters should be reduced for this example by including experiments with separate additions of synthetic substrates, for example ammonium and nitrite. In this way it would be possible to fix these kinetic parameters in the characterisation

of the complex wastewater, similar to the approach of Spanjers and Vanrolleghem (1995).

Finally, an application with industrial wastewater (no nitrification) was presented by Coen *et al.* (1998), where a model-based interpretation approach was applied for the determination of kinetic parameters and substrate concentrations of simultaneous degradation of three COD wastewater fractions.

4.3.2. Nitrate utilisation rates

Characterisation of reaction kinetics via analysis of the nitrate utilisation rate is basically very similar to the methodology based on oxygen respiration rate, and different studies have dealt with the comparison of $r_{O,ex}$ and $r_{NO_3,ex}$ (e.g. McClintock *et al.*, 1988; Kristensen *et al.*, 1992; Orhon *et al.*, 1996; Sözen *et al.*, 1998). In ASM1, the same kinetic expressions are applied for nitrate utilisation processes as for oxygen, with the only difference that a correction factor η is incorporated in the equations for anoxic processes. This factor allows to describe that only a fraction of the total biomass is capable of respiring with nitrate and/or that the anoxic rate is lower than the aerobic one. Typically, one applies the relationship given in Eq. 30 in order to relate $r_{O,ex}$ with $r_{NO_3,ex}$.

$$h = 2.86 \cdot \frac{r_{NO_3,ex}}{r_{O,ex}} \quad (30)$$

Correction factors for anoxic growth and hydrolysis h .

It has been shown that the value of η can vary significantly for different activated sludge systems. In different studies values have been recorded in the range 0 - 0.95 (Van Haandel *et al.*, 1981; Henze, 1986; Henze *et al.*, 1987, 1995; McClintock *et al.*, 1988; Kristensen *et al.*, 1992; Sözen *et al.*, 1998; Spérandio *et al.*, 1999). Some theories were developed based on general mass balances that allowed for an estimation of η from wastewater characteristics, treatment plant layout and operation (Henze, 1986). It was shown that the dominating factor for η is the potential inlet fraction of denitrifiers, which includes the denitrifying fraction of the influent biomass plus the primary produced anoxic biomass. Based on some practical constraints concerning e.g. minimum anoxic sludge age and minimum aerobic sludge age to keep both nitrification and denitrification in the system, it was estimated that in practice η might be in the order of 0.4 - 0.9 (Henze, 1986).

An underlying assumption behind Eq. 30 is that the aerobic and anoxic yields are equal. As discussed above significant evidence exists that the anoxic yield may be lower than the aerobic one. In the studies by Orhon *et al.* (1996) and Sözen *et al.* (1998) very high values (>1) for the conversion factor η were related to possible lower anoxic yields for which correction will be needed. The occurrence of lower anoxic biomass yields was already discussed above, in the section about application of nitrate utilisation rates for the determination of readily or slowly biodegradable substrate S_S and X_S .

4.3.3. Titrimetry

Maximum specific autotrophic growth rate $\mu_{\max A}$ and half-saturation concentration

K_{NH}

So far, the titrimetric technique based on pH control and monitoring of the cumulative amount of base or acid added to keep the pH set-point, proposed by Ramadori *et al.* (1980), and introduced in more detail above, has only been applied to the determination of the nitrification kinetic parameters $\mu_{\max A}$ and K_{NH} . As illustrated in Fig. 12 and 13 and by Eq. 12, the cumulative amount of base added can be used to calculate the nitrification rate and thereby provide kinetic information. In the work of Gernaey *et al.* (1998) a model-based data interpretation was applied for the estimation of $\mu_{\max A}$ and K_{NH} . The model is similar to the one applied to describe respirometric and nitrate utilisation rate data. The only difference is the stoichiometric coefficient relating the ammonium degradation to proton production Hp (Eq. 31).

$$r_{Hp} = \frac{2 + Y_A \cdot i_{XB}}{14} \cdot \frac{\mu_{\max A} \cdot X_{BA}}{Y_A} \cdot \frac{S_{NH}}{K_{NH} + S_{NH}} \quad (31)$$

4.3.4. Summary and discussion of biological characterisation of stoichiometric and kinetic parameters

Summarising, the review on biological characterisation has illustrated that, theoretically, nearly all parameters can be determined with biological methods. Especially respirometry stands as a powerful characterisation method but other methods too are useful for the characterisation of specific processes, e.g. titrimetry for the characterisation of nitrification and application of nitrate utilisation rates for the determination of the correction factor for denitrification.

One of the challenges in the application of the biological methods is how to interpret and relate the experimental data to the different processes that may take place simultaneously. It is obvious that experiments with addition of known and simple substrate such as ammonium or acetate are easier to interpret in terms of determination of stoichiometric and kinetic parameters than experiments with real wastewater. For example, it is difficult to assess the heterotrophic yield Y_H by experiments with real wastewater, and in some cases it was therefore suggested to determine it from an experiment with known substrate in the form of acetate (Brands *et al.*, 1994; Liebeskind *et al.*, 1996). It has also been suggested to determine the maximum specific growth rate $\mu_{\max H}$ based on experiments with acetate in respirometric experiments (e.g. Vanrolleghem and Verstraete, 1993). However, acetate does not represent the actual wastewater very well. As already stressed above it is generally questionable to use a single substrate to represent complex wastewater. Furthermore it is a known phenomenon that acetate easily gets directed towards the storage process instead of directly being consumed for growth (Majone *et al.*, 1999). This means that if such data are only interpreted in terms of the growth process, the estimated parameters

related to growth will be erroneous. E.g. the stoichiometric growth yield (Y_H) will be overestimated (Dircks *et al.*, 1999). On the other hand, characterisation of the stoichiometric and kinetic parameters for nitrification can be done by respirometric or titrimetric experiments with single additions of pure ammonium. It is of course advantageous if several parameters (kinetic or stoichiometric) and some wastewater components can be obtained from the same experiment. This was illustrated in studies with municipal wastewater by e.g. Spanjers and Vanrolleghem (1995) and Brouwer *et al.* (1998), and also for an industrial COD removal case (Coen *et al.*, 1998).

In Table 8 (adopted and modified from Vanrolleghem *et al.*, 1999) the experiments described above for characterisation of stoichiometry and kinetics are concisely represented. Attention is drawn to

- (i) The method (respirometry, nitrate utilisation rates, titrimetry)
- (ii) The type of reactor set-up (continuous or batch experiment) and the additions performed;
- (iii) The requirement for other information collected from other experiments (or assumed);
- (iv) Major assumptions made during the interpretation of the data;
- (v) The reference where more information can be found.

From Table 8 it can for example be seen that in the work of Spanjers and Vanrolleghem (1995) with wastewater (reference SV95 and experiment type "B, WW add.") the parameters $\mu_{\max H}$, K_S , $\mu_{\max A}$, K_{NH} and k_h , and the substrate components S_S , X_S and S_{NH} could be retrieved from a single experiment.

It will now be attempted to evaluate whether the approaches for characterisation of the kinetic and stoichiometric parameters as reviewed for ASM1 can hold for ASM3 too.

As reviewed above, it should be theoretically possible to assess the ammonification rate from respirometric data, provided that ammonification is the rate limiting step. However, in most applications this is not the case making it difficult to quantify the kinetics of ammonification. Furthermore, ammonification does not affect the model predictions significantly, since it is usually a fast process. Thus, with this in mind the ammonification process was not included in ASM3, thereby also eliminating the need to determine its kinetic rate.

Another simplification in ASM3 is the way the decay process is described. Instead of the more complex death regeneration concept it was chosen to describe decay with a more traditional and simple endogenous decay process. This means that the results from a simple long-term aeration test (Marais and Ekama, 1976), where the endogenous respiration rate is monitored over a period of several days, can be applied more directly. In this way a transformation of the data from the endogenous test to the death regeneration concept is no longer needed. Furthermore, the exclusion

Table 8. Overview of biological methods for estimation of (combinations of) ASM1 parameters. (Fields with grey background indicate that a respirometric method is not applicable or not relevant)

	Method	Type of experiment	Additional information	Assumptions	References
Stoichiometric parameters					
Y_H	R	B, WW add. B, Ac add.	S_I	Ac representative of S_s	SG91 Br94
Y_A	R	B, NH_4 add. B, NH_4 +Ac add.	i_{XB}, Y_H	$i_{XB} \approx 0$	SV95 SV95
f_p	R	B	MLVSS		K98
i_{XB}	R	B, COD add.	$Y_H, Y_A, \Delta COD^{Deg}$		this paper
i_{XP}					
Kinetic parameters					
μ_{maxH}	R	B, n S,Ac adds. B, S, Ac add. B, WW add. B, WW add.	Y_H, X_{BH} Y_H, X_{BH} b_H Y_H, X_{BH}	μ_H represent original X_{BH}	C84; VG90 K94; E96; Sm96 KG92 SV95, B98
K_S	R	B, n S,Ac adds. B, S, Ac add. B, WW add. B, WW add.	Y_H, X_{BH} Y_H, X_{BH} b_H Y_H, X_{BH}	K_S represent original X_{BH}	C84; VG90 K94; E96; Sm96 KG92 SV95, B98
K_{OH}	R	B, n S_O	S_O	S_S sufficiently high	KG92
K_{NO}					
b_H	R	B, no add. B, n Ac add. B, no add.	f_p, Y_H f_p, Y_H	Y_H, μ_H constant	ME76; SG91 SV95 V92
μ_{maxA}	R	B, n NH_4 adds. B, NH_4 add.	Y_A, X_{BA} Y_A, X_{BA}		C84 D93; SV95
	T	B, NH_4 add.	Y_A, X_{BA}		G98
	A	B, NH_4 add.	Y_A, X_{BA}		K92
K_{NH}	R	B, n NH_4 adds. B, NH_4 add. B, WW add.	Y_A Y_A Y_A		N94 D93; SV95 SV95, B98
K_{OA}	R	B, n S_O	S_{NH}	S_{NH} sufficiently high	KG92
b_A	R	B, NH_4 add. B, n NH_4 +Ac add.			H87; N94 SV95
η_g	R+N	B, WW add.			K92; S99
k_a	R	B, S add.			This paper
k_h	R	C (on/off) C, WW add. B, WW add.	Y_H, X_{BH} Y_H	max. hydrolysis rate K_X very large K_X very large	E86 SG91 KG92; SV95; B98
K_X	R	C (on/off)	Y_H, X_{BH}		E86
η_h	R+N	B, WW add			K92

Explanation to Table 8

Method:

R: Respirometry N: Nitrate respiration test A: Ammonia uptake test T: Titrimetry

Type of experiment:

Ac: acetate B: batch reactor add.: addition adds.: additions

C: continuous system WW: wastewater S: synthetic substrate

References

B94	Brands <i>et al.</i> , 1994	B98	Brouwer <i>et al.</i> , 1998	C84	Cech <i>et al.</i> , 1984
D93	Drtil <i>et al.</i> , 1993	E86	Ekama <i>et al.</i> , 1986	E96	Ellis <i>et al.</i> , 1996
G98	Gernaey <i>et al.</i> , 1998	H87	Henze <i>et al.</i> , 1987	KG92	Kappeler and Gujer, 1992
K98	Keesman <i>et al.</i> , 1998	K94	Kong <i>et al.</i> , 1994	K92	Kristensen <i>et al.</i> , 1992
ME76	Marais and Ekama, 1976	N94	Nowak <i>et al.</i> , 1994	Sm96	Smets <i>et al.</i> , 1996
SG91	Sollfrank and Gujer, 1991	SV95	Spanjers and Vanrolleghem, 1995	S99	Spérandio <i>et al.</i> , 1999
V92	Vanrolleghem <i>et al.</i> , 1992	VG	Volskay and Grady, 1990		

of the death regeneration concept also resulted in a simplification of the hydrolysis process, since this process is now only involved in hydrolysis of slowly biodegradable substrate (X_S) contained in the influent.

However, with the introduction of the storage model concept it becomes difficult to separate between the kinetics of storage and growth. Already in the discussion of wastewater characterisation it was pointed out that the yield obtained from a respirometric test is composed of two factors $Y_{net} = Y_{STO} \cdot Y_H$. Furthermore, it does not seem clear how to differentiate between the storage rate and growth rate from e.g. a respirometric test.

4.4. Is characterisation via lab-scale experiments relevant?

In previous sections the sources of information that can be used for calibration of ASM1 were reviewed and attention was especially focused on how to characterise the different wastewater components, stoichiometric and kinetic parameters. Different problems were already highlighted.

The focus is now turned back to calibration of ASM1 and the aim of describing a full-scale WWTP. It should be remembered that the purpose of the model calibration determines the degree of detail of the information that is needed, e.g. which wastewater components and parameters need a more accurate determination than others. Even though it may be possible to characterise some components or parameters it may not always be relevant for the actual purpose. Or to apply the terminology suggested by Grady *et al.* (1996); do the lab-scale experiments provide extant kinetic parameters, i.e. parameters representative for the biomass prior to the experiments? Furthermore it will be discussed how the relations are between lab- and full-scale observations, and how the biological processes are presented in ASM1:

- (a) Transferability between lab-scale and full-scale observations: Are the different components and parameters that may be determined via lab-scale experiments representative, i.e. transferable to the full-scale system? That is, do the experiments provide extant parameters.
- (b) Transferability between full-scale observations and modeled processes: Are the full-scale processes described in a biologically realistic way in the model or are the model processes lumping different biological processes? If so, it may be impossible to characterise them by any experiment.
- (c) Transferability between model processes and lab-scale observations: Are the processes defined in the model reflected by the lab-scale experiments?

These conflicts of transferability are illustrated in Fig. 22, and the discussion is taken below considering the different wastewater components, kinetic and stoichiometric parameters. The aim of this discussion is to decide which information source is most relevant for the different components and parameters. Of course, in principle all the components and parameters can be obtained from the model, e.g. via the default parameter set or via adjustment of the values during the model calibration exercise.

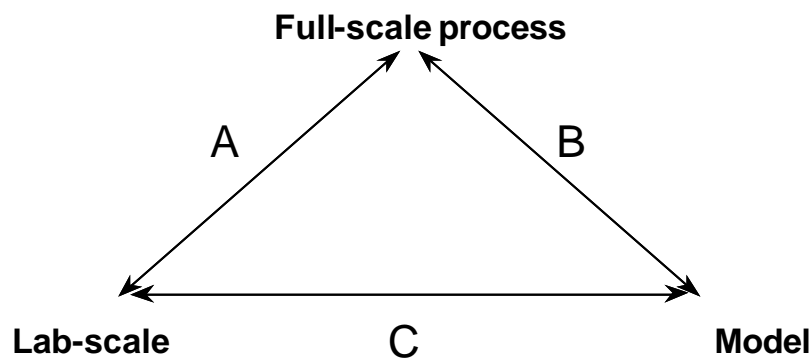


Figure 22. Schematic representation of discussion on transferability

However, some model processes do not reflect reality completely, although they enable a mathematical description of the biological observations. The model components and parameters related to such processes can not be characterised reliably via either lab-scale or full-scale data and should preferably be tuned during the model calibration with the full ASM1. Then there are some components and parameters that readily and reliably can be transferred from a lab-scale experiment. For others the lab-scale results are difficult to transfer to the model of the full-scale system, and for instance a mass balance with full-scale data may be more appropriate as information source. Whether a certain component or parameter should be obtained via lab-scale or full-scale data or should be tuned directly via the model will depend on what the component or parameter in question is depending on. In this discussion it is assumed that the values of the components and parameters can depend on either the actual biomass in the activated sludge system or the actual WWTP operation. It should be stressed that only the actual state of the system is considered in this

discussion, since this is what the calibrated model is aimed at describing. Obviously, the biomass character (e.g. maximum specific growth rate, decay rate etc.) of the WWTP is determined by both the incoming wastewater and WWTP operation. However, changes in biomass characteristics caused by changing WWTP operation or wastewater character are more long-term effects. Description of these effects is not within the scope of the ASM models. Thus, the actual wastewater considered for the model calibration is assumed to be representative for the general wastewater composition to which the biomass has adapted and by which the biomass character is determined.

4.4.1. Kinetic and stoichiometric parameters

Below, the information sources for the most relevant kinetic and stoichiometric parameters will be discussed in relation to Fig. 22. Furthermore, the discussion on whether a parameter is depending on the wastewater, biomass and/or WWTP operation is summarised in Table 9. Finally, the most relevant information source is indicated in Table 9. Brackets in Table 9, i.e. (X) indicates that a lab-scale experiment is possible for determination but the transferability of the obtained parameters to the full-scale situation is uncertain for different reasons, as explained below. Finally, as mentioned above all parameters can in principle be determined based on the model alone without additional supporting information.

Table 9. Discussion on relevant information sources for kinetic and stoichiometric parameters. A bracket around X indicates that a lab-scale experiment is possible for determination but the transferability of the obtained parameters to the full-scale situation is uncertain due to different reasons (see text for further explanation)

	Dependency		Relevant information source		
	Sludge/biomass	Plant operation	Lab-scale experiment	Full-scale data Mass balances	Model calibration
$\mu_{\max H}$	X		X		X
$\mu_{\max A}$	X		X		X
K_S, K_{NO}	X	X	(X)	(X)	X
K_{NH}	X	X	(X)	(X)	X
K_{OH}, K_{OA}	X	X	(X)	(X)	X
b_H, b_A	X		X		X
Y_H	X		(X)		X
Y_A	X		(X)		X
k_h	X				X
K_X	X				X
η_g	X		X	X	X
η_h	X				X

The maximum specific heterotrophic growth rate, $\mu_{\max H}$

The observed actual specific growth rate in the full-scale system, $\mu'_{\max H}$, depends on the sludge age and therefore depends both on the actual wastewater and the WWTP operation. If the wastewater contains a significant amount of biomass, $\mu'_{\max H}$ will depend primarily on the wastewater, whereas it will depend on the operation if the biomass is primarily produced within the plant. On the contrary, the maximum specific growth rate, $\mu_{\max H}$, is the maximum possible specific growth rate of the actual sludge, and is only influenced by the actual kind of bacteria present. It may be important to distinguish here between $\mu_{\max H}$ and the growth rate, μ , which is influenced by the mixed liquor substrate concentration. Thus, $\mu_{\max H}$ is not depending on the wastewater whereas μ is.

This means that the problem of transferability between the lab-scale and the full-scale observations will not be significant (conflict a in Fig. 22) if the lab-scale experiment is carried out under conditions that are comparable to the full-scale system (e.g. with respect to pH, temperature, ratio between substrate and biomass concentration etc.). In other words, if the lab-scale experiments are performed in a way that allows measurement of extant parameter values, then little or no conflict will arise.

As described earlier, the death regeneration concept in the model has the effect that the cell mass turnover rate increases, resulting in a higher growth rate than if a more traditional concept of endogenous decay was applied. Thus, this should be taken into account in the interpretation of lab-scale experiments and in the transferability of results to the full-scale model (conflict C in Fig. 22). Similarly the death regeneration model concept and the way it influences the maximum specific growth rate may not reflect the full-scale process completely (conflict B in Fig. 22), but may allow for an adequate description of observations.

Summarising, the $\mu_{\max H}$ is one of the most relevant parameters to study in lab-scale experiments and can be considered to be a biological parameter, which is only determined by the actual bacteria present (see Table 9).

The maximum specific autotrophic growth rate, $\mu_{\max A}$

Although specific bacterial groups undertake nitrification, they adapt to the actual environment and the bacterial species can therefore vary. Therefore, the discussion on the maximum specific autotrophic growth rate $\mu_{\max A}$ is rather similar to the one of $\mu_{\max H}$. Thus, it is possible to determine the value of $\mu_{\max A}$ from lab-scale experiments, and transfer the value to the model of the full-scale system.

Half-saturation coefficients : K_S , K_{NH} , K_{NO} , K_{OA} and K_{OH}

In pure cultures the half-saturation coefficients can be regarded as pure biological parameters that give measures of the affinity of the biomass for substrates. However, in cultures where the bacteria grow in flocs (as in activated sludge), the floc size and structure play a role in the diffusion of substrate to the cell and

thereby on the apparent value of saturation coefficients. Especially in full-scale systems mixing characteristics will further influence the apparent values. Even in lab-scale tests under simpler mixing characteristics, mixing may play a role and influence the obtained values of the half-saturation coefficients. Thus, the different mixing characteristics of the lab-scale and full-scale system make it difficult to transfer the lab-scale observation to the full-scale system (conflict A in Fig. 22). If the floc size decreases due to e.g. a more intensive mixing in the small batch-scale experiments, the obtained coefficients will be smaller than required to describe the full-scale behaviour (Henze *et al.*, 1998). This makes it difficult to obtain a model relevant value of the half-saturation coefficients from lab-scale experiments (conflict C in Fig. 22). The saturation coefficients in ASM1 describing a full-scale situation may therefore be regarded more as model parameters with the purpose of preventing unrealistically high substrate uptake and growth rates. Thus, the biological meaning of the model half-saturation coefficients is mixed with the hydraulics of the system (conflict B in Fig. 22). Obviously, if a very detailed model is available to describe the hydraulics of a system accurately, it may be possible to separate the effects of biomass affinity for a substrate and the hydraulic effects from mixing. However, usually the hydraulic pattern is approximated by a simple tanks-in-series model that may be sufficient for a mathematical description but not accurate enough for a complete elimination of hydraulic effects on the biological parameters.

Thus, all half-saturation coefficients of the full-scale system will depend on both the WWTP operation (mixing) and the actual kind of biomass present. The coefficients can be determined by lab-scale experiments but the values obtained may not be very representative. It may therefore be better to estimate these parameters from full-scale data, via the operational rate of COD removal found by mass balances as function of the operational range of COD concentrations. The question is of course whether the full-scale data is informative enough for such determinations. Thus, in practice these values may have to be tuned during the model calibration.

Decay rate of heterotrophs b_H and autotrophs b_A .

The decay rate in a full-scale WWTP is in principle a characteristic of the actual biomass, and can, similarly to the maximum specific growth rate, be considered as a biological parameter. However, it may be difficult to obtain a representative value of the decay rates of a full-scale system from the lab-scale tests presented above (conflict A in Fig. 22), since decay and growth due to substrate inflow (and internal production) take place simultaneously in the full-scale WWTP. On the contrary, decay is typically investigated under starving conditions (endogenous respiration) in lab-scale experiments. Furthermore, the decay rate in the full-scale plant is typically influenced by grazing, i.e. presence of protozoa, which may not be present or may not be able to survive in the lab-scale experiment.

In ASM1, the death regeneration concept includes both lysis combined with hydrolysis of released substrate and, subsequently, growth on this substrate. As discussed earlier, this interaction of different

processes makes it difficult to determine the decay coefficient related to the death regeneration concept (conflict B in Fig. 22). However, according to ASM1 it is possible to transfer the decay rate obtained from a lab-scale experiment with decreasing endogenous respiration as function of time for determination of the endogenous decay rate to the death regeneration model concept (via Eq. 23, conflict C in Fig. 22). Obviously, the change in ASM3 to the endogenous respiration decay concept makes it more straightforward to determine the decay rate of the model by a lab-experiment.

Conclusively, it is possible to determine the decay rate via lab-scale experiments, and to convert the obtained value to the death regeneration concept of ASM1, but the value may to some extent have to be adjusted during the model calibration procedure.

Maximum heterotrophic and autotrophic yield, Y_H and Y_A .

The observed yields in a full-scale WWTP, Y'_H and Y'_A , are depending on the process operation, i.e. the actual wastewater load and the sludge age. On the other hand, the actual maximum yields (Y_H and Y_A) are depending on the kind of biomass present. For municipal WWTP's the parameters Y_H and Y_A are typically assumed to be rather constant, indicating that the biomass character is rather similar among different municipal WWTP's. However, it may still be needed in some cases to determine the biomass yields. This can be carried out in lab-scale experiments, but there may be some experimental difficulties, e.g. caused by the possible influence of storage which may be induced by the conditions in the lab-scale experiment (Majone *et al.*, 1999), as earlier described (conflict A in Fig. 22).

In fact the typical maximum heterotrophic yield of 0.67 for municipal wastewater (Henze *et al.*, 1987) is higher than the yields observed with pure cultures. The reason for this may be that the model yield covers different processes as storage, death regeneration etc. and may thereby be considered more as a model yield (van Loosdrecht and Henze, 1999) (conflict B and C in Fig. 22). Although the heterotrophic biomass yield seems to be influenced by the available electron acceptors (the anoxic yield is reported to be lower than the aerobic one, Koike and Hattori, 1975; Orhon *et al.*, 1996; McClintock *et al.*, 1998; Spérandio *et al.*, 1999), the yield may be more influenced by storage than by the type of electron acceptor.

Hydrolysis rate k_h and half-saturation coefficient K_x

Although only limited knowledge is available about hydrolysis, the process is needed in ASM1 to describe the degradation of slowly biodegradable organic matter originating from the influent COD and from internal turnover of substrate in the death regeneration cycle.

As described above attempts have been made to analyse hydrolysis in lab-scale experiments. It may be possible to compare the real enzymatic hydrolysis as it takes place in lab-scale with the full-scale hydrolysis process. However, the real enzymatic hydrolysis is not the same as the hydrolysis process in the model, as it might also cover consumption of storage polymers, hydrolysis of decayed biomass (death regeneration),

protozoan activity etc. (conflict B and C in Fig. 22) (van Loosdrecht and Henze, 1999). Thus, it remains problematic to design an experiment that is representative for both the model concept and the hydrolysis process as it takes place in full-scale. If this is compared to the determination of e.g. the maximum specific growth rate, we note that this parameter also covers many details but still only describes one process, i.e. growth.

Conclusively, the real hydrolysis process is probably determined by the actual biomass that produces the enzymes, but for the model calibration of ASM1 it does not seem relevant to attempt to characterise this process in lab-scale tests. Hence, the hydrolysis as it is described in ASM1 should be considered as a model process that has to be adjusted during the model calibration procedure. It should be remembered that the definition of hydrolysis has changed in ASM3 and is closer to the real biological hydrolysis. Thus, a characterisation of the hydrolysis parameters from a lab-scale experiment will be more relevant for ASM3. The problem remains, however, to design a good experiment for characterising the real biological hydrolysis.

Correction factors for denitrification η_g and η_h

The correction factors for denitrification can be found via a combination of respirometric and nitrate utilisation rate experiments for the determination of the growth and hydrolysis process, although some problems may be encountered in the case where the aerobic and anoxic yields can not be considered equal. It was also referred above that the correction factors can be determined based on some general mass balances of the full-scale system (Henze, 1986). Both correction factors will depend on the actual biomass character. However, no particular conflicts, as indicated in Fig. 22, are apparent concerning the correction factor for growth, η_g . Determination of the correction factor for hydrolysis will suffer from the same problems as indicated above for the hydrolysis itself, and may therefore also be considered more as a model parameter.

4.4.2. Relevant kinetic and stoichiometric parameters for lab-scale characterisation

In the discussion on the relevance of characterisation of the stoichiometric and kinetic parameters of ASM1 via lab-scale experiments, one has to remember that none of the ASM model processes are pure or microbiologically correct. They are all bulk processes to some extent. It has clearly been illustrated above that experiments oriented in identifying mechanisms introduced in the model might easily lead to conflict with the actual model coefficients (van Loosdrecht and Henze, 1999). Thus, although possible, it may not always be relevant to retrieve the model parameters from lab-scale tests.

Above the discussion was taken on these conflicts between lab- and full-scale observations and the links to the model processes. Table 9 summarised the dependency of the parameters on the biomass and WWTP

operation, and it was attempted to indicate the most relevant information source based on these discussions. Notice the difference to Table 8 that listed how the different parameters could be estimated from lab-scale tests, whereas Table 9 indicates whether this is relevant or not, considering that the parameter should correspond reasonably well both with the full-scale behaviour, i.e. extant parameters are sought, and the model concepts.

From Table 9 it is deduced that it may be relevant to determine the following list of stoichiometric and kinetic parameters from lab-scale experiments. It is not judged whether it is always needed to characterise these parameters since that will depend on the purpose of the model calibration. For the same reason it is not attempted to make an indicative order of parameter importance.

- $\mu_{\max H}$
- $\mu_{\max A}$
- η_g
- b_A
- b_H
- (Y_H)
- (Y_A)

The yields are included in the list, knowing that they are not easy to determine in lab-scale tests and that they are usually assumed to be rather constant. However, it should also be realised that the yield coefficients have an important influence on nearly all the processes (see Table 6), and therefore it would be rather relevant to have a more accurate determination of these.

The remaining parameters can be determined via either full-scale data or directly via the model calibration, as indicated in Table 9. It is important to notice that the above parameter list is significantly reduced compared to the list of parameters retrieved from experiments based on Table 8, basically due to the fact that the half-saturation coefficients and hydrolysis parameters are left out.

4.4.3. Relevant wastewater components for lab-scale characterisation

Only the side of the triangle dealing with the conflict between lab-scale observations and model concepts (conflict C) outlined in Fig. 22 is relevant when it comes to characterisation of wastewater components. Also, the discussion summarised in Table 9 is not relevant here, since the wastewater components are neither depending on the biomass or the WWTP operation. Therefore, the discussion on wastewater components is less extensive here (see also the earlier discussion and summary of wastewater characterisation methods) and is not divided according to the different components.

As discussed above in the review of wastewater characterisation a conflict may indeed exist between the need for quantification of some of the ASM1 wastewater components and what is practically obtainable from lab-scale experiments. The origin of this problem mainly lays in the way the components are defined in ASM1. The death regeneration cycle and the hydrolysis processes of ASM1 are model processes that are not directly measurable in lab-scale experiments, as discussed above. Thus, the slowly biodegradable substrate and inert particulate matter components, X_S and X_I respectively, that are related to these processes may then also be regarded as model components that should rather be quantified during the model calibration exercise than through dedicated experiments. Indeed, it was proposed by Henze *et al.* (1995) to estimate X_I in the influent via the complete model during the calibration of the sludge balance and, subsequently, estimate X_S from the difference between total COD and the other COD components, as discussed earlier. A determination of the heterotrophic biomass (X_{BH}) in the wastewater is possible via lab-scale experiments, as described above. However, in most cases the X_{BH} present in wastewater is not of great importance, since the growth rates are so high that washout of X_{BH} never occurs in practice. Thus, an inclusion of X_{BH} in the X_S component does not affect the modelling significantly, although it will affect the value of the heterotrophic yield coefficient (a slightly smaller yield may need to be chosen) (Henze *et al.*, 1998). On the contrary, the presence of autotrophic biomass (X_{BA}) in the wastewater may be of importance to prevent wash out of the nitrifiers. The concentration of X_{BA} can in principle be determined via lab-scale experiments, but in practice the procedure may not be straightforward and X_{BA} may rather be adjusted during the model calibration.

In general there is no need for a detailed characterisation of the nitrogen components since the main part of nitrogen in wastewater is ammonium without any coupling to the organic matter (Henze *et al.*, 1998). An exception to this may, however, exist for some industrial wastewater. Thus, the wastewater components relevant to be characterised separately via lab-scale experiments are listed below. Again, an indicative order of importance is not aimed for, since this will depend on the actual case.

- S_{NH}
- S_S
- S_I
- (S_{ND}, X_{ND})

The relevance of determining the inert soluble matter (S_I) is linked to the determination of the soluble readily biodegradable substrate (S_S) since S_I may be needed for the mass balance of soluble COD.

5. Biological experimental constraints

In the previous section wastewater components, stoichiometric and kinetic parameters were listed that are

most relevant to be determined in lab-scale experiment were listed. This list was compiled on the basis of considerations that the component or parameter resulting from the lab-scale experiment should be relevant to full-scale behaviour and fit within the model concepts.

Here we will further zoom in on the problem of transferability between lab-scale results and full-scale behaviour. As discussed above care should be taken in the transfer of results derived from lab-scale experiments to a model of the full-scale system. Summarising, the reason for problems with transferability are on the one hand differences in biological experimental conditions between lab-scale and full-scale experiments (conflict A in Fig. 22) and, on the other hand, differences in the models used (conflict C in Fig. 22).

At the experimental level the lab-scale behaviour may not equal the full-scale behaviour due to, for instance, differences in feeding pattern resulting in other concentration profiles, differences in environmental conditions such as pH, temperature or mixing behaviour, or differences in sludge history. One of the most discussed biological experimental factors is the ratio between initial substrate concentration (S_0) and the initial biomass concentration (X_0). This $S(0)/X(0)$ ratio is considered to be one of the important factors determining (1) the response of the sludge with a certain wastewater or substrate and (2) whether the experimental response is sufficiently informative for adequate interpretation. The first point is of a more basic nature since it has been observed that the $S(0)/X(0)$ ratio directly influences the behaviour of the sludge, leading to different characteristics (Chudoba *et al.*, 1992; Grady *et al.*, 1996, Pollard *et al.*, 1998). The second point is more related to the practical identifiability of model parameters, i.e. it affects the quality of the experimental data (Spanjers and Vanrolleghem, 1995; Spérandio and Paul, 2000). For instance, if $S(0)/X(0)$ is very high the measured response (e.g. the respiration rate) may be too small and the experiment may take too long. On the other hand, if $S(0)/X(0)$ is very low the respirometric response may be too short for a reliable measurement, or it may be swamped into the endogenous respiration rate. Below, special attention is paid to the first point, where the $S(0)/X(0)$ problem will be discussed in more detail.

At the modelling level the results from lab-scale experiments may be described with a model different from the model used to describe the full-scale behaviour. Although not obvious at first sight, the use of a simple model for interpretation of the lab-scale data increases calculation speeds significantly, resulting in, for instance, a faster and more straightforward parameter estimation. Problems arise when the model uses different concepts that may not allow to transfer the estimated parameters from one model to the other, e.g. the death regeneration versus endogenous respiration concept (Yuan and Stenström, 1996).

5.1. Transferability between model concepts: an example

In ASM1 the death regeneration concept is applied, whereas the model to describe the lab-scale results

may only include the degradation of substrates, i.e. decay and death regeneration are omitted, because they are considered insignificant in relation to the time scale used in the experiment (Spanjers and Vanrolleghem, 1995). In ASM1 oxygen is consumed for growth on incoming substrate plus growth on substrate produced due to death regeneration, whereas in a lab-scale model one may only consider that oxygen is consumed for growth on incoming substrate. This is illustrated in Fig. 23.

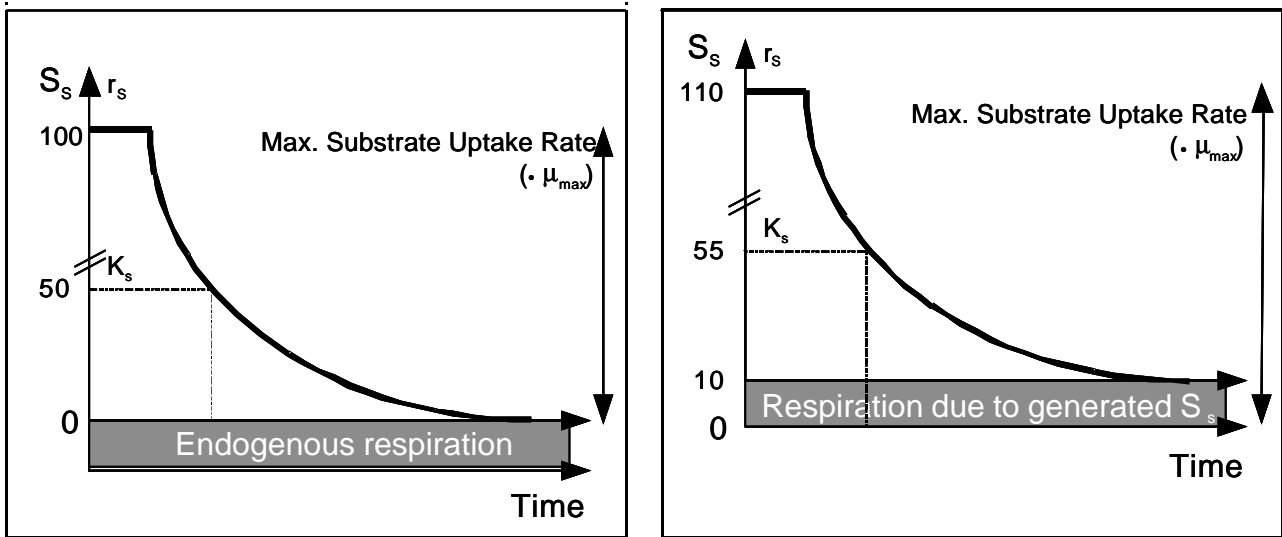


Figure 23. Illustration of difference in interpretation of substrate uptake rate in lab-scale (endogenous respiration) model versus ASM1 (death regeneration)

In Fig. 23 the line illustrates substrate uptake rate r_s as function of time and the values at the left hand side of the y-axes indicate the corresponding substrate concentrations S_s . The left figure illustrates how the substrate uptake rate is interpreted in the lab-scale (batch) experiments whereas the right figure gives the ASM1 interpretation. In both cases the total oxygen consumption rate is the same, but it is interpreted differently in the lab and full-scale model. In the lab-scale model oxygen is consumed to degrade the incoming substrate and the substrate concentration will eventually go to zero. Apart from oxygen for substrate degradation ($r_{O,ex}$), oxygen is also used for endogenous respiration ($r_{O,end}$). In ASM1 substrate will also be degraded. However the concentration will not reach zero since there will be some production of substrate from the death regeneration process. Thus, according to the ASM1 model concept oxygen will be consumed for degradation of both the incoming substrate and the produced substrate. In Fig. 23 it is assumed for clarity that the concentration of the produced substrate is 10 mg COD/l. This slightly higher substrate availability in ASM1 means that the contribution of the observed total r_b to degradation of incoming substrate is lower in ASM1 than in the lab-scale model. As a consequence the estimated maximum growth rate, which is proportional to the maximum r_b , will be lower in the batch system. This is illustrated with the size of the double arrow at the right hand side of both graphs in Fig. 23. Also, the value of the half-saturation coefficient K_s will be underestimated in the batch model compared to ASM1. In the

batch model this is illustrated by a K_S value of 50 whereas it may be 55 in ASM1.

As discussed earlier, it is possible to derive analytical transformations between both model concepts for the decay and growth rates, the yield and the fraction of inerts produced (Henze *et al.*, 1987). However, a transformation for K_S is more complicated.

5.2. Review and discussion of $S(0)/X(0)$ ratio

Depending on the experimental conditions the organic substrate (COD) uptake rate in both lab- and full-scale may consist of different responses. This is illustrated in Fig. 24.

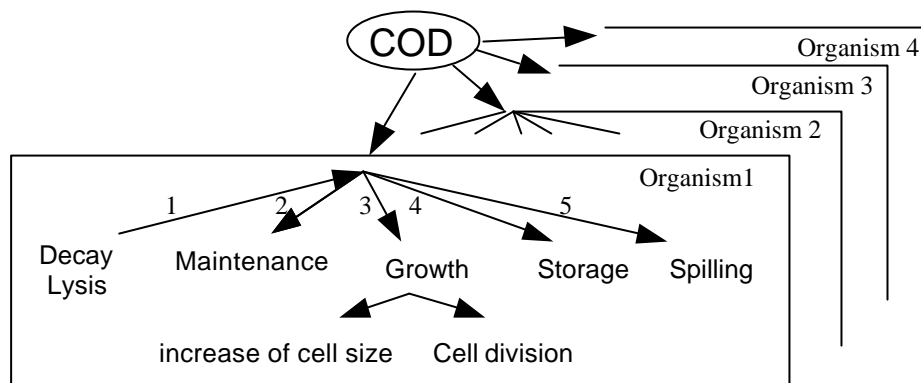


Figure 24. Different flows of external COD in the organisms

In the concept presented in that figure COD is produced from decay (flow 1). Maintenance (flow 2) is defined as the external substrate requirements to maintain the organisms in their current state. Note the difference here to endogenous respiration, which can be defined as the respiration in absence of external substrate (for a detailed review see van Loosdrecht and Henze, 1999). However, here it is assumed that external substrate is present. Growth (flow 3) is divided in two; (i) increase in biomass due to production of cell constituents (e.g. proteins etc.) but without cell multiplication, (ii) increase in biomass caused by cell multiplication. Storage (flow 4) is defined as the accumulation of polymers, e.g. poly-hydroxy-alkanoates and glycogen. Energy spilling (flow 5) (Zeng *et al.*, 1995) is defined as substrate waste that may take place when the organisms are exposed to very high substrate concentrations. In such cases the organisms may not be able to regulate the catabolism rate to the needs for anabolism, resulting in inefficient use of substrate and possible excretion of metabolites. Fig. 24 illustrates the possible COD flows in the single organisms. Depending on the experimental conditions one of the flows may dominate in a single organism (Fig. 24). The same experimental conditions also provoke a particular distribution of COD over the different organisms. Competition may eventually lead to a shift in the population (Novák *et al.*, 1994).

As mentioned above the $S(0)/X(0)$ ratio is considered to be one of the determining factors for the way the organisms respond in a system. However, even though the importance of this ratio has been recognised,

only few references that deal with the subject in more detail can be found (Chudoba *et al.*, 1992; Novák *et al.* 1994; Zeng *et al.*, 1995; Grady *et al.*, 1996; Liu, 1996). They all deal with the subject from a more theoretical point of view without much experimental support, and there is still a lack of both qualitative and especially quantitative explanation of the exact role of the S(0)/X(0) ratio. The discussion on the effect of S(0)/X(0) can be considered from a reaction stoichiometry or reaction kinetic point of view.

Effect of S(0)/X(0) on stoichiometry

Both Chudoba *et al.* (1992) and Liu (1996) explain the importance of the S(0)/X(0) ratio from a thermodynamic point of view based on the observations that the observed yield (Y'_H) decreased with increasing S(0)/X(0) ratio (Fig. 25).

In the work of Chudoba *et al.* (1992) substrate (COD) profiles versus time were measured. Here it was assumed that autocatalytic growth would cause substrate uptake at an increasing rate whereas substrate uptake at a constant rate was assumed to be an indirect evidence of storage. It was hypothesised that at low S(0)/X(0) ratio the main response is storage (flow 4 in Fig. 24) since the energy level in the cell will be too low to trigger cell multiplication, resulting in less substrate being oxidised (Daigger and Grady, 1982) and thereby a higher Y'_H . At high S(0)/X(0) ratios on the contrary, the growth response where cell multiplication (flow 3 in Fig. 24) is dominating results in lower observed yields (Chudoba *et al.*, 1992). However, the lower Y'_H at higher S(0)/X(0) ratios may as well be explained by less energy being required for growth without associated cell multiplication (flow 3) and without the involvement of storage (flow 4). A second possible explanation of the data of Chudoba *et al.* (1992) is that the contribution of endogenous respiration to the total amount of oxygen consumed is higher at high S(0)/X(0) ratio. This could also result in lower Y'_H , since the experiments at high S(0)/X(0) ratios take longer time and therefore the amount of decayed biomass (flow 1) is higher.

Still, a different explanation of the decreasing observed yield with increasing S(0)/X(0) is found in the work of Liu (1996), who presented an attempt to quantify the importance of S(0)/X(0). Here the decrease in Y'_H is explained by an increase in energy spilling (flow 5) with increasing S(0)/X(0) (Liu, 1996). However, the problem in verifying this approach is to define at which S(0)/X(0) energy spilling will start to take place. In the study of Liu (1996) the ratio is assumed to be 1. The proposed model was tested on literature data, but the S(0)/X(0) ratios of all the literature data used in the study were higher than 1, making the evidence for the model incomplete. It should be noted that none of these studies attempted to explain the observed behaviour with a more complex model, such as ASM1.

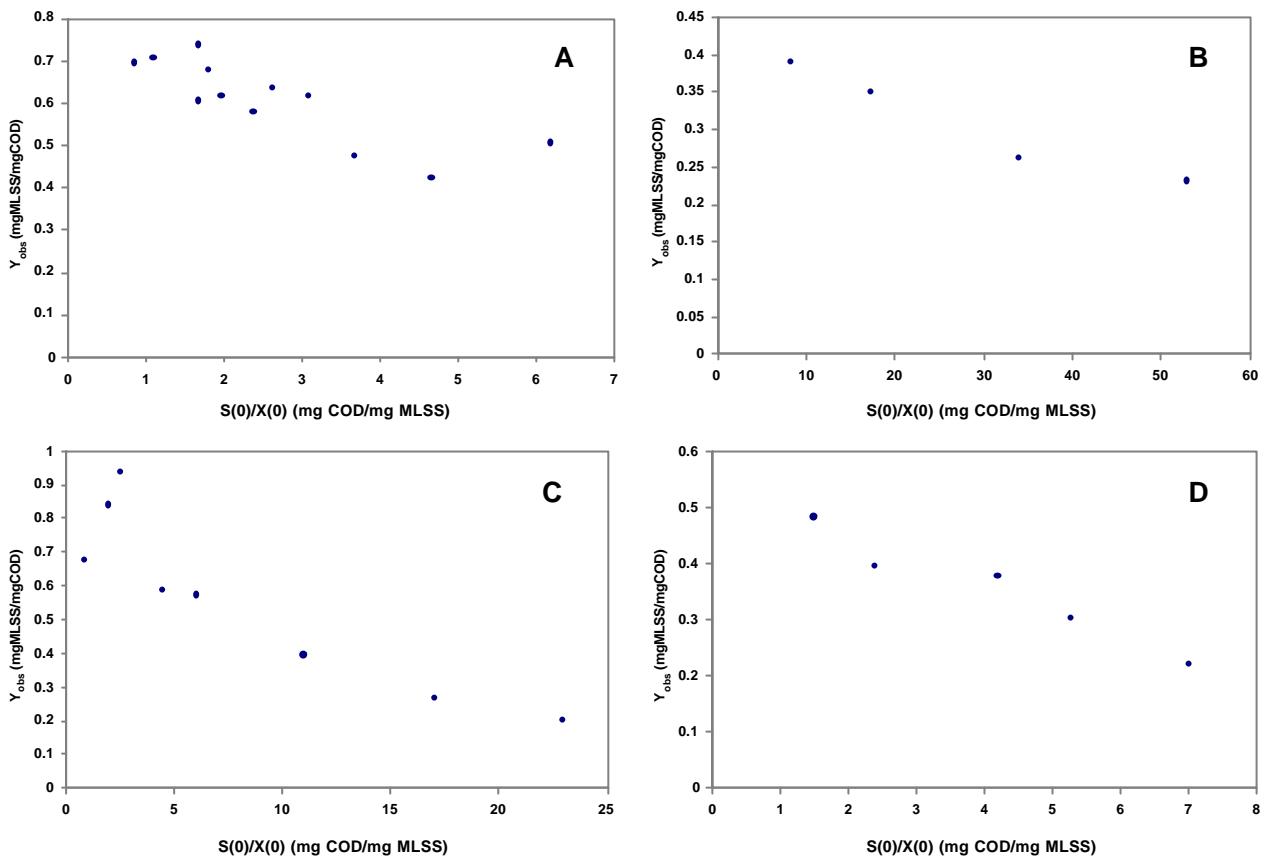


Figure 25. Literature data of Y_{obs} as function of $S(0)/X(0)$ ratio: **A:** Rao and Gaudy, 1966; **B:** Chudoba, 1969; **C:** Chang *et al.*, 1993; **D:** Chudoba *et al.*, 1991. Data digitised from Liu (1996)

Effect of $S(0)/X(0)$ on kinetics

Another way of looking at the influence of $S(0)/X(0)$ is from a kinetic point of view focusing on the physiological, i.e. enzymatic, state and adaptation. In order to describe these phenomena, the concept of the machinery necessary for protein synthesis (PSS) has been introduced (Grady *et al.*, 1996). This should basically be understood as follows. If the organisms are adapted to grow under substrate limited conditions, its PSS will not be sufficient to quickly increase the growth rate if the substrate limitation is removed. Thus, the PSS and eventually the specific growth rate will gradually increase during time, until the maximum possible value according to the new conditions, i.e. physical adaptation has taken place. It has been stated that the synthesis of storage polymers requires less physiological adaptation than the growth response (Daigger and Grady, 1982). Thus, this would mean that if a substrate limitation is removed, as described above, a storage response may be triggered as a fast response and as an alternative mechanism when the growth response is too slow.

A simple example of physiological adaptation is illustrated in Fig. 26 where three pulses of acetate were added consecutively to a sludge sample (Vanrolleghem *et al.*, 1998). Each of the three responses is

characterised by a fast start-up of about two minutes. These two minutes are assumed to be the time needed by a cell to take up fresh substrate and oxidise it (Vanrolleghem *et al.*, 1998). In the first two responses a more gradual increase of $r_{O,ex}$ is observed for about 10 minutes, presumably due to an increased conversion capacity (e.g. enzyme activation or synthesis). In the third response (after 40 minutes) this capacity has become constitutive. Starvation of the culture for one night turned the capacity down (the organisms “forgot”) and a similar behaviour could be observed when acetate was added again (results not shown).

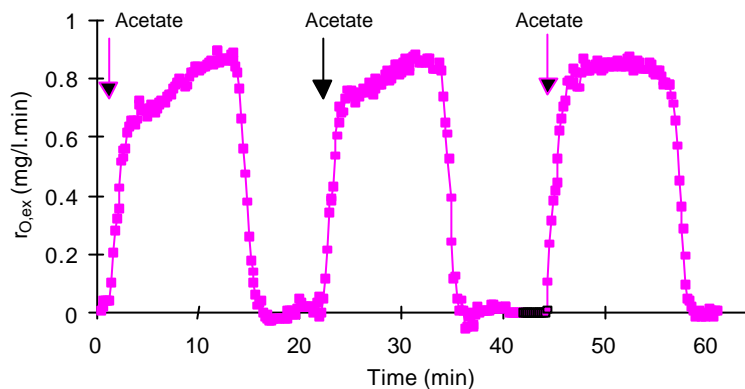


Figure 26. $r_{O,ex}$ profiles obtained by addition of acetate to an activated sludge sample (Vanrolleghem *et al.*, 1998)

In both Chudoba *et al.* (1992) and Liu (1996) the applied $S(0)/X(0)$ ratios are very high (above 1), whereas in the example of Fig. 26 the $S(0)/X(0)$ ratio was very low (below $1/20$). It is commonly assumed that it is necessary to work under low $S(0)/X(0)$ ratios (Chudoba *et al.*, 1992; Novák *et al.*, 1994; Spanjers and Vanrolleghem, 1995; Grady *et al.*, 1996). Indeed, if the $S(0)/X(0)$ ratio is high this may result in a change of maximum specific growth and substrate removal rate due to physiological adaptation, which eventually may result in changes of the proportions among slow-growers and fast-growers leading to population shifts (Novák *et al.*, 1994). The kinetics measured under such conditions will more represent the ultimate capabilities of the organisms (intrinsic kinetics), whereas kinetics measured in experiments performed under low $S(0)/X(0)$ ratio may be more representative of the physiological state of the cells prior to the experiments (extant kinetics) (Grady *et al.*, 1996). In the example of Kappeler and Gujer (1992) a very high $S(0)/X(0)$ ratio was applied resulting in an overestimation of the growth rates, due to a shift in biomass composition towards fast-growers. In addition, population shifts will also take place if the substrate source is changed.

Discussion on $S(0)/X(0)$ ratio

As illustrated above the discussion on the effect of the $S(0)/X(0)$ ratio is looked at from many angles and it seems difficult to draw a coherent picture. However, instead of focusing on a threshold value for the

$S(0)/X(0)$ ratio it may be more relevant to consider the following factors in the discussion of what kind of response can be expected in a lab-scale experiment:

1. ΔS : how big is the change of substrate concentration in the lab-scale system compared to the full-scale system, i.e. to what extent are organisms subjected to a drastic change in their environmental conditions.
2. Time: for how long is ΔS maintained, i.e. what is the time frame of the experiments.
3. History: how strong is the history of the sludge, e.g. starvation periods prior to the experiment

These three factors should be understood as follows. If ΔS is low and the experiment is performed over short-term, the risk for changing the response of the sludge compared to the full-scale system is probably low and extant parameters can be obtained. If ΔS is high and the time is short the risk for excess substrate uptake not resulting in immediate growth increases (maybe induction of storage or spilling). Finally, if ΔS is high and the experiment is performed over long-term the risk for physiological adaptation due to enzymatic changes is increasing, eventually leading to a population shift. The specific growth rate may increase during the experiment resulting in an increase in growth response and a decrease in excess substrate uptake response, i.e. the initial stress reaction such as storage or energy spilling will decrease as the organisms get adapted to the new environment. Thus, somehow a compromise between ΔS and time is needed.

Furthermore, the history of the sludge will play a role in the experimental designs, since for example starvation periods prior to the experiment will result in an initial slower response of the sludge. It is, however, not really clear if for example starvation periods can lead to an initial different response.

The above discussion on $S(0)/X(0)$ focused on heterotrophic organisms and their response to a carbon substrate. However, the discussion can easily be extended to autotrophic organisms where the substrate is ammonium. In this case a too high ΔS may result in inhibition of the nitrification process. However, the risk for a population shift may be lower since the nitrifying group of organisms is supposed to be rather uniform in character. Still, adaptations to new environments will take place and the bacterial species can vary.

The problem of choosing an appropriate $S(0)/X(0)$ value will be addressed further in chapter 7.

6. Summary

In this extensive review numerous aspects of activated sludge model calibration have been touched upon. As an introduction the industry-standard Activated Sludge Model No. 1 was introduced to set the scene and it was compared to the more recent update ASM3. The wastewater and sludge fractions considered in these models were described and the processes taking place among them were given. All these items are focused upon when calibrating such model.

In a next section an overview was given on the descriptions of calibration procedures that were found in

literature. Surprisingly, it is not possible to find a single paper where a comprehensive overview is given. The information is only available as “bits and pieces” and is scattered in a vast amount of literature. The information sets that are typically required were presented and a 10-step calibration procedure was proposed.

The multitude of methods for model calibration was structured along three lines: (1) wastewater characterisation, (2) sludge composition analysis and (3) stoichiometric and kinetic parameters.

The wastewater characterisation is typically done either by physical-chemical or biological characterisation methods. Whereas the former appear the easiest to apply, even in routine lab analysis, their results are not directly related to the model concepts and, moreover, the results need to be augmented with specific characteristics obtained from biological characterisation methods. Among these biological methods attention was particularly given to the respirometric tests as they form the core technique, but nitrate utilisation tests and the upcoming titrimetric tests were presented as well. For the extraction of the model-related information, either direct or model-based analysis is needed. Whereas the former is really simple, the latter allows extracting multiple characteristics from a single experiment.

For the sludge composition analysis, mainly in-out mass balancing methods are being used. The estimation of stoichiometric and kinetic parameters is typically based on dedicated batch experiments using respirometers. Special attention was drawn to the simultaneous estimation of parameters from well-designed single experiments. Especially for this, model-based analysis is required. It is also noteworthy that these more complex approaches not only lead to stoichiometric and kinetic parameter estimates, but typically also lead to estimates on wastewater composition.

In the last section of this review attention was focused upon the problem of transferring the results of the specific tests to a model apt to describe the full-scale behaviour. It was indeed argued that quite some estimation results give a near-perfect description of what happened in the batch test. However this result could not be applied in the practical situation because, for instance, the insufficiently modelled mixing characteristics have to be lumped into the biological parameters of the full-scale model. Still, it was attempted to point towards the parameters whose values can most likely be assessed realistically from lab-scale tests and transferred to the full-scale model.

All in all, this review has led to the belief that a considerable potential exists for efficient characterisation of Activated Sludge Models, provided that precautions are taken with respect to constraining the experimental conditions. The further work of this thesis is entirely devoted to this question. The thesis focuses on the design of optimal experiments that not only lead to high-information content data sets with good identifiability properties, but that also take into account the biological constraints to guarantee transferability of calibration results to the full-scale model.

Chapter 3

-

Activated sludge monitoring with combined respirometric - titrimetric measurements

Parts of this chapter were presented as:

Petersen B., Gernaey K. and Vanrolleghem P.A. (1999) Modelling of activated sludge process kinetics using a combination of hybrid respirometric and titrimetric data. In: Proceedings 9th European Congress on Biotechnology. Brussels, Belgium, July 11-15 1999.

The main part of this chapter was published as:

Gernaey K., Petersen B., Ottoy J.P. and Vanrolleghem P.A. (2001) Activated sludge monitoring with combined respirometric - titrimetric measurements. *Water Research*, **35**, 1280-1294.

Chapter 3

Activated sludge monitoring with combined respirometric-titrimetric measurements

Abstract - A short review of different respirometric methods is presented, and advantages and disadvantages of different principles are discussed. In this study a combined respirometric – titrimetric set-up was applied to monitor degradation processes during batch experiments with activated sludge. The respirometer consists of an open aerated vessel and a closed non-aerated respiration chamber. It is operated with two oxygen probes resulting in two sources of information on the oxygen uptake rate, both collected at a high frequency. The respirometer is combined with a titrimetric unit that keeps the pH of the activated sludge sample at a constant value through addition of acid and/or base. The cumulative amount of added acid and base serves as a complementary information source on the degradation processes. Interpretation of respirometric data resulting from validation experiments (additions of acetate and urea as ammonium source) showed that the set-up provided reliable data. Data interpretation was approached in two ways: (1) via a basic calculation procedure, in which the oxygen uptake rates were obtained by an oxygen mass balance over the respiration chamber, and (2) via a model-based procedure in which substrate transport was included for a more accurate data interpretation. Simulation examples showed that the presence of substrate transport in the model may be crucial for a correct data interpretation, since experimental conditions (e.g. low flow rate) and/or the biodegradation kinetic parameters (e.g. high K_S) may otherwise lead to data interpretation errors. Earlier studies already pointed out that titrimetric data can be related to nitrification, and this was also confirmed in this study. However, in addition, it was shown here for experiments with acetate that the amount of acid dosed was clearly related to the amount of acetate degraded. This indicates that titrimetric data can be used to study carbon source degradation. For the titrimetric data in this study, a model-based analysis was however only applied for the nitrification process. For an experiment with ammonium, it was illustrated that estimation of biodegradation kinetics on a combined respirometric-titrimetric data set significantly improves confidence intervals of the parameters compared to parameter estimation based on respirometric or titrimetric data separately.

1. Introduction

In the following respirometric techniques are reviewed. The advantages and disadvantages of different respirometric approaches are discussed with respect to their applicability for wastewater and sludge

kinetics characterisation. In addition recent applications of a titrimetric measuring principle for activated sludge is presented shortly.

1.1. Respirometry

Respirometry is the measurement and interpretation of the respiration rate of activated sludge, and is defined as the amount of oxygen per unit of volume and time that is consumed by the microorganisms in activated sludge. It is a frequently used tool for the characterisation of wastewater and activated sludge kinetics. The resulting data can for example be applied in the frame of modelling and control of the aerobic parts of the activated sludge process (Henze *et al.*, 1987; Spanjers *et al.*, 1998; Vanrolleghem *et al.*, 1999). Several respirometric principles were developed in the past, and one can classify them into a number of basic measurement principles depending on two criteria: 1) The phase where oxygen is measured (gas or liquid), and 2) The flow regime of both gas and liquid phase, which can be either flowing or static (Spanjers *et al.*, 1998). Fig. 1 shows a schematic representation of a respirometer.

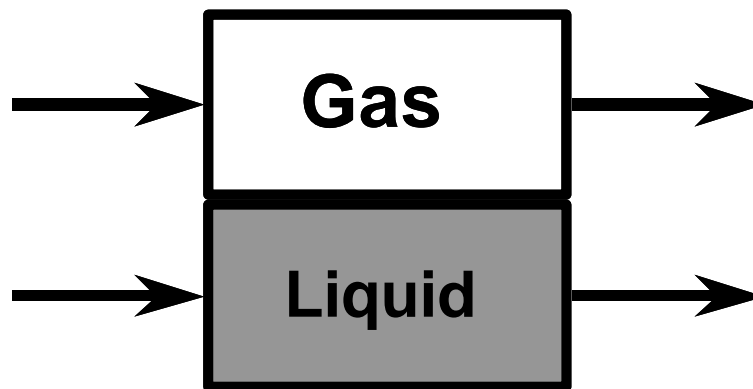


Figure 1. Schematic representation of a respirometer (Spanjers *et al.*, 1998)

For most practical applications oxygen measurements are performed in the liquid phase. Hence, respirometric methods described in the sequel of this introduction will be limited to respirometers where oxygen is measured in the liquid phase using a dissolved oxygen electrode. The respiration rate is calculated by making a general mass balance for oxygen over the liquid phase (Eq. 1). The equation includes, in that order, a transport term, an aeration term and a term describing the oxygen uptake rate (r_o) by the microorganisms. However, depending on the design of the respirometer the transport and aeration term may not be needed as will be illustrated below.

$$\frac{dS_o}{dt} = \frac{Q_{in}}{V} (S_{o,in} - S_o) + K_L a (S_o^o - S_o) - r_o \quad (1)$$

1.1.1. Static gas - static liquid

A static gas - static liquid respirometer is typically operated by monitoring the decline in dissolved oxygen

concentration S_O with time in a closed vessel after a short aerated phase (Vernimmen *et al.*, 1967; Cech *et al.*, 1984; Kappeler and Gujer, 1992; Kristensen *et al.*, 1992; Kroiss *et al.*, 1992; Drtil *et al.*, 1993; Ubay Çokgör *et al.*, 1998). In this type of respirometer the mass balance of Eq. 1 becomes very simple because the transport and aeration term can be omitted, resulting in Eq. 2.

$$\frac{dS_O}{dt} = -r_o \quad (2)$$

A completely closed respiration chamber with no headspace is needed because no aeration of the activated sludge sample (e.g. through surface aeration or air bubbles in the liquid phase) may take place during the experiment. In case an open respiration chamber is used surface aeration may influence the measured data, and in that case Eq. 3 (see below) applies for a correct data interpretation. However, the contribution of the surface aeration is typically neglected (Farkas, 1969; Takamatsu *et al.*, 1981; Randall *et al.*, 1991). Alternatively one can try to limit the oxygen transfer through the liquid-air interface of the open vessel, for example by covering the surface with small plastic balls (Wentzel *et al.*, 1995), or through use of a narrow respiration chamber that has about the same diameter as the dissolved oxygen electrode (Gernaey *et al.*, 1997b).

Because of the absence of aeration, and thereby danger of oxygen limitation, application of this type of respirometer is limited, especially for the determination of sludge kinetics and wastewater characteristics. Typically, experiments with these set-ups are carried out with high substrate concentrations and low biomass concentrations (high S_O/X_O ratio) to avoid limitation of oxygen. However, the sludge behaviour when subjected to a very high S_O/X_O ratio may not be representative for the full-scale system (Novák *et al.*, 1994). Furthermore, experiments with high S_O/X_O ratio will most often only allow a determination of maximum growth rate and not of the half-saturation substrate concentration (K_S) since the substrate concentration may never drop to values near the value of K_S . Alternatively, oxygen limitation can be avoided by a regular reaeration of the sample (Suschka and Ferreira, 1986; Watts and Garber, 1993). This will allow higher sludge concentrations and thereby more realistic S_O/X_O ratios. Another way to solve the oxygen limitation problem is to oversaturate the activated sludge sample with pure oxygen or increased air pressure and in that way achieve a higher initial S_O concentration (Ellis *et al.*, 1996). The disadvantage may however be that the microorganisms are exposed to S_O levels different from their natural environment. A closed respiration vessel is also very important in this case to avoid transfer of oxygen from the oversaturated liquid phase to the gas phase. It should be added here that the respirometric methodology of Ellis *et al.* (1996) is not based on Eq. 2. In their approach the cumulative oxygen consumption (expressed in mg/l as function of time) is calculated as the difference between the initial and actual oxygen concentration. Finally, static gas - static liquid respirometers have been developed where the activated sludge in the closed vessel is replaced when the S_O concentration drops below a certain minimum, or when the retention time in the vessel exceeds a preset maximum (Dircks *et al.*, 1999).

The r_O sampling frequency is often rather low in these different kinds of static gas – static liquid respirometers since one will typically obtain one r_O value per aeration – measurement cycle. A low r_O sampling frequency is a disadvantage especially when the data are to be used to estimate activated sludge kinetic parameters (Vanrolleghem and Spanjers, 1998).

1.1.2. Flowing gas - static liquid

Flowing gas - static liquid respirometers are continuously aerated and have the advantage that higher sludge concentrations can be used, because there is a continuous input of oxygen to avoid oxygen limitation (Blok, 1974; Farkas, 1981; Ros *et al.*, 1988; Vanrolleghem *et al.*, 1990, 1994). A higher sludge concentration will typically allow a shortening of the experiment. The transport term of Eq. 1 is not needed and the mass balance over the liquid phase becomes:

$$\frac{dS_O}{dt} = K_L a(S_O^\circ - S_O) - r_O \quad (3)$$

It should be noted that the oxygen dynamics might not be visible in case the oxygen transfer coefficient $K_L a$ is too high. Moreover, too high aeration intensity may increase the risk of measurement noise. It is thus important to optimise the aeration in the respirometer in such a way that a reliable r_O value can be obtained. In general, the oxygen uptake rate (r_O) may be considered to consist of two components (Spanjers, 1993): The exogenous oxygen uptake rate ($r_{O,ex}$), which is the immediate oxygen uptake needed to degrade a substrate, and the endogenous oxygen uptake rate ($r_{O,end}$). The $r_{O,ex}$ is zero when no substrate is present, and in that case the oxygen concentration in the flowing gas – static liquid respirometer reaches a steady-state concentration $S_{O,eq}$ representing the equilibrium between oxygen transfer and endogenous respiration. Therefore, Eq. 3 can be transformed into Eq. 4 (Vanrolleghem *et al.*, 1994), under the assumption that $r_{O,end}$ is constant, which is a reasonable assumption for short-term experiments.

$$\frac{dS_O}{dt} = K_L a(S_{O,eq} - S_O) - r_{O,ex} \quad (4)$$

By applying Eq. 4 attention can be focused on the substrate degradation induced respiration ($r_{O,ex}$) only. A flowing gas - static liquid respirometer allows to record r_O data with a higher frequency compared to most static gas – static liquid respirometers (e.g. one measurement every 10 s as in Vanrolleghem *et al.*, 1994). According to Eq. 4, $r_{O,ex}$ can be calculated from S_O data measured during substrate degradation when the values of dS_O/dt , $S_{O,eq}$ and $K_L a$ are known. The factor dS_O/dt is the slope of the S_O curve, and is typically obtained by a moving data window regression on the S_O data. The $S_{O,eq}$ can be obtained easily from the respirogram as the S_O concentration measured during the endogenous respiration phase. In the example in Fig. 2, $S_{O,eq}$ corresponds to the S_O concentration measured at $t = 70$ min. For the oxygen transfer coefficient $K_L a$ several methods can be used to obtain its value (ASCE, 1996). The $K_L a$ can for example be obtained from a separate reaeration experiment with sludge in endogenous state (Bandyopadhyay *et al.*,

1967). Alternatively, the $K_L a$ value can be estimated from a reaeration curve obtained after addition of a known readily biodegradable substrate to an activated sludge sample (Vanrolleghem, 1994), as illustrated in Fig. 2. This $K_L a$ estimation method requires the assumption that the degradation of the added known readily biodegradable substrate is completed at a certain point in time, and that r_O is constant during the reaeration phase. The S_O curve in Fig. 2 consists of two parts: 1) S_O values are decreasing, and both substrate degradation and aeration influence the S_O concentration; 2) S_O values increase due to aeration of the activated sludge. The bending point in the upward part of the S_O curve is subsequently determined as the point where $d^2 S_O/dt^2$ changes sign (after 23 min. in Fig. 2). From this point on $K_L a$ values are calculated by applying Eq. 4 at each time instant, assuming that $r_{O,ex}$ is zero. Thus, when the $K_L a$ value calculated this way becomes constant (judged by a statistical test) this is seen as an indication that the reaeration is the only process that takes place. In Fig. 2 this assumption is valid from the very first point after the bending point, and this estimated $K_L a$ value is used in the further calculations. The increased noise on the estimated $K_L a$ values at the end of the respirogram is mainly because S_O approaches the value of $S_{O,eq}$, eventually resulting in unreliable $K_L a$ estimates.

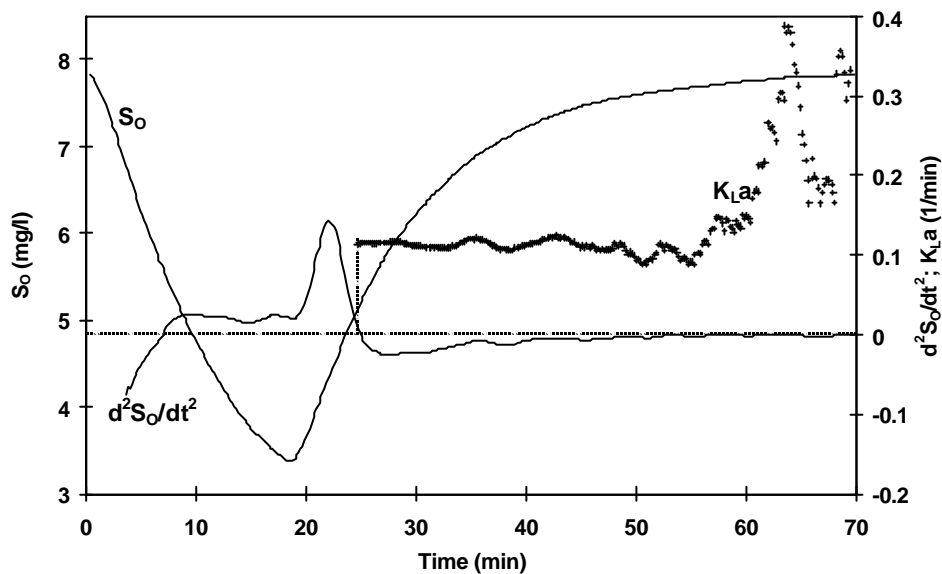


Figure 2. Illustration of the $K_L a$ determination principle for a flowing gas - static liquid respirometer following the addition of a readily biodegradable substrate at $t = 0$

The $K_L a$ value obtained this way is substituted in Eq. 4 to calculate r_O for other experiments in which unknown substrates are added to the activated sludge sample in the respirometer. This approach may however give practical problems. An addition of an unknown substrate (e.g. a complex wastewater containing surfactants) or a change in the liquid volume in the sensor (e.g. by adding a large volume of wastewater sample) can result in $K_L a$ changes that will not be taken into account during the r_O calculations. Finally, the question remains if the assumption of constant $K_L a$ also holds while the degradation of complex

wastewater samples is ongoing. Research is currently going on to investigate the problems concerning the assumptions behind this $K_L a$ estimation method.

1.1.3. Static gas - flowing liquid

In static gas - flowing liquid respirometers the S_O concentration at both the inlet and the outlet of a closed respiration chamber is measured (Spanjers, 1993). Aerated sludge is pumped continuously through the respiration chamber. The r_O is calculated by making an oxygen mass balance over the respiration chamber using the inlet ($S_{O,in}$) and outlet (S_O) dissolved oxygen concentration and the residence time (V/Q_{in}) in the chamber (Eq. 5).

$$\frac{dS_O}{dt} = \frac{Q_{in}}{V} (S_{O,in} - S_O) - r_O \quad (5)$$

Knowledge of $K_L a$ is not necessary, which gives this type of respirometer an advantage in the study of more complex substrates such as wastewater for which $K_L a$ estimation may be problematic. The residence time (V/Q_{in}) is assumed to be known in this approach, and should be properly chosen to avoid oxygen limitation in the respiration chamber. A disadvantage is that a relatively small difference ($S_{O,in} - S_O$) must be calculated from the signals of two different dissolved oxygen probes, indicating that drift of the electrodes may cause erroneous r_O data. To deal with this, the S_O concentrations in inlet and outlet of the respiration chamber are measured by the same dissolved oxygen probe in the static gas - flowing liquid respirometer of Spanjers (1993). This was achieved by regular switching of the flow direction in the respiration vessel (e.g. once every minute). However, the frequent flow direction switch means that the response time of the electrode itself becomes important for the data interpretation (Spanjers and Olsson, 1992). Moreover, it is the cause of a lower measurement frequency of r_O (Vanrolleghem and Spanjers, 1998), typically one data point per minute (Spanjers, 1993). As an alternative to this respirometric principle, where the residence time in the respiration chamber is kept constant, Kalte (1990) proposed a respirometer in which the flow rate is varied to maintain a constant ($S_{O,in} - S_O$) set-point in order to assess the short term biochemical oxygen demand (BOD_{st}).

1.1.4. Hybrid respirometer

As a compromise, taking the good and leaving the bad elements of the different existing respirometers, the theoretical concept of a hybrid respirometric measurement principle was proposed (Vanrolleghem and Spanjers, 1998). In the hybrid respirometer, the principles of a flowing gas - static liquid and a static gas - flowing liquid respirometer are combined. The respirometer consists of an open aerated vessel and a closed non-aerated respiration chamber, and is equipped with two dissolved oxygen probes (Fig. 3). Sludge is continuously pumped between the aeration vessel and the respiration chamber. The advantages of the different respirometer principles are combined (Table 1): Use of two dissolved oxygen probes results in

the high r_O data collection frequency of the flowing gas - static liquid respirometer. At the same time r_O can be calculated with a similar procedure as the static gas - flowing liquid respirometer because a mass balance for oxygen over the closed respiration chamber (Eq. 6) avoids the need to estimate $K_L a$ values. In addition, a second mass balance for oxygen can be made over the aeration vessel as a second source of r_O data on condition that the $K_L a$ value can be estimated (Eq. 7).

$$\frac{dS_{O,2}}{dt} = \frac{Q_{in}}{V_2}(S_{O,1} - S_{O,2}) - r_{O,2} \quad (6)$$

$$\frac{dS_{O,1}}{dt} = \frac{Q_{in}}{V_1}(S_{O,2} - S_{O,1}) + K_L a(S_O^o - S_{O,1}) - r_{O,1} \quad (7)$$

Vanrolleghem and Spanjers (1998) proposed different implementations of the hybrid respirometer principle by changing the position of the dissolved oxygen probes in the set-up (Fig. 3). An obvious disadvantage of the hybrid respirometer is that it involves two dissolved oxygen probes with the risk that the measured S_O outputs drift away from each other. However, each of the proposed configurations had different possibilities for fault detection and respirometer calibration aiming at reducing errors due to pump flow rate and/or dissolved oxygen probe drift. The “ultimate” hybrid respirometer has the two dissolved oxygen probes in the tubes transporting sludge from aeration vessel to respiration chamber and vice versa (Fig. 3).

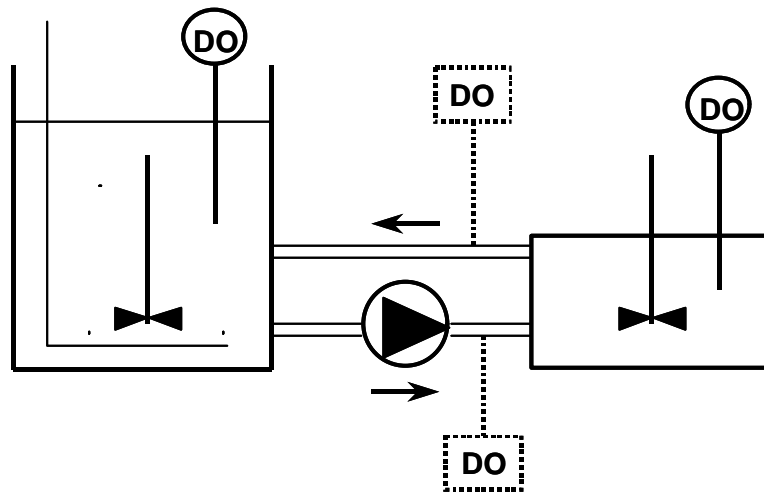


Figure 3. Scheme of the operation of two different hybrid respirometer principles (Vanrolleghem and Spanjers, 1998). Full line = respirometer configuration with dissolved oxygen electrodes in aeration vessel and respiration chamber; dotted line = “ultimate” hybrid respirometer configuration with dissolved oxygen electrodes in the lines between the vessels

The practical development of the hybrid respirometer resulted however in the configuration shown in Fig. 3 where the dissolved oxygen electrodes are placed in the aeration vessel and the respiration chamber. This development will be discussed further below. The hybrid respirometric principle with a dissolved oxygen probe in the aeration vessel and a dissolved oxygen probe in a closed respiration chamber has already

been described by Clarke *et al.* (1978), Hissett *et al.* (1982) and Sollfrank and Gujer (1990). Both Clarke *et al.* (1978) and Hissett *et al.* (1982) applied a rather simple data interpretation based only on the difference between the two measured S_O concentrations. Sollfrank and Gujer (1990) connected a respiration chamber to the aeration basin of an activated sludge pilot plant. They used the system to measure r_O of the biomass and the oxygen transfer coefficient in the aeration basin. However, in none of these cases has a model-based interpretation of the data been carried out.

Table 1. Comparison of advantages and disadvantages of different respirometric principles

Respirometer type	Advantages	Disadvantages
Static gas – static liquid	- Easy to operate	- Danger for oxygen limitation - Low r_O measurement frequency
Flowing gas – static liquid	- High r_O measurement frequency	- K_La estimation needed
Static gas – flowing liquid	- No K_La needed	- Low r_O measurement frequency
Hybrid respirometer	- No K_La needed - High r_O measurement frequency	- Two dissolved oxygen probes

1.2. Titrimetry

Besides respirometry, titration experiments can also yield information about biological nitrogen removal processes in activated sludge (Ramadori *et al.*, 1980; Bogaert *et al.*, 1997; Gernaey *et al.*, 1997a). Indeed, the pH value of a biological system responds to microbial reactions and the evolution of the pH of a system often provides a good indication of some of the ongoing biological reactions. For activated sludge wastewater treatment plants the processes that mostly influence the pH of the liquid phase are: 1) Nitrification which causes a pH decrease due to proton production (Ramadori *et al.*, 1980; Gernaey *et al.*, 1997a), 2) Denitrification which causes a pH increase due to proton consumption (Bogaert *et al.*, 1997), 3) Degradation of organic matter which affects pH due to a) the uptake of the carbon source through the cell wall of the bacteria, b) the release of CO_2 resulting from respiration processes in the liquid phase, c) the uptake of ammonium for growth (San and Stephanopoulos, 1984; Iversen *et al.*, 1994; Siano, 1995 among others), 4) Stripping of CO_2 due to aeration.

The pH effects observed in a liquid medium can be related to the biological process rates and kinetics. However, one difficulty encountered with the observation of pH changes is the variable buffer capacity of the liquid medium due to the presence of several acid-base buffer systems with pH depending buffer capacity (Stumm and Morgan, 1981). The pH variation of the liquid medium during biological reactions is thus difficult to convert into a precise number of protons that is released or consumed. The problems

caused by the pH depending buffer capacity of the liquid medium can be avoided by controlling the pH of a liquid medium at a constant pH setpoint through addition of acid and/or base. In that case, monitoring the acid and/or base consumption rate, needed to keep the pH constant, provides the rate of proton formation or consumption due to biological reactions.

Model-based analysis of titration data can be used to estimate parameters of the reactions. This approach has been used in fermentation (Iversen *et al.*, 1994), and specifically for wastewater treatment, a model-based analysis of titration data has already successfully been applied to the nitrification process (Gernaey *et al.*, 1998).

The main goal of this paper is to demonstrate and validate the methodology of combined respirometric and titrimetric experiments. The validation is performed with additions of simple substrates, as acetate and urea as ammonium source, to an activated sludge sample. Both a basic spread-sheet calculation and a model-based data interpretation will be applied for the interpretation of the data. Kinetic parameters will be estimated both on separate and combined data sets to investigate the parameter accuracy. First however, the practical implementation of the “ultimate” hybrid respirometer principle as proposed by Vanrolleghem and Spanjers (1998) will be described, and the problems of its implementation highlighted. The more practical implementation, used in the study, is subsequently described.

2. Respirometer development

Initially it was attempted to realise the “ultimate” respirometer described by Vanrolleghem and Spanjers (1998) where the two dissolved oxygen electrodes are located in the inlet and outlet of the respiration chamber (Fig. 3). This configuration has the important advantage that errors between different experiments and within one experiment can be minimised easily instead of relying on pre- and post-calibrations. By switching the flow direction and changing the flow rate at the same time the quality of pump and electrode calibrations (e.g. electrode response time and drifts) can be checked while the experiment is running. However, some basic problems related to the change of flow rate and flow direction were experienced, and as a consequence it was finally chosen to apply a simpler configuration. These problems are illustrated below to support future attempts of building the “ultimate” respirometer.

2.1. Problems related to flow rate change in the “ultimate” respirometer

It became clear from tests with tap water that the flow rate was affecting the readings of the dissolved oxygen electrode (see Fig. 4). With the available peristaltic pump (flow rate adjustable from 0 to 0.550 l/min) a liquid flow rate of about 2–10 cm/sec could be obtained over the membrane surface of the dissolved oxygen electrodes. As can be seen in Fig. 4, the flow rate change had a clear effect on the S_0

readings, with an increase of S_{O_2} concentration as the flow increased. An increase in flow rate can normally result in higher S_{O_2} readings because the liquid film at the surface of the electrode is renewed more frequently. Indeed, for some electrodes stable S_{O_2} readings are only possible when the liquid flow rate over the electrode membrane is higher than 15 cm/sec (Willems and Ottoy, 1998) or even 30 – 40 cm/sec (Bogaerts, 1998). It should be stressed that these tests were carried out with electrodes with a rather large membrane surface (about 0.8 cm²) and with a cathode surface of about 0.2 cm². A simple calculation shows that a 20 times larger respiration chamber would be needed (a volume of 10 liters instead of 0.5 liters) in order to keep: (1) a safe liquid flow rate of minimum 40 cm/sec over the electrode surface to avoid a dependency between liquid flow rate and S_{O_2} readings, (2) the flexibility to increase the liquid flow rate with a factor 5, and (3) a similar residence time in the respiration chamber. An alternative could be to reduce the diameter of the gap below the electrode where the liquid is passing by (in the set-up the tube diameter is about 0.5 cm) which however would increase the risk for clogging.

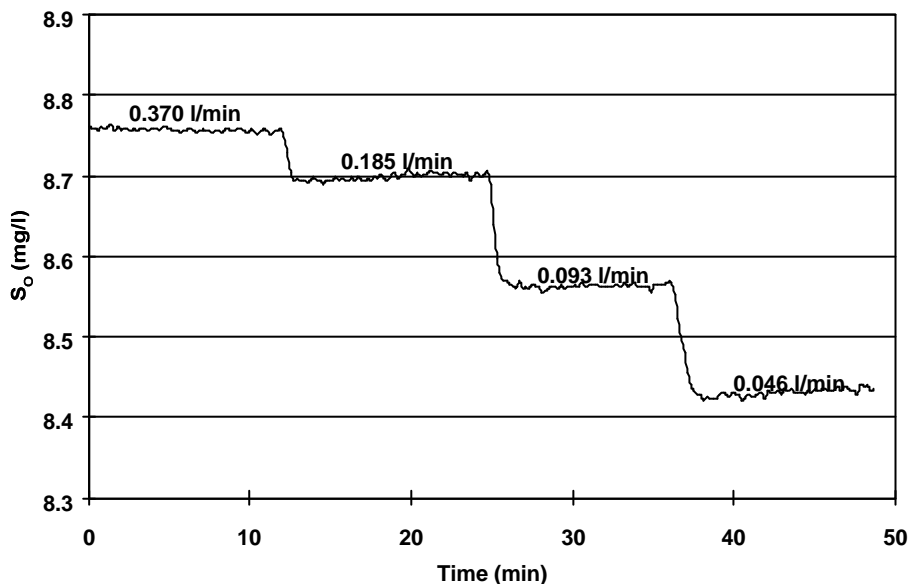


Figure 4. Influence of liquid flow rate variations on dissolved oxygen probe readings

Otherwise, the increase of measured S_{O_2} concentrations with increasing flow rates (Fig. 4) could be explained by a pressure increase in the set-up when liquid flow rates increase, thereby leading to higher measured S_{O_2} values. Indeed, applying Daltons law and taking a flow rate of 0.046 l/min as a reference point, a pressure increase of about 40 mbar in the set-up could explain the increase of S_{O_2} from 8.42 (flow rate = 0.046 l/min) to 8.77 mg/l (flow rate = 0.370 l/min).

2.2. Problems related to flow direction change in the “ultimate” respirometer

In other tap water experiments, where the flow rate was kept constant, it was observed that the S_{O_2}

readings changed when the liquid flow direction was switched. The dissolved oxygen electrodes consistently measured a higher S_O concentration in the inlet flow to the respiration chamber compared to the outlet flow (data not shown). A slightly higher liquid temperature in the respiration chamber (in comparison with the aeration vessel) could explain these observations. The temperature increase of the liquid in the respiration chamber (liquid residence time 1.5 – 6 min) can be due to heat produced by the stirrer of the respiration chamber. Although more important was probably the fact that only the aeration vessel was cooled.

It is possible that the effects of flow rate changes illustrated in Fig. 4 could have been caused by temperature differences as well, due to different residence times in the respiration chamber. However, the S_O data in Fig. 4 is obtained from the outlet of the aeration vessel. The temperature there, and therefore also the S_O readings, is normally constant (confirmed by other data, not shown here) due to the cooling of the aeration vessel. This indicates that the observed effects in Fig. 4 are only caused by the change in flow rate, and not by temperature changes of the liquid in the aeration vessel.

Another problem with the dissolved oxygen electrodes was a short instantaneous disturbance of the electrode readings upon flow direction changes before reaching a stable value. This disturbance could be explained by pressure differences on the membrane of the electrode caused by the change of flow direction. A pressure increase pushes more electrolyte away between membrane and electrode surface (Bogaerts, 1998). This decrease in the contact surface (the mV generating surface of the electrode) gives a decrease in the S_O readings.

2.3. Change of electrodes

Because of the above mentioned problems related to flow rate and direction changes, it was decided to change to electrodes with a hard surface membrane and a smaller cathode surface, thereby leading to a lower dissolved oxygen consumption (see below in Materials and Methods section).

2.4. Change of set-up and confirmation of temperature problem.

The problems related to flow direction change, possibly caused by a temperature difference between the aeration vessel and respiration chamber, prevented that the “ultimate” respirometer concept was realised. E.g. the flexibility of checking for dissolved oxygen electrode drifts would not make much sense under such conditions. It was instead decided to build a simpler configuration with a dissolved oxygen electrode in each vessel, as already illustrated in Fig. 3. However, it should be noted that with this configuration the flexibility of changing the flow rate and direction is lost.

In this set-up the calibration of the dissolved oxygen electrodes is done in two steps while aerated tap water is pumped through the set-up. First, the electrode in the aeration vessel is calibrated, and secondly

the electrode in the respiration vessel is calibrated to give identical readings as the electrode in the aeration vessel. In this way it is sought to compensate for the temperature difference between the two vessels (about 0.6 °C) during the electrode calibration.

A last check of the set-up concerned the adjustment of the stirrer speed in both vessels to a level that did not influence the electrode readings. It was indeed observed that a too low stirrer speed also influences the S_{O_2} readings of the electrode in the respiration chamber. This can be explained again by a too low liquid exchange rate around the membrane surface (data not shown).

With this new set-up the temperature hypothesis was indeed further confirmed by a tap water experiment, during which the flow rate was varied and the temperature of the liquid in the two vessels was recorded. Note that the flow rate can no longer influence the S_{O_2} readings of the electrodes in this experiment as was described above, since the electrodes are now placed in the aeration vessel and respiration chamber respectively. The flow rate only influences the residence time in the respiration chamber. The measured S_{O_2} concentrations of the tap water in the aeration vessel and respiration chamber should theoretically be identical regardless of the flow rate, and thereby the residence time, in the respiration chamber. This was however not the case, as illustrated in Fig. 5. The results of Fig. 5 should be interpreted as follows: Two reference experiments were carried out with a flow rate of 0.185 l/min. In these experiments the dissolved oxygen electrodes were calibrated to the same values, thus the difference in S_{O_2} ($\Delta S_{O_2,ref}$ with $\Delta S_{O_2} = S_{O_2,1} - S_{O_2,2}$) is zero for this flow rate. The temperature difference (0.6 °C) in the reference experiments is noted as ΔT_{ref} but set to zero in Fig. 5. Two experiments were then carried out with half (0.0925 l/min) and double (0.370 l/min) flow rate compared to the reference experiment. The ΔS_{O_2} and ΔT of these experiments were compared to the reference experiment as illustrated in Fig. 5. It was observed that both ($\Delta S_{O_2,ref} - \Delta S_{O_2}$) and ($\Delta T_{ref} - \Delta T$) increased with decreasing flow rate but on the contrary decreased when the flow rate was increased. It was indeed observed that it were primarily temperature changes in the respiration chamber that caused the changes of ($\Delta T_{ref} - \Delta T$). Summarising, at a decreased flow rate, i.e. increase of residence time, the temperature of the respiration chamber increased with a decrease of S_{O_2} as a consequence, in accordance to the theoretical relation between temperature and dissolved oxygen concentration. The opposite was observed for a flow rate increase. This was verified by calculations of S_{O_2} at flow 0.0925 and 0.370 l/min considering the change of temperature. The errors between these predicted S_{O_2} values and the measure ones were below 1%.

The temperature problem could probably be solved by cooling the whole set-up. However this was technically difficult to realise. Based on the experience gained during the practical development of the hybrid respirometer principle it can be concluded that to realise the “ultimate” respirometer of Vanrolleghem and Spanjers (1998) care has to be taken to: a) the quality of the dissolved oxygen electrode (especially the sensitivity to low flow velocity and pressure changes), b) a sufficiently high pump flow rate (to avoid influence of pump flow rate on measured S_{O_2} values), c) the stirrer speed, d) accurate and

constant temperature of the whole system, to achieve accurate and reliable S_O measurements. It is important to stress that these rather basic factors are not only important for the hybrid respirometer, but should be of general concern and checked for all types of respirometers. In simpler respirometer configurations, which at first sight may seem more robust, problems with the above mentioned elements may remain unnoticed and result in erroneous r_O data.

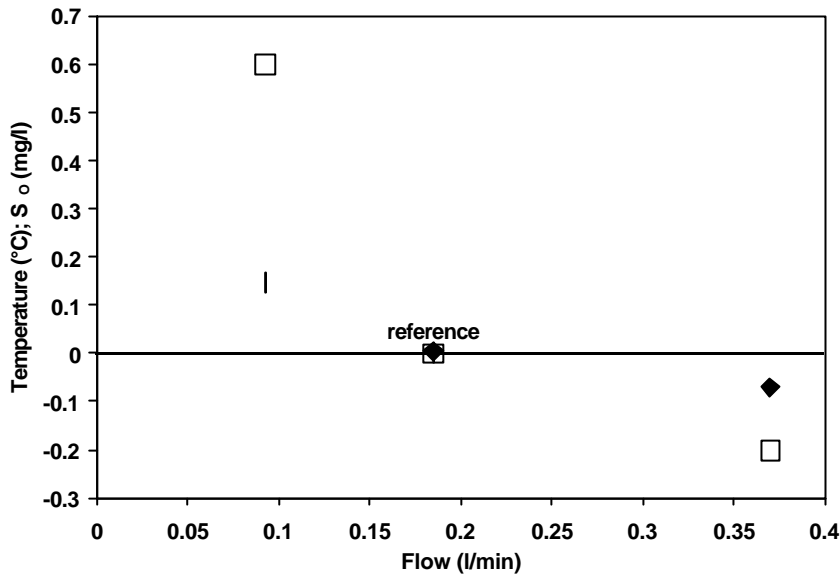


Figure 5. Temperature difference between the liquid in the respiration vessel and the aeration chamber, and calculated endogenous respiration rate as a function of liquid flow rate ($\square = \Delta T_{ref} - \Delta T$; $\blacklozenge = \Delta S_{O,ref} - \Delta S_O$)

3. Materials and Methods

3.1. Set-up

A schematic overview of the different components of the set-up is shown in Fig. 6. The set-up consists of an aeration vessel ($V = 2$ l) and a respiration chamber ($V = 0,5$ l). The respiration chamber is completely closed and does not contain air. Magnetic stirrers with adjustable speed mix the contents of both vessels. A peristaltic pump with adjustable speed (pump 1 in Fig. 6) is used to continuously pump the activated sludge around in the set-up. A cooling system (Lauda WK1400) is used to control the temperature in the aeration vessel. The aeration vessel as well as the respiration chamber is equipped with a dissolved oxygen electrode (Ingold/Mettler Toledo, Inpro 6400). The dissolved oxygen probes are connected to a transmitter (Knick 73 O_2 for the aeration vessel and Knick Stratos 2401 Oxy for the respiration chamber). The 4-20 mA signals from the transmitters are logged by a PC equipped with the Labview software package (National Instruments) and a combined A/D I/O card (National Instruments, AT-MIO-16XE-

50).

The pH controller is installed in the aeration vessel. The pH in the aeration vessel is measured with a Mettler Toledo HA 405-DXK-S8/120 Xerolyte pH electrode connected to a Knick 73 pH transmitter. The 4-20 mA signal is logged with the same Labview software. pH control was also implemented in Labview. The pH was controlled within a narrow pH setpoint $\pm \Delta\text{pH}$ region, as described by Gernaey *et al.* (1997a). Only the base dosage system is shown in Fig. 6 to avoid the scheme to be overloaded. The pH setpoint was typically chosen between 7.5 and 8.3, and a ΔpH value of 0.03 pH units was used. When the pH was out of the pH setpoint $\pm \Delta\text{pH}$ region, dosage of acid (0.05 N) or base (0.05 N) was done by opening an electromagnetic pinch valve for a short period (typically 1.5 s = 1 pulse). Acid and base solutions were continuously pumped around by a peristaltic pump (pump 2 in Fig. 6) to keep a constant liquid pressure in the tubes and thus a constant dosage rate. When the valves are closed the acid and base flows are recycled to the storage vessels. Opening a valve diverts the acid or base flow to the aeration vessel. Calibration of the dosage system was done by collecting the volume of acid or base dosed during 50 subsequent pulses (average dosage = 3.32 ± 0.013 ml/50 pulses for 19 calibrations). The cumulative amount of acid and base dosed during an experiment was logged with the Labview software package.

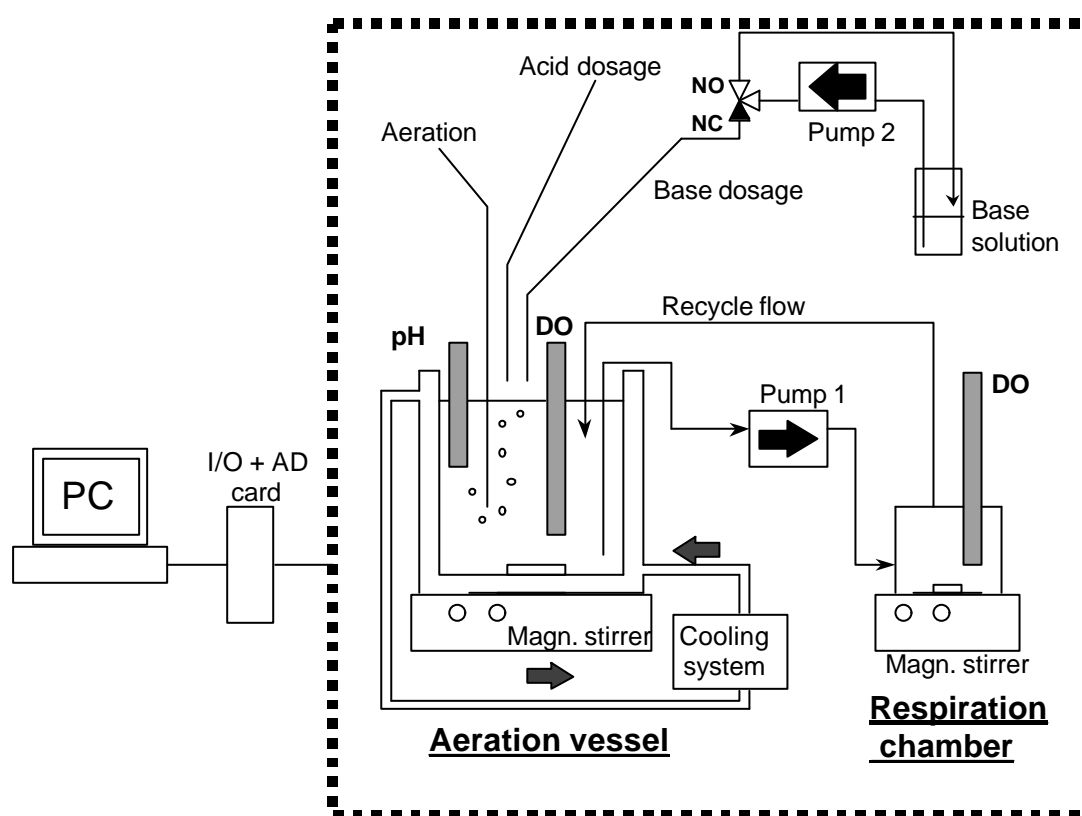


Figure 6. Overview of the components of the combined respirometric - titrimetric set-up that was used to collect experimental data

3.2. Experimental work

Activated sludge was sampled at the combined municipal-industrial wastewater treatment plant of Zele (operated by Aquafin NV, Aartselaar, Belgium) and transported to the lab. At the start of an experiment the set-up was filled with 2.5 liters of activated sludge. The activated sludge was aerated until the endogenous respiration phase was reached. During the experiments small substrate pulses (e.g. 10 ml) of acetate (10 g COD/l), ammonium (1 g N/l) and urea (1 g N/l) stock solutions were dosed to the activated sludge.

4. Basic and model-based data interpretation

Data derived from each experiment were interpreted using both a spreadsheet program (Excell) and a model-based data interpretation method. The modelling work was done with the WEST™ software tool (Hemmis NV, Kortrijk, Belgium).

4.1. Basic data interpretation

The dissolved oxygen and titration data were processed using a spreadsheet program. The r_{O_2} values were calculated by making a mass balance over the respiration vessel using the available S_O data of the aeration vessel ($S_{O,1}$) and the respiration chamber ($S_{O,2}$), as described in Eq. 6. The S_O measurements were corrected for the electrode response time, according to Spanjers and Olsson (1992), and $dS_{O,2}/dt$ was simply calculated with a moving window regression (over three data points). The BOD_{st} for each substrate addition was obtained as the area under the r_{O_2} curve. The value of $r_{O,end}$ was subtracted from $r_{O,2}$ in this last calculation step. The titration data was interpreted by extrapolating the different slopes of the titration curves to obtain the amounts of base or acid needed to compensate the production or consumption during substrate degradation, as described by Gernaey *et al.* (1997a). A more detailed explanation on this method can also be found in chapter 2. Note that the titrimetric data are collected for the total volume of the set-up (values in meq) and converted to the unit meq/l via division by the total reactor volume.

4.2. Model-based data interpretation

Respirometric data (the r_{O_2} values that were calculated in the basic data interpretation step) were modelled by applying the model structure that is summarised in Table 2. The model in Table 2 is based on ASM1 (Henze *et al.*, 1987), with some modifications:

- Nitrification was modelled as a two-step process. In the first nitrification step ammonium (S_{NH}) is oxidised to nitrite (S_{NO_2}), which is subsequently oxidised to nitrate (S_{NO_3}) in the second nitrification step.
- Incorporation of S_{NH} into new biomass was neglected for the second nitrification step. It has been

estimated that the error introduced by this assumption is less than 0.5%.

- Biomass decay was included in the model as endogenous respiration, and was assumed to be constant during the short duration of each experiment.
- The active biomass was lumped into one fraction X, instead of subdividing it into a separate fraction of nitrifiers ($X_{BA} = f_{BA} \cdot X$) and heterotrophs ($X_{BH} = f_{BH} \cdot X$) as proposed by Henze *et al.* (1987). The main reason for this is that biomass fractionation is difficult to perform for activated sludge, and on the other hand the main interest is usually focused on the maximum substrate removal rate of the total sludge (e.g. $X \cdot \mu_{\max H} / Y_H$ for the heterotrophs).
- In this study, a detailed model for the titrimetric data is only applied for the nitrification process (see Table 2). In the model protons (Hp) replace the ASM1 S_{ALK} component, which means that the signs of the stoichiometric factors in the Hp column are the opposite of the signs that appear in the S_{ALK} column in the ASM1 matrix (Henze *et al.*, 1987). In the model S_{NH} oxidation and uptake of S_{NH} for biomass growth during nitrification will produce Hp. A constant background Hp production is included in the titrimetric model to take CO_2 stripping into account, as was introduced by Gernaey *et al.* (1998). The effect of CO_2 stripping is assumed to be constant during the short duration of each experiment (Gernaey *et al.*, 1998). For heterotrophic growth, the standard ASM1 conversion term is included in the Hp column of Table 2 (uptake of S_{NH} to be incorporated into new biomass produces Hp). However, as stated above heterotrophic substrate (here acetate) degradation is not modelled in this study. For more details on this topic the reader is referred to Gernaey *et al.* 2000a and 2000b.
- In the model, the oxygen mass balances for the aeration vessel and the respiration chamber were described by Eq. 6 and 7. Furthermore, the model includes terms to describe (i) the first order dissolved oxygen probe dynamics (Spanjers and Olsson, 1992) and (ii) the biological start-up phenomena, that are typically observed in batch experiments, before the oxygen uptake rate has reached its maximum value. This start-up phase, which typically lasts 0.5 – 2 min, was assumed to be the time needed by a cell to take up fresh substrate and oxidise it and can be described with a simple first order equation (Vanrolleghem *et al.*, 1998). Whether $r_{O,1}$ and $r_{O,2}$ are identical will depend on the experimental design. This will be illustrated and explained below for a better understanding of the experimental results and their interpretation.

Besides substrate degradation and endogenous respiration (Table 2), substrate transport was included in the model, similar to the mass balances for oxygen (Eq. 6 and 7). As an example the mass balance over the respiration chamber for the biodegradable substrate is given in Eq. 8.

$$\frac{dS_{S,2}}{dt} = \frac{Q_{in}}{V_2}(S_{S,1} - S_{S,2}) - \frac{m_{maxH} \cdot X}{Y_H} \cdot \frac{S_{S,2}}{K_S + S_{S,2}} \quad (8)$$

In this paper the model-based interpretation is applied in three steps:

1. Model-based evaluation of the behaviour of the respirometer
2. Model-based interpretation and evaluation of the experimental data to validate the respirometric method.
3. Model based interpretation of the combined respirometric-titrimetric data including the calculation of confidence intervals.

Table 2. Model used for interpretation of the respirometric and titrimetric data. Processes 1, 2, 3, 4 and 5 were necessary to model respirometric data. For titrimetric data, processes 2 and 6 were used to model nitrification experiments

Component → Process ↓	1. X	2. S	3. S _O	4. S _{NH}	5. S _{NO2}	6. S _{NO3}	7. H _p	Process rate
1. Heterotrophic growth on S _s	1	$-\frac{1}{Y_H}$	$-\frac{1-Y_H}{Y_H}$	$-i_{XB}$			$\frac{i_{XB}}{14}$	$\mu_{maxH} \cdot \frac{S_S}{K_S + S_S} \cdot X$
2. Nitrification step 1, S _{NH} oxidation	1		$-\frac{3.43 - Y_{A1}}{Y_{A1}}$	$-\frac{1}{Y_{A1}} - i_{XB}$	$\frac{1}{Y_{A1}}$		$\frac{i_{XB}}{14} + \frac{1}{7 \cdot Y_{A1}}$	$\mu_{maxA1} \cdot \frac{S_{NH}}{K_{SA1} + S_{NH}} \cdot X$
3. Nitrification step 2, S _{NO2} oxidation	1		$-\frac{1.14 - Y_{A2}}{Y_{A2}}$		$-\frac{1}{Y_{A2}}$	$\frac{1}{Y_{A2}}$		$\mu_{maxA2} \cdot \frac{S_{NO2}}{K_{SA2} + S_{NO2}} \cdot X$
4. Endogenous respiration	-1		-1					$b \cdot X$
5. Aeration			1					$K_L a \cdot (S_o^0 - S_o)$
6. CO ₂ stripping							1	r_{HpB}

5. Results

5.1. Model-based evaluation of the behaviour of the respirometer

At the start of an experiment substrate is added in the aeration vessel, and not to the respiration chamber as stated above. Hence, the substrate concentration in the respiration chamber must build up from zero through substrate supply from the aerated vessel via the liquid flow. Obviously, the oxygen uptake rate in the two vessels ($r_{O,1}$ and $r_{O,2}$ respectively) is only equal when the substrate concentration is identical in both vessels.

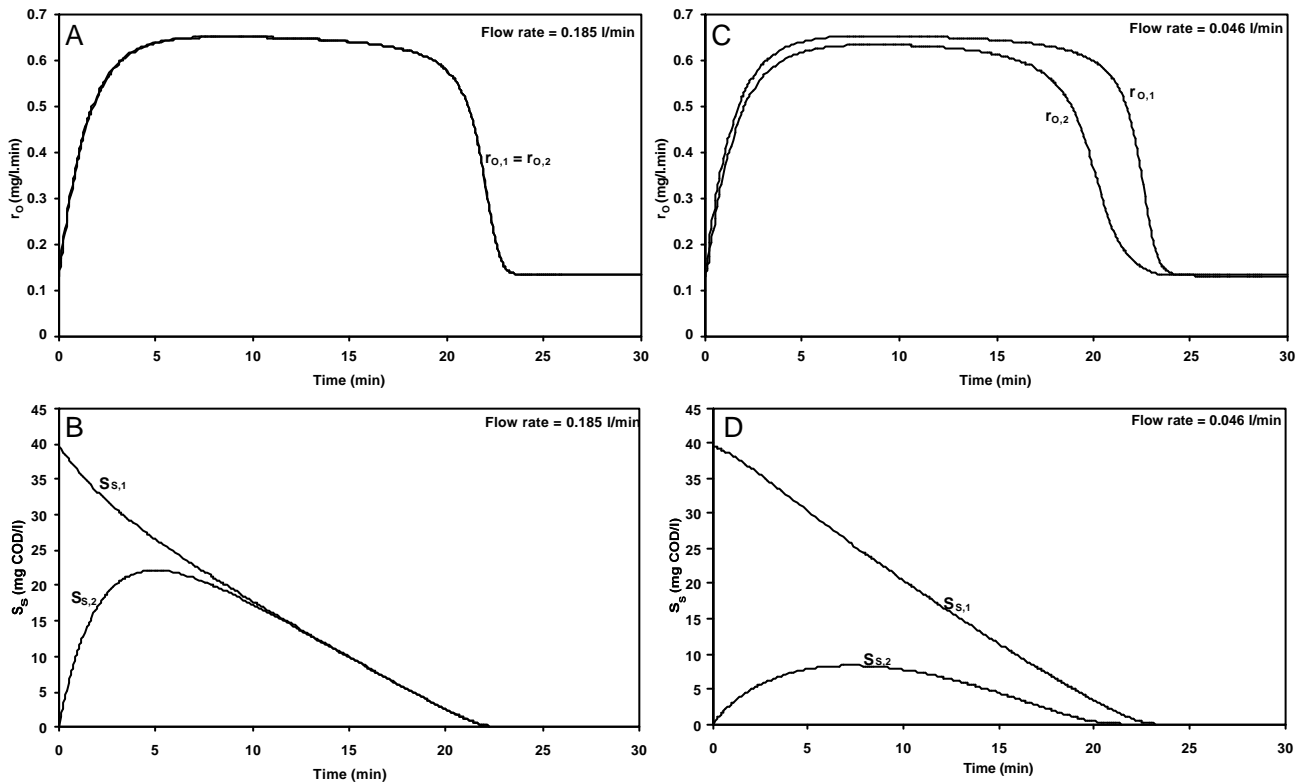


Figure 7. Results of simulations with the respirometer model for an addition of readily biodegradable substrate to the aeration vessel at time zero. $S_{S,1}$ at time zero is 39.6 mg COD/l, $K_S = 0.5$ mg COD/l, $(\mu_{\max} \cdot X) = 1.084$ g/l.min. **A:** $r_{O,1}$ and $r_{O,2}$ as a function of time for a liquid flow rate of 0.185 l/min; **B:** $S_{S,1}$ and $S_{S,2}$ as a function of time for a liquid flow rate of 0.185 l/min; **C:** $r_{O,1}$ and $r_{O,2}$ as a function of time for a liquid flow rate of 0.046 l/min; **D:** $S_{S,1}$ and $S_{S,2}$ as a function of time for a liquid flow rate of 0.046 l/min

Fig. 7 and 8 show simulation results for an addition of biodegradable substrate to the aeration vessel at time zero. In Fig. 7 the results are given for two simulations obtained with different liquid flow rates (0.185 l/min and 0.046 l/min). In the high flow rate experiment the initial substrate concentration in the respiration vessel ($S_{S,2}$) is zero, and it takes a little while before the substrate is properly mixed and the concentrations in the

two vessels become identical (see Fig. 7B). Thus, initially $r_{O,1}$ and $r_{O,2}$ are not identical. However, as can be observed in Fig. 7A this difference is negligible at a flow rate of 0.185 l/min. In contrast, a flow rate of 0.046 l/min results in a situation where the substrate concentration never reaches the same value in the two vessels (Fig. 7D). As a consequence the values of $r_{O,1}$ and $r_{O,2}$ remain different during the whole experiment (Fig 7C).

Whether $r_{O,1}$ is equal to $r_{O,2}$ will also depend on the value of the half saturation concentration K_S for the particular substrate under study. In the simulations given in Fig. 7A and 7B the K_S value was set low to 0.5 mg COD/l, and as noticed above $r_{O,1}$ and $r_{O,2}$ were similar. However, a higher K_S value of 10 mg COD/l (Fig. 8A and B) resulted in an initial difference between $r_{O,1}$ and $r_{O,2}$ even at the high flow rate. A flow rate higher than 0.185 l/min would result in a smaller initial difference between $r_{O,1}$ and $r_{O,2}$ whereas a lower flow rate would increase the difference again.

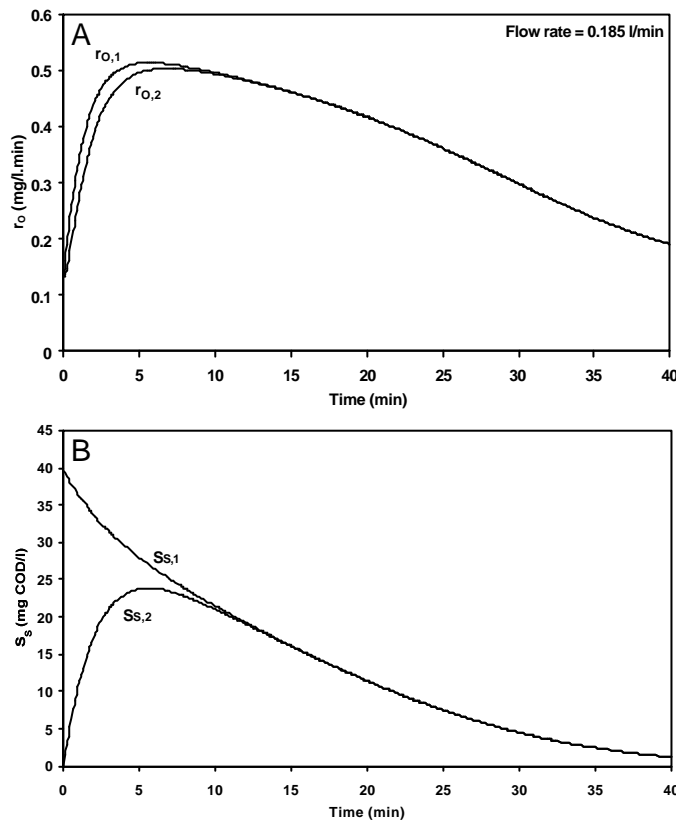


Figure 8. Results of simulations with the respirometer model for an addition of readily biodegradable substrate to the aeration vessel at time zero. $S_{S,1}$ at time zero is 39.6 mg COD/l, $K_S = 10.0$ mg COD/l, $(\mu_{maxH^+} \cdot X) = 1.084$ g/l.min. **A:** $r_{O,1}$ and $r_{O,2}$ as a function of time for a liquid flow rate of 0.185 l/min; **B:** $S_{S,1}$ and $S_{S,2}$ as a function of time for a liquid flow rate of 0.185 l/min

It is important to remember that r_O values calculated with the basic method are based on the S_O mass balance over the respiration vessel only (Eq. 6). The calculation thus yields $r_{O,2}$ values. This means that the

BOD_{st} calculated based on the area under this $r_{O,2}$ profile may underestimate the real value depending on the experimental conditions and the biodegradation kinetics (e.g. K_S), as shown with the simulation examples. Besides an underestimation of BOD_{st} there may also be a risk to underestimate μ_{maxH} (see Fig 7C), and to overestimate K_S values (Fig 7C, tail of $r_{O,2}$ profile).

It should be noticed that the initial phase in the $r_{O,1}$ profile, before $r_{O,1}$ has reached a maximum, can only be due to biological start-up phenomena (Vanrolleghem *et al.*,1998). The initial phase of the $r_{O,2}$ profile, on the contrary, is due to a combination of biological start-up and substrate mixing phenomena, as described above. Thus, for a complete and accurate analysis of the respirometric data derived from the hybrid respirometer a model-based data interpretation, as will be illustrated below, may be needed.

5.2. Basic interpretation of experimental data

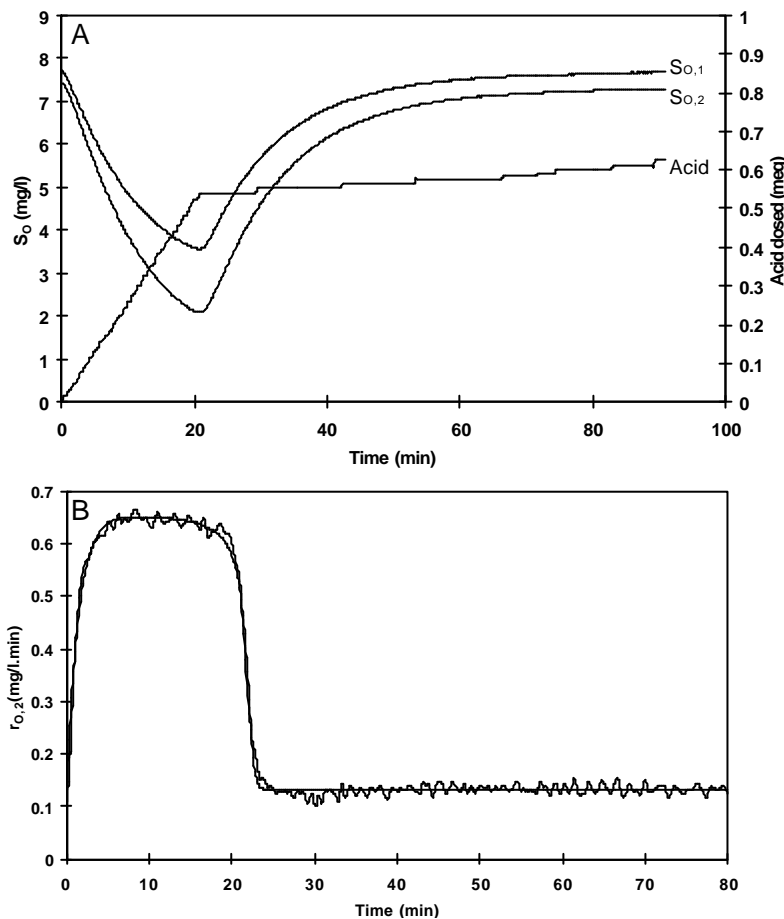


Figure 9. Response of the combined respirometric - titrimetric sensor following a 100 mg COD acetate addition to the aeration vessel at $t = 0$. **A:** S_O and titrimetric data; **B:** $r_{O,2}$ values calculated based on the S_O data using a mass balance for S_O over the respiration vessel. The smooth line represents the model fit to the $r_{O,2}$ data

A typical raw data set recorded from an acetate dosage is shown in Fig. 9A. At time zero 100 mg acetate

COD was added in the aeration vessel of the respirometer. The corresponding $r_{O,2}$ profile in Fig. 9B is rather typical, with a steep decrease from maximum r_O to endogenous $r_{O,end}$ as soon as the substrate is completely degraded (Vanrolleghem *et al.*, 1995). The pH controller also shows a clear response (Fig. 9A). During acetate degradation dosage of acid is needed to keep the pH of the mixed liquor at the pH setpoint (8.25 in this case). This is clearly related to the acetate degradation since acid dosage and $r_{O,2}$ drop at the same moment ($t = 22$ min). From $t = 22$ min on acid dosage fell back to the background dosage rate that was also observed before acetate addition. The background acid dosage rate is due to CO_2 stripping and is assumed to be constant during the experiment (Gernaey *et al.*, 1997a, 1998).

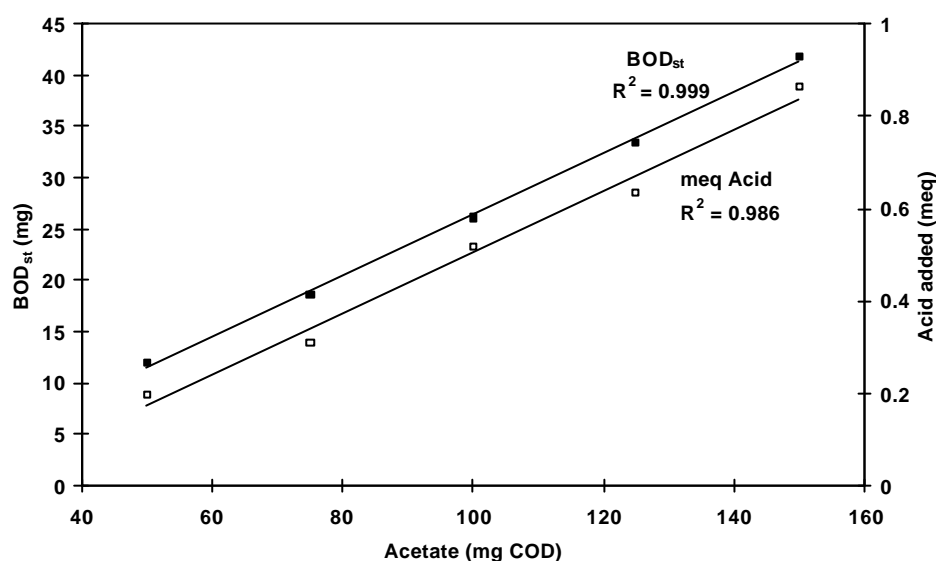


Figure 10. BOD_{st} (calculated based on the area under the $r_{O,2}$ profiles) and total amount of acid dosed during degradation as a function of the initial amount of acetate added

A linear relationship between the amount of substrate added and BOD_{st} is usually observed (Spanjers, 1993). The slope of this curve represents the oxygen demand per unit of COD or N, and allows the calculation of the biomass yield (via $BOD_{st} = (1 - Y_H) \cdot COD$ or $BOD_{st} = (4.57 - Y_A) \cdot S_{NH}$). The BOD_{st} values were calculated as the area under the $r_{O,2}$ curve. A linear increase of BOD_{st} was indeed observed when increasing amounts of acetate were added to the respirometer (Fig. 10). The maximum average yield for this data series is 0.74 with a standard deviation of 0.016. This yield is slightly higher but still comparable to the range of Y_H values (0.24 - 0.72) mentioned in literature for aerobic acetate degradation (Brands *et al.*, 1996; Liebeskind *et al.*, 1996; Xu and Hasselblad; 1996; Dircks *et al.*, 1999). Furthermore, a linear increase of the amount of acid (in meq) added during the degradation was observed as a function of the initial amount of acetate added (Fig. 10).

A data set collected from an addition of 11 mg urea NH_4-N in the aeration vessel of the respirometer is shown in Fig. 11A, and the corresponding $r_{O,2}$ profile is given in Fig. 11B. The $r_{O,2}$ profile has a tail

indicating that the second nitrification step (oxidation of S_{NO_2} to S_{NO_3}) is slower compared to the first step. To verify the respirometric method the linearity between calculated BOD_{st} values and NH_4-N concentrations added is illustrated in Fig. 12. The slope ($4.57 - Y_A$) of this curve is typically expected to be $4.33 \text{ g O}_2/\text{g NH}_4-N$ for nitrification (Henze *et al.*, 1987). The slope of the curve in Fig. 12 is $4.44 \pm 0.16 \text{ g O}_2/\text{g NH}_4-N$ (95% confidence interval) which is slightly higher (2.5%) than expected, but acceptable considering that 4.33 lays within the confidence boundaries.

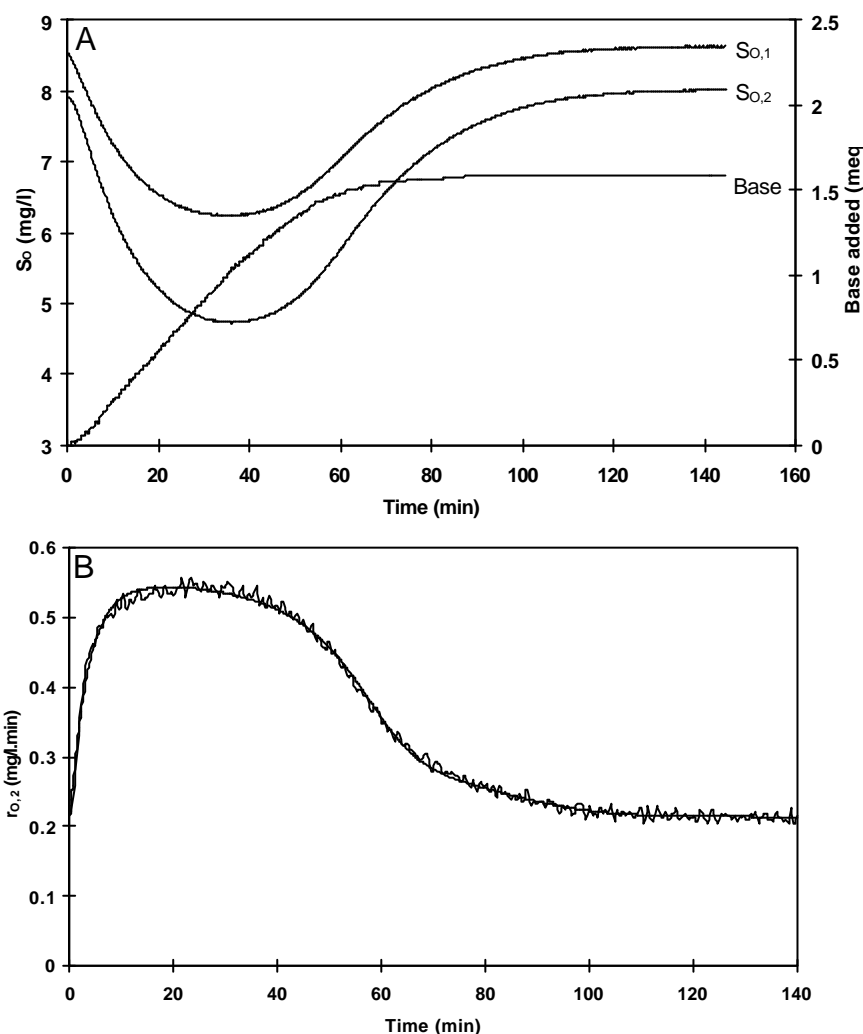


Figure 11. Response of the combined respirometric - titrimetric sensor following an 11 mg N urea addition to the aeration vessel at $t = 0$. **A:** S_0 and titrimetric data; **B:** $r_{O,2}$ values calculated based on the S_0 data using a mass balance for S_0 over the respiration vessel. The smooth line represents the model fit to the $r_{O,2}$ data

During nitrification dosage of base is needed to compensate for the proton production in the first nitrification step, as already observed in earlier literature (Ramadori *et al.*, 1980). For a series of NH_4-N additions to activated sludge, an average recovery of 1.01 with a standard deviation of 0.05 has been obtained from titration data. Calculations were done assuming a production of 2 protons per NH_4-N

oxidised, according to the method described by Gernaey *et al.* (1997a). This confirms that the stoichiometric conversion factor of 2 protons per mg NH₄-N, in accordance with earlier observations (Massone *et al.*, 1995; Gernaey *et al.*, 1997a).

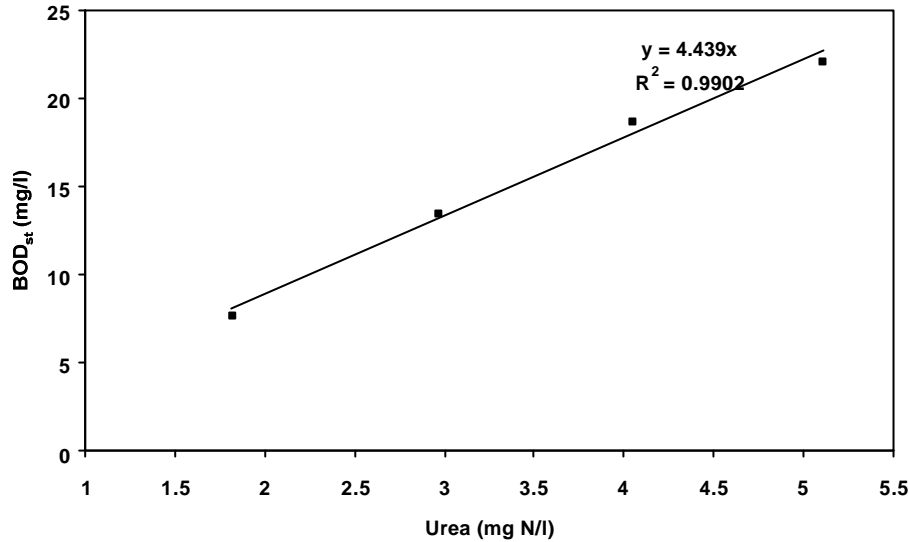


Figure 12. BOD_{st} (calculated based on the area under the r_{O_2} profiles) as a function of the initial urea concentration in the respirometer (expressed as mg N/l)

5.3. Model-based interpretation and evaluation of experimental data.

Examples of the model fit on r_{O_2} data obtained for an acetate and an urea addition are given in Fig. 9B and 11B together with the respective r_{O_2} data. To illustrate the two-step nitrification model further, the estimated evolution of the S_{NH} concentration in both reactors and the build up of S_{NO_2} are shown in Fig. 13.

The theoretically identifiable parameter combinations of a respirometric model describing the degradation of a single carbon substrate with Monod kinetics have been shown to be $(1-Y_H)/Y_H \cdot \mu_{maxH} \cdot X_{BH}$, $(1-Y_H) \cdot K_S$ and $(1-Y_H) \cdot S_S(0)$, assuming that only $r_{O,ex}$ data are available, (Dochain *et al.*, 1995), see Table 3. For the two-step nitrification model assuming no growth, identifiable parameter combinations are discussed in detail in chapter 4. Values for the identifiable parameter combinations are shown in Table 4.

The values of the parameter combinations estimated on acetate and urea r_{O_2} profiles are given in Table 3 and 4. In both cases the reproducibility of the estimates is good. Observed coefficient of variation (C.V.) values are low for μ_{max} related parameter combinations. In the literature C.V. values of 15.0 % (Kong *et al.*, 1996) and 10.3 % (Gernaey *et al.*, 1998) are mentioned from a similar estimation procedure with respirometric and titrimetric data respectively. The C.V. values calculated for the K_S related parameter combinations are higher compared to C.V. values of μ_{max} related parameter combinations. This has been observed before in estimation of kinetic parameters based on respirometric data (Kong *et al.*, 1996), titrimetric data (Gernaey *et al.*, 1998) or substrate concentration data measured during a substrate

depletion experiment (Robinson and Tiedje, 1982; Simkins and Alexander, 1985). The reason for the generally higher C.V. values for the K_S related parameter combinations compared to the μ_{\max} related parameter combinations is probably that the confidence intervals on the estimated K_S values is larger than the confidence intervals on μ_{\max} (see chapter 5). Note also that the C.V. for the parameters of the second nitrification step is higher than for the first nitrification step. This is related to the lower amount of available data points related to the second step (i.e. the tail in the r_O profile) and thereby a poorer practical parameter identifiability.

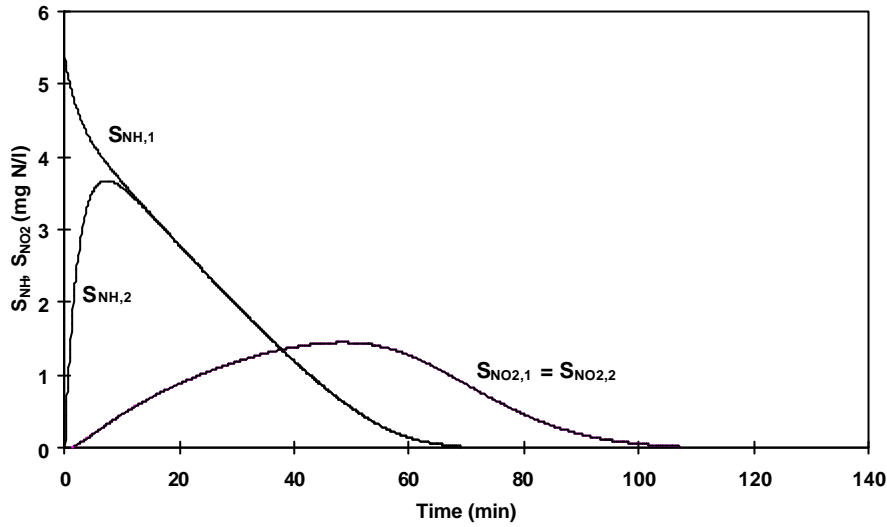


Figure 13. Results of a simulation with the respirometer model for an addition of urea to the aeration vessel at time zero. $S_{NH,1}$ at time zero is 5.30 mg N/l, $K_{SA1} = 0.43$ mg N/l, $(\mu_{\max A1} \cdot X) = 0.318$ mg/l.min, $K_{SA2} = 0.62$ mg N/l, $(\mu_{\max A2} \cdot X) = 0.090$ mg/l.min, liquid flow rate = 0.18 l/min. **A:** Evolution of $r_{O,1}$ and $r_{O,2}$ as a function of time; **B:** Evolution of $S_{NH,1}$, $S_{NH,2}$, $S_{NO2,1}$ and $S_{NO2,2}$ as a function of time

It is also important to compare the calculated BOD_{st} (basic interpretation of $r_{O,2}$ values) with estimated BOD_{st} values. Estimated BOD_{st} is defined as $(1 - Y_H) \cdot S_{S,1}(0)$ for acetate and as $((3.43 - Y_{A1}) + (1.14 - Y_{A2})) \cdot S_{NH,1}(0)$ for nitrification. Note that the estimated substrate concentration is the initial substrate concentration in the aeration vessel at time zero and that the estimated BOD_{st} values therefore have to be multiplied with $V_1/(V_1 + V_2)$ to enable a comparison with the calculated BOD_{st} . When the calculated BOD_{st} values were regressed against the estimated BOD_{st} the slopes were close to 1, both in the case of urea and acetate and, furthermore, the correlation coefficients were close to 1 (0.99). This indicates that the experimental conditions applied in the experiments described in this study were such that the BOD_{st} values calculated as the area under the $r_{O,2}$ profile, obtained from a mass balance over the respiration vessel only, were sufficiently accurate.

Table 3. Values of parameter combinations resulting from estimations on acetate r_{O_2} profiles. The last 3 columns give a comparison between BOD_{st} values resulting from the model-based and basic data interpretation procedure respectively

Parameter combinations→ mg COD↓ (Exp. No.)	$\frac{1 - Y_H}{Y_H} \cdot \mu_{maxH} \cdot X$	$(1 - Y_H) \cdot K_s$	BOD _{st} (model)		% deviation
			$\frac{V_1}{V_1 + V_2} (1 - Y_H) \cdot S_{S,1}(0)$	BOD _{st} (basic)	
50 (1)	0.489	0.177	4.895	4.743	-3.1
75 (2)	0.506	0.160	7.560	7.388	-2.3
100 (3)	0.534	0.163	10.342	10.273	-0.7
125 (4)	0.558	0.155	13.066	13.017	-0.4
150 (5)	0.579	0.189	15.421	16.073	+4.2
Average	0.533	0.169	Correlation	0.999	
C.V. (%)	6.9	8.2			

Table 4. Values of parameter combinations for $\mu_{\max A1}$, $\mu_{\max A2}$, K_{SA1} , and K_{SA2} resulting from estimations on urea r_{O_2} profiles. The last 3 columns give a comparison between BOD_{st} values resulting from the model-based and basic data interpretation procedure respectively

Parameter combinations → mg NH ₄ -N ↓ (Exp. No.)	$\mu_{\max A1}$ ¹	$\mu_{\max A2}$ ²	K_{SA1} ³	K_{SA2} ⁴	BOD_{st} (model) ⁵	BOD_{st} (basic)	% deviation ⁶
5 (4)	0.334	0.098	1.872	1.285	8.106	7.712	-4.9
8 (1)	0.322	0.113	1.427	1.170	13.677	13.517	-1.2
11 (2)	0.318	0.090	1.398	0.666	18.467	18.651	+1.0
14 (3)	0.304	0.103	1.277	0.993	22.072	22.033	-0.2
Average	0.319	0.101	1.493	1.028	Correlation	0.999	
C.V. (%)	3.8	9.4	17.4	26.2			

Parameter combinations:

$$1) \frac{3.43 - Y_{A1}}{Y_{A1}} \cdot \mu_{\max A1} \cdot X$$

$$3) (3.43 - Y_{A1}) \cdot K_{SA1}$$

$$5) \frac{V_1}{V_1 + V_2} \cdot ((3.43 - Y_{A1}) + (1.14 - Y_{A2})) \cdot S_{NH,1}(0)$$

$$2) \frac{1.14 - Y_{A2}}{Y_{A2}} \cdot \mu_{\max A2} \cdot X$$

$$4) (1.14 - Y_{A2}) \cdot K_{SA2}$$

$$6) \frac{BOD_{st}(\text{model}) - BOD_{st}(\text{basic})}{BOD_{st}(\text{model})} \cdot 100\%$$

5.4. Model-based interpretation of combined respirometric-titrimetric data

The two-step nitrification model was applied to describe and estimate parameters for an experiment with addition of ammonium. Parameters were estimated on r_{O_2} and H_p data separately as well as on the combined r_{O_2} and H_p data set. The data and model fit resulting from parameter estimation on the combined data set are illustrated in Fig. 14. The resulting values of the parameters $\mu_{\max A1}$ and K_{SA1} together with their 95% confidence interval are given in Table 5. The derivation of the confidence interval is discussed in detail in chapter 5, and was also applied by Weijers (1999). However, details on the confidence calculations are beyond the scope of this chapter but are described and discussed in chapter 4 where this example is further developed. From Table 5 it becomes clear that the confidence intervals on $\mu_{\max A1}$ and K_{SA1} are slightly improved when based on H_p data compared to parameter estimation based on r_{O_2} data. More importantly, it appears that the confidence intervals improve significantly when r_{O_2} and H_p data are combined for parameter estimations. The confidence on $\mu_{\max A1}$ and K_{SA1} improves 46% and 37% respectively compared to estimation on only r_{O_2} , and compared to estimation on H_p the confidence improvements are 24% and 35% on $\mu_{\max A1}$ and K_{SA1} respectively.

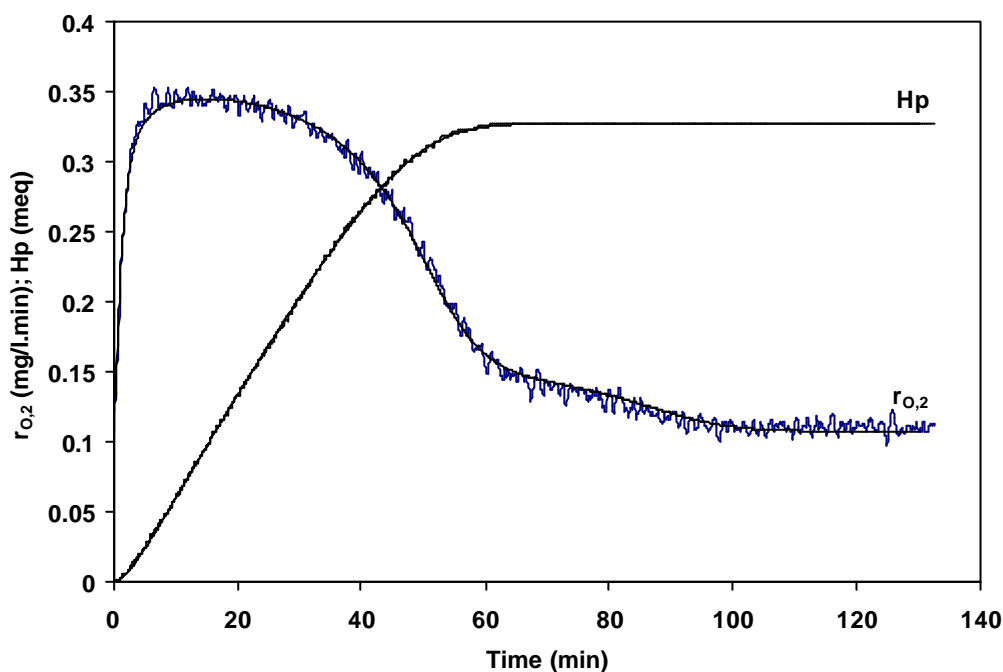


Figure 14. Model fit to r_{O_2} and base addition data collected in an experiment with addition of 7.5 mg NH_4-N to the respiration vessel at $t = 0$. Parameter combinations were estimated on the combined respirometric-titrimetric data.

Table 5. Results of parameter estimations on $r_{O,2}$ and Hp data separately and on combined data for an addition of NH_4-N to activated sludge. R.S.D. = relative standard deviation

Estimated parameter → Data source ↓	μ_{maxA1} min^{-1}	K_{SA1} mg NH_4-N/l
$r_{O,2}$ data	3.27E-06	0.299
Hp data	3.11E-06	0.253
$r_{O,2}$ + Hp data	3.26E-06	0.295
95 % confidence intervals (R.S.D., %)	μ_{maxA1}	K_{SA1}
$r_{O,2}$ data	1.19	5.88
Hp data	0.84	5.66
$r_{O,2}$ + Hp data	0.64	3.70

6. Discussion

In the results section an experimental set-up with combined respirometric and titrimetric measurements was validated with simple substrates (acetate, and urea as N source). For practical implementations the advantages of the proposed respirometer are the high r_0 measuring frequency, and the possibility to calculate $r_{O,2}$ based on a simple oxygen mass balance over the respiration chamber without the need for an estimated $K_L a$ value. However, in case the $K_L a$ in the aeration vessel is known, a second information source, $r_{O,1}$, is available based on a mass balance for oxygen over the aeration vessel. It is investigated further in chapter 4 how this second data source can contribute with respect to parameter identifiability.

The obvious disadvantage of the proposed respirometer is that it involves two dissolved oxygen electrodes with the risk that the measured S_O outputs drift away from each other. With the respirometric approach that was applied in this study, it is important to calibrate and frequently compare the response of the two dissolved oxygen electrodes. It is clear that the reliability of the respirometer output mainly depends on the quality of the dissolved oxygen electrodes used in the set-up. In the “ultimate” hybrid respirometer concept proposed by Vanrolleghem and Spanjers (1998) checks of the dissolved oxygen electrode responses and re-calibrations could be carried out automatically during an experiment by changing the liquid flow rate and its direction. However, the realisation of this respirometer could not be achieved due to practical problems, as described above in the section about the development of the hybrid respirometer.

A second disadvantage of the set-up is that a model-based data interpretation may be needed for a

completely correct data interpretation. The necessity for a model-based data interpretation depends on the liquid flow rate applied in the set-up and the K_S of the biodegradation process, as was shown with simulation examples (Fig. 7 and 8). However, in case one is only interested in values of BOD_{st} a sufficiently high flow rate can be applied, and in this way a model-based analysis can be avoided.

The respirometric data benefit from the implementation of the titration method in the hybrid respirometer. It automatically leads to pH control, and consequently, the possible effect of pH changes (e.g. due to proton consumption or production during biological reactions) on r_O data can be excluded. However, the most important advantage of a combination of respirometric and titrimetric measurements is that two independent measurements are obtained simultaneously for the same process. This results in higher information content, and therefore, more accurate determination of wastewater composition and biodegradation kinetics. It was indeed illustrated in this study that the confidence intervals on the estimated parameters improve significantly when combined respirometric and titrimetric data are applied (Table 5). It has also been shown that Y_A became theoretically identifiable by combining the information available from the separate data sets without exact knowledge of the initial substrate concentration (Devisscher, 1997). Mathematical and experimental verification of the improved parameter identifiability with combined respirometric-titrimetric data sets will be investigated in more detail in chapter 4 and 5.

A linear increase of the amount of acid (in meq) added during the acetate degradation was observed as a function of the initial amount of acetate added (Fig. 10). Initially it was believed that this could be explained fully by the proton consumption during acetate uptake (Cramer and Knaff, 1991). However, the amount of acid added was lower than one meq per mmol of acetate, which is the expected amount assuming that one proton is consumed for each mmol of acetate taken up by the cells. Obviously, factors other than substrate uptake affect the proton balance in the mixed liquor. Production of protons due to CO_2 formation and uptake of NH_3 by the cells are processes that will also influence the proton balance (Iversen *et al.*, 1994). The contribution of these processes needs to be investigated in more detail. It should be clear that the ASM1 approach, taking only into account that H_p is produced (or S_{ALK} is consumed) during acetate degradation due to incorporation of S_{NH} into new biomass, cannot be used to model the titrimetric data that were obtained for acetate. The best illustration is that ASM1 would predict production of H_p during carbon source degradation, while experimental data show H_p consumption since acid needed to be added to keep the pH of the activated sludge constant during acetate degradation (Fig. 9A). The available titration data for acetate were modelled, and acetate degradation kinetics was extracted via a parameter estimation procedure (Gernaey *et al.*, 2000a, 2000b). In addition, a model-based interpretation of acetate titration profiles was combined with already existing models for interpretation of r_O data. Similar to nitrification (Devisscher, 1997; see also chapter 4), the full information of a combined respirometric-titrimetric data set allows to extract the heterotrophic biomass yield Y_H immediately from the available data (provided i_{XB} is assumed to be known), i.e. without knowing the initial substrate concentration.

Summarising, the combination of respirometric and titrimetric measurements certainly opens perspectives towards a more informative, reliable and accurate characterisation of wastewater and sludge kinetics. Future work will focus on applying the proposed methodology in the study of complex substrates and wastewaters. Yuan *et al.* (1999) presented an approach to combine information of titrimetric and respirometric experiments to determine the nitrifiable nitrogen content of wastewater. However, it can be foreseen that titrimetric data can be rather complex to interpret for a wastewater, and it may appear more difficult to generalise results obtained with titrimetry compared to respirometry. During wastewater degradation different processes, proton producing as well as proton consuming, may affect the pH, contrary to the case where only nitrification occurs. The latter allows a more straightforward interpretation (Massone *et al.*, 1995; Gernaey *et al.*, 1997a, 1998).

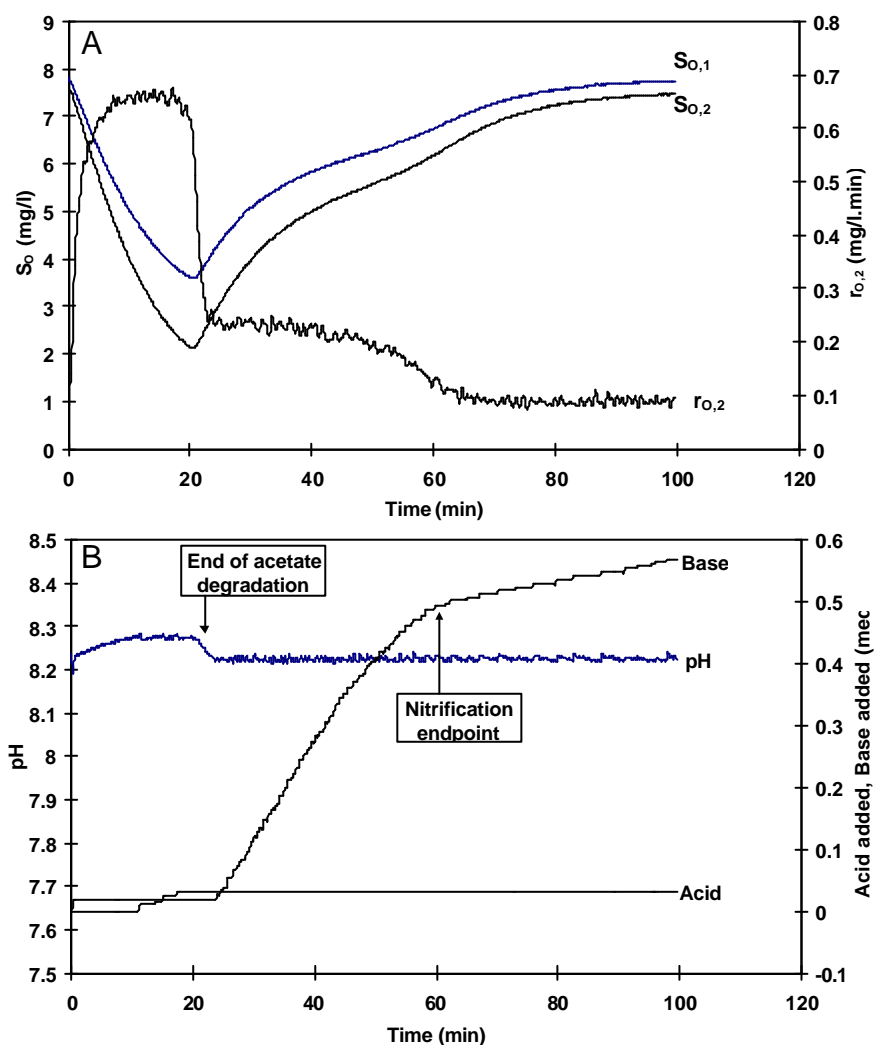


Figure 15. Example of combined respirometric-titrimetric data obtained after addition of acetate (30 mg COD/l) and ammonium (2 mg N/l) at $t = 0$. **A:** Respirometric data; **B:** Titrimetric data (Gernaey *et al.*, 1999)

Indeed, the results of this paper already illustrate that pH effects of nitrification and acetate uptake and degradation are opposite. When these two substrates are mixed the proton effects of the two processes may simply compensate for each other. An example of combined respirometric-titrimetric data collected after addition of a mixture of acetate and $\text{NH}_4\text{-N}$ to activated sludge is given in Fig. 15. It is clear from both the S_{O} and $r_{\text{O},2}$ curves (Fig. 15A) that the substrate degradation phase can be divided in two parts. First, both acetate and $\text{NH}_4\text{-N}$ are oxidised simultaneously, and secondly only degradation of $\text{NH}_4\text{-N}$ continues. From the titration data (Fig. 15B) it can indeed be seen that the pH effects of both processes (acetate degradation and nitrification) almost compensate for each other, and only a slight amount of acid has to be added. However, as soon as acetate is degraded, base is added to compensate for the protons produced during the nitrification process. Thus, the titrimetric information obtained from this experiment will be more complex to interpret, especially since the information content of the titration profile is low during the phase of simultaneous acetate degradation and nitrification. Finally, there is a bend in the base curve at the nitrification endpoint.

However, in general when one knows that acetate oxidation consumes protons, while ammonium oxidation produces them, titrimetric data can immediately serve to identify the different shoulders in r_{O} profiles without knowing the initial composition of the added substrate. Such titrimetric data thus give information on the different processes, and combined with respirometry it becomes a powerful and very information rich method for characterisation of biological wastewater treatment processes.

7. Conclusions

A respirometric technique was applied that allows high frequency sampling of respiration rates by making an oxygen mass balance over a non-aerated flow-through respiration chamber without the need for $K_L a$ estimation. The respirometer was combined with a titrimetric technique and via validation experiments it was proven that the set-up produced reliable data sets.

Simulations showed that a model-based data interpretation, which takes substrate transport in the respirometer into account, is necessary to exclude that operating conditions (e.g. flow rate) or degradation kinetics (e.g. high K_S) interfere during interpretation of the respiration rate data.

Consecutive acetate additions to activated sludge showed that titrimetric data can also yield information about carbon source degradation processes.

Applying a combined respirometric-titrimetric measurement approach resulted in improved confidence intervals when the parameter values are obtained from the combined data set compared to estimations on the separate respirometric or titrimetric data sets.

Chapter 4

-

Improved theoretical identifiability of Monod model parameters by combined respirometric – titrimetric measurements. A generalisation of results

A revised version of this chapter has been submitted for publication as:

Petersen B., Gernaey K., Devisscher M., Dochain D. and Vanrolleghem P.A. (2002) A simplified method to assess structurally identifiable parameters in Monod-based activated sludge models. Water Research (submitted).

A condensed version of this chapter was presented as:

Petersen B., Gernaey K. and Vanrolleghem P.A. (2000) Improved theoretical identifiability of model parameters by combined respirometric-titrimetric measurements. A generalisation of results. In: Proceedings IMACS 3rd Symposium on Mathematical Modelling, February 2-4, 2000, Vienna University of Technology, Austria. Vol.2, 639-642.

Chapter 4

Improved theoretical identifiability of Monod model parameters by combined respirometric – titrimetric measurements. A generalisation of results

Abstract – The first step in estimation of parameters of models applied for data interpretation should always be an investigation of the identifiability of the model parameters. In this study the theoretical identifiability of the model parameters of the two-step nitrification Monod model was studied. It was assumed that respirometric (dissolved oxygen or oxygen uptake rates) measurements from two types of respirometer and titrimetric (cumulative proton production) measurements were available. Two model structures including presence and absence of significant growth for description of long- and short-term experiments respectively were considered. The theoretical identifiability was studied via the Taylor series expansion and generating series methods. It was proven that the autotrophic yield becomes uniquely identifiable when combined respirometric and titrimetric data are considered. In one of the respirometric methods an input was considered, and it was illustrated that the generating series method resulted in simpler equations with respect to the parameters that were easier to solve for the identifiable (or combinations of) parameters. Most remarkable result of the study was however that the identifiability results could be generalised by applying a set of ASM1 matrix based generalisation rules. It appeared that the identifiable parameter combinations could be predicted directly based on knowledge of the process model under study (in ASM1-like matrix representation), the measured variables and the biodegradable substrate considered. This generalisation reduces the time-consuming task of deriving the theoretically identifiable model parameters significantly and helps the user to obtain these directly without the necessity to go too deeply into the mathematical background of theoretical identifiability.

1. Introduction

In the characterisation of wastewater degradation and many other biological degradation processes Monod-type growth kinetics, as described in the Activated Sludge Model No.1 (ASM1) (Henze *et al.*, 1987) are most often used to describe the observations. In this study the focus will be on the theoretical

identifiability of the parameters in Monod based models.

A study of the theoretical identifiability of model parameters prior to practical model application, e.g. in the frame of parameter estimation or model calibration, is very important in order to obtain reliable parameter estimates. The key question of the theoretical and practical identifiability analysis can be formulated as follows (Dochain *et al.*, 1995): "Assume that a certain number of state variables are available for measurements; on the basis of the model structure (theoretical identifiability) or on the basis of the type and quality of available data (practical identifiability), can we expect to obtain unique values for the model parameters?". It is important to notice the distinction between theoretical and practical identifiability in this statement. In the study of theoretical identifiability perfect noise-free data is assumed whereas in practice the data may be noise corrupted. As a result, parameters may be practically unidentifiable although they are theoretically identifiable (Holmberg, 1982; Jeppsson, 1996).

For linear systems the theoretical identifiability is well understood and there are several methods available for testing the identifiability (see e.g. Bellman and Åström (1970), and for an overview of different methods Godfrey and DiStefano (1985)). On the contrary, the theoretical identifiability of non-linear models is more complex to assess, and only a few methods are currently available to test the identifiability. In the case of non-linear models the approach has more been to work out different necessary and/or sufficient conditions for local and/or global theoretical identifiability that may allow for some conclusions (Walter, 1982). The following list summarises the available methods for non-linear models, including both theoretical and application oriented references that have focused on Monod kinetic models.

1. Transformation of the non-linear model into a linear model (Walter, 1982; Godfrey and DiStefano, 1985; Ljung and Glad, 1994). Applications: Dochain *et al.*, 1995; Bourrel *et al.*, 1998; Sperandio and Paul, 2000.
2. Series expansions:
 - 2.1. Taylor series expansion (Pohjanpalo, 1978; Walter, 1982; Godfrey and DiStefano, 1985; Chappell *et al.*, 1990; Walter and Pronzato, 1995). Applications: Holmberg, 1982; Dochain *et al.* 1995; Jeppsson, 1996; Bourrel *et al.*, 1998; Sperandio and Paul, 2000.
 - 2.2. Generating series (Walter, 1982; Walter and Lecourtier, 1982; Walter and Pronzato, 1995). No practical applications have been found.
3. Similarity transformation approach or local state isomorphism (Vajda *et al.*, 1989; Chappell *et al.*, 1990; Chappell and Godfrey, 1992; Walter and Pronzato, 1995). Applications: Julien, 1997; Julien *et al.*, 1998.
4. Study of the observability properties of non-linear system (Casti, 1985). Applications: Bourrel *et al.*, 1998.

In general, for both linear and non-linear models, it can be very difficult to predict which approach involves the least efforts for a particular example (Chappell *et al.*, 1990). In this study the series expansion methods were chosen since these methods are relatively simple to apply. In the Taylor approach the series is generated with respect to the time domain whereas the series is generated with respect to the input domain in the generating series approach. In fact the generating series approach can be considered as an extension of the Taylor series expansion method for the case where a class of inputs is considered (Raksanyi *et al.*, 1985). Thus, it appears that in the specific case of a model with zero inputs, the generating series approach becomes equivalent to the Taylor series expansion (Walter, 1982; Vajda *et al.*, 1989). The principles behind both series expansion methods will be briefly described below.

As stressed by Dochain *et al.* (1995) the theoretical identifiability will only depend on the model structure and on which variables are measured. In the study of heterotrophic substrate degradation via the Monod model carried out by Holmberg (1982), measurements of both substrate and biomass were assumed to be available, and it was proven that all parameters were theoretically identifiable under such conditions. However, in a similar study assuming only biomass measurements it was not possible to identify all parameters theoretically (Chappell and Godfrey, 1992). In both studies (Holmberg, 1982; Chappell and Godfrey, 1992) it was assumed that growth took place. In the work by Dochain *et al.* (1995) growth was neglected in the heterotrophic substrate degradation model, and oxygen uptake rate data was considered as measurements. It appeared that in this situation only certain parameter combinations were theoretically identifiable. If, however, growth is assumed to take place the theoretical parameter identification improves because the identifiable parameter combinations obtained assuming no growth (Dochain *et al.*, 1995) can be split up further (Sperandio and Paul, 2000). Bourrel *et al.* (1998) studied the theoretical identifiability of the Monod kinetics for the denitrification process in a biofilm model assuming steady state with respect to growth, and it was shown that depending on the measured state variables (nitrate, nitrite, carbon substrate) different parameter combinations were identifiable. In another study the identifiability of a reduced order model, to be used to control nitrification and denitrification by applying measurements of oxygen and nitrate, was investigated (Julien, 1997; Julien *et al.*, 1998). Also in this study it appeared that some parameters were identifiable uniquely whereas others were only identifiable in combination with other parameters.

The objective of this study is to analyse the theoretical identifiability of the two-step nitrification Monod kinetics using outputs from two types of respirometer (oxygen concentration data, S_o , or oxygen uptake rate data, r_o), output from a titrimetric method (cumulative proton production data, H_p) and combined respirometric and titrimetric data. The generating series and the Taylor expansion method were applied to investigate the theoretical identifiability. Two situations will be considered: first a model structure that excludes biomass growth, which simplifies the study significantly, and secondly a model structure where biomass growth is included in the model. These two model structures allow the description of short- and

long-term experiments respectively. Furthermore, the results of the identifiability study for the two-step nitrification model will be generalised based on an ASM1-like stoichiometric matrix. It will be proven with examples that the identifiable parameter combinations can be predicted by applying simple generalisation rules, based on only knowledge of the process under study, the measured variables and the substrate considered.

The chapter is organised as follows: First the definition of theoretical identifiability is presented in section two together with the principles of the two methods that are applied in this study, Taylor expansion and generating series, are described in section two. The two-step nitrification process is presented in section three together with the model and the measurement principles of the two respirometers and the titrimetric technique (mainly repetition from chapter 3). The theoretical identifiability of the models considering different outputs is studied in a section four. This section is subdivided according to the different studies carried out: (1) Respirometric data (r_O , applicable for both respirometers) or titrimetric data (Hp), considering both growth and no growth, (2) Combined r_O and Hp data and, (3) Respirometric data from both respirometers (S_O) and titrimetric data (Hp), considering both growth and no growth. The principle of the Taylor expansion method and the generating series approach are illustrated in detail for the first identifiability studies where growth is not included. For the remaining studies the principles are lined up but the equations are not written out fully due to the increasing complexity of the expressions. The power of the generating series approach over the Taylor series will be illustrated for the specific case of the second respirometer. Finally the results of the identifiability studies are generalised in section five, and the results of this generalisation are compared to literature results.

2. Theory

There is substantial literature on theoretical identifiability (e.g. Pohjanpalo, 1978; Walter, 1982; Godfrey and DiStefano, 1985), and different definitions have been given in the literature, however all being variants of the following considerations. Assuming that the general model $M(\underline{p})$ (Eq.1) is considered:

$$M(\underline{p}) : \begin{cases} \frac{d}{dt} \underline{x}(t) = \underline{f}(\underline{x}(t), \underline{u}(t), t, \underline{p}), & \underline{x}(0) = \underline{x}_0(\underline{p}) \\ \underline{y}(t, \underline{p}) = \underline{g}(\underline{x}(t), \underline{p}) \end{cases} \quad (1)$$

where \underline{x} , \underline{u} , \underline{y} and \underline{p} represent the state vector, the input vector, the output (measured variables) vector and the (unknown) parameter vector respectively. Two models, $M(\underline{p})$ and $M(\hat{\underline{p}})$, are considered which have the same structure, e.g. the same parameterisation, same input \underline{u} , which belongs to an admissible input class U , and identical outputs $\underline{y} \equiv \hat{\underline{y}}$ for any input \underline{u} . If it is furthermore considered that the vector \underline{p} to be identified belongs to some admissible parametric space P , the definitions for identifiability can be

formulated as follows (Walter, 1982):

Definition 1

The parameter p_i is *theoretically locally identifiable* for the input class U , if and only if for almost any value $\underline{p} \in P$ there exists a neighbourhood $V(\underline{p})$ such that:

$$\left. \begin{array}{l} \hat{\underline{p}} \in V(\underline{p}) \subset P \\ \hat{\underline{y}}(\hat{\underline{p}}, t) \equiv \underline{y}(\underline{p}, t), \quad \forall t > 0, \forall \underline{u} \in U \end{array} \right\} \Rightarrow \hat{p}_i = p_i \quad (2)$$

This means that, if there exists another parameter vector $\hat{\underline{p}}$ which belongs to a local sub-domain, i.e. a neighbourhood $V(\underline{p})$ of the admissible parametric space P , and if the outputs \underline{y} with both parameter vectors \underline{p} and $\hat{\underline{p}}$ are equal for all time t and all inputs \underline{u} , then (each component of) both parameter vectors are equal and thereby uniquely identifiable. On the contrary, if the parameter vectors are not equal for all inputs, then the system is not identifiable. E.g. if there exists at least one $\hat{\underline{p}} \neq \underline{p}$ such that the output of $M(\underline{p})$ can not be distinguished from the output of $M(\hat{\underline{p}})$, this would question any further use of \underline{p} .

Definition 2

The parameter p_i is *theoretically globally identifiable* for the input class U , if and only if for almost any value $\underline{p} \in P$ one has:

$$\left. \begin{array}{l} \hat{\underline{p}} \in P \\ \hat{\underline{y}}(\hat{\underline{p}}, t) \equiv \underline{y}(\underline{p}, t), \quad \forall t > 0, \forall \underline{u} \in U \end{array} \right\} \Rightarrow \hat{p}_i = p_i \quad (3)$$

Definition 2 is very similar to the one above, except that the domain is now expanded to the whole parametric space P to access the *global* identifiability.

Definition 3

The model $M(\underline{p})$ is theoretically globally and/or locally identifiable if and only if all the parameters p_i are globally and/or locally identifiable.

2.1. Taylor series expansion

The Taylor series expansion approach to study the theoretical identifiability was originally developed by

Pohjanpalo (1978). The general model as defined in Eq.1 is considered. The basis of the Taylor approach is that the output vector and its derivatives with respect to time, typically developed around initial time $t = 0$, can be assumed to be known and unique. The successive Taylor derivatives, $\underline{a}_k(\underline{p})$, are defined as described in Eq. 4, and the Taylor series approximation of the output \underline{y} around time t is given in Eq. 5.

$$\underline{a}_k(\underline{p}) = \lim_{t \rightarrow 0} \frac{d^k}{dt^k}(\underline{y}(t, \underline{p})) \quad k = 0, 1, \dots, \infty \quad (4)$$

$$\underline{y}(t, \underline{p}) = \underline{y}(t) + t \cdot \frac{d\underline{y}}{dt}(t) + \frac{t^2}{2!} \cdot \frac{d^2\underline{y}}{dt^2}(t) + \dots + \frac{t^k}{k!} \cdot \frac{d^k\underline{y}}{dt^k}(t) \quad k = 0, 1, \dots, \infty \quad (5)$$

Thus, the Taylor derivatives, $\underline{a}_k(\underline{p})$, are functions of \underline{p} and the method simply consists of solving a set of algebraic equations (consisting of the Taylor derivatives) with respect to the parameters or combinations thereof. A sufficient condition for the model to be theoretically identifiable is that there exists a unique solution for \underline{p} (Pohjanpalo, 1978; Walter, 1982).

2.2. Generating series

The generating series approach generalises in some sense the Laplace transform approach for identifiability of linear models (Walter, 1982; Walter and Lecourtier, 1982; Walter and Pronzato, 1995). In the generating series approach it is considered that the model equations are written as Eq. 6.

$$\begin{cases} \frac{d}{dt} \underline{x}(t) = \underline{f}^0(\underline{x}(t), \underline{p}) + \sum_{i=1}^m u_i(t) \underline{f}^i(\underline{x}(t), \underline{p}), & \underline{x}(0) = \underline{x}_0(\underline{p}) \\ \underline{y}(t, \underline{p}) = \underline{g}(\underline{x}(t), \underline{p}) \end{cases} \quad (6)$$

In this equation \underline{x} , \underline{y} and \underline{p} represent the state vector with n states, the output (measured variables) vector and the (unknown) parameter vector respectively, while u_i represents the input with $i = 0, 1, \dots, m$. Note that the model is defined to be linear with respect to the inputs. The generating series is based on the output function $\underline{g}(\underline{x}(t), \underline{p})$ and its successive Lie derivatives, typically evaluated at $t = 0$ (Eq. 7).

$$L_{f_i} \underline{g}(\underline{x}, \underline{p}) \Big|_{t=0} = \sum_{k=1}^n f^{i,k}(\underline{x}, \underline{p}) \frac{\partial}{\partial x_k} \underline{g}(\underline{x}, \underline{p}) \Big|_{t=0} = s_i(\underline{p}) \quad (7)$$

In Eq. 7 $f^{i,k}$ is the k 'th component of \underline{f}^i , e.g. in $f^{1,2}$: (1) refers to the function of the first input and (2) to the second state. If $\underline{s}(\underline{p})$ denotes the vector of all the coefficients of the series of successive derivatives, a sufficient condition for the model to be theoretically identifiable is that there exists a unique solution for \underline{p} from $\underline{s}(\underline{p})$, similar to the Taylor series expansion method (Walter, 1982; Walter and Lecourtier, 1982;

Walter and Pronzato, 1995).

2.3. Practical application of the series expansions methods

The practical procedure for application of the two methods can be described by the following steps:

1. Computation of the successive derivatives of the output function.
2. Choice of the parameter set \underline{p} to be identified.
3. Evaluation of the successive derivatives by inserting already known quantities and derivatives of lower orders.
4. Express the successive derivatives as function of the parameter combinations that were chosen in step 2.
5. Solve the set of equations resulting from step 4 with respect to \underline{p} .
6. If a unique solution can be found from step 5 the parameter set selected in step 2 is theoretically identifiable.

Typically, the Taylor or generating series are developed around $t = 0$. However, systems that are singular (i.e. not solvable) around zero can not be termed unidentifiable by the argument that a unique solution for \underline{p} is lacking around $t = 0$, since later observations at $t > 0$ may provide additional information on \underline{p} (Pohjanpalo, 1978; Walter, 1982). In addition, it should be stressed that it is the user that defines the parameters or parameter combinations \underline{p} that are to be identified in step 2. Thus, the procedure becomes iterative, since so far there are no general rules for selecting the “right” combinations (Dochain *et al.*, 1995).

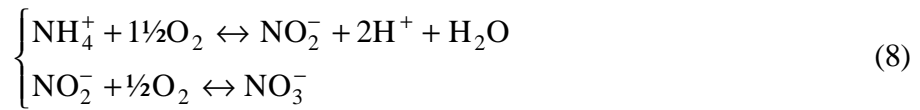
Another disadvantage is that the upper bound on the number of equations that may be required is unknown. One usually starts with a limited number of coefficients and adds more if necessary. There is, however, no guarantee that new information could not have been obtained by including derivatives from an even higher order (Godfrey and DiStefano, 1985; Vajda *et al.*, 1989; Chappell *et al.*, 1990). This lack of an upper bound means that this condition is only sufficient, but not necessary, for identifiability (Walter and Lecourtier, 1982; Vajda *et al.*, 1989). Moreover, the structure of the resulting equations is most often far from simple, even for models of moderate complexity. Although symbolic manipulation software packages have proven very useful, this problem can not always be resolved making it difficult to establish the identifiability properties (Raksanyi *et al.*, 1985).

For a model with zero input the generating series approach is equivalent to the Taylor series expansion method, as mentioned above. However, for models that include inputs, the generating series approach usually results in simpler equation structures than those of the Taylor series approach (Raksanyi *et al.*,

1985; Walter and Prozato, 1995), although this was questioned by Godfrey and DiStefano (1985). In general, it can be difficult beforehand to judge which approach is the most suitable one for a particular model (Chappell *et al.*, 1990).

3. Case study: Two-step nitrification

Nitrification takes place in two steps (1) oxidation of ammonium (NH_4^+) to nitrite (NO_2^-) and (2) oxidation of nitrite (NO_2^-) to nitrate (NO_3^-). This process is illustrated in a simple form in Eq. 8 without considering that a small part of NH_4^+ is incorporated into the biomass during growth.



Note that both nitrification steps can be characterised by measurements of oxygen uptake whereas it is only during the first step that protons are produced. This makes it possible to characterise the first step by its proton production. Measurements of oxygen uptake rate (r_o) can be carried out via respirometry, and proton production (Hp) can be quantified via a titrimetric technique (Gernaey *et al.*, 1998). In this study two slightly different respirometers were considered. Detailed information on the difference between the two respirometric principles can be found in chapter 3.

The first respirometer consists of a continuously aerated batch reactor and is illustrated in Fig. 1 together with a typical data set. For this type of respirometer the mass balance for dissolved oxygen (S_o) consists of two parts: a term for the oxygen transfer due to aeration and a term for the oxygen uptake rate, r_o (Eq. 9).

$$\frac{dS_o}{dt} = K_L a (S_o^o - S_o) - r_o \quad (9)$$

The r_o in Eq. 9 consists of two processes: (1) the immediate uptake of oxygen due to the consumption of a readily biodegradable substrate, i.e. the exogenous oxygen uptake rate $r_{o,ex}$, and (2) the endogenous oxygen uptake rate $r_{o,end}$. The endogenous oxygen uptake is also observed in absence of a readily biodegradable substrate. It is assumed that this rate is associated with e.g. oxidation of biodegradable matter produced internally during lysis of dead biomass etc. When no readily biodegradable substrate is present $r_{o,ex}$ is zero, and in that case the oxygen concentration in the respirometer reaches a steady-state concentration ($S_{o,eq}$) representing the equilibrium between oxygen transfer and endogenous respiration. With this knowledge Eq. 9 can be transformed into Eq. 10 (Vanrolleghem, 1994), under the assumption that $K_L a$, S_o^o and $r_{o,end}$ are constant during the observed time period.

$$\frac{dS_o}{dt} = K_L a (S_{o,eq} - S_o) - r_{o,ex} \quad (10)$$

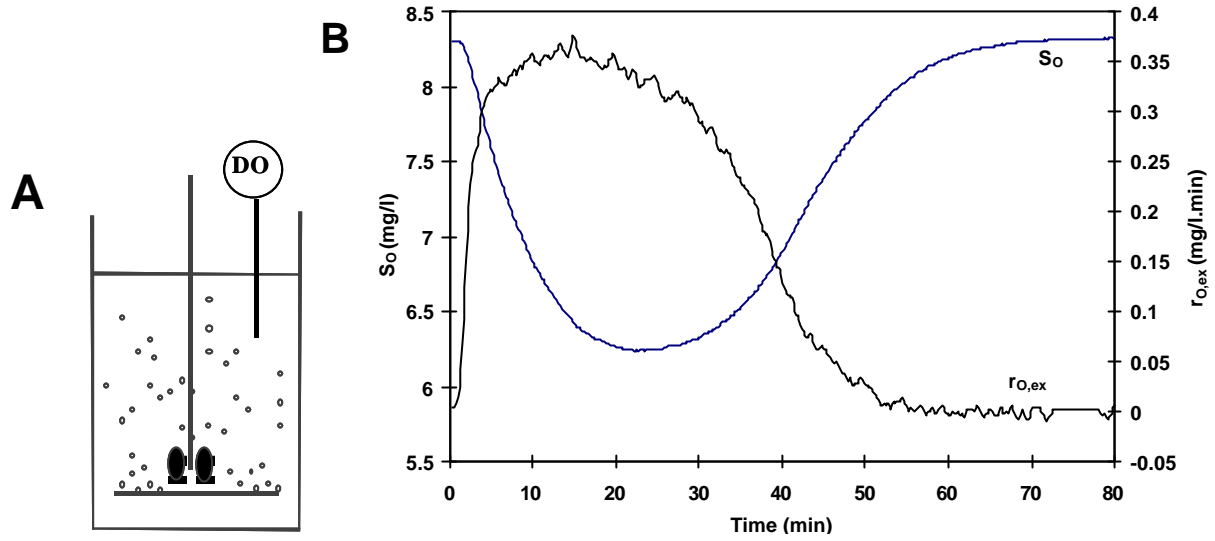


Figure 1. A: Schematic representation of respirometer 1. **B:** Typical S_{O} and $r_{O,ex}$ data set obtained following the addition of S_{NH} to the activated sludge in respirometer 1 at $t = 0$

In this respirometer the value of $r_{O,ex}$ can be calculated from the measured S_{O} data when the values of dS_{O}/dt , $S_{O,eq}$ and $K_{L}a$ are known. The factor dS_{O}/dt is the slope of the S_{O} curve, and is typically obtained by a moving window regression on the S_{O} data. $S_{O,eq}$ can be obtained from the respirogram as the S_{O} concentration measured during the endogenous respiration phase. For the oxygen transfer coefficient $K_{L}a$ several methods can be used to obtain its value. However, the estimation of a reliable $K_{L}a$ value is not without problems (ASCE, 1996) which is the disadvantage of applying this type of respirometer.

The second respirometer, called the hybrid respirometer, is more advanced. An illustration of its configuration and a typical data set ($S_{O,1}$, $S_{O,2}$ data and calculated $r_{O,2}$ values) are given in Fig. 2A and 2B (see also chapter 3 for a more detailed explanation). The respirometer consists of an open continuously aerated vessel and, connected to it, a closed non-aerated respiration chamber. It is equipped with two dissolved oxygen probes. Mixed liquor is continuously pumped between the aeration vessel and the respiration chamber, and vice versa. The S_{O} mass balances are given in Eq. 11 and 12, where 1 refers to the aeration vessel and 2 to the respiration chamber.

$$\frac{dS_{O,1}}{dt} = \frac{Q_{in}}{V_1} (S_{O,2} - S_{O,1}) + K_L a (S_O^o - S_{O,1}) - r_{O,1} \quad (11)$$

$$\frac{dS_{O,2}}{dt} = \frac{Q_{in}}{V_2} (S_{O,1} - S_{O,2}) - r_{O,2} \quad (12)$$

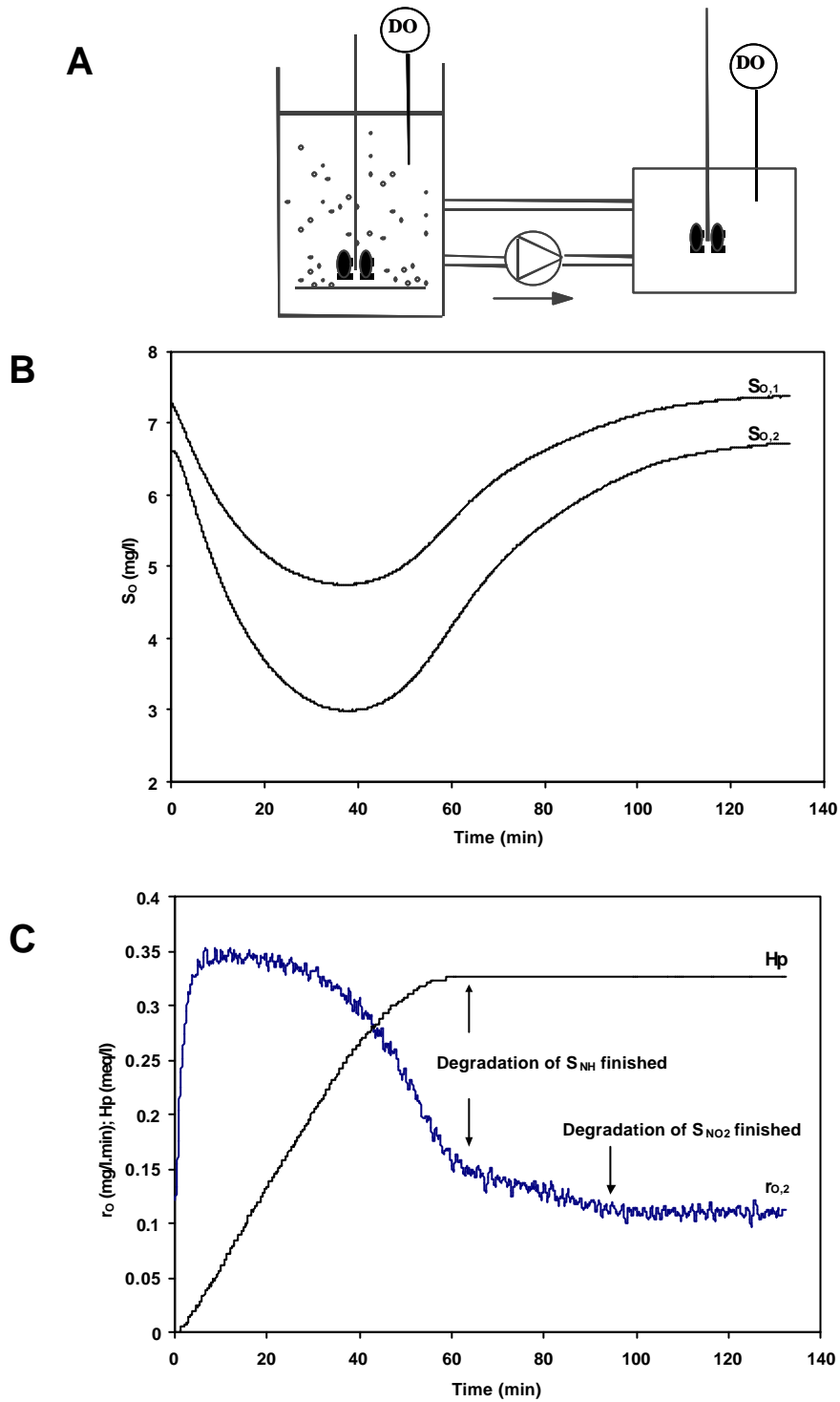


Figure 2. **A:** Schematic representation of respirometer 2. **B:** Typical S_O data set obtained following the addition of S_{NH} to the activated sludge in the aeration vessel of respirometer 2 at $t = 0$. **C:** H_p and $r_{O,2}$ data resulting from the same experiment

The main advantage of this respirometer is that r_O can be calculated from a simple S_O mass balance over the closed respiration vessel (Eq. 12), thereby avoiding the need to estimate $K_L a$ values. In the hybrid

respirometer substrate is added as a pulse in the aeration vessel at the start of an experiment ($t = 0$), and not to the respiration chamber. Thus, the substrate concentration in the respiration chamber builds up from zero through the substrate flow from the aerated vessel. The r_O in the two vessels ($r_{O,1}$ and $r_{O,2}$ respectively) is obviously only equal when the substrate concentrations in both vessels are identical. The substrate transport is illustrated in Fig. 3, where simulated profiles of ammonium (S_{NH}) are given for the experimental data of Fig. 2. In fact, at time zero, $r_{O,2}$ is equal to $r_{O,end}$ (see chapter 3).

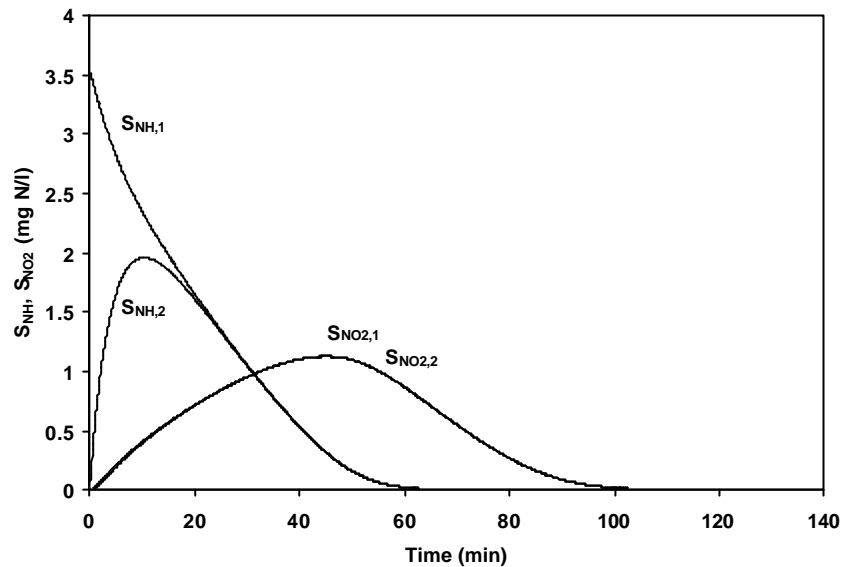


Figure 3. Simulated S_{NH} and S_{NO_2} profiles in aeration vessel ($S_{NH,1}$, $S_{NO_2,1}$) and respiration chamber ($S_{NH,2}$, $S_{NO_2,2}$) for the experimental data of Fig. 2 (no S_{NO_2} added at $t = 0$)

An illustration of a typical Hp data set is given in Fig. 2C. Hp data are collected in parallel with respirometric data during an experiment with an addition of ammonium at $t = 0$. As mentioned above, only the first nitrification step has an effect on the pH. This is clearly illustrated in Fig. 2C, where the cumulative proton production stops when the degradation of S_{NH} is finished. The respirometric and titrimetric data were modelled by applying the model structure that is summarised in Table 1. The model in Table 1 is based on ASM1 (Henze *et al.*, 1987), with some modifications:

- Nitrification was modelled as a two-step process. In the first nitrification step S_{NH} is oxidised to nitrite (S_{NO_2}), which is subsequently oxidised to nitrate (S_{NO_3}) in the second nitrification step, as described above.
- For the second nitrification step nitrogen taken from S_{NO_2} is incorporated into new biomass.
- Biomass decay was included in the model as endogenous respiration.

Table 1. Model used for interpretation of the respirometric and titrimetric data. Processes 1, 2, 3, 4 and 5 were necessary to model respirometric data. For titrimetric data, processes 2 and 6 were used to model nitrification experiments

Component (measurement, i) (substrate, k)→ Process(j)↓	1.	2.	3.	4.	5.	6.	7.	Process rate
	X	S _S	S _O	S _{NH}	S _{NO2}	S _{NO3}	H _p	
1. Heterotrophic growth on S _S	1	$-\frac{1}{Y_H}$	$-\frac{1-Y_H}{Y_H}$	$-i_{XB}$			$\frac{i_{XB}}{14}$	$\mu_{maxH} \cdot \frac{S_S}{K_S + S_S} \cdot X$
2. Nitrification step 1, S _{NH} oxidation	1		$-\frac{3.43 - Y_{A1}}{Y_{A1}}$	$-\frac{1}{Y_{A1}} - i_{XB}$	$\frac{1}{Y_{A1}}$		$\frac{i_{XB}}{14} + \frac{1}{7 \cdot Y_{A1}}$	$\mu_{maxA1} \cdot \frac{S_{NH}}{K_{SA1} + S_{NH}} \cdot X$
3. Nitrification step 2, S _{NO2} oxidation	1		$-\frac{1.14 - Y_{A2}}{Y_{A2}}$		$-\frac{1}{Y_{A2}} - i_{XB}$	$\frac{1}{Y_{A2}}$		$\mu_{maxA2} \cdot \frac{S_{NO2}}{K_{SA2} + S_{NO2}} \cdot X$
4. Endogenous respiration	-1		-1	i_{XB}			$-\frac{i_{XB}}{14}$	$b \cdot X$
5. Aeration			1					$K_L a \cdot (S_O^0 - S_O)$
6. CO ₂ stripping							1	Γ_{HpB}

- In this study, a detailed model for the titrimetric data is only applied for the nitrification process (see Table 1). In the model protons (Hp) replace the ASM1 S_{ALK} component, which means that the signs of the stoichiometric factors in the Hp column are the opposite of the signs that appear in the S_{ALK} column in the ASM1 matrix (Henze *et al.*, 1987). In the model S_{NH} oxidation and uptake of S_{NH} for biomass growth during nitrification will produce Hp. A constant background Hp production is also included in the titrimetric model to take CO_2 stripping into account, similar to Gernaey *et al.* (1998). This effect of CO_2 stripping is assumed to be constant during the short duration of each experiment (Gernaey *et al.*, 1998).
- For heterotrophic growth, the standard ASM1 conversion term for S_{ALK} is included in the Hp column of Table 1 (uptake of S_{NH} to be incorporated in new biomass produces Hp).

4. Results

All symbolic manipulations were carried out with the MAPLE V software package (Waterloo Maple Software).

4.1. Measurements of $r_{O,ex}$ or Hp – No net growth model

In the model used in the first study growth and decay are not included, i.e. column 1 and row 4 in Table 1 are excluded which means that X is considered as a constant. Moreover, incorporation of S_{NH} for biomass growth is not considered ($i_{XB} = 0$). It will appear that these assumptions simplify the study significantly. However, it should be noted that the mass balances of organic substrate and ammonium strictly speaking are not correct since it is only assumed that the substrate degradation induces oxygen consumption and proton production or consumption. The assumptions are, however, reasonable, and no significant errors will be induced in the case of short-term experiments where significant growth can be assumed not to take place.

4.1.1. Respirometric data ($r_{O,ex}$)

In the work of Dochain *et al.* (1995) the theoretical identifiability of the model for heterotrophic growth on a readily biodegradable carbon substrate, S_S , (process 1 in Table 1) was studied. The expression for $r_{O,ex}$ according to Table 1 is given in Eq. 13.

$$r_{O,ex}(t) = (1 - Y_H) \cdot \frac{m_{maxH} \cdot X}{Y_H} \cdot \frac{S_S(t)}{K_S + S_S(t)} \quad (13)$$

Only S_S was considered to vary as function of time in the application of the Taylor series expansion since biomass growth was not considered in the model. It was concluded that the following three parameter combinations were identifiable (Eq. 14 – 16) (Dochain *et al.*, 1995).

$$q_1 = \frac{1 - Y_H}{Y_H} \cdot m_{\max H} \cdot X \quad (14)$$

$$q_2 = (1 - Y_H) \cdot K_S \quad (15)$$

$$q_3 = (1 - Y_H) \cdot S_S(0) \quad (16)$$

For the two-step nitrification considering no net biomass growth (process 2 - 3 in Table 1, but with $i_{XB} = 0$) the expression for $r_{O,ex}$ is given in Eq. 17.

$$r_{O,ex} = (3.43 - Y_{A1}) \cdot \frac{m_{\max A1} \cdot X}{Y_{A1}} \cdot \frac{S_{NH}(t)}{K_{SA1} + S_{NH}(t)} + (1.14 - Y_{A2}) \cdot \frac{m_{\max A2} \cdot X}{Y_{A2}} \cdot \frac{S_{NO2}(t)}{K_{SA2} + S_{NO2}(t)} \quad (17)$$

It became however too complex for Maple V to simultaneously solve for identifiable parameter combinations for the two nitrification steps. The theoretical identifiability was therefore considered in a two stage approach, i.e. the first and second nitrification step were dealt with separately, similar to the study of a double Monod model with two readily biodegradable carbon substrates by Dochain *et al.* (1995). However, there are two major differences between the two-step nitrification process and the double Monod example of Dochain *et al.* (1995): (1) At $t = 0$ the concentration of the substrate for the second nitrification step, S_{NO2} , is zero. Hence, only information on the kinetics of the first nitrification step is available at $t = 0$. (2) The two nitrification steps are closely linked in the way that S_{NO2} is produced from the first step, i.e. as long as S_{NH} is still present there will be a time varying input of S_{NO2} .

The study of the theoretical identifiability was therefore approached as follows. First, $t = 0$ is considered and the identifiability of the first step can be analysed. Secondly, it is assumed that S_{NH} is completely eliminated from the mixed liquor at a certain time instant $t > 0$, i.e. $S_{NH} = 0$ and S_{NO2} is no longer produced. However degradation of accumulated S_{NO2} still takes place and, consequently the identifiability of the second nitrification step can be studied. Thus, this is an example where later observations ($t > 0$) can give further information on the set of possible identifiable parameters, as discussed earlier (Pohjanpalo, 1978; Walter, 1982). As a side note, to be practically identifiable, a necessary condition for this approach will obviously be that the second nitrification step is slower than the first step resulting in a build-up of S_{NO2} that is “observable” as a shoulder in the $r_{O,ex}$ profile. This situation is illustrated in Fig. 2 and 3. From the simulated S_{NO2} concentrations in Fig. 3 one can clearly see the build-up of S_{NO2} . Degradation of S_{NH} is finished at $t = 60$ min while S_{NO2} degradation continues. In case the second nitrification step is faster than the first step, then the amount of S_{NO2} available upon the complete degradation of S_{NH} will be too low to result in a visible $r_{O,ex}$ response, leading to impossible practical identification of the second step parameters.

Finally, one may have the situation where sufficient S_{NO2} is added initially together with S_{NH} to cause a second shoulder in the $r_{O,ex}$ profile. In this case the $r_{O,ex}$ profile can be subdivided in two parts corresponding to the degradation of S_{NH} and S_{NO2} (see Fig. 4). In this situation the theoretical identifiability

study could be approached as follows. First, the identifiability of the second step is carried out assuming that S_{NH} is completely degraded at a point $t_1 > 0$ (e.g. at $t = 65$ min in Fig. 4). The $r_{O,ex}$ of the second step, which can be assumed constant in the first period where both nitrification steps occur in parallel, can then be subtracted from the total $r_{O,ex}$, allowing the identifiability of the first step to be studied.

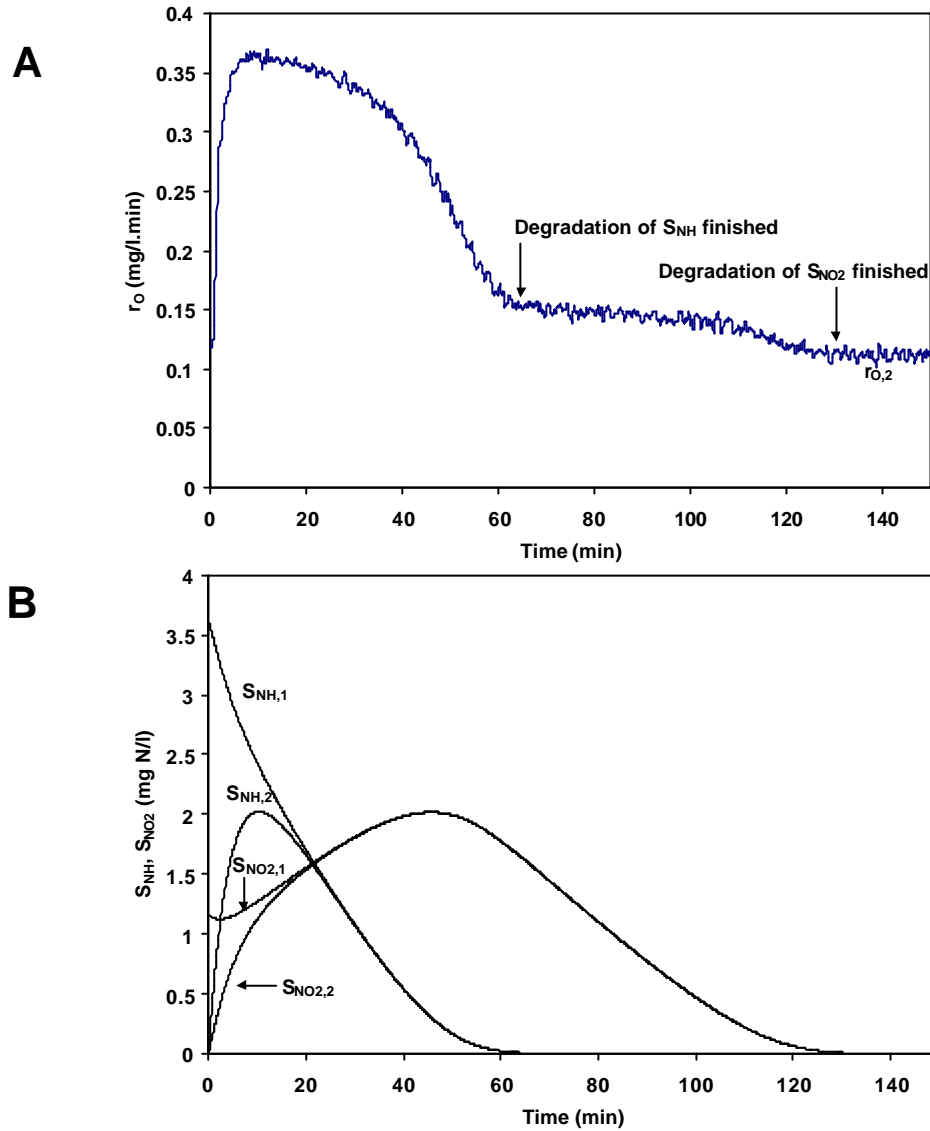


Figure 4. A: $r_{O,2}$ data resulting from an experiment with addition of a mixture of S_{NH} and S_{NO_2} at $t = 0$ in the aeration vessel of respirometer 2. **B:** Simulated S_{NH} and S_{NO_2} profiles in aeration vessel ($S_{NH,1}$, $S_{NO_2,1}$) and respiration chamber ($S_{NH,2}$, $S_{NO_2,2}$)

In the following the first situation ($S_{NO_2}(0) = 0$) is considered. Thus, first $t = 0$ is considered and the identifiability analysis is based on the first part of Eq. 17. In the following the exogenous oxygen uptake rate concerning only the first nitrification step is denoted $r_{O,ex}^{NI}$. The Taylor series expansion was applied, and Eq. 18 - 20 list the first three successive derivatives of $r_{O,ex}^{NI}$ with respect to time at $t = 0$.

$$r_{O,ex}^{NI}(0) = \frac{m_{maxA1} \cdot X \cdot (3.43 - Y_{A1})}{Y_{A1}} \cdot \frac{S_{NH}(0)}{K_{SA1} + S_{NH}(0)} \quad (18)$$

$$\frac{dr_{O,ex}^{NI}(0)}{dt} = - \frac{m_{maxA1}^2 \cdot X^2 \cdot (3.43 - Y_{A1})}{Y_{A1}^2} \cdot \frac{K_{SA1} \cdot S_{NH}(0)}{(K_{SA1} + S_{NH}(0))^3} \quad (19)$$

$$\frac{d^2 r_{O,ex}^{NI}(0)}{dt^2} = \frac{m_{maxA1}^3 \cdot X^3 \cdot (3.43 - Y_{A1})}{Y_{A1}^3} \cdot \frac{K_{SA1} \cdot S_{NH}(0) \cdot (K_{SA1} - 2 \cdot S_{NH}(0))}{(K_{SA1} + S_{NH}(0))^5} \quad (20)$$

The parameter combinations that were considered as potentially identifiable in the study are given in Eq. 21 – 23.

$$\mathbf{b}_1 = \frac{3.43 - Y_{A1}}{Y_{A1}} \cdot m_{maxA1} \cdot X \quad (21)$$

$$\mathbf{b}_2 = (3.43 - Y_{A1}) \cdot K_{SA1} \quad (22)$$

$$\mathbf{b}_3 = (3.43 - Y_{A1}) \cdot S_{NH}(0) \quad (23)$$

It is now sought to express the derivatives (Eq. 18 - 20) as a function of the parameter combinations (Eq. 21 – 23) as generally expressed in Eq. 24, where i is equal to the order of the derivative. The expressions for the actual case are given in Eq. 25 - 27:

$$v_i = \frac{d^i r_{O,ex}}{dt^i}(0) \quad (24)$$

$$v_0 = \frac{\mathbf{b}_1 \cdot \mathbf{b}_3}{\mathbf{b}_2 + \mathbf{b}_3} \quad (25)$$

$$v_1 = - \frac{\mathbf{b}_1^2 \cdot \mathbf{b}_2 \cdot \mathbf{b}_3}{(\mathbf{b}_2 + \mathbf{b}_3)^3} \quad (26)$$

$$v_2 = - \frac{\mathbf{b}_1^3 \cdot \mathbf{b}_2 \cdot \mathbf{b}_3 \cdot (2\mathbf{b}_3 - \mathbf{b}_2)}{(\mathbf{b}_2 + \mathbf{b}_3)^5} \quad (27)$$

The equations 25 - 27 are finally solved for the parameter combinations, resulting in Eq. 28 – 30.

$$\mathbf{b}_1 = \frac{v_0 \cdot (v_0 \cdot v_2 - 3v_1^2)}{v_0 \cdot v_2 - v_1^2} \quad (28)$$

$$\mathbf{b}_2 = \frac{-4v_0^2 \cdot v_1^3}{(v_0 \cdot v_2 - 3v_1^2)(v_0 \cdot v_2 - v_1^2)} \quad (29)$$

$$\mathbf{b}_3 = \frac{-2v_0^2 \cdot v_1}{v_0 \cdot v_2 - 3v_1^2} \quad (30)$$

Conclusively, this study shows that the parameter combinations for the first nitrification step given by Eq. 21 - 23 are indeed theoretically identifiable, considering $r_{D,ex}$ measurements and no net biomass growth. The results are similar to the parameter combinations obtained by Dochain *et al.* (1995), only replacing the factor $(1-Y_H)$ in Eq. 14 – 16 by $(3.43-Y_{A1})$ in Eq. 21 – 23.

The theoretical identifiability of the second nitrification step assuming $t > 0$ follows very much the same patterns as illustrated above, and results in the identifiable parameter combinations listed in Eq. 31 – 33. In this case Eq. 33 is not really relevant, since $S_{NO_2}(0) = 0$. However, in the case where $S_{NO_2}(0) \neq 0$ the identifiability study yields identical results, and it may be relevant to identify a combination including $S_{NO_2}(0)$.

$$\mathbf{b}_4 = \frac{1.14 - Y_{A2}}{Y_{A2}} \cdot m_{maxA2} \cdot X \quad (31)$$

$$\mathbf{b}_5 = (1.14 - Y_{A2}) \cdot K_{SA2} \quad (32)$$

$$\mathbf{b}_6 = (1.14 - Y_{A2}) \cdot S_{NO_2}(0) \quad (33)$$

4.1.2. Titrimetric data – Hp

The model that describes the proton production rate for the first nitrification step is given in column 7 in Table 1 (no net growth and therefore $\dot{x}_B=0$ is still considered). The structure of this model is in fact rather similar to the model for respirometric data described above, only is the output now the concentration of Hp (meq/l) instead of $r_{D,ex}$. It is thus expected that the structure of the identifiable parameter combinations becomes similar to the ones derived in the previous example. The generating series principle will be illustrated for this study.

The equation set for the generating series approach, according to the general formula of Eq. 6, is given in Eq. 34 considering the states S_{NH} and Hp respectively. Note that there are no inputs considered in this case.

$$\underline{f}^0 = \begin{pmatrix} f^{01} \\ f^{02} \end{pmatrix} = \begin{pmatrix} -\frac{\mathbf{m}_{\max A1} \cdot X}{Y_{A1}} \cdot \frac{S_{NH}(t)}{K_{SA1} + S_{NH}(t)} \\ \frac{2}{14} \frac{\mathbf{m}_{\max A1} \cdot X}{Y_{A1}} \cdot \frac{S_{NH}(t)}{K_{SA1} + S_{NH}(t)} \end{pmatrix}, \quad f^1 = \begin{pmatrix} 0 \\ 0 \end{pmatrix}, \quad g = Hp \quad (34)$$

The initial value for the output Hp is zero and the initial value of S_{NH} (at $t = 0$) is $S_{NH}(0)$.

The first Lie derivative operator can now be written as generally stated in Eq. 35. In this equation x_1 refers to S_{NH} and x_2 to Hp (see also Eq. 36). The first Lie derivative operator is written out completely in Eq. 36 for this example.

$$L_{f_0} = f^{01} \cdot \frac{\partial}{\partial x_1} + f^{02} \cdot \frac{\partial}{\partial x_2} \quad (35)$$

$$L_{f_0} = \left[-\frac{\mathbf{m}_{\max A1} \cdot X}{Y_{A1}} \cdot \frac{S_{NH}(0)}{K_{SA1} + S_{NH}(0)} \right] \cdot \frac{\partial}{\partial S_{NH}} + \left[\frac{2}{14} \cdot \frac{\mathbf{m}_{\max A1} \cdot X}{Y_{A1}} \cdot \frac{S_{NH}(0)}{K_{SA1} + S_{NH}(0)} \right] \cdot \frac{\partial}{\partial Hp} \quad (36)$$

The Lie derivative of the output g in its general form is given in Eq. 37 and the corresponding expression for this example in Eq. 38 - 39.

$$L_{f_0} g(0) = f^{01} \cdot \frac{\partial}{\partial x_1} (g(0)) + f^{02} \cdot \frac{\partial}{\partial x_2} (g(0)) \quad (37)$$

$$L_{f_0} g(0) = \left[-\frac{\mathbf{m}_{\max A1} \cdot X}{Y_{A1}} \cdot \frac{S_{NH}(0)}{K_{SA1} + S_{NH}(0)} \right] \cdot \frac{\partial Hp}{\partial S_{NH}} + \left[\frac{2}{14} \frac{\mathbf{m}_{\max A1} \cdot X}{Y_{A1}} \cdot \frac{S_{NH}(0)}{K_{SA1} + S_{NH}(0)} \right] \cdot \frac{\partial Hp}{\partial Hp} \quad (38)$$

$$\Leftrightarrow L_{f_0} g(0) = \frac{2}{14} \frac{\mathbf{m}_{\max A1} \cdot X}{Y_{A1}} \cdot \frac{S_{NH}(0)}{K_{SA1} + S_{NH}(0)} \quad (39)$$

The successive Lie derivatives of the output g follow the general formula (Eq. 40) and for this specific example the expressions for the second and third derivative are given in Eq. 41 and 42.

$$L_{f_0} L_{f_0} g(0) = f^{01} \cdot \frac{\partial}{\partial x_1} (L_{f_0} g(0)) + f^{02} \cdot \frac{\partial}{\partial x_2} (L_{f_0} g(0)) \quad (40)$$

$$L_{f_0} L_{f_0} g(0) = -\frac{2}{14} \frac{S_{NH}(0) \cdot K_{SA1}}{(K_{SA1} + S_{NH}(0))^3} \left(\frac{\mathbf{m}_{\max A1} \cdot X}{Y_{A1}} \right)^2 \quad (41)$$

$$L_{f_0} L_{f_0} L_{f_0} g(0) = -\frac{2}{14} \frac{S_{NH}(0) \cdot K_{SA1} \cdot (2 \cdot S_{NH}(0) - K_{SA1})}{(K_{SA1} + S_{NH}(0))^5} \cdot \left(\frac{\mathbf{m}_{\max A1} \cdot X}{Y_{A1}} \right)^3 \quad (42)$$

The parameter combinations that were evaluated for theoretical identifiability are listed in Eq. 43 - 45.

$$\mathbf{d}_1 = \frac{2}{14} \frac{\mathbf{m}_{\max A1} \cdot X}{Y_{A1}} \quad (43)$$

$$\mathbf{d}_2 = \frac{2}{14} S_{\text{NH}}(0) \quad (44)$$

$$\mathbf{d}_3 = \frac{2}{14} K_{\text{SA1}} \quad (45)$$

Similar to the Taylor series expansion the derivatives (Eq. 39, 41 and 42) are now expressed as function of the parameter combinations (Eq. 43 – 45), resulting in Eq. 46 – 48. Equations 46 – 48 are again solved for the parameter combinations, and solutions are given in Eq. 49 – 51.

$$u_0 = \frac{\mathbf{d}_1 \cdot \mathbf{d}_3}{\mathbf{d}_2 + \mathbf{d}_3} \quad (46)$$

$$u_1 = -\frac{\mathbf{d}_1^2 \cdot \mathbf{d}_2 \cdot \mathbf{d}_3}{(\mathbf{d}_2 + \mathbf{d}_3)^3} \quad (47)$$

$$u_2 = -\frac{\mathbf{d}_1^3 \cdot \mathbf{d}_2 \cdot \mathbf{d}_3 \cdot (2\mathbf{d}_3 - \mathbf{d}_2)}{(\mathbf{d}_2 + \mathbf{d}_3)^5} \quad (48)$$

$$\Leftrightarrow \mathbf{d}_1 = \frac{u_0 \cdot (3u_1^2 - u_0 \cdot u_2)}{u_1^2 - u_0 \cdot u_2} \quad (49)$$

$$\mathbf{d}_2 = \frac{-4u_0^2 \cdot u_1^3}{(u_0 \cdot u_2 - 3u_1^2)(u_0 \cdot u_2 - u_1^2)} \quad (50)$$

$$\mathbf{d}_3 = \frac{-2u_0^2 \cdot u_1}{3u_1^2 - u_0 \cdot u_2} \quad (51)$$

Thus, the parameter combinations given in Eq. 43 – 45 are theoretically identifiable. As could be expected, the structure of these parameter combinations and its solutions (Eq. 49 – 51) are similar to the ones derived in the previous example considering $r_{\text{O,ex}}$ data, except for the stoichiometric factors.

The results of the theoretical identifiability studies of the two-step nitrification model considering a model structure with no growth and separate measurements of $r_{\text{O,ex}}$ or H_p are summarised in Table 2.

Table 2. Schematic overview of the theoretically identifiable parameter combinations for nitrification step 1 and 2, depending on r_{O} and H_p measurements, and for a model structure excluding biomass growth

Process (j)	Nitrification step 1		Nitrification step 2
Measurement (i) →	$r_{O,ex}$	H_p	$r_{O,ex}$
Model structure ↓			
No growth	$\frac{3.43 - Y_{A1}}{Y_{A1}} m_{\max A1} X$ $(3.43 - Y_{A1}) K_{SA1}$ $(3.43 - Y_{A1}) S_{NH}(0)$	$\frac{2}{14} \frac{m_{\max A1} X}{Y_{A1}}$ $\frac{2}{14} K_{SA1}$ $\frac{2}{14} S_{NH}(0)$	$\frac{1.14 - Y_{A2}}{Y_{A2}} m_{\max A2} X$ $(1.14 - Y_{A2}) K_{SA2}$ $(1.14 - Y_{A2}) S_{NO2}(0)$

4.2. Measurements of $r_{O,ex}$ or H_p – Growth model

In the theoretical identifiability studies presented in this subsection net growth will be explicitly taken into account. It will be assumed that $r_{O,end}$ (i.e. $b \cdot X(t)$) and the background proton production, which in the case of growth will be time varying, are known and that $r_{O,ex}$ or H_p data are available.

4.2.1. Respirometric data ($r_{O,ex}$)

The same approach is applied as for the model that did not consider biomass growth, however, with the difference that X is now also a function of time with a known initial biomass concentration $X(0)$. This complicates the expression of the successive derivatives significantly and below only the first two derivatives for the first nitrification step are illustrated (Eq. 52 – 53).

$$r_{O,ex}^{NI}(0) = \frac{m_{\max A1} \cdot X(0) \cdot (3.43 - Y_{A1})}{Y_{A1}} \cdot \frac{S_{NH}(0)}{K_{SA1} + S_{NH}(0)} \quad (52)$$

$$\frac{dr_{O,ex}^{NI}(0)}{dt} = \frac{m_{\max A1}^2 \cdot X(0) \cdot S_{NH}(0) \cdot (3.43 - Y_{A1}) \cdot (X(0) \cdot K_{SA1} \cdot (1 + i_{XB} \cdot Y_{A1}) - S_{NH}(0) \cdot Y_{A1} \cdot (S_{NH}(0) + K_{SA1}))}{Y_{A1}^2 \cdot (K_{SA1} + S_{NH}(0))^3} \quad (53)$$

It appeared that it was possible to express the parameter combinations given in Eq. 54 - 57 as a function of derivatives evaluated at $t = 0$. Hence, these parameter combinations are theoretically identifiable. When growth is considered explicitly it appeared possible to separate $\mu_{\max A1}$ and $X(0)$ in the identifiable

parameter combinations. Further, an extra term including the parameter i_{XB} appears in the parameter combinations for $S_{NH}(0)$ and K_{SA1} .

$$\mathbf{b}_7 = \mathbf{m}_{\max A1} \quad (54)$$

$$\mathbf{b}_8 = \frac{3.43 - Y_{A1}}{Y_{A1}} \cdot X(0) \quad (55)$$

$$\mathbf{b}_9 = \frac{3.43 - Y_{A1}}{1 + i_{XB} \cdot Y_{A1}} \cdot K_{SA1} \quad (56)$$

$$\mathbf{b}_{10} = \frac{3.43 - Y_{A1}}{1 + i_{XB} \cdot Y_{A1}} \cdot S_{NH}(0) \quad (57)$$

For the second nitrification step the theoretically identifiable parameter combinations are similar to the ones of the first nitrification step (see Table 3).

4.2.2. Titrimetric data – Hp

The generating series approach was again applied, but now growth was included in the model which alters the equation set for the generating series (Eq. 58) compared to the study with no growth (see Eq. 34), since now an equation for the state X has to be included.

$$\mathbf{f}^0 = \begin{pmatrix} f^{01} \\ f^{02} \\ f^{03} \end{pmatrix} = \begin{pmatrix} \mathbf{m}_{\max A1} \cdot X(t) \cdot \frac{S_{NH}(t)}{K_{SA1} + S_{NH}(t)} - \mathbf{b}_H \cdot X(t) \\ -\frac{\mathbf{m}_{\max A1} \cdot X(t)}{Y_{A1}} \cdot \frac{S_{NH}(t)}{K_{SA1} + S_{NH}(t)} \cdot (1 + i_{XB} \cdot Y_{A1}) + i_{XB} \cdot \mathbf{b} \cdot X(t) \\ \frac{2 + i_{XB} \cdot Y_{A1}}{14} \cdot \frac{\mathbf{m}_{\max A1} \cdot X(t)}{Y_{A1}} \cdot \frac{S_{NH}(t)}{K_{SA1} + S_{NH}(t)} \end{pmatrix} \quad \mathbf{g} = \text{Hp} \quad (58)$$

The first two Lie derivatives with respect to the output Hp are listed in Eq. 59 – 60 for illustration purposes only.

$$L_{f^0} \mathbf{g}(0) = \frac{(2 + i_{XB} \cdot Y_{A1})}{14} \cdot \frac{\mathbf{m}_{\max A1} \cdot X(0)}{Y_{A1}} \cdot \frac{S_{NH}(0)}{K_{SA1} + S_{NH}(0)} \quad (59)$$

$$L_{f0} L_{f0} g(0) = \frac{(2 + i_{XB} \cdot Y_{A1}) \cdot m_{\max A1}^2 \cdot X(0) \cdot S_{NH}(0) \cdot (X(0) \cdot K_{SA1} \cdot (1 + i_{XB} \cdot Y_{A1}) - S_{NH}(0) \cdot Y_{A1} \cdot (S_{NH}(0) + K_{SA1}))}{14 \cdot Y_{A1}^2 \cdot (K_{SA1} + S_{NH}(0))^3} \quad (60)$$

The corresponding identifiable parameter combinations are rather similar to Eq. 54 – 57, and are listed in Eq. 61 - 64. Again, i_{XB} appears in the parameter combinations since S_{NH} incorporation for biomass growth is now explicitly considered for the first nitrification step.

$$d_4 = m_{\max A1} \quad (61)$$

$$d_5 = \frac{2 + i_{XB} \cdot Y_{A1}}{14 \cdot Y_{A1}} \cdot X(0) \quad (62)$$

$$d_6 = \frac{2 + i_{XB} \cdot Y_{A1}}{14(1 + i_{XB} Y_{A1})} \cdot K_{SA1} \quad (63)$$

$$d_7 = \frac{2 + i_{XB} \cdot Y_{A1}}{14(1 + i_{XB} Y_{A1})} \cdot S_{NH}(0) \quad (64)$$

Table 3 summarises the results of the theoretical identifiability studies of the two-step nitrification model considering a model structure with biomass growth and separate measurements of $r_{O,ex}$ or H_p .

Table 3. Schematic overview of the theoretically identifiable parameter combinations for nitrification step 1 and 2, depending on r_O and H_p measurements and for a model structure excluding biomass growth.

Process (j)	Nitrification step 1		Nitrification step 2
Measurement (i) → Model structure ↓	r_O	H_p	r_O
Growth	$m_{\max A1}$ $\frac{3.43 - Y_{A1}}{Y_{A1}} X(0)$ $\frac{3.43 - Y_{A1}}{1 + i_{XB} Y_{A1}} K_{SA1}$ $\frac{3.43 - Y_{A1}}{1 + i_{XB} Y_{A1}} S_{NH}(0)$	$m_{\max A1}$ $\frac{2 + i_{XB} Y_{A1}}{14 \cdot Y_{A1}} X(0)$ $\frac{2 + i_{XB} Y_{A1}}{14(1 + i_{XB} Y_{A1})} K_{SA1}$ $\frac{2 + i_{XB} Y_{A1}}{14(1 + i_{XB} Y_{A1})} S_{NH}(0)$	$m_{\max A2}$ $\frac{1.14 - Y_{A2}}{Y_{A2}} X(0)$ $\frac{1.14 - Y_{A2}}{1 + i_{XB} Y_{A2}} K_{SA2}$ $\frac{1.14 - Y_{A2}}{1 + i_{XB} Y_{A2}} S_{NO2}(0)$

4.3. Combined measurements of $r_{O,ex}$ and H_p

In this section it is assumed that $r_{O,ex}$ and H_p are measured simultaneously in the same system. The measurements of $r_{O,ex}$ and H_p are assumed to be independent. Consequently, the information on identifiable parameter combinations (derived in the previous sections) based on $r_{O,ex}$ and H_p data separately, can be combined in the search for possibly new and improved parameter identification. It should be remembered that improved identifiability can not be expected for the parameters of the second nitrification step (Eq. 8) since the cumulative proton production only yields information on the first nitrification step. Again, the situation with no initial addition of S_{NO_2} is considered ($S_{NO_2}(0)=0$), i.e. at $t = 0$ $r_{O,ex}$ contains information on the first nitrification step only.

The theoretically identifiable parameter combinations obtained under the assumption that biomass growth does not take place are given in Eq. 65 – 68. The first three combinations are identical to the ones derived for $r_{O,ex}$ measurements (Eq. 21 – 23). The new parameter combination α_1 (Eq. 68) is proposed and, if identifiable, would allow an identification of Y_{A1} . Inserting Y_{A1} in Eq. 65 – 67 would subsequently result in unique identification of $m_{maxA1} \cdot X$, K_{SA1} and $S_{NH}(0)$.

$$\mathbf{b}_1 = \frac{3.43 - Y_{A1}}{Y_{A1}} \cdot m_{maxA1} \cdot X \quad (65)$$

$$\mathbf{b}_2 = (3.43 - Y_{A1}) \cdot K_{SA1} \quad (66)$$

$$\mathbf{b}_3 = (3.43 - Y_{A1}) \cdot S_{NH}(0) \quad (67)$$

$$\mathbf{a}_1 = \frac{14}{2} \cdot (3.43 - Y_{A1}) \quad (68)$$

The successive derivatives as functions of the parameter combinations are listed in Eq. 69 - 72, where $v_0 - v_2$ are the three first derivatives based on $r_{O,ex}$ measurements (identical to Eq. 25 – 27) whereas z_0 is based on the first derivative of H_p .

$$v_0 = \frac{\mathbf{b}_1 \cdot \mathbf{b}_3}{\mathbf{b}_2 + \mathbf{b}_3} \quad (69)$$

$$v_1 = -\frac{\mathbf{b}_1^2 \cdot \mathbf{b}_2 \cdot \mathbf{b}_3}{(\mathbf{b}_2 + \mathbf{b}_3)^3} \quad (70)$$

$$v_2 = -\frac{\mathbf{b}_1^3 \cdot \mathbf{b}_2 \cdot \mathbf{b}_3 \cdot (2\mathbf{b}_3 - \mathbf{b}_2)}{(\mathbf{b}_2 + \mathbf{b}_3)^5} \quad (71)$$

$$z_0 = \frac{\mathbf{b}_1 \cdot \mathbf{b}_2}{\mathbf{a}_1 \cdot (\mathbf{b}_2 + \mathbf{b}_3)} \quad (72)$$

It was found that the equation set v_0 , v_1 , v_2 and z_0 (Eq. 69 – 72) could be solved with respect to the parameters β_1 , β_2 , β_3 and α_1 , proving that the parameter combinations listed in Eq. 65 – 68 are theoretically identifiable. The solutions that were found for β_1 , β_2 , β_3 and α_1 are given in Eq. 73 - 76. Equations 73 – 75 are in fact identical to Eq. 28 – 30.

$$\mathbf{b}_1 = \frac{v_0 \cdot (3v_1^2 - v_0 \cdot v_2)}{v_1^2 - v_0 \cdot v_2} \quad (73)$$

$$\mathbf{b}_2 = -\frac{2v_0^2 \cdot v_1}{3v_1^2 - v_0 \cdot v_2} \quad (74)$$

$$\mathbf{b}_3 = \frac{-4v_0^2 \cdot v_1^3}{(v_0 \cdot v_2 - 3v_1^2)(v_0 \cdot v_2 - v_1^2)} \quad (75)$$

$$\mathbf{a}_1 = \frac{v_0}{z_0} \quad (76)$$

It is noteworthy that it was not possible to identify the parameters based on the first two successive derivatives with respect to $r_{O,ex}$ and Hp data respectively, indicating that information from higher order derivatives was needed. The analysis was also tried using the first three derivatives of the Hp measurements and the first derivative of $r_{O,ex}$. This equation set could also be solved for the parameter combinations given in Eq. 65 - 68.

Important to notice is that in fact α_1 (Eq. 76), the parameter combination which will allow to identify Y_{A1} , is nothing else but the ratio between the stoichiometric factors relating $r_{O,ex}$ and the first derivative of Hp to $\frac{dS_{NH}}{dt}$ (see Table 2).

The identifiability study considering growth followed the same pattern. However, the equations became more complicated and they are therefore not written out fully. The parameter combinations that were found to be identifiable are listed in Eq. 77 - 81. Again, the parameter α_2 that contains the information on Y_{A1} is defined by the ratio between the stoichiometric factors relating $r_{O,ex}$ and the first derivative of Hp to $\frac{dS_{NH}}{dt}$ (see Table 3).

$$\mathbf{b}_7 = \mathbf{m}_{\max A1} \quad (77)$$

$$\mathbf{b}_8 = \frac{3.43 - Y_{A1}}{Y_{A1}} \cdot X(0) \quad (78)$$

$$\mathbf{b}_9 = \frac{3.43 - Y_{A1}}{1 + i_{XB} \cdot Y_{A1}} \cdot K_{SA1} \quad (79)$$

$$\mathbf{b}_{10} = \frac{3.43 - Y_{A1}}{1 + i_{XB} \cdot Y_{A1}} \cdot S_{NH}(0) \quad (80)$$

$$\mathbf{a}_2 = \frac{2 + i_{XB} \cdot Y_{A1}}{3.43 - Y_{A1}} \quad (81)$$

Summarising, by considering growth and combined measurements of $r_{O,ex}$ and H_p the parameters μ_{maxA1} , $X(0)$, K_{SA1} , $S_{NH}(0)$ and Y_{A1} become theoretically identifiable under the assumption that i_{XB} is known.

Finally, the unique identification of Y_{A1} will also result in a unique identification of Y_{A2} based on the following simple reasoning. The integral of $r_{O,ex}$, which is a known quantity, is defined as (Eq. 82):

$$\int_0^t r_{O,ex} dt = (3.43 - Y_{A1}) \cdot S_{NH}(0) + (1.14 - Y_{A2}) \cdot S_{NH}(0) \quad (82)$$

As a result of Y_{A1} and thereby also $S_{NH}(0)$ being uniquely identifiable, Y_{A2} is the only unknown in Eq. 82 and becomes identifiable as well. Note that in the case where S_{NO2} is added initially ($S_{NO2}(0) \neq 0$) an identification of Y_{A2} will only be possible if $S_{NO2}(0)$ is known.

4.4. Measurements of S_O and H_p

From a practical point of view it is an advantage to consider measurements of oxygen concentrations, S_O , for parameter estimation as an alternative to $r_{O,ex}$ measurements. Indeed, S_O is the direct output from the dissolved oxygen electrode(s) in the respirometer and thus the differentiation step, which is needed to convert S_O data into $r_{O,ex}$ data, but at the same time also increases the noise on the data, could be avoided. In the following the theoretical parameter identifiability based on S_O measurements will be considered for both types of respirometer. The parameter identifiability should not depend on whether one focuses on S_O or its derivative, r_O , as output. However the fact that a few extra parameters related to oxygen transfer and biomass decay will need to be considered simultaneously, compared to the situations illustrated above, may complicate the matter slightly. For simplicity, only the identifiability of the first nitrification step will be considered in the following. However, the identifiability of the biodegradation kinetic parameters of the second nitrification step can also be carried out according to the procedure described above.

4.4.1. Respirometer 1 – S_O and H_p measurements

For the first respirometric technique the equation set for the generating series approach excluding growth is given in Eq. 83. The successive derivatives with respect to time for the Taylor series approach will follow the patterns initiated in Eq. 84 – 86, where the derivatives of $r_{O,ex}$ are similar to the ones that were derived

above (Eq. 18 – 20).

$$f^0 = \begin{pmatrix} f^{01} \\ f^{02} \\ f^{03} \end{pmatrix} = \begin{pmatrix} \mathbf{m}_{\max A1} \cdot X \cdot \frac{S_{NH}(t)}{K_{SA1} + S_{NH}(t)} \\ -\frac{\mathbf{m}_{\max A1} \cdot X}{Y_{A1}} \cdot \frac{S_{NH}(t)}{K_{SA1} + S_{NH}(t)} \\ K_L a \cdot (S_{O,eq} - S_O(t)) - (3.43 - Y_{A1}) \cdot \frac{\mathbf{m}_{\max A1} \cdot X}{Y_{A1}} \cdot \frac{S_{NH}(t)}{K_{SA1} + S_{NH}(t)} \end{pmatrix}, f^1 = \begin{pmatrix} 0 \\ 0 \\ 0 \end{pmatrix}, \underline{g} = (S_O) \quad (83)$$

$$\frac{dS_O(0)}{dt} = K_L a \cdot (S_{O,eq} - S_O(0)) - r_{O,ex}^{N1}(0) \quad (84)$$

$$\frac{d^2 S_O(0)}{dt^2} = -K_L a \cdot \frac{dS_O(0)}{dt} - \frac{dr_{O,ex}^{N1}(0)}{dt} \quad (85)$$

$$\frac{d^3 S_O(0)}{dt^3} = -K_L a \cdot \frac{d^2 S_O(0)}{dt^2} - \frac{d^2 r_{O,ex}^{N1}(0)}{dt^2} \quad (86)$$

The complexity of the equations increases significantly and the equations are therefore not written out fully. It was sought to identify the parameter combinations given in Eq. 87 – 91, with Eq. 87 – 89 containing the kinetic information identical to the earlier applied Eq. 21 – 23.

$$\mathbf{b}_1 = \frac{3.43 - Y_{A1}}{Y_{A1}} \cdot \mathbf{m}_{\max A1} \cdot X \quad (87)$$

$$\mathbf{b}_2 = (3.43 - Y_{A1}) \cdot K_{SA1} \quad (88)$$

$$\mathbf{b}_3 = (3.43 - Y_{A1}) \cdot S_{NH}(0) \quad (89)$$

$$\mathbf{b}_{15} = K_L a \quad (90)$$

$$\mathbf{b}_{16} = S_{O,eq} \quad (91)$$

Five successive derivatives were needed to solve for the parameter sets given above. However, MAPLE V was not able to achieve this and a slightly different approach was applied to show that identification of the parameter combinations given in Eq. 87 - 91 is possible. This approach consisted of including a second time instant in the identifiability study. This point, t_i , is defined as the point in time where all substrate is degraded (i.e. $r_{O,ex} = 0$ at point t_i), but S_O is still unequal to $S_{O,eq}$. It is reasonable to assume that such a point t_i exists since complete re-aeration to the equilibrium oxygen concentration $S_{O,eq}$ is only possible when substrate degradation is terminated, resulting in the mass balance given in Eq. 92.

$$\frac{dS_O(t_1)}{dt} = K_L a \cdot (S_{O,eq} - S_O(t_1)) \quad (92)$$

By including this equation in the identifiability study, it becomes possible to identify the parameter combinations given in Eq. 87 – 91. This is again an example that later observations at $t > 0$ may give additional information needed to identify some parameters.

If, on the other hand, growth is assumed to take place, the equilibrium concentration of oxygen $S_{O,eq}$ will change with time and one will have to consider the unreduced form of Eq. 9 for the oxygen mass balance (Eq. 93)

$$\frac{dS_O(t)}{dt} = K_L a(S_O^o - S_O(t)) - r_{O,end}(t) - r_{O,ex}(t) \quad (93)$$

It will be necessary to assume that either the oxygen transfer coefficient $K_L a$ or the saturation concentration S_O^o is known in order to identify the kinetic parameters related to $r_{O,ex}$. For example, the $K_L a$ can be determined via separate tests (ASCE, 1996). The endogenous respiration $r_{O,end}$ is defined by $r_{O,end} = b \cdot X(t)$. If $X(0)$ is assumed to be known, the decay rate b will be identifiable at the time instant where the substrate is not added yet. Thus, based on these assumptions the parameter combinations given in Eq. 94 - 97 (identical to Eq. 54 - 57) become identifiable.

$$\mathbf{b}_7 = \mathbf{m}_{\max A1} \quad (94)$$

$$\mathbf{b}_8 = \frac{3.43 - Y_{A1}}{Y_{A1}} \cdot X \quad (95)$$

$$\mathbf{b}_9 = \frac{(3.43 - Y_{A1})}{(1 + i_{XB} \cdot Y_{A1})} \cdot K_{SA1} \quad (96)$$

$$\mathbf{b}_{10} = \frac{(3.43 - Y_{A1})}{(1 + i_{XB} \cdot Y_{A1})} \cdot S_{NH}(0) \quad (97)$$

Finally, it was proven (results not shown) that the yield of the first nitrification step, Y_{A1} , becomes uniquely identifiable by combining S_O and H_p measurements. To achieve this result a similar approach was applied as described for the combination of r_O and H_p measurements including successive derivatives of S_O and the first derivative of H_p .

4.4.2. Respirometer 2 – S_O and H_p measurements

For the second respirometer the complexity of the mass balance equations is increasing further, because two oxygen measurements are included together with transport terms as described earlier in Eq. 9 and 10. If Q_{in} is considered to be a known input, the resulting complete equation set for the generating series

approach (including biomass growth) is given in Eq. 98.

$$\begin{aligned}
 f^0 = & \begin{pmatrix} f^{01} \\ f^{02} \\ f^{03} \\ f^{04} \\ f^{05} \\ f^{06} \end{pmatrix} = \begin{pmatrix} m_{\max A1} \cdot X_1(t) \cdot \frac{S_{NH,1}(t)}{K_{SA1} + S_{NH,1}(t)} \\ m_{\max A1} \cdot X_2(t) \cdot \frac{S_{NH,2}(t)}{K_{SA1} + S_{NH,2}(t)} \\ -\frac{m_{\max A1} \cdot X_1(t)}{Y_{A1}} \cdot \frac{S_{NH,1}(t)}{K_{SA1} + S_{NH,1}(t)} \cdot (1 + i_{XB}) \\ -\frac{m_{\max A1} \cdot X_2(t)}{Y_{A1}} \cdot \frac{S_{NH,2}(t)}{K_{SA1} + S_{NH,2}(t)} \cdot (1 + i_{XB}) \\ K_L a \cdot (S_{O,1}^0 - S_{O,1}) - (3.43 - Y_{A1}) \cdot \frac{m_{\max A1} \cdot X_1(t)}{Y_{A1}} \cdot \frac{S_{NH,1}(t)}{K_{SA1} + S_{NH,1}(t)} - b \cdot X_1(t) \\ - (3.43 - Y_{A1}) \cdot \frac{m_{\max A1} \cdot X_2(t)}{Y_{A1}} \cdot \frac{S_{NH,2}(t)}{K_{SA1} + S_{NH,2}(t)} - b \cdot X_2(t) \end{pmatrix}, \\
 f^1 = & \begin{pmatrix} f^{11} \\ f^{12} \\ f^{13} \\ f^{14} \\ f^{15} \\ f^{16} \end{pmatrix} = \begin{pmatrix} \frac{1}{V_1} (X_2(t) - X_1(t)) \\ \frac{1}{V_2} (X_1(t) - X_2(t)) \\ \frac{1}{V_1} (S_{NH,2}(t) - S_{NH,1}(t)) \\ \frac{1}{V_2} (S_{NH,1}(t) - S_{NH,2}(t)) \\ \frac{1}{V_1} (S_{O,2}(t) - S_{O,1}(t)) \\ \frac{1}{V_2} (S_{O,1}(t) - S_{O,2}(t)) \end{pmatrix}, \quad \underline{g} = \begin{pmatrix} S_{O,1} \\ S_{O,2} \end{pmatrix} \quad (98)
 \end{aligned}$$

The two first Lie derivatives (L_{f_0}) with respect to the two outputs are given in equations 99 and 100.

$$L_{f_0} \cdot g_1(0) = K_L a \cdot (S_{O,1}^0 - S_{O,1}) - r_{O,ex1}^{NI} - r_{O,end} \quad (99)$$

$$L_{f_0} \cdot g_2(0) = -r_{O,end} = -b \cdot X_1(0) = -b \cdot X_2(0) \quad (100)$$

It should be remembered that the substrate concentration in the respiration chamber at $t = 0$, $S_{NH,2}(0)$, is zero, resulting in Eq. 100, because substrate is only added in the aeration vessel at $t = 0$ for this respirometer. Thus, it is clear that based on Eq. 100, $r_{O,end}$ is identified since the biomass concentrations $X_1(0)$ and $X_2(0)$ are assumed to be equal. As a consequence, the successive Lie derivatives (L_{f_0}) with respect to the first output $S_{O,1}$ (Eq. 99) are similar to the derivatives considered for the first respirometer

(Eq. 84 – 86) and are leading to the same identifiable parameter sets. Alternatively, one could have considered equations of the type L_{fi} based on the input functions in Eq. 98. However, in this case this choice does not give any further information on the kinetic parameters but only yields information on the volumes, information that is considered known already.

It should be obvious that the Taylor series approach is much more complex in this case since the transport terms have to be differentiated with respect to time as well, as illustrated by Eq. 101 and 102 giving the second order derivatives for the Taylor approach.

$$\frac{d^2S_{O,1}(0)}{dt^2} = \frac{Q_{in}}{V_1} \cdot \left(\frac{dS_{O,2}(0)}{dt} - \frac{dS_{O,1}(0)}{dt} \right) - K_{La} \cdot \frac{dS_{O,1}(0)}{dt} - \frac{dr_{O,ex1}^{NI}(0)}{dt} \quad (101)$$

$$\frac{d^2S_{O,2}(0)}{dt^2} = \frac{Q_{in}}{V_2} \cdot \left(\frac{dS_{O,1}(0)}{dt} - \frac{dS_{O,2}(0)}{dt} \right) - \frac{dr_{O,ex2}^{NI}(0)}{dt} \quad (102)$$

It appeared indeed that the equations based on the Taylor approach reached such a complexity that the problem was not solvable in MAPLE V. Hence, in this particular example applying the Lie derivatives has a big advantage compared to the Taylor series approximation.

5. Generalisation of theoretically identifiable parameter combinations

A summary of the theoretically identifiable parameter combinations resulting from this study is listed in Table 4. The investigation of the theoretical identifiability via the series expansion methods is an iterative procedure, as mentioned in the introduction and further illustrated in the different examples, since the parameter combinations initially have to be “guessed” by the user. No rules seem to exist yet for selection of possible identifiable parameter combinations.

In the evaluation of the results obtained in this study however, it appears possible to generalise the parameter identifiability results listed in Table 4 based on the ASM1-like stoichiometric matrix (Table 1). Indeed, the identifiable parameter combinations can be predicted based on knowledge of the process under study, the measured component and the substrate component that is degraded. The rules of this generalisation are illustrated in Table 5. With reference to Table 1, v denotes the stoichiometric coefficient, j the process, i the measured component, while the substrate under study is denoted k . Considering that some components are consumed (e.g. S_O , S_S) whereas others are produced (e.g. X , Hp), the absolute values of the stoichiometric coefficients v should be taken. In case two components are measured for the same process, the parameter combinations for a single measurement listed in Table 5 still hold, but with the additional identifiable parameter combination $v_{i(1),j}/v_{i(2),j}$, where (1) and (2) indicate the two measured components respectively. The generalisation of Table 5 was confirmed with the identifiable parameter

combinations listed in Table 4, but also with examples from literature as will be illustrated below.

Table 4. Schematic overview of the theoretically identifiable parameter combinations for nitrification step 1 and 2, depending on the available measurement(s) and the model structure

Process (j)	Nitrification step 1			Nitrification step 2
	S _O or r _O	Hp	S _O + Hp or r _O + Hp	S _O or r _O
Measurement (i) → Model structure ↓				
No growth	$\frac{3.43 - Y_{A1}}{Y_{A1}} m_{\max A1} X$ $(3.43 - Y_{A1}) K_{SA1}$ $(3.43 - Y_{A1}) S_{NH}(0)$	$\frac{2}{14} \frac{m_{\max A1} X}{Y_{A1}}$ $\frac{2}{14} K_{SA1}$ $\frac{2}{14} S_{NH}(0)$	$\frac{3.43 - Y_{A1}}{Y_{A1}} m_{\max A1} X$ $(3.43 - Y_{A1}) K_{SA1}$ $(3.43 - Y_{A1}) S_{NH}(0)$ $\frac{14}{2} (3.43 - Y_{A1})$	$\frac{1.14 - Y_{A2}}{Y_{A2}} m_{\max A2} X$ $(1.14 - Y_{A2}) K_{SA2}$ $(1.14 - Y_{A2}) S_{NO2}(0)$
Growth	$\frac{m_{\max A1}}{Y_{A1}} X(0)$ $\frac{3.43 - Y_{A1}}{1 + i_{XB} \cdot Y_{A1}} K_{SA1}$ $\frac{3.43 - Y_{A1}}{1 + i_{XB} \cdot Y_{A1}} S_{NH}(0)$	$\frac{m_{\max A1}}{Y_{A1}} X(0)$ $\frac{2 + i_{XB} Y_{A1}}{14(1 + i_{XB} Y_{A1})} K_{SA1}$ $\frac{2 + i_{XB} Y_{A1}}{14(1 + i_{XB} Y_{A1})} S_{NH}(0)$	$\frac{m_{\max A1}}{Y_{A1}} X(0)$ $\frac{3.43 - Y_{A1}}{1 + i_{XB} Y_{A1}} K_{SA1}$ $\frac{3.43 - Y_{A1}}{1 + i_{XB} Y_{A1}} S_{NH}(0)$ $\frac{2 + i_{XB} Y_{A1}}{14(3.43 - Y_{A1})}$	$\frac{m_{\max A2}}{Y_{A2}} X(0)$ $\frac{1.14 - Y_{A2}}{1 + i_{XB} \cdot Y_{A2}} K_{SA2}$ $\frac{1.14 - Y_{A2}}{1 + i_{XB} \cdot Y_{A2}} S_{NO2}(0)$

Example 1:

The first nitrification step is considered (see Table 1), S_{NH} is added, Hp is measured and biomass growth is assumed to take place. Thus, in this case we have, i=7, j=2 and k=4 (see Table 1). According to Table 5 the identifiable parameter combinations are as follows:

1. $m_{\max j}$, i.e. the maximum specific growth rate related to process 2 which is $\mu_{\max A1}$.

$$2. \left| \mathbf{n}_{i,j} \right| \cdot X(0) \Leftrightarrow \left| \mathbf{n}_{7,2} \right| \cdot X(0) \Leftrightarrow \left(\frac{i_{XB}}{14} + \frac{1}{7 \cdot Y_{A1}} \right) \cdot X(0) = \frac{2 + i_{XB} \cdot Y_{A1}}{14 \cdot Y_{A1}} X(0).$$

$$3. \frac{\left| \mathbf{n}_{i,j} \right|}{\left| \mathbf{n}_{k,j} \right|} \cdot K_j \Leftrightarrow \frac{\left| \mathbf{n}_{7,2} \right|}{\left| \mathbf{n}_{4,2} \right|} \cdot K_2 \Leftrightarrow \frac{2 + i_{XB} \cdot Y_{A1}}{14 \cdot Y_{A1}} \cdot \frac{Y_{A1}}{1 + i_{XB} \cdot Y_{A1}} K_{A1} = \frac{2 + i_{XB} \cdot Y_{A1}}{14 \cdot (1 + i_{XB} \cdot Y_{A1})} K_{A1}.$$

$$4. \frac{\left| \mathbf{n}_{i,j} \right|}{\left| \mathbf{n}_{k,j} \right|} \cdot S_k(0) \Leftrightarrow \frac{\left| \mathbf{n}_{7,2} \right|}{\left| \mathbf{n}_{4,2} \right|} \cdot S_4(0) \Leftrightarrow \frac{2 + i_{XB} \cdot Y_{A1}}{14 \cdot (1 + i_{XB} \cdot Y_{A1})} S_{NH}(0).$$

These parameter combinations are completely in accordance with the ones derived in this study for the case where Hp is measured and biomass growth is considered in the model (see Table 4).

Table 5. Parameter combinations for Monod degradation kinetics based on ASM1-like matrix notation.

See text for a detailed explanation of the generalisation rules

S ₀ /r ₀ or Hp measurements		S ₀ /r ₀ and Hp measurements	
Model structures			
No growth	Growth	No growth	Growth
$\left \mathbf{n}_{i,j} \right \cdot \mathbf{m}_{\max,j} \cdot X$	$\mathbf{m}_{\max,j}$	$\left \mathbf{n}_{i,j} \right \cdot \mathbf{m}_{\max,j} \cdot X$	$\mathbf{m}_{\max,j}$
$\frac{\left \mathbf{n}_{i,j} \right }{\left \mathbf{n}_{k,j} \right } \cdot K_j$	$\left \mathbf{n}_{i,j} \right \cdot X(0)$	$\frac{\left \mathbf{n}_{i,j} \right }{\left \mathbf{n}_{k,j} \right } \cdot K_j$	$\left \mathbf{n}_{i,j} \right \cdot X(0)$
$\frac{\left \mathbf{n}_{i,j} \right }{\left \mathbf{n}_{k,j} \right } \cdot S_k(0)$	$\frac{\left \mathbf{n}_{i,j} \right }{\left \mathbf{n}_{k,j} \right } \cdot K_j$	$\frac{\left \mathbf{n}_{i,j} \right }{\left \mathbf{n}_{k,j} \right } \cdot S_k(0)$	$\frac{\left \mathbf{n}_{i,j} \right }{\left \mathbf{n}_{k,j} \right } \cdot K_j$
	$\frac{\left \mathbf{n}_{i,j} \right }{\left \mathbf{n}_{k,j} \right } \cdot S_k(0)$		$\frac{\left \mathbf{n}_{i,j} \right }{\left \mathbf{n}_{k,j} \right } \cdot S_k(0)$
		$\frac{\left \mathbf{n}_{i(1),j} \right }{\left \mathbf{n}_{i(2),j} \right }$	$\frac{\left \mathbf{n}_{i(1),j} \right }{\left \mathbf{n}_{i(2),j} \right }$

Example 2:

The first nitrification step is again considered (see Table 1), S_{NH} is added, Hp and S₀ are measured and growth is not considered (i.e. i_{XB} = 0). Thus, i(1)=3, i(2)=7, j=2 and k=4. The parameter combinations become:

1. $\left| \mathbf{n}_{i,j} \right| \cdot \mathbf{m}_{\max,j} \cdot X$. Now both i(1) and i(2) can be considered to write up a series of theoretically identifiable parameter combinations. In this example i(1)=3 will be chosen $\Rightarrow \left| \mathbf{n}_{3,2} \right| \cdot \mathbf{m}_{\max,2} \cdot X \Leftrightarrow \frac{3.43 - Y_{A1}}{Y_{A1}} \cdot \mathbf{m}_{\max A1} \cdot X$
2. $\frac{\left| \mathbf{n}_{i,j} \right|}{\left| \mathbf{n}_{k,j} \right|} \cdot K_j \Leftrightarrow \frac{\left| \mathbf{n}_{3,2} \right|}{\left| \mathbf{n}_{4,2} \right|} \cdot K_2 \Leftrightarrow \left(\frac{3.43 - Y_{A1}}{Y_{A1}} \cdot Y_{A1} \right) \cdot K_{SA1} = (3.43 - Y_{A1}) \cdot K_{SA1}$

$$3. \frac{\left| \mathbf{n}_{i,j} \right|}{\left| \mathbf{n}_{k,j} \right|} \cdot S_k(0) \Leftrightarrow \frac{\left| \mathbf{n}_{3,2} \right|}{\left| \mathbf{n}_{4,2} \right|} \cdot S_4(0) \Leftrightarrow \left(\frac{3.43 - Y_{A1}}{Y_{A1}} \cdot Y_{A1} \right) \cdot S_{NH}(0) = (3.43 - Y_{A1}) \cdot S_{NH}(0)$$

$$4. \frac{\left| \mathbf{n}_{i(1),j} \right|}{\left| \mathbf{n}_{i(2),j} \right|} \Leftrightarrow \frac{\left| \mathbf{n}_{3,2} \right|}{\left| \mathbf{n}_{7,2} \right|} \Leftrightarrow \frac{3.43 - Y_{A1}}{Y_{A1}} \cdot \frac{14 \cdot Y_{A1}}{2} = \frac{14}{2} (3.43 - Y_{A1})$$

These results are in accordance with the results of the Maple V developments that were obtained earlier (Table 4). Identical results would have been obtained in case $i(2)=7$ was chosen for the derivation.

Example 3:

If we now look beyond the identifiability studies carried out in this study, then an obvious example to check

is the situation where both $r_{O,ex}$ and S_S are measured. Since $\int_0^t r_{O,ex} dt = \frac{S_S(0)}{(1 - Y_H)}$ one would expect that

the biomass yield Y_H becomes identifiable from such a measurement set-up. The integral of $r_{O,ex}$ indicates how much oxygen is consumed and can be regarded as oxygen measurement. Furthermore, heterotrophic growth is considered and S_S is the substrate, i.e. $i(1)=2$, $i(2)=3$, $j=1$, $k=2$. The yield should now appear from the following combination:

$$1. \frac{\left| \mathbf{n}_{i(1),j} \right|}{\left| \mathbf{n}_{i(2),j} \right|} \Leftrightarrow \frac{\left| \mathbf{n}_{2,1} \right|}{\left| \mathbf{n}_{3,1} \right|} \Leftrightarrow \frac{1}{Y_H} \cdot \frac{Y_H}{1 - Y_H} = \frac{1}{1 - Y_H}.$$

This is proving, as expected, that the yield becomes identifiable if both S_O and S_S are measured.

Example 4:

If we return to literature, Holmberg (1982) proved that all the parameters μ_{maxH} , K_S , $S_S(0)$, $X(0)$ and Y_H were identifiable in the case where S_S and X measurements were available and biomass growth was considered. Hence, heterotrophic growth is considered, S_S is substrate and S_S and X are measured. In this example $i(1)=1$, $i(2)=2$, $j=1$ and $k=2$ and, according to the generalisation, the identifiable parameter set should be:

$$1. \mathbf{m}_{max,j} \Leftrightarrow \mathbf{m}_{maxH}.$$

$$2. \left| \mathbf{n}_{i,j} \right| \cdot X(0). \text{ As in example 2 both } i(1) \text{ and } i(2) \text{ can be considered, here } i(1)=1 \text{ will be chosen } \Leftrightarrow \left| \mathbf{n}_{1,1} \right| \cdot X(0) = X(0)$$

$$3. \frac{\left| \mathbf{n}_{i,j} \right|}{\left| \mathbf{n}_{k,j} \right|} \cdot K_j \Leftrightarrow \frac{\left| \mathbf{n}_{1,1} \right|}{\left| \mathbf{n}_{2,1} \right|} \cdot K_1 \Leftrightarrow \left(1 \cdot \frac{1}{Y_H} \right) \cdot K_S = \frac{1}{Y_H} \cdot K_S$$

$$4. \frac{|n_{i,j}|}{|n_{k,j}|} \cdot S_k(0) \Leftrightarrow \frac{|n_{1,1}|}{|n_{2,1}|} \cdot S_2(0) \Leftrightarrow \left(1 \cdot \frac{1}{Y_H}\right) \cdot S_S(0) = \frac{1}{Y_H} \cdot S_S(0)$$

$$5. \frac{|n_{i(1),j}|}{|n_{i(2),j}|} \Leftrightarrow \frac{|n_{1,1}|}{|n_{2,1}|} \Leftrightarrow 1 \cdot \frac{Y_H}{1} = Y_H$$

Thus, since the biomass yield Y_H becomes identifiable from step 5 all the parameters $\mu_{\max H}$, K_S , $S_S(0)$, $X(0)$ and Y_H become identifiable by applying the generalisation rules, similar to the results obtained by Holmberg (1982).

Example 5:

In the work of Sperandio and Paul (2000), the theoretical identifiability was also studied for heterotrophic growth but here assuming only measurements of $r_{O,ex}$. The identified parameters were $\mu_{\max H}$, $\frac{1 - Y_H}{Y_H} \cdot X(0)$, $(1 - Y_H) \cdot K_S$ and $(1 - Y_H) \cdot S_S(0)$, which is in fact equivalent to the ones obtained in this study for growth during the nitrification process. The parameter combinations derived by Sperandio and Paul (2000) could also be obtained directly based on the generalisation rules outlined above with $i=3$, $j=1$ and $k=2$.

$$1. \mathbf{m}_{\max,j} \Leftrightarrow \mathbf{m}_{\max H}$$

$$2. |n_{i,j}| \cdot X(0) \Leftrightarrow |n_{3,1}| \cdot X(0) \Leftrightarrow \frac{1 - Y_H}{Y_H} \cdot X(0)$$

$$3. \frac{|n_{i,j}|}{|n_{k,j}|} \cdot K_j \Leftrightarrow \frac{|n_{3,1}|}{|n_{2,1}|} \cdot K_1 \Leftrightarrow \frac{1 - Y_H}{Y_H} \cdot Y_H \cdot K_S = (1 - Y_H) \cdot K_S$$

$$4. \frac{|n_{i,j}|}{|n_{k,j}|} \cdot S_k(0) \Leftrightarrow \frac{|n_{3,1}|}{|n_{2,1}|} \cdot S_1(0) \Leftrightarrow \frac{1 - Y_H}{Y_H} \cdot Y_H \cdot S_S(0) = (1 - Y_H) \cdot S_S(0)$$

6. Discussion

The theoretical identifiability of a two-step nitrification model was studied assuming that respirometric and titrimetric measurements were available. The choice for a two-step nitrification model to describe nitrification in activated sludge was motivated by the observation that a two-step nitrification model is often required in practice to describe experimental data adequately. The two-step nitrification model is a more detailed version of the one-step nitrification model that is included in ASM1 (Henze *et al.*, 1987).

The Taylor and generating series approach were both applied to assess the theoretical identifiability of the

model parameters. In the last example of the hybrid respirometer (respirometer 2) it was illustrated that the generating series method may be more powerful than the Taylor method in cases where inputs are considered. The complexity of the equations decreased when applying the generating series approach since the input functions did not contain information on the kinetic parameters for the example that was studied, and could therefore be left out of the study, contrary to the Taylor method. When the inputs contain information on the parameters of interest, the generating series method allows to look at the different inputs separately (by taking derivatives to each input separately and combining them afterwards) whereas for the Taylor method the whole output function is derived with respect to time. The generating series method results in more, but simpler equations with respect to the parameters. On the contrary, in case no inputs are defined in the model the Taylor expansion method and the generating series give identical results, in agreement with Walter (1982). Thus, in that case the Taylor method is to be preferred since the derivation of the Taylor coefficients appears easier to apply than the Lie derivation.

For the two-step nitrification model the theoretical identifiability study was carried out for (i) a model structure that did not include net biomass growth and (ii) a model structure where biomass growth was explicitly taken into account. With respect to parameter identifiability, the difference between the two model structures was that the no-growth parameter combination including $X(0)$, Y and μ_{\max} can be split up further into μ_{\max} on the one hand, and a parameter combination including $X(0)$ and Y on the other hand.

Brouwer *et al.* (1998) also estimated nitrification kinetic parameters for a two-step nitrification model. In that study the assumed theoretically identifiable parameter combinations were defined to be the ones related to no growth although growth was considered in the model applied for parameter estimation. The same goes for the study of a one-step nitrification model by Vanrolleghem and Verstraete (1993), and also for the parameter estimations presented by Spanjers and Vanrolleghem (1995). From a theoretical point of view, a wrong approach was taken by including growth in the model (e.g. \dot{x}_B appears in the model) whereas the assumed theoretically identifiable parameter combinations were based on a no-growth model structure (\dot{x}_B did not appear in the identifiable combinations although it should have). However, the experiments considered in these studies were all of short-term character where significant growth is unlikely to take place. Thus, the practical identifiability, based on a model incorporating growth, of the theoretically identified parameter combinations resulting from a no-growth model structure would not have suffered much. The possible error in these studies is in fact related to the factor $(1 + \dot{x}_B Y_{A1})$.

Indeed, to be able to practically identify the theoretically identifiable parameters assuming growth, the available data must show a significant increase of the amount of biomass, e.g. visible in an increase of $r_{O,ex}$ during a long-term experiment. If the data do not reflect such significant biomass growth, the separation of the parameters μ_{\max} and $X(0)$ will not work in practice, causing high correlation between these two estimates. A good example for a respirometric experiment that does show significant biomass growth is presented in the work of Kappeler and Gujer (1992) and is also applied by Spérandio and Paul (2000).

An important result of this study is that the autotrophic yield, Y_{A1} (and Y_{A2} as well in case $S_{NO_2}(0)$ is known) becomes uniquely identifiable by combining respirometric and titrimetric data when studying nitrification. This is an important finding since the yield is an essential parameter in substrate degradation models. Indeed, the yield determines the distribution of consumed substrate between biomass growth and energy production. It is in fact not surprising that a unique identification of the biomass yield requires two kinds of measurements, since the yield coefficient relates two measures, that can link how much biomass is produced per unit of substrate degraded. Holmberg (1982), who identified the yield coefficient uniquely by assuming combined measurements of biomass and substrate already proved this. In the present case with combined respirometric and titrimetric measurements, both measurements reflect how much biomass is produced per unit of substrate degraded. The biomass yield becomes identifiable for the combined measurements because an additional parameter combination becomes identifiable compared to a situation where only a single measurement is available. This additional parameter combination appears to be nothing else than the ratio of the two stoichiometric factors that relate the respective measured variables to substrate degradation.

Finally and most substantially, it was proven and illustrated that it is possible to generalise the theoretical parameter identifiability based on an ASM1-like stoichiometric matrix. As stressed above one of the bottlenecks of the application of the series expansion methods is that the user initially has to “guess” which parameter combinations may be identifiable. If the problem is not solvable under these assumptions, other parameter combinations have to be assumed and tried out resulting in an iterative procedure. Thus, the generalisation rules are a very powerful tool to assess the theoretical identifiable parameter combinations directly, only based on knowledge of the process under study, the measured component(s) and the substrate component(s) that is degraded. Thereby the rather time-consuming task of assessing the theoretical identifiability of parameters of models, described by the Monod growth kinetics in ASM1-like matrix presentations, has been reduced significantly.

7. Conclusions

An essential first step in parameter estimation of models that are applied for data description is the assessment of the theoretical identifiability of the model parameters. In this study the theoretical identifiability of the two-step nitrification model was studied, via the Taylor series expansion and generating series methods, considering data resulting from two different types of respirometer and a titrimetric measurement. Initially, the parameter identifiability of the Monod kinetic parameters was studied based on measurements of oxygen uptake rates and cumulative proton consumption. It appeared that the parameter identifiability improves when combined respirometric and titrimetric data are available. It was proven that the autotrophic yield becomes uniquely identifiable in this situation. When oxygen concentration data are applied instead of oxygen uptake rates, it was further proven that the volumetric oxygen transfer coefficient

$K_L a$ was theoretically identifiable together with the Monod kinetic parameters.

In the theoretical identifiability study including the hybrid respirometer (respirometer 2), where an input was considered, it was illustrated that the generating series method was more powerful than the Taylor series expansion, since it resulted in simpler equations with respect to the parameters. On the contrary, in case no inputs were defined the Taylor expansion method and the generating series gave identical results.

The most important result of the study was however that the results of the theoretical identifiability study could be generalised. Based on simple generalisation rules the theoretically identifiable parameter combinations can be assessed directly from an ASM1-like matrix representing the model under study, thereby reducing the time needed for a theoretical identifiability study significantly. Thus, the theoretical identifiable parameters can be obtained directly without even considering the mathematical aspects of theoretical identifiability.

Chapter 5

-

Practical identifiability of model parameters by combined respirometric-titrimetric measurements

This chapter was published as :

Petersen B., Gernaey K. and Vanrolleghem P.A. (2001) Practical identifiability of model parameters by combined respirometric - titrimetric measurements. *Water Science and Technology*, **43**(7), 347-356.

Chapter 5

Practical identifiability of model parameters by combined respirometric-titrimetric measurements

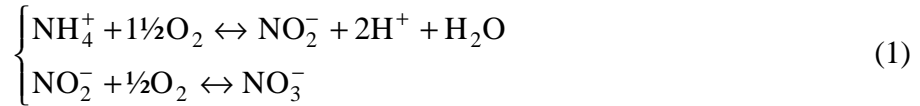
Abstract - A study on theoretical identifiability of parameters for a two-step nitrification model showed that a unique estimation of the yield Y_{A1} is possible with combined respirometric-titrimetric data, contrary to the case where only one type of measurement is available (chapter 4). Here, the practical identifiability of model parameters has been evaluated. The study was carried out via evaluation of the output sensitivity functions and the corresponding Fisher Information Matrix (FIM). It appeared that the FIM is not sufficiently powerful to predict the practical identifiability of this case with combined measurements as parameters can indeed be identified despite the fact that the FIM became singular. In the second part of the chapter the accuracy of parameter estimates based on respirometric and titrimetric data and combination thereof was investigated. It appeared that estimation on titrimetric data (H_p) is very accurate and a fast convergence of the objective function towards a minimum is obtained. The same holds for estimation on oxygen uptake rate data (r_O), however with a lower accuracy. Parameter estimation based on oxygen concentration data (S_O) is more complex but results in a higher accuracy. Thus, when the highest accuracy is needed it is recommended to estimate parameters initially on H_p and/or r_O data, and to subsequently use these parameters as initial values for final, and more accurate estimation on S_O data.

1. Introduction

The theoretical identifiability of model parameters is based on the model structure and the available outputs, and gives an indication of the maximum amount of information that can be obtained from a given (theoretical) experiment (see chapter 4). The practical identifiability on the contrary not only depends on the model structure, but is also related to the experimental conditions together with the quality and quantity of the measurements. For a given practical case or experiment one can obtain a direct answer on the parameter identifiability by studying the practical parameter identifiability. It should be stressed that the practical parameter identifiability often does not correspond with the theoretically derived one due to poor data quality (Holmberg, 1982).

The theoretical identifiability of the parameters of a two-step nitrification model based on Monod kinetics

has been studied via the series expansion methods: Taylor and generating series expansions (see chapter 4). The two-step nitrification model consists of the following steps: (1) oxidation of ammonium (NH_4^+) to nitrite (NO_2^-), and (2) oxidation of nitrite (NO_2^-) to nitrate (NO_3^-). This process is illustrated in a simple form in Eq. 1, without considering that a small part of NH_4^+ may be incorporated into the biomass during growth. Note that both nitrification steps can be characterised by measurements of oxygen uptake whereas only the first step can be characterised by its proton production.



The theoretical identifiability study was undertaken for two different model structures, assuming absence and presence of biomass growth respectively. It was considered that only respirometric data (measurements of dissolved oxygen, S_{O} , or oxygen uptake rate, r_{O}), only titrimetric data (cumulative proton production, H_{p}) or a combination of both were available. Table 1 summarises the results of the theoretical identifiability study for a model structure that assumed no biomass growth, typically applicable for description of short-term experiments.

Table 1. Schematic overview of the theoretically identifiable parameter combinations for nitrification step 1 and 2, depending on the available measurement(s), and assuming that no biomass growth takes place (chapter 4)

Process	Nitrification step 1			Nitrification step 2
Measurement → Model structure ↓	S_{O} or r_{O}	H_{p}	S_{O} + H_{p} or r_{O} + H_{p}	S_{O} or r_{O}
No growth	$\frac{3.43 - Y_{\text{A1}}}{Y_{\text{A1}}} m_{\text{maxA1}} X$ $(3.43 - Y_{\text{A1}}) K_{\text{SA1}}$ $(3.43 - Y_{\text{A1}}) S_{\text{NH}}(0)$	$\frac{2}{14} \frac{m_{\text{maxA1}} X}{Y_{\text{A1}}}$ $\frac{2}{14} K_{\text{SA1}}$ $\frac{2}{14} S_{\text{NH}}(0)$	$\frac{3.43 - Y_{\text{A1}}}{Y_{\text{A1}}} m_{\text{maxA1}} X$ $(3.43 - Y_{\text{A1}}) K_{\text{SA1}}$ $(3.43 - Y_{\text{A1}}) S_{\text{NH}}(0)$ $\frac{14}{2} (3.43 - Y_{\text{A1}})$	$\frac{1.14 - Y_{\text{A2}}}{Y_{\text{A2}}} m_{\text{maxA2}} X$ $(1.14 - Y_{\text{A2}}) K_{\text{SA2}}$ $(1.14 - Y_{\text{A2}}) S_{\text{NO2}}(0)$

An important result of the theoretical identifiability study was that the autotrophic yield for the first nitrification step, Y_{A1} , becomes uniquely identifiable when a combination of respirometric and titrimetric measurements is available. This can be concluded from the “ S_{O} + H_{p} or r_{O} + H_{p} ” column in Table 1, where the 4. expression results in a unique identification of Y_{A1} . The autotrophic yield coefficient Y_{A1} is only identifiable in a combination with other parameters in case only one kind of measurement is available, as can be seen in the “ S_{O} or r_{O} ” and the “ H_{p} ” column in Table 1. It is in fact not surprising that a unique

identification of Y_{A1} requires two kinds of measurements, since the yield coefficient links the amount of produced biomass to the number of degraded substrate units.

The methods by which the theoretical identifiability can be studied (e.g. the series expansions) may however not be that straightforward to apply, and may result in sets of non-linear equations that are far from simple, even for models of moderate complexity (Raksanyi *et al.*, 1985). This was also realised in the study presented in chapter 4. Consequently, the theoretical identifiability analysis may not be very “practical” as a preliminary step towards parameter estimation. Alternatively, the practical parameter identifiability can be evaluated directly based on the sensitivity functions (Holmberg and Ranta, 1982; Marsilli-Libelli, 1989) and the corresponding Fisher Information Matrix (FIM), which is a known measure for practical identifiability (Spriet and Vansteenkiste, 1982; Munack, 1991).

In this chapter, the theoretical identifiability results obtained with the series expansion methods in chapter 4 are evaluated for a specific case study through interpretation of the sensitivity functions and the corresponding FIM. This evaluation was carried out as a preliminary step to apply the results of the theoretical identifiability study in the context of optimal experimental design for combined respirometric and titrimetric experiments (see chapter 7). Furthermore, the accuracy of parameter estimates based on respirometric or titrimetric data and combined measurements was investigated.

2. Theoretical background

Consider the general model $M(\underline{p})$ (Eq. 2) :

$$M(\underline{p}) : \begin{cases} \frac{d}{dt} \underline{x}(t) = \underline{f}(\underline{x}(t), \underline{u}(t), t, \underline{p}), & \underline{x}(0) = \underline{x}_0(\underline{p}) \\ \underline{y}(t, \underline{p}) = \underline{g}(\underline{x}(t), \underline{p}) \end{cases} \quad (2)$$

Parameter estimation typically aims for a minimisation of a weighted sum $J(\underline{p})$ of squared errors between model outputs $\underline{y}(t_i, \underline{p})$ and measured outputs $\underline{y}_m(t_i)$ with the weights \underline{Q}_i and N the number of measurements (Eq. 3). The minimisation is obtained by optimal choice of the parameter vector \underline{p} .

$$J(\underline{p}) = \sum_{i=1}^N \left(\underline{y}(t_i, \underline{p}) - \underline{y}_m(t_i) \right)^T \underline{Q}_i \left(\underline{y}(t_i, \underline{p}) - \underline{y}_m(t_i) \right) \quad (3)$$

For a given \underline{p} the effect of a small deviation of the parameters, $\partial \underline{p}$, on the model fit, described by $J(\underline{p})$, can be evaluated by introducing a linearisation of the model with respect to the parameters along the trajectory (Eq. 4).

$$E[J(\underline{p} + \partial \underline{p})] = \sum_{i=1}^N \left(\underline{y}(t_i, \underline{p} + \partial \underline{p}) - \underline{y}_m(t_i) \right)^T \underline{Q}_i \left(\underline{y}(t_i, \underline{p} + \partial \underline{p}) - \underline{y}_m(t_i) \right) \quad (4)$$

where :

$$\underline{y}(t_i, \underline{p} + \partial \underline{p}) \approx \underline{y}(t_i, \underline{p}) + \left[\frac{\partial \underline{y}(t_i, \underline{p})}{\partial \underline{p}} \right]_{\underline{p}} \partial \underline{p} \approx \underline{y}(t_i, \underline{p}) + Y_p(t_i, \underline{p}) \partial \underline{p} \quad (5)$$

In Eq. 5 $Y_p(t_i, \underline{p})$ denotes the output sensitivity functions with respect to the parameters. Thus, the output sensitivity functions are defined by Eq. 6. They can be obtained analytically by differentiating Eq. 2 with respect to \underline{p} resulting in Eq. 7 (Posten and Munack, 1989; Munack, 1991). Simultaneous integration of Eq. 2 and Eq. 7 results then in the output sensitivity functions. The sensitivity functions of the states can be derived similarly.

$$Y_p(t_i, \underline{p}) = \frac{\partial \underline{y}(t_i, \underline{p})}{\partial \underline{p}} \quad (6)$$

$$\frac{dY_p}{dt}(t, \underline{p}) = \frac{\partial \underline{y}}{\partial \underline{x}} \Big|_{\underline{x}^o, \underline{p}} \underline{x}_p + \frac{\partial \underline{y}}{\partial \underline{p}} \Big|_{\underline{x}^o, \underline{p}}, \quad \underline{x}_p(0) = \frac{\partial \underline{x}_0}{\partial \underline{p}} \quad (7)$$

For a non-linear model, such as the Monod model, the sensitivity functions are dependent on the model parameters. This is in fact a general characteristic of non-linear models and can be used to define non-linearity (Robinson, 1985).

In practice one may approximate the sensitivity functions numerically via Eq. 8, an approximate form of Eq. 6.

$$\frac{\partial \underline{y}}{\partial \underline{p}} \approx \frac{\Delta \underline{y}}{\Delta \underline{p}} \quad (8)$$

Returning to Eq. 4 - 5, the expected value of the objective function $J(\underline{p})$ can be reformulated (Eq. 9).

$$E[J(\underline{p} + \partial \underline{p})] = J(\underline{p}) + \partial \underline{p}^T \left(\sum_{i=1}^N Y_p(t_i, \underline{p})^T \underline{Q}_i Y_p(t_i, \underline{p}) \right) \partial \underline{p} \quad (9)$$

Consequently, to obtain a reliable minimum for $J(\underline{p})$ the difference between $J(\underline{p})$ and $J(\underline{p} + \partial \underline{p})$ should be maximised, i.e. a minimum is sought where $J(\underline{p})$ is sensitive towards changes in \underline{p} . The reliability of the minimum can thus be increased by maximising the term between brackets in Eq. 9.

If the weighting matrix \underline{Q}_i in Eq. 9 is chosen as the inverse measurement error covariance matrix, assuming that the measurement noise is white (i.e. independent and normally distributed with zero mean), and uncorrelated (i.e. the measurement error covariance matrix is a diagonal matrix), the term between brackets in Eq. 9 is defined as the Fisher Information Matrix (FIM). This choice of \underline{Q}_i means that the more a

measurement is noise corrupted the less it will count in the FIM. The FIM is given in Eq. 10 (Munack, 1991).

$$\text{FIM} = \sum_{i=1}^N Y_p(t_i, \underline{p})^T \underline{Q}_i Y_p(t_i, \underline{p}) \quad (10)$$

Moreover, the FIM is the inverse of the parameter estimation error covariance matrix, COV, and provides the Cramer-Rao lower bound on the parameter estimation errors, Eq. 11 (Ljung, 1999; Walter and Pronzato, 1999).

$$\text{COV}(\underline{p}) \geq \text{FIM}^{-1}(\underline{p}) \quad (11)$$

Thus, the FIM can be regarded as a summary of the output sensitivity functions and the measurement accuracy, thereby summarising the information concerning the model parameters gained from an experiment. The rank of the FIM gives an indication of the theoretical parameter identifiability because the FIM is an approximation of the Hessian matrix of J (Söderström and Stoica, 1989). Local parameter identifiability requires that the rank of the FIM is full. This can for example be checked by computation of the determinant. If the $\text{Det}(\text{FIM}) \neq 0$ the parameters are locally identifiable (Spriet and Vansteenkiste, 1982; Söderström and Stoica, 1989). In case $\text{Det}(\text{FIM}) = 0$ (FIM is singular) some of the sensitivity functions are proportional, i.e. they are multiples of one another. According to the FIM it will be impossible in that situation to obtain unique estimates of the parameters from the data. Unique parameter estimates may be obtained when the sensitivity equations are almost proportional, but they will be highly correlated. This situation is rather undesirable since it implies that several combinations of parameters may describe the data almost equally well (Robinson and Tiedje, 1983). Several scalar functions of FIM can be defined as a measure of the “quality” of the estimated parameters, e.g. the determinant, condition number and trace. They play a key role in the theory of optimal experimental design. Application of FIM in that respect is however outside the scope of this chapter but has been dealt with in other studies (e.g. Munack, 1991; Vanrolleghem *et al.*, 1995; Versyck *et al.*, 1997), see also chapter 7. Here, however, another use is made of the calculated FIM. Its inverse will be applied in the derivation of confidence intervals. Indeed, the standard deviation of the i 'th estimated parameter \hat{p}_i can be obtained from the square root σ_i of the i 'th diagonal element of the inverse FIM. An approximate confidence interval at level α is then given by Eq. 12, where t indicates the t-distribution, which converges to the normal distribution when the number of measurements N is high.

$$\left[\hat{p}_i - t_{\mathbf{a}(N-p)} \mathbf{S}_i, \hat{p}_i + t_{\mathbf{a}(N-p)} \mathbf{S}_i \right] \quad (12)$$

3. Case study

In the case under study data was obtained with a hybrid respirometer that was combined with a titrimetric measurement technique (see chapter 3). The set-up is illustrated in Fig. 1. It consists of an open continuously aerated vessel and, connected to it, a closed non-aerated respiration chamber. It is equipped with two electrodes for measurement of dissolved oxygen. Mixed liquor is continuously pumped between the aeration vessel and the respiration chamber. The oxygen (S_O) mass balances for the aeration vessel and the respiration chamber are given in Eq. 13 and 14 respectively. In these equations, the suffixes 1 and 2 refer to the aeration vessel and the respiration chamber respectively.

$$\frac{dS_{O,1}}{dt} = \frac{Q_{in}}{V_1} (S_{O,2} - S_{O,1}) + K_L a (S_O^o - S_{O,1}) - r_{O,1} \quad (13)$$

$$\frac{dS_{O,2}}{dt} = \frac{Q_{in}}{V_2} (S_{O,1} - S_{O,2}) - r_{O,2} \quad (14)$$

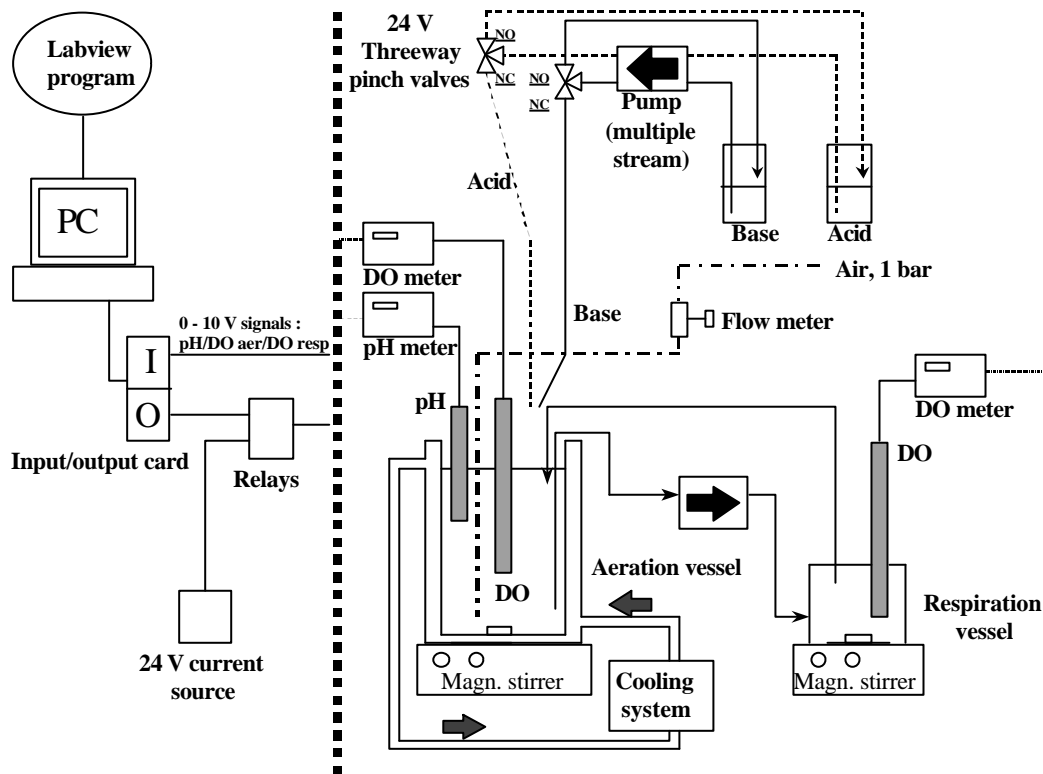


Figure 1. Experimental set-up used to collect combined respirometric-titrimetric data

The main advantage of this respirometer is that the oxygen uptake rate $r_{O,2}$ can be calculated by a simple S_O mass balance over the closed respiration vessel (Eq. 14), thereby avoiding the need to estimate $K_L a$ values (see chapter 3). In the hybrid respirometer substrate is added in the aeration vessel at the start of an experiment (time zero), and not to the closed respiration chamber. Thus, the substrate concentration in the

respiration chamber builds up from zero through the substrate flow from the aerated vessel. The r_O values in both vessels ($r_{O,1}$ and $r_{O,2}$ respectively) are obviously only equal when the substrate concentrations in both vessels are identical. The r_O value in Eq. 13 and 14 consists of two processes: (1) the immediate uptake of oxygen due to the consumption of a readily biodegradable substrate, i.e. the exogenous oxygen uptake rate $r_{O,ex}$, and (2) the endogenous oxygen uptake rate $r_{O,end}$. The $r_{O,ex}$, can be modelled via a Monod expression and the $r_{O,end}$ is typically modelled as a first order decay process $b \cdot X$.

The basic concept behind the titrimetric measurement technique is that the pH of the activated sludge sample is kept at a constant pH set-point while the cumulative amount of base and/or acid needed to keep that set-point is measured (Ramadori *et al.*, 1980). The cumulative amount of base or acid added contains kinetic information that is comparable to respirometric data in the case of nitrification, and can be modelled similarly (Gernaey *et al.*, 1998).

For this case study respirometric and titrimetric data were modelled by applying the model structure that is summarised in Table 2. The model in Table 2 is based on ASM1 (Henze *et al.*, 1987), with some modifications, and included also equations for the substrate transport in the hybrid respirometer and a first order equation to describe the biological start-up until r_O reaches its maximum value. A more detailed description of the model can be found in chapter 3.

Table 2. Model used for interpretation of the respirometric and titrimetric data assuming that no biomass growth takes place

Component → Process ↓	1. S_O	2. S_{NH}	3. S_{NO2}	4. S_{NO3}	5. H_p	Process rate
1. Nitrification step 1	$-\frac{3.43 - Y_{A1}}{Y_{A1}}$	$-\frac{1}{Y_{A1}}$	$\frac{1}{Y_{A1}}$		$\frac{1}{7 \cdot Y_{A1}}$	$m_{maxA1} \frac{S_{NH}}{K_{SA1} + S_{NH}} X$
2. Nitrification step 2	$-\frac{1.14 - Y_{A2}}{Y_{A2}}$		$-\frac{1}{Y_{A2}}$	$\frac{1}{Y_{A2}}$		$m_{maxA2} \frac{S_{NO2}}{K_{SA2} + S_{NO2}} X$

The actual experiment under study consisted of an ammonium addition to activated sludge. Data interpretation was done assuming that no biomass growth takes place, by applying the model summarised in Table 2. The data set is presented in Fig. 2 together with the model fits. In Fig. 2 it may be difficult to distinguish the model fit from the data. This is due to a combination of a low noise level on the S_O data and a good model fit.

A tail is observed in the $r_{O,2}$ profile (from $t = 60$ min to about $t = 100$ min in Fig. 2) which indicates that in this case the second nitrification step is slower than the first step. In this study we will only focus on the estimation of the parameters of the first nitrification step. Therefore, the parameters for the second step were fixed at known values obtained from a separate experiment with addition of nitrite. Consequently,

according to the theoretical identifiability analysis summarised in Table 1, the parameters $\mu_{\max A1}$, K_{SA1} , Y_{A1} and $S_{NH}(0)$ could be estimated when considering combined $r_{O,2}$ and H_p data. If S_O data was considered instead of $r_{O,2}$ the parameters $K_{L,a}$, b and S_O^0 had to be estimated additionally, as can be concluded from Eq. 13 – 14 (see also chapter 4).

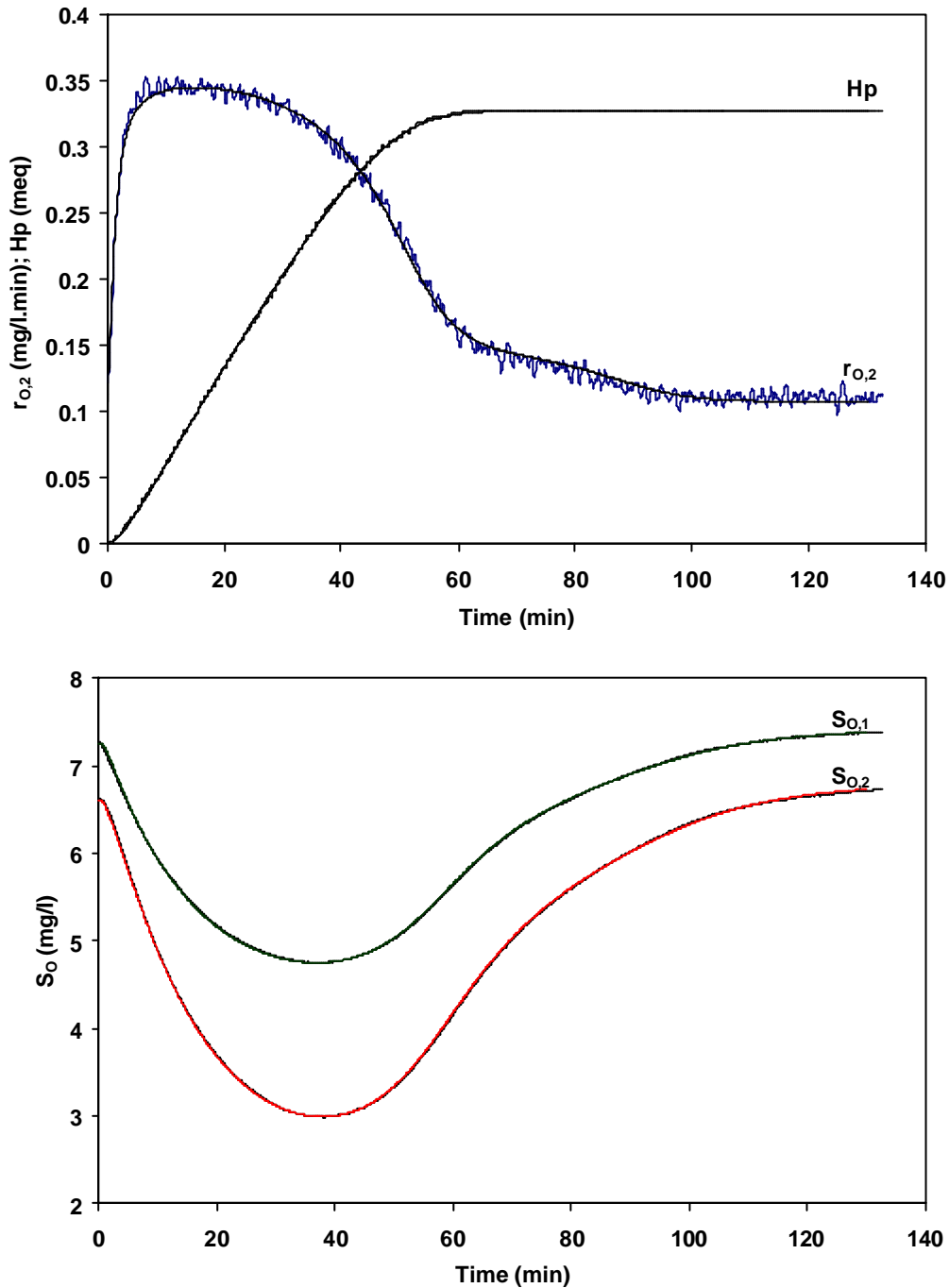


Figure 2. Experimental data ($r_{O,2}$, H_p , $S_{O,1}$ and $S_{O,2}$) obtained after adding ammonium to activated sludge at time = 0 and model fit to experimental data

4. Results and discussion

4.1. Sensitivity functions and practical identifiability

The output sensitivity functions of S_O , $r_{O,2}$ and H_p with respect to the different parameters were analytically derived in MAPLE V (Waterloo Maple Software) according to Eq. 6 – 7 (see Appendix 5.1). In this analytical derivation only the model considering the first nitrification step was included. The analytically derived sensitivity functions were verified numerically (via Eq. 8), and it was found that the analytical and numerical sensitivity functions were identical. This numerical check is recommended for complex models, as the one under study, because errors easily slip into the analytical derivation.

The well-known almost linear dependency between the sensitivities of the different outputs with respect to $\mu_{\max A1}$ and K_{SA1} was observed (data not shown, see Appendix 5.1). This is indicating that these two parameters will be correlated, and that it may be difficult to identify these two parameters in practice (Holmberg, 1982; Robinson and Tiedje, 1983). Furthermore, it can be observed in Fig. 3A and 3B that the sensitivity functions of the outputs $r_{O,2}$ and H_p with respect to $\mu_{\max A1}$ and Y_{A1} appear proportional. This is confirmed by the equations of the sensitivity functions which are proportional (see Appendix 5.1). Consequently, based on this information it will not be possible to obtain unique estimates for these two parameters. Note here that this finding is in conflict with the results of the theoretical identifiability study. Below, after a more thorough discussion of the sensitivity functions, this finding will be discussed in more detail.

As mentioned above, the sensitivity functions can pinpoint the experimental conditions under which the dependency of the outputs on the parameters is largest, and thereby under which conditions most information can be obtained on the parameters. E.g. the sensitivities of $r_{O,2}$ outputs with respect to the kinetic parameters exhibit rather sharp peaks indicating that at certain points the sensitivity of the outputs towards the parameters is significant (see Fig. 3A). This in fact indicates that the full information contained in the data is only available during a rather short part of a typical batch experiment and, further, that large estimation errors may be generated if one does not collect sufficient data during this “sensitive” time interval (Marsilli-Libelli, 1989). The sensitivities of the H_p output on the other hand do not exhibit such sharp peaks (Fig. 3B). The information is not only concentrated in a limited time interval and, in case of equidistant measurements, this may indicate that with H_p outputs better advantage is taken of the information provided by the entire data set.

The sensitivity functions with respect to the initial substrate concentration seemed to be clearly distinguishable from the other sensitivities indicating that a unique estimate can be expected (Fig. 3C). The rather different shapes of the sensitivity functions of $r_{O,2}$ compared to H_p illustrate the difference between the sensitivity of concentration (given by H_p) versus rate data (given by $r_{O,2}$). The sensitivity functions of S_O

with respect to S_O^0 and b in Fig. 3D show that these are proportional, whereas it was found that the shape of the sensitivity function with respect to $K_L a$ was distinguishable (Appendix 5.1). This indicates that a unique estimate of $K_L a$ would be possible (see also chapter 4).

Summarising, it can be expected from the detailed sensitivity analysis study that the estimation of $\mu_{\max A1}$ and K_{SA1} may cause practical problems. Y_{A1} is not identifiable when considering separate measurements of $r_{O,2}$, S_O or Hp . Furthermore, it was indicated that a separation of the parameters S_O^0 and b may be problematic.

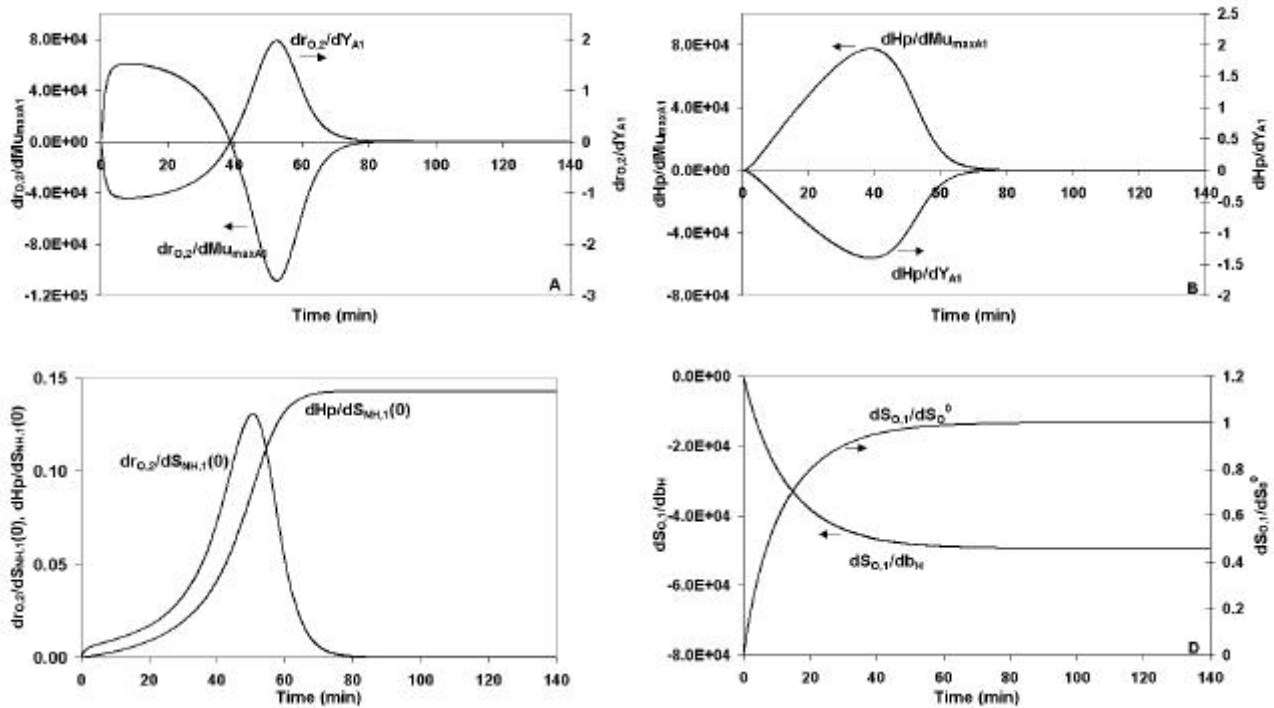


Figure 3. Sensitivity functions for $r_{O,2}$, Hp and S_O obtained for the nitrification case study. **A:** $dr_{O,2}/d\mu_{\max A1}$ and $dr_{O,2}/dY_{A1}$; **B:** $dHp/d\mu_{\max A1}$ and dHp/dY_{A1} ; **C:** $dr_{O,2}/dS_{NH,1}(0)$ and $dHp/dS_{NH,1}(0)$; **D:** $dS_{O,1}/dS_O^0$ and $dS_{O,1}/db$

According to the findings from the theoretical identifiability study (see Table 1) Y_{A1} should become uniquely identifiable when measurements are combined. Surprisingly, however, when summarising the information of the sensitivity functions in the FIM for combined respirometric (S_O or $r_{O,2}$) and titrimetric (Hp) measurements, the FIM becomes singular indicating an unidentifiable situation. It was found that it is the inclusion of the sensitivity functions with respect to Y_{A1} that is causing the singularity due to the fact that the sensitivity functions of $\mu_{\max A1}$ and Y_{A1} are proportional. Thus, there seems to appear a conflict between the application of FIM as a measure for local parameter identifiability and the results derived from the theoretical identifiability studies (Table 1). The FIM does not seem to reflect the improved theoretical identifiability achieved by combining measurements. A similar observation was observed with the

parameters S_O^0 and b . The parameter b is theoretically identifiable when combining two oxygen measurements in the hybrid respirometer (chapter 4). However, the inclusion of the sensitivity function of b also causes singularity of the FIM.

The reason for this discrepancy is not clear. It may however be hypothesised that information on parameter identifiability obtained from the combination of measured outputs may be lost due to the local first order linearisation of the model with respect to the parameters on which FIM is based (see Eq. 5 and 9).

To further investigate the practical identifiability of Y_{A1} for the example under study, simultaneous estimation of $\mu_{\max A1}$, K_{A1} , $S_{NH,1}(0)$ and Y_{A1} was carried out. A contour plot of the objective function J as a function of the possibly correlated parameters $\mu_{\max A1}$ and Y_{A1} is given in Fig. 4. As would be expected from the FIM results, it appears that the parameters $\mu_{\max A1}$ and Y_{A1} are highly correlated in practice since a long valley is observed, indicating a severe practical identifiability problem. However, it is also obvious that the contour is closed. Hence, the result that Y_{A1} is theoretically identifiable is confirmed if one evaluates the non-linear objective function and not its linear approximation close the minimum as done when applying a FIM-based analysis. Obviously this conflict between methods for identifiability analysis deserves further theoretical analysis.

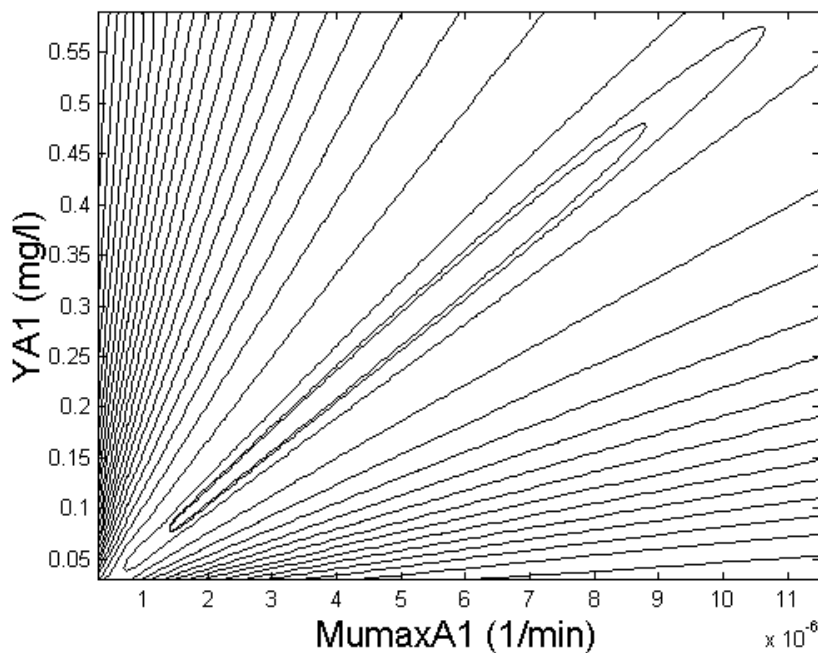


Figure 4. Contour plot of the objective function plotted as a function of $\mu_{\max A1}$ and Y_{A1}

4.2. Evaluation of parameter estimation accuracy with respirometric-titrimetric data

In the following, the confidence intervals of the estimated parameters are evaluated based on Eq. 11 - 12 and it will be discussed whether respirometric data (S_O or $r_{O,2}$) may be more powerful than titrimetric data (H_p) for accurate parameter estimations.

First, it will be described how the measurement error covariance matrix Q in Eq. 10 is practically estimated for S_O , $r_{O,2}$ and H_p data of the example given in Fig. 2. For S_O and $r_{O,2}$ data the measurement error (s^2) is estimated from a data series obtained during endogenous respiration (typically before or after the substrate addition). In the case under study the measurement errors of $r_{O,2}$ were estimated from $t=100 - 120$ min where $r_{O,end}$ can be considered constant. This data series for $r_{O,2}$ is illustrated in Fig. 5 together with the average value and the residuals. The s^2 is estimated via Eq. 13, where N is the number of measurements and p is the number of estimated parameters (here $p=1$, the average).

$$s^2 = \frac{SSE}{N - p} \quad (13)$$

For H_p data it would, however, give an unrealistic, optimistic picture to estimate the measurement error from data after the point where substrate degradation is terminated, since the H_p profile in the case under study is a perfect horizontal line. As a consequence s^2 is estimated based on the data series from $t = 15 - 35$ min where the slope can be assumed constant. Thus, the data are not evaluated with respect to an average value but to a model of the simple form $H_p = a \cdot t + b$ (calculated via the slope and intercept of the data series). The data series, model and residuals are illustrated in Fig. 5. In the estimation of s^2 p is now equal to 2. Note that it appears from Fig. 5 that the residuals seem to be auto-correlated. This is in fact violating the white measurement noise condition in Eq. 10, and it may result in optimistic confidence intervals (Glasbey, 1980). Note that the auto-correlation is only visible due to the high sampling frequency implemented.

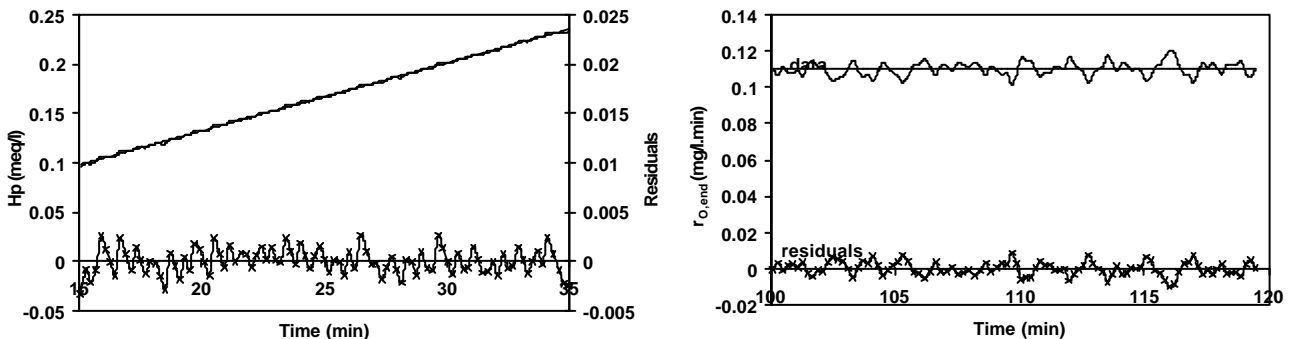


Figure 5. Data and residuals used to estimate the measurement noise on H_p and $r_{O,2}$ data

The covariance among the residuals and the corresponding correlation matrix were estimated and are given in Eq. 14 - 15 respectively for the example of combined $r_{0,2}$ and Hp measurements.

$$\underline{\underline{\Sigma}} = \begin{bmatrix} s_{r_{0,2}}^2 & s_{r_{0,2}} \cdot s_{Hp} \\ s_{r_{0,2}} \cdot s_{Hp} & s_{Hp}^2 \end{bmatrix} = \begin{bmatrix} 1.385 \cdot 10^{-5} & 2.541 \cdot 10^{-7} \\ 2.541 \cdot 10^{-7} & 1.617 \cdot 10^{-6} \end{bmatrix} \quad (14)$$

$$\underline{\underline{\Sigma}} = \begin{bmatrix} 1 & 5.367 \cdot 10^{-2} \\ 5.367 \cdot 10^{-2} & 1 \end{bmatrix} \quad (15)$$

It was verified, via a t-test for correlation, that the correlation between the two data sets was insignificant at test level 5%. Thus, the measurement covariance matrix Q was determined to be (Eq. 16):

$$\underline{\underline{\Sigma}} = \begin{bmatrix} s_{r_{0,2}}^2 & s_{r_{0,2}} \cdot s_{Hp} \\ s_{r_{0,2}} \cdot s_{Hp} & s_{Hp}^2 \end{bmatrix} = \begin{bmatrix} 1.385 \cdot 10^{-5} & 0 \\ 0 & 1.617 \cdot 10^{-6} \end{bmatrix} \Leftrightarrow \underline{\underline{\Sigma}}^{-1} = Q = \begin{bmatrix} 72199 & 0 \\ 0 & 618047 \end{bmatrix} \quad (16)$$

A test of the correlation between the residuals of the two $S_{O,1}$ and $S_{O,2}$ and Hp data also showed to be insignificant, resulting in the measurement covariance matrix Q given in Eq. 17.

$$\underline{\underline{\Sigma}}^{-1} = Q = \begin{bmatrix} s_{S_{O,1}}^2 & s_{S_{O,1}} \cdot s_{S_{O,2}} & s_{S_{O,1}} \cdot s_{Hp} \\ s_{S_{O,1}} \cdot s_{S_{O,2}} & s_{S_{O,2}}^2 & s_{S_{O,2}} \cdot s_{Hp} \\ s_{S_{O,1}} \cdot s_{Hp} & s_{S_{O,2}} \cdot s_{Hp} & s_{Hp}^2 \end{bmatrix}^{-1} = \begin{bmatrix} 76108 & 0 & 0 \\ 0 & 90350 & 0 \\ 0 & 0 & 618047 \end{bmatrix} \quad (17)$$

From Eq. 16 and 17 it can be seen that the actual measurement error on $S_{O,1}$ and $S_{O,2}$ is in the same order of magnitude, however relatively the measurement error on $r_{0,2}$ data is about 100 times bigger than the relative error on $S_{O,1}$ data. On the contrary, it is difficult to compare the measurement variance of titrimetric and respirometric data since they are two different kinds of measurements. The 95% confidence intervals (expressed as percentage of the parameter values, Table 3) are now retrieved by calculation of the inverse FIM via Eq. 10 and 11, and by inserting the diagonal values into Eq. 12. It should be noted that due to the singularity problems with the FIM, the sensitivity functions of Y_{A1} and b were excluded from the calculation of the FIM.

These results indicate that it is more accurate to estimate the parameters based on Hp data than on $r_{0,2}$ data. This is especially the case for $S_{NH,1}(0)$ where the 95% confidence interval is as low as +/- 0.074% with Hp data. If one considers the Hp profile in Fig. 2 this is not surprising since $S_{NH,1}(0)$ is in fact determined by the location of the constant horizontal plateau and many data contain this information. Furthermore, it becomes obvious from Table 3 that the confidence intervals improve by the application of combined $r_{0,2}$ and Hp measurements. This is especially the case for the parameters μ_{maxA1} and K_{SA1} , where an improvement of about 50% is observed compared to measurements of $r_{0,2}$ alone. The accuracy of the $S_{NH}(0)$ estimate does, however, not improve significantly further by applying combined $r_{0,2}$ and Hp

measurements. When the accuracy based on S_{O_2} data is compared with the accuracy obtained by using the S_{O_2} derived r_{O_2} , it becomes obvious that it is more accurate to estimate on the S_{O_2} concentration data. This is clearly due to the much higher measurement noise on r_{O_2} data, as mentioned above. Furthermore, a significant improvement in accuracy is observed when two dissolved oxygen measurements are available ($S_{O_1} + S_{O_2}$) compared to a situation where only one measurement is available (S_{O_1}). This confirms the statement made by Vanrolleghem and Spanjers (1998) that in this set-up basically two independent measures of the respiration rate can be obtained, thus duplicating the information on the kinetic parameters. The added value of H_p to combined S_{O_1} and S_{O_2} measurements seems however to be insignificant.

Table 3. 95% confidence intervals expressed as percentage of the parameter values, Q via measurement errors

Data	$\mu_{\max A1}$	K_{SA1}	$S_{NH,1}(0)$	K_{La}	$S_{O_2}^{\circ}$
r_{O_2}	1.385	6.328	0.510	-	-
H_p	0.905	5.780	0.074	-	-
$r_{O_2} + H_p$	0.696	3.942	0.070	-	-
S_{O_1}	0.231	0.943	0.241	0.293	0.064
$S_{O_1} + S_{O_2}$	0.093	0.506	0.028	0.094	0.028
$S_{O_1} + S_{O_2} + H_p$	0.091	0.511	0.026	0.090	0.028

The accuracy reported in Table 3 are quite impressive and warrant some verification. First of all, it was evaluated whether the confidence intervals were too optimistic due to the occurrence of auto-correlated residuals. However, the measurement noise of the applied experimental method is indeed not very significant, as indicated in Fig. 2. The confidence intervals were verified via simulations where the parameter values were set to the limits of the 95% confidence intervals. The resulting simulated curves indeed just laid within the edges of the measurement noise, confirming that the calculated 95% confidence intervals are calculated correctly. A final element of discussion is that in the calculation of confidence intervals in Table 3, the weighting matrix Q is based on the measurement errors only and does not include the model errors. Therefore, as a second evaluation of the parameter accuracy Q was based on the values of the objective function $J(\underline{p})$ obtained from the parameter estimation, thereby including both measurement noise and model errors, as also applied in the study of Weijers (1999). The resulting 95% confidence intervals are given in Table 4.

Table 4. 95% confidence intervals expressed as percentage of the parameter values, Q via objective function $J(\underline{p})$

Data	$\mu_{\max A1}$	K_{SA1}	$S_{NH,1}(0)$	K_{La}	S_O^o
$r_{O,2}$	1.884	8.805	2.433	-	-
Hp	0.911	5.820	0.074	-	-
$r_{O,2} + Hp$	0.826	4.740	0.077	-	-
$S_{O,1}$	0.308	1.255	0.321	0.389	0.085
$S_{O,1} + S_{O,2}$	0.335	1.821	0.104	0.321	0.094
$S_{O,1} + S_{O,2} + Hp$	0.264	1.503	0.066	0.246	0.076

In general the differences between the 95% confidence intervals obtained with the two error calculation approaches are not very large when considering $r_{O,2}$, Hp, $r_{O,2}+Hp$ and $S_{O,1}$ data. This indicates that the model has been able to describe these data adequately since the main part of the errors is included in the measurement noise. This is especially the case for Hp measurements, where the confidence intervals obtained with both approaches are almost identical. An exception is the estimation of $S_{NH,1}(0)$ based on $r_{O,2}$ data where the model error seems to play a significant role. On the contrary the difference in 95% confidence intervals with $S_{O,1} + S_{O,2}$ data seems significant, and when model errors are considered the accuracy does not improve compared to $S_{O,1}$ data alone (Table 4). However, compared to Table 3 including the Hp data now improves the accuracy. The reason for the lack of improvement in accuracy when considering two oxygen measurements is the fact that the complexity of the parameter estimation procedure increases drastically in this case. Furthermore, the model may not be adequate enough to describe the data as well as in the other cases.

Consequently, based on Table 3, and thus only considering measurement errors, one may conclude that the most accurate parameters are obtained by applying the two oxygen measurements, $S_{O,1}$ and $S_{O,2}$, from the hybrid set-up. This is however contradicted by the results given in Table 4 which point more in the direction of applying only one set of oxygen measurements, i.e. $S_{O,1}$.

Another important factor to consider before choosing the most adequate measured variables for a parameter estimation problem is the rate of convergence of $J(\underline{p})$ towards a minimum and, quite related, the sensitivity for local minima. From experience it has appeared that convergence is significantly faster when $r_{O,2}$ and/or Hp data are used rather than S_O data. This is due to the increased complexity of the estimation problem when using S_O data, since K_{La} and S_O^o both need to be estimated simultaneously with the kinetic parameters $\mu_{\max A1}$ and K_{SA1} and $S_{NH,1}(0)$. Especially the parameter estimation based on Hp data alone is very fast and is, in addition, also very accurate, as indicated in Table 3 and 4. Thus, in practice one may

initially choose to estimate the kinetic parameters on H_p and/or $r_{O,2}$ data, and to obtain an even higher accuracy, especially for $\mu_{\max A1}$ and K_{SA1} , apply these parameter values as initial guesses for parameter estimations based on S_O data. The introduction of a second S_O data source, however, may seem questionable based on the case under study, due to the increased complexity of the parameter estimation problem and the effects this has on convergence rates.

5. Conclusions

In this chapter the practical identifiability was studied on a nitrification example considering combined respirometric and titrimetric measurements. The practical identifiability was evaluated via output sensitivity functions and the corresponding Fisher Information Matrix (FIM). It appeared that the FIM became singular indicating an unidentifiable situation despite the fact that a theoretical identifiability study had shown that the chosen parameter set, including a unique identifiability of the yield Y_{A1} , should be identifiable with combined respirometric-titrimetric measurements. The FIM seemed, however, inadequate to evaluate this improved theoretical identifiability since the inclusion of the sensitivity of Y_{A1} in the calculation of FIM caused the singularity. It was hypothesised that some information on the parameters may be lost when applying FIM due to the local first order linearisation of the model with respect to the parameters on which the FIM is based. It was found that, estimation of the Y_{A1} was indeed possible in practice, as the theoretical identifiability analysis predicted, although it was strongly correlated with $\mu_{\max A1}$. For the case under study it thus seemed that an evaluation of parameter identifiability based on FIM gave a too pessimistic picture. This has some implications on the application of FIM in Optimal Experimental Design, as will be dealt with further in chapter 7.

Furthermore, the accuracy of parameter estimates based on respirometric and titrimetric data was evaluated. In this evaluation considerations and experience were included, concerning (i) measurements errors, (ii) model errors and (iii) the complexity of the parameter estimation as characterised by the convergence of the estimation algorithm towards a minimum. From this it could be concluded that estimation of parameters on H_p data is very accurate and a fast convergence is obtained. The same holds for $r_{O,2}$ data although the accuracy is less. It is suggested that an even higher accuracy can be obtained when the parameter estimates based on H_p and/or $r_{O,2}$ are applied as initial values for the more complex parameter estimation based on S_O data. Thus, these findings may be kept in mind in the choice of measurement.

Appendix 5.1

-

Output sensitivity functions of single step nitrification model

Appendix 5.1

Output sensitivity functions of single step nitrification model

In this appendix the output sensitivity functions of $r_{O,ex}$, S_O , and H_p are derived. Concerning the output functions of $r_{O,ex}$ it should be remembered that $r_{O,ex}$ in the hybrid set-up is derived from the mass balance over the respiration chamber ($r_{O,ex2}$) (see chapter 3). In the study on practical identifiability of model parameters by combined respirometric-titrimetric measurements, the applied model was a two step nitrification model. However, in the presented case only the parameters of the first step could be identified, and the parameters for the second nitrification step were therefore fixed at known values obtained from a separate experiment where only nitrite was added. Thus, in the calculation of the FIM only the sensitivity functions related to the first step were included (see chapter 5 for the details), which in fact makes the derivations below similar to the derivations considering a single step nitrification model.

In this study only short-term experiments were considered. It can therefore be assumed that significant growth can be neglected which means that the biomass concentration X is not considered as a function of time (see chapter 4). In case the experiments are not short-term the output sensitivity functions will be significantly more complicated (i.e. it will have to be considered that $X(t)$ is depending on the parameters as well). Furthermore, the experiments under study are all performed under oxygen sufficient conditions ($S_O > 2\text{mg/l}$) which means that $r_{O,ex}$ is independent of S_O . All analytically derived sensitivity functions have been carefully verified via a numerical procedure, as described in chapter 5.

1. Sensitivity functions of $r_{O,ex2}$

The sensitivity of $r_{O,ex2}$ with respect to $\mu_{\max A1}$ and K_{SA1} were obtained following the same procedure as given in Vanrolleghem and Dochain (1998) with the difference however that a 1.order description of the biological start-up is included (Vanrolleghem *et al.*, 1998).

$$\frac{\partial r_{O,ex2}^{NI}(t)}{\partial \mathbf{m}_{\max A1}} = -(3.43 - Y_{A1}) \frac{\partial}{\partial \mathbf{m}_{\max A1}} \left(- (1 - e^{-t/\tau}) \frac{\mathbf{m}_{\max A1} X}{Y_{A1}} \frac{S_{NH,2}(t)}{K_{SA1} + S_{NH,2}(t)} \right) \quad (1)$$

The substrate concentration is calculated by integration of the dynamic model for the hybrid set-up including substrate transport (Eq. 2 illustrates the substrate equation for the respiration chamber).

$$\frac{dS_{NH,2}(t)}{dt} = \frac{Q_{in}}{V_2} \cdot (S_{NH,1}(t) - S_{NH,2}(t)) - (1 - e^{-t/\tau}) \frac{m_{maxA1} \cdot X}{Y_{A1}} \frac{S_{NH,2}(t)}{K_{SA1} + S_{NH,2}(t)} \quad (2)$$

Eq. 1 results in Eq. 3.

$$\frac{\partial r_{O,ex2}^{NI}(t)}{\partial m_{maxA1}} = \frac{(3.43 - Y_{A1}) \cdot (1 - e^{-t/\tau}) \cdot X}{Y_{A1}} \left(\frac{S_{NH,2}(t)}{K_{SA1} + S_{NH,2}(t)} + \frac{m_{maxA1} \cdot K_{SA1} \cdot \frac{\partial S_{NH,2}(t)}{\partial m_{maxA1}}}{(K_{SA1} + S_{NH,2}(t))^2} \right) \quad (3)$$

The factor $\frac{\partial S_{NH}(t)}{\partial m_{maxA1}}$ in Eq. 3 is defined as an additional state variable, and $\frac{\partial r_{O,ex2}(t)}{\partial m_{maxA1}}$ can therefore be obtained by a simultaneous solution of Eq. 2 and 3. The sensitivity with respect to Y_{A1} is very similar to the sensitivity function of μ_{maxA1} (Eq. 4), and it is obvious by comparing Eq. 3 and 4 that they appear to be proportional (see chapter 5).

$$\frac{\partial r_{O,ex2}^{NI}(t)}{\partial Y_{A1}} = \frac{(3.43 - Y_{A1}) \cdot (1 - e^{-t/\tau}) \cdot m_{maxA1} \cdot X}{Y_{A1}^2} \left(\frac{S_{NH,2}(t)}{K_{SA1} + S_{NH,2}(t)} + \frac{Y_{A1} \cdot K_{SA1} \cdot \frac{\partial S_{NH,2}(t)}{\partial Y_{A1}}}{(K_{SA1} + S_{NH,2}(t))^2} \right) \quad (4)$$

The sensitivity of $r_{O,ex2}$ with respect to K_{SA1} follows the same principle and is given in Eq. 5.

$$\frac{\partial r_{O,ex2}^{NI}}{\partial K_{SA1}} = \frac{(3.43 - Y_{A1}) \cdot (1 - e^{-t/\tau}) \cdot m_{maxA1} \cdot X}{Y_{A1}} \left(\frac{K_{SA1} \cdot \frac{\partial S_{NH,2}(t)}{\partial K_{SA1}} - S_{NH,2}(t)}{(K_{SA1} + S_{NH,2}(t))^2} \right) \quad (5)$$

For the sensitivity of $r_{O,ex2}$ with respect to the initial substrate concentration $S_{NH,1}(0)$, it should be remembered that the substrate is added in the aeration vessel only. Thus, the sensitivity of $r_{O,ex2}$ should be derived with respect to the initial ammonium concentration in the aerated vessel $S_{NH,1}(0)$ (Eq. 6).

$$\frac{\partial r_{O,ex2}^{NI}(t)}{\partial S_{NH,1}(0)} = -(3.43 - Y_{A1}) \frac{\partial}{\partial S_{NH,1}(0)} \left(- (1 - e^{-t/\tau}) \frac{m_{maxA1} X}{Y_{A1}} \frac{S_{NH,2}(t)}{K_{SA1} + S_{NH,2}(t)} \right) \quad (6)$$

In the study of Vanrolleghem and Dochain (1998) the model of heterotrophic substrate (S_S) degradation was considered, however, for a simpler respirometer with only (aerated) vessel yielding one value of $r_{O,ex}$. The relationship of the form given in Eq. 7 was introduced to be able to solve the sensitivity function of $r_{O,ex}$ with respect to the initial substrate concentration.

$$S_S(t) = S_S(0) - \frac{\int_0^t r_{O,ex} dt}{(1 - Y_H)} \quad (7)$$

An important difference between the hybrid respirometer and the respirometric principle studied in Vanrolleghem and Dochain (1998) is that it only contains one vessel to which the substrate is added. However, in the hybrid respirometer $r_{O,ex}$ is calculated from a mass balance of the respiration chamber yielding $r_{O,ex2}$, whereas the substrate initially is added in the aeration vessel, i.e. $S_{NH,1}(0)$ and $S_{NH,2}(0)=0$. Thus, an equivalent of Eq. 7 for the hybrid becomes (Eq. 8) :

$$S_{NH,2}(t) = S_{NH,1}(0) - \frac{\int_0^t r_{O,ex2}^{NI} dt}{(3.43 - Y_{A1})} \quad (8)$$

For the hybrid model Eq. 7 will strictly speaking only be valid from the point on where $r_{O,ex1}$ equals $r_{O,ex2}$, i.e. $S_{NH,1}(t) = S_{NH,2}(t)$. Alternatively, it could be considered that substrate was added to both vessels to make Eq. 7 valid for the whole experimental period. This is, however, not in accordance with reality, and therefore this study it constrained to the situation where the transport phase is not significantly long in the hybrid respirometer, i.e. the flow between aeration vessel and respiration chamber is sufficiently high to allow a converging of $r_{O,2}$ to $r_{O,1}$ within a short time (see also discussion on the flow effect in chapter 3). Thus, an overall mass balance for $S_{NH}(t)$ in the system can be written as Eq. 9.

$$V_1 \cdot S_{NH,1}(t) + V_2 \cdot S_{NH,2}(t) = V_1 \cdot S_{NH,1}(0) + V_2 \cdot S_{NH,2}(0) - V_1 \cdot \frac{\int_0^t r_{O,ex1}^{NI} dt}{(3.43 - Y_{A1})} - V_2 \cdot \frac{\int_0^t r_{O,ex2}^{NI} dt}{(3.43 - Y_{A1})} \quad (9)$$

When $S_{NH,1}(t) = S_{NH,2}(t)$, i.e. $r_{O,ex1} = r_{O,ex2}$ and $S_{NH,2}(0)=0$, then Eq. 9 results in Eq. 10, and Eq. 6 results in Eq. 11.

$$S_{NH,2}(t) = \frac{V_1}{V_1 + V_2} S_{NH,1}(0) - \frac{\int_0^t r_{O,ex2}^{NI} dt}{(3.43 - Y_{A1})} \quad (10)$$

$$\frac{\partial r_{O,ex2}^{NI}(t)}{\partial S_{NH,1}(0)} = \frac{(1 - e^{-t/\tau}) \mathbf{m}_{\max A1} X \cdot K_{SA1}}{Y_{A1}} \left(\frac{(3.43 - Y_{A1}) \frac{V_1}{V_1 + V_2} - \int_0^t \frac{\partial r_{O,ex2}^{NI} dt}{\partial S_{NH,1}(0)}}{(K_{SA1} + S_{NH,2}(t))^2} \right) \quad (11)$$

2. Sensitivity functions of S_o

The sensitivity functions of S_o in the hybrid model with respect to the different parameters ($\mu_{\max A1}$, K_{SA1} , Y_{A1} , $S_{NH,1}(0)$, K_{La} , S_o^o and b_H) are given in the following Eq. 12 – 19.

$$\frac{d}{dt} \frac{\partial S_{O,1}}{\partial \mathbf{m}_{\max A1}} = -K_{La} \frac{\partial S_{O,1}}{\partial \mathbf{m}_{\max A1}} - \frac{\partial r_{O,ex1}^{N1}}{\partial \mathbf{m}_{\max A1}} + \frac{Q_{in}}{V_1} \left(\frac{\partial S_{O,2}}{\partial \mathbf{m}_{\max A1}} - \frac{\partial S_{O,1}}{\partial \mathbf{m}_{\max A1}} \right) \quad (12)$$

$$\frac{d}{dt} \frac{\partial S_{O,2}}{\partial \mathbf{m}_{\max A1}} = -\frac{\partial r_{O,ex2}^{N1}}{\partial \mathbf{m}_{\max A1}} + \frac{Q_{in}}{V_2} \left(\frac{\partial S_{O,1}}{\partial \mathbf{m}_{\max A1}} - \frac{\partial S_{O,2}}{\partial \mathbf{m}_{\max A1}} \right) \quad (13)$$

where $\frac{\partial r_{O,ex1}^{N1}}{\partial \mathbf{m}_{\max A1}}$ and $\frac{\partial r_{O,ex2}^{N1}}{\partial \mathbf{m}_{\max A1}}$ are obtained via the approach given in Eq. 1. The sensitivity functions concerning K_{SA1} , Y_{A1} and $S_{NH,1}(0)$ follow the same system as outlined in Eq. 12 – 13. The sensitivity functions of K_{La} , S_o^o and b are given in Eq. 14 - 19. Note that $r_{O,ex}$ is independent of S_o as mentioned above which means that $\frac{\partial r_{O,ex1}^{N1}}{\partial K_{La}}$ and $\frac{\partial r_{O,ex1}^{N1}}{\partial S_o^o}$ are zero. Furthermore, since insignificant growth is assumed,

the endogenous respiration is constant and thereby $\frac{\partial r_{O,ex1}^{N1}}{\partial b_H}$ is zero.

$$\frac{d}{dt} \frac{\partial S_{O,1}}{\partial K_{La}} = (S_o^o - S_{O,1}) - K_{La} \frac{\partial S_{O,1}}{\partial K_{La}} + \frac{Q_{in}}{V_1} \left(\frac{\partial S_{O,2}}{\partial K_{La}} - \frac{\partial S_{O,1}}{\partial K_{La}} \right) \quad (14)$$

$$\frac{d}{dt} \frac{\partial S_{O,2}}{\partial K_{La}} = \frac{Q_{in}}{V_2} \left(\frac{\partial S_{O,1}}{\partial K_{La}} - \frac{\partial S_{O,2}}{\partial K_{La}} \right) \quad (15)$$

$$\frac{d}{dt} \frac{\partial S_{O,1}}{\partial S_o^o} = K_{La} - K_{La} \frac{\partial S_{O,1}}{\partial S_o^o} + \frac{Q_{in}}{V_1} \left(\frac{\partial S_{O,2}}{\partial S_o^o} - \frac{\partial S_{O,1}}{\partial S_o^o} \right) \quad (16)$$

$$\frac{d}{dt} \frac{\partial S_{O,2}}{\partial S_o^o} = \frac{Q_{in}}{V_2} \left(\frac{\partial S_{O,1}}{\partial S_o^o} - \frac{\partial S_{O,2}}{\partial S_o^o} \right) \quad (17)$$

$$\frac{d}{dt} \frac{\partial S_{O,1}}{\partial b} = -K_{La} \frac{\partial S_{O,1}}{\partial b} - X + \frac{Q_{in}}{V_1} \left(\frac{\partial S_{O,2}}{\partial b} - \frac{\partial S_{O,1}}{\partial b} \right) \quad (18)$$

$$\frac{d}{dt} \frac{\partial S_{O,2}}{\partial b} = -X + \frac{Q_{in}}{V_2} \left(\frac{\partial S_{O,1}}{\partial b} - \frac{\partial S_{O,2}}{\partial b} \right) \quad (19)$$

3. Sensitivity functions of Hp

Before developing the sensitivity functions of Hp, it should be reminded that pH control in the hybrid set-up is installed in the aerated vessel only, i.e. only Hp₁ is measured. Thus, in reality the protons produced in the respiration chamber is only compensated for, by addition of base, in the aerated vessel. This also means that in reality Hp₂ > Hp₁ despite complete mixing, i.e. S_{NH,1}(t) = S_{NH,2}(t). However, in the treatment of the data this difference between Hp₁ and Hp₂ is neglected and the amount of added base (in meq) to compensate the proton production is divided with the total volume (V₁+V₂) and interpreted as an overall proton production (in meq/l). Thus, in the data analysis it is assumed that the mixing of the system is instantaneous, i.e. S_{NH,1}(t) = S_{NH,2}(t) and Hp₁ = Hp₂. Altogether this small discrepancy between reality and data analysis will be insignificant as long as the flow is sufficiently high allowing S_{NH,2}(t) to converge to S_{NH,1}(t) within short time (see chapter 3), and thereby permitting the flow term in the model to be neglected.

Finally, since insignificant growth is considered, incorporation of S_{NH} into biomass is not considered. The sensitivity functions of Hp then very much follow the same procedure as for r_{O,ex2}. The solutions with respect to μ_{maxA1} and K_{SA1} are given in Eq. 20 - 24.

$$\frac{\partial}{\partial m_{\max A1}} \frac{dHp_1(t)}{dt} = \frac{2 \cdot (1 - e^{-t/\tau}) \cdot X}{14 \cdot Y_{A1}} \left(\frac{S_{NH,1}(t)}{K_{SA1} + S_{NH,1}(t)} + \frac{m_{\max A1} \cdot K_{SA1} \cdot \frac{\partial S_{NH,1}(t)}{\partial m_{\max A1}}}{(K_{SA1} + S_{NH,1}(t))^2} \right) \quad (20)$$

$$\frac{\partial Hp_1(t)}{\partial m_{\max A1}} = \frac{2}{14} \frac{\partial S_{NH,1}(t)}{\partial m_{\max A1}} \quad (21)$$

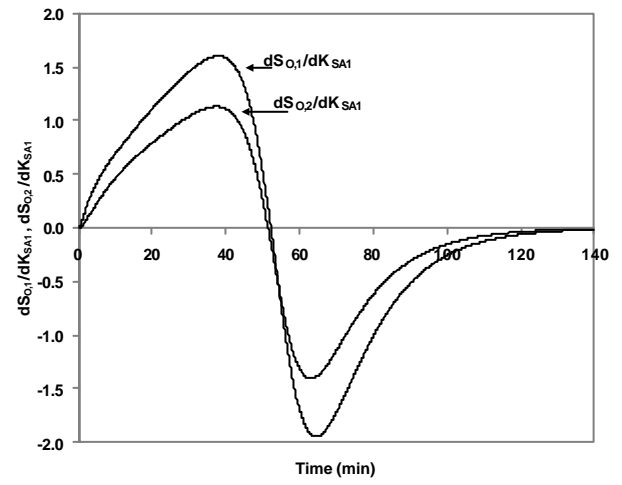
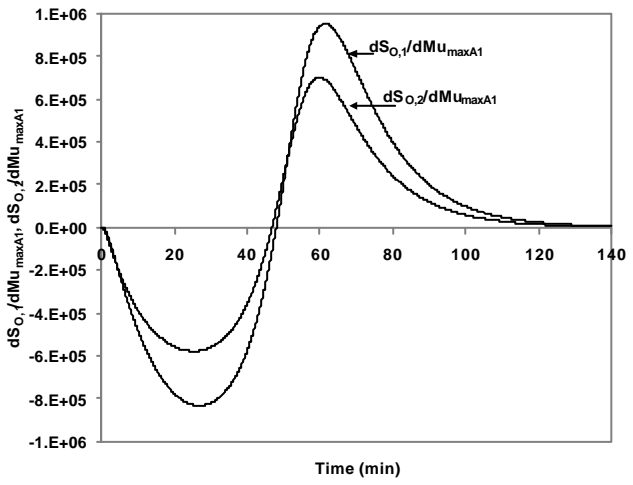
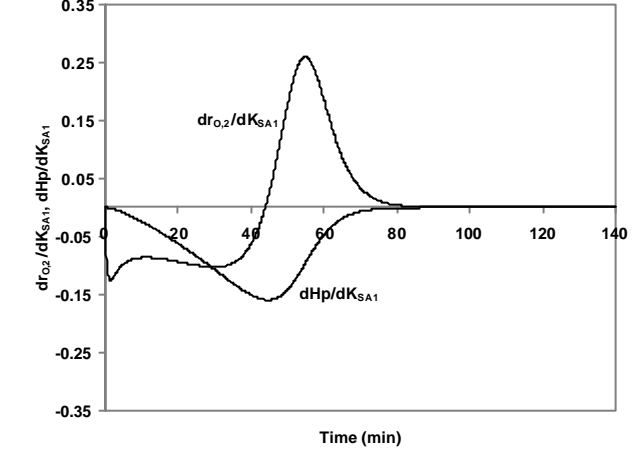
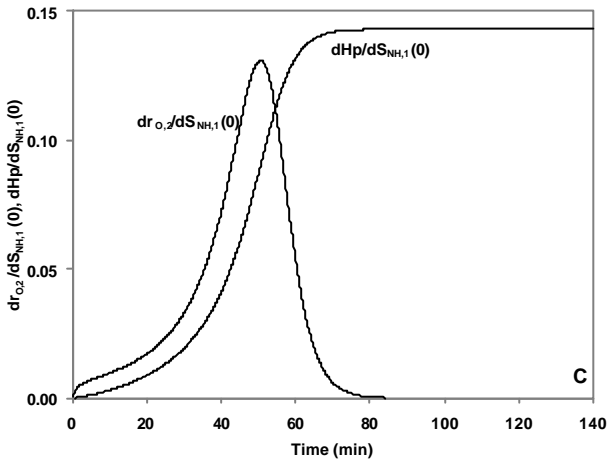
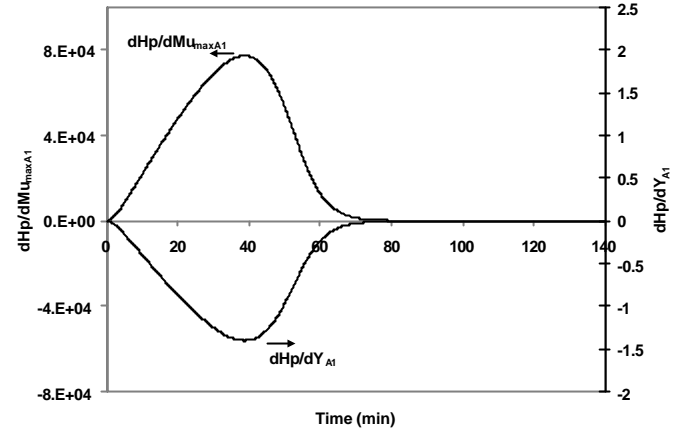
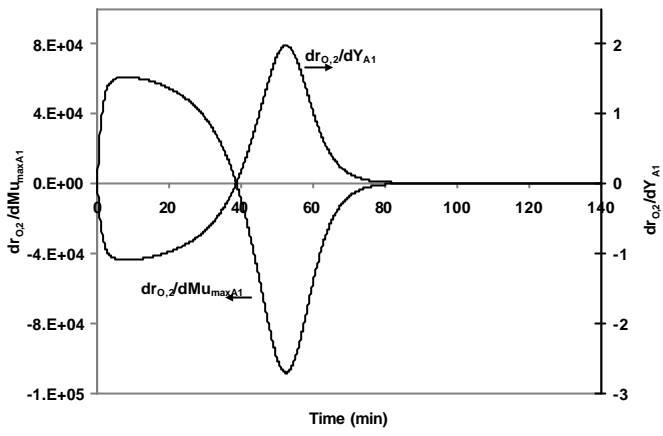
$$\frac{\partial}{\partial K_{SA1}} \frac{dHp_1(t)}{dt} = \frac{2 \cdot (1 - e^{-t/\tau}) \cdot m_{\max A1} \cdot X}{14 \cdot Y_{A1}} \cdot \left(\frac{K_{SA1} \cdot \frac{\partial S_{NH,1}(t)}{\partial K_{SA1}} - S_{NH,1}(t)}{(K_{SA1} + S_{NH,1}(t))^2} \right) \quad (22)$$

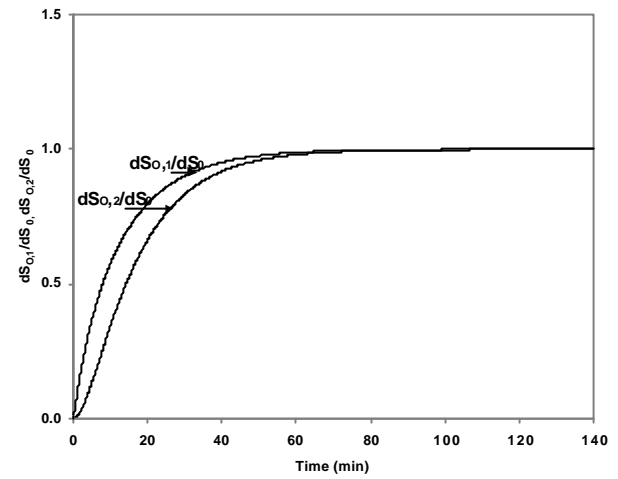
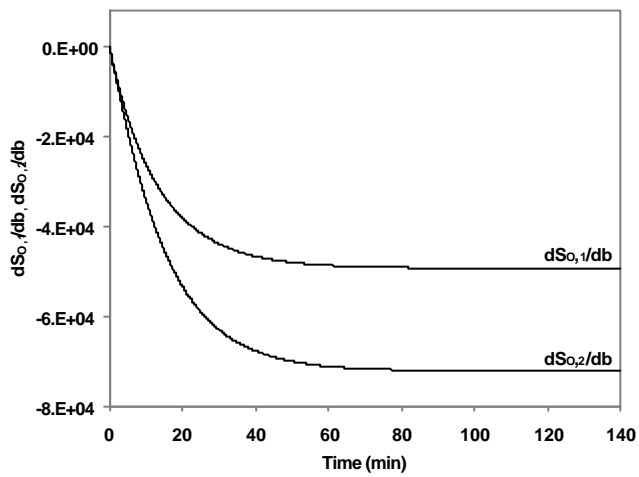
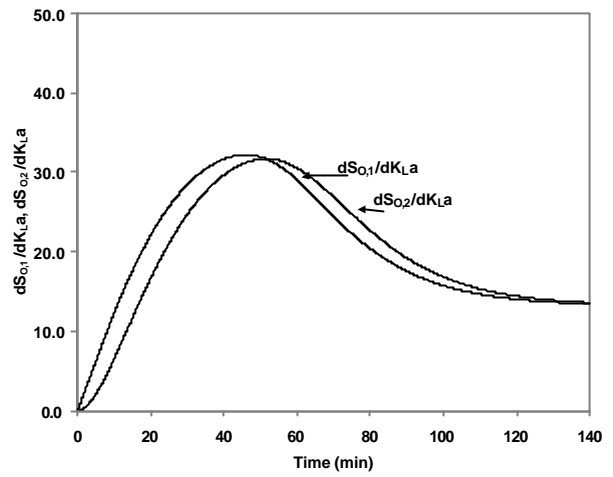
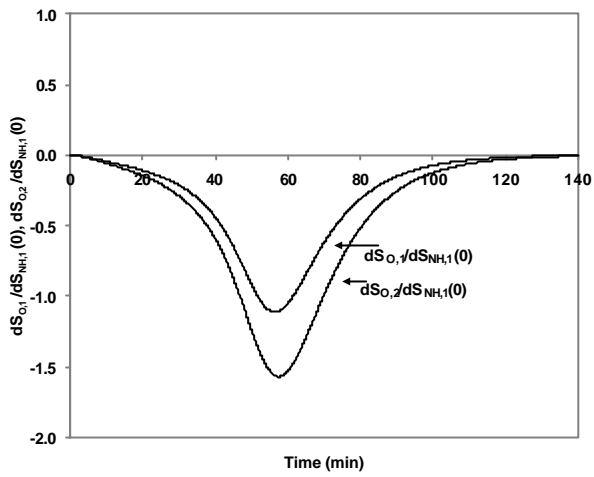
$$\frac{\partial Hp_1(t)}{\partial K_{SA1}} = \frac{2}{14} \frac{\partial S_{NH,1}(t)}{\partial K_{SA1}} \quad (23)$$

For the sensitivity with respect to the initial substrate concentration Eq. 24 replaces Eq. 10.

$$S_{NH,1}(t) = \frac{V_1}{V_1 + V_2} S_{NH,1}(0) - \frac{14}{2} Hp_1(t) \quad (24)$$

Figures of the output sensitivity functions are given below.





Chapter 6

-

Effect of parameter scaling on the Fisher Information Matrix (FIM) and FIM based experimental designs

Chapter 6

Effect of parameter scaling on the Fisher Information Matrix (FIM) and FIM based experimental designs

Abstract – Simple rescaling of parameter units is shown in this study to affect the numerical properties of the Fisher Information Matrix (FIM) and its inverse, the parameter estimation error covariance matrix (COV). Only parameters expressed in time units can be re-scaled usefully, e.g. min to days. Parameter rescaling can be used to the advantage of more reliable covariance assessment because the numerical problems related to inversion of the FIM can be minimised by proper rescaling. However, the effect of rescaling on the FIM also affects the optimal experimental design (OED) methodology based on FIM. In the OED theory different scalar functions (e.g. determinant, condition number, trace) of the FIM are used as measures of the accuracy of the estimated parameters. Different OED criteria can be defined all aiming at reducing the COD. In this study it is shown that most OED-criteria are sensitive to rescaling, with the noticeable exception of the D-criterion, that focuses on a maximisation of the determinant of FIM. It means that the optimal experiments calculated according to an OED-criterion will be different if the model is written in different time units. Obviously, this is not very practical and rescaling should be carried out carefully. This sensitivity to rescaling was most pronounced for the modified E criterion that focuses on a minimisation of the condition number of the FIM with the optimal minimum equal 1. A classic OED example of a simple single substrate batch biodegradation model was re-evaluated and it was found that the theoretically best possible experiment according to this criterion, i.e. modified E criterion = 1, could be obtained just by rescaling of the parameter units. However, the corresponding optimal experiments could not be considered “optimal”, since it is just the result of changing the time units. This work stresses that care should be taken when OED-criteria other than the D-criterion are used to optimise an experimental plan.

1. Introduction

The Fisher Information Matrix (FIM) is the cornerstone in the optimal experimental design (OED) theory, since it summarises information on the measurement errors and parameter sensitivities thereby permitting a quantification of the quality of parameter estimation. Under certain conditions the FIM is equal to the

inverse of the parameter estimation error covariance matrix (COV). This property is basically the rationale for the use of FIM as a suitable characterisation of parameter uncertainty (Goodwin and Payne, 1977; Goodwin, 1987; Walter and Pronzato, 1990, 1999). Different optimal experimental design criteria have been defined to improve the quality of parameter estimation based on scalar functions of the FIM, or in other words the shape of the confidence region (e.g. Goodwin, 1987; Munack, 1989, 1991).

For non-linear models the FIM is per definition parameter dependent and, thereby, the actual matrix elements depend on the actual parameter units. A question that can be asked therefore is whether the OED criteria are dependent on the parameter units (e.g. minutes rather than hours). In this respect it has been stated in literature that OED's based on the D-optimal criterion, which focus on maximisation of the determinant of the FIM, are independent of reparametrisation (Goodwin and Payne, 1977; Walter and Pronzato, 1990 and 1999). However, as far as known, the remaining criteria have not been addressed with respect to the effect of parameter rescaling.

In this study a scaling of parameter units only was intentionally introduced to allow for a more stable numerical inversion of the FIM, as we use it to access the parameter error covariance matrix COV. The condition number (i.e. the ratio between the largest and the smallest eigenvalue of the FIM) is considered as a measure of the "robustness" of the inversion. Because of its central role in optimal experimental design it was further investigated how such scaling of units affects the FIM properties (e.g. the eigenvalues, trace and determinant), and thereby potentially the results of different optimal experimental design approaches. Finally, special attention was paid to effects on the modified E (modE) criterion, which focuses on minimisation of the condition number of FIM.

2. Theoretical background

Parameter estimation typically aims for a minimisation of a weighted sum $J(\underline{p})$ of squared errors between model outputs $\underline{y}(t_i, \underline{p})$ and measured outputs $\underline{y}_m(t_i)$ with the weights \underline{Q}_i and N the number of measurements, also denoted the objective function (Eq. 1). The minimisation is obtained by optimal choice of the parameter vector \underline{p} .

$$J(\underline{p}) = \sum_{i=1}^N \left(\underline{y}(t_i, \underline{p}) - \underline{y}_m(t_i) \right)^T \underline{Q}_i \left(\underline{y}(t_i, \underline{p}) - \underline{y}_m(t_i) \right) \quad (1)$$

For the analysis of the information content with respect to the parameters, the Fisher Information Matrix (FIM) can be used (Eq. 2):

$$\text{FIM} = \sum_{i=1}^N \underline{Y}_p(t_i, \underline{p})^T \underline{Q}_i \underline{Y}_p(t_i, \underline{p}) \quad (2)$$

where $Y_p(t_i, \underline{p})$ denotes the output sensitivity functions with respect to the parameters. The weighting matrix Q_i is typically chosen as the inverse of the measurement error covariance matrix. Then, the FIM is the inverse of the parameter estimation error covariance matrix (COV). Thus, the FIM can be regarded as a summary of the output sensitivity functions and the measurement accuracy, thereby summarising the information concerning the model parameters gained from an experiment. For a more thorough derivation and discussion of the FIM the reader is referred to Chapter 5 and e.g. Munack (1989 and 1991).

Several scalar functions of FIM have been defined as a measure of the quality of the estimated parameters, e.g. the determinant, condition number and trace. They play key roles in the theory of optimal experimental design (OED). Different OED criteria have been defined based on these scalar functions which, in different ways, give measures of the shape of the confidence region (e.g. Goodwin, 1987; Munack, 1989 and 1991; Walter and Pronzato, 1990 and 1999). Basically, these OED criteria all aim at a reduction of the COV of the parameter estimates (i.e. maximisation of FIM) by focusing on different conditions. Once the constraints on the experiment and the OED criterion have been specified, the experimental design simply reduces to a constrained optimisation problem. Note that *a priori* knowledge of the model parameters is both advisable and unavoidable since the FIM is parameter dependent (Goodwin, 1977; Walter and Pronzato 1990).

A – optimal criterion : min Tr(FIM⁻¹)

In this criterion the focus is on a minimisation of the trace, and thereby the sum of eigenvalues, i.e. the squares of the lengths of the axes of the confidence ellipsoids, of the inverse FIM (i.e. COV). This is equivalent to minimisation of the arithmetic average of the parameter errors. Note that this criterion is based on an inversion of the FIM. Thus, this may lead to numerical problems in case the FIM is ill-conditioned, i.e. singular.

modA – optimal criterion : max Tr(FIM)

This criterion is similar to the A criterion, only is the trace of FIM maximised. The problem with this criterion is, however, that in case an unidentifiable experiment is conducted, i.e. a case where FIM becomes singular and one of the eigenvalues becomes zero, which means that the confidence region goes to infinite in a certain direction, the trace may still be optimised and the problem of unidentifiability will not be noticed (Goodwin and Payne, 1977). This is less of a problem with the A criterion since an inversion will not be possible if FIM becomes singular and the problem of unidentifiability will thereby be exposed.

D - optimal criterion : max Det(FIM)

Here it is aimed to maximise the determinant of FIM. The determinant is proportional to the volume of the confidence region. Thus, by maximising Det(FIM) one minimises the volume of the confidence ellipsoids, and, correspondingly, one minimises the geometric average of the parameter errors. Moreover, D –

optimal experiments possess the property of being invariant with respect to any rescaling of the parameters, as mentioned above (Goodwin and Payne, 1977; Walter and Pronzato, 1990 and 1999).

E – optimal criterion : max $\lambda_{\min}(\text{FIM})$

The lengths of the axes of the confidence ellipsoids are proportional to the inverse of the square roots of the corresponding eigenvalues. The E criterion maximises the smallest eigenvalue of the FIM and thereby minimises the length of the largest axis of the confidence ellipsoids. Thus, this design aims at minimising the largest parameter error and thereby at maximising the distance from the singular, unidentifiable, case.

modE – optimal criterion : min $\lambda_{\max}(\text{FIM})/\lambda_{\min}(\text{FIM})$

This criterion is also related to the shape of the confidence region. Here, the focus is on a minimisation of the condition number, i.e. the ratio between the largest and the smallest eigenvalue. The minimum of this ratio is 1 indicating the case where the shape of the confidence ellipsoids is a (hyper)sphere. The ratio $\lambda_{\max}(\text{FIM})/\lambda_{\min}(\text{FIM})$ expresses the stiffness of the FIM. The more important the stiffness becomes, the more problematic it becomes numerically to invert FIM until finally a singular matrix is obtained ($\lambda_{\min}(\text{FIM})=0$) and the information content becomes zero, i.e. the ratio is infinite.

3. Scaling of FIM

The model applied to study and illustrate the effect of scaling was a simple one step Monod model describing the heterotrophic degradation of a readily biodegradable substrate S_S and the resulting exogenous oxygen uptake rate, $r_{O,ex}$ (Eq. 3 and 4). Note further that the area under the $r_{O,ex}$ profile divided with the factor $(1 - Y_H)$ is a measure of the initially added substrate $S_S(0)$.

$$\frac{dS_S}{dt} = - \frac{\mu_{\max H} \cdot X}{Y_H} \frac{S_S}{K_S + S_S} \quad (3)$$

$$r_{O,ex} = (1 - Y_H) \frac{\mu_{\max H} \cdot X}{Y_H} \frac{S_S}{K_S + S_S} \quad (4)$$

Fig. 1 illustrates this example where the applied parameter values and units were:

- $\mu_{\max H}$ maximum specific growth rate (min^{-1}); $2.64 \cdot 10^{-4} \text{ min}^{-1}$
- Y_H yield coefficient (mg COD(biomass)/mg COD(substrate)); 0.67 mg COD/mg COD
- S_S substrate (mg COD(substrate)/l), 34 mg COD/l
- X biomass (mg COD(biomass)/l), 4000 mg COD/l
- K_S half saturation coefficient (mg COD(substrate)/l), 1 mg COD/l

For the Monod model given in Eq. 3 - 4, it was found that only a rescaling on the time units, i.e. the specific growth rate and time itself, has an effect on the condition number of the FIM. A parameter scaling of either the half saturation coefficient (K_S), the substrate concentration (S_S), the yield (Y_H) or the biomass concentration (X) requires that the values of all these remaining parameters are scaled as well. However, such scaling cancels itself out (e.g. since the Monod factor $\frac{S_S}{K_S + S_S}$ is dimensionless), and can therefore not affect the condition number.

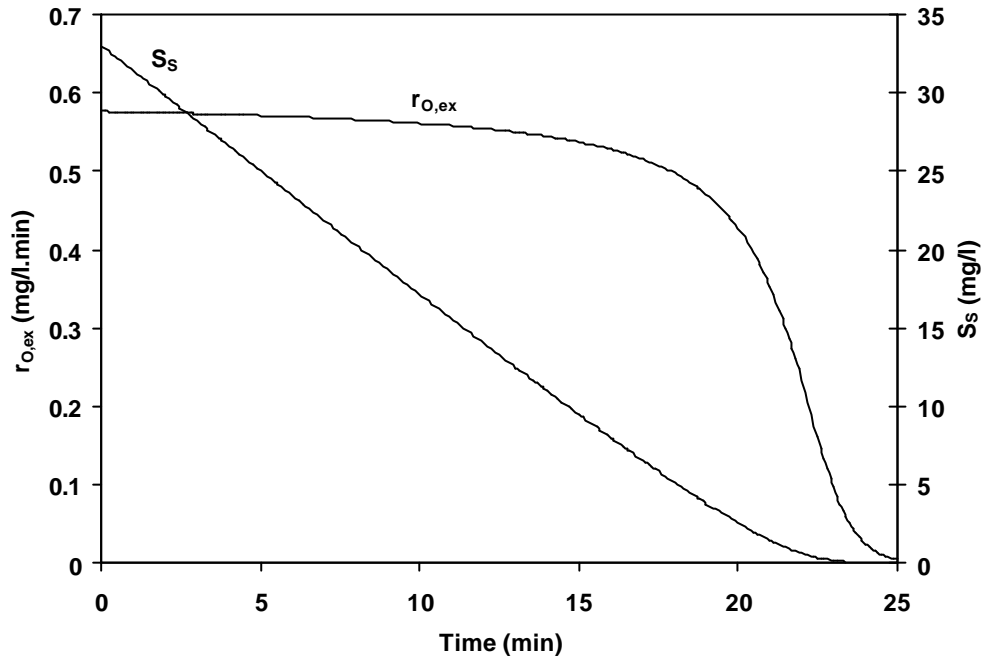


Figure 1. Profile of S_S and $r_{O,ex}$ for case study

The approach of scaling is first outlined in general below. Eq. 5 indicates a typical sensitivity function of an output y with respect to a parameter p as a function of a specific growth rate μ_{max} .

$$\frac{d\left(\frac{\partial y}{\partial p}\right)}{dt} = f(\mathbf{m}_{max}, \dots) \quad (5)$$

A scaling factor α is introduced in Eq. 6 to scale μ_{max} and time to new time units defined as $t' = \frac{t}{\alpha}$ and

$$\mathbf{m}'_{max} = \alpha \cdot \mathbf{m}_{max}.$$

$$\frac{d\left(\frac{\partial y}{\partial p}\right)}{dt'} = f(\mathbf{m}'_{max}, \dots) \quad (6)$$

Thus, it is now the purpose to seek the minimum condition number of the FIM by a change of the time units

allowing for the most stable numerical FIM inversion. Instead of a trial and error approach, a numerical search algorithm was used to find a scaling factor that gave the smallest possible condition number. However, in order to apply an optimisation routine the simulation time must be kept constant. Thus, by division with α on both sides of Eq. 6, the original time unit can be kept in the model and the output y together with its scaled sensitivity differential equations (such as Eq. 7) can be solved for different values of α . Hence, an optimisation routine can be used to search for the best value of α via minimisation of the condition number.

$$\frac{d\left(\frac{\partial y}{\partial p}\right)}{\mathbf{a} \cdot dt'} = \frac{d\left(\frac{\partial y}{\partial p}\right)}{dt} = \frac{1}{\mathbf{a}} \cdot f(\mathbf{m}'_{\max}, \dots) \quad (7)$$

Note that the scaling in Eq. 7 appears explicitly w.r.t. μ_{\max} but implicitly on $\frac{dy}{dt}$, i.e. the values and shape of $\frac{dy}{dt}$ stays the same whereas μ_{\max} is changing with α . Note that in case of a double Monod model with two specific growth rates, the scale α must be the same for both μ_{\max} parameters, since only one time unit can be used in a model.

4. Results

4.1. Scaling of FIM applied on the single Monod case study

The case study is based on a simple illustrative example, slightly modified from Vanrolleghem *et al.* (1995), where only $r_{O,ex}$ is measured to characterise heterotrophic degradation of the substrate S_S (Eq. 3 - 4). For the calculation of the FIM only the sensitivities of $r_{O,ex}$ with respect to two parameters, $\mu_{\max H}$ and K_S , are considered. Eq. 8 shows the sensitivity function of $r_{O,ex}$ with respect to $\mu_{\max H}$ (Vanrolleghem and Dochain, 1998) and Eq. 9 - 11 introduces the scaling factor α , as in Eq. 6 - 7. Eq. 12 gives the sensitivity function of K_S (Vanrolleghem and Dochain, 1998) and Eq. 13 - 15 give the resulting scaled versions of the equations.

Sensitivity function of $r_{O,ex}$ with respect to $\mu_{\max H}$:

$$\frac{\partial r_{O,ex}(t)}{\partial \mathbf{m}_{\max H}} = -(1 - Y_H) \frac{d}{dt} \frac{\partial S_S(t)}{\partial \mathbf{m}_{\max H}} = \frac{(1 - Y_H) \cdot X}{Y_H} \left(\frac{S_S(t)}{K_S + S_S(t)} + \frac{\mathbf{m}_{\max H} \cdot K_S \cdot \frac{\partial S_S(t)}{\partial \mathbf{m}_{\max H}}}{(K_S + S_S(t))^2} \right) \quad (8)$$

Rescaling to new time units:

$$\frac{\partial r_{O,ex}(t')}{\partial (\dot{\mathbf{m}}_{maxH})} = -(1 - Y_H) \frac{d}{dt'} \frac{\partial S_S(t')}{\partial (\dot{\mathbf{m}}_{maxH})} = \frac{(1 - Y_H) \cdot X}{Y_H} \left(\frac{S_S(t')}{K_S + S_S(t')} + \frac{\dot{\mathbf{m}}_{maxH} \cdot K_S \cdot \frac{\partial S_S(t')}{\partial (\dot{\mathbf{m}}_{maxH})}}{(K_S + S_S(t'))^2} \right) \quad (9)$$

Division with α :

$$\frac{1}{\mathbf{a}} \frac{\partial r_{O,ex}(t')}{\partial (\dot{\mathbf{m}}_{maxH})} = -(1 - Y_H) \frac{1}{\mathbf{a}} \frac{d}{dt'} \frac{\partial S_S(t')}{\partial (\dot{\mathbf{m}}_{maxH})} = \frac{1}{\mathbf{a}} \frac{(1 - Y_H) \cdot X}{Y_H} \left(\frac{S_S(t')}{K_S + S_S(t')} + \frac{\dot{\mathbf{m}}_{maxH} \cdot K_S \cdot \frac{\partial S_S(t')}{\partial (\dot{\mathbf{m}}_{maxH})}}{(K_S + S_S(t'))^2} \right) \quad (10)$$

Time units of $\frac{dS_S}{dt}$ back to original units to allow for optimisation of α :

$$\frac{1}{\mathbf{a}} \frac{\partial r_{O,ex}(t)}{\partial (\dot{\mathbf{m}}_{maxH})} = -(1 - Y_H) \frac{d}{dt} \frac{\partial S_S(t)}{\partial (\dot{\mathbf{m}}_{maxH})} = \frac{1}{\mathbf{a}} \left(\frac{(1 - Y_H) \cdot X}{Y_H} \left(\frac{S_S(t)}{K_S + S_S(t)} + \frac{\dot{\mathbf{m}}_{maxH} \cdot K_S \cdot \frac{\partial S_S(t)}{\partial (\dot{\mathbf{m}}_{maxH})}}{(K_S + S_S(t))^2} \right) \right) \quad (11)$$

Sensitivity function of $r_{O,ex}$ with respect to K_S :

$$\frac{\partial r_{O,ex}(t)}{\partial K_S} = -(1 - Y_H) \frac{d}{dt} \frac{\partial S_S(t)}{\partial K_S} = \frac{(1 - Y_H) \cdot \dot{\mathbf{m}}_{maxH} \cdot X}{Y_H} \cdot \left(\frac{K_S \cdot \frac{\partial S_S(t)}{\partial K_S} - S_S(t)}{(K_S + S_S(t))^2} \right) \quad (12)$$

Rescaling to new time units:

$$\frac{\partial r_{O,ex}(t')}{\partial K_S} = -(1 - Y_H) \frac{d}{dt'} \frac{\partial S_S(t')}{\partial K_S} = \frac{(1 - Y_H) \cdot \dot{\mathbf{m}}_{maxH} \cdot X}{Y_H} \cdot \left(\frac{K_S \cdot \frac{\partial S_S(t')}{\partial K_S} - S_S(t')}{(K_S + S_S(t'))^2} \right) \quad (13)$$

Division with α :

$$\frac{1}{\mathbf{a}} \frac{\partial r_{O,ex}(t')}{\partial K_S} = -(1 - Y_H) \frac{1}{\mathbf{a}} \frac{d}{dt'} \frac{\partial S_S(t')}{\partial K_S} = \frac{1}{\mathbf{a}} \frac{(1 - Y_H) \cdot \dot{\mathbf{m}}_{maxH} \cdot X}{Y_H} \cdot \left(\frac{K_S \cdot \frac{\partial S_S(t')}{\partial K_S} - S_S(t')}{(K_S + S_S(t'))^2} \right) \quad (14)$$

Time units of $\frac{dS_S}{dt}$ back to original units to allow for optimisation of α :

$$\frac{1}{\mathbf{a}} \frac{\partial r_{O,ex}(t)}{\partial K_S} = -(1-Y_H) \frac{d}{dt} \frac{\partial S_S(t)}{\partial K_S} = \frac{(1-Y_H) \cdot \mathbf{m}_{maxH} \cdot X}{Y_H} \cdot \left(\frac{K_S \cdot \frac{\partial S_S(t)}{\partial K_S} - S_S(t)}{(K_S + S_S(t))^2} \right) \quad (15)$$

4.2. Optimisation of scaling factor

Eq. 16 illustrates the original FIM of this example, with a condition number ($\lambda_{max}/\lambda_{min}$) of $8.05 \cdot 10^8$ (see Table 1).

$$FIM_{original} = \begin{bmatrix} \sum_{i=1}^N \frac{\partial r_{O,ex}}{\partial \mathbf{m}_{maxH}} \cdot \frac{\partial r_{O,ex}}{\partial \mathbf{m}_{maxH}} & \sum_{i=1}^N \frac{\partial r_{O,ex}}{\partial K_S} \cdot \frac{\partial r_{O,ex}}{\partial \mathbf{m}_{maxH}} \\ \sum_{i=1}^N \frac{\partial r_{O,ex}}{\partial K_S} \cdot \frac{\partial r_{O,ex}}{\partial \mathbf{m}_{maxH}} & \sum_{i=1}^N \frac{\partial r_{O,ex}}{\partial K_S} \cdot \frac{\partial r_{O,ex}}{\partial K_S} \end{bmatrix} = \begin{bmatrix} 3.0133 \cdot 10^8 & -5837 \\ -5837 & 0.15051984 \end{bmatrix} \quad (16)$$

The condition number was subsequently minimised by optimising the value of the scaling factor α . As a result a condition number as low as 14.018 was obtained for a α value of 44750. This scaling guarantees a more stable matrix inversion. From Table 1 it is clear that this reduction in condition number seems mainly to be caused by a reduction of λ_{max} . Correspondingly, the actual values of the FIM properties Det(FIM), Tr(FIM) and Tr(FIM⁻¹) change.

Table 1. Properties of original and scaled FIM

α	Det(FIM)	λ_{min}	λ_{max}	$\lambda_{max}/\lambda_{min}$	Tr(FIM)	Tr(FIM ⁻¹)
1	$1.13 \cdot 10^7$	0.037	$3.01 \cdot 10^8$	$8.05 \cdot 10^8$	$3.01 \cdot 10^8$	26.72
44750	$5.63 \cdot 10^{-3}$	0.020	0.281	14.018	0.300	53.45

The resulting FIM is given in Eq. 17 (according to Eq. 11 and 15). From Eq. 17 and 18 it is clear that only these FIM elements in which the sensitivity function of μ_{maxH} is involved, are affected by the scaling.

$$FIM_{scaled} = \begin{bmatrix} \sum_{i=1}^N \frac{1}{\mathbf{a}^2} \frac{\partial r_{O,ex}}{\partial \mathbf{m}_{maxH}} \cdot \frac{\partial r_{O,ex}}{\partial \mathbf{m}_{maxH}} & \sum_{i=1}^N \frac{1}{\mathbf{a}} \frac{\partial r_{O,ex}}{\partial K_S} \cdot \frac{\partial r_{O,ex}}{\partial \mathbf{m}_{maxH}} \\ \sum_{i=1}^N \frac{1}{\mathbf{a}} \frac{\partial r_{O,ex}}{\partial \mathbf{m}_{maxH}} \cdot \frac{\partial r_{O,ex}}{\partial K_S} & \sum_{i=1}^N \frac{\partial r_{O,ex}}{\partial K_S} \cdot \frac{\partial r_{O,ex}}{\partial K_S} \end{bmatrix} = \begin{bmatrix} 0.15047296 & -0.13045455 \\ -0.13045455 & 0.15051984 \end{bmatrix} \quad (17)$$

$$= \begin{bmatrix} \frac{1}{\mathbf{a}^2} \cdot 3.0133 \cdot 10^8 & -\frac{1}{\mathbf{a}} \cdot 5837 \\ -\frac{1}{\mathbf{a}} \cdot 5837 & 0.15051984 \end{bmatrix}$$

(18)

4.3. Effect of scaling on OED criteria

Next it was investigated, via symbolic manipulation (MAPLE V, Waterloo Software), how the scaling of the FIM (Eq. 18) affects the different optimal experimental design (OED) criteria.

For simplicity the factor $\sum_{i=1}^N \frac{\partial r_{O,ex}}{\partial \mathbf{m}_{maxH}} \frac{\partial r_{O,ex}}{\partial \mathbf{m}_{maxH}}$ is denoted A, $\sum_{i=1}^N \frac{\partial r_{O,ex}}{\partial \mathbf{m}_{maxH}} \frac{\partial r_{O,ex}}{\partial K_S}$ is denoted B and the factor $\sum_{i=1}^N \frac{\partial r_{O,ex}}{\partial K_S} \frac{\partial r_{O,ex}}{\partial K_S}$ is called C. Thus Eq. 17 simplifies to Eq. 19:

$$\text{FIM}_{\text{scaled}} = \begin{bmatrix} \frac{1}{\mathbf{a}^2} A & \frac{1}{\mathbf{a}} B \\ \frac{1}{\mathbf{a}} B & C \end{bmatrix} \quad (19)$$

The corresponding eigenvalues, determinant and trace of this matrix are given in Eq. 20, 21 and 22 respectively.

$$\mathbf{l}_{1,2} = \frac{A + \mathbf{a}^2 C \pm \sqrt{A^2 - 2\mathbf{a}^2 AC + \mathbf{a}^4 C^2 + 4\mathbf{a}^2 B^2}}{2\mathbf{a}^2} \quad (20)$$

$$\text{Det}(\text{FIM}_{\text{scaled}}) = \frac{1}{\mathbf{a}^2} (AC - B^2) \quad (21)$$

$$\text{Tr}(\text{FIM}_{\text{scaled}}) = \frac{1}{\mathbf{a}^2} A + C \quad (22)$$

Finally, the effect of the scaling on the COV matrix (i.e. $\text{FIM}_{\text{scaled}}^{-1}$) and the $\text{Tr}(\text{COV})$ is given in Eq. 23 - 24.

$$\text{COV}_{\text{scaled}} = \begin{bmatrix} \mathbf{a}^2 \frac{C}{AC - B^2} & \mathbf{a} \frac{B}{AC - B^2} \\ \mathbf{a} \frac{B}{AC - B^2} & \frac{A}{AC - B^2} \end{bmatrix} \quad (23)$$

$$\text{Tr}(\text{FIM}_{\text{scaled}}^{-1}) = \mathbf{a}^2 \frac{C}{AC - B^2} + \frac{A}{AC - B^2} \quad (24)$$

From Eq. 20 - 24 it appears that only the optimal experimental design w.r.t. the D-criterion, i.e. maximising the Det(FIM), will remain unaffected by the scaling, in accordance with Goodwin and Payne (1977); Walter and Prozato (1990, 1999). The value of the Det(FIM) changes with α but the location of the optimum experiment does not, see Eq. 21. For the remaining criteria, which involve the eigenvalues and trace (A-, modA-, E- and modE-criteria), the scaling factor α appears in a non-linear way in the resulting expressions. Consequently, it may be expected that the resulting optimal experiments are different from the optimal experiments calculated for the original time units (without a scaling factor, i.e $\alpha = 1$). From Eq. 23 it can be seen that the COV of the original parameter values can readily be obtained by dividing e.g. the COV11 element with α^2 .

In the study of Vanrolleghem *et al.* (1995) the degree of freedom for the OED was the initial substrate concentration that should be chosen in an optimal way. For this particular case, it was thoroughly investigated whether the scaling of the FIM affects the properties of the FIM and thereby the optimal experimental design results, as indicated in Eq. 20 - 24. The optimal initial substrate concentrations obtained via the different optimal experimental design criteria for the initial and optimal α value (corresponding to the lowest condition number, see Table 1) are given in Table 2.

Table 2. Effect of scaling on the optimal initial substrate concentration considering different OED criteria

Optimal experimental design criteria					
α	A	modA	D	E	modE
1	33.42	35.21	34.37	33.42	2.35
44750	34.24	34.51	34.37	34.21	40.05

These results confirm that the D criterion based OED is unaffected by the scaling (Eq. 21), whereas the other criteria are affected, resulting in slightly different experiments. Thus, it is clear that the D criterion is the most robust experimental design w.r.t. scaling of units. Scaling is especially critical when applying the modE criterion, as it results in a radically different experiment especially in the absence of scaling but also when the scaling of the time units is introduced. Notice though that both for $\alpha = 1$ and $\alpha = 44750$ the corresponding experiments will yield the best condition numbers possible. Therefore, the most reliable matrix inversion will be achieved (for the given time unit). Special focus will be paid to the modE criterion below.

4.4. Focus on modE criterion

Returning to the symbolic manipulation result (Eq. 19 – 20) the expression for α can be solved for a condition number of 1 (modE criteria) which is the ultimate value one can achieve. Thus, if α full-fills Eq.

25 a condition number of 1 is obtained.

$$\mathbf{a} = \pm \frac{\sqrt{AC - 2B^2 \pm 2\sqrt{-ACB^2 + B^4}}}{A} \quad (25)$$

Thus, there appear to be four possible values of α ; two positive and two negative values respectively, for which a condition number of 1 can theoretically be obtained. Evidently, only positive real scaling values are relevant.

For the example illustrated above, the solution to Eq. 25 are complex numbers of $-1.25 \cdot 10^5 \pm 2.19 \cdot 10^5 \cdot i$ (the minimum of $\lambda_{\max}/\lambda_{\min}$ was 14.018, see Table 1). However, for other values of A, B and C it is possible that the optimal condition number of 1 can be achieved. To illustrate the approach, A, B and C-values were changed by varying the initial substrate concentration in the simulated experiments. Indeed, different $S_S(0)$ values lead to different trajectories of the sensitivity functions and, consequently, lead to other A, B and C entries in the FIM. Contour plots of the condition number as function of the initial substrate concentration $S_S(0)$ and the scaling factor α are given in Fig. 2. A minimum condition number of 3.63 was reached for a $S_S(0)$ concentration of 39.69 mg/l. The optimal scaling factor α was in this case equal to 66730. Thus, with a FIM defined by the sensitivity functions of $r_{O,ex}$ with respect to the parameters $\mu_{\max H}$ and K_S and with the initial substrate concentration as degree of freedom, the minimum value of 1 for the condition number could not be reached. Still, a rather significant reduction of the condition number was possible with scaling on the time units alone.

The minimum of the modE criterion implies that in the neighbourhood of the parameter vector a complete decorrelation between the parameter estimates is achieved, i.e. the non-diagonal elements of the COV matrix are insignificant (Munack, 1991). It is a well-known phenomenon that the Monod parameters $\mu_{\max H}$ and K_S are correlated (Holmberg, 1982) and, apparently, it is not possible to break this correlation completely when the experimental degree of freedom is the initial substrate concentration $S_S(0)$. In this case it could indeed be tested via a standard statistical test for significance of correlation that the correlation coefficient between $\mu_{\max H}$ and K_S was significant at a standard 5% test level.

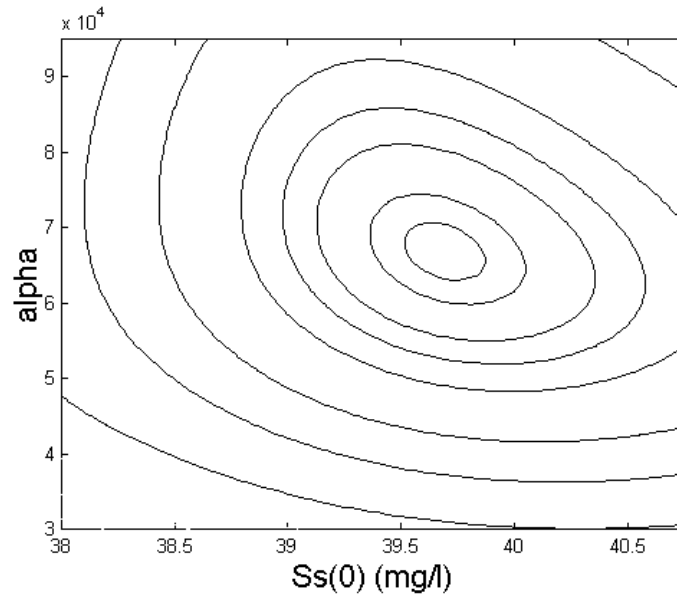


Figure 2. The condition number, $\lambda_{\max}/\lambda_{\min}$, as function of $S_S(0)$ and scaling factor α for the case where FIM includes sensitivity functions of $r_{O,ex}$ with respect to $\mu_{\max H}$ and K_S . Minimum is obtained for $\lambda_{\max}/\lambda_{\min} = 3.63$, $\alpha = 66730$ and $S_S(0) = 39.69$ mg COD/l.

Suppose next that the FIM is defined by the sensitivity functions of $r_{O,ex}$ with respect to $\mu_{\max H}$ and $S_S(0)$ instead of $\mu_{\max H}$ and K_S , i.e. stepping from a $\mu_{\max H}$ and K_S estimation problem into a $\mu_{\max H}$ and $S_S(0)$ estimation problem. These parameters are typically non-correlated. In this case the minimum condition number of 1 could be readily obtained by optimisation of the initial substrate concentration $S_S(0)$ and the scaling factor α . Fig. 3 - 4 illustrate the contour plots of the condition number as function of the values of $S_S(0)$ and α . Two positive real minima for α were found, according to Eq. 25, for which a condition number of 1 was obtained (see Table 3). These minima were obtained with initial substrate concentrations of 2.45 mg/l and 41.13 mg/l respectively.

However, a closer look at the $r_{O,ex}$ profiles corresponding to these two minima indicates that they are not very optimal for parameter estimation (Fig. 5 and 6). In the case of an initial substrate concentration of 2.45 mg/l (Fig. 5) the $r_{O,ex}$ profile does not reach a plateau and thereby contains little information on $\mu_{\max H}$. On the contrary, with an initial substrate addition of 41.13 mg/l (Fig. 6) the corresponding optimal $r_{O,ex}$ is not terminated within the experimental time. Thus, in this case the information on $S_S(0)$ does not seem sufficient since this is related to the area under the $r_{O,ex}$ profile which becomes hard to assess from such data. The FIM characteristics and the corresponding COV are given in Table 3 and Table 4.

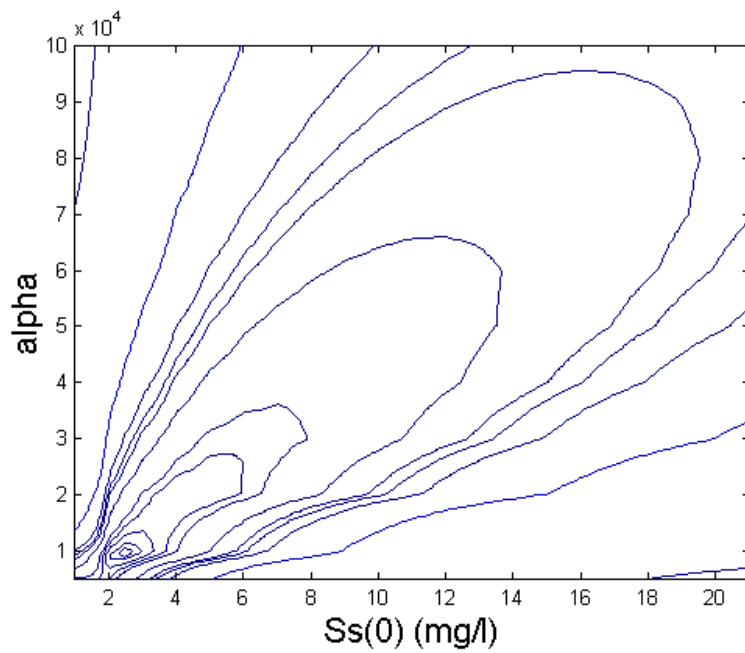


Figure 3. The condition number, $\lambda_{\max} \backslash \lambda_{\min}$, as function of $S_s(0)$ and scaling factor α for the case where FIM includes sensitivity functions of $r_{O,ex}$ with respect to $\mu_{\max H}$ and $S_s(0)$. Minimum is obtained for $\lambda_{\max} \backslash \lambda_{\min} = 1$, $\alpha = 9594$ and $S_s(0) = 2.45$ mg COD/l

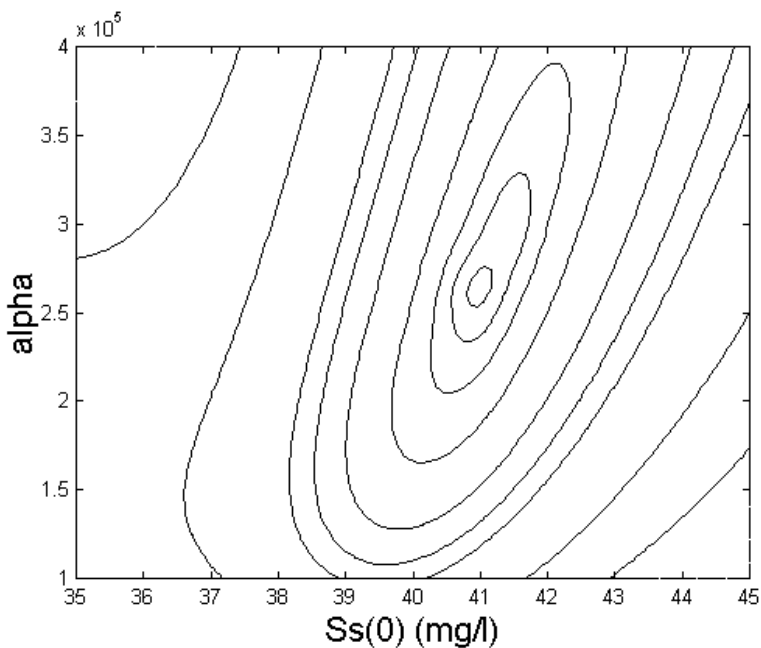


Figure 4. The condition number, $\lambda_{\max} \backslash \lambda_{\min}$, as function of $S_s(0)$ and scaling factor α for the case where FIM includes sensitivity functions of $r_{O,ex}$ with respect to $\mu_{\max H}$ and $S_s(0)$. Minimum is obtained for $\lambda_{\max} \backslash \lambda_{\min} = 1$, $\alpha = 273374$ and $S_s(0) = 41.13$ mg COD/l

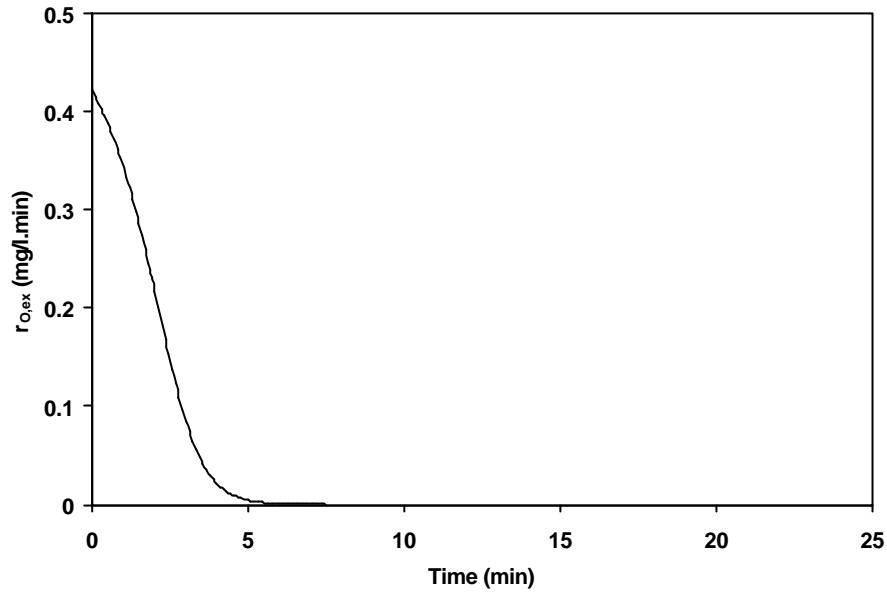


Figure 5. $r_{O,ex}$ profile of optimal experiment according to $ModE=1$, $S_S(0)=2.45$ mg COD/l

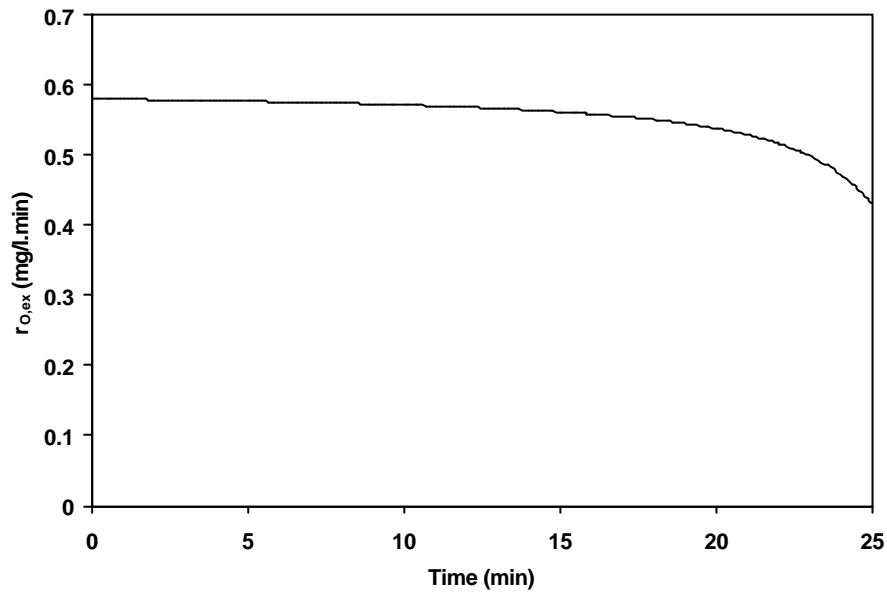


Figure 6. $r_{O,ex}$ profile of optimal experiment according to $ModE=1$, $S_S(0)=41.13$ mg COD/l

Table 3 Properties of original and scaled FIM in case where FIM is defined by the sensitivity function of $r_{O,ex}$ with respect to μ_{maxH} and $S_S(0)$.

$S_S(0)$	α	Det(FIM)	λ_{min}	λ_{max}	$\lambda_{max}/\lambda_{min}$	Tr(FIM)	Tr(FIM ⁻¹)
2.45	1	$9.8 \cdot 10^4$	0.03263	$3.0 \cdot 10^6$	$9.2 \cdot 10^7$	$3.0 \cdot 10^6$	30.64
	9594	1.0×10^{-3}	0.03263	0.03263	1	0.065	61.29
41.13	1	$1.1 \cdot 10^5$	0.001234	$9.2 \cdot 10^7$	$7.5 \cdot 10^{10}$	$9.2 \cdot 10^7$	810.65
	273374	1.5×10^{-6}	0.001234	0.001234	1	$2.5 \cdot 10^{-3}$	1621

Table 4 Properties of original and scaled COV in case where FIM is defined by the sensitivity function of $r_{O,ex}$ with respect to μ_{maxH} and $S_S(0)$.

$S_S(0)$	α	COV11	COV12	COV22
2.45	1	$3.33 \cdot 10^{-7}$	$7.41 \cdot 10^{-12}$	30.64
	9594	30.64	$7.11 \cdot 10^{-8}$	30.64
41.13	1	1.0810^{-8}	$3.63 \cdot 10^{-10}$	810.65
	273374	810.65	$9.92 \cdot 10^{-5}$	810.65

From Table 3 it is clear that the $ModE=1$ is reached by a decrease of λ_{max} down to the value of λ_{min} . This is corresponding to an increase in the actual value of COV11 related to μ_{maxH} . Thus, in both cases we are increasing the actual value of the covariance on μ_{maxH} to the one of $S_S(0)$. Apparently, there are two points where $modE=1$ is possible, the first one at $S_S(0) = 2.45$ and the second one with $S_S(0) = 41.13$, where the COV22 related to $S_S(0)$ is much larger. The latter seems intuitively right considering Fig. 5 - 6, since the information on $S_S(0)$ is not complete. Further, the $Det(FIM)$ is a measure for the generalised variance and is largest for $S_S(0) = 2.45$. Thus, the variance is smallest in this case, as verified in Table 4. Finally, it was again tested via a standard statistical test that the correlation between $S_S(0)$ and μ_{maxH} is insignificant at a 5% test level.

It should be noted here that the optimal $S_S(0)$ of 39.69 mg/l in the case where FIM was calculated on the basis of sensitivity functions with respect to μ_{maxH} and K_S (see above) also resulted in a $r_{O,ex}$ profile that was not terminated and thereby contained insufficient information on K_S . Here too the minimum condition number of 3.63 was mainly obtained by a decrease of λ_{max} with corresponding increase of COV1. Similar observations with the $modE$ criterion were done by Vanrolleghem *et al.* (1995).

The two eigenvalues are given as function of the scaling factor in Fig. 7 and 9 and the evolution of COV as function of the scaling is given in Fig. 8 and 10. These figures confirm that the largest initial eigenvalue is reduced to the value of the smallest one to obtain $ModE = 1$, and, furthermore, that this takes place with a corresponding increase in COV11. Obviously what happens is that the confidence ellipsoid approaches a sphere. However this does not take place due to a decrease of parameter variance but as a results of covariance increase, which is the opposite of what is typically aimed for in OED.

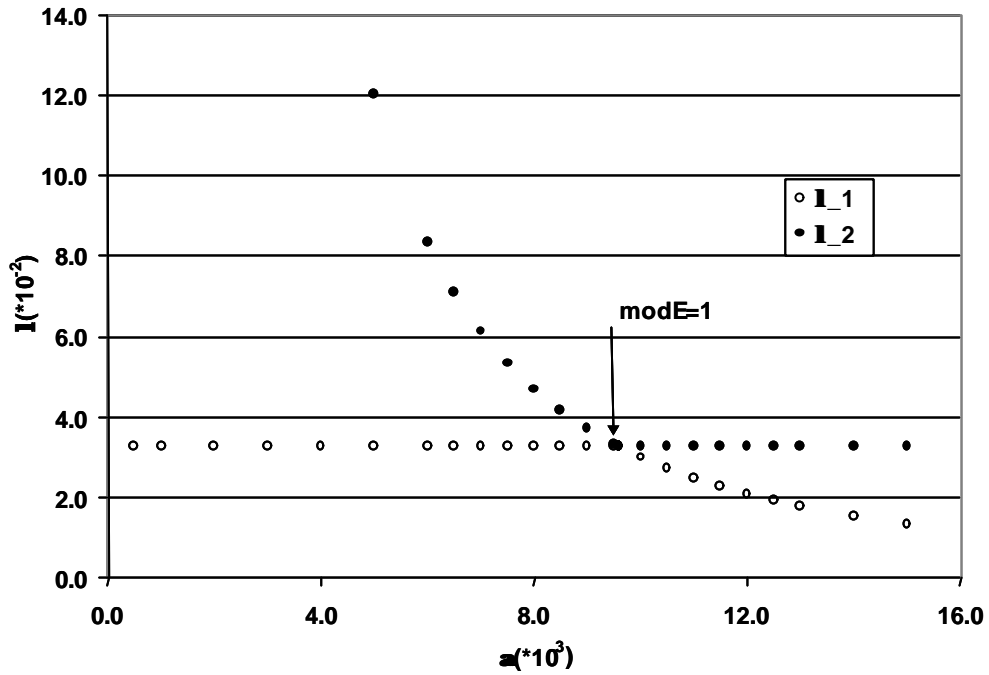


Figure 7. The eigenvalues λ_1 and λ_2 as function of the scaling factor α for $S_S(0) = 2.45$ mg COD/l

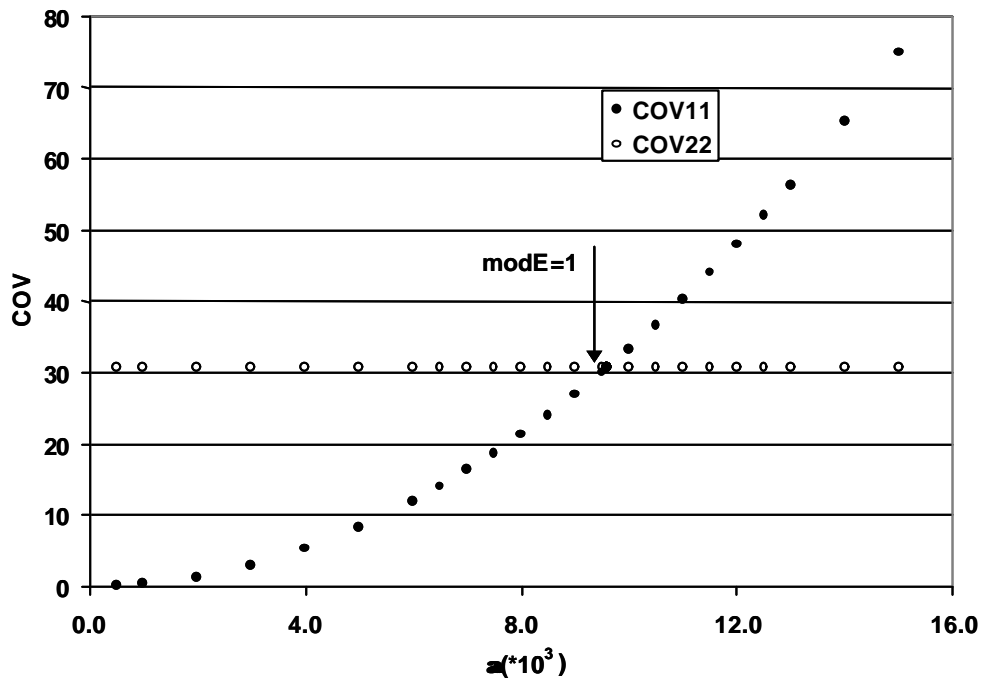


Figure 8. The COV as function of the scaling factor α for $S_S(0) = 2.45$ mg COD/l

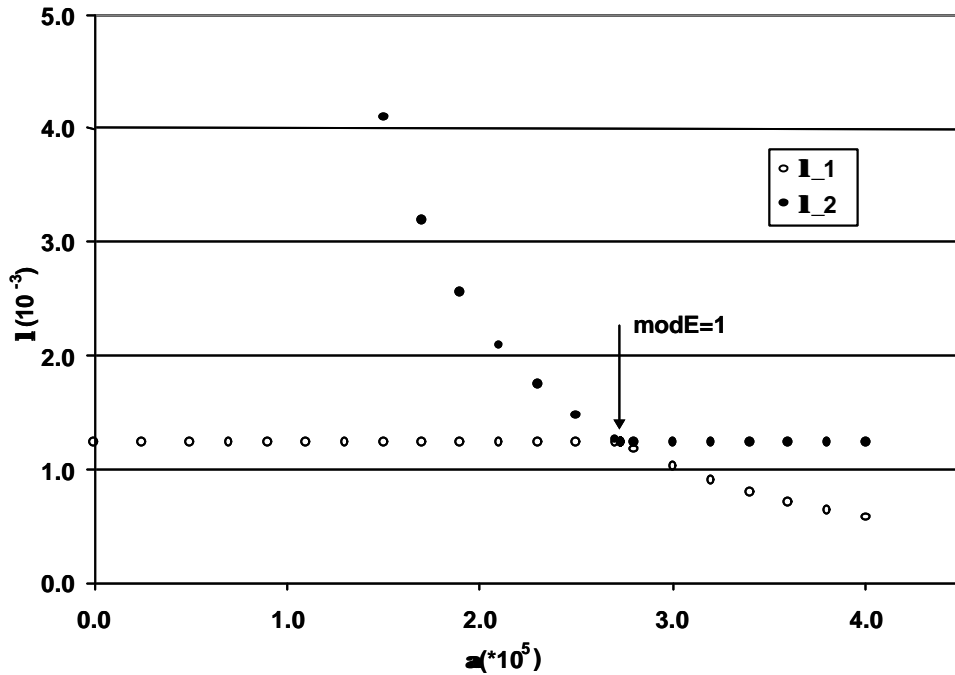


Figure 9 The eigenvalues λ_1 and λ_2 as function of the scaling factor α for $S_5(0) = 41.13$ mg COD/l

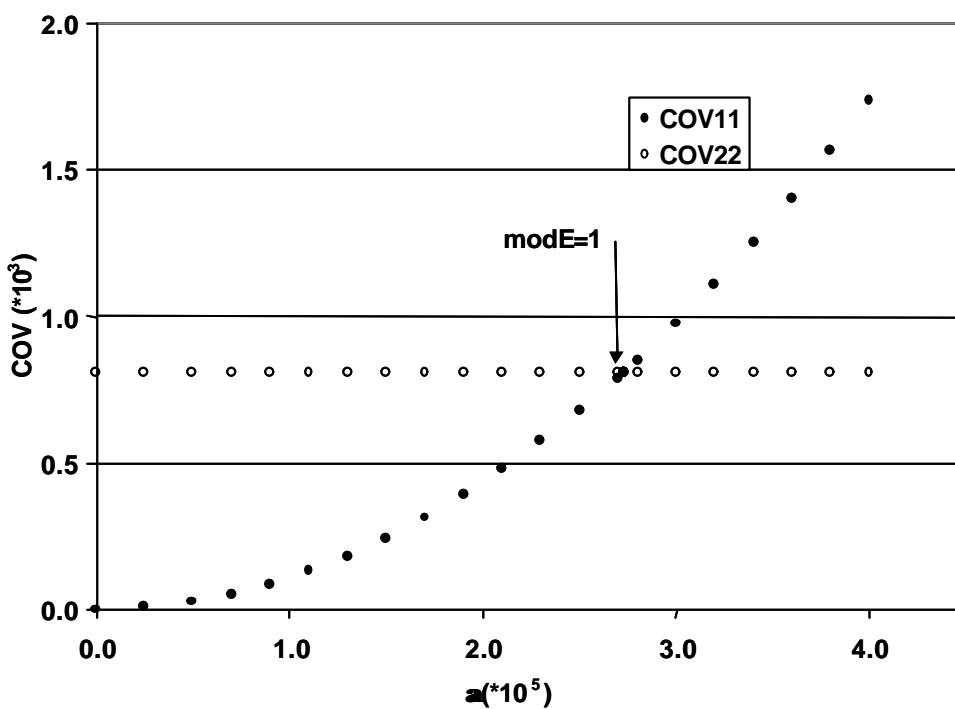


Figure 10. The COV as function of the scaling factor α for $S_5(0) = 41.13$ mg COD/l. **Discussion**

By definition, the Fisher Information Matrix (FIM) depends on the model parameters and their actual values. In this study a simple single Monod model was used as case study in the investigation of changes (scaling) of the time units. The original purpose of this parameter scaling was simply to obtain a more numerically stable inversion of FIM for the application of FIM in designing optimal experiment (see chapter

7). Indeed, it was observed that a significant reduction of the condition number could be obtained just by changing the time units. In the case under study the condition number could for example be reduced from $8.05 \cdot 10^8$ to 14.018, which should guarantee a more stable numerical matrix inversion.

The FIM is basically the cornerstone of optimal experimental design (OED), and it was therefore investigated how this simple scaling of time units had an effect on the FIM properties, i.e. the eigenvalues of FIM and the corresponding determinant and trace. These factors play an essential role in the OED criteria. Via symbolic manipulation it appeared that only the D-criterion (maximisation of the $\text{Det}(\text{FIM})$) was unaffected by the scaling, as supported also by the literature (Goodwin and Payne, 1977; Walter and Pronzato, 1990 and 1999). These findings were confirmed by optimisations of the initial substrate added in the experiment under study. Here, the D-criterion remained unaffected by the scaling, whereas the A-, modA- and E- criteria resulted in slightly different experiments.

Most critical, however, was the modE criterion, which yielded completely different experiments depending on the scaling of the time units. The modE criterion is related to the condition number and aims at obtaining the optimal condition number of 1. Via symbolic manipulation it was found that, theoretically, two positive minima could be obtained for which modE is equal to 1. Initially, the case study involved a FIM based on sensitivity functions of $r_{O,ex}$ with respect to the parameters μ_{maxH} and K_S . For these parameters and the conditions tested, it appeared not to be possible to obtain a condition number of 1 (a condition number of 3.63 was reached though).

Instead, for the FIM based on the sensitivity functions of $r_{O,ex}$ with respect to μ_{maxH} and the initial substrate concentration $S_S(0)$ two cases leading to $\text{modE}=1$ could be detected. The two optimal experiments for which $\text{modE}=1$ was obtained did, however, not seem very “optimal” for parameter estimation, since the $r_{O,ex}$ profile was either rather short or not terminated within the experimental time. Via a more detailed analysis of the properties of the FIM and the evolution of the eigenvalues as function of the scaling factor, it appeared that the $\text{modE}=1$ was achieved in both cases by increasing the actual covariance value of μ_{maxH} and thereby decreasing the value of the initially largest eigenvalue to the value of the smallest. Hence, the situation where modE equals 1 could be created just by scaling of the parameter units. The experimental designs, although optimal with respect to the modE criterion, could, however, not really be characterised as “optimal” for parameter estimation and were just the result of parameter scaling. It should be noted that it may be difficult (or even impossible) to find necessary scaling if more than one parameter with a time unit is defined in the model, since only one time unit can be dealt with.

These results certainly stress that care should be taken with the scale of parameter units, since the FIM is depending on their actual values. Only the D-criterion based OED is unaffected by scaling, confirming that this OED criterion is the most reliable one and may be the best one to apply in practice (see chapter 7) since considerations concerning the effect of parameter units can be avoided. Care should especially be

taken in application of the modE criterion. In the work of Munack (1989), Baltes *et al.* (1994), Versyck *et al.* (1997) and Versyck and Van Impe (1999) feeding rates to fed-batch systems have been optimised based on the modE criterion. In the work of Versyck *et al.* (1997) modE=1 OED's was obtained (for further review on these OED example, see chapter 5). It should be stressed that the results of the study conducted here indicate that one may find a scaling factor that improves the condition number. Moreover, in certain cases the optimal value of the modE (i.e. 1) can just be obtained by changes in parameter units. However, such an experiment can not be considered to be an optimal experiment unless the condition number of the estimation problem is the only concern.

6. Conclusion

In this chapter a study was conducted on the effect of rescaling of the parameter units in parameter estimation exercises. The example applied was the estimation of parameters in a simple single substrate batch biodegradation model. The study was originally initiated to evaluate whether rescaling could be used to improve the numerical properties of the Fisher Information Matrix in view of its inversion, as this is used to obtain the parameter estimation error covariance matrix. Only rescaling of the time unit was found to be useful to change the condition number of the FIM. Significant improvements in condition number, up to a factor 10^{10} , could be obtained by rescaling the time unit of parameters. Moreover, it was shown that in some cases it is possible to reach the best possible condition number, i.e. a value = 1.

This result has quite some implications for the optimal experimental design methodology. It was found that, among the 5 OED-criteria evaluated, only the D-criterion based experimental design is not affected by rescaling of the parameter units. For all other criteria, and especially the modified E criterion, which focuses on a minimisation of the condition number of FIM, the optimal experiment design is quite different for different parameter units. Hence, OED results should be compared with care in case different units are used to express model parameters.

Chapter 7
-
Optimal Experimental Design

Chapter 7

Optimal Experimental Design

Abstract - In this chapter a conceptual methodology for optimal FIM based experimental design was developed. This methodology was applied in two case studies focusing on the two step nitrification process and simultaneous nitrification and degradation of wastewater COD respectively. In both cases simple experimental degrees of freedom to be optimised was defined. In the first case study it was aimed to optimise the initial addition of nitrite to allow for simultaneous estimation of the kinetics of both nitrification steps. The second case focused on optimising an additional amount of ammonium to be added together with the wastewater with the aim to simultaneously estimate the kinetics of COD degradation and nitrification. The experiments were optimised via the D-criterion in which the determinant of FIM is maximised. Improvements in parameter accuracy up to 50% were found for both case studies. The theoretical results were successfully validated with experiments carried out according to the predicted optimal experimental design. Finally, the sensitivity of the optimal experimental design to changes in parameter values or substrate concentrations was investigated. Here it was found that some safety margins existed, thus, the designs were rather robust against parameter variations. Still, however, some critical situations were encountered, which would result in rather inaccurate parameter estimates. Thus, it was concluded that either frequent updating of the optimal experiment may be required or more robust designs may be strived for.

1. Introduction

The study on theoretical identifiability in chapter 4 and the evaluation of these results by practical identifiability analysis in chapter 5 and 6 can be considered as preliminary steps towards the design of optimal experiments. The purpose and conceptual idea of optimal experimental design, as it is applied in this study, is illustrated in Fig. 1. This figure will be explained step by step in the following. First, however, consider a range of different experimental conditions that eventually will lead to an experimental response. Initially experimental conditions can be understood rather broadly, since it can be any imaginary conditions under which the experiments can be carried out. Thus, in principle the experimental conditions are only limited by the reality (e.g. it would not be possible to carry out experiments under unrealistic or extreme conditions such as negative oxygen concentrations etc.). In practice of course the experimental condition space will also be limited by the experimental set-up and its flexibility, e.g. with respect to availability of

different equipment elements, sampling frequency, total number of samples that can be analysed etc.

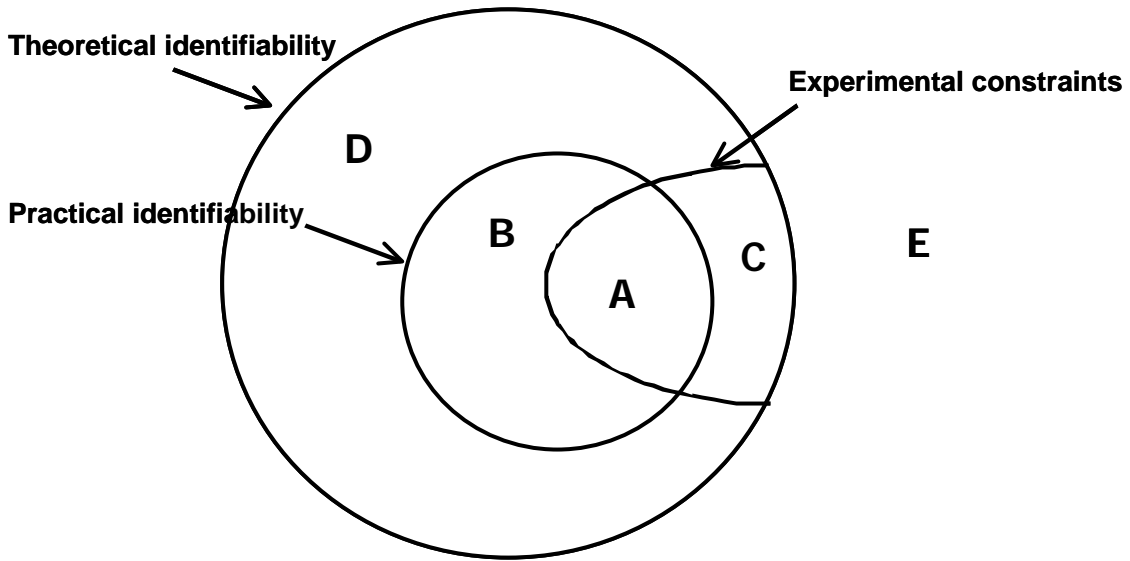


Figure 1. Conceptual idea of optimal experimental design

The experimental conditions consist of both environmental and measured variables. Examples of experimental conditions are listed below:

- Experimental conditions:
 - Measured variables:
 - Oxygen concentration (S_O)
 - Oxygen uptake rate (r_O)
 - pH
 - Alkalinity
 - Redox potential
 - Conductivity
 - etc.
 - Environmental variables:
 - Origin and concentration of sludge
 - History of sludge
 - Origin of substrate
 - Initial substrate to biomass ratio ($S(0)/X(0)$)
 - Change in substrate concentrations or load (ΔS)
 - pH
 - Temperature

- Oxygen concentration
- Availability of nutrients (e.g. N, P)
- etc.

The environmental variables are determining the response of the system, whereas the measured variables and the frequency of the measurements will determine what kind of information is obtained for the experimental response.

In chapter 2 a thorough discussion on the $S(0)/X(0)$ ratio was made. Basically, this ratio, or maybe more precisely the change in substrate concentrations or load, ΔS , that the organisms are subjected to, has an important influence on the resulting experimental response and may influence both the observed yield and kinetic parameters. Drastic changes of the environment may eventually lead to population shifts. This especially applies to organic substrate, which can flow into different mechanisms depending on the environmental conditions, as repeated in Fig. 2. In addition, sludge history can be important to consider, since it also influences the state of the organisms and thereby their response. For the more detailed discussion on this matter the reader is referred to chapter 2.

Examples of some possible experimental responses are listed below:

- Experimental responses:
 - Heterotrophic substrate degradation
 - Nitrification
 - Significant or insignificant growth
 - Storage of substrate
 - Decay
 - etc.

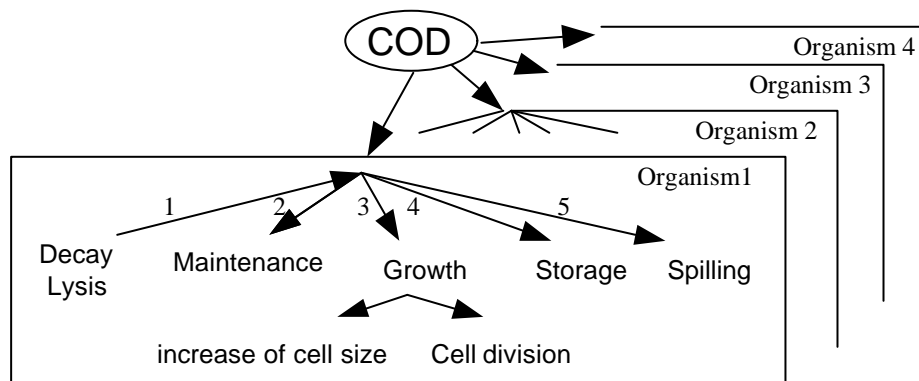


Figure 2. Different flows of external COD in the organisms

The experimental conditions are all user-defined and will depend on the purpose of the actual experiment, i.e. what kind of experimental response and information content are pursued to allow estimation of certain

model parameters with a certain accuracy.

The space of Fig. 1 is now considered to consist of a range of different experimental conditions as described above. Thus, a point located at a certain position in Figure 1 is defined by a certain set of experimental conditions, resulting in a certain experimental response and related information content. If these experimental conditions comply with the purpose of the study, the point will lay within one of the given regions (A - D), and if the experimental conditions do not comply with the purpose the point will lay somewhere outside the region (E).

The first region (A - D) to consider is summarising the results of the theoretical identifiability analysis of the model which parameters are sought. Thus, this region frames the experimental conditions for which unique parameters can theoretically be obtained from the data. Moreover, this theoretical identifiability region can be considered as a hard, ultimate bound on the experimental conditions since the theoretical identifiability is determined by the model structure and the available measurements only. This region was thoroughly studied in chapter 4.

On the other hand, the region (A - B), that delineates the practical identifiability, is determined by the experimental data and their information content. The quality of the data may not be high enough to allow for a determination of all the theoretically identifiable parameters, which is why this region is a sub-set of the theoretical identifiability. Moreover, contrary to the region of theoretical identifiability, the region of practical identifiability is not fixed at a certain position in the experimental condition space, but can be located elsewhere. For instance when the actual model parameter values are different or the collected data and their properties, e.g. noise level, change.

Finally, the half-region (A, C) indicates that certain constraints can be imposed on the experimental conditions to fulfil a certain experimental purpose. The purpose could for example be to obtain kinetic parameters that are representative for, and thereby transferable, to a full-scale system. In other words extant parameters are sought (Grady *et al.*, 1996). In that case the experiments should be carried out under conditions that are as close as possible to the full-scale system, e.g. with respect to pH, temperature, load etc. Obviously such a purpose will put some constraints on the experimental conditions under which the experiments should be performed. Note that the model may still be able to describe data that are collected under experimental conditions that are outside these constraints, e.g. conditions that would favour the maximum capacity of the biomass thereby providing intrinsic parameters (Grady *et al.*, 1996). However, the information obtained will not be in accordance with the purpose of the modelling exercise.

The optimal experiments can now be defined as those experiments for which the conditions belong to the intersection of the three regions, and within this set of possible experiments the best one is selected. Thus, it is aimed to maximise the information content of the experimental data within given constraints. The Fisher Information Matrix (FIM) is central in the theory of Optimal Experimental Design (OED) for parameter

estimation. Indeed, the inverse of the FIM is, under certain conditions, equal to the parameter estimation error covariance matrix (COV) and the essence of OED is typically to reduce the COV. Different optimal experimental design criteria have been defined based on different scalar functions of the FIM (e.g. Walter and Pronzato, 1990; Munack, 1989, 1991).

Applications of the FIM and the different OED criteria can be found within many different disciplines and with various purposes. For example, in the work of Munack (1991) it was clearly illustrated how the amount of sampling points, best positions and type of measurements were investigated and optimised via analysis of the FIM properties for a microbial growth process in an aerated column reactor. In the following, however, the focus is more on the literature that has dealt with the Monod model, and, furthermore, some cases are reviewed where the objective of optimising the practical identifiability of model parameters has been combined with other constraints.

In the work of Munack (1989) the aim was to obtain an optimal feeding profile to increase the quality of the estimation of the Monod parameters μ_{\max} and K_S from a fed-batch experiment. It is well known that these two parameters tend to be correlated resulting in practical identifiability problems (Holmberg, 1982). However, by introduction of a feed profile where the initial batch phase is extended by a fed-batch phase with drastically changes of the feed rates, the substrate concentration was repeatedly driven near the value of K_S . Thereby, the correlation between the two Monod parameters could be broken to a large extent (Munack, 1989). This experimental idea was illustrated and confirmed by experimental data in the study of Vanrolleghem *et al.* (1995).

It was, however, questioned that too steep gradients in the feeding pattern, as proposed by Munack (1989), may result in invalidity of the Monod model, since this model is based on balanced growth operating under steady state (Baltes *et al.*, 1994). Thus, the proposed fed-batch experiments may be restricted to only small rates of change in substrate concentrations to ensure the validity of the Monod model. A combined objective function was defined in the study of Baltes *et al.* (1994), where an optimisation of the experimental design should answer two questions: (i) How to guarantee sufficient accuracy of the estimated parameters? and (ii) Can the optimal experimental design guarantee model validity. The restriction that balanced growth must exist to allow for model validity was shown to put a strong limitation on the rate of substrate change that was needed for improvement of parameter estimation accuracy. A critical biological criterion with regard to balanced growth was defined as the gradient of the specific growth rate as function of time and was therefore incorporated into the objective function of the OED. In the study it was concluded that a constant feeding rate after an initial batch phase was the most robust design towards changes of parameters. However, the model validity improved remarkably by the application of time varying feeding rates. Therefore, a compromise had to be made between security for parameter accuracy and model validity. Experimental verification with fermentation of yeast showed that in this case the constant feeding rate gave satisfactory results (Baltes *et al.*, 1994).

Another study focused on combining optimal process performance (maintenance of optimal yield or productivity) with optimal information on the model parameters (Versyck *et al.*, 1997; Versyck and Van Impe, 1999). In this study the optimal feeding rate appeared to be one where the substrate concentration was kept constant, but in an initial phase, preceding this phase, a disturbance was introduced either in the form of a batch phase or a feeding phase with a maximum feed rate level. In this way it was possible to combine optimal process performance with optimal parameter estimation accuracy.

Summarising, the model validity concept as presented in Baltes *et al.* (1994) can be seen as an expression for the delineation of the first region (D) in Fig.1. Indeed, provided ideal measurements are available, all parameters of the model could be estimated and the model could be applied for its purpose, i.e. the model would be valid. However, when the rate of change of the substrate would be too fast, i.e. the experimental conditions were outside the region (D), the model would be invalid. In other words, if unbalanced growth takes place the Monod model may no longer be able to describe the data (Baltes *et al.*, 1994) and the experiment can no longer be considered to lay within the region of theoretical identifiability but lays outside as an E experiment in Fig. 1. By combining an objective of model validity and optimisation of practical parameter identifiability, Baltes *et al.* (1994) aims at the region of practical identifiability in Fig. 1 (experiment B). In the work of Versyck *et al.* (1997) and Versyck and Van Impe (1999) a further constraint is imposed in the search for both optimal process performance and optimal parameter information. Thus, to relate their work to Fig. 1, they aim for the half region indicating that certain constraints can be imposed on the experimental conditions to fulfil a certain experimental purpose (experiment A in Fig. 1).

In this study the concept outlined in Fig. 1 is concretised for two case studies with different aims. The first case study deals with a classical example; the two step nitrification where the aim is to identify the second nitrification step. Secondly, a combined municipal-industrial wastewater is studied with the aim of determining the kinetics of heterotrophic substrate degradation and nitrification. Moreover, the aim in these studies is to design experiments that give responses that can be considered representative for the full-scale system under study. In this way it is pursued to obtain extant kinetic parameters for a model describing the full-scale system. Finally, an additional aim was to investigate the effect of the variation of the wastewater and reaction kinetics on the experimental designs. The aim here was to judge whether the developed optimal experimental designs were robust or whether the designs had to be adjusted often to maintain the quality of the parameter estimates as the system's characteristic change.

2. Theoretical background

Parameter estimation typically aims for a minimisation of a weighted sum $J(\underline{p})$ of squared errors between model outputs $\underline{y}(t_i, \underline{p})$ and measured outputs $\underline{y}_m(t_i)$ with the weights \underline{Q}_i and N the number of

measurements, also denoted the objective function (Eq. 1). The minimisation is obtained by optimal choice of the parameter vector \underline{p} .

$$J(\underline{p}) = \sum_{i=1}^N \left(\underline{y}(t_i, \underline{p}) - \underline{y}_m(t_i) \right)^T \underline{Q}_i \left(\underline{y}(t_i, \underline{p}) - \underline{y}_m(t_i) \right) \quad (1)$$

For the analysis of the information content with respect to the parameters, the Fisher Information Matrix (FIM) can be used (Eq. 2):

$$\text{FIM} = \sum_{i=1}^N Y_p(t_i, \underline{p})^T \underline{Q}_i Y_p(t_i, \underline{p}) \quad (2)$$

where $Y_p(t_i, \underline{p})$ denotes the output sensitivity functions with respect to the parameters. The weighting matrix \underline{Q}_i is typically chosen as the inverse measurement error covariance matrix. In this case the FIM is the inverse of the parameter estimation error covariance matrix (COV). Thus, the FIM can be regarded as a summary of the output sensitivity functions and the measurement accuracy, thereby summarising the information concerning the model parameters gained from an experiment. For a more thorough derivation and discussion of the FIM the reader is referred to chapter 5 and e.g. Munack (1989 and 1991).

Several scalar functions of FIM have been defined as a measure of the quality of the estimated parameters, e.g. the determinant, condition number and trace. They play key roles in the theory of optimal experimental design (OED). Different OED criteria have been defined based on these scalar functions which in different ways give measures of the shape of the confidence region (e.g. Goodwin, 1987; Munack, 1989 and 1991; Walter and Pronzato, 1990, 1999). Basically these OED criteria all aim at a reduction of the COV of the parameter estimates (i.e. maximisation of FIM) by focusing on different conditions. Once the constraints on the experiment and the OED criterion have been specified the experimental design simply reduces to a constrained optimisation problem. Note that *a priori* knowledge of the model parameters is both advisable and unavoidable since the FIM is parameter depending (Goodwin, 1977; Walter and Pronzato 1990). This dependency seems natural since on one hand the ability to design a good experiment should depend upon prior knowledge regarding the nature of the experiment, and on the other hand any model structure can already be considered as prior knowledge.

A – optimal criterion: min Tr(FIM⁻¹)

In this criterion the focus is on a minimisation of the trace, and thereby the sum of eigenvalues of the inverse FIM (i.e. COV), i.e. the squares of the lengths of the axes of the confidence ellipsoids, This is equivalent to minimisation of the arithmetic average of the parameter errors. Note that this criterion is based on an inversion of the FIM. Thus, this may lead to numerical problems in case the FIM is badly conditioned.

modA – optimal criterion: max Tr(FIM)

This criterion is similar to the A criterion, only is the trace of FIM maximised. The problem with this criterion is, however, that in case an unidentifiable experiment is conducted, i.e. a case where FIM becomes singular and one of the eigenvalues becomes zero, which means that the confidence region goes to infinity in a certain direction, the trace may still be optimised and the problem of unidentifiability will not be noticed (Goodwin and Payne, 1977). This is less of a problem with the A criterion since if FIM becomes singular an inversion will not be possible and the problem of unidentifiability will thereby be exposed.

D - optimal criterion : max Det(FIM)

Here it is aimed to maximise the determinant of FIM. The determinant is proportional to the volume of the confidence region, thus by maximising Det(FIM) one minimises the volume of the confidence ellipsoids, and, correspondingly, one minimises the geometric average of the parameter errors. Moreover, D-optimal experiments possess the property of being invariant with respect to any rescaling of the parameters, as mentioned above, see also the detailed analysis in chapter 6 (Goodwin and Payne, 1977; Walter and Pronzato, 1990 and 1999).

E – optimal criterion : max λ_{\min} (FIM)

The lengths of the confidence ellipsoids are proportional to the inverse of the square roots of the corresponding eigenvalues. The E criterion maximises the smallest eigenvalue of the FIM and thereby minimises the length of the largest axis of the confidence ellipsoids. Thus, these designs aims at minimising the largest parameter error and thereby at maximising the distance from the singular, unidentifiable, case.

modE – optimal criterion : min λ_{\max} (FIM)/ λ_{\min} (FIM)

This criterion is also related to the shape of the confidence region. Here the focus is on a minimisation of the condition number, i.e. the ratio between the largest and the smallest eigenvalue. The minimum of this ratio is 1 indicating the case where the shape of the confidence ellipsoids is a (hyper) sphere. The ratio $\lambda_{\max}(\text{FIM})/\lambda_{\min}(\text{FIM})$ expresses the stiffness of the FIM. The more important the stiffness becomes, the more problematic it becomes numerically to invert FIM until finally a singular matrix is obtained ($\lambda_{\min}(\text{FIM})=0$) and the information content becomes zero, i.e. the ratio is infinite.

Finally, it should be stressed that also other design criteria can be proposed. The above criteria do not focus on the estimation error of a particular parameter but focus more on the “overall” error. However, other criteria could easily be designed where, for example, the variance of a particular parameter is in focus.

In this work the inverse of the calculated FIM is also used for calculation of the parameter confidence

intervals (see also chapter 5). Indeed, the standard deviation of the i 'th estimated parameter \hat{p}_i can be obtained from the square root σ_i of the i 'th diagonal element of the inverse FIM. An approximate confidence interval at level α is then given by Eq. 3, where t indicates the t -distribution.

$$\left[\hat{p}_i - t_{\alpha, (N-p)} \mathbf{S}_i, \hat{p}_i + t_{\alpha, (N-p)} \mathbf{S}_i \right] \quad (3)$$

3. Methodology

The OED methodology applied in this study is summarised in Fig. 3 and includes the following steps:

1. Model-based analysis of the reference experiment.
2. Define experimental conditions and constraints.
3. Investigation of theoretical identifiability of the model parameters (see chapter 4).
4. Investigation of practical identifiability of the model parameters (see chapter 5).
 - 4.1 Derivation of output sensitivity functions with respect to the theoretically identifiable parameters from step 3.
 - 4.2 Calculation of FIM based on the output sensitivity functions of step 4.1.
5. Scaling on the time related parameters in the FIM to ensure a more stable numerical inversion (see chapter 6).
6. Investigate if FIM is singular as a check whether the FIM can cope with the results of the theoretical identifiability study (see chapter 5 - 6).
7. Define experimental degrees of freedom.
8. Optimisation of OED criterion to obtain the optimal experiment by modifying the given experimental degrees of freedom.
9. Investigation of the sensitivity of the optimal experimental design obtained in step 8, to check how robust the design is towards parameter changes of the reference experiment. This can for example be investigated by quantifying how much a specific parameter can vary while still allowing a sufficiently accurate parameter estimation.

Steps 1 - 4 in this procedure are already thoroughly described in the introduction and theoretical background given above. Step 5 deals with the fact that the FIM, by definition, is parameter dependent. Thus, the actual values of the FIM elements depend on the parameter units. In chapter 6 it was shown how a simple scaling (via a scaling factor α) on the time units enabled a significant reduction of the condition number of the FIM, and thereby increased the mathematical robustness of the FIM inversion. Moreover,

the effect of the scaling of the time units on the FIM properties, and thereby the results of potentially optimal experimental design, was investigated. From this study it was concluded that only the optimal experiments obtained with the D-criterion, i.e. maximisation of $\text{Det}(\text{FIM})$, remain unaffected by the scaling of time units (see chapter 6 for further details). Therefore, only this optimal experimental design criterion will be considered in this study.

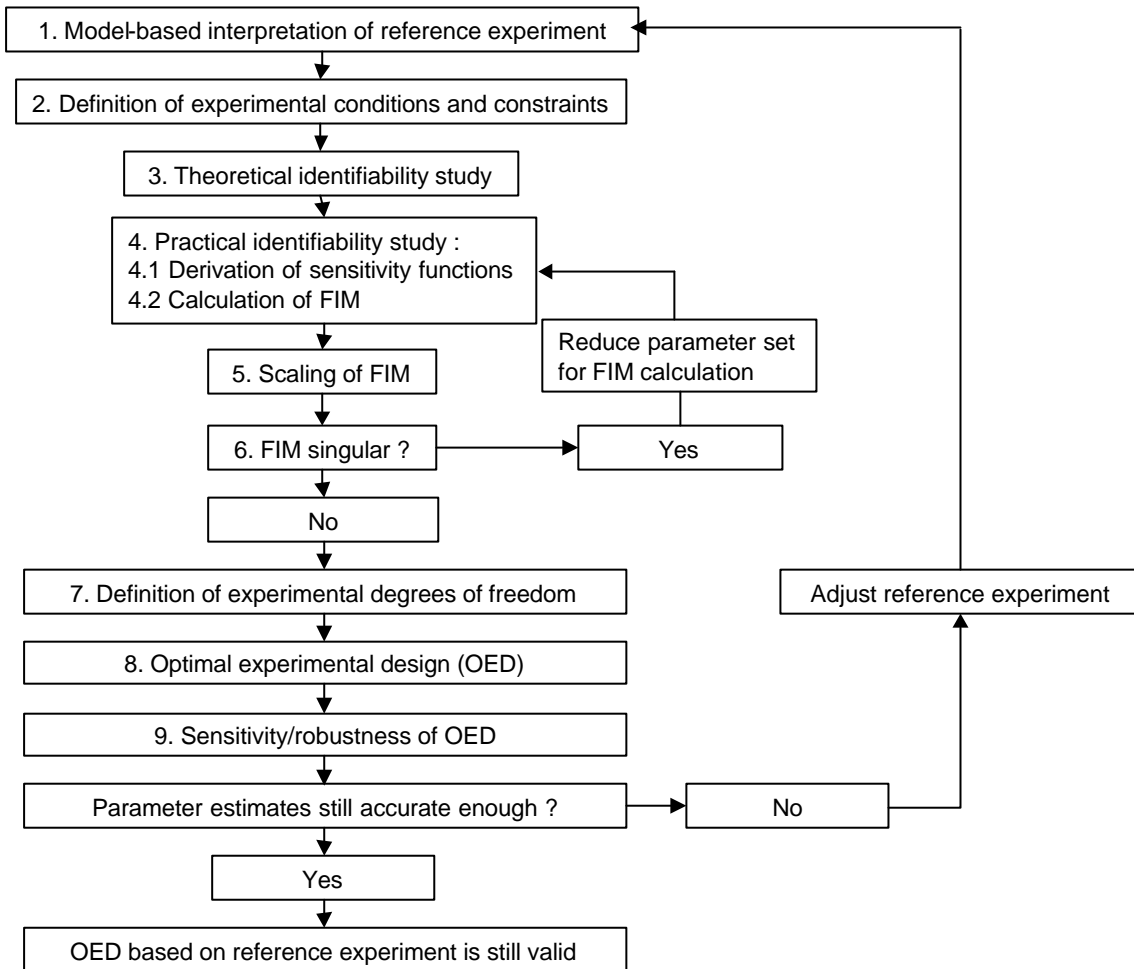


Figure 3. Flow-scheme of OED procedure

In step 6 it is checked whether the FIM becomes singular when it is calculated using the output sensitivity functions that were derived earlier in step 4.1, which is again based on the theoretical identifiability study. In chapter 5 it was observed that the FIM may become singular when composed of the output functions with respect to all theoretically identifiable parameters. Thus, it seemed that in some cases the FIM is inadequate to deal with all theoretically identifiable parameters. If this is the case, a reduced set of output functions with respect to the theoretically identifiable parameters must be selected instead for the calculation of the FIM, as was also illustrated in chapter 5.

Now the experimental degree of freedom can be defined (step 7). The $\text{Det}(\text{FIM})$ is maximised in step 8 via

a numerical optimisation routine implemented in the WEST modelling and simulation environment (Hemmis NV, Kortrijk, Belgium).

Finally, in step 9 it is investigated how robust the optimal experiment is towards changes in parameter values. If the parameters or measurement noise have changed too much, the optimal experiment may no longer yield a sufficient accurate estimation of the parameters, and the experimental design may have to be adjusted.

4. Case study 1 – Two-step nitrification

4.1. Step 1: Reference experiment

The nitrification of the combined municipal-industrial full-scale WWTP of Zele (Aquafin NV, Aartselaar, Belgium) was characterised by combined respirometric-titrimetric measurements. A typical experimental profile, already presented and investigated in chapter 3 and 5, is illustrated in Fig. 4. The r_o profile could not be adequately described as a single step nitrification due to the “tail” in the r_o profile, indicating that the second nitrification step was slower than the first one. Therefore, to describe this profile a model including nitrification in two steps was applied (see Table 1).

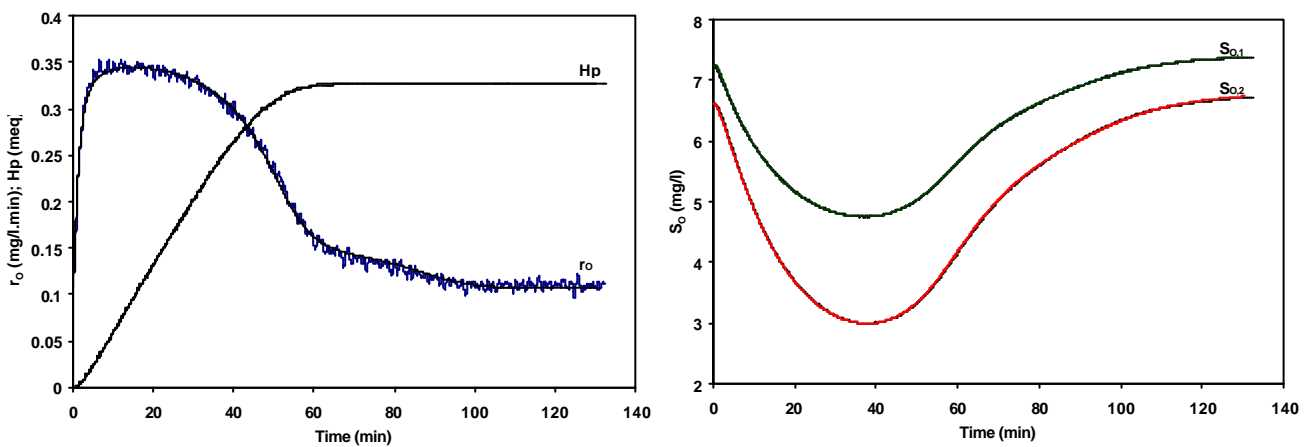


Figure 4. Experimental data (r_o , H_p , $S_{O,1}$ and $S_{O,2}$) of ammonium addition and model fit

Table 1. Two step nitrification model for interpretation of respirometric and titrimetric data, assuming that no biomass growth takes place

Component → Process ↓	1.	2.	3.	4.	5.	Process rate
	S_O	S_{NH}	S_{NO2}	S_{NO3}	H_p	
1. Nitrification step 1	$-\frac{3.43 - Y_{A1}}{Y_{A1}}$	$-\frac{1}{Y_{A1}}$	$\frac{1}{Y_{A1}}$		$\frac{1}{7Y_{A1}}$	$m_{\max A1} \frac{S_{NH}}{K_{SA1} + S_{NH}} X$
2. Nitrification step 2	$-\frac{1.14 - Y_{A2}}{Y_{A2}}$		$-\frac{1}{Y_{A2}}$	$\frac{1}{Y_{A2}}$		$m_{\max A2} \frac{S_{NO2}}{K_{SA2} + S_{NO2}} X$

However, it appeared that the “tail” in the r_O profile is not sufficiently pronounced to allow for reliable estimation of the kinetic parameters of the second nitrification step. Thus, in previous work the parameters of the second nitrification step were fixed at values obtained from a separate experiment where only nitrite was added (see chapter 3 and 5). This means that more experimental work was necessary to characterise the process.

One may of course assume that the nitrite build-up is a phenomenon only related to the batch lab-scale experiments and is not relevant for the full-scale behaviour. However, at the full-scale WWTP nitrite was observed in the final effluent too, indicating that a slower second nitrification step is also characteristic of the full-scale behaviour.

The purpose of this study was to design a single experiment that allowed for simultaneous characterisation of the reaction kinetics of both nitrification steps. In this case the obvious optimal experimental design (A) in Fig. 1 is the one where the degradation of nitrite results in a more visible second shoulder, “tail”, in the r_O profile. Such profile would contain sufficient information to identify the kinetics of the second nitrification step. Secondly, the experiments should be performed under conditions that are representative for the full-scale system under study. Thus, extant parameters are sought for. Combined respirometric (r_O) and titrimetric (Hp) measurements were applied to monitor the reactions to obtain a high accuracy on the model parameters, and the accuracy was compared to measurements of only r_O or S_O . The concept outlined in Fig. 1 is now concretised for this case study and is illustrated in Fig. 5.

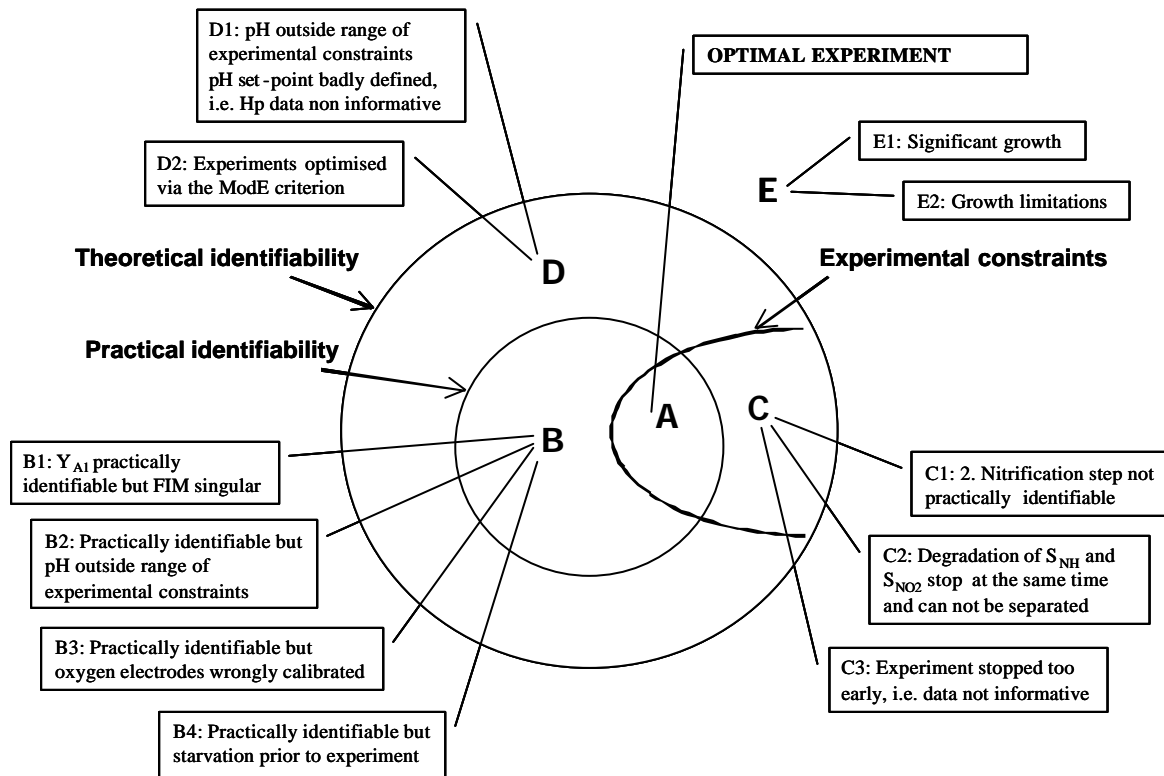


Figure 5. Optimal experimental design for two step nitrification. Illustrations of experiments: A - D

4.2. Step 2: Experimental conditions and constraints

As defined above the purpose of this case study is to obtain accurate estimation of the kinetic parameters for the two step nitrification process. Furthermore, it is aimed that these parameters are representative for the full-scale system under study. As discussed more in detail in chapter 2 it is typically recommended to work under low $S(0)/X(0)$ ratio, or expressed in another way low ΔS , to obtain responses that are representative for the physiological state prior to the experiments, i.e. extant parameters are sought (Grady *et al.*, 1996). This may not be as severe for nitrification as for COD degradation (see chapter 2) since ammonium basically only flows into nitrification or is incorporated into the cell compounds. Still, if ΔS is too high there is a risk for substrate inhibition or changes in the nitrifying population. Therefore in this study it will be aimed to carry out the experiments with low ΔS to allow for conditions that are not too different from the full-scale system under study with respect to substrate levels. Furthermore, no significant growth is allowed to take place during the experiment. A model structure assuming insignificant growth (i.e. X is not a function of time) is thereby chosen as the one for which unique parameters are sought (see Table 1).

Below the list of valid experimental conditions is defined:

- Experimental conditions :
 - Measured variables :
 - Oxygen concentration (S_O)
 - Oxygen uptake rate (r_O)
 - Cumulative proton production (H_p)
 - Environmental variables :
 - Nitrifying sludge.
 - The ammonium load, ΔS , and $S(0)/X(0)$ ratio should not be too different compared to the full-scale system to ensure that the nitrifiers are not subjected to too drastic changes in their environmental conditions.
 - Substrates should be added in such amounts that the increase in nitrifying biomass does not exceed 5% to avoid significant growth. Thus, a growth of less than 5% is here considered negligible.
 - Ammonium and/or nitrite as substrate should be dosed such that the concentrations of ammonia (NH_3) and nitrous acid (HNO_2) are below 0.1 gN/m^3 and 0.2 gN/m^3 respectively to avoid inhibition. Note that the critical concentrations of NH_3 and HNO_2 are pH dependent (Anthonisen, 1976).

- pH in the range 5.5 – 10 to avoid growth limitation (Henze *et al.*, 1997).
- Temperature 5 – 40 °C to avoid growth limitation (Henze *et al.*, 1997).
- Oxygen concentration above 2 mg/l to avoid growth limitation.
- No presence of nitrifying inhibiting components.

The first purpose of this study was to obtain an experiment that allowed for a simultaneous characterisation of both nitrification steps. To fulfil this purpose, no additional experimental constraints had to be defined, since this purpose can be achieved by ensuring practical identifiability. However, a few further constraints have to be imposed on the experimental conditions already mentioned above in order to achieve the second part of the purpose, i.e. impose experimental conditions that are rather similar to the full-scale system in order to obtain extant kinetic parameters. In this case these constraints can be rather readily deduced and are very simple:

- Experimental constraints:
 - pH in range 7.5 - 8.5
 - Temperature in full-scale system is 10°C
 - Sludge history

Concerning the temperature constraint a compromise was made between the temperature of the full-scale system and what was practically feasible in lab-scale. Thus, the experiments were temperature controlled at 17.5°C.

The sludge history is included as an experimental constraint since e.g. starvation periods prior to the lab-scale experiment may influence the results. This was simply illustrated in chapter 2 (Fig. 26) where the results from an experiment with three pulses of acetate to an activated sludge sample, that had been in the state of endogenous respiration overnight, showed that the r_0 of the first substrate pulse did not reach the maximum rate. Thus, the sludge first had to be “activated” (e.g. enzyme activation or synthesis). Clearly, these results proved that storage or starvation of the sludge prior to experimentation, which is often the case in practice and in most cases unavoidable, effects the initial experimental results. This does not mean that the model given in Table 1 is not able to describe the data. The experimental response may still be the one of growth without cell multiplication, and practical identifiability may still be obtained, but the results are not expressing the actual capacity of the sludge organisms. These phenomena have also been observed with additions of ammonium and wastewater in this study (data not shown). Consequently, in practice one would activate the sludge with one or two substrate additions before data are collected for determination of the kinetic parameters. Provided that the amount of added substrate do not cause significant growth.

4.3. Step 3: Theoretical Identifiability

The theoretical identifiability of the two step nitrification model was thoroughly investigated in chapter 4,

considering both respirometric (measurements of either S_O or r_O) and titrimetric (H_p) measurements. Moreover, model structures assuming insignificant and significant growth were studied. The results concerning the system with insignificant growth are summarised in Table 2 below.

Thus, for the experimental conditions defined above the hard bound region relates to the theoretically identifiable parameter combinations given in the first, third and fourth column in Table 2 respectively. This region defines the experimental conditions, given above, for which it is theoretically possible to obtain unique model parameters from the data (A - D in Fig.5), i.e. the conditions have to be such that a nitrification response is achieved without significant growth nor inhibition of any kind. Experiments in which significant growth or inhibition takes place, resulting in data that can not be described by the model, lay outside the region of theoretical identifiability and are exemplified with experiment E in Fig. 5.

Table 2. Schematic overview of the theoretically identifiable parameter combinations for nitrification step 1 and 2, depending on the available measurement(s) and with a model structure assuming insignificant growth (chapter 4)

Process (j)	Nitrification step 1			Nitrification step 2
Measurement (i) →	S_O or r_O	H_p	$S_O + H_p$ or $r_O + H_p$	S_O or r_O
Model structure ↓				
No growth	$\frac{3.43 - Y_{A1}}{Y_{A1}} m_{\max A1} X$ $(3.43 - Y_{A1}) K_{SA1}$ $(3.43 - Y_{A1}) S_{NH}(0)$	$\frac{2}{14} \frac{m_{\max A1} X}{Y_{A1}}$ $\frac{2}{14} K_{SA1}$ $\frac{2}{14} S_{NH}(0)$	$\frac{3.43 - Y_{A1}}{Y_{A1}} m_{\max A1} X$ $(3.43 - Y_{A1}) K_{SA1}$ $(3.43 - Y_{A1}) S_{NH}(0)$ $\frac{14}{2} (3.43 - Y_{A1})$	$\frac{1.14 - Y_{A2}}{Y_{A2}} m_{\max A2} X$ $(1.14 - Y_{A2}) K_{SA2}$ $(1.14 - Y_{A2}) S_{NO2}(0)$

4.4. Step 4 - 6: Practical Identifiability

The practical identifiability of model parameters for the example given in Fig. 4 was evaluated in chapter 5. This study was carried out via evaluation of the output sensitivity functions and the corresponding Fisher Information Matrix (FIM) constructed for all theoretically identifiable parameter combinations. It appeared, however, that the FIM became singular indicating a practically unidentifiable situation despite the fact that the theoretical identifiability study had shown that the chosen parameter set, including unique identifiability

of the yield Y_{A1} , is identifiable with combined respirometric-titrimetric measurements (see Table 2). The FIM seemed, however, inadequate to deal with this theoretical identifiability result since the inclusion of the sensitivity of Y_{A1} in the calculation of FIM caused the singularity. It was found that estimation of the Y_{A1} was indeed possible in practice, as the theoretical identifiability analysis predicted, although it was strongly correlated with $\mu_{\max A1}$. For the case under study it thus seemed that an evaluation of parameter identifiability based on FIM gave a too pessimistic picture. For the development of OED this result is rather crucial, since the FIM is the cornerstone in the search for optimal experiments. Based on the results of chapter 5 it is, however, not possible to include the fact that the Y_{A1} becomes uniquely identifiable with combined respirometric-titrimetric measurements in the FIM and, thus, in the OED.

We can now exemplify the experiment B in Fig. 5 by the experiment where the combined respirometric-titrimetric data is of such high quality that the parameters of both nitrification steps, including Y_{A1} , are practically identifiable. It is obvious that if the aim of the experiment would be to identify Y_{A1} then this would in fact be the optimal experimental design. Only, we would not be able to find it using a FIM based OED approach. Thus, for the OED the FIM is based on the sensitivity functions of the outputs (r_O , combined r_O and H_p or S_O) with respect to the theoretically identifiable parameters listed in column 1 and 4 in Table 2 only. In addition the parameters $K_L a$ and saturation coefficient of oxygen S_O^0 are considered in the case of S_O measurements.

Next, the optimal scaling factors α applied to the time units in the reference experiment to allow for a more stable inversion of the FIM are given in Table 3. The optimal scaling factors were found according to chapter 6 by minimisation of the condition number ($\lambda_{\max}/\lambda_{\min}$) of FIM.

Table 3. Applied scaling factors α and the condition number of the FIM for case study 1

Measurements	α	$\lambda_{\max}/\lambda_{\min}$
r_O	1	$3.55 \cdot 10^{13}$
	$7.72 \cdot 10^5$	$2.07 \cdot 10^2$
r_O+H_p	1	$9.79 \cdot 10^{13}$
	$7.21 \cdot 10^5$	$7.85 \cdot 10^2$
S_O	1	$1.15 \cdot 10^{14}$
	$5.46 \cdot 10^3$	$1.99 \cdot 10^{10}$

Obviously, the condition number of the FIM considering r_O or combined r_O and H_p measurements can be reduced significantly by scaling of the time units, in accordance with the findings of chapter 6. However, the

condition number of the scaled FIM when measurements of S_O are used for parameter estimation remains rather high ($1.99 \cdot 10^{10}$). In this respect it should be remembered that only one scaling factor α can be considered for all parameters related to time, since it is only possible to deal with one time unit (see chapter 6). When dealing with S_O data three parameters have a time unit, i.e. $\mu_{\max A1}$, $\mu_{\max A2}$ and $K_L a$. The value of $K_L a$ is in general of another order of magnitude than $\mu_{\max A1}$ and $\mu_{\max A2}$ (in this case $K_L a = 9.35 \cdot 10^{-2} \text{ min}^{-1}$, $\mu_{\max A1} = 3.12 \cdot 10^{-6} \text{ min}^{-1}$ and $\mu_{\max A2} = 6.93 \cdot 10^{-7} \text{ min}^{-1}$). Therefore, scaling of the time units can not reduce the condition number of the FIM as significantly as in the case where only r_O or combined r_O and H_p data are considered. This means that the results considering S_O data may have to be taken with some reservation since the FIM is not as numerically stable as in the case of r_O and combined r_O and H_p data.

4.4.1. Examples of experiments B - D

In the following some illustrative examples are given for the non-optimal experiments B – D in Fig. 5.

First, experiment B can be illustrated by the case where the kinetic parameters of the two step nitrification are practically identifiable, but where the experimental conditions do not comply with the constraints, e.g. pH outside the range of 7.5 – 8.5. An experiment of type B can also occur if the dissolved oxygen electrodes are wrongly calibrated. Thus, the data may be of sufficient quality to allow for a practical identifiability of the model parameters but the results will still be erroneous. Finally, experiment B can also be illustrated by the case where the sludge has been exposed to significant starvation prior to the experiment. The parameters may be practically identifiable but still not describing the actual capacity of the sludge.

Experiment C can be exemplified by experiments of a single ammonium addition where the experimental constraints are fulfilled, but where the second nitrification step is not practically identifiable (as in Fig. 4). Thus, experiment C is not within the region of practical identifiability but it is within the region of experimental constraints. Furthermore, the pathological case where the degradation of added ammonium and nitrite complete exactly at the same time not allowing a separation of the responses, is also represented by an experiment C in Fig. 5. A final example of an experiment C would be an experiment that is stopped too early to allow for complete termination of the S_O , r_O or H_p profile (a typical experimental error) or where only a very small amount of substrate is added not allowing for informative profiles. This experiment may be within the experimental constraints but the parameters may not be practically identifiable.

Finally, before aiming for the optimal experiment, experiment D can be exemplified by an experiment where the pH set-point is also outside the range of 7.5 – 8.5, but where the set-point is badly chosen resulting in non-informative H_p data. However, an even more illustrative example of a D experiment is the case thoroughly discussed in the previous chapter 6 where the optimal value of the ModE criterion (=1) was obtained just by rescaling the parameter units. The ModE=1 optimal experiment is optimal considering the numerical properties of the estimation problem since it secures a stable numerical inversion of the FIM.

Thus, if this is the primary aim such experiments are the optimal ones (A). However, if the aim is to obtain reliable parameter estimates, as in this case, the resulting so-called optimal r_O profile clearly illustrated that it would not be possible to estimate parameters reliably based on such data. The optimal experiment was either too short to even reach the maximum r_O or too long to allow a termination of the $r_{O,ex}$ profile within the defined experimental time. Indeed, it was also found in chapter 6 that the A-, modA- and E- criteria were affected by parameter rescaling, although to a lesser extent than the modE criterion. Consequently, care should be taken with the application of these criteria since they may result in misleading, theoretically optimal, experiments.

4.5. Step 7: Experimental degrees of freedom

In this case study the experimental degree of freedom to reach an optimal experiment (A) is chosen as the addition of an optimal amount of nitrite together with ammonium. Thus, the aim of the OED exercise is to optimise the initial addition of nitrite, $S_{NO_2,1}(0)$, to obtain a r_O profile which contains sufficient information to identify the kinetics of both nitrification steps simultaneously. The initial ammonium concentration, $S_{NH_4,1}(0)$, is assumed to be fixed at the same value as in the reference experiment of Fig. 4 and the pH set-point was 8.2. Furthermore, no significant growth may take place during the experiment as defined above. For nitrification this condition is not that severe since the yield of nitrification is low. In this example the amount of $S_{NH_4,1}(0)$ is fixed to be 3.5 mg NH_4-N/l . It has been calculated that the concentration of nitrifiers is about 40 g $COD_{NIT}(biomass)/l$ (see chapter 8). Thus, with a total nitrification yield of 0.24 mg $COD/mg N$ an addition of 3.5 mg NH_4-N/l will only yield an increase in biomass of about 2%. An extra simultaneous addition of nitrite will not increase the growth significantly since the growth yield on nitrite is as low as 0.06 mg $COD/mg N$ (Sharma and Ahlert, 1977). The nitrogen load at the full-scale WWTP is about 0.02 – 0.025 kg $N/kg MLSS.d$ calculated on the basis of average full-scale data. In the lab-scale experiments the nitrogen load was about 0.015-0.025 kg $N/kg MLSS.d$ calculated as the mass of nitrogen added per mass of MLSS divided with the duration of the experiment. Thus, the difference in substrate load, ΔS , which the nitrifiers are exposed to under the lab-scale conditions, does not differ significantly from the full-scale situation. One may therefore expect that the experimental response is representative for the full-scale system and that extant parameters can be obtained.

The maximal experimentation time for the optimal experimental design was fixed to 130 minutes, similar to the experimentation time of the single ammonium addition of the experiment in Fig. 4.

4.6. Step 8: Optimal Experimental Design

The results of the D criterion based OED and the reference experiment are given in Table 4, considering r_O , combined r_O and H_p and S_O measurements and applying the α values of Table 3. The values of all the other FIM characteristics for the same D-optimal experiment are reported as well.

Table 4. Values of the OED criteria for different experimental set-ups and with the D criterion (Det(FIM)) as optimisation criterion. $S_{NO_2,1}(0)$ is the degree of freedom in the experimental design. The optimised value for the D criterion is given in bold

Meas.	Criterion	Tr (FIM ⁻¹)	Tr (FIM)	Det(FIM)	λ_{max}	λ_{min}	$\lambda_{max}\backslash\lambda_{min}$	$S_{NO_2,1}(0)$
r_O	reference	$2.39 \cdot 10^{-3}$	$1.75 \cdot 10^5$	$8.47 \cdot 10^{19}$	$1.09 \cdot 10^5$	$5.27 \cdot 10^2$	$2.07 \cdot 10^2$	0
	D	$1.35 \cdot 10^{-3}$	$2.35 \cdot 10^5$	3.88×10^{20}	$1.17 \cdot 10^5$	$1.22 \cdot 10^3$	$9.56 \cdot 10^1$	1.98
r_O+Hp	reference	$1.51 \cdot 10^{-3}$	$1.02 \cdot 10^6$	$8.54 \cdot 10^{22}$	$5.69 \cdot 10^5$	$7.25 \cdot 10^2$	$7.85 \cdot 10^2$	0
	D	$9.05 \cdot 10^{-4}$	$1.08 \cdot 10^6$	3.41×10^{23}	$5.67 \cdot 10^5$	$1.26 \cdot 10^3$	$4.47 \cdot 10^2$	1.98
S_O	reference	$6.31 \cdot 10^{-2}$	$4.86 \cdot 10^{11}$	$4.12 \cdot 10^{48}$	$3.16 \cdot 10^{11}$	$1.59 \cdot 10^1$	$1.99 \cdot 10^{10}$	
	D	$7.36 \cdot 10^{-2}$	$8.49 \cdot 10^{11}$	1.87×10^{49}	$6.74 \cdot 10^{11}$	$1.36 \cdot 10^1$	$4.96 \cdot 10^{10}$	1.59

As can be expected, the optimal $S_{NO_2,1}(0)$ addition considering both r_O and combined r_O and Hp measurements is the same (1.98 mg N/l) since Hp data do not give extra information on the second nitrification step. However, as will be seen below, the Hp measurements improve the identification of the first nitrification step and thereby also the accuracy of the parameters related to the second nitrification step. The optimal $S_{NO_2,1}(0)$ addition considering S_O measurements and the same experimental time of 130 min. is lower (1.59 mg N/l) since here re-aeration has to take place as well within the experimental time to allow for estimation of K_{La} and S_O^0 . Hence, less time is available for complete degradation of S_{NO_2} .

In all three cases the Det(FIM) of the optimal experiment is larger (about four times) than in the reference experiment indicating that the overall generalised parameter variance has decreased.

Furthermore, the minimum eigenvalue λ_{min} increases, indicating that the largest parameter error has decreased by OED. It is, however, not possible to trace specifically which parameters the largest parameter error, i.e. λ_{min} , and minimum parameter error, i.e. λ_{max} , is corresponding to (Brouwer *et al.*, 1998). In the case of S_O measurements it was observed that also the value of λ_{max} increased with a factor 2 indicating that the minimum parameter error had increased. This was not observed in the case considering r_O or combined r_O and Hp measurements. This increase in λ_{max} in the case of S_O data had an effect on the trace of FIM (i.e. the sum of eigenvalues, equivalent to the average of the parameter errors), which also increased more than in the case of r_O and combined r_O and Hp data. However, the trace of FIM⁻¹ increased a bit considering S_O measurements. This was not expected, since Tr (FIM⁻¹) ideally should decrease for an optimal experiment. Most remarkable is, however, that the value of $\lambda_{max}\backslash\lambda_{min}$ increased when S_O measurements are considered and a D-optimal experiment is conducted.

These inconsistent and unexpected observations when considering S_O data are most probably related to the

rescaling of time unit. For comparison the OED results for S_O data not incorporating the scaling factor are given in Table 5.

Table 5. Evaluation of the effect of parameter rescaling on the OED criteria in case of S_O measurements, OED results obtained for $\alpha=1$

Meas.	Criterion	Tr (FIM ⁻¹)	Tr (FIM)	Det(FIM)	λ_{\max}	λ_{\min}	$\lambda_{\max}/\lambda_{\min}$	$S_{NO_2,1}(0)$
S_O	reference	$1.49 \cdot 10^{-6}$	$1.45 \cdot 10^{19}$	$1.09 \cdot 10^{71}$	$9.41 \cdot 10^{18}$	$8.19 \cdot 10^4$	$1.15 \cdot 10^{14}$	
	D	$7.81 \cdot 10^{-6}$	$2.53 \cdot 10^{19}$	$4.93 \cdot 10^{71}$	$2.01 \cdot 10^{19}$	$2.18 \cdot 10^5$	$9.19 \cdot 10^{13}$	1.59

It is obvious that the properties of FIM are in accordance to expectation for the unscaled case. Thus, again, this confirms the danger of rescaling and how changing time units may interfere with the OED criteria related to the eigenvalues and trace (A-, modA-, E- and modE-criterion). Only the D-criterion is invariant to rescaling of parameters, as stated in chapter 6.

The expected 95% confidence intervals for the reference experiment and the experiments with optimal addition of S_{NO_2} are given in Table 6. The confidence intervals are calculated based on the inverse of the FIM and the assumption that the measurement error remains the same for the optimal experiment (see Eq. 3).

Table 6. Expected 95% confidence intervals for the two step nitrification experiments optimised according to the D criterion, see Table 3, expressed as percentage of parameter values

Meas.	Criterion	$\mu_{\max A1}$	K_{SA1}	$S_{NH,1}(0)$	$\mu_{\max A2}$	K_{SA2}	S_O^0	K_{La}
r_O	reference	1.50	6.80	0.59	7.12	29.44		
	D	1.37	6.36	0.61	3.08	21.43		
r_O+Hp	reference	0.72	4.04	0.09	6.39	26.18		
	D	0.70	3.97	0.09	3.00	21.18		
S_O	reference	0.12	0.67	0.03	0.66	2.67	0.03	0.10
	D	0.10	0.53	0.03	0.24	1.64	0.03	0.10

First, considering the reference experiment, it is obvious from Table 6 that combined r_O and Hp measurements result in more narrow confidence intervals for the parameters related to the first nitrification step (i.e. $\mu_{\max A1}$, K_{SA1} and $S_{NH,1}(0)$) than with r_O data alone, as already observed (see chapter 5). It can further be observed that the confidence intervals for the parameters related to the second nitrification step (i.e. $\mu_{\max A2}$ and K_{SA2}) are slightly smaller considering combined r_O and Hp measurements. Thus, apparently the improved parameter identifiability of the first nitrification step, due to the inclusion of Hp data, helps the identification of the second nitrification step in the reference experiment, where the “shoulder” in the r_O

profile related to the second nitrification step was poorly identified (see Fig. 4). The optimal experiment compared to the reference experiment results in improvements of 56% and 53% for $\mu_{\max A2}$ and 27% and 19% for K_{SA2} considering r_O and combined r_O and H_p measurements respectively. If S_O data are considered an improvement of 74% for $\mu_{\max A2}$ and 38% for K_{SA2} can be obtained. Furthermore, slight improvements of the accuracy of the parameters related to the first step were observed in all three cases.

If S_O is measured rather than combined r_O and H_p measurements it is obvious that the parameter accuracy improves significantly with about a factor 10. This is caused by the fact that the measurement noise relatively is about 100 times smaller for S_O measurements than with r_O measurements as discussed earlier (see chapter 5).

4.7. Validation of optimal experimental design

The actual experiments carried out to validate the procedure were made with $S_{NO2,1}(0)$ additions of 0.35; 0.70; 1.40 and 2.55 mg N/l. The experimental data together with the model fits are illustrated in Figure 6 – 7. Table 7 lists the estimated parameter combinations, and also reports the parameters of the reference experiment ($S_{NO2,1}(0) = 0$).

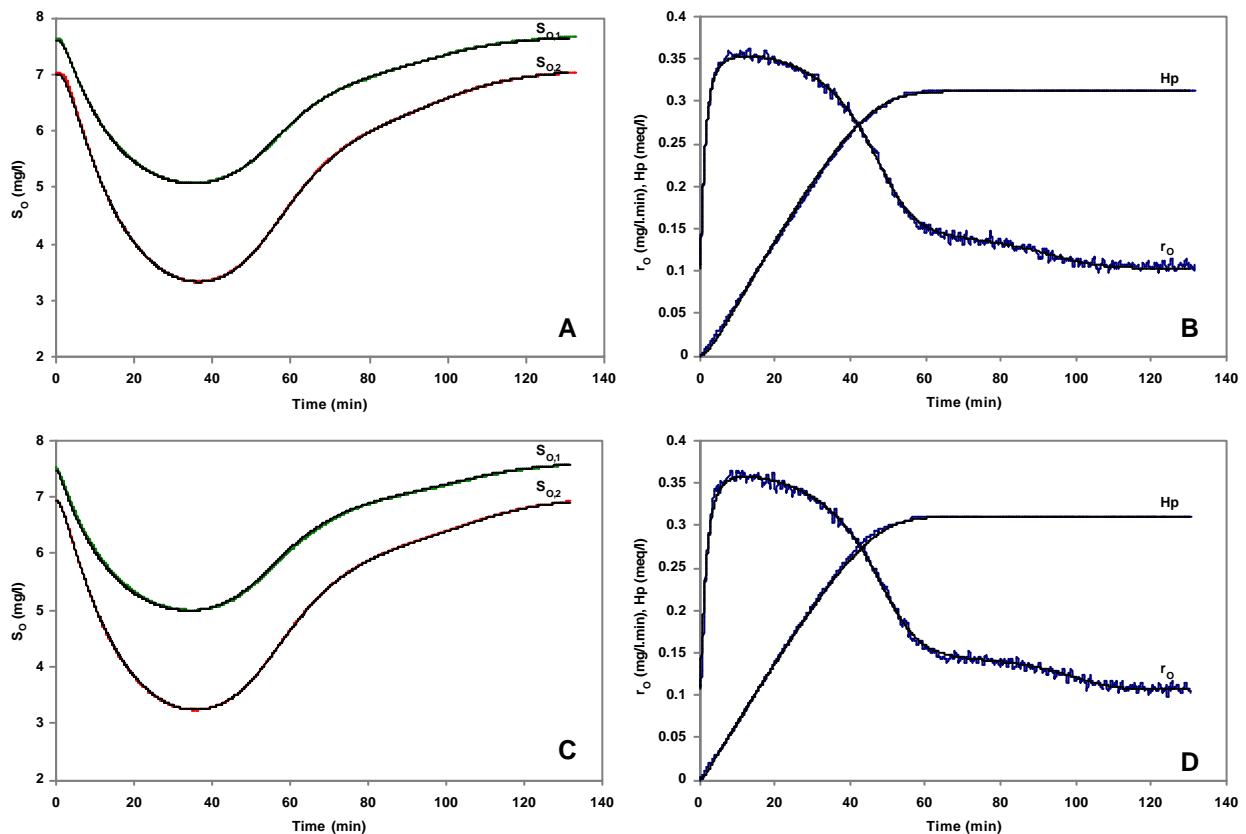


Figure 6. Validation experiments. Profiles of S_O , r_O and H_p experimental data and model fits. **A-B:** addition of $S_{NO2} = 0.35$ mg N/l, **C-D:** addition of $S_{NO2} = 0.70$ mg N/l.

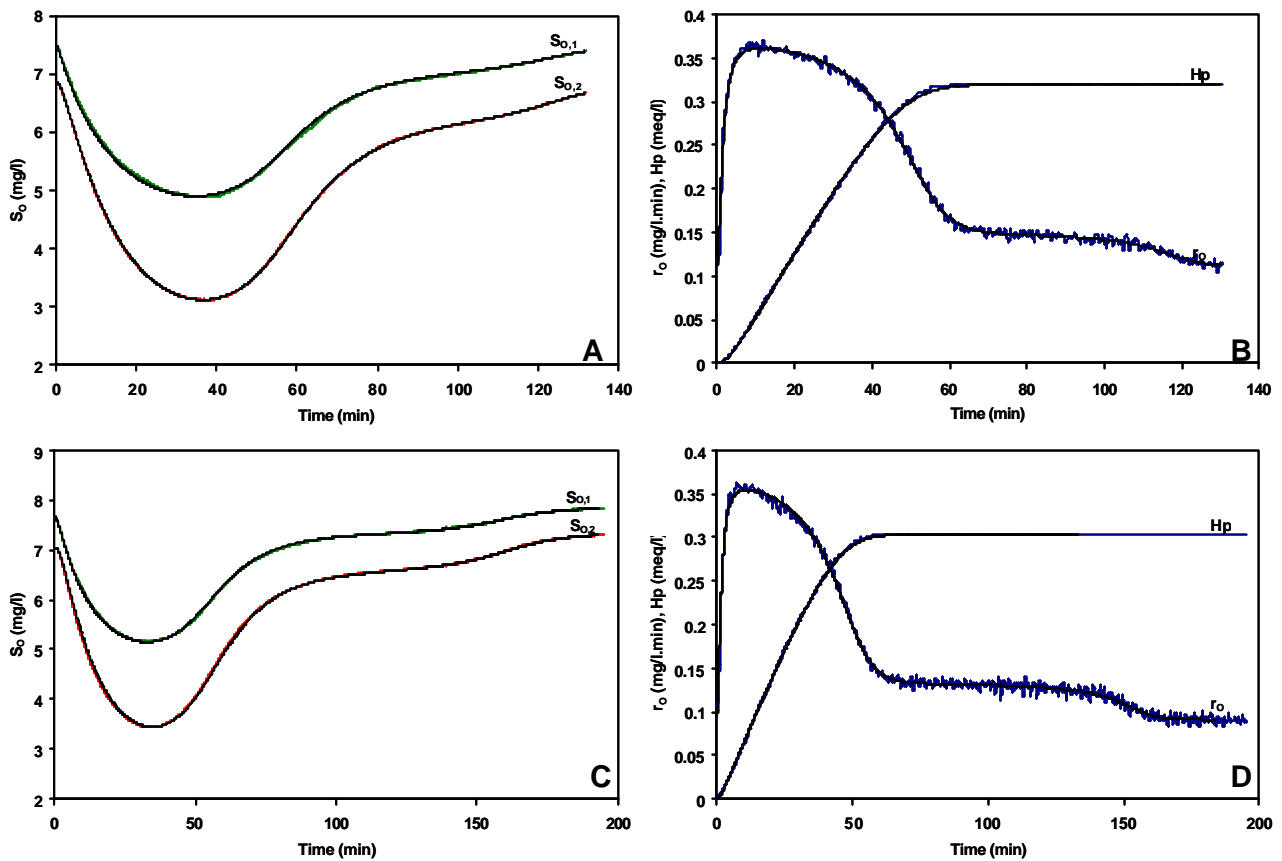


Figure 7. Validation experiments. Profiles of S_O , r_O and H_p experimental data and model fits. **A-B:** addition of $S_{NO_2} = 1.40$ mg N/l, **C-D:** addition of $S_{NO_2} = 2.55$ mg N/l

As can be observed from Table 7 the estimated parameter combinations for the experiments with addition of different amounts of S_{NO_2} are very close and in accordance with the reference experiment, confirming that these experiments can be used as validation of the procedure. Notice that it seems as if the parameter estimates based on S_O data are slightly lower than the ones based on r_O data. The reason for this is not clear.

For these validation experiments Table 8 lists the actual 95% confidence intervals on the estimated kinetic parameter combinations. Here the combinations are not written out fully but e.g. μ_{maxA1} indicates the combination related to μ_{maxA1} (i.e. $\frac{3.43 - Y_{A1}}{Y_{A1}} m_{maxA1} X$).

Table 7. Estimated parameter combinations for reference ($S_{\text{NO}_2,1}(0)=0$) and validation experiments with different $S_{\text{NO}_2,1}(0)$ (values in italic were fixed and not estimated)

	$S_{\text{NO}_2,1}(0)$ mg/l	$\frac{3.43 - Y_{A1}}{Y_{A1}} \mu_{\text{max},A1} X$	$(3.43 - Y_{A1}) K_{SA1}$	$(3.43 - Y_{A1}) S_{\text{NH}_4,1}(0)$	$\frac{1.14 - Y_{A2}}{Y_{A2}} \mu_{\text{max},A2} X$	$(1.14 - Y_{A2}) K_{SA2}$	S_0^0	K_{La}
r_0	0	0.2360	0.970	11.500	<i>0.0498</i>	<i>0.271</i>		
$r_0 + \text{Hp}$		0.2355	0.960	11.492	<i>0.0498</i>	<i>0.271</i>		
S_0		0.2256	0.911	11.396	<i>0.0498</i>	<i>0.271</i>	8.86	0.0935
r_0	0.35	0.2344	1.061	11.028	0.0514	0.410		
$r_0 + \text{Hp}$		0.2394	1.127	11.358	0.0450	0.287		
S_0		0.2221	0.989	10.831	0.0447	0.221	8.97	0.0974
r_0	0.70	0.2419	1.141	11.408	0.0424	0.218		
$r_0 + \text{Hp}$		0.2390	1.080	11.324	0.0425	0.215		
S_0		0.2213	0.984	10.910	0.0438	0.249	9.04	0.0952
r_0	1.40	0.2422	1.127	11.860	0.0379	0.139		
$r_0 + \text{Hp}$		0.2393	1.073	11.767	0.0396	0.170		
S_0		0.2214	0.930	11.313	0.0419	0.177	8.98	0.0962
r_0	2.55	0.2489	1.306	11.517	0.0403	0.180		
$r_0 + \text{Hp}$		0.2466	1.252	11.451	0.0405	0.198		
S_0		0.2263	1.132	11.031	0.0439	0.277	8.99	0.0965

Table 8. Confidence intervals as percentage of parameter values for different additions of $S_{NO_2,1}(0)$

	$S_{NO_2,1}(0)$ mg/l	μ_{maxA1}	K_{SA1}	$S_{NH,1}(0)$	μ_{maxA2}	K_{SA2}	S_O^0	K_{La}
r_O	0.35	1.54	6.21	0.62	8.17	39.14		
r_O+Hp		0.80	3.99	0.10	5.72	25.98		
S_O		0.11	0.57	0.03	0.39	2.20	0.03	0.10
r_O	0.70	1.50	6.58	0.59	4.70	27.34		
r_O+Hp		0.75	3.98	0.10	4.44	25.58		
S_O		0.11	0.54	0.03	0.32	1.75	0.03	0.09
r_O	1.40	1.39	6.23	0.58	3.66	31.90		
r_O+Hp		0.74	3.90	0.09	3.09	25.32		
S_O		0.09	0.51	0.03	0.18	1.67	0.02	0.08
r_O	2.55	1.54	6.32	0.59	1.82	18.95		
r_O+Hp		0.80	3.84	0.08	1.92	20.66		
S_O		0.10	0.48	0.03	0.11	1.03	0.02	0.07

Considering the accuracy of the parameters related to the first nitrification step, the same conclusions, as discussed above, hold concerning the comparison of r_O , combined r_O and Hp and S_O measurements. It is not expected that the accuracy of the first step changes significantly as more S_{NO_2} is added. When focusing on the parameters of the second nitrification step, it is obvious that the more S_{NO_2} is added initially the smaller the confidence interval of both μ_{maxA2} and K_{SA2} . When comparing the addition of 0.35 mg N/l with an addition of 2.55 mg N/l an improvement in accuracy of about 77% for μ_{maxA2} and 52% for K_{SA2} is achieved. Evidently, with this experimental design the largest improvements in parameter accuracy can be achieved for the maximum specific growth rate μ_{maxA2} , since a higher $S_{NO_2,1}(0)$ results in more data containing information on the maximum respiration rate related to the second nitrification step, and thereby on μ_{maxA2} .

The theoretically predicted confidence intervals of the optimal experiment according to Table 6, considering S_O data ($S_{NO_2,1}(0) = 1.59$), match well with the confidence intervals calculated for the evaluation experiment with $S_{NO_2,1}(0) = 1.4$ mg N/l (Table 8). Also, the theoretically predicted confidence intervals for an addition of 1.98 mg N/l considering either r_O or combined r_O and Hp measurements lay in between the calculated confidence intervals for the validation experiments with additions of 1.4 mg N/l and 2.55 mg N/l.

Obviously, one can further optimise the experiment by increasing the amount added, to e.g. 2.55 mg N/l. However, this experiment takes about 40 or 90 minutes longer (depending on whether r_O or S_O data are

used respectively) than the experimental time constraint set to 130 min. Thus, a compromise must be sought between the desired accuracy and the experimentation time.

4.8. Step 9: Sensitivity of the optimal experimental design to parameter variation

Above an optimal experimental design was determined and an optimal initial addition of nitrite was defined to be 1.98 mg N/l or 1.59 mg N/l depending on whether r_O or S_O was measured respectively. The reference and validation experiments above were all carried out on the date 151198 and as could be seen from Table 7 the parameter variation among these experiments was minor. It is, however, interesting to pose the question whether this experimental design would hold in case the kinetic parameters of the first or second nitrification step would change. Or said in other words “How large parameter variation is possible still allowing for an accurate estimation of the parameters, especially of these related to the second nitrification step”. If one imagines that the value of $\mu_{\max A1}$ decreases, the length of the tail in the r_O profile related to the second nitrification step will become less pronounced, resulting in a worse practical parameter identifiability of the second step. Thus, a higher amount of $S_{NO,1}(0)$ may have to be added to allow for the same parameter accuracy as the optimal experiment derived above. On the other hand, if $\mu_{\max A1}$ increases, the r_O tail will become more pronounced resulting in even more accurate parameter estimates and less $S_{NO,1}(0)$ could thus be added to maintain the same accuracy. A similar reasoning can be made in case it is $\mu_{\max A2}$ that either decreases or increases.

Experiments with addition of ammonium for detection of the nitrification kinetics were carried out daily during a measuring campaign at the full-scale WWTP of Zele (see chapter 8). The estimated parameter combinations based on r_O measurements are listed in Table 9. Despite the fact that more accurate estimates are obtained with S_O data, parameters of the validation experiments were estimated based on r_O data due to the faster convergence of the objective function towards a minimum (see chapter 5). The parameters of the second nitrification step were estimated based on independent experiments with nitrite additions and their values were fixed during the parameter estimations using the experimental results of ammonium additions (similar to the reference experiment).

Some variation in the kinetics can be observed with a variation in the parameter combination related to $\mu_{\max A1}$ from 0.1036 to 0.2603 (with 0.236 for the reference and optimal experiment) and for the combination related to $\mu_{\max A2}$ a variation from 0.0354 to 0.0630. Especially the experiments carried out on 181198 and 221198 are deviating. The reason for the deviation of 181198 can be that the sludge sample for this experiment was taken at the full-scale plant after a heavy rain fall in the beginning of the measuring campaign (see also chapter 8). This may have had a dilution effect on the viable fraction of the sludge. There seems no obvious reason for the deviation of the experiment 221198. However, in this context the main point of interest is not why the sludge kinetics change but rather whether the optimal experiment is still

valid if and when the reaction kinetics changes. Finally, it should be noted that despite addition of similar amounts of $S_{NH,1}(0)$ the related parameter combination $((3.43 - Y_{A1})S_{NH,1}(0))$ vary with about 25%.

Table 9. Estimated parameter combinations for different experiments with an addition of $S_{NH,1}(0) = 7.5$ mg N/l and $S_{NO,1}(0)=0$ mg N/l (values in italic were fixed, the biomass concentration is corrected for changes in-between the experiments to allow for a comparison of parameter combinations).

Experiment 151198 is the reference experiment

Date	$\frac{3.43 - Y_{A1}}{Y_{A1}} \mu_{maxA1} X$	$(3.43 - Y_{A1}) K_{SA1}$	$\frac{1.14 - Y_{A2}}{Y_{A2}} \mu_{maxA2} X$	$(1.14 - Y_{A2}) K_{SA2}$	$(3.43 - Y_{A1}) S_{NH,1}(0)$
151198	0.2360	0.970	<i>0.0499</i>	<i>0.271</i>	11.500
161198	0.2603	1.091	0.0540	<i>0.223</i>	11.801
181198	0.1036	1.081	0.0354	<i>0.438</i>	14.438
191198	0.2331	1.150	0.0666	<i>0.223</i>	14.484
201198	0.2500	1.206	0.0630	<i>0.223</i>	14.686
211198	0.2637	1.148	0.0630	<i>0.223</i>	14.550
221198	0.1089	0.952	0.0486	<i>0.223</i>	11.566

The optimal experiment ($S_{NO2,1}(0) = 1.98$ mg N/l, optimal for the sludge of 151198) is now simulated again, but with parameter combinations $\frac{3.43 - Y_{A1}}{Y_{A1}} \mu_{maxA1} X$ and $\frac{1.14 - Y_{A2}}{Y_{A2}} \mu_{maxA2} X$ changed according to the observed minimum and maximum of Table 9. For these conditions, the expected 95 % confidence intervals are calculated and given in Table 10.

Table 10. Expected 95% confidence intervals expressed as percentage of parameter values for validation experiments (1 - 4) (changes of μ_{maxA1} and μ_{maxA2}) of the optimal experiment ($S_{NO2}(0)=1.98$ mg N/l), considering r_O measurements

	$\frac{3.43 - Y_{A1}}{Y_{A1}} \mu_{maxA1} X$	$\frac{1.14 - Y_{A2}}{Y_{A2}} \mu_{maxA2} X$	μ_{maxA1}	K_{SA1}	$S_{NH,1}(0)$	μ_{maxA2}	K_{SA2}
D optimal	0.2360	<i>0.0499</i>	1.37	6.36	0.61	3.08	21.43
Exp. 1	0.1036	0.0499	7.96	28.85	0.74	23.30	83.58
Exp. 2	0.2603	0.0499	1.31	6.13	0.58	2.98	21.06
Exp. 3	0.2360	0.0354	1.38	6.38	0.62	3.34	24.99
Exp. 4	0.2360	0.0630	1.36	6.38	0.58	2.89	19.82

From Table 10 it is obvious that when the combination related to $\mu_{\max A1}$ decreases (Exp. 1), the parameter identifiability suffers significantly since the tail in the r_O profile related to the second nitrification step is now no longer visible (see Fig. 8A). The increase in $\mu_{\max A1}$ (Exp. 2) results in a slight improvement of parameter accuracy compared to the D-optimal experiment. Also, the changes in $\mu_{\max A2}$ to the minimum (Exp. 3) and maximum (Exp. 4) observed result in the expected changes in parameter estimation accuracy, i.e. increase and decrease of accuracy respectively. However, for both cases the accuracy is rather comparable to the one of the optimal experiment.

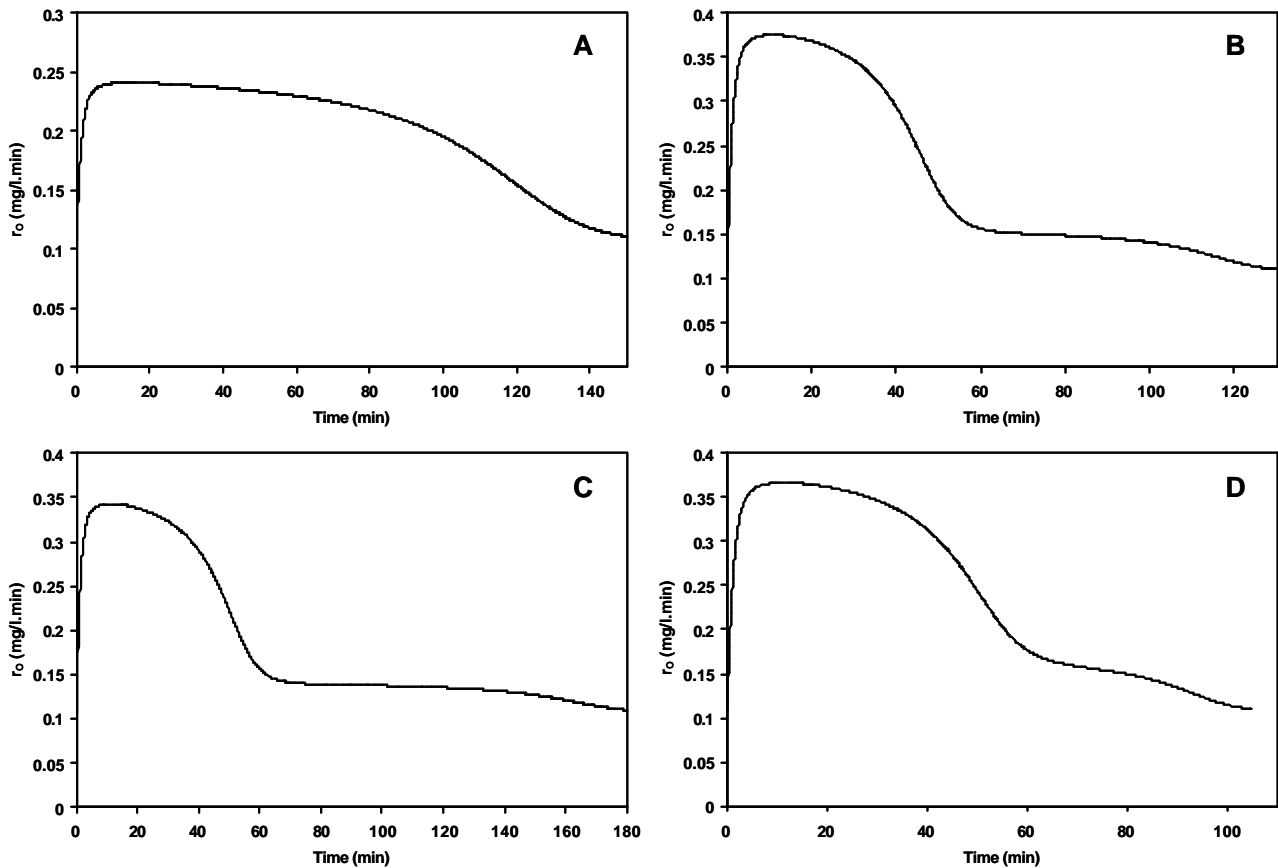


Figure 8 Sensitivity of optimal experiment to parameter changes. Simulated r_O profiles. **A:** $\mu_{\max A1}$ decrease, **B:** $\mu_{\max A1}$ increase, **C:** $\mu_{\max A2}$ decrease, **D:** $\mu_{\max A2}$ increase.

Thus, obviously the most critical situation is the one where $\mu_{\max A1}$ decreases and $\mu_{\max A2}$ remains at a high value. The maximum possible value of the parameter combination of $\mu_{\max A2}$, still allowing parameter estimation accuracy comparable to the optimal experiment, has been detected to be 0.0252 for the minimum observed $\mu_{\max A1}$. The corresponding expected 95% confidence intervals are listed in Table 11. Indeed, as observed from Table 9 this critical value for $\mu_{\max A2}$ is exceeded in the experiment of 181198 for which the minimum $\mu_{\max A1}$ is observed.

Table 11. Expected 95% confidence intervals expressed as percentage of parameter values for the critical experiment

	$\frac{3.43 - Y_{A1}}{Y_{A1}} m_{\max A1} X$	$\frac{1.14 - Y_{A2}}{Y_{A2}} m_{\max A2} X$	$\mu_{\max A1}$	K_{SA1}	$S_{NH,1}(0)$	$\mu_{\max A2}$	K_{SA2}
D optimal	0.2360	0.0499	1.37	6.36	0.61	3.08	21.43
Critical exp	0.1036	0.0252	1.91	9.13	0.90	4.59	31.98

5. Case study 2 – combined COD degradation and nitrification

5.1. Step 1: Reference experiment

The degradation of the readily biodegradable compounds in the combined municipal-industrial wastewater of the WWTP of Zele (Aquafin NV, Aartselaar, Belgium) was characterised by respirometric measurements. Titrimetric measurements were also carried out, but these data were not included in this study since it was not yet evident how to interpret the titrimetric effects of COD degradation. The titrimetric effect related to degradation of COD will highly depend on the kind of carbon compounds present, e.g. it was shown in the work of Gernaey *et al.* (2000a) that acetate and dextrose degradation result in completely opposite titrimetric effects. Obviously, it is not known which specific carbon compounds the wastewater COD consists of. In experiments where nitrification was suppressed it was indeed observed that the wastewater COD also resulted in a titrimetric effect (data not shown). However, it was not within the scope of this work to interpret and model this.

A typical experimental r_0 profile of a wastewater from the Zele WWTP is given in Fig. 9. Based on an analysis of the wastewater it is known that ammonium is present and probably also some readily biodegradable COD (see chapter 8). From the section above (case study 1) it was realised that a model including nitrification in two steps was needed to describe the nitrification in this plant adequately. However, it is clear from the “tailing” wastewater profile in Fig. 9 that it would not be possible to separate the contributions of (i) the nitrification and (ii) the degradation of readily biodegradable COD to the total r_0 from each other. Thus, to analyse the example of Fig. 9 the nitrification parameters were fixed at values obtained from a separate experiment where only ammonium and nitrite were added (from case study 1). In this way kinetic parameters related to the COD degradation could be estimated (Spanjers and Vanrollegem, 1995).

However, in general the respirograms of wastewater were not informative enough to describe the degradation of COD via Monod kinetics, since no zero order respiration rate plateau (i.e. constant respiration rate) was reached in the experiments. Consequently, the degradation of COD was instead described via a first order model (Eq. 4), where the first order rate constant k replaces the Monod

parameter combination $\frac{m_{\max H}}{K_S}$. The model applied to describe the wastewater data is given in Table 12.

$$\begin{cases} \frac{dS_S}{dt} = -\frac{k \cdot X}{Y_H} S_S(t) \\ r_{O,ex} = \frac{1 - Y_H}{Y_H} \cdot k \cdot X \cdot S_S(t) \end{cases} \quad (4)$$

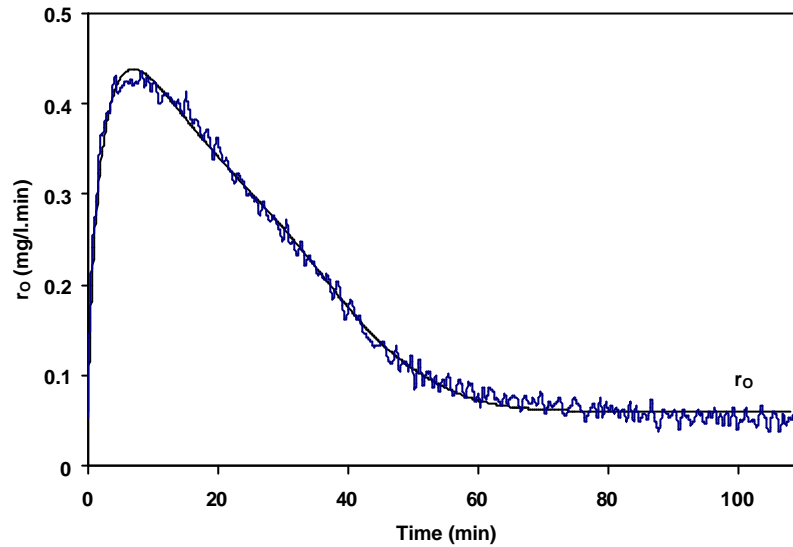


Figure 9. Experimental data and model fit of a wastewater r_o profile

Table 12. COD degradation and nitrification model for interpretation of respirometric data, assuming that no biomass growth takes place

Component → Process ↓	1. S_O	2. S_{NH}	3. S_{NO2}	4. S_{NO3}	5. S_S	Process rate
1. COD degradation	$-\frac{1 - Y_H}{Y_H}$				$-\frac{1}{Y_H}$	$k \cdot X$
2. Nitrification step 1	$-\frac{3.43 - Y_{A1}}{Y_{A1}}$	$-\frac{1}{Y_{A1}}$	$\frac{1}{Y_{A1}}$			$m_{\max A1} \frac{S_{NH}}{K_{SA1} + S_{NH}} X$
3. Nitrification step 2	$-\frac{1.14 - Y_{A2}}{Y_{A2}}$		$-\frac{1}{Y_{A2}}$	$\frac{1}{Y_{A2}}$		$m_{\max A2} \frac{S_{NO2}}{K_{SA2} + S_{NO2}} X$

The purpose of this study was to design an experiment that would allow for a simultaneous characterisation of the reaction kinetics for both the first nitrification step and the degradation of readily biodegradable COD. Here, we will not aim for a simultaneous identification of the second nitrification step. Thus, the parameters related to the second nitrification step will be fixed at values obtained in the case study above.

As in the case study of the two step nitrification above, the most obvious experimental design (A) is the one where the nitrification results in a more visible shoulder in the r_o profile. Secondly, the purpose is to design an experiment from which extant parameters can be obtained. That is, the conditions have to be such that they are representative for the full-scale system to be able to transfer the lab-scale results to a model of the full-scale WWTP. Finally, emphasis is put on the sensitivity of the experimental design to analyse the effect of changes in wastewater concentration and character. Because of the faster convergence of the objective function toward a minimum for the parameter estimation only measurements of r_o will be considered in this study. Again, the concept of optimal experimental design defined in Fig. 1 is now concretised for this case and illustrated in Fig. 10.

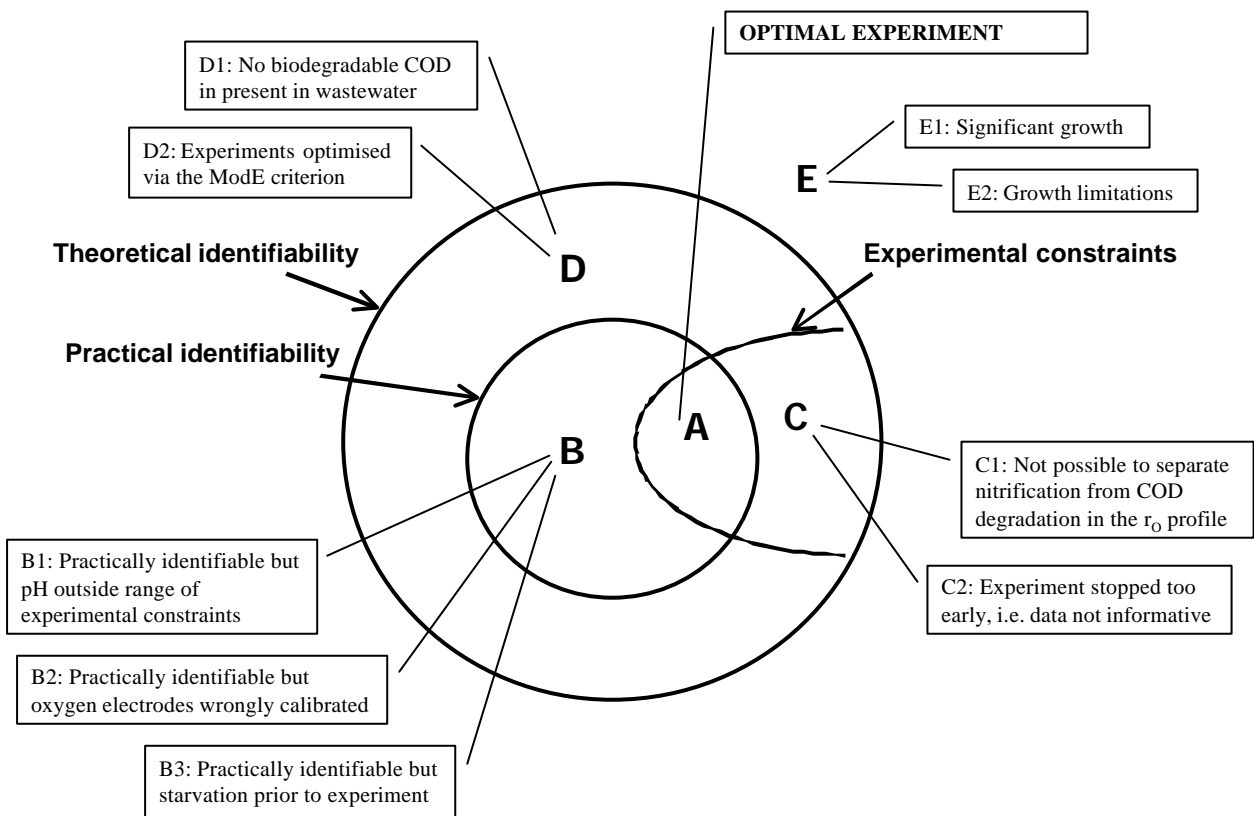


Figure 10. Optimal experimental design for combined COD degradation and nitrification. Illustrations of experiments : A – D

5.2. Step 2: Experimental conditions and constraints

The purpose of the experiments is to achieve accurate estimation of the kinetic parameters for COD degradation and the first nitrification step. In addition, these parameters should be representative for the full-scale system under study. As discussed above the $S(0)/X(0)$ and ΔS are two critical factors that are influencing the experimental response. Also, here it will be attempted to work at the lowest $S(0)/X(0)$ and ΔS possible to avoid significant growth and nitrification inhibition. Thus, concerning the COD degradation process the growth process without cell multiplication (Fig. 2) is aimed for. Again, the model for which unique parameters are sought does not consider growth (i.e. X is not a function of time), see Table 12.

The list of valid experimental conditions is rather similar to the one of the two step nitrification example above:

- Experimental conditions :
 - Measured variables :
 - Oxygen uptake rate (r_O)
- Environmental variables :
 - Nitrifying and COD removing sludge from the full-scale WWTP under study.
 - The substrate load of ammonium and COD, ΔS , and $S(0)/X(0)$ ratio should not be too different compared to the full-scale system to ensure that the organisms are not subjected to too drastic changes in their environmental conditions, and thereby changes of experimental responses (considering COD see Fig. 2).
 - Substrates should be added in such amounts that the biomass increase does not exceed 5% to avoid significant growth. Thus, a growth of less than 5% is here considered negligible.
 - Ammonium and/or nitrite as substrate should be dosed such that the concentrations of ammonia (NH_3) and nitrous acid (HNO_2) are below 0.1 gN/m^3 and 0.2 gN/m^3 respectively to avoid inhibition of nitrification Note that the critical concentrations of NH_3 and HNO_2 are pH dependent (Anthonisen, 1976).
 - pH in the range 5.5 – 10 to avoid growth limitation (Henze *et al.*, 1997).
 - Temperature 5 – 40 °C to avoid growth limitation (Henze *et al.*, 1997).
 - Oxygen concentration above 2 mg/l to avoid limitation.
 - No presence of inhibiting components.

The purpose concerning simultaneous characterisation of the reaction kinetics for the first nitrification step and COD degradation can be fulfilled by designing an experiment for which the practical identifiability is ensured. Thus, no further experimental constraints will have to be imposed on the experimental conditions already listed above. Similar to the case of two step nitrification, however, the second purpose dealing with

the transferability of the lab-scale results to the full-scale system requires a few additional constraints to frame the experimental conditions. Again, these extra experimental constraints are rather simple and similar to the two step nitrification case, since the main issues of ensuring a lab-scale result that is transferable to the full-scale system are already defined by the conditions above.

- Experimental constraints:
 - pH in range 7.5 - 8.5
 - Temperature in full-scale system is 10°C
 - Sludge history

The comments on these experimental constraints given above for the two step nitrification case also apply here. Hence, for example a pH outside the defined range, or an experiment carried out with sludge that has been starved in endogenous state prior to the experiment to an extent that leads to a response significantly different from the full-scale behaviour, are both conditions that do not comply with the defined constraints.

5.3. Step 3: Theoretical Identifiability

The theoretical identifiability of Monod models was investigated in detail in chapter 4. For this case study the theoretical identifiability of the first order model for COD degradation was investigated and it appeared that the combinations $k \cdot X$ and $(1 - Y_H) \cdot S_S(0)$ are theoretically identifiable. Table 13 summarises the results given the assumption of insignificant growth and measurements of r_O only. Thus, column one and two in Table 13 defines the hard bound region of the theoretically identifiable parameter combinations considered in this case study (Fig. 10).

Table 13. Schematic overview of the theoretically identifiable parameter combinations for heterotrophic growth and nitrification, assuming measurements of r_O and a model structure with insignificant growth (see also chapter 4)

Process (j)	Heterotrophic growth	Nitrification step 1	Nitrification step 2
Measurement (i) →	r_O	r_O	r_O
Model structure ↓			
No growth	kX $(1 - Y_H)S_S(0)$	$\frac{3.43 - Y_{A1}}{Y_{A1}} m_{\max A1} X$ $(3.43 - Y_{A1})K_{SA1}$ $(3.43 - Y_{A1})S_{NH}(0)$	$\frac{1.14 - Y_{A2}}{Y_{A2}} m_{\max A2} X$ $(1.14 - Y_{A2})K_{SA2}$ $(1.14 - Y_{A2})S_{N02}(0)$

This region of theoretical identifiability frames the experimental conditions (A - D), defined above, for which unique parameters of the chosen model can be obtained. Again, experiments that do not comply with these restrictions, i.e. in case significant growth or inhibition takes place, can not be described with this model. Thus, such experiments lay outside the region of theoretical identifiability (experiment E in Fig. 10).

5.4. Step 4 – 6: Practical Identifiability

In the two step nitrification case above problems with singularity of the FIM were encountered caused by the introduction of combined respirometric-titrimetric measurements. Here, only respirometric measurements (r_O) are considered and thereby the problem of the FIM being singular did not appear.

Obviously, an experiment where the respirometric data contain sufficient information for practical identifiability of both the heterotrophic degradation of COD and the first nitrification step is represented by experiment B in Fig. 10.

The scaling factor α that was applied on the time units in the reference experiment to allow for a more stable inversion of the FIM are given in Table 14. As dealt with in chapter 6 this optimal scaling factor was found by minimisation of the condition number ($\lambda_{\max}/\lambda_{\min}$) of the FIM.

Table 14 Applied scaling factor α and the corresponding condition number of the FIM for case 2.

Measurements	α	$\lambda_{\max}/\lambda_{\min}$
r_O	1	$4.15 \cdot 10^{14}$
	$3.88 \cdot 10^5$	$1.02 \cdot 10^4$

Again, the condition number of the FIM can be reduced significantly by scaling of the time units.

5.5. Examples of experiments B - D

Experiments of the type B2 - B4 from Fig. 5 related to (1) pH outside defined range, (2) wrong calibration of oxygen electrodes and (3) starvation prior to experimentation respectively, but with ensured practical identifiability, are also relevant for this case.

An experiment in accordance with the experimental constraints but where the first step nitrification is not practically identifiable from the r_O profile (as in Fig. 9) is illustrated by experiment C in Fig. 10. Also, experiments yielding non-informative r_O profiles due to a too early termination of the experiment or too little substrate added are represented by experiment C, similar to the two step nitrification case.

Finally, in this case experiment D can be exemplified by an experiment where the wastewater added does not contain any readily biodegradable COD. Thus, in such an experiment the reaction kinetics related to the

first nitrification step can still be identified with the model, but the purpose of simultaneous estimation of degradation kinetics of readily biodegradable COD can naturally not be fulfilled excluding the experiment from the region of experimental constraints. Finally, a D-type experiment can also be illustrated by an experiment optimised via the ModE criterion, as described in the two step nitrification case.

5.6. Step 7: Experimental degrees of freedom

The experimental degree of freedom to obtain the optimal experiment (A) is here chosen as the optimal additional amount of ammonium to be added initially together with the wastewater. The aim of the OED is then to optimise the additional initial addition of ammonium, $S_{NH,1}(0)$, to obtain a r_O profile which contains enough information to allow for simultaneous estimation of the kinetic parameters related to the first nitrification step and the degradation of the readily biodegradable COD. It is assumed that the amount of wastewater is fixed although the wastewater may contain a varying COD content. The pH set-point was between 8.0 – 8.2.

The sludge load of the full-scale WWTP was calculated on the basis of average full-scale data and was found to be about 0.32 – 0.48 kgCOD/kgMLSS.d (see chapter 8). However, only an average of about 16% of the total COD is readily biodegradable (see chapter 8), which gives a load of readily biodegradable COD of about 0.05 – 0.08 kgCOD/kgMLSS.d. The load of readily biodegradable COD in the lab-scale experiments was calculated to be 0.05 – 0.20 kgCOD/kgMLSS.d. Thus, in some cases the lab-scale load has been higher than the average full-scale load. Still, the differences are not considered to be significant enough to change the response of the organisms. The applied $S(0)/X(0)$ ratios were in the range 1:100 – 1:200 mg COD(substrate)/mg COD(total). The heterotrophic biomass concentration was calculated to be about 0.217 mg COD_{HET}/mg COD(total) (see chapter 8), resulting in a $S(0)/X(0)$ ratio of about 1:20 – 1:40 mg COD(substrate)/mg COD_{HET}. With a heterotrophic yield coefficient, Y_H , of 0.67 mg COD(biomass)/ mg COD(substrate), such $S(0)/X(0)$ ratios will result in a biomass increase of less than about 3 %. Thus, the experimental constraint that no biomass growth should take place is clearly fulfilled.

The experimentation time for the optimal experimental designs was fixed to 85 minutes, which is the time needed to terminate the degradation of COD and the first step nitrification step in the reference experiment (Fig. 9).

5.7. Step 8: Optimal Experimental Design

The results of the D-criterion based OED and the reference experiment are listed in Table 15, considering r_O measurements and applying the α value of Table 14.

Thus, according to the D-criterion the optimal $S_{NH,1}(0)$ value is 5.24 mg N/l. This corresponds to an extra addition of 2.88 mg N/l, since the wastewater contains 2.46 mg N/l according to the estimation. For this

optimal experiment the Det(FIM) is about ten times larger than for the reference experiment, indicating that the generalised parameter variance has decreased as expected. In addition the λ_{\min} has increased, $\text{Tr}(\text{FIM}^{-1})$ has decreased and $\text{Tr}(\text{FIM})$ has increased in the optimal experiment, in accordance with expectations. However, similar to the case with S_{O} measurements in the two step nitrification case study above, the value of the condition number, $\lambda_{\max}/\lambda_{\min}$, increased. This is contrary to what is expected and indicates that the reference experiment is more optimal with respect to the modE criterion (minimisation of $\lambda_{\max}/\lambda_{\min}$) than the experiment predicted via the D-criterion. Again, this inconsistency may be caused by the rescaling of the time unit that has a negative effect on the performance of especially the modE criterion (see chapter 5).

Table 15. Values of the OED criteria for different experimental set-ups and with the D criterion (Det(FIM)) as optimisation criterion. $S_{\text{NH},1}(0)$ is the degree of freedom in the experimental design. The optimised value for the D-criterion is given in bold

Meas.	Criterion	$\text{Tr}(\text{FIM}^{-1})$	$\text{Tr}(\text{FIM})$	$\text{Det}(\text{FIM})$	λ_{\max}	λ_{\min}	$\lambda_{\max}/\lambda_{\min}$	$S_{\text{NH},1}(0)$	$S_{\text{S},1}(0)$
r_{O}	reference	$1.38 \cdot 10^{-1}$	$9.26 \cdot 10^4$	$1.15 \cdot 10^{15}$	$7.97 \cdot 10^4$	7.85	$1.02 \cdot 10^4$	2.46	17.30
	D	$8.82 \cdot 10^{-2}$	$2.07 \cdot 10^5$	1.48×10^{16}	$1.94 \cdot 10^5$	12.10	$1.60 \cdot 10^4$	5.24	17.30

The expected 95% confidence intervals for the reference experiment and the optimal experiments with the extra addition of S_{NH} are given in Table 16. These confidence intervals are calculated based on the inverse of the FIM^{-1} assuming that the measurement error on r_{O} remains the same as for the reference experiment (see Eq. 3).

Table 16 Expected 95% confidence intervals for the experiments of combined COD degradation and nitrification optimised according to the D criterion, see Table 15, expressed as percentage of parameter values.

Measurements	Experiment	$\mu_{\max A1}$	$K_{\text{SA}1}$	$S_{\text{NH}}(0)$	k	$S_{\text{S}}(0)$
r_{O}	reference	3.33	10.86	1.63	6.34	3.05
	D-optimal	1.48	6.31	1.78	4.94	2.49

From Table 16 it is clear that the confidence intervals for the parameters $\mu_{\max A1}$ and $K_{\text{SA}1}$ will significantly improve when an extra amount of S_{NH} is added initially. The improvement of the confidence intervals is 55% and 42% respectively. It is not clear why the confidence interval of $S_{\text{NH},1}(0)$ increases for the optimal experiment, although the difference is not very large. Finally, the improved identifiability of the nitrification

parameters helps to improve the confidence intervals of the first order degradation rate for COD degradation and the estimated initial concentration of readily biodegradable COD (S_S) in the wastewater. These improve with 22% and 18% respectively.

5.8. Validation of optimal experimental design

The extra amount of ammonium added in the experiment carried out to validate the procedure was 2.20 mg N/l. The experimental data together with the model fits are illustrated in Fig. 11. The results of the estimated parameter combinations for the reference and validation experiment are given in Table 17.

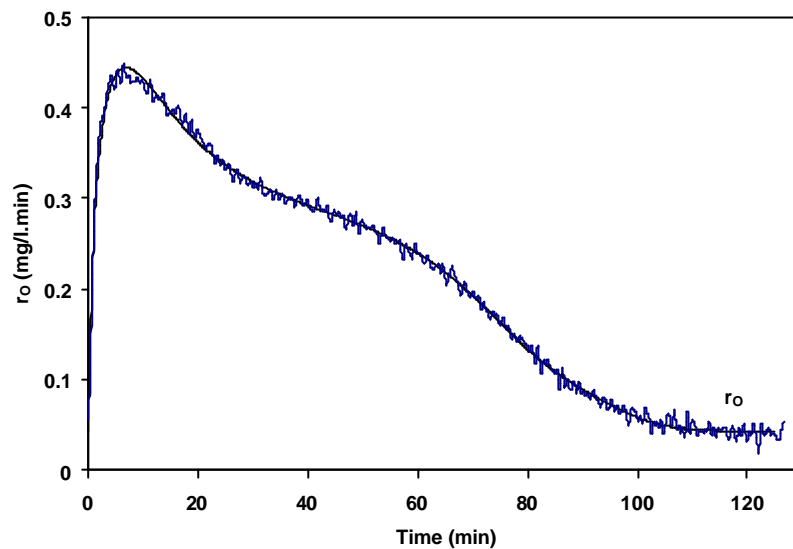


Figure 11. Validation experiment. Experimental r_o data and model fit of an addition of wastewater and extra ammonium

Table 17. Estimated parameter combinations for reference ($\text{NH}_4\text{-N}$ and WW) and validation experiment (WW + $\text{NH}_4\text{-N}$) for combined COD degradation and nitrification (values in italic were fixed and not estimated). The amount originating from the wastewater is calculated based on chemical analysis of ammonium-nitrogen in the wastewater and indicated between brackets for WW+ NH_4

Addition	$S_{\text{NH}_4}(0)$ mg/l	BOD_{st} (theory)	BOD_{st} (model)	$\frac{3.43 - Y_{\text{A1}}}{Y_{\text{A1}}} m_{\text{max A1}} X$	$(3.43 - Y_{\text{A1}})K_{\text{SA1}}$	kX	$(1 - Y_{\text{H}})S_{\text{S},i}(0)$
$\text{NH}_4\text{-N}$	4.54	19.65	19.30	0.2331	1.150		
WW	1.80	7.79	10.66	<i>0.2331</i>	<i>1.150</i>	0.0779	5.711
WW+ NH_4	(1.80+2.20)	17.32	21.88	0.2036	1.410	0.0735	5.518

As can be observed from Table 17 the estimated parameter combinations are very similar. This confirms that these experiments can be used as a validation of the OED procedure. The estimated BOD_{st} for the

single ammonium addition matches well the theoretically expected one ($4.33 \cdot S_{NH,1}(0)$). However, the BOD_{st} related to the ammonium added with the wastewater seems to be overestimated. This can be caused by the fact that the amount of ammonium added with the wastewater is calculated on the basis of chemical analysis of ammonium-nitrogen (1.80 mg N/l). It is likely that parts of the organic nitrogen (for this wastewater the concentration of TKN is about three times higher than the NH_4-N concentration) in the wastewater is nitrifiable and thereby results in oxygen consumption. Note that the value of $S_{NH}(0)$ in Table 15 is the model value. Indeed, if one compares the experiment of the wastewater addition with the wastewater plus extra ammonium (2.20 mg N/l) experiment, then it is observed that the difference in estimated BOD_{st} ($21.88 - 10.66 = 11.22$) corresponds reasonably well with the theoretically expected ($17.32 - 7.79 = 9.53$).

The actual 95% confidence interval for the validation experiment is given in Table 18.

Table 18. Confidence intervals as percentage of parameter values for the validation experiment for combined COD degradation and nitrification.

Measurements	Experiment	μ_{maxA1}	K_{SA1}	$S_{NH}(0)$	k	$S_S(0)$
r_O	validation	1.88	7.28	0.95	5.42	2.95

Obviously the confidence intervals for μ_{maxA1} , K_{SA1} , $S_{S,1}(0)$ and k are slightly larger than the theoretically predicted ones (see Table 16) since the actual amount of S_{NH} added was a bit lower than the amount calculated by the OED procedure. However, the actual confidence interval on $S_{NH,1}(0)$ is smaller than predicted.

5.9. Step 9: Sensitivity of the optimal experimental design to variation in parameters and wastewater concentrations

In this study, the robustness of the optimal experimental design derived above was first investigated in general by checking the sensitivity of the parameter estimation accuracy, indicated by COV and Det(FIM), to changes in the kinetic parameters for degradation of COD and ammonium, i.e. k and μ_{maxA1} , and changes in wastewater concentrations, i.e. S_S and S_{NH} . The sensitivity was evaluated using relative sensitivity functions, RSF (see Eq. 5). The optimal experiment was used as the reference, and the model output obtained after increasing the value of a specific parameter with 1% was used to obtain the relative sensitivity functions (Eq. 5).

$$RSF = \frac{\Delta y}{y} \cdot \frac{p}{\Delta p} \quad (5)$$

The results of this evaluation are shown in Table 19. The influence of a parameter or substrate

concentration on the COV or Det(FIM) was interpreted as proposed by Julien (1997): If $RSF = 0$ the parameter has no influence at all, for $RSF < 0.25$ the influence of the parameter is not considered to be significant; if $0.25 \leq RSF < 1$, the parameter is considered to be influential; if $1 \leq RSF < 2$ the parameter is considered to be very influential and, finally, if $2 \leq RSF$ the parameter is considered to be extremely influential. When the value of a parameter or initial substrate concentration and the COV or Det(FIM) change in the same direction, this is indicated with a positive sign in Table 19, and when they move in the opposite direction this is indicated with a negative sign.

Table 19. Results sensitivity analysis of the D-optimal experimental design (0 = no influence, +, - = not very significant, ++, -- = influential; +++, --- = very influential; + + + +, - - - - = extremely influential). See text for a further explanation of the results

Parameter	COV($\mu_{\max A1}$)	COV(K_{SA1})	COV($S_{NH,1}(0)$)	COV(k)	COV($S_{S,1}(0)$)	Det(FIM)
k	-	+	---	+++	----	++
$\mu_{\max A1}$	+	----	+	++	++	++++
$S_{S,1}(0)$	0	0	0	----	0	+++
$S_{NH,1}(0)$	--	++	++	-	--	+

From Table 19 it becomes clear that a decrease in the degradation rate of COD (k) will increase COV($S_{S,1}(0)$) and COV($S_{NH,1}(0)$), i.e. the accuracy of both the $S_{S,1}(0)$ and $S_{NH,1}(0)$ determination will decrease. Indeed, if k decreases then the part of the $r_{O,ex}$ profile related to COD degradation will last longer, i.e. it will become more difficult to separate the area of the $r_{O,ex}$ profile in two fractions related to the $S_{S,1}(0)$ and $S_{NH,1}(0)$ concentrations respectively. This effect is not compensated by the increased number of data points available for the estimation of this parameter since the COD degradation will last longer for a lower value of k. The accuracy for $\mu_{\max A1}$ will decrease slightly when k decreases. An increase of k will have the opposite effects on the covariance.

When the value of $\mu_{\max A1}$ decreases it means that the $r_{O,ex}$ profile is not terminated within the defined experimental time of 85 minutes. Obviously, this has a very negative effect on the accuracy of K_{SA} . On the contrary, if $\mu_{\max A1}$ increases this will result in slightly more data points for the K_{SA1} determination, yielding a higher accuracy. Further, a decrease of $\mu_{\max A1}$ means that the degradation of COD and nitrification processes are better separated in the $r_{O,ex}$ profile, resulting in improved accuracy of k and $S_{S,1}(0)$. Finally, note that the value of $\mu_{\max A1}$ also determines its own accuracy: when $\mu_{\max A1}$ decreases more data points are available, yielding a better $\mu_{\max A1}$ estimate.

Wastewater changes with respect to $S_{S,1}(0)$ only have a strong effect on the accuracy of k. There are no

effects on the remaining parameters. This can be explained because the sensitivity functions of $r_{O,ex}$ with respect to $S_S(0)$ are constant functions for the first order degradation model (see Appendix 7.1).

If the concentration of $S_{NH,1}(0)$ increases, the accuracy of μ_{maxA1} , k and $S_{S,1}(0)$ increase (their covariance decreases) because more data points will be available to describe the nitrification process, thus allowing for an improved separation between COD degradation and nitrification. However, again the $r_{O,ex}$ profile will then not terminate within the preset experimental time resulting in a worse parameter accuracy for K_{SA1} and $S_{NH,1}(0)$.

Finally, μ_{maxA1} is the parameter that has the largest influence on the overall generalised variance expressed by $\text{Det}(\text{FIM})$. Thus, if μ_{maxA1} for example increases the $\text{Det}(\text{FIM})$ will also increase significantly.

5.10. Validation of sensitivity of the optimal experimental design to variation in parameters and wastewater concentrations

In the following the effects of parameter and initial substrate changes, discussed above, are evaluated with a set of experiments carried out with wastewater and extra ammonium additions during a measuring campaign at the combined municipal – industrial WWTP of Zele (Aquafin NV, Aartselaar, Belgium). Table 20 lists the estimated parameter combinations.

The variations in the parameter combination including k are considered to be related to changes in the wastewater organic compounds. However, the COD degradation could still be described by the first order model. Some variations are observed for the nitrification kinetics as well, as discussed in the previous section. Finally, it is again observed for some cases that the estimated BOD_{st} related to ammonium oxidation is larger than theoretically predicted. As described above this can be caused by the fact that the theoretical values are based on the concentration of the analytically measured ammonium-nitrogen, not including possible nitrifiable organic nitrogen. The experimental data and model fits for the experiments with wastewater and ammonium added are given in Fig. 12 – 13.

Table 20. Estimated parameter combinations for different experiments with addition of wastewater and extra initial ammonium, the $S_{NH}(0)$ value between brackets indicates the amount of ammonium present in the wastewater alone

Exp	Addition	Time (min)	$S_{NH,1}(0)$ mg/l	BOD_{st} (theory)	BOD_{st} (model)	$\frac{3.43 - Y_{A1}}{Y_{A1}} \mu_{max A1} X$	$(3.43 - Y_{A1})K_{SA1}$	$(3.43 - Y_{A1})S_{NH,1}(0)$	kX	$(1 - Y_H)S_{S,1}(0)$
191198(ref)	NH ₄		4.54	19.65	19.30	0.2331	1.150	14.484		
	WW		1.80	7.79	10.66	0.2331	1.150	7.997	0.0779	5.711
Validation	WW+NH ₄	85	(1.80)+2.20	17.32	21.88	0.2036	1.410	16.422	0.0735	5.518
161198	NH ₄		3.06	13.80	15.72	0.2603	1.091	11.801		
	WW+NH ₄	50	(2.25)+0.75	12.97	13.21	0.2823	1.400	9.913	0.3200	1.678
201198	NH ₄		3.60	15.61	19.57	0.2500	1.206	14.686		
	WW+NH ₄	75	(1.16)+3.16	18.75	20.27	0.2465	1.160	17.815	0.0589	5.778
211198	NH ₄		3.78	16.40	19.38	0.2637	1.148	14.550		
	WW+NH ₄	100	(1.26)+2.54	20.08	29.61	0.2344	1.580	22.227	0.0810	4.611
221198	NH ₄		3.78	16.40	15.41	0.1089	0.952	11.566		
	WW+NH ₄	125	(1.67)+2.21	16.80	19.02	0.1361	1.530	14.277	0.0697	6.062
241198	NH ₄		3.79	16.40	16.95	0.2146	1.425	12.720		
	WW+NH ₄	120	(1.78)+2.93	20.43	27.10	0.2069	1.500	20.340	0.0850	3.602

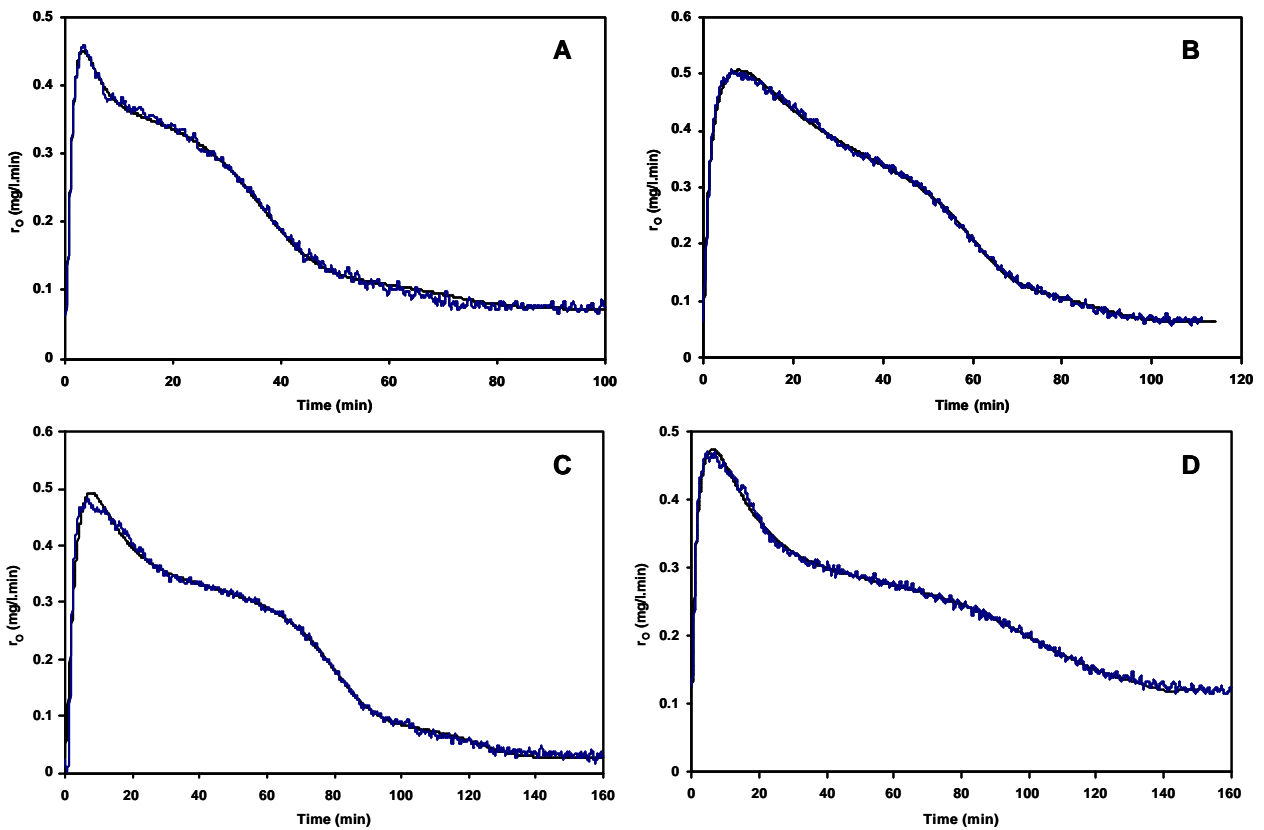


Figure 12. Experimental data (r_o) of wastewater and ammonium addition together with model fits. **A:** 161198, **B:** 201198, **C:** 211198, **D:** 221198

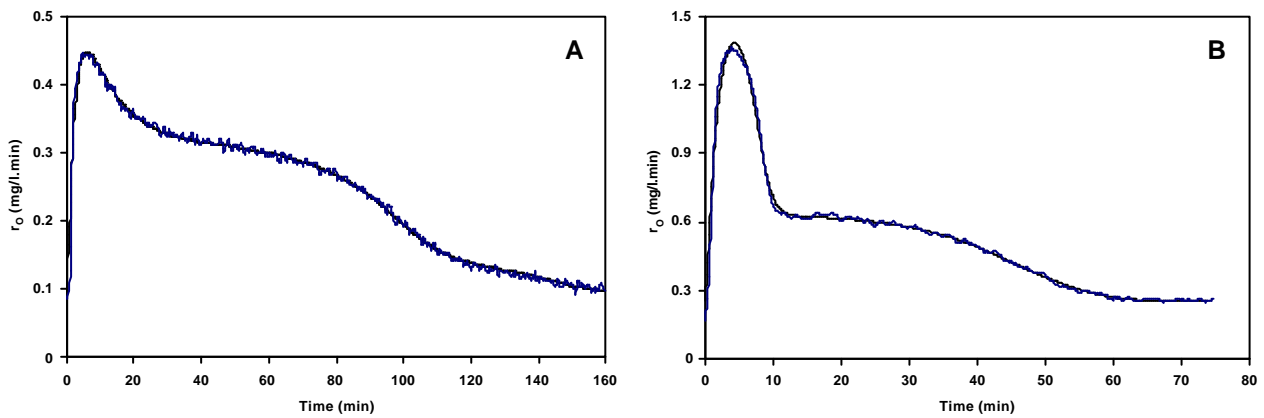


Figure 13. Experimental data (r_o) of wastewater and ammonium addition together with model fits, **A:** 241198, **B:** Change in wastewater character

The confidence intervals were calculated for the experiments in which the first order rate constant k differed most from the reference case (Table 21).

Table 21 Confidence intervals as percentage of parameter values for the validation of robustness of the optimal-D experiment

Experiment	$\mu_{\max A1}$	K_{SA1}	$S_{NH,1}(0)$	k	$S_{S,1}(0)$	Det(FIM)
D optimal	1.48	6.31	1.78	4.94	2.49	$1.48 \cdot 10^{16}$
161198	2.98	9.26	0.97	13.19	4.07	$9.61 \cdot 10^{13}$
201198	1.86	6.68	1.42	5.14	3.53	$9.07 \cdot 10^{15}$
221198	2.57	8.30	1.07	4.40	2.59	$5.65 \cdot 10^{15}$

From Table 21 it can be observed that the changes of parameters or substrate concentrations may be somewhat more complex to interpret since more than one parameter change at a time. Still, it is possible to draw some lines and evaluate the results based on the general sensitivity analysis in Table 19.

For the experiment of 161198 the estimated value of the parameter combination including the first order degradation rate k is about four times larger compared to the k value of the D-optimal experiment. Furthermore, the concentration of $S_{S,1}(0)$ is about three times lower. According to Table 19, both an increase of k and a decrease of $S_{S,1}(0)$ will lead to a lower accuracy of the estimated k. Indeed, it can be observed from Table 21 that the confidence interval of k for the experiment 161198 is significantly larger than for the D-optimal experiment, as expected from the sensitivity results. Furthermore, both the estimated value of the parameter combination including $\mu_{\max A1}$ and the $S_{NH,1}(0)$ concentration are lower for the experiment of 161198 than for the D-optimal experiment. Especially, a lower $\mu_{\max A1}$ has a negative effect on the accuracy of the K_{SA1} estimate as seen from Table 19. The results in Table 21 indeed confirm this prediction. The decrease in $S_{NH,1}(0)$ results in a lower accuracy of $\mu_{\max A1}$ according to Table 19, as was confirmed for experiment 161198 (see Table 21). Summarising, the experiment 161198 is generally resulting in less accurate parameter estimates as generally confirmed with the lower Det(FIM) that was obtained for this experiment.

For the experiments of 201198 and 221198 the values of Det(FIM) are closer to the optimal one. The accuracy of the parameters is also closer to the optimal ones compared to the experiment of 161198. A significant decrease in the parameter combination including $\mu_{\max A1}$ is observed for experiment 221198, which according to Table 19 should induce a significant reduction of the accuracy for the K_{SA1} . This is indeed observed in Table 21. However, it should also be noted that the experimental time was allowed to be longer (125 min) compared to the defined optimal time of 85 min. It is obvious that the accuracy decrease of K_{SA1} would have been more drastic in case the experiment of 221198 had been forced to end after 85 min.

5.11. Sensitivity of the optimal experimental design to variation in wastewater character

Above, the effect of a variation in wastewater concentration has been investigated. In such cases the optimal experimental design can be adjusted in case the resulting parameter estimates become too inaccurate. However, if the wastewater character (rather than its concentration) changes, e.g. the degradation can no longer be described by a first order model, then the OED becomes significantly more complicated and the whole OED procedure has to be adjusted. An example of change in wastewater character is given in Fig. 13B. Here, the data had to be described via a Monod model instead of the first order model. Thus, the region of theoretical identifiability in Fig. 10 will have to be adjusted accordingly.

A final example of an unfortunate situation, with respect to the sensitivity of the proposed OED, is the case where the wastewater does not contain sufficient readily biodegradable COD (a typical weekend phenomenon) exemplified by experiment D in Fig. 10. In this case the aim of the OED procedure has to be revised since it is now only possible to identify the nitrification process.

6. Discussion

In this study a conceptual and general methodology for optimal experimental design was developed. The concept was illustrated in Fig. 1 and specifically outlined for FIM based optimal experimental designs in Fig. 3. The outlined procedure consists of 9 steps. In fact the procedure is a culmination of the previous chapters 3 – 6. The first and very important step is to define the purpose of the experiment. The purpose determines further (step 2) the appropriate experimental conditions, e.g. measurement technique (see chapter 3), possible constraints and, thereby, the model for which accurate parameter estimates is sought. Next the theoretical identifiability of the model parameters has to be investigated indicated by step 3 (see also chapter 4), and the practical identifiability is considered in step 4 – 6. The practical identifiability analysis includes investigation of the FIM properties, i.e. whether the FIM becomes singular (chapter 5) and also the effect of the rescaling of parameter units (chapter 6). If FIM becomes singular the parameter set, on which it is based, has to be reduced. Now the experimental degrees of freedom to reach an optimal experiment can be defined (step 7). The optimal experimental criterion is chosen in step 8 and is optimised by changing the experimental degree of freedom, in this case via a numerical optimisation routine implemented in the WEST software. Finally, it is considered how sensitive the suggested optimal experimental design is towards changes in e.g. parameters and substrate concentrations (step 9). If the parameter accuracy has decreased significantly it may be needed to update the optimal experiment and, thereby, re-run the procedure.

In this work the procedure for optimal experimental design, outlined above, was concretised for two case studies. The first case study focused on the two step nitrification process and it was aimed to design an

experiment that allowed for simultaneous characterisation of the reaction kinetics of both nitrification steps. Here, the experimental degree of freedom was chosen as the addition of an optimal amount of nitrite together with ammonium. The second case study dealt with simultaneous characterisation of the reaction kinetics of the first nitrification step and readily biodegradable wastewater COD. In this study the experimental degree of freedom was an optimal additional amount of ammonium to be added initially together with the wastewater.

In both cases the main issue of the OED was, of course, to improve the accuracy of the parameter estimates. Table 22 summarises and combines the expected accuracy (95% confidence intervals) of the two case studies (according to Table 6 – 16).

In general it was found that the accuracy of parameter estimates is highest when oxygen measurements are applied for the estimations. The confidence intervals are narrower for the maximum specific growth rates ($\mu_{\max A1}$ and $\mu_{\max A2}$) than for the half saturation coefficients (K_{SA1} and K_{SA2}). This is in accordance with earlier findings (see chapter 3 and 5) and also reported in literature (Kong *et al.*, 1996; Gernaey *et al.*, 1998). It is also noticeable that the parameter accuracy is lower on the parameters related to the second nitrification step, i.e. $\mu_{\max A2}$ and K_{SA2} , compared to the parameters of the first step. This is caused by a lower number of data points for characterisation of the second step. Finally, combined r_O and H_p measurements result in increased accuracy of the parameter related to the first nitrification step compared to single measurements of r_O (see also chapter 5).

Table 22. Summary of expected parameter estimation accuracy (95% confidence interval)

Parameter	Case study 1	Case study 1	Case study 1	Case study 2
	r_O	$r_O + H_p$	S_O	r_O
$\mu_{\max A1}$	1.50	0.70	0.10	1.48
K_{SA1}	6.36	3.97	0.53	6.31
$S_{NH,1}(0)$	0.61	0.09	0.03	1.78
$\mu_{\max A2}$	3.08	3.00	0.24	
K_{SA2}	21.43	21.18	1.64	
S_O^0			0.03	
K_{La}			0.10	
k				4.94
$S_{S,1}(0)$				2.49

Considering the first case study, the main improvements of about 50%, compared to the reference experiment, in parameter accuracy were found for the parameter $\mu_{\max A2}$. This was in accordance with the goal of the optimal experimental design. Moreover, the optimised experimental degree of freedom, $S_{NO,1}(0)$, results in more data containing information on the maximum respiration rate of the second nitrification step, and thereby on the parameter $\mu_{\max A2}$. In addition, a significant improvement of about 20 - 30% was found for the parameter K_{SA2} .

For the second case study, the confidence interval of both $\mu_{\max A1}$ and K_{SA1} are reduced with about 50%, whereas the parameter related to the first order degradation of COD was estimated with an accuracy that is about 20% better. Again, these results are in agreement with the purpose of the study, since the experimental degree of freedom, $S_{NH,1}(0)$, focuses on a separation of the nitrification process from the degradation of COD to allow for an improved identification.

These theoretical predictions were validated with independent parameter estimations on the basis of experiments conducted according to the optimal experimental design.

In these validation experiments of the two step nitrification case study it was found that rather similar experiments conducted with the same sludge source and wastewater lead to highly reproducible parameter estimates. The same applied for the second case study. Here, an interesting side remark is that the analytical ammonia measurement was not a good indicator of the actual nitrifiable nitrogen in the wastewater, since the amount analytical ammonia consistently was lower than the results of the model-based analysis of the respirometric data.

However, if the parameters estimated with sludge collected at different dates within the same week are compared large differences in parameter estimates was observed (up to a factor 2 between min and max value of the same parameter) for both case studies. In view of the fact that the estimates are highly accurate and reproducible, it can be concluded that either the sludge parameters or in the second case study the wastewater composition are varying very significantly over time. Indeed, the variation in the degradation rate of the wastewater COD may be caused by changes in wastewater composition, however this can not be the cause of the differences in nitrification kinetics. Further research is then certainly desired to elucidate the reasons for these short-term changes. In a study of industrial wastewater (Coen *et al.*, 1998) the influent characteristics and the kinetic parameters of the sludge were assessed from on-line respirometric experiments over a 40 hours period (approximately one data set per hour). Here it was found that the wastewater composition and sludge kinetics did not change that drastically, so that the identification algorithm applied on the on-line data was allowed to "follow" the changes. In this situation the wastewater composition did not seem to change significantly during the investigated period, whereas differences in parameters up to a factor 2 also were observed during this 40 hours period. It is likely that the specific organic compounds contained in the total wastewater COD may change over short-term in this specific

case resulting in varying kinetic parameters. However, this was not clear from the study (Coen *et al.*, 1998).

In the studies conducted on the sensitivity of the OED to parameter changes it was found that quite some safety margin exists for the experimental design, i.e. it is rather robust against parameter variations. In the two step nitrification case it was obvious that a combination of a low $\mu_{\max A1}$ and high $\mu_{\max A2}$ was critical and a maximum value of $\mu_{\max A2}$ was determined that still allowed for accurate parameter estimates. One example was recorded (181198) where an application of the optimal experiment would have resulted in really inaccurate parameter estimates.

In the case of combined COD degradation and nitrification a more systematic sensitivity study was carried out to check the effect of the changes of parameters and substrate concentration on the parameter accuracy. Here it was found that changes of the first order degradation rate of COD especially influences the accuracy of the estimation of initial substrates $S_{s,1}(0)$ and $S_{NH,1}(0)$, whereas for example changes of $\mu_{\max A1}$ influence the parameter accuracy of K_{SA1} significantly. A change in the initial substrate concentration $S_{NH,1}(0)$ had the least effect on the overall variances measured by the Det(FIM).

The conclusion in both cases is that frequent updating of optimal experiments may be required or that one must strive for more robust experimental designs.

In this study the experiments were optimised by the D-criterion which maximises the generalised variance expressed by Det(FIM). However, to obtain a robust experimental design an extended OED-criterion could be created in which the sensitivity to parameter or wastewater changes is punished for.

In addition, in this study the defined experimental constraints, e.g. low $S(0)/X(0)$ and ΔS , were checked manually. Such constraints of e.g. no significant growth could also be incorporated into the objective function together with the Det(FIM). In the study of Baltes *et al.* (1994) a critical biological criterion with regard to balanced growth was defined as the gradient of the specific growth rate as function of time, and was incorporated into the objective function of the OED. Something similar could be suggested for the case studies investigated here.

However, in case the model structure changes, as exemplified in the second case study, the whole region of theoretical identifiability will move in the experimental condition space of Fig. 1. Thus, in such a case the whole OED procedure will have to be revised, since it will not be possible to create a criterion that can account for model structure changes. This is contrary to the suggestions above where it is discussed to keep the optimal experiment within the region of practical identifiability by a more robust experiment, however with the same model structure.

7. Conclusion

A conceptual methodology for optimal experimental design was developed and specifically outline for FIM based optimal experimental designs. The procedure was applied in two case studies. The first case focused on the classical problem of identification of both nitrification steps in the two step nitrification process. A simple experimental degree of freedom was chosen as the addition of an optimal amount of nitrite together with ammonium. In the second case study it was aimed to simultaneously characterise the kinetics of the first nitrification step and degradation of the readily biodegradable COD in a wastewater. Also here a simple experimental degree of freedom was chosen as an optimal additional amount of ammonium to be added together with the wastewater. In both cases it was found that the optimised experiment resulted in significant improvements of the parameter estimates. For the case study on the two step nitrification process an improvement of about 50% in the accuracy of the $\mu_{\max A2}$ estimates was obtained. Also for the second case study improvements of about 50% was achieved for the parameters related to the first nitrification step, i.e. $\mu_{\max A1}$ and K_{SA1} . The confidence intervals of the parameters related to the COD degradation improved about 20% in this case. These theoretical predictions were successfully validated with experiments carried out according to the optimal experimental design. Furthermore, it was found that the parameter estimates were highly reproducible for experiments performed with the same sludge source. On the contrary, some variation in estimated parameter values (up to a factor 2) was found for experiments carried out within the same week. Thus, apparently either the sludge parameters or wastewater composition vary significantly over short term. Finally, the sensitivity of the optimal experiment towards changes in values of the kinetic parameters or wastewater concentrations was evaluated for both case studies. For the two step nitrification example it was clear that a situation where the value of $\mu_{\max A1}$ is low combined with a high value of $\mu_{\max A2}$ is critical and would lead to inaccurate parameter estimates. In the second case study a more systematic sensitivity analysis was made. Here it was for example found that changes in the first order degradation rate of COD was very influential on the estimates of the substrate concentrations, whereas changes in $\mu_{\max A1}$ was extremely influential on the K_{SA1} estimate. Conclusively, either frequent updates or more robust optimal experimental design must be aimed for, and it was discussed how more robust experimental designs might be predicted via extension of the objective function of the OED.

Appendix 7.1

-

**Output sensitivity functions of two-step
nitrification model and first order substrate
degradation model**

Appendix 7.1

Output sensitivity functions of two-step nitrification model and first order substrate degradation model

In this appendix the output sensitivity functions of $r_{O,ex2}$ are derived considering the two-step nitrification model. Furthermore, the output sensitivity functions of $r_{O,ex2}$ for a model describing first order degradation of substrate S_S are developed. Growth is considered to be insignificant and it is assumed that the processes are not limited by oxygen. All analytically derived sensitivity functions have been carefully verified via a numerical procedure, as described in chapter 5.

1. Two-step nitrification model

1.1. Sensitivity functions of $r_{O,ex2}$

First, note that the concentration of S_{NO_2} is depending on both μ_{maxA1} , K_{SA1} and $S_{NH,1}(0)$. The sensitivity function of $r_{O,ex2}$ with respect to μ_{maxA1} is defined in Eq. 1

$$\begin{aligned} \frac{\partial r_{O,ex2}(t)}{\partial \mathbf{m}_{maxA1}} = & -(3.43 - Y_{A1}) \frac{\partial}{\partial \mathbf{m}_{maxA1}} \left(- (1 - e^{-t/\tau}) \frac{\mathbf{m}_{maxA1} X}{Y_{A1}} \frac{S_{NH,2}(t)}{K_{SA1} + S_{NH,2}(t)} \right) \\ & - (1.14 - Y_{A2}) \frac{\partial}{\partial \mathbf{m}_{maxA1}} \left(- (1 - e^{-t/\tau}) \frac{\mathbf{m}_{maxA2} X}{Y_{A2}} \frac{S_{NO_2,2}(t)}{K_{SA2} + S_{NO_2,2}(t)} \right) \end{aligned} \quad (1)$$

The concentration of S_{NH} and S_{NO_2} are calculated by integration of the dynamic model for the hybrid set-up including substrate transport (Eq. 2 and 3 illustrate the substrate equations for the respiration chamber).

$$\frac{dS_{NH,2}(t)}{dt} = \frac{Q_{in}}{V_2} \cdot (S_{NH,1}(t) - S_{NH,2}(t)) - (1 - e^{-t/\tau}) \frac{\mathbf{m}_{maxA1} \cdot X}{Y_{A1}} \frac{S_{NH,2}(t)}{K_{SA1} + S_{NH,2}(t)} \quad (2)$$

$$\frac{dS_{NO2,2}(t)}{dt} = \frac{Q_{in}}{V_2} \cdot (S_{NO2,1}(t) - S_{NO2,2}(t)) + (1 - e^{-t/\tau}) \left(\frac{m_{maxA1} \cdot X}{Y_{A1}} \frac{S_{NH,2}(t)}{K_{SA1} + S_{NH,2}(t)} - \frac{m_{maxA2} \cdot X}{Y_{A2}} \frac{S_{NO2,2}(t)}{K_{SA2} + S_{NO2,2}(t)} \right) \quad (3)$$

Eq. 1 results in Eq. 4.

$$\frac{\partial r_{O,ex2}(t)}{\partial m_{maxA1}} = \frac{(3.43 - Y_{A1}) \cdot (1 - e^{-t/\tau}) \cdot X}{Y_{A1}} \left(\frac{S_{NH,2}(t)}{K_{SA1} + S_{NH,2}(t)} + \frac{m_{maxA1} \cdot K_{SA1} \cdot \frac{\partial S_{NH,2}(t)}{\partial m_{maxA1}}}{(K_{SA1} + S_{NH,2}(t))^2} \right) + \frac{(1.14 - Y_{A2}) \cdot (1 - e^{-t/\tau}) \cdot m_{maxA2} \cdot X}{Y_{A2}} \cdot \frac{K_{SA2} \cdot \frac{\partial S_{NO2,2}(t)}{\partial m_{maxA1}}}{(K_{SA2} + S_{NO2,2}(t))^2} \quad (4)$$

The sensitivity function of $r_{O,ex2}$ with respect to K_{SA1} is derived similarly leading to Eq. 5.

$$\frac{\partial r_{O,ex2}}{\partial K_{SA1}} = \frac{(3.43 - Y_{A1}) \cdot (1 - e^{-t/\tau}) \cdot m_{maxA1} \cdot X}{Y_{A1}} \cdot \left(\frac{K_{SA1} \cdot \frac{\partial S_{NH,2}(t)}{\partial K_{SA1}} - S_{NH,2}(t)}{(K_{SA1} + S_{NH,2}(t))^2} \right) + \frac{(1.14 - Y_{A2}) \cdot (1 - e^{-t/\tau}) \cdot m_{maxA2} \cdot X}{Y_{A2}} \cdot \frac{K_{SA2} \cdot \frac{\partial S_{NO2,2}}{\partial K_{SA1}}}{(K_{SA2} + S_{NO2,2}(t))^2} \quad (5)$$

To be able to solve the sensitivity functions of $r_{O,ex}$ with respect to the initial ammonium concentration $S_{NH,1}(0)$ Eq. 6 is introduced, see further details on the underlying assumptions in the appendix of chapter 5, resulting in Eq. 7.

$$S_{NH,2}(t) = \frac{V_1}{V_1 + V_2} S_{NH,1}(0) - \frac{\int_0^t r_{O,ex2}^{N1} dt}{(3.43 - Y_{A1})} \quad (6)$$

$$\frac{\partial r_{O,ex2}(t)}{\partial S_{NH,1}(0)} = \frac{(1 - e^{-t/\tau}) \cdot \mathbf{m}_{maxA1} \cdot X \cdot K_{A1}}{Y_{A1}} \left(\frac{(3.43 - Y_{A1}) \frac{V_1}{V_1 + V_2} - \int_0^t \frac{\partial r_{O,ex2}^{N1}}{\partial S_{NH,1}(0)} dt}{(K_{SA1} + S_{NH,2}(t))^2} \right) + \frac{(1.14 - Y_{A2}) \cdot (1 - e^{-t/\tau}) \cdot \mathbf{m}_{maxA2} \cdot X}{Y_{A2}} \cdot \frac{K_{SA2} \cdot \frac{\partial S_{NO2,2}(t)}{\partial S_{NH,1}(0)}}{(K_{SA2} + S_{NO2,2}(t))^2} \quad (7)$$

Only the second nitrification step is depending on the parameters μ_{maxA2} , K_{SA2} and the initial nitrite concentration $S_{NO2,1}(0)$ (if added). Thus, the sensitivity functions of $r_{O,ex2}$ follow the same patterns as listed in the appendix of chapter 5 for the single step nitrification, leading to Eq. 8 – 11.

$$\frac{\partial r_{O,ex2}(t)}{\partial \mathbf{m}_{maxA2}} = \frac{(1.14 - Y_{A2}) \cdot (1 - e^{-t/\tau}) \cdot X}{Y_{A2}} \left(\frac{S_{NO2,2}(t)}{K_{SA2} + S_{NO2,2}(t)} + \frac{\mathbf{m}_{maxA2} \cdot K_{SA2} \cdot \frac{\partial S_{NO2,2}(t)}{\partial \mathbf{m}_{maxA1}}}{(K_{SA2} + S_{NO2,2}(t))^2} \right) \quad (8)$$

$$\frac{\partial r_{O,ex2}}{\partial K_{SA2}} = \frac{(1.14 - Y_{A2}) \cdot (1 - e^{-t/\tau}) \cdot \mathbf{m}_{maxA2} \cdot X}{Y_{A2}} \left(\frac{K_{SA2} \cdot \frac{\partial S_{NO2,2}(t)}{\partial K_{SA2}} - S_{NO2,2}(t)}{(K_{SA2} + S_{NO2,2}(t))^2} \right) \quad (9)$$

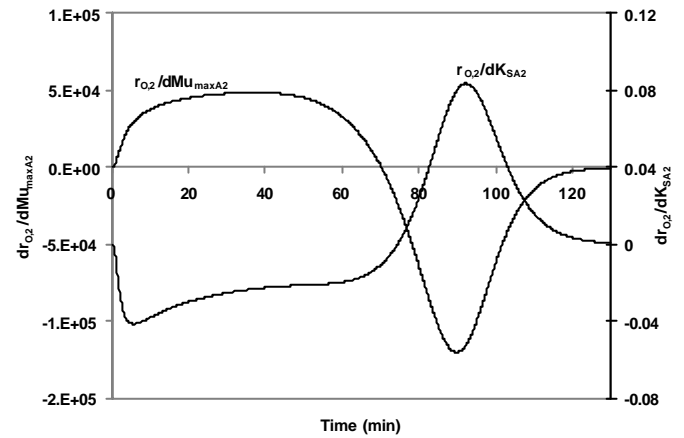
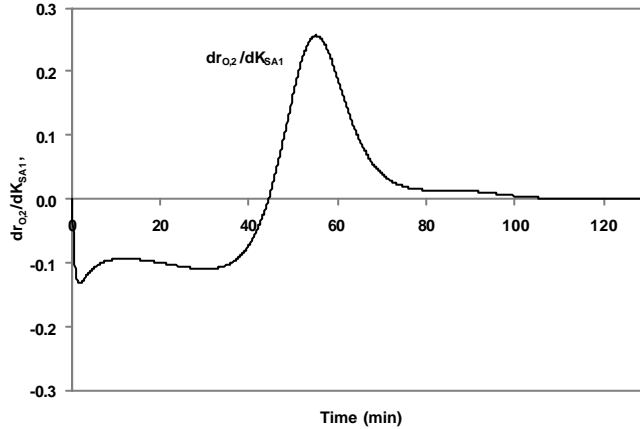
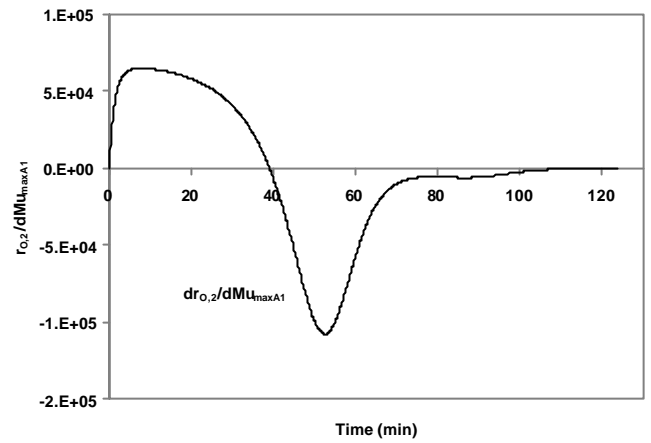
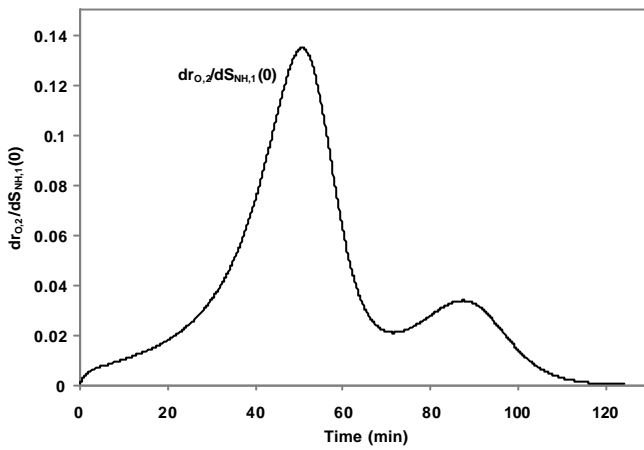
For the sensitivity functions with respect to initial nitrite concentration, $S_{NO2}(0)$, Eq. 10 is introduced (again see appendix of chapter 5 for underlying assumptions).

$$S_{NO2,2}(t) = \frac{V_1}{V_1 + V_2} S_{NO2,1}(0) + \frac{\int_0^t r_{O,ex2}^{N1} dt}{(3.43 - Y_{A1})} - \frac{\int_0^t r_{O,ex2}^{N2} dt}{(1.14 - Y_{A2})} \quad (10)$$

Note that the factor $\frac{\int_0^t r_{O,ex2}^{N1} dt}{(3.43 - Y_{A1})}$ is not influenced by $S_{NO2}(0)$, resulting in Eq. 11.

$$\frac{\partial r_{O_2,ex2}(t)}{\partial S_{NO2,1}(0)} = \frac{(1 - e^{-t/\tau}) \cdot m_{maxA2} \cdot X \cdot K_{SA2}}{Y_{A2}} \left(\frac{(1.14 - Y_{A2}) \frac{V_1}{V_1 + V_2} - \int_0^t \frac{\partial r_{O_2,ex2} dt}{\partial S_{NO2,1}(0)}}{(K_{SA1} + S_{NO2,2}(t))^2} \right) \quad (11)$$

The figures of the sensitivity functions are given below.



2. First order substrate degradation

The only relevant parameter to consider here is the first order degradation constant k and the initial substrate concentration $S_{S,1}(0)$. The sensitivity function with respect to k is simply derived in Eq. 12 – 13.

$$\frac{\partial r_{O,ex2}(t)}{\partial k} = -(1 - Y_H) \frac{\partial}{\partial k} \left(-(1 - e^{-t/\tau}) \cdot k \cdot S_{S,2} \right) \quad (12)$$

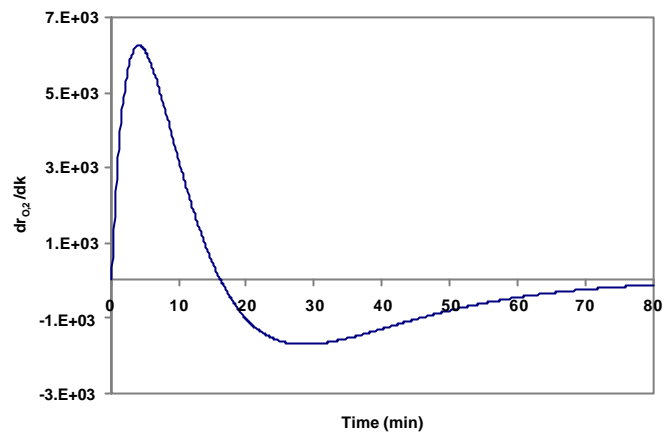
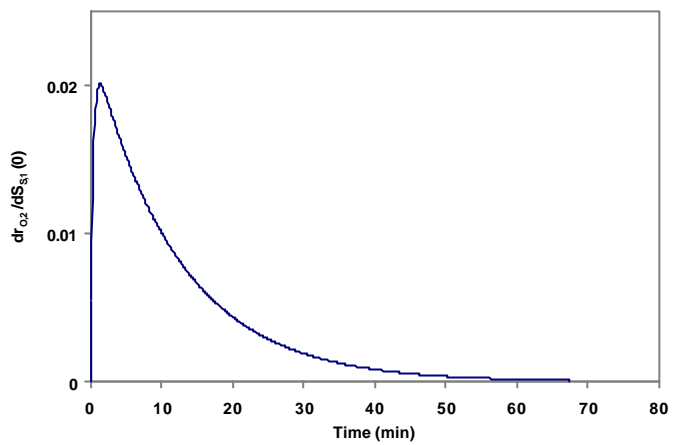
$$\frac{\partial r_{O,ex2}(t)}{\partial k} = (1 - Y_H)(1 - e^{-t/\tau}) \cdot \left(S_{S,2} + k \frac{\partial S_{S,2}}{\partial k} \right) \quad (13)$$

Concerning the initial substrate concentration $S_{S,1}(0)$ Eq. 14 is again introduced to be able to achieve a solution (see underlying assumptions in appendix of chapter 5), resulting in Eq. 15.

$$S_{S,2}(t) = \frac{V_1}{V_1 + V_2} S_{S,1}(0) - \frac{\int_0^t r_{O,ex} dt}{(1 - Y_H)} \quad (14)$$

$$\frac{\partial r_{O,ex2}(t)}{\partial S_{S,1}(0)} = k \cdot X \cdot (1 - e^{-t/\tau}) \left((1 - Y_H) \cdot \frac{V_1}{V_1 + V_2} - \int_0^t \frac{\partial r_{O,ex2}}{\partial S_{S,1}(0)} dt \right) \quad (15)$$

Note that the sensitivity function with respect to $S_{S,1}(0)$ is a constant function independent on the actual value of $S_{S,1}(0)$. Figures are given below.



Chapter 8

-

Evaluation of an ASM1 model calibration procedure on a municipal-industrial wastewater treatment plant

This chapter was published as:

Petersen B., Gernaey K., Henze M. and Vanrolleghem P.A. (2002) Evaluation of an ASM1 model calibration procedure on a municipal-industrial wastewater treatment plant. *Journal of Hydroinformatics*, **4**, 15-38.

Chapter 8

Evaluation of an ASM1 model calibration procedure on a municipal-industrial wastewater treatment plant

Abstract - The purpose of the calibrated model determines how to approach a model calibration, e.g. which information is needed and to which level of detail the model should be calibrated. A systematic model calibration procedure was therefore defined, and evaluated for a municipal-industrial wastewater treatment plant. In the case that was studied it was important to have a detailed description of the process dynamics, since the model was to be used as the basis for optimisation scenarios in a later phase. Therefore, a complete model calibration procedure was applied including: (1) a description of the hydraulics in the system via a tracer test, (2) an intensive measuring campaign and (3) supporting lab-scale experiments to obtain and confirm kinetic parameters for the model. In this paper the model calibration procedure for this case study is described step by step, and the importance of the different steps is discussed. The calibrated model was evaluated via a sensitivity analysis on the influence of model parameters and influent component concentrations on the model output. The sensitivity analysis confirmed that the model output was sensitive to the parameters that were modified from the default parameter values. The calibrated model was finally reduced from 24 tanks in series to a 12 tanks in series configuration, resulting in a 50% reduction of the simulation time.

1. Introduction

Implementation of biological nutrient removal on wastewater treatment plants (WWTP's) resulted in an increased knowledge on the biological degradation processes. This resulted in the development and use of more advanced dynamic mathematical models that may be able to describe the biological nutrient removal processes. These activated sludge models allow to study and to further increase the understanding of the influence of process modifications on treatment process efficiency. The dynamic models are for example increasingly used for scenario evaluations aiming at the optimisation of activated sludge processes (Stokes *et al.*, 1993; de la Sota *et al.*, 1994; Coen *et al.*, 1997 among many others). The Activated Sludge Model No.1 (ASM1) presented by the IAWQ Task Group on Mathematical Modelling for Design and Operation of Biological Wastewater Treatment Processes (Henze *et al.*, 1987) is generally accepted as state-of-the-

art. ASM1 was primarily developed for municipal activated sludge wastewater treatment plants to describe the removal of organic carbon substances and nitrogen with simultaneous consumption of oxygen and nitrate as electron acceptors, and to yield a good description of the sludge production. ASM1 has been extended to include a description of biological phosphorus removal, resulting in ASM2 and ASM2d (Henze *et al.*, 1995, 1998). Recently, some of the model concepts behind ASM1 have been altered in ASM3 (Gujer *et al.*, 1998), a model that also focuses on the degradation of carbon and nitrogen but allows the introduction of processes describing the storage of bio-polymers under transient conditions.

In this study model calibration is understood as the adaptation of the model to fit a certain set of informations obtained from the full-scale WWTP under study. This task is often rather time-consuming, and typically the time needed for a model calibration is underestimated. Even though more than a decade has passed since the publication of ASM1, a fully developed model calibration procedure has not been defined yet. We have not been able to find a complete model calibration report in literature. There may be many reasons for this. Important to realise is that the purpose of the model is very much determining on how to approach the calibration, making it difficult to generalise (Henze *et al.*, 1995). Still, considering the wide application of these activated sludge models there are surprisingly few references that contain details on the applied model calibration procedure. Often one has to collect bits and pieces from various sources to obtain an overview.

In this study it was attempted to gather and summarise the information needed to achieve a successful model calibration. The set of informations listed below was extracted and combined from different sources (Henze *et al.*, 1987; Lesouef *et al.*, 1992; Pedersen and Sinkjær, 1992; Siegrist and Tschui, 1992; Stokes *et al.*, 1993; de la Sota *et al.*, 1994; Dupont and Sinkjær, 1994; Weijers *et al.*, 1996; Xu and Hultman, 1996; Kristensen *et al.*, 1998):

1. Design data: e.g. reactor volumes, pump flows and aeration capacities.
2. Operational data:
 - 2.1. Flow rates, as averages or dynamic trajectories, of influent, effluent, recycle and waste flows.
 - 2.2. pH, aeration and temperatures.
3. Characterisation for the hydraulic model, e.g. the results of tracer tests.
4. Characterisation for the settler model: e.g. zone settling velocities at different mixed liquor suspended solids concentrations
5. Characterisation for the biological model, ASM1, of:

5.1. Wastewater concentrations of full-scale WWTP influent and effluent (as well as some intermediate streams between the WWTP's unit processes), as averages or dynamic trajectories: e.g. SS, COD, TKN, NH₄-N, NO₃-N, PO₄-P etc.

5.2. Sludge composition: e.g. SS, VSS, COD, N and/or P content.

5.3. Reaction kinetics: e.g. growth and decay rates.

5.4. Reaction stoichiometry : e.g. yields

As mentioned above, the required quality and quantity of the information will depend very much on the purpose of the modelling. In case the model is to be used for educational purposes (e.g. to increase basic understanding of the processes), for comparison of design alternatives for non-existing plants or in other situations where qualitative comparisons are sufficient, the default parameter values defined by Henze *et al.* (1987) can be applied. A reasonably good description can most often be obtained with this default parameter set for typical municipal cases without significant industrial influences (Henze *et al.*, 1997). However, if the calibrated model is going to be used for process performance evaluation and optimisation, it may be necessary to have a more accurate description of the actual processes under study. Some processes may need a more adequate description than others, again depending on the purpose of the study. This may especially apply for models that are supposed to describe the processes in an industrial or combined municipal and industrial treatment plant.

The information needed for the characterisation of the biological model, listed in point 5 above, can basically be gathered from three sources:

1. Default values from literature (e.g. Henze *et al.*, 1987).
2. Full-scale plant data
 - 2.1. Average or dynamic data from grab or time/flow proportional samples.
 - 2.2. Conventional mass balances of the full-scale data.
 - 2.3. On-line data.
 - 2.4. Measurements in reactors to characterise process dynamics (mainly relevant for SBR's and other alternating systems).
3. Information obtained from different kinds of lab-scale experiments with wastewater and activated sludge from the full-scale plant under study.

Again, the intended use of the model will determine which information source to choose for the characterisation of the different biological processes in the model. In addition, the purpose will decide to which level the model has to be calibrated, since the quality of the desired model predictions will depend

strongly on the quality of the model calibration. Fig. 1 illustrates the different general steps in a model calibration procedure. It should be stressed that, depending on the purpose, not all steps may have to be taken.

Steps 1 - 5 in Fig. 1 indicate the collection of information. Design (1) and operational (2) data are in general always needed for a model calibration. E.g. the flow and load variations are important in the design of measuring campaigns for hydraulic, sludge settling and biological characterisation of the full-scale WWTP. The hydraulics (3) are typically characterised via tracer tests at the full-scale installation (De Clercq *et al.*, 1999). The settling characteristic (4) can be characterised via on-line or lab-scale settling tests (Vanderhasselt *et al.*, 1999a, 1999b). Finally, the biology can be obtained via different information sources as indicated above. A review of the information that can be obtained from different kinds of lab-scale experiments is presented in detail elsewhere (see chapter 2), and for information especially obtained from respirometric tests the reader is referred to Vanrolleghem *et al.* (1999).

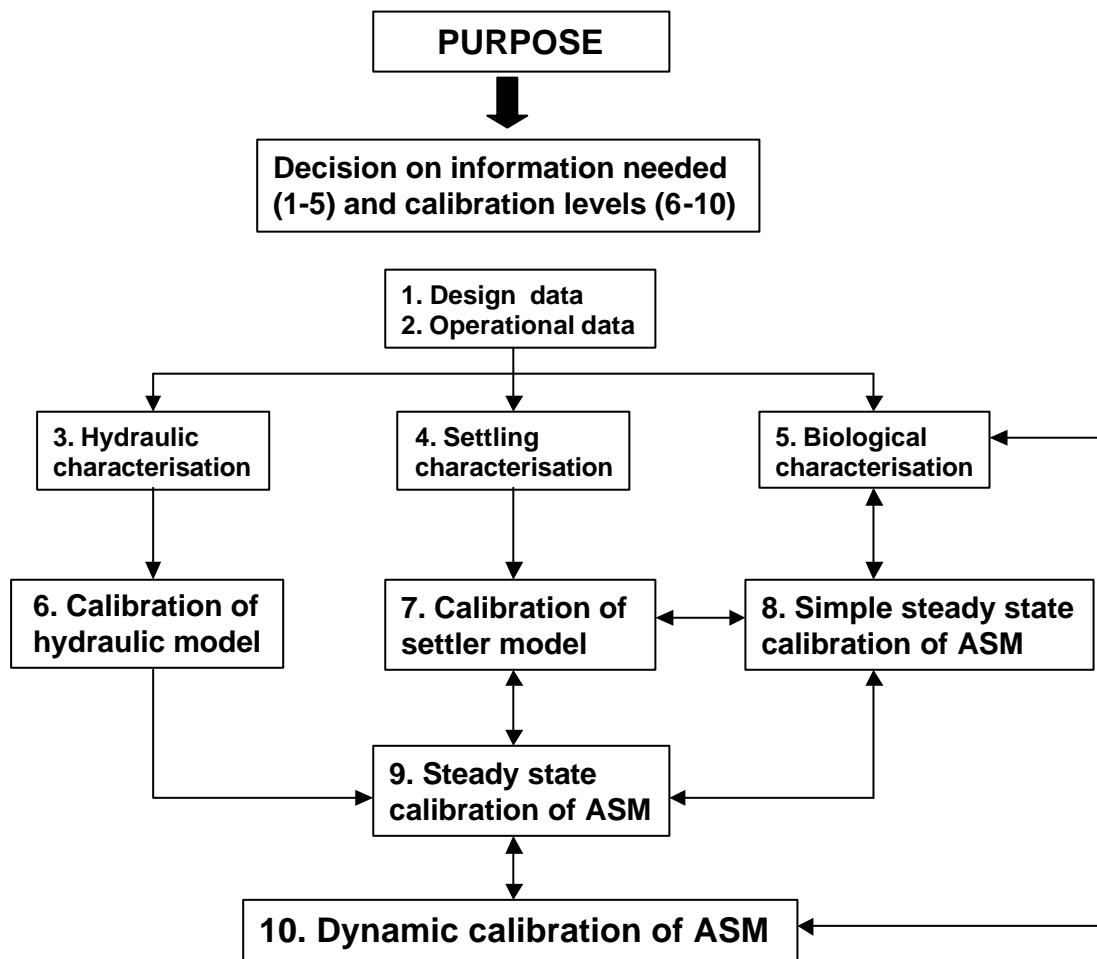


Figure 1. Schematic overview of the different general steps in an activated sludge model calibration procedure

In Fig. 1 steps 6 - 10 illustrate different calibration levels. The calibration of the hydraulic model via tracer

test results, and the settler model calibration via results from sludge settling tests are indicated in steps 6 and 7 respectively. A first ASM calibration level is typically a simple steady state model calibration step (8). In this phase of the model calibration the different reactors in the treatment plant are each represented by an ideal perfectly mixed tank, resulting in a simple treatment plant configuration. Here data obtained from the full-scale WWTP are averaged, thereby assuming that this average represents a steady state, and the model is calibrated to fit to average effluent and sludge waste data. Typically, the calibration of the ASM and the settler are linked together, since the aim is most often to describe the final effluent quality. Moreover, the recycle from the settler has an influence on the activated sludge system. Thus, at this stage, there may be an interaction between the steady state calibration and the settler model calibration, indicated with the double arrow. Finally, the characterisation of wastewater components may be adjusted according to the calibration of the full-scale model, indicated with the double arrow between (8) and (5) in Fig. 1.

The next step in the calibration procedure is a steady state model calibration that includes the hydraulic model (9). In general, with a steady state model calibration, only parameters responsible for long-term behaviour of the WWTP can be determined, i.e. Y_H , f_p , b_H and X_I in the influent (Henze *et al.*, 1998; Nowak *et al.*, 1999). These parameters are correlated to a certain degree, meaning that a modification of one parameter value can be compensated by a modification of another parameter value. In the study of Nowak *et al.* (1999) on mass balances of full-scale data, it was therefore chosen to fix Y_H and f_p leaving X_I in the influent and b_H to be determined from the steady state data. In the study of Lesouef *et al.* (1992) two WWTP models were calibrated via steady state calibration only, and this calibrated model was applied to simulate dynamic process scenarios. However, if one relies entirely on a steady state calibration to dynamic data, some problems may be encountered since the real input variations are usually faster than the slow process dynamics that were focused upon during the steady state calibration. In other words, the process does not operate in steady state but one still attempts to fit a steady state simplification of the model to an unsteady situation. A steady state calibration may, however, be very useful for the determination of initial conditions prior to a dynamic model calibration and for the initiation of a first parameter estimation (e.g. Pedersen and Sinkjær, 1992; Stokes *et al.*, 1993; Dupont and Sinkjær, 1994; Xu and Hultman, 1996; Kristensen *et al.*, 1998).

If it is the aim to describe and predict more short-term and dynamic situations, a model calibration to dynamic data will be needed since such data contain more information than steady state data, especially on fast dynamic behaviour. The important point in model calibration based on dynamic data is to obtain a more reliable estimation of the maximum specific growth rates $\mu_{\max H}$ and $\mu_{\max A}$ (Henze *et al.*, 1998), which are the most important parameters in predicting dynamic situations.

At WWTP's data are most often collected routinely with a daily or weekly sampling frequency. This sampling frequency may, however, not be high enough, and for more accurate modelling it may therefore be required to run special measuring campaigns (e.g. Pedersen and Sinkjær 1992; de la Sota *et al.*, 1994;

Dupont and Sinkjær, 1994; Xu and Hultman, 1996; Coen *et al.*, 1997). The sampling frequencies should be chosen in relation to the time constants of the process and influent variations. One of the important time constants of the process is the hydraulic retention time. Various lengths of measuring campaigns are recorded in literature. Ideally, one should choose to sample about five times faster than the hydraulic retention time and have a test duration of 3 - 4 times this key time constant (Ljung, 1987). However, since measurements on full-scale WWTP's are relatively expensive these recommendations may not always be completely fulfilled.

Furthermore, data from the full-scale installation alone may be insufficient for a dynamic model calibration since the reaction kinetics can not be readily obtained from such data, except for specific designs like SBR's and alternating systems (Vanrolleghem and Coen, 1995). For a dynamic model calibration on a full-scale WWTP the modeller is therefore typically aiming at combining more information rich results derived from lab-scale experiments (carried out with sludge and wastewater from the full-scale installation) with data obtained from measuring campaigns on the WWTP under study (Dupont and Sinkjær, 1994; Xu and Hultman, 1996; Kristensen *et al.*, 1998).

In this paper the model calibration procedure presented in Fig. 1 is illustrated for the combined municipal-industrial activated sludge WWTP of Zele (Aquafin NV, Aartselaar, Belgium). The purpose of the model calibration was to obtain a good description of the N removal capacity and to a lesser extent of the COD removal. In a second phase the model was to be applied for process optimisation of the N removal (Gernaey *et al.*, 2000c). Based on this purpose the necessary information set and calibration strategy were defined. A tracer test was carried out first, to have an adequate description of the hydraulic flow pattern, which is especially important if dynamic situations are to be predicted. The sludge at the Zele WWTP is settling reasonably well, and it was therefore found adequate to describe the settler with a simple point settler model. Thus, no specific tests were carried out to characterise the settling properties, i.e. step 4 of Fig. 1 is not included in this study. With respect to the wastewater characterisation an intensive measuring campaign was designed to obtain sufficient dynamic data. The variation in readily biodegradable organic substrate was characterised, since the model was to be applied later on for optimisation of N removal, including the start-up of denitrification. The sludge composition was analysed to support the calibration of the sludge balance. Moreover, lab-scale experiments were planned for the determination of the sludge kinetics related to nitrification and degradation of COD, and a decay experiment was carried out to support the description of biomass decay in the treatment plant. No specific experiments were carried out for the determination of stoichiometric coefficients. A sensitivity analysis was carried out on the calibrated model to check whether the parameters that were modified during the model calibration procedure were indeed influencing the model output. It was finally investigated if the calibrated model could be reduced, to increase simulation speed while maintaining the same accuracy of the full model.

2. Case study

The municipal activated sludge WWTP of Zele was constructed in 1983 for a design capacity of 50000 inhabitant equivalents (IE). Fig. 2 gives a schematic overview of the process layout. The influent of the WWTP consists for 40 % of household wastewater and 60 % industrial wastewater (slaughterhouses, industrial laundry, textile cleaning, textile painting etc.). The influent is divided over two parallel rectangular primary clarifiers after the pretreatment step (coarse grit removal, fine grit removal, sand and grease removal). The effluent of the primary clarifier flows to the biological activated sludge treatment, where it is mixed with recycle sludge. The activated sludge tank consists of one plug flow aeration tank that is divided into 6 lanes of about 400 m³ each. The mixed liquor flows to two secondary clarifiers through an open aerated channel of about 200 m³. The clarifiers each have a diameter of 33 m and a volume of 2050 m³. The final effluent is discharged into a nearby stream. The underflow from the secondary clarifier flows back to the aeration tank through an aerated sludge recycle channel with a volume of 400 m³. The primary and secondary sludge are thickened prior to anaerobic digestion.

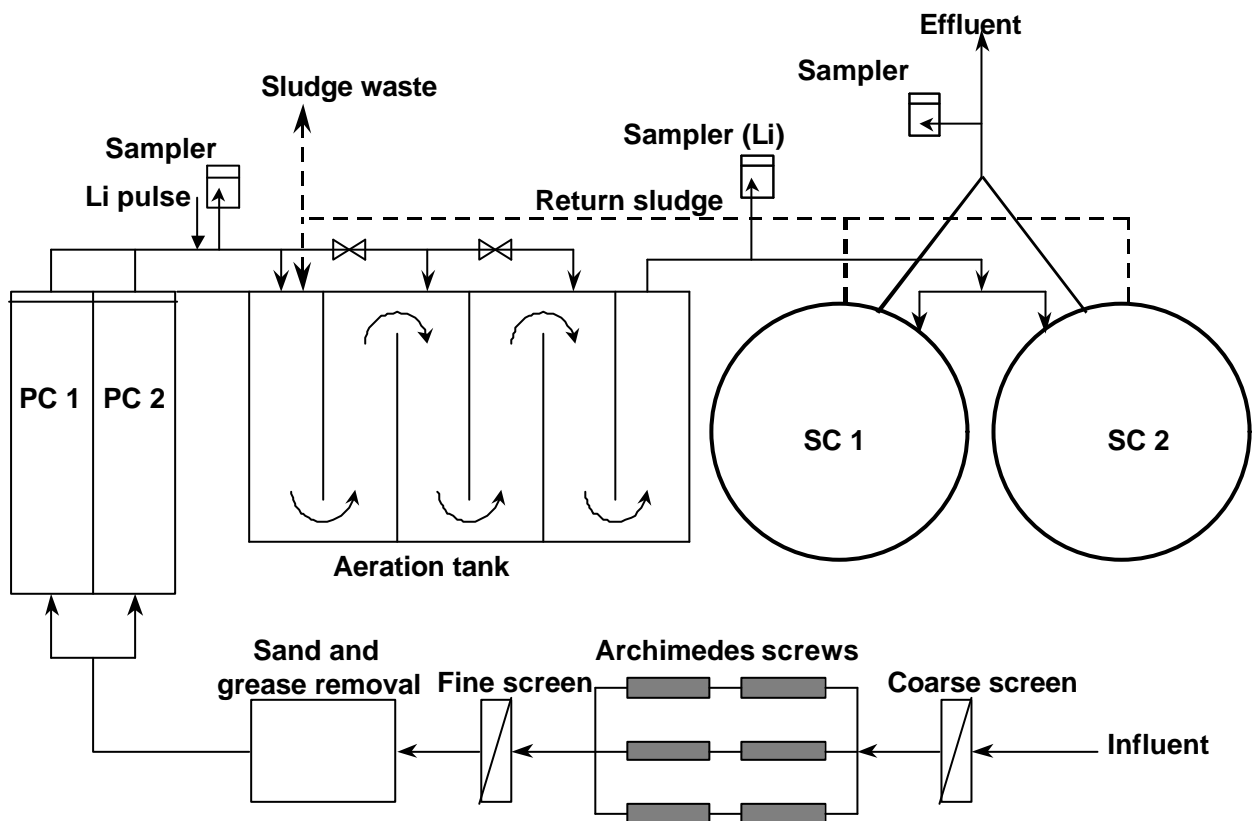


Figure 2. Schematic overview of the process layout of the Zele wastewater treatment plant (Aquafin NV, Aartselaar, Belgium)

The Zele WWTP is going through a stepwise renovation process with the aim to obtain an effluent quality that complies with the Flemish effluent standard for total N (15 mg total N per litre as yearly average). A

first step in the renovation process was the installation of a fine bubble aeration system in 1997. This had an immediate positive effect on the nitrification capacity resulting in a decrease of the effluent $\text{NH}_4\text{-N}$ concentration. However, the effluent total N concentration remained too high to comply with the effluent standard. For the period January 1997 till November 1998 an average total N concentration of 19.6 mg/l was calculated (average of 53 effluent samples). The absence of a denitrification compartment in the WWTP is believed to be the main reason for the high effluent total N concentrations.

3. Materials and methods

3.1. Tracer test

A tracer test with lithium chloride (LiCl) was carried out to characterise the hydraulics of the activated sludge tank. The tracer was added as a pulse at the beginning of the aeration tank, where presettled influent is mixed with return sludge (indicated on Fig. 2). During the test mixed liquor samples were taken at the point where the activated sludge flows over into the secondary clarifiers (see Fig. 2). The sampling frequency took into account the worst case scenario (with respect to obtaining detectable Li concentrations) of an ideally mixed situation, although the expectation in view of the design was plug-flow mixing behaviour. Thus, frequent sampling (one sample every 5 to 10 minutes) was undertaken for 0 - 1.5 times the hydraulic retention time

3.2. Measuring campaign

The measuring campaign was carried out in November 1998. First, a 1-day test campaign was done in order to test the planned strategy, e.g. to evaluate whether the planned measurement frequency of one sample every two hours was high enough to observe the dynamics, and to check if the installed measuring/sampling equipment worked properly. Only afterwards a detailed one-week measuring campaign was carried out. Two automatic samplers with built-in refrigerator (4°C) were installed on the treatment plant. Time proportional samples (100 ml every 6 minutes) were taken every second hour on the effluent of the primary clarifier (= influent to activated sludge tank) and on the effluent of the secondary clarifier (see Fig. 2). The influent samples were analysed for the following parameters via standard methods: Suspended solids (SS), ammonium nitrogen ($\text{NH}_4\text{-N}$), total Kjeldahl nitrogen (TKN), total and soluble chemical oxygen demand (COD_{tot} and COD_{sol}). The effluent samples were analysed for SS, $\text{NH}_4\text{-N}$, nitrate nitrogen ($\text{NO}_3\text{-N}$), nitrite nitrogen ($\text{NO}_2\text{-N}$), COD_{tot} and COD_{sol} . In addition, mixed liquor and return sludge were sampled at regular times (once or twice per day) to measure the COD, TKN, SS and volatile suspended solids (VSS) content of the sludge.

Effluent flow data were collected with a data logger that was temporarily connected to the effluent flow sensor. Sludge waste flows were obtained from treatment plant operation logbooks. Temperature and pH

of the activated sludge in the aeration tank were measured daily.

3.3. Lab-scale experiments

Respirometric lab-scale experiments with wastewater and activated sludge were carried out during the measuring campaign. Experiments were performed in the RODTOX (Vanrolleghem *et al.*, 1994) and the hybrid respirometer (chapter 3). The purposes of these experiments were two fold:

3.3.1. Wastewater characterisation – Determination of readily biodegradable COD

The first purpose was to measure the short-term biochemical oxygen demand (BOD_{st}), to determine the readily biodegradable COD of the influent, denoted COD_{st} . The BOD_{st} was determined as the area under the oxygen uptake rate profile related to substrate degradation as function of time (called a respirogram). Only unfiltered influent samples were subjected to respirometric analysis. Some of the samples (typically the ones with a high COD concentration) were also analysed after inhibiting nitrification with ATU. The measured BOD_{st} values were converted to COD units via an assumed yield factor Y_H of 0.67 (Henze *et al.*, 1987) (Eq.1)

$$COD_{st} = \frac{BOD_{st}}{(1 - Y_H)} \quad (1)$$

In case BOD_{st} was available from experiments in the presence of ATU, the value was immediately used as an estimate for the COD_{st} concentration. In case the BOD_{st} value resulted from an experiment in which no ATU was added, the COD_{st} concentration was determined according to Eq. 2. The BOD_{st} requirement for the oxidation of NH_4 -N (BOD_{st,NH_4}) was determined using the NH_4 -N concentrations obtained from the chemical analyses of the wastewater (Eq. 3). The value of Y_A was set to 0.24 (Henze *et al.*, 1987).

$$BOD_{st} = BOD_{st,total} - BOD_{st,NH_4} \quad (2)$$

$$BOD_{st,NH_4} = (4.57 - Y_A) \cdot NH_4 - N \quad (3)$$

3.3.2. Activated sludge kinetics

Maximum specific growth rates

Experiments were carried out to obtain data to estimate the kinetic parameters related to nitrification. The design of these experiments is described in more detail elsewhere (see chapter 7), but consisted of simultaneous addition of wastewater and ammonium, thus allowing to estimate the nitrification kinetics and the degradation of COD in a single experiment. The exogenous oxygen uptake rate, $r_{O,ex}$, caused by the wastewater and ammonium addition can be described by Eq. 4.

$$r_{O,ex} = (1 - Y_H) \cdot \frac{m_{maxH} X}{Y_H} \cdot \frac{S_S}{K_S + S_S} + (4.57 - Y_A) \cdot \frac{m_{maxA} X}{Y_A} \cdot \frac{S_{NH}}{K_{NH} + S_{NH}} \quad (4)$$

Decay rate

The endogenous respiration rate, $r_{O,end}$, was measured as function of time in a long term (5 days) aerated batch experiment without substrate supply. The endogenous decay rate, b_H' , was determined as the slope of the curve consisting of $\ln(r_{O,end}(0))/\ln(r_{O,end}(t))$ data points plotted as function of time (Ekama *et al.*, 1986). This decay rate was transformed into the model decay rate based on the death regeneration concept via Eq. 5 (Henze *et al.*, 1987), where Y_H was set to 0.67 and f_p to 0.08 according to the ASM1 default parameters.

$$b_H = \frac{b_H'}{1 - Y_H (1 - f_p)} \quad (5)$$

Temperature correction of the parameters determined from the lab-scale experiments (18 °C) were carried out according to standard procedures (Henze *et al.*, 1997).

4. Results

The results of the different model calibration steps, out-lined in Fig. 1, are described for the example that was studied.

4.1. Step 1-2: Design and operational data

The volumes are repeated in Table 1, and Table 2 lists the operational data during the 6 day measuring campaign (November 18 – 23 1998). The data includes a rain event on the first day of the measuring campaign, as can be seen from the flow data (2 hour averages) in Fig. 3. Therefore some key parameters were calculated both including and excluding the data obtained during this rain event (Table 2). Table 2 clearly shows that the daily COD load, and thereby the sludge load, increased significantly during the rain period. The sludge age seems low for a nitrifying WWTP. It is the experience at the WWTP, however, that it is difficult to maintain a higher sludge age during winter due to a decrease in sludge settleability and thereby an increased risk for sludge wash-out. The observed yield is also slightly higher than expected according to the sludge load (Henze *et al.*, 1997) but is probably related to the low sludge age.

Table 1. Design data Zele WWTP

Design parameter	Unit	Value
Volume activated sludge tank	m ³	2600
Volume of recycle channel	m ³	400
Volume of secondary clarifier	m ³	2*2050

Table 2. Operational data Zele WWTP obtained during the measuring campaign

Variable	Unit	Value (incl. rain period)	Value (excl. rain period)
Influent flow average	m ³ /d	12559	10255
Waste flow average	m ³ /d	248	241
Temperature	°C	10.5	10.5
pH		7.2	7.2
Sludge concentration average *	g SS/l	4.0	3.9
COD load	kg COD/d	5607	3730
TKN load	kg TKN/d	342	258
Sludge load	kg COD/kg SS.d	0.48	0.32
Sludge production	kg SS/d	2394	2300
Sludge age	d	6.2	8.6
Observed yield	kg SS/ kg COD	0.42	0.62

* see also Table 3

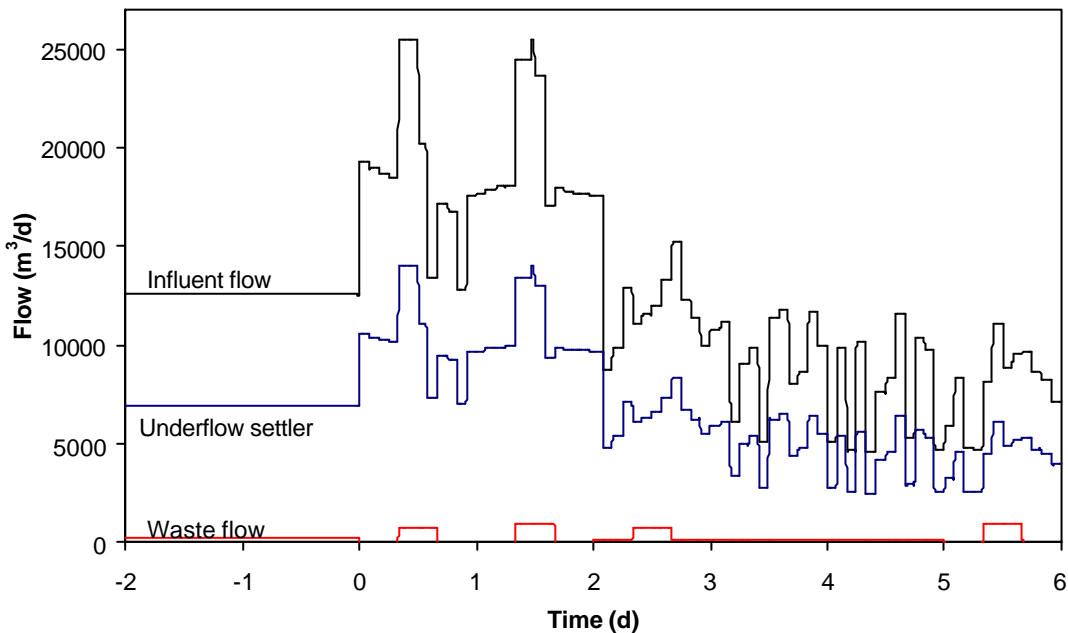


Figure 3. Simulated flow rates during the measuring campaign (t = 0 corresponds to the beginning of the measuring campaign). Influent flow rates (2 hour averages) were collected at the treatment plant. Settler underflow rates are obtained as 0.55 * influent flow (proportional recycle flow controller). The discontinuous waste flow rates were obtained from treatment plant operation logbook data

4.2. Step 3 and 6: Characterisation of hydraulics and calibration of hydraulic model

The data resulting from the tracer test are shown in Fig. 4. A sharp peak was recorded with a maximum Li concentration of 1.2 mg/l at $t = 0.1$ d. The increase of the Li concentration around $t = 0.27$ d is due to the Li that is recycled internally in the treatment plant with the sludge recycle.

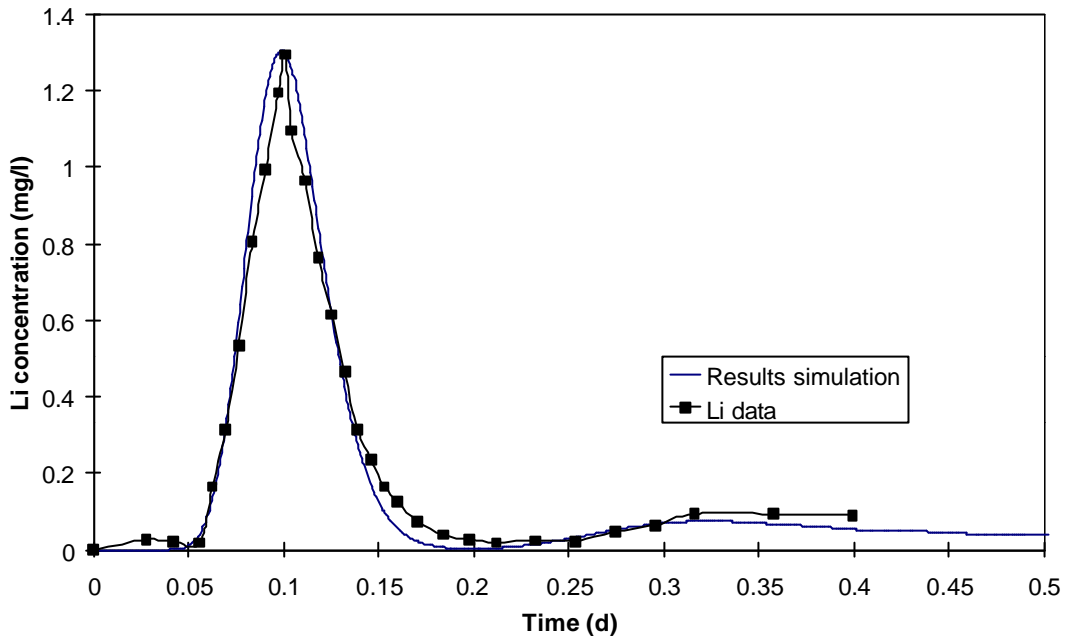


Figure 4. Data resulting from the tracer test on the aeration tank of the Zele WWTP, together with the best model fit that was obtained. See text for explanation of the model

The tracer test data were normalised by C_0 (Eq. 6, where M is the total mass of Li added at $t = 0$), and the time was normalised by the average hydraulic residence time (θ_H) during the test, which was 2.6 hours. First, a simple data interpretation was applied. The N tanks-in-series model (Eq. 7) was fitted to the normalised Li data via the solver function in MSExcel and $N = 19$ was found to give the best fit.

$$C_0 = \frac{M}{V} \quad (6)$$

$$C_{Nt} = \frac{N}{(N-1)!} * (N * \mathbf{q}_t)^{(N-1)} * e^{(-N\mathbf{q}_t)} \quad (7)$$

This simple approach however assumes constant flow rate and, thus, does not include the flow variations that occurred during the tracer test. Moreover, the sludge recycle (including the LiCl that is recycled via the underflow of the settlers) and the residence time of the recycle liquid flow in the secondary clarifiers were not considered in this simplified approach. Thus, to obtain a better hydraulic description different

configurations were simulated in the WEST++ modelling and simulation environment (Hemmis NV, Kortrijk, Belgium). The value of $N = 19$ obtained from the simple data interpretation was used as a starting point for this more detailed model-based interpretation. The resulting plant configuration that gave the best description consisted of the following components:

- A plug flow aeration tank consisting of 24 tanks in series (6 lanes, each consisting of 4 tanks in series, where each tank has a volume of 100 m^3)
- The sludge channel that transports the sludge from the aeration tank to the secondary clarifiers consists of two 100 m^3 tanks in series.
- An ideal point-settler and a “buffer tank” of 1000 m^3 to take the residence time into account for the liquid that is recycled together with the recycle sludge (settler underflow).
- The recycle channel that transports the recycle sludge from the secondary clarifiers to the aeration tank consists of five tanks in series of 80 m^3 each.

The model fit on the Li tracer data for this configuration is shown in Fig. 4, and the hydraulic scheme is illustrated in Fig. 14 in the process configuration for the dynamic model.

4.3. Step 5: Biological characterisation

4.3.1. Wastewater characterisation

Results of measuring campaign

Fig. 5, 6 and 7 show the chemical analysis results for the influent samples (presettled wastewater). The influent COD_{tot} , TKN and SS concentrations were highest on Wednesday afternoon and Thursday morning as a result of the rain event. The COD_{sol} and $\text{NH}_4\text{-N}$ concentrations were, however, not higher during the rain event compared to the other working days, indicating that the increase of COD_{tot} and TKN concentrations during the rain event were related to the extra suspended solids load. The high SS content of the presettled wastewater during the rain event indicates that the primary clarifiers are overloaded when the influent flow is high, e.g. due to rainfall.

For both COD (Fig. 5) and N (Fig. 6) a diurnal pattern can be distinguished with lower concentrations during the night and higher during daytime. The concentration variations are much lower in the weekend due to the absence of industrial discharges. The start-up of industrial activity after the weekend again caused an increase of the influent pollutant concentrations. In Fig. 5 it can furthermore be seen that the COD_{st} , obtained via BOD_{st} from respirometric tests (Eq. 1), is related to COD_{sol} . Moreover, the COD_{st} seems to be related to the industrial discharges since there is hardly any COD_{st} present in the influent during the weekend.

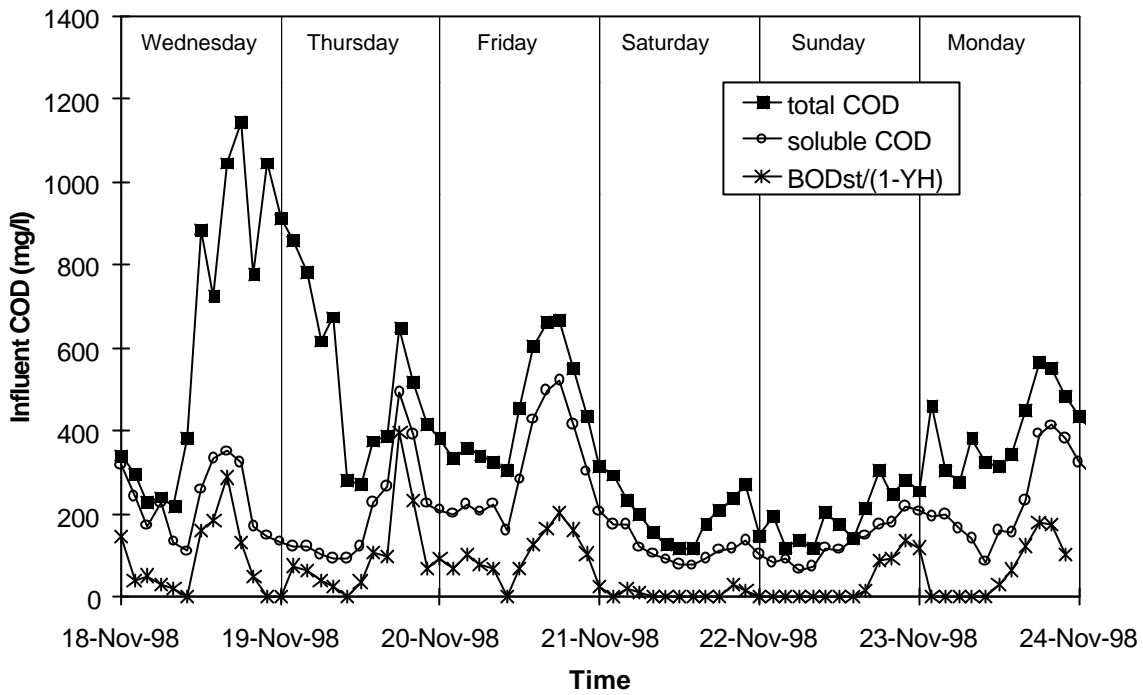


Figure 5. COD_{tot} and COD_{sol} concentrations measured on the influent of the Zele WWTP during the measuring campaign. COD_{st} values were calculated using the BOD_{st} values resulting from respirometric experiments with unfiltered wastewater (see Eq. 1)

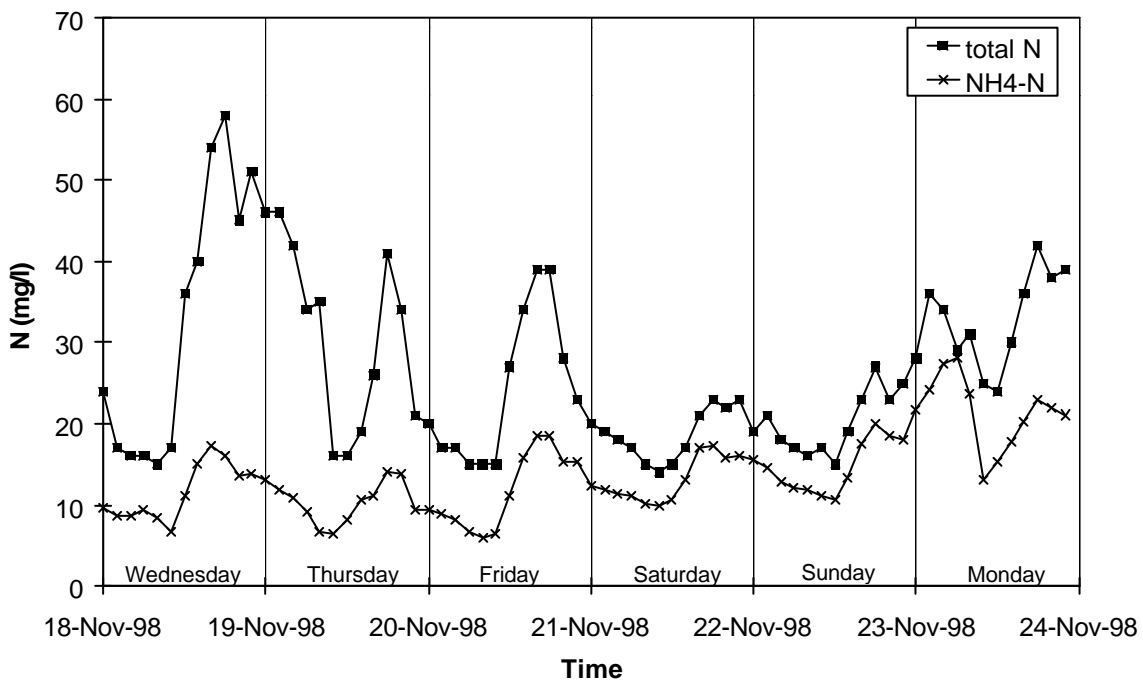


Figure 6. TKN and NH₄-N concentrations measured on the influent of the Zele WWTP during the measuring campaign

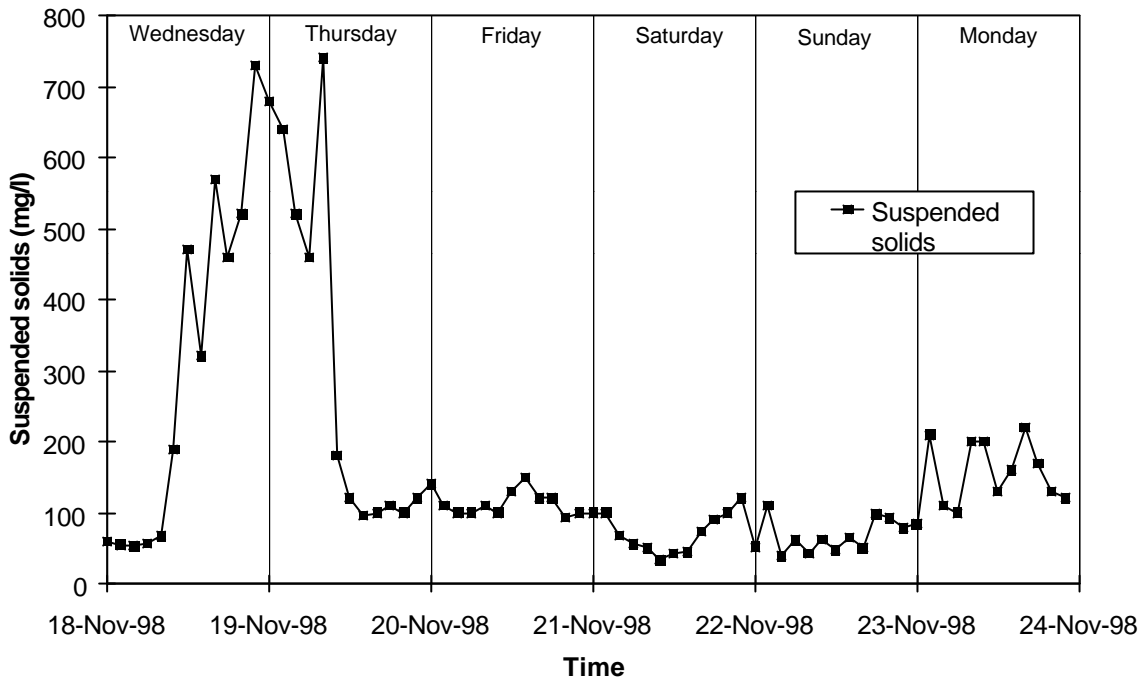


Figure 7. SS concentration measured on the influent of the Zele WWTP during the measuring campaign

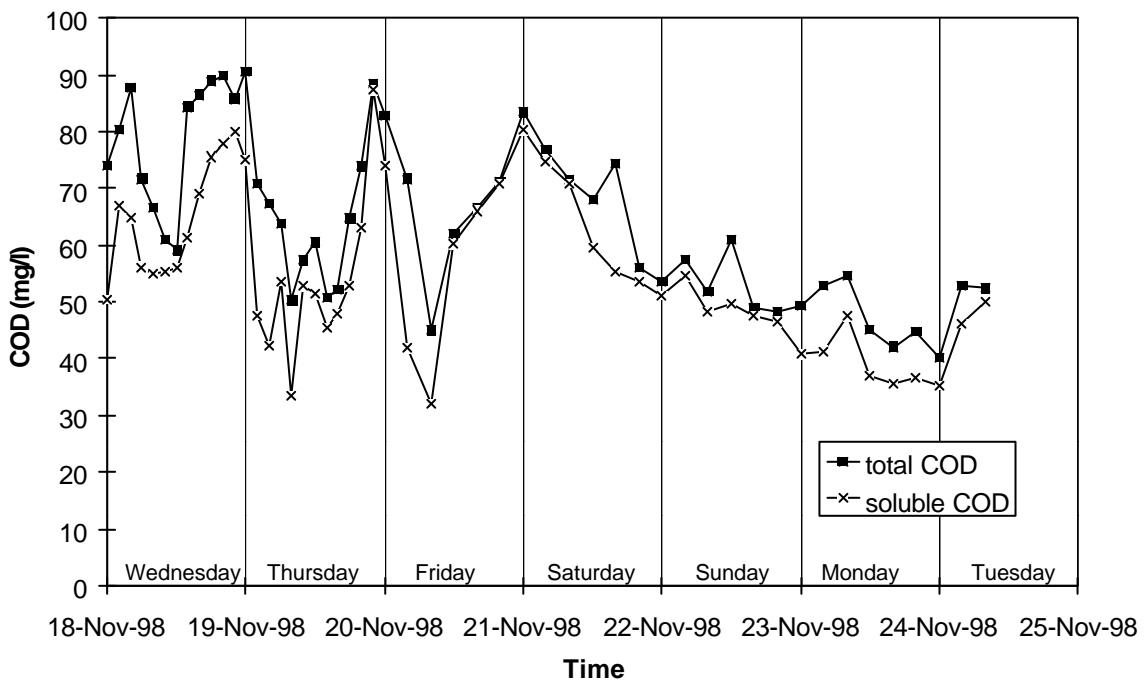


Figure 8. COD_{tot} and COD_{sol} concentrations measured on the effluent of the Zele WWTP during the measuring campaign

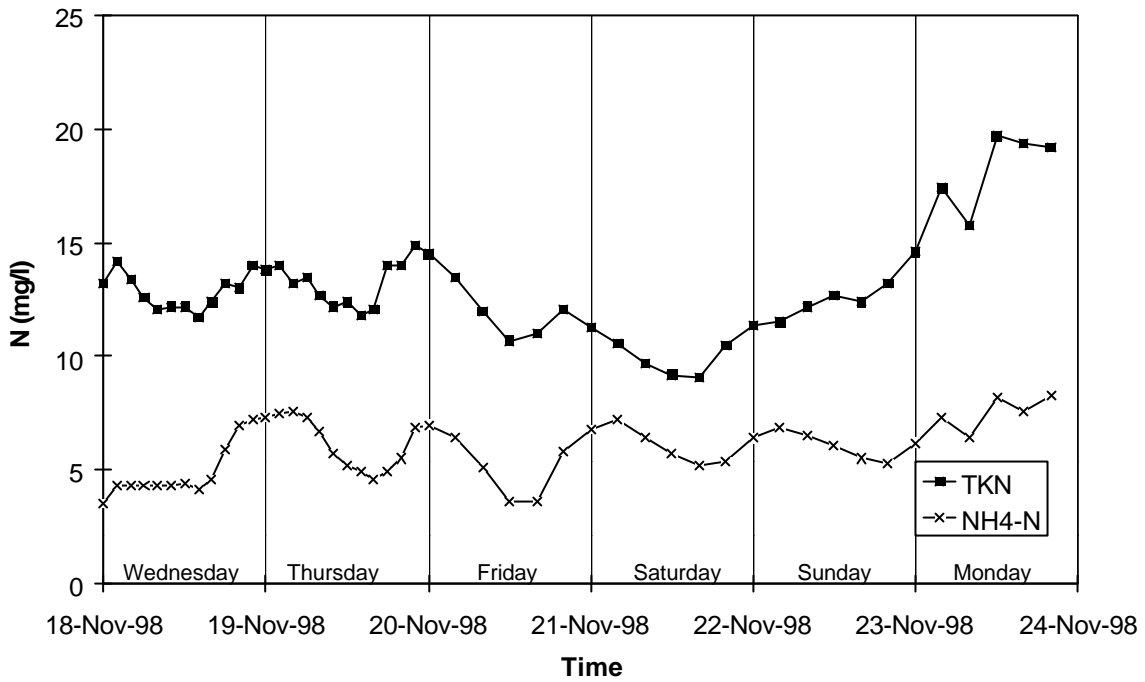


Figure 9. TKN and NH₄-N concentrations measured on the effluent of the Zele WWTP during the measuring campaign

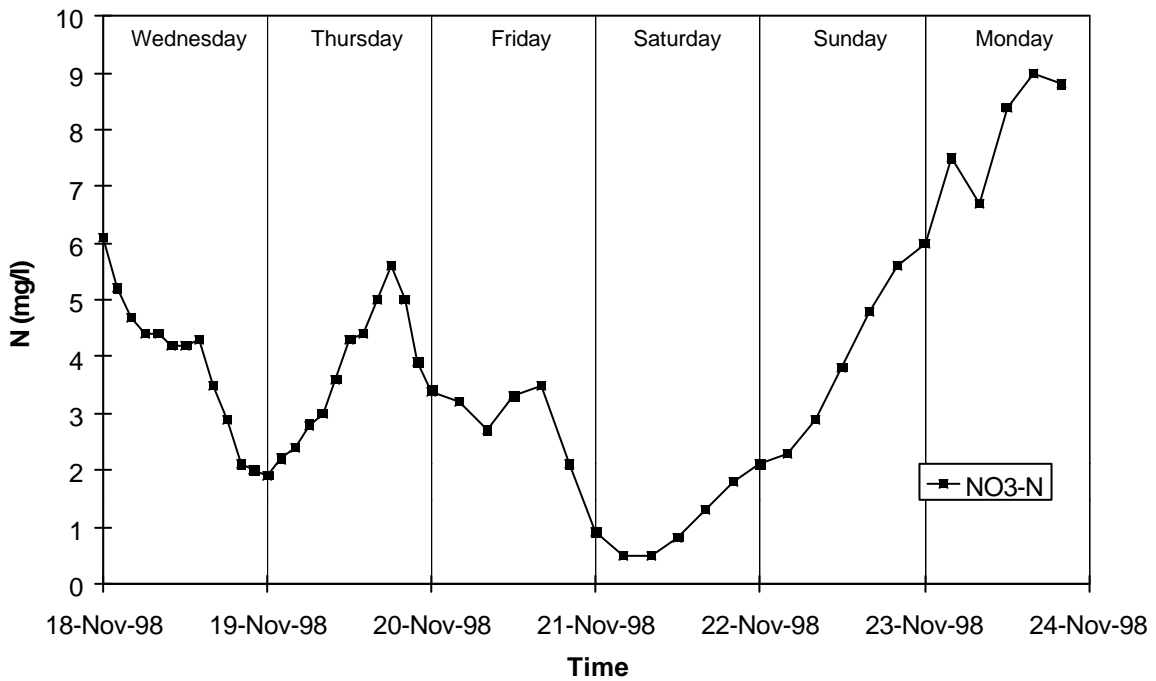


Figure 10. NO₃-N concentrations measured on the effluent of the Zele WWTP during the measuring campaign

The results of the chemical analyses on the effluent are shown in Fig. 8, 9 and 10. Effluent COD and N concentrations show a diurnal pattern, but, as expected, the variations were rather small compared to the concentration variations measured in the presettled influent. During the measuring campaign the effluent total N concentration was, in general, lower than the 15 mg/l total N effluent standard (Fig. 9). However, on Monday, a day with normal dry weather flow, the effluent total N concentration exceeded the 15 mg/l total N standard. Also, in Fig. 9 it can be seen that full nitrification was not reached. Besides $\text{NH}_4\text{-N}$, $\text{NO}_3\text{-N}$ contributed significantly to the effluent total N concentrations during the measuring campaign (Fig. 10).

4.3.2. Conversion of wastewater data into model components

The next step in the wastewater characterisation is the conversion of the available data from the measuring campaign into a data set that can be used as input for ASM1. It is assumed that the oxygen concentration (S_{O}) in the incoming wastewater is zero. Furthermore, the conversion of alkalinity (S_{ALK}) is not considered in this study. Thus, the ASM1 wastewater components to consider are related to the organic carbon (COD) and nitrogen components.

COD components

The total COD in the model includes the components described in Eq. 8 (Henze *et al.*, 1987).

$$\text{COD}_{\text{tot}} = S_{\text{S}} + S_{\text{I}} + X_{\text{S}} + X_{\text{I}} \quad (8)$$

The presence of heterotrophic and autotrophic biomass (X_{BH} and X_{BA}) in the influent wastewater was not considered in the ASM1 report (Henze *et al.*, 1987). Activated sludge may, however, be inoculated significantly by X_{BH} in the influent, especially in cases where no primary settling is present. However, it can be difficult to determine the amount of biomass in the wastewater, and the biomass fraction is therefore often lumped into X_{S} (Henze *et al.*, 1995). This does not influence the modelling significantly but it may affect the value of the biomass yield. Contrary to the heterotrophic biomass, the presence of autotrophic biomass (X_{BA}) can be important to keep sufficient nitrification in the system in cases where the sludge retention time is too low to sustain the nitrifying biomass. Model results may reveal whether this is the case. As an initial approximation X_{BH} and X_{BA} were assumed to be zero in this study. The methods for characterisation of the organic wastewater components are summarised in Fig. 11.

- Inert soluble organic matter (S_{I}), influent and effluent.

Influent S_{I} was determined via effluent data (Henze, 1992). The weekly BOD_5 results of the effluent (available from samples that are routinely taken on the effluent of the WWTP) were used to determine the effluent S_{S} concentration. An average effluent BOD_5 concentration of 6.2 ± 3.0 mg/l had been measured, and an average $\text{BOD}_5/\text{COD}_{\text{tot}}$ ratio of 7 ± 3 % was calculated for the effluent data. Assuming a BOD yield (Y) of 0.20 (STOWA, 1996), the corresponding effluent S_{S} concentrations were calculated

according to Eq. 9. The influent S_I was obtained by combining Eq. 9 and 10.

$$S_{S,\text{effluent}} = \frac{0.07 * \text{COD}_{\text{tot}}}{(1 - Y)} = 0.0875 * \text{COD}_{\text{tot,effluent}} \quad (9)$$

$$S_{I,\text{effluent}} = S_{I,\text{influent}} = (\text{COD}_{\text{sol,effluent}} - S_{S,\text{effluent}}) \quad (10)$$

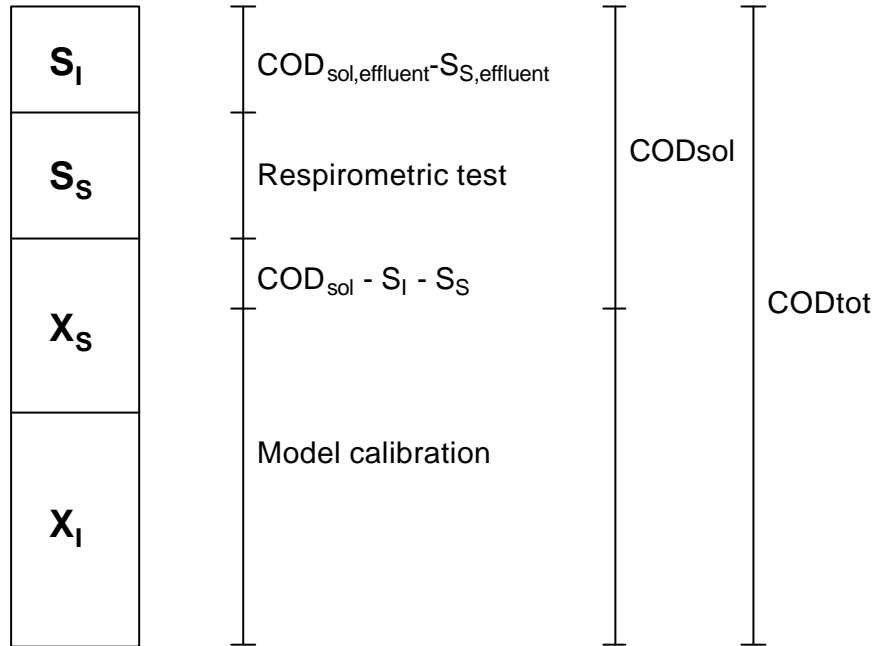


Figure 11. Summary of influent characterisation methods for organic wastewater components

- Readily biodegradable substrate (S_S), influent

Based on the results of the respirometric tests, the influent readily biodegradable COD (Eq. 1) is set equal to the model component S_S .

In the next step, the mass balance for influent COD_{sol} ($\text{COD}_{\text{sol,influent}}$) was checked (Eq. 11).

$$\text{COD}_{\text{sol,influent}} = S_S + S_I + S_{\text{rest}} \quad (11)$$

In case $\text{COD}_{\text{sol,influent}}$ in Eq. 11 is higher than $S_S + S_I$, S_{rest} can be added to the slowly biodegradable substrate, X_S . On the contrary, if $\text{COD}_{\text{sol,influent}}$ is lower than $S_S + S_I$, part of the measured BOD_{st} may be considered to be originating from X_S . For the wastewater under study it appeared that $\text{COD}_{\text{sol,influent}} > (S_S + S_I)$, thus S_{rest} was added to the X_S component.

- Slowly biodegradable substrate (X_S), influent

Contribution to the X_S concentration partly came from the mass balance in Equation 11 as S_{rest} , but was also partly determined from the steady state model evaluations (see also X_I).

- Inert suspended organic matter (X_I), influent

The best estimate for X_I is obtained by comparing the measured and predicted sludge concentration and sludge production (Henze *et al.*, 1987; Henze *et al.*, 1995). The X_I influent concentration is typically used as a “tuning component” in the model calibration of the sludge balance (Henze *et al.*, 1995; Nowak *et al.*, 1999), and the X_S concentration is adjusted accordingly via mass balance Eq. 12 (assuming that X_{BH} and X_{BA} are negligible, see above).

$$\text{COD}_{\text{tot}} - \text{COD}_{\text{sol}} = X_S + X_I \quad (12)$$

Initially X_I was assumed to be 50 % of the particulate COD. However, this was adjusted during the model calibration (see below).

Nitrogen components

For the nitrogen fractions a similar approach was used for both influent and effluent characterisation. It was assumed that the influent contains negligible concentrations of nitrate (S_{NO}). The total Kjeldahl nitrogen could then be fractionated according to Eq. 13 (Henze *et al.*, 1987).

$$\text{TKN} = X_{NI} + X_{ND} + S_{NI} + S_{ND} + S_{NH} \quad (13)$$

- Ammonia nitrogen (S_{NH})

The analytically measured $\text{NH}_4\text{-N}$ concentration was considered to be equal to S_{NH} .

- Soluble biodegradable organic nitrogen (S_{ND})

Only TKN measurements were available. It was assumed that the ratio of soluble to total TKN was proportional with the ratio of COD_{sol} to COD_{tot} . Thus, the soluble Kjeldahl nitrogen (SKN) can be approximated via Eq. 14, and by assuming that the nitrogen content of inert soluble organic matter (i_{NSI}) equals 1.5% (Henze *et al.*, 1995) the concentration of S_{ND} can be determined via Eq. 15.

$$\text{SKN} = \frac{\text{COD}_{\text{sol}}}{\text{COD}_{\text{tot}}} \cdot \text{TKN} = S_{NI} + S_{ND} + S_{NH} \quad (14)$$

$$S_{ND} = \text{SKN} - i_{NSI} \cdot S_I - S_{NH} \quad (15)$$

- Slowly biodegradable organic nitrogen (X_{ND})

The nitrogen content of inert suspended organic matter (i_{NXI}) is initially assumed to be 1% (Henze *et al.*, 1995) resulting in Eq. 16 for the determination of X_{ND} .

$$X_{ND} = \text{TKN} - i_{NXI} \cdot X_I - \text{SKN} \quad (16)$$

4.3.3. Sludge composition

The average results of the sludge composition analysis, based on ten measurements of the COD, SS and VSS content of the activated sludge and recycle sludge, are given in Table 3. The measured COD/VSS ratio is slightly higher than typical values, although Stokes *et al.* (1993) observed similar values. This highly reduced matter content could be due to industrial discharges (e.g. discharge of fat from the slaughterhouses).

Table 3. Analysis results on activated sludge and recycle sludge (average and 95% confidence interval, resulting from 10 measurements)

	SS (g/l)	VSS/SS	COD/SS	COD/VSS	TKN/COD (%)
Activated sludge	4.01 ± 1.20	0.70 ± 0.02	1.38 ± 0.26	1.99 ± 0.36	3.90 ± 1.31
Recycle sludge	10.05 ± 5.27	0.69 ± 0.02	1.37 ± 0.12	1.98 ± 0.17	3.45 ± 1.38

4.3.4. Kinetic characterisation

In Fig. 12 a typical respirogram of a wastewater and a respirogram obtained after addition of wastewater plus extra ammonium are illustrated. It is obvious that the wastewater respirogram can not be separated clearly into two parts, i.e. one part that describes the oxygen consumption due to COD degradation and one part that describes the nitrification. Thus, the wastewater respirogram alone is not informative enough for the identification of both the nitrification kinetics and the degradation kinetics related to COD removal. Therefore optimal experiments were designed where extra ammonium was added together with the wastewater to simultaneously identify both processes from one set of experimental data. For a complete description of the lab-scale experiments and their interpretation, including the estimation of kinetic parameters, the reader is referred to chapter 7.

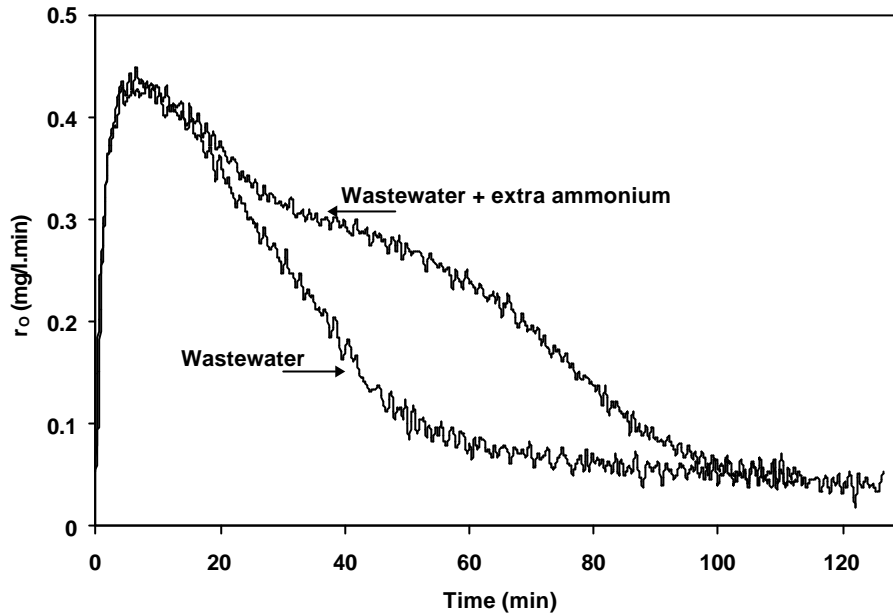


Figure 12. Example of respirograms obtained from respirometric tests with wastewater and wastewater mixed with ammonium

The respirograms were in general not informative enough to describe the degradation of COD in the wastewater via Monod kinetics, as described in Eq. 4 (no zero order respiration rate plateau was reached in the experiment). Consequently, the degradation of COD was instead described via a first order model (Eq. 17), where the first order rate constant k replaces the Monod parameter combination $\frac{m_{\max H}}{K_S}$.

$$r_{O,ex} = \frac{1 - Y_H}{Y_H} \cdot k \cdot X_{BH} \cdot S_S(t) \quad (17)$$

4.4. Step 7-9: Steady state model calibration

For the steady state model calibration a simple WWTP configuration was constructed in WEST++ (Fig. 13). The steady state configuration consists of one aeration tank ($V = 2600 \text{ m}^3$), a point-settler, an internal recycle line ($V = 400 \text{ m}^3$), and a constant average sludge waste flow from the recycle line.

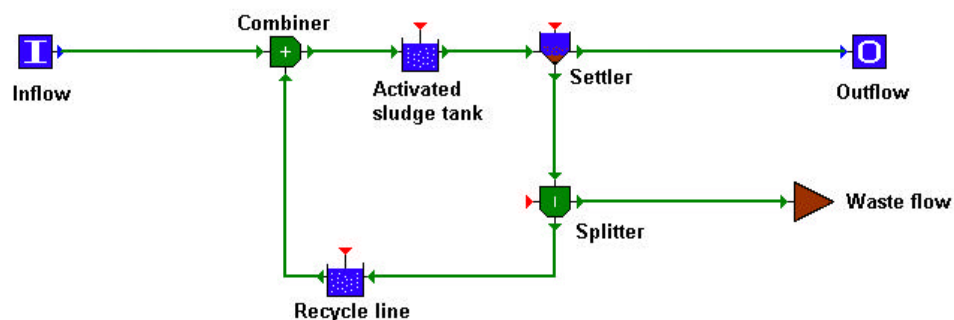


Figure 13. Treatment plant configuration used for the steady state model calibration

As mentioned above, the main aim of the steady state model is to fit the modelled sludge production to the sludge production calculated from plant data collected during the measuring campaign (based on waste flow data and sludge concentration measurements). This is done by adjusting parameters responsible for long-term behaviour, i.e. the decay rates b_H and b_A , together with the influent concentration of X_I . The experimental value of the decay rate determined based on the lab-scale test was 0.41 d^{-1} (corrected for temperature and transformed to the death regeneration concept, as described in Eq. 5), and was used as a guideline for the model calibration. The influent for the steady state model was obtained by averaging the dynamic influent data. Initially, these averages were calculated using only the dry weather flow data (influent data from 11/19/98 at 10.00 a.m. until the end of the measuring campaign, and with the wastewater characterisation as described above). For this period of the measuring campaign a total sludge production of 10342 kg SS was calculated, with an average waste flow rate of $241 \text{ m}^3/\text{day}$. Converting into COD units, using the SS to COD conversion factor of 1.38 resulting from the COD analyses done on the recycle sludge samples, the sludge production was calculated to be equivalent with 14065 kg COD. However, during the initial calibration of the steady state model only about half of this sludge production could be predicted no matter the values applied for b_H and b_A . Adjustment of the specific growth rates did not solve the sludge balance problem either. The simulated average sludge concentration in the aeration tank and the recycle line were much lower than the measured concentrations. It was tried to increase the model sludge production by assuming that all particulate COD consisted of X_I (instead of 50% as initially assumed), but the sludge balance did not improve sufficiently to solve the problem.

The resulting distribution of the different COD components in the influent is summarised in Table 4. Initially, X_I consisted of 30% of the total COD and X_S of 42 %, assuming that X_S consisted of S_{rest} plus 50% of the particulate COD, as described above.

Table 4. The average COD composition of the influent during the measuring campaign

COD component	%
S_I	12 %
S_S	16 %
X_S	22 %
X_I	50 %

It was then tried to find other reasons for the imbalance in the sludge production. As mentioned above (Fig. 5 and 7) the COD and SS concentrations together with the influent flow (Fig. 3) were very high during the first 2 days of the measuring campaign due to the rainfall. This indicates that the primary clarifiers did not retain the solids sufficiently during the rain event. This high load during the rain event could be due to a flush

effect in the sewers. This extra load of COD and SS contributed significantly to the sludge production, and this extra sludge production was most probably only wasted during the following dry weather flow days. To take this into account for the sludge balance during the model calibration it was therefore decided to include the data measured during the rain event for the calculation of the average influent composition.

The sludge production too was recalculated to include the data of the rain event. A total sludge production of 14364 kg SS (19535 kg COD) was now obtained with an average waste flow rate of 248 m³/d. A new series of steady state simulations resulted in a sludge production of 19177 kg COD, which was comparable to the sludge production measured at the WWTP (with the wastewater composition of Table 3).

The final calibrated value of b_H was 0.5 d⁻¹ which is higher than the default value for 10 °C (Henze *et al.*, 1987) but in accordance with the experimental value of 0.41 d⁻¹. Furthermore, initial adjustments of the maximum specific growth rates, μ_{maxA} and μ_{maxH} , were carried out during the steady state calibration. However, it should be stressed that final values can only be assigned to these parameters in the dynamic model calibration, which is the last part of the model calibration procedure (Fig. 1).

The fraction of autotrophic biomass, f_{BA} , in the activated sludge of the full-scale installation can be approximated by Eq. 18 (Sinkjær *et al.*, 1994).

$$f_{BA} = Y_A \cdot \frac{q_X}{1 + b_A \cdot q_X} \cdot \frac{N_{NIT}}{MLVSS \cdot V} \quad (18)$$

The calculated fraction became 0.0085 mg COD_{NIT}/mg COD. This value is very comparable with the steady state model calibration that yielded an autotrophic biomass fraction of 0.0086 mg COD_{NIT}/mg COD. The fraction of heterotrophic biomass was calculated similarly and a value of 0.217 mg COD_{HET}/mg COD was obtained comparable to a model value of 0.182 mg COD_{HET}/mgCOD.

4.5. Step 10: Dynamic model calibration

The configuration of the dynamic model (see Fig. 14) consists of a plug flow reactor (6 times 4 reactors in series of 100 m³ each), a sludge line (2 reactors in series of 100 m³ each), a pointsettler, an effluent buffer tank ($V = 3500$ m³), and a sludge recycle line (5 reactors in series of 80 m³ each). The effluent buffer tank was added to the configuration to simulate the liquid retention time in the settlers, however no reactions were assumed to take place there.

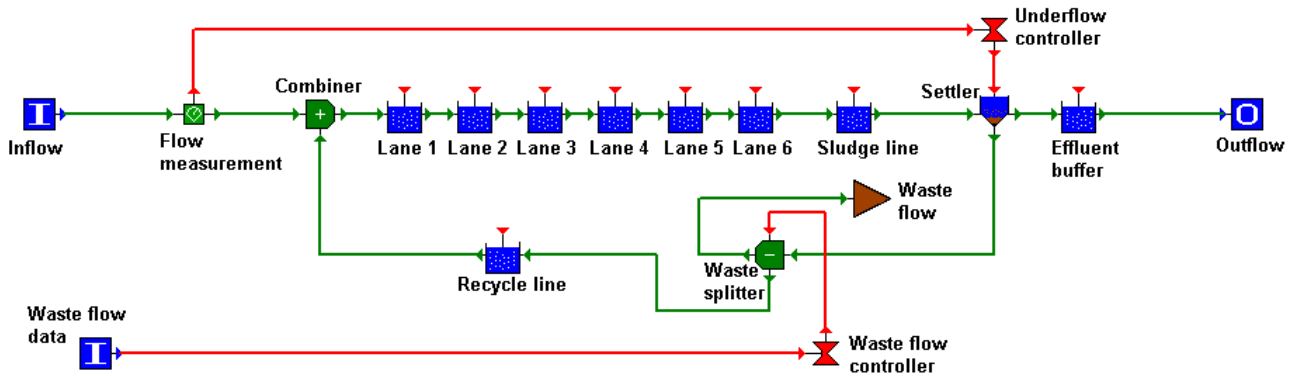


Figure 14. Model configuration for the calibrated model

The recycle flow was controlled at 55 % of the influent flow rate, to simulate the behaviour of the full-scale WWTP. To this purpose an influent flow measurement coupled to a proportional underflow controller was included in the model. Furthermore, a waste flow controller (see Fig. 14) was implemented in the model to simulate the discontinuous sludge waste from the recycle line. This on/off controller was fed with a data flow that indicated the sludge waste rate (data obtained from plant operation logbook).

A problem with the nitrogen balance appeared during the rain period, since a rather high simulated effluent S_{NH} peak occurred (20 - 25 mg NH_4-N/l) which was not observed in the measured ammonium data. To solve the problem, it was assumed that the nitrogen content of the high X_t load during the rain period was higher than the assumed 1%. By adjustment of i_{NXI} to 3% during the rain weather period the problem of the nitrogen balance could be solved, because less nitrogen was thus released by hydrolysis and ammonification. Note, that a fraction of inert nitrogen of 3% is considerably higher than the typical value of 0.5 - 1% (Henze *et al.*, 1995).

The maximum specific growth rates μ_{maxH} and μ_{maxA} were calibrated to $2.8 d^{-1}$ and $0.31 d^{-1}$ respectively and the K_S was adjusted to 15 mg COD/l.

The parameter combination involving μ_{maxA} identifiable from the lab-scale experiments is given by

$$(4.57 - Y_A) \cdot \frac{\mu_{maxA} \cdot X_{BA}}{Y_A} \quad (\text{see chapter 4}), \text{ which in fact is equal to the maximum oxygen uptake rate for}$$

nitrification assuming no substrate limitations. Thus, a way to validate the parameters of the full-scale model with the ones derived from lab-scale experiments (corrected for temperature differences) is to compare the parameter combination just described. With a μ_{maxA} of $0.31 d^{-1}$ and an average simulated X_{BA} of about 40 mg COD/l, the simulated maximum oxygen uptake rate becomes 225 mg/l.d. This is in very good agreement with the parameter combination derived from lab-scale experiments which had an average of 237 mg/l.d (n=21) with a 95% confidence interval of 175-300 mg/l.d. The simulated S_{NH} concentration in the aeration tanks was always higher than about 3 mg N/l (i.e. the minimum measured concentration of the

final effluent, see Fig. 9). Thus, in this case the influence of the half saturation coefficient, K_{NH} , is insignificant.

In the lab-scale experiments the heterotrophic substrate degradation was described with a first order expression since the data were not informative enough to be described with the Monod model, as explained above. An evaluation of the calibrated parameters of the full-scale model versus the lab-scale parameters can however still be carried out. The substrate degradation rate was calculated based on both the lab-scale model and its parameters on the one hand (Eq. 17), and the Monod model and its parameters on the other hand (Eq. 19).

$$r_S = \frac{\mu_{\max H} \cdot X_{BH}}{Y_H} \frac{S_S(t)}{K_S + S_S(t)} \quad (19)$$

The calculated profiles can be seen in Fig. 15. The lab-scale parameters are estimated on 16 different lab tests and the corresponding 95% confidence interval is given in Fig. 15 as well. For the Monod model the average simulated biomass concentration was used for X_{BH} . It is clear from Eq. 15 that as S_S increases, the model result based on the lab-scale parameters deviates from the Monod model. However, important to notice is that for the smaller S_S concentrations in the first order region of the Monod model, $S_S < K_S$, the Monod profile lies within the results of the lab-scale experiments, confirming that a value of 2.8 d^{-1} for $\mu_{\max H}$ and 15 mg/l for K_S are reasonable. The simulated S_S concentrations in the main part of the aeration tanks were indeed below the value of K_S . Thus, the experimental first order description of the S_S removal is realistic.

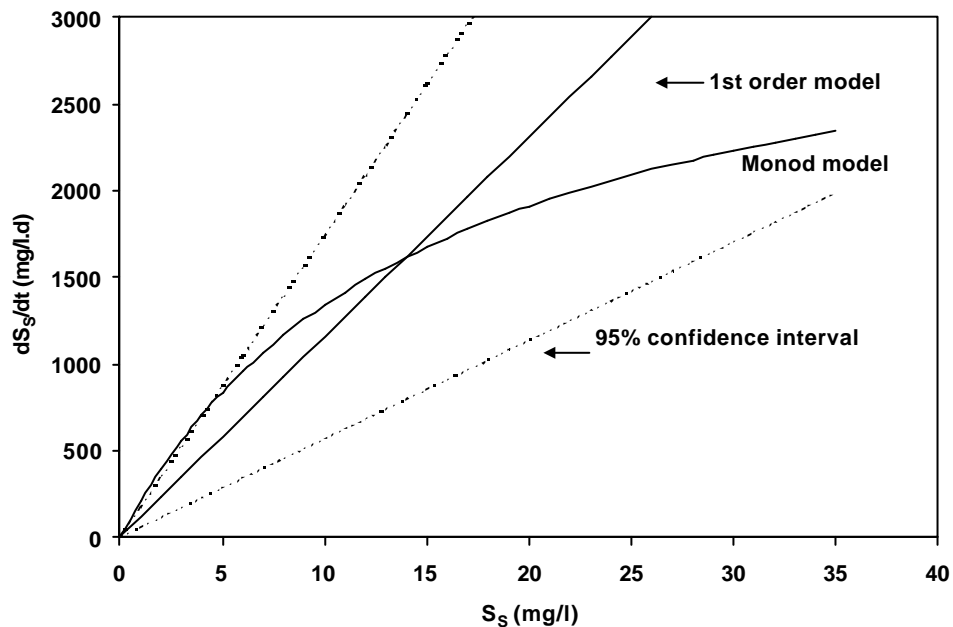


Figure 15. Substrate removal rate (dS_S/dt) plotted as a function of the substrate concentration for the Monod model (used in the calibrated model) and the 1st order model (used for the interpretation of respirometric data)

Both the description of the effluent S_{NH} and S_S data are good (Fig. 16 and 17). Only on one occasion do the simulations result in a S_S peak that is not present in the data. This S_S peak results from a high influent concentration together with a high flow rate, which could not be modelled adequately. One explanation could be that degradation of S_S could have continued for a while in the secondary clarifiers, while the model assumes that no degradation reactions take place in the clarifiers. Initially the model predicted too high S_{NO} concentrations in the final effluent. Although the activated sludge system is fully aerated it is likely that some simultaneous denitrification can take place in the system, e.g. in the less intensively aerated recycle channel. E.g. the NO_3 -N effluent concentration decreased to about 1 mg N/l on Friday evening and Saturday morning. This was probably due to an increased residence time in the aeration tank (lower flow) combined with availability of sufficient readily biodegradable carbon for denitrification entering the WWTP on Friday afternoon (see Fig. 3). The effluent NO_3 -N concentration increased again on Sunday and Monday (Fig. 10) due to lack of readily biodegradable COD (see Fig. 5).

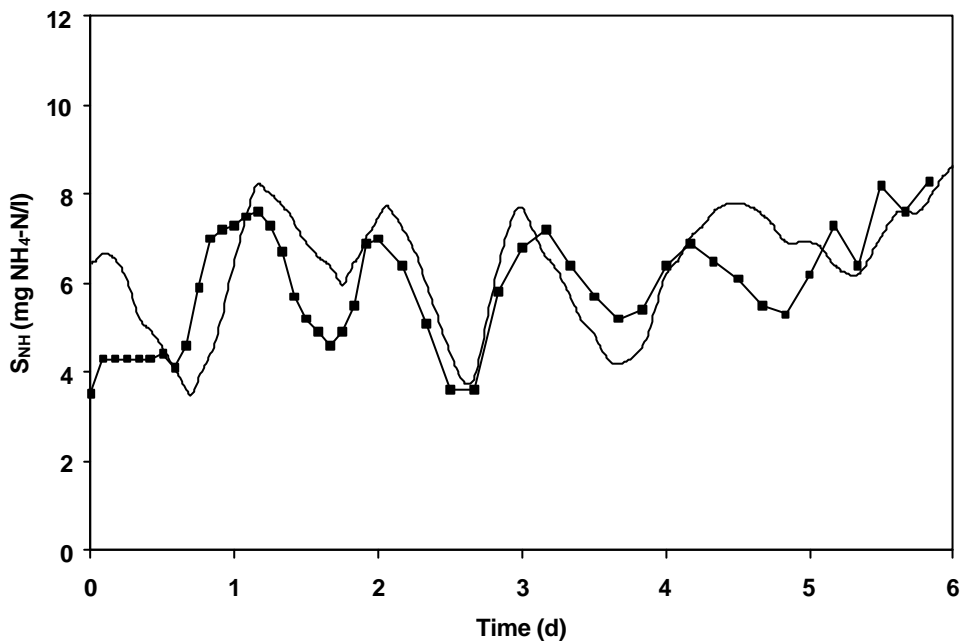


Figure 16. Effluent S_{NH} data (squares) and model effluent S_{NH} predictions

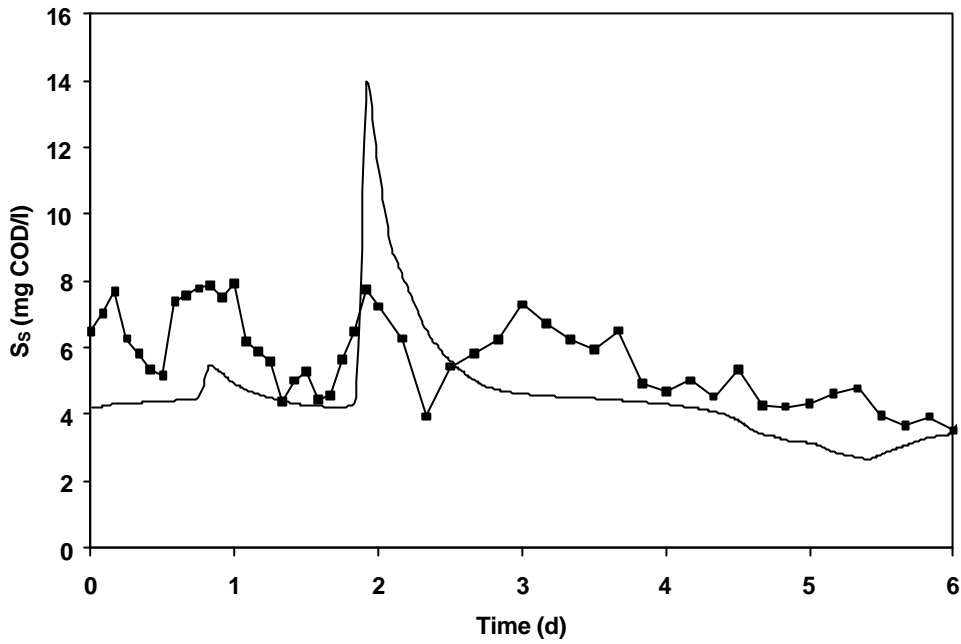


Figure 17. Effluent S_s data (squares) and model effluent S_s predictions

The saturation coefficient for oxygen, K_{OH} , was increased slightly to 0.5 mg O_2/l to decrease the inhibition of denitrification by O_2 , and the fraction of denitrifiers, η_g , was decreased to 0.6, to make the simulated S_{NO} concentration in the effluent approach the measured values. The resulting description of effluent S_{NO} is not perfect but follows the trend of the data reasonably (Fig. 18). Table 5 shows the complete parameter list for the dynamic model.

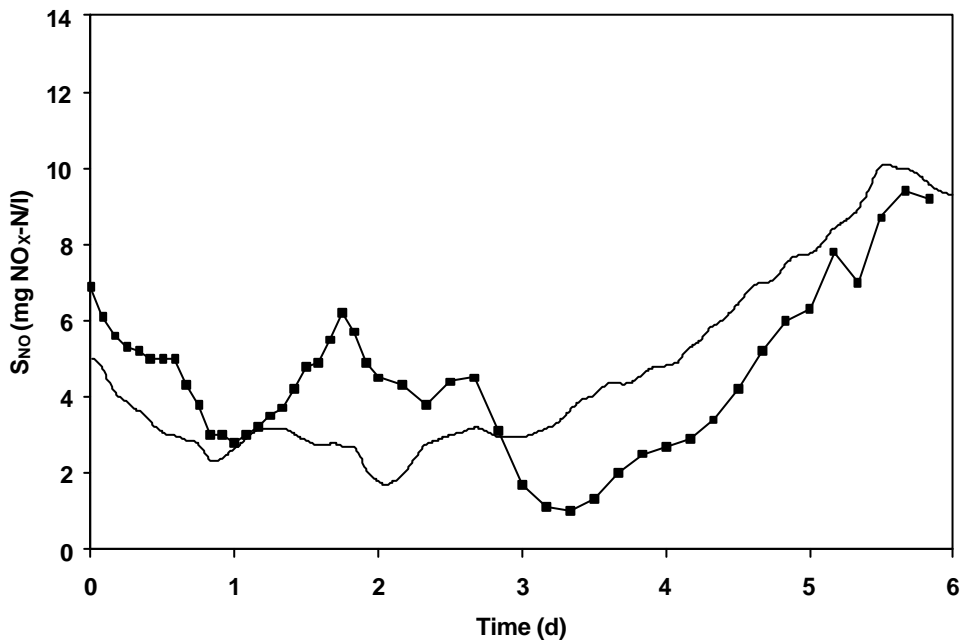


Figure 18. Effluent S_{NO} data (squares) and model effluent S_{NO} predictions

Table 5. List of main parameters for dynamic model (10 °C)

Parameter	Default (10 °C)	Calibrated	Units
Y_H	0.67		g cell COD formed/g COD oxidized
Y_A	0.24		g cell COD formed/g N oxidized
$\mu_{\max H}$	3.0	2.8	d ⁻¹
$\mu_{\max A}$	0.3	0.31	d ⁻¹
b_H	0.2	0.5	d ⁻¹
b_A	0.05	0.02	d ⁻¹
K_S	20	15	g COD/m ³
K_{NH}	1.0		g NH ₄ -N/m ³
K_{NO}	0.5		g NO ₃ -N/m ³
K_{OH}	0.2	0.5	g O ₂ /m ³
K_{OA}	0.4		g O ₂ /m ³
k_h	1.0		g slowly biodegradable COD/g cell COD.d
K_X	0.01		g slowly biodegradable COD/g cell COD
η_g	0.8	0.6	Dimensionless

Finally, the removal efficiencies for COD_{tot}, COD_{sol}, TKN and NH₄-N have been calculated based on the actual measured and averaged data on the one hand, and based on averaged results of the dynamic simulation including the whole measuring campaign on the other hand. From these results, it has been calculated how close the model describes the removal of COD_{tot}, COD_{sol}, TKN and NH₄-N (see Table 6). As it can be seen from Table 6 the model describes 94 - 100% of the actual removal, which can be considered to be very satisfactory.

Table 6. Removal efficiency based on measurements and simulation, expressed as percentage of the observed removal that is described by the model

Removal efficiency	COD _{tot}	COD _{sol}	TKN	NH ₄ -N
Measurements	84%	73%	68%	58%
Simulation	83%	72%	67%	54%
Model description	99%	100%	99%	94%

4.6. Sensitivity analysis

The parameter values of the calibrated model given in Table 5 did not seem very different from the default parameter set. Therefore, it was investigated if the parameters that were modified during the model calibration were indeed influencing the model outputs significantly. To this purpose a sensitivity analysis was carried out with the calibrated model, to check the sensitivity of the model output (effluent S_S , S_{NH} and S_{NO} concentrations) and the predicted sludge concentration (X) to changes in the model parameters and influent pollutant concentrations. The sensitivity was evaluated using relative sensitivity functions, RSF (see Eq. 20). The calibrated model was used as the reference simulation, and the model output obtained after increasing the value of a specific parameter with 1% was used to obtain the relative sensitivity functions (Eq. 20).

$$RSF = \frac{\Delta y}{y} * \frac{p}{\Delta p} \quad (20)$$

The value of the relative sensitivity function at the beginning of the period with dynamic data was used for the evaluation (= output corresponding to the end of the steady state simulation). One can comment that this leads to a steady state sensitivity analysis. However, it should be added here that a similar sensitivity analysis was done for the period with dynamic data (calculation of the average model deviation Δy based on the simulation data obtained for the period with dynamic data). The results of this analysis were rather similar to the results of the steady state analysis presented here. The results of this evaluation are shown in Table 7. The influence of a parameter on the model output was interpreted as proposed by Julien (1997): For $RSF < 0.25$ a parameter is considered to have no significant influence on a certain model output; if $0.25 \leq RSF < 1$, the parameter is considered to be influential; if $1 \leq RSF < 2$ the parameter is considered to be very influential; if $2 \leq RSF$ the parameter is considered to be extremely influential. When the value of a parameter and the output change in the same direction, this is indicated with a positive sign in Table 7, when they move in the opposite direction this is indicated with a negative sign.

The sludge concentration is only significantly influenced by the value of Y_H and by the influent X_I concentration. The latter confirms that a modification of the influent fractionation (the fraction of X_I was increased) was indeed one of the most appropriate things to do to increase the sludge concentration in the system (and consequently also the sludge production) during the steady state model calibration. Besides the sludge concentration, Y_H also influences the output S_S , S_{NO} and S_{NH} concentrations. However, at the beginning of the calibration it was decided not to change Y_H (and Y_A). The sensitivity analysis shows furthermore that all but one (η_g) of the parameters that were modified from their default values in the final calibrated model (μ_{maxH} , μ_{maxA} , b_H , b_A , K_S , K_{OH} , η_g) influence one or several of the simulated effluent concentrations. This confirms (at least for 6 out of 7 parameters, μ_{maxH} , μ_{maxA} , b_H , b_A , K_S , K_{OH}) that a modification of these parameter values resulted in a considerable change in the simulated model output. Finally, it should be stressed that both μ_{maxH} and μ_{maxA} are very influential on effluent S_S and extremely

influential on effluent S_{NH} and S_{NO} concentrations respectively. In other words, this confirms that even a slight modification of the value of these parameters, as in the presented model calibration, can have an important effect on the model output.

Table 7. Results sensitivity analysis with the calibrated model of the Zele WWTP. (+, - = influential; ++, - - = very influential; + + +, - - - = extremely influential). See text for a further explanation of the results

Parameter	X	Effluent S_S	Effluent S_{NO}	Effluent S_{NH}
Y_H	+	- -	+	- -
Y_A				
μ_{maxH}		- -		
μ_{maxA}			+ + +	- - -
b_H		+ + +		
b_A			-	+
K_S		+ +		
K_{NH}			-	+
K_{OH}				-
K_{OA}			-	+
k_a				
k_h		- -		+
K_X				
η_g				
Influent component	X	Effluent S_S	Effluent S_{NO}	Effluent S_{NH}
S_S			-	+
S_{NH}			+ +	+
X_I	+			
X_S		+	- -	+

4.7. Model reduction

It was investigated whether the number of tanks could be reduced in the hydraulic model to increase the calculation speed of the model. To evaluate the effect of model reduction, the quality of the fit between simulated values and available data was evaluated by calculating the average relative deviation (ARD)

between model predictions of S_{NH} and available data points (Eq. 21).

$$ARD = \frac{1}{n} \cdot \sum_{i=1}^n \left(\frac{|X_{i_{obs}} - X_{i_{sim}}|}{X_{i_{obs}}} \right) \cdot 100\% \quad (21)$$

For the calibrated model ARD was 16.5% when considering the effluent S_{NH} concentration. For a reduction of the number of tanks from 24 to 12 in the activated sludge lanes, and from 5 to 3 in the recycle channel, the same ARD (16.5%) was obtained for effluent S_{NH} . Thus, this model reduction gave the same accuracy as the full model. However a further reduction of the number of tanks to 8 in the activated sludge lanes and 2 in the recycle channel gave a significantly worse description with an ARD of 73.5%. Although the dynamics of the effluent S_{NH} data could still be described, the simulated S_{NH} concentrations were in general higher than the measured data with the last model. The reason for this is simply that the mixing patterns are more approaching an ideally mixed situation compared to the original model. In general, except for the case of zero order degradation kinetics, an ideally mixed tank results in a lower substrate removal efficiency in comparison with an ideal plug-flow tank when the same reactor volume is available. Conclusively, the model reduction resulted in a model that needed about 50% less calculation time for a simulation than the original calibrated model.

In principle, one could imagine that if the value of μ_{maxA} is increased then a similar model fit for the reduced 8 tanks in series model could be reached as for the calibrated model, since an increase of μ_{maxA} would decrease the outlet $S_{NH}(0)$. Thus, this means that a “wrong” hydraulic characterisation could be compensated by a change of parameter values.

5. Discussion

In this study it was stressed that the purpose of the model should determine how the model is calibrated, e.g. which information is needed and to which level the model should be calibrated. A systematic and general model calibration procedure was proposed, and illustrated for a combined municipal-industrial WWTP. ASM1 was applied in the case under study, but the proposed general model calibration procedure is applicable for any activated sludge model.

The purpose of the case study was to obtain a good description of the biological N removal, since the model was to be used for process optimisations focusing on an improvement of the N-removal capacity, including start-up of denitrification (Gernaey *et al.*, 2000c). Therefore, it was also important to describe the variation in readily biodegradable COD. Biodegradation of COD will influence the N components in the activated sludge system, e.g. because S_{NH} is incorporated into new biomass and S_{NO} is consumed during denitrification. It was observed that the presence of readily biodegradable COD in the influent was mainly related to industrial activity, resulting in a lack of biodegradable COD during the weekend. For future implementation of denitrification in the WWTP this may cause problems in maintaining the denitrification

efficiency during weekends. This weekend effect was reported previously for another Flemish municipal WWTP by Coen *et al.* (1997).

In this study it was obviously important to have a good description of the hydraulic patterns to describe the dynamics of the system adequately. Indeed, a model reduction study showed that the number of tanks could be halved, from 24 to 12, still giving the same description of the effluent data with the same parameter set as the calibrated model. However, it also became clear that a further model reduction would not be possible without a compensating change in the kinetic parameters. In other words, for a further model reduction (a decrease of the number of tanks below 12) errors in hydraulics have to be compensated by “wrong” biological parameters deviating from the lab-scale results, e.g. increase of $\mu_{\max A}$ to decrease the effluent S_{NH} concentration. Thus, in case a hydraulic model would not have been available at all, e.g. the hydraulics were described with a 4 tanks in series model, the calibrated parameter set might have been rather different and not corresponding at all to the results of the lab-scale experiments. This is immediately linked to the importance of evaluating the key kinetic parameters with lab-scale experiments. In this case study the decay rate and the two specific growth rates $\mu_{\max A}$ and $\mu_{\max H}$ were determined. It was illustrated how to compare these parameters obtained from lab-scale experiments with the parameters of the full-scale model, thereby verifying that the parameters of the full-scale model were realistic.

Thus, as just described above the information obtained from different tests for hydraulic, sludge settling (if needed) and biological characterisation help to frame the model calibration, and in fact reduces the apparently high degree of freedom of the model parameters significantly.

For this case study, it could be questioned, however, whether it was necessary to determine some kinetic parameters in lab-scale experiments, since the resulting calibrated parameters were not far from the ASM1 default parameter set (Henze *et al.*, 1987). Still, even in this case the lab-scale results gave extra confirmation on the parameter set of the calibrated model, thereby increasing the quality and confidence of the model calibration. Moreover, the sensitivity analysis clearly showed that the calibrated model was indeed sensitive to changes of the parameters that were modified during the model calibration procedure. Two of the most influential parameters were $\mu_{\max A}$ and $\mu_{\max H}$, which confirmed that even the small deviations of these parameters from their default values (Henze *et al.*, 1987) in the calibrated model has a considerable influence on the model output. It should be stressed that such a sensitivity analysis is case specific, since the results of the analysis can be influenced by the data set that is studied. This can be illustrated with the parameter K_{NH} . The calibrated model presented here is not sensitive to a change of K_{NH} because the S_{NH} concentrations in the plant are always considerably higher than the value of K_{NH} (1 mg N/l). However, one could imagine that the influence of K_{NH} could be larger for a model that describes a treatment plant with almost complete nitrification (e.g. effluent S_{NH} concentration around 1 mg N/l).

It was clear from this study that there is an interaction between wastewater characterisation and calibration

of the full-scale model to the available data (effluent and sludge wasted). For instance, the influent concentration of X_I and X_S were adjusted during the steady state model calibration to be able to describe the sludge production data. In this phase it became clear that it was important to include the data of the rain weather period prior to the dry weather period, since a high COD load originating from the rain period contributed significantly to the sludge that was wasted during the following days.

6. Conclusions

A systematic model calibration procedure was presented and evaluated for a combined municipal-industrial WWTP. It was underlined that it is very important to define the purpose of the model carefully since this will determine how to approach the model calibration. In this study it was clearly illustrated how additional information obtained from tests specifically designed to describe the hydraulics and the biology of the system help to decide on realistic model parameters during the model calibration procedure.

The aim of this study was to obtain a good description of the N removal capacity, since the model was to be applied for process optimisation in a later stage. It was thus important to have a good description of the process dynamics. Therefore, the hydraulic behaviour of the system was investigated, resulting in a 24 tanks-in-series model to describe the plug flow aeration tank. It was shown that this hydraulic model could be reduced to a 12 tanks-in-series model, yielding a 50% reduction of the calculation time for the scenario simulations. Two of the most important parameters to adjust to correctly describe the dynamics were the specific growth rates, as was also evidenced by a sensitivity analysis carried out with the calibrated model. Consequently, additional information on the specific growth rates derived from lab-scale experiments is important to confirm that the calibrated parameters of the full-scale model are realistic.

Chapter 9
-
Conclusions and perspectives

Chapter 9

Conclusions and perspectives

The task of model calibration is often rather time-consuming and the time and resources needed for a reliable calibrated model, that can be applied for different purposes, is very often under-estimated. In this thesis it was aimed to set-up a more methodological approach for model calibration with special focus to the investigation, illustration and solution of the problems encountered when deriving information from lab-scale experiments.

The study focused especially on the development of a general methodology to apply optimal experimental design on lab-scale experiments with activated sludge aiming at accurate parameter estimates for biological models. The concept of the proposed method can be illustrated by Fig. 1.

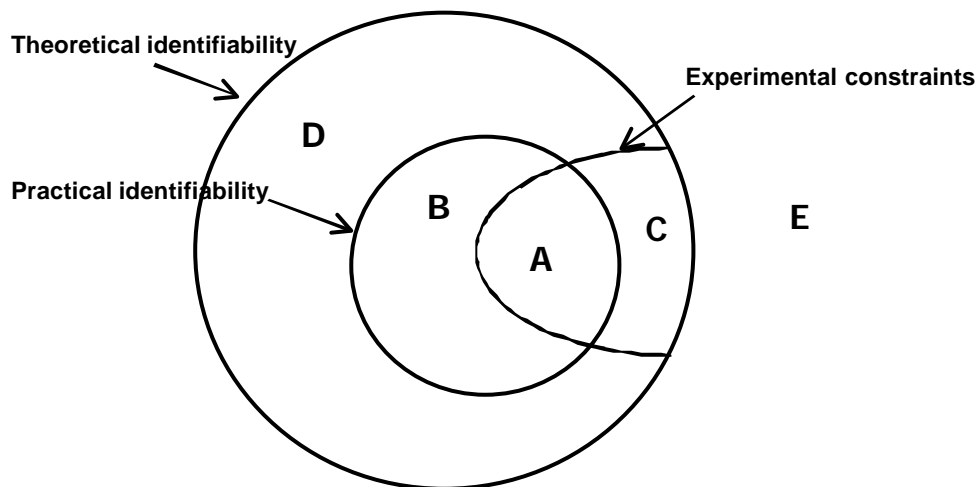


Figure 1. Conceptual idea of parameter identifiability and optimal experimental design

The first step in this conceptual methodology consists of a thorough analysis of the purpose of the experiment, i.e. which experimental response is sought. This purpose determines the conditions under which the experiments should ideally be carried out. Each point in Fig. 1 corresponds to a set of experimental conditions leading to an experimental response with a certain information content. If these experimental conditions are in accordance with the defined purpose, the point will lay within one of the defined regions (A - D) in Fig. 1. The exact position will depend on the experimental conditions and on the information content of the data. The point will, however, be located outside the defined regions if the

experimental conditions do not comply with the purpose (point E in Fig. 1).

In Fig. 1 the region to investigate first is the region defining the theoretical identifiability of the model for which accurate parameters are sought. This region, outlined by the outer circle in Fig 1 (A – D) frames the experimental conditions that allow theoretically to obtain unique parameter values from the selected and available measurements. The bound on this region is considered to be a hard, ultimate one since the theoretical identifiability is entirely defined by the structure of the model under study and the chosen measurements.

On the other hand, the practical identifiability region (indicated by A and B in Fig. 1) is related to the quality and thereby the information content of the experimental data. Even when the theoretical identifiability analysis has shown that some given parameters are identifiable, they may not be practically identifiable, for instance if the data are too noise corrupted (Holmberg, 1982). Therefore, the practical identifiability region is a sub-set of the theoretical identifiability region. Furthermore, this region is not fixed at a certain position but can be located elsewhere within the theoretical identifiability region in case the actual model parameter values or the collected data and their properties, e.g. the noise level on the data, change.

At last, the region (C – A) indicates that in addition certain constraints can be imposed on the experimental conditions, to ensure that the experiment fulfils a defined purpose.

The optimal experiment (A) is now determined as the one for which the experimental conditions belong to the intersection of the three regions in Fig. 1: practically identifiable, theoretically identifiable and obeying to the experimental constraints.

These conceptual ideas on a methodology for optimal experimental designs are very general and can be applied to any case where the aim is to obtain accurate parameters from an experiment (lab-scale as well as full-scale).

In this study the conceptual methodology was investigated and illustrated for lab-scale experiments with the purpose of obtaining accurate parameter estimates of activated sludge reaction kinetics and wastewater component concentrations. Two case studies were carried out. The first one focused on the classical example of the two-step nitrification process, and the second case study aimed at characterisation of combined COD degradation and nitrification kinetics. For determination of the optimal experiments the theory of Optimal Experimental Design (OED) was applied. The cornerstone in OED is the Fisher Information Matrix (FIM) which under some conditions equals the parameter estimation error covariance matrix (COV). The essence of most OED is basically to reduce the COV, and different optimal experimental design criteria have been defined based on different scalar functions of the FIM (e.g. Walter and Pronzato, 1990; Munack, 1989 and 1991). In general, of course, different other experimental design procedures for optimisation of experiments can be applied depending on the purpose and model under study.

Since measurements are the basis on which parameter estimation is conducted, the study started by focusing on the available measuring techniques. After a thorough literature review, it was concluded that respirometric and titrimetric methods were the most powerful data generators for the processes that were studied. To maximise the data quality, a methodology of combined respirometric-titrimetric measurements was developed and evaluated (see chapter 3) and applied in this study. With respect to the respirometric method one of the hybrid respirometer principles proposed by Vanrolleghem and Spanjers (1998) was implemented. The hybrid respirometer consists of an open aerated vessel and a closed non-aerated respiration chamber. It is operated with two oxygen electrodes resulting in two sources of information on the oxygen uptake rate, both collected at a high frequency. The obvious advantage of this respirometer is that the oxygen uptake rate (r_O) can be obtained by making a simple oxygen mass balance over the respiration chamber, without the need to estimate the oxygen transfer coefficient (K_{La}).

Especially for characterisation of the nitrification process titrimetric data are straightforward to interpret (e.g. Gernaey *et al.*, 1997a) due to the well-defined proton production during the first nitrification step. In chapter 3 the potential of this method for characterisation of organic carbon compounds was illustrated with acetate. However, an application of this titrimetric method for organic carbon and wastewater COD characterisation may eventually not be without problems due to the more complex and compound dependent titrimetric effects caused by the degradation of organic matter. Further work is currently done in this direction (Gernaey *et al.*, 2000a, 2000b), but it was, however, out of the scope of this thesis to analyse this subject in more detail.

It was already noticed in chapter 3, and investigated in more detail in chapter 5, that the accuracy of the parameter estimates increased significantly when combined measurements (respirometric and titrimetric data) were considered for characterisation of the nitrification kinetic parameters rather than single measurements (respirometric or titrimetric data). For example the accuracy of the parameters μ_{maxA1} and K_{SA1} improved with about 50% when combined r_O and H_p data were used compared to measurements of r_O alone. In chapter 5 the accuracy was evaluated based on (i) the measurement errors, (ii) model errors and (iii) the complexity of the parameter estimation as characterised by the rate of convergence of the estimation algorithm towards a minimum. Here it was concluded that especially parameter estimation based on H_p data was very accurate and fast convergence was obtained. The same holds for r_O data, but in that case the accuracy of the parameters was lower. However, in general, the accuracy based on S_O data was much higher. This was clearly caused by the much lower measurement noise compared to the r_O data. Furthermore, a significant improvement in accuracy was observed when two dissolved oxygen measurements were available ($S_{O,1} + S_{O,2}$) compared to a single measurement ($S_{O,1}$). This confirms the statement made by Vanrolleghem and Spanjers (1998) that basically two independent measures of the respiration rate can be obtained in the hybrid respirometer, thus duplicating the information on the kinetic parameters. The added value of H_p to combined $S_{O,1}$ and $S_{O,2}$ measurements was not significant, because

it did not improve the parameter accuracy any further. However, the complexity of the parameter estimation procedure increased significantly when based on S_0 data only with a much slower rate of convergence towards the final parameter estimates. It was therefore suggested that parameter estimates based on H_p and/or r_0 could be applied as initial values for the more complex parameter estimation based on S_0 data, in case the highest possible parameter accuracy is aimed for.

The next step in the thesis, after having developed and evaluated the measuring methodology, was to analyse the theoretical identifiability of the models that were applied for data interpretation (chapter 4). Again, the nitrification process was selected as the example under study due to the possibility of characterising this process via combined respirometric-titrimetric measurements. In chapter 4 a thorough study of the theoretical identifiability of the two-step nitrification model based on Monod kinetics was undertaken considering respirometric outputs (dissolved oxygen or oxygen uptake rates) from two types of respirometer and titrimetric outputs (cumulative proton production). In the analysis two model structures including presence or absence of biomass growth were investigated for the interpretation of long- and short-term experiments respectively. The theoretical identifiability was studied by the series expansion methods: both the Taylor and generating series methods were applied. It was illustrated in the analysis of the hybrid respirometer that the generating series method was more powerful than the Taylor series expansion when an input is considered, since it resulted in simpler equations with respect to the parameters. This is in accordance with Walter (1982).

From this study of the nitrification process it appeared that the parameter identifiability improves significantly when combined respirometric and titrimetric data are available. It was proven that the yield of the first nitrification step (Y_{A1}) becomes uniquely identifiable. This was not a complete surprise since in general the yield coefficient relates amounts of produced biomass to amounts of degraded substrate. The possibility for a unique identification of Y_{A1} is important, since it means that all parameters that are typically identified in combination with the biomass yield coefficient when considering respirometric measurements alone (Dochain *et al.*, 1995), could now be uniquely identified. An exception to this is the maximum specific growth rate, which in case no biomass growth is considered (i.e. short-term experiments), would only be identifiable as a parameter combination involving the biomass concentration. However, in case biomass growth is considered (i.e. long-term experiments) all parameters become uniquely identifiable with combined respirometric-titrimetric measurements.

The most important result of the theoretical identifiability analysis reported in chapter 4 was that the results could be generalised. Indeed, an important disadvantage of the series expansion methods to evaluate the theoretical identifiability is that the user initially has to “guess” which parameter combinations may be the “right”, i.e. theoretically identifiable, ones. If the problem is not solvable with this “guess”, other parameter combinations may have to be assumed resulting in an iterative time-consuming trial and error procedure. It appeared, however, that by applying a set of simple generalisation rules the theoretical identifiable

parameter combinations could be assessed directly, only based on (i) knowledge of the process under study, (ii) the measured component(s) and (iii) the substrate component(s) that is degraded. The generalisation was proven to work with several examples, also taken from literature data. This result significantly reduces the time consuming task of analysing the theoretical identifiability of models described by Monod growth kinetics in ASM1-like matrix presentations. Thus the generalisation of theoretically identifiable parameter combinations may become a powerful tool in future identifiability studies since it can help the users to obtain the identifiable parameter combinations directly without the need to go too deeply into the mathematical background of theoretical identifiability. This study of theoretical identifiability has focused on Monod models. However, it may be possible to extend the generalisation rules, to also cover the theoretically identifiable parameter combinations of non-Monod kinetic models. This would for sure be a topic that is worth investigating further.

The practical identifiability of a specific nitrification example was investigated in more detail in chapter 5. The investigation was carried out by evaluation of the output sensitivity functions and the corresponding FIM. Local parameter identifiability requires that the rank of FIM is full. This can, for instance, be investigated by calculation of the determinant of the FIM, i.e. if the $\text{Det}(\text{FIM}) \neq 0$ the parameters are locally identifiable (Spriet and Vansteenkiste, 1982; Söderström and Stoica, 1989). In this study it appeared that the FIM became singular, when calculated on the basis of output sensitivity functions with respect to all parameters that are theoretically identifiable considering combined respirometric – titrimetric measurements, i.e. including the sensitivity function of Y_{A1} . The reason for the singularity was that the output sensitivity functions of the respirometric or titrimetric output with respect to $\mu_{\max A1}$ and Y_{A1} , as expected, were proportional. By definition this results in a singular FIM. However, the theoretical identifiability analysis in chapter 4 had clearly shown that the Y_{A1} becomes identifiable with combined measurements. Moreover, by investigation of the sum of squared error objective function as a function of the parameters $\mu_{\max A1}$ and Y_{A1} , it was clearly observed that the Y_{A1} was practically identifiable although strongly correlated with $\mu_{\max A1}$. The FIM approach was obviously not able to deal with this and the FIM analysis gave a too pessimistic picture of the practical parameter identifiability. Thus, in further studies of practical identifiability using FIM properties, the theoretical result that Y_{A1} becomes uniquely identifiable could not be included.

Hence, this work clearly illustrated some limitations in the application of FIM as a measure of practical identifiability and care should be taken in using the FIM as a measure of identifiability since the method may not be sensitive enough.

Another problem related to the application of the properties of the FIM in different optimal experimental design criteria was encountered and analysed in depth in chapter 6. Different optimal experimental design criteria have been developed based on scalar functions of the FIM (e.g. Goodwin, 1987; Munack, 1989, 1991). Initially, the study reported in chapter 6 aimed at evaluating whether rescaling of parameter units could be used to improve the numerical properties of the FIM giving a more stable inversion and thereby

more reliable assessment of the parameter estimation error covariance matrix. The condition number (i.e. the ratio between the largest and the smallest eigenvalue of the FIM) is a measure of the “robustness” of the inversion. It was found that improvements in condition number up to a factor 10^{10} could be obtained just by rescaling the time unit of the parameters. In addition, it was found that in some cases it is possible to reach the most optimal condition number (=1). This result has some serious implications for optimal experimental design methodology and certainly stresses that care should be taken with scaling of parameter units since the FIM is dependent on the actual parameter values. Via a simple parameter estimation example of a single substrate batch model with Monod kinetics it was proven that both the A-, modA-, E- and modE-criteria were affected by rescaling, and that only the D-criterion (which focuses on maximisation of the determinant of FIM) was unaffected by rescaling. The invariance of the D-criterion with respect to parameter rescaling was in fact already addressed by Goodwin (1987) and repeated in Walter and Pronzato (1999). However, as far as known, no evaluation was made with respect to the remaining criteria. The rescaling is especially critical for the modE criterion that focuses on the optimisation of the condition number of the FIM. In the work of Munack (1989), Baltes *et al.* (1994), Versyck *et al.* (1997) and Versyck and Van Impe (1999) feeding rates to fed-batch systems have exactly been optimised based on the modE criterion. In the work of Versyck *et al.* (1997) the optimum of the modE (=1) was obtained. Although these results can not be questioned, it must be stressed that it may be possible in some cases to obtain the optimum value for this criterion just by parameter rescaling, which, of course, has nothing to do with optimal design of an experiment.

Following the investigation of different aspects and details of the theoretical and practical identifiability, the focus was turned to the conceptual procedure for optimal experimental design (Fig. 1). The concept was specially outlined for FIM based optimal experimental designs. This procedure consisted of 9 steps, and the procedure was applied in practice for two simple case studies in chapter 7. In both case studies, the purpose was to obtain parameter estimates that were as accurate as possible, and in addition these estimated parameters should be representative for the full-scale system under study.

Some emphasis was put on the definition of the experimental conditions that would lead to the desired experimental response for which parameters would be theoretically identifiable. For instance, one of the important factors to be considered was the ratio between the initial substrate and biomass concentration, $S(0)/X(0)$. The influence of this ratio on the experimental response was discussed in detail in chapter 2. It was discussed there that it could be more relevant to focus on the change in substrate concentrations or load, ΔS , which the organisms are subjected to. It is typically recommended to work under low $S(0)/X(0)$ ratio, or expressed in another way low ΔS , to obtain responses that are representative for the physiological state of the biomass prior to the experiments (Grady *et al.*, 1996), i.e. the physiological state of the biomass in the activated sludge plant in order to obtain what are called “extant kinetic parameters”. This $S(0)/X(0)$ ratio may have an important influence on the resulting experimental responses and may influence

both the observed biomass yield and the kinetic parameters. Drastic changes of the environment may eventually even lead to biomass population shifts. The latter applies especially to organic substrate (COD), which can flow into different mechanisms depending on the environmental conditions. For nitrification on the other hand, a too high change in substrate load may lead to substrate inhibition of the nitrification process.

In case study 1 the aim was to design a simple experiment that allowed for simultaneous characterisation of the reaction kinetics of both nitrification steps. The experimental degree of freedom to be optimised was selected as the addition of an optimal amount of nitrite together with the ammonium at the beginning of the experiment. The purpose of the second case study was to design an experiment that would allow for a simultaneous characterisation of the reaction kinetics for both the first nitrification step and the degradation of readily biodegradable wastewater COD. In the second case study the experimental degree of freedom was defined as the optimal amount of ammonium to be added initially together with the wastewater.

In both case studies the experiment was optimised via application of the D-criterion (maximisation of $\text{Det}(\text{FIM})$ or in other words minimisation of the generalised parameter covariance), and it was thoroughly investigated and evaluated how the confidence intervals on the estimated parameters improved in the optimal experimental designs. For the first case study the main improvement in parameter accuracy (about 50%) compared to the reference experiment was found for the parameter $\mu_{\text{maxA}2}$. This was in agreement with the purpose of the optimal experiment, where the optimised experimental degree of freedom was the initial amount of nitrite ($S_{\text{NO}_2}(0)$) added. Indeed, an increase of $S_{\text{NO}_2}(0)$ results in more information on the maximum respiration rate of the second nitrification step, and thereby on the parameter $\mu_{\text{maxA}2}$. Moreover, a significant improvement in accuracy (about 20 - 30 %) was obtained for the parameter $K_{\text{SA}2}$. In the second case study, a reduction of about 50% of the confidence intervals of the kinetic parameters related to the first nitrification step, $\mu_{\text{maxA}1}$ and $K_{\text{SA}1}$, was found. Furthermore, the accuracy of the parameter related to the first order degradation of COD improved with about 20%. These results were also in accordance with the aim of the study where the experimental degree of freedom was chosen as the additional amount of ammonium, $S_{\text{NH}}(0)$, to be added together with the wastewater. Indeed, an increase of $S_{\text{NH}}(0)$ focuses on a better separation of the nitrification process from COD degradation in the respirogram to allow for a better identification of both processes.

These theoretical predictions were validated with independent parameter estimations based on experiments that were carried out according to the optimal experimental design. In both case studies it was found that rather similar experiments conducted with the same sludge source and wastewater lead to highly reproducible parameter estimates. However, rather large differences (up to a factor 2) in parameter estimates were found for experiments in both case studies, when using sludge collected at different days within the same week. Considering that the parameter estimates are highly accurate and reproducible, it was concluded that either the sludge parameters or, in the second case study, the wastewater varied

significantly, even over such a short-term period.

Interesting to discuss is how sensitive the proposed optimal experimental design is towards changes of reaction kinetics or changes in wastewater substrate concentrations. This was investigated in both case studies. It was found that some safety margin exists for the experimental design, which means that it is rather robust against parameter variations. However, for the two step nitrification case it was for example found that a combination of a low $\mu_{\max A1}$ and high $\mu_{\max A2}$ was critical and could result in experimental data that would not allow to practically identify the kinetic parameters of both nitrification step. One example was recorded where the optimal experiment indeed would have resulted in very inaccurate parameter estimates.

In the second case study dealing with combined COD degradation and nitrification, a more systematic sensitivity study was carried out to evaluate the effect of changes of parameters and substrate concentrations on the parameter estimation accuracy. In that study it was concluded that changes in the first order degradation rate of the wastewater COD especially influenced the accuracy of the estimation of initial substrates (in this case $S_{S,1}(0)$ and $S_{NH,1}(0)$). On the other hand changes of $\mu_{\max A1}$ influenced the parameter accuracy of K_{SA1} significantly and changes of the initial substrate concentration $S_{NH}(0)$ had the least effect on the overall variances as quantified by the $\text{Det}(\text{FIM})$.

The conclusion of the sensitivity study was that depending on the acceptable accuracy of the parameter estimates, the optimal experimental designs may need frequent updating to ensure the practical parameter identifiability, or more robust experimental designs must be developed.

The situation of frequent updating versus robust OED will be considered in more detail below. As mentioned above in the presentation of the conceptual methodology the region of practical identifiability may move but, as long as the model structure does not change, only within the hard bound region of theoretical identifiability. This adaptation of the optimal experimental design is illustrated in Fig. 2. To make the discussion more concrete in the example used in Fig.2, one can imagine that the ratio between the ammonium content of the wastewater S_{NH} and the wastewater character, expressed by the first order degradation rate k , changes. Indeed, in case study 2 short-term variations were observed for both the parameter k and the ammonium concentration in the wastewater. Suppose now that a model was calibrated under some experimental conditions, and that these parameters were used to design the next experiment. However, in the mean time the system has changed its properties, e.g. change of k or S_{NH} , and the experiment conducted according to this design will lead to an experimental response that may not allow an accurate estimation of the parameters. In Fig. 2, it is illustrated how the region of practical identifiability moves within the region of theoretical identifiability in case the parameters, here either S_{NH} or k , change. Thus, in this situation, the optimal experiment, illustrated by experiment A, will have to be adapted. One can even imagine that the parameters change to such an extent that the experiment no longer complies with

the experimental constraints, as illustrated in Fig. 2. This can be exemplified with the situation where a practical identification of the parameters is only possible under such experimental conditions that the sludge is no longer reacting as it would do in the full-scale system. Thus, “intrinsic” parameters are obtained instead of extant parameters.

The direction in which the practical identifiability region moves may be predictable based on e.g. the sludge history or daily variations of e.g. wastewater composition. Ideally, the adjustment of the optimal experiment should be carried out so often that the regions of practical identifiability overlap to obtain the most reliable update. This is illustrated in Fig. 3.

As an alternative to the frequent update of the optimal experimental design, a more robust experimental design can be applied, illustrated in Fig. 4. In the two studied cases a robust experiment would be one where a large amount of either S_{NO_2} or S_{NH} is added initially, but still allowing the experiment to comply with the defined experimental conditions and constraints. As an example the added amount should be such that no biomass growth or other changes in the experimental response occur. In such robust experimental design the accuracy of parameter estimates may be lower, but the adaptation of the design will not have to take place as frequently. Thus, a compromise between accuracy and adaptation frequency will have to be made.

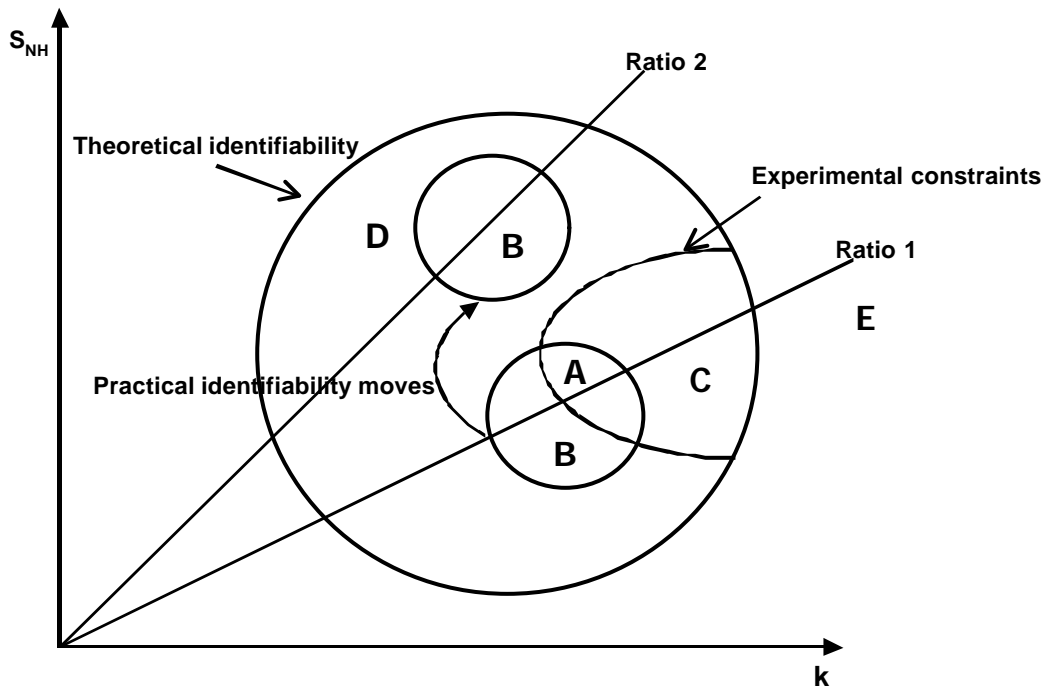


Figure 2. The region of practical identifiability moves in case the rate between S_{NH} and wastewater character, expressed by the degradation rate k , changes

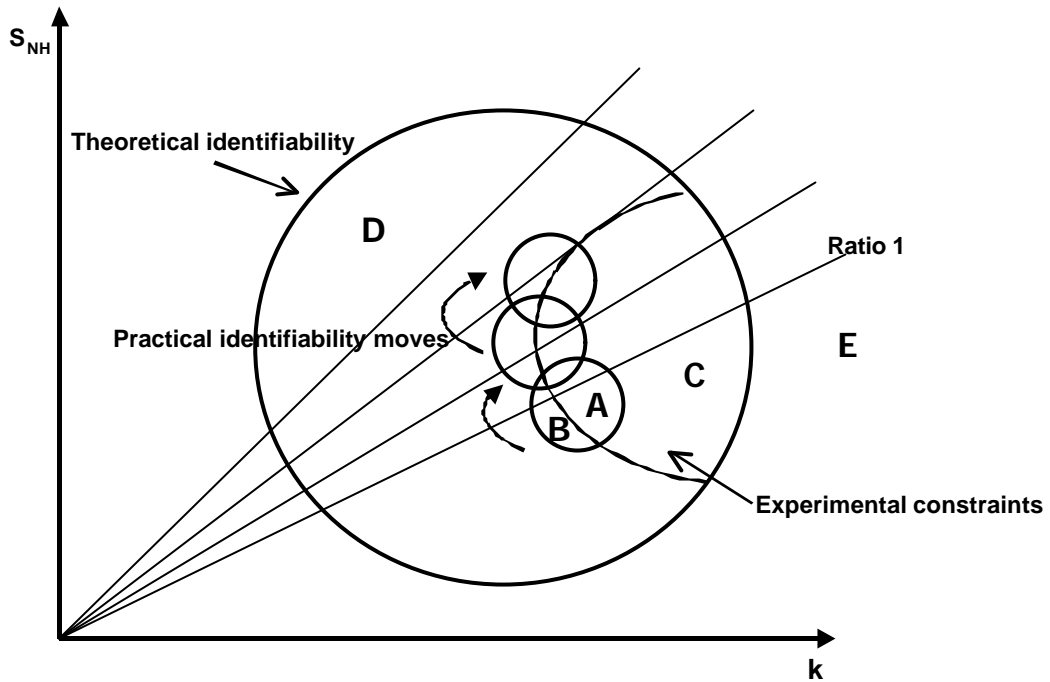


Figure 3. Frequent update of the region of practical identifiability in case the rate between S_{NH} and wastewater character, expressed by the degradation rate k , changes

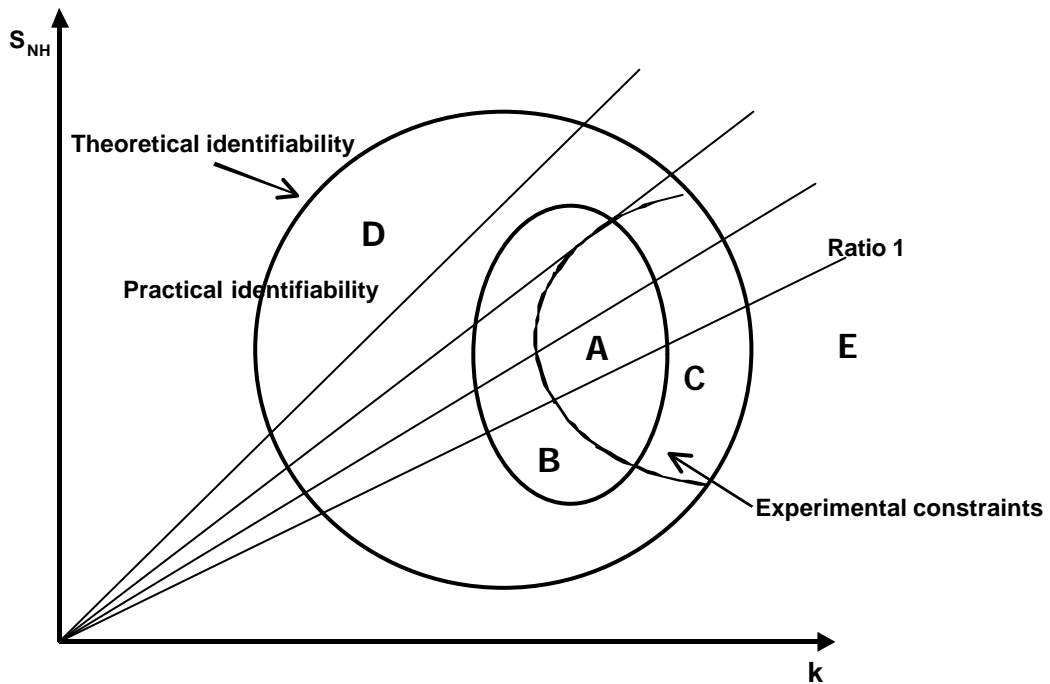


Figure 4. Robust experimental design for practical identifiability in case the rate between S_{NH} and wastewater character, expressed by the degradation rate k , changes

In this study the D-criterion, which focuses on maximisation of the determinant of FIM ($\text{Det}(\text{FIM})$), was

applied to optimise the experiment. A more extended OED-criterion could however be created in which the sensitivity of the OED to parameter or wastewater changes is leading to increased penalties to ensure a robust experimental design. Moreover, in this study one of the required experimental conditions was that no biomass growth must take place during the experiment, e.g. low $S(0)/X(0)$ and low ΔS were strived for. Such conditions could also be incorporated into a combined objective function of the OED together with the $\text{Det}(\text{FIM})$. For example in the study of Baltes *et al.* (1994) a critical biological criterion with regard to balanced growth was defined and incorporated into the objective function of the OED. Certainly, development of combined OED criteria opens perspectives for more advanced and reliable experimental designs in which the classical OED criteria, e.g. $\text{Det}(\text{FIM})$, which includes parameter accuracy alone, can be combined with different other constraints focusing for example on specific biological factors.

In the last part of the thesis the focus was on evaluating an ASM1 model calibration procedure for a combined municipal-industrial WWTP. A systematic model calibration procedure was defined in chapter 2, based on a thorough literature review. The kind of information that is needed, and the way model calibrations have been approached in literature. It was stressed that the purpose of the model calibration is determining how the calibration can be approached in a step-wise way. In the full-scale case under study it was important to have a detailed description of the process dynamics, since the model was to be used as the basis for optimisation scenarios in a later phase (Gernaey *et al.*, 2000c). Therefore, a complete model calibration procedure was applied in this case including : (1) a description of the hydraulics in the system via a tracer test, (2) an intensive measuring campaign and (3) supporting lab-scale experiments to obtain and confirm kinetic parameters for the model. In this model calibration it was clearly demonstrated how the information obtained from different tests for hydraulic, sludge settling (if needed) and biological characterisation can help to frame the model calibration, and in fact reduce the apparently high degree of freedom of the model parameters significantly.

In this study, the calibrated parameters $\mu_{\max A}$, $\mu_{\max H}$ and b_H were compared to the parameters obtained from lab-scale experiments. It was illustrated how these parameters could be compared to the parameters of the full-scale model, thereby verifying via lab-scale experimental data that the parameter values of the calibrated full-scale model were realistic.

In the literature review in chapter 2 it was discussed in detail which wastewater components and parameters are most relevant to be characterised via lab-scale experiments for an ASM1 model calibration. This discussion included the problem of transferability between lab-scale and full-scale observations and potentially different model concepts. Here it was deduced that it may be relevant to determine the parameters $\mu_{\max A}$, $\mu_{\max H}$, η_g , b_A , b_H and possibly also Y_A and Y_H , whereas e.g. the half-saturation coefficients derived from lab-scale experiments are not representative for the full-scale system, mainly due to different mixing characteristics. The yields were included in the list, knowing that they are not easy to determine in lab-scale tests and that they are usually assumed to be rather constant. However, it

was also realised that the yield coefficients have an important influence on nearly all the processes, and therefore it could be relevant in some cases to have a more accurate determination of these values.

In this model calibration it was chosen to determine $\mu_{\max A}$, $\mu_{\max H}$ and b_H via lab-scale tests, as mentioned above, whereas the determination of the anoxic correction factor for denitrification, η_g was adjusted during the model calibration. It was not aimed to determine the yield coefficients in this case.

In the study in chapter 8 the resulting calibrated parameters did not differ a lot from the ASM1 default parameter set (Henze *et al.*, 1987). Thus, one could question whether it was necessary to determine some of the parameters in lab-scale experiments at all. Still, even in this case the lab-scale results gave useful confirmation on the validity of the parameter set of the calibrated model, thereby, increasing the quality and confidence of the model calibration. The calibrated model was evaluated via a sensitivity study on the influence of model parameters and influent component concentrations on the model output. This analysis clearly showed that the calibrated model was sensitive to changes of the parameters that were modified during the model calibration procedure. The two most influential parameters were $\mu_{\max A}$ and $\mu_{\max H}$ which confirmed that even the small deviations of these parameters from their default values had a considerable influence on the model output. Furthermore, this confirmed the importance of having an extra information source on the values of these parameters via lab-scale tests.

Finally, the focus is returned to the figure outlined in the problem statement that illustrated the problems of transferability between lab-scale experiments and the full-scale system (Fig. 5).

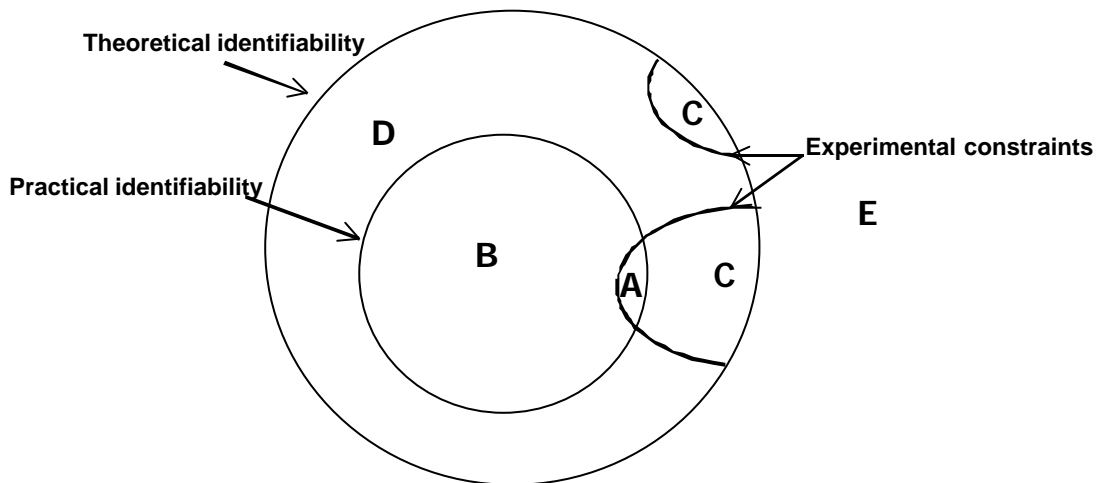


Figure 5. Conceptual idea of parameter identifiability and optimal experimental design in case information is retrieved from lab-scale experiments

Via this figure it was hypothesised that lab-scale experimental conditions may allow for a larger region of practical identifiability, but problems may arise whether the obtained parameters are transferable to full-scale applications. Indeed in the study presented in this thesis we have seen that it was possible to transfer the values of the parameters $\mu_{\max A}$, $\mu_{\max H}$ and b_H from the lab-scale test to the full-scale model, although

the lab-scale experiment used to validate $\mu_{\max H}$ was interpreted with a different model (first order degradation kinetics) than the full-scale model (Monod kinetics). Thus, for these parameters it was possible to find an optimal experiment (A) that yielded values that complied with the experimental constraints on transferability. However, it has also been discussed that for some ASM1 parameters it may not be relevant or possible to retrieve realistic parameter values from lab-scale experiments. A typical example is the half-saturation coefficients which may not describe the same phenomena in lab-scale compared to full-scale systems, due to the different mixing patterns. Thus, in this case it is difficult to create an experiment (A) and the regions of practical parameter identifiability of the lab-scale experiment may not overlap with the region of experimental constraints, as also illustrated in Fig. 5. Certainly further research is needed in the direction of characterisation of the different ASM parameters and components to solve the transferability problems related to differences in lab-scale and full-scale behaviours.

References

References

- Anthonisen A.C., Loehr R.C., Prakasam T.B.S. and Srinath E.G. (1976) Inhibition of nitrification by ammonia and nitrous acid. *J. Water Pollut. Control Fed.*, **48**, 835 – 852.
- ASCE (1996). *Standard Guidelines for In-Process Oxygen Transfer Testing*. American Society of Civil Engineers, ASCE-18-96, pp.48.
- Avcioglu E., Orhon D. and Sözen S. (1998) A new method for the assesment of heterotrophic endogenous respiration rate under aerobic and anoxic conditions. *Water Sci. Technol.*, **38**(8-9), 95 – 103.
- Baltes M., Schneider R., Sturm C. and Reuss M. (1994) Optimal experimental design for parameter estimation in unstructured growth models. *Biotechnol. Prog.*, **10**, 480 – 488.
- Bandyopadhyay B., Humphrey A.E. and Taguchi H. (1967) Dynamic measurement of the volumetric oxygen transfer coefficient in fermentation systems. *Biotechnol. Bioeng.*, **9**, 533 - 544.
- Bellman R. and Åström K.J. (1970) On structural identifiability. *Mathematical Biosciences*, **7**, 329 – 339.
- Bjerre H.L., Hvitved-Jacobsen T., Teichgräber B. and te Heesen D. (1995) Experimental procedures characterizg transformations of wastewater organic matter in the Emscher river. Germany. *Water Sci. Technol.*, **31**(7), 201 – 212.
- Blok J. (1974) Respirometric measurements on activated sludge. *Water Res.*, **8**, 11 – 18.
- Boero V.J., Eckenfelder W.W. Jr. and Bowers A.R. (1991) Soluble microbial product formation in biological systems. *Water Sci. Technol.*, **23**, 1067 – 1076.
- Bogaert H., Vanderhasselt A., Gernaey K., Yuan Z., Thoeye C. and Verstraete W. (1997) New sensor based on pH effects of denitrification process. *J. Environ. Engineering.*, **123**, 884 – 891.
- Bogaerts N. (1998) Personal communication.
- Bortone G., Cech J.S., Germirli F., Bianchi R, and Tilche A. (1994) Experimental approaches for the characterisation of a nitrification/denitrification process on industrial wastewater. *Water. Sci. Technol.*, **29**(7), 129 – 136.
- Bourrel S.V., Babary J.P., Julien S., Nihtilä M.T. and Dochain D. (1998) Modelling and identification of a fixed-bed denitrification bioreactor. *System Analysis Modelling Simulation (SAMS)*, **30**, 289 – 309.
- Brands E., Liebeskind M and Dohmann M. (1994) Parameters for dynamic simulation of wastewater treatment plants with high-rate and low-rate activated sludge tanks. *Water Sci. Technol.*, **30**(4), 211 – 214.
- Brouwer H., Klapwijk A. and Keesman J. (1998) Identification of activated sludge and wastewater characteristics using respirometric batch-experiments. *Water Res.*, **32**, 1240 – 1254.
- Bunch B. and Griffin D.M. Jr. (1987) Rapid removal of colloidal substrate from domestic wastewater. *J. Water Pollut. Control Fed.*, **59**, 957 – 963.

- Casti J.L. (1985) Non linear system theory, volume 175. Mathematics in Science and Engineering, Academic Press, Orlando.
- Cech J.S., Chudoba J. and Grau P. (1984) Determination of kinetic constants of activated sludge microorganisms. *Water Sci. Technol.*, **17**, 259 – 272.
- Chang J., Chudoba P. and Capdeville B. (1993) Determination of the maintenance requirements of activated sludge. *Water Sci. Technol.*, **28**, 139 – 142.
- Chappell M.J., Godfrey K.R. and Vajda S. (1990) Global identifiability of the parameters of nonlinear systems with specified inputs: A comparison of methods. *Mathematical Biosciences*, **102**, 41 – 73.
- Chappell M.J. and Godfrey K.R. (1992) Structural identifiability of the parameters of a nonlinear batch reactor model. *Mathematical Biosciences*, **108**, 241 – 251.
- Chudoba J. (1969) Residual organic matter in activated sludge processes effluents V-effluent of the initial food-to-microorganisms ratio. *Sci. Paper, Inst. Chem. Technol. Prague F1-F5*, 23 – 34.
- Chudoba J. (1985) Quantitative estimation in COD units of refractory organic compounds produced by activated sludge microorganisms. *Water Res.*, **19**, 37-43.
- Chudoba P., Chevalier J.J., Chang J. and Capdeville B. (1991) Effect of anaerobic stabilisation of activated sludge on its production under batch conditions at various S_0/X_0 . *Water Sci. Technol.*, **23**, 917 – 926.
- Chudoba P., Capdeville B. and Chudoba J. (1992) Explanation of biological meaning of the S_0/X_0 ratio in lab-scale cultivation. *Water Sci. Technol.*, **26**(3-4), 743 – 751.
- Ciaccio L.L. (1992) Instrumental determination of energy oxygen and BOD_5 . *Water Sci. Technol.*, **26**(5-6), 1345 – 1353.
- Clarke A.N., Eckenfelder W.W., McMullen E.D., Roth J.A. and Young B.A. (1978) Development of a continuous respirometer. *Water Res.*, **12**, 799 – 804.
- Coen F., Vanderhaegen B., Boonen I., Vanrolleghem P.A. and Van Meenen P. (1997) Improved design and control of industrial and municipal nutrient removal plants using dynamic models. *Water Sci. Technol.*, **35**(10), 53 – 61.
- Coen F., Petersen B., Vanrolleghem P.A., Vanderhaegen B. and Henze M. (1998) Model-based characterisation of hydraulic, kinetic and influent properties of an industrial WWTP. *Water Sci. Technol.*, **39**(1), 195 – 214.
- Copp J.B. and Dold P.L. (1998) Confirming the nitrate-to-oxygen conversion factor for denitrification. *Water Res.*, **32**, 1296 – 1304.
- Cramer W.A. and Knaff D.B. (1991) Energy transduction in biological membranes. A textbook of bioenergetics. Springer-Verlag, New York.
- Daigger G.T. and Grady C.P.L. (1982) The dynamics of microbial growth on soluble substrates. A unifying theory. *Water Res.*, **16**, 365 – 382.
- De Clercq B., Coen F., Vanderhaegen B. and Vanrolleghem P.A. (1999) Calibrating simple models for mixing and flow propagation in waste water treatment plants. *Water Sci. Technol.*, **39**(4), 61 – 69.

- de la Sota A., Larrea L., Novak L., Grau P. and Henze M. (1994) Performance and model calibration of R-D-N processes in pilot plant. *Water Sci. Technol.*, **30**(6), 355 – 364.
- Devisscher M. (1997) pH effect sensoren voor de controle van biologische stikstofverwijderingsprocessen in de waterzuivering. Engineers thesis. University Gent, Belgium, 110 p. (In Dutch)
- Dhaene R. (1996) Een nieuwe biosensor voor het denitrificatieproces gebaseerd op een pH-regelaar. M.Sc. thesis at Hogeschool West-Vlaanderen, Kortrijk, Belgium. (in Dutch)
- Dircks K., Pind P.F., Mosbæk H. and Henze M. (1999) Yield determination by respirometry - The possible influence of storage under aerobic conditions in activated sludge. *Water SA*, **25**, 69 – 74.
- Dochain D., Vanrolleghem P.A. and Van Daele M. (1995) Structural identifiability of biokinetic models of activated sludge respiration. *Water Res.*, **29**, 2571 – 2579.
- Dold P. (1980) A general model for the activated sludge process. *Prog. Wat. Tech.*, **12**(6), 47 – 77.
- Drtil M., Németh P. and Bodík I. (1993) Kinetic constants of nitrification. *Water Res.*, **27**, 35 – 39.
- Dupont R. and Sinkjar O. (1994) Optimisation of wastewater treatment plants by means of computer models. *Water Sci. Technol.*, **30**(4), 181 – 190.
- Ekama G.A., Dold P.L. and Marais G.v.R. (1986) Procedures for determining influent COD fractions and the maximum specific growth rate of heterotrophs in activated sludge systems. *Water Sci. Technol.*, **18**(6), 91 – 114.
- Ellis T.G., Barbeau D.S., Smets B.F. and Grady C.P.L. Jr. (1996) Respirometric techniques for determination of extant kinetic parameters describing biodegradation. *Water Environ. Res.*, **38**, 917 – 926.
- Farkas P. (1969) Method for measuring aerobic decomposition activity of activated sludge in an open system. In: Proceedings 4th International Conference on Water Pollution Control Research, Prague, *Adv. Water Pollut. Res.*, 309 – 327.
- Farkas P. (1981) The use of respirography in biological treatment plant control. *Water Sci. Technol.*, **13**, 125 – 131.
- Funamizu N. and Takakuwa T. (1994) Simulation of the operating conditions of the municipal wastewater treatment plant at low temperatures using a model that includes the IAWPRC activated sludge model. *Water Sci. Technol.*, **30**(4), 150 – 113.
- Germirli F., Orhon D. and Artan N. (1991) Assessment of the initial inert soluble COD in industrial wastewaters. *Water Sci. Technol.*, **23**(4-6), 1077 – 1086.
- Gernaey K., Bogaert H., Massone A., Vanrolleghem P. and Verstraete W. (1997a) On-line nitrification monitoring in activated sludge with a titrimetric sensor. *Environ. Sci. Technol.*, **31**, 2350 – 2355.
- Gernaey K., Verschuere L., Luyten L. and Verstraete W. (1997b) Fast and sensitive acute toxicity detection with an enrichment nitrifying culture. *Water Environ. Res.*, **69**, 1163 – 1169.
- Gernaey K., Vanrolleghem P.A. and Verstraete W. (1998) On-line estimation of *Nitrosomonas* kinetic parameters in activated sludge samples using titration in-sensor-experiments. *Water Res.*, **32**, 71 – 80.
- Gernaey K., Petersen B., Ottoy J.-P. and Vanrolleghem P.A. (1999) Biosensing activated sludge. *WQI*, May/June 1999, 16 – 21.

- Gernaey K., Petersen B., Nopens I., Comeau Y. and Vanrolleghem P. (2000a) Modelling aerobic carbon source degradation processes using titrimetric data and combined respirometric-titrimetric data: experimental data and model structure. Submitted to *Biotechnology and Bioengineering*.
- Gernaey K., Petersen B. and Vanrolleghem P. (2000b) Modelling aerobic carbon source degradation processes using titrimetric data and combined respirometric-titrimetric data: theoretical and practical identifiability. Submitted to *Biotechnology and Bioengineering*.
- Gernaey K., Petersen B., Parmentier G., Bogaert H., Ottoy J.P. and Vanrolleghem P.A. (2000c) Application of dynamic models (ASM1) and simulation to minimize renovation costs of a municipal activated sludge wastewater treatment plant. Proceedings 1st World Congress of the International Water Association, 3-7 July 2000, Paris, France.
- Glasbey C.A. (1980) Nonlinear regression with autoregressive time series error. *Biometrics*, **36**, 135 – 140.
- Godfrey K.R. and DiStefano III J.J. (1985) Identifiability of model parameters. In: *Identification and System Parameter Estimation*, 89 – 144. Pergamon Press, Oxford.
- Goodwin G.C. (1987) Identification: Experiment design. In: *Systems and Control Encyclopedia*, Vol. 4. Ed. Singh M., Pergamon Press, Oxford. 2257 – 2264.
- Goodwin G.C. and Payne R.L. (1977) *Dynamic system identification. Experiment design and data analysis*. Academic Press. New York.
- Grady C.P.L., Smets B.F and Barbeau D.S. (1996) Variability in kinetic parameter estimates : a review of possible causes and a proposed terminology. *Water Res.*, **30**, 742 – 748.
- Gujer W., Henze M., Mino T. and van Loosdrecht M. (1998) Activated sludge model No. 3. In: *Proceedings 4th Kollekolle Seminar on Activated Sludge Modelling (Modelling and Microbiology of Activated Sludge Processes)*, March 16-18 1998, Copenhagen (Denmark).
- Gujer W., Henze M., Mino T. and van Loosdrecht M.C.M. (1999) Activated sludge model No. 3. *Water Sci. Technol.*, **39**(1), 183 – 193.
- Haider S. (2000) CSB-Elimination in A-stufen und ihre Auswirkung auf die Stickstoffelimination von AB-Anlagen unter dem Gesichtspunkt der mathematischen Modellierung. PhD. Thesis. TU Wien, Austria. (in preparation)
- Heijnen J.J., Van Loosdrecht M.C.M., Tijhuis L. (1992) A black box mathematical model to calculate auto- and heterotrophic yields based on Gibbs energy dissipation. *Biotechnol. Bioeng.* **40**, 1139 – 1154.
- Henze M. (1986) Nitrate versus oxygen utilisation rates in wastewater and activated sludge systems. *Water Sci. Technol.*, **18**(6), 115 – 122..
- Henze M. (1992) Characterization of wastewater for modelling of activated sludge processes. *Water Sci. Technol.* **25**(6), 1 – 15.
- Henze M., Grady C.P.L. Jr., Gujer W., Marais G.v.R. and Matsuo T. (1987) *Activated Sludge Model No. 1*. IAWQ Scientific and Technical Report No. 1, London, UK.

- Henze M., Gujer W., Mino T., Matsuo T., Wentzel M.C.M. and Marais G.v.R. (1995) Activated Sludge Model No. 2. IAWQ Scientific and Technical Report No. 3, London, UK.
- Henze M., Harremoës P., la Cour Janssen J. and Arvin E. (1997) Biological and chemical wastewater treatment, 2nd edition, Springer, Berlin.
- Henze M., Gujer W., Mino T., Matsuo T., Wentzel M.C., Marais G.v.R. and van Loosdrecht M.C.M. (1998) Activated sludge model No. 2D, ASM2D. Proceedings of the 4th IAWQ Seminar on Modelling and Microbiology of Activated Sludge Processes, March 16 – 18, Kollokole, Denmark.
- Henze M., Gujer W., Mino T., Matsuo T., Wentzel M.C., Marais G.v.R. and van Loosdrecht M.C.M. (1999) Activated sludge model No. 2D, ASM2D. Water Sci. Technol., **39**(1), 165 – 182.
- Hissett R., Deans E.A. and Evans M.R. (1982) Oxygen consumption during batch aeration of piggery slurry at temperatures between 5 and 50 °C. Agricultural Wastes, **4**, 477 – 487.
- Holmberg A. (1982) On the practical identifiability of microbial growth models incorporating Michaelis-Menten type nonlinearities. Mathematical Biosciences, **62**, 23 – 43.
- Holmberg A. and Ranta J. (1982) Procedures for parameter and state estimation of microbial growth process models. Automatica, **18**(2), 181 – 183.
- Iversen J.J.L., Thomsen J.K. and Cox R.P. (1994) On-line growth measurements in bioreactors by titrating metabolic proton exchange. Appl. Microbiol. Biotechnol., **42**, 256 – 262.
- Jeppsson U. (1996). Modelling aspects of wastewater treatment processes. Ph.D. thesis: Department of Industrial Electrical Engineering and Automation, Lund Institute of Technology, Sweden. pp. 428.
- Julien S. (1997). Modelisation et estimation pour le contrôle d'un procédé boues activées éliminant l'azote des eaux résiduaires urbaines. Ph.D. thesis: Laboratoire d'Analyse et d'Architecture des Systèmes du C.N.R.S., Rapport LAAS No. 97499.
- Julien S., Babary J.P. and Lessard P. (1998) Theoretical and practical identifiability of a reduced order model in an activated sludge process doing nitrification and denitrification. Water Sci. Technol., **37**(12), 309 – 316.
- Kalte P. (1990) The continuous measurement of short-time BOD. In: Advances in Water Pollution Control. Ed. Briggs R., Pergamon Press, London. 59 – 65.
- Kappeler J. and Gujer W. (1992) Estimation of kinetic parameters of heterotrophic biomass under aerobic conditions and characterization of wastewater for activated sludge modelling. Water Sci. Tech., **25**(6), 125 – 139.
- Keesman K.J., Spanjers H. and van Straten G. (1998) Analysis of endogenous process behavior in activated sludge. Biotechnol. Bioeng., **57**, 155 – 163.
- Koike I. and Hattori A. (1975) Growth yield of a denitrifying bacterium, *Pseudomonas denitrificans*, under aerobic and denitrifying conditions. J. Gen. Microbiol., **88**, 1 – 10.
- Kong Z., Vanrolleghem P.A. and Verstraete W. (1994) Automated respiration inhibition kinetics analysis (ARIKA) with a respirographic biosensor. Water Sci. Tech., **30**(4), 275 – 284.
- Kong Z., Vanrolleghem P., Willems P. and Verstraete W. (1996) Simultaneous determination of inhibition kinetics of carbon oxidation and nitrification with a respirometer. Water Res., **30**, 825 – 836.

- Krishna C. and van Loosdrecht M.C.M. (1999) Substrate flux into storage and growth in relation to activated sludge modelling. *Water Res.*, **33**, 3149 – 3161.
- Kristensen H.G., Elberg Jørgensen P. and Henze M. (1992) Characterisation of functional micro-organism groups and substrate in activated sludge and wastewater by AUR, NUR and OUR. *Water Sci. Technol.*, **25**(6), 43 – 57.
- Kristensen H.G., la Cour Janssen J. and Elberg Jørgensen P. (1998) Batch test procedures as tools for calibration of the activated sludge model – A pilot scale demonstration. *Water Sci. Technol.*, **37**(4-5), 235 – 242.
- Kroiss H., Schweighofer P., Frey W. and Matsche N. (1992) Nitrification inhibition - a source identification method for combined municipal and/or industrial wastewater treatment plants. *Water Sci. Technol.*, **26**(5-6), 1135 – 1146.
- Kujawa K. and Klapwijk B. (1999) A method to estimate denitrification potential for predenitrification systems using NUR batch test. *Water Res.*, **33**(10), 2291 – 2300.
- Larrea L., Garcia-Heras J.L., Ayesa E. and Florez J. (1992) Designing experiments to determine the coefficients of activated sludge models by identification algorithms. *Water. Sci. Technol.*, **25**(6), 149 – 165.
- Leenen E.J., Boogert A.A. van Lammeren A.A., Tramper J. and Wijffels R.H. (1997) Dynamics of artificially immobilized *Nitrosomonas europaea*: Effect of biomass decay. *Biotechnol. Bioeng.*, **55**, 630 – 641.
- Lesouef A., Payraudeau M., Rogalla F. and Kleiber B. (1992) Optimizing nitrogen removal reactor configurations by on-site calibration of the IAWPRC activated sludge model. *Water Sci. Technol.*, **25**(6), 105 – 123.
- Levine A.D., Tchobanoglous G. and Asano T. (1985) Characterisation of the size distribution of contaminants in wastewater: treatment and reuse implications. *Journal WPCF*, **57**(7), 805 – 816.
- Liebeskind M., Schäpers D., Bornemann C., Brands E., Freund M. and Rolfs T. (1996) Parameter determination and model fitting – two approaches for modelling processes in wastewater treatment plants. *Water Sci. Technol.*, **34**(5-6), 27 – 33.
- Liu Y. (1996) Bioenergetic interpretation on the S_o/X_o ratio in substrate-sufficient lab-scale culture. *Water Res.*, **30**, 2766 – 2770.
- Ljung L. (1987) *System Identification - Theory for the User*. Prentice-Hall, Englewood Cliffs, New Jersey.
- Ljung (1999) *Experiment design. System Identification – Theory for the User*. Prentice-Hall, Englewood Cliffs, New Jersey.
- Ljung L. and Glad T. (1994) On global identifiability for arbitrary model parametrisations. *Automatica*, **30**(2), 265 – 276.
- Lukasse L.J.S., Keesman K.J. and van Straten G. (1997) Estimation of BOD_{st}, respiration rate and kinetics of activated sludge. *Water Res.*, **31**, 2278 – 2286.
- Majone M., Dircks K. and Beun J.J. (1999) Aerobic storage under dynamic conditions in activated sludge processes. The state of the art. *Water Sci. Technol.*, **39**(1), 61 – 73.

- Mamais D., Jenkins D. and Pitt P. (1993) A rapid physical-chemical method for the determination of readily biodegradable soluble COD in municipal wastewater. *Water Res.*, **27**, 195 – 197.
- Marais G.v.R. and Ekama G.A. (1976) The activated sludge process. Part 1 – Steady state behaviour. *Water SA*, **2**, 163 – 199.
- Marsilli-Libelli S. (1989) Modelling, identification and control of the activated sludge process. *Adv. Biochem. Eng. Biotechnol.*, **38**, 90 – 148.
- Massone A., Gernaey K., Rozzi A., Willems P. and Verstraete W. (1995) Ammonium concentration measurements using a titrimetric biosensor. *Med. Fac. Landbouww. Univ. Gent*, **60**, 2361 – 2368.
- McClintock S.A., Sherrard J.H., Novak J.T. and Randall C.W. (1988) Nitrate versus oxygen respiration in the activated sludge process. *J. Water Pollut. Control Fed.*, **60**, 342 – 350.
- Melcer H. (1999) Full scale experience with biological process models - calibration issues. *Water Sci. Technol.*, **39**(1), 245 – 252.
- Mino T., San Pedro D.C., Yamamoto S. and Matsuo T. (1997) Application of the IAWQ activated sludge model to nutrient removal process. *Water Sci. Technol.*, **35**(8), 111 – 118.
- Munack A. (1989) Optimal feeding strategy for identification of Monod-type models by fed-batch experiments. In: *Computer applications in fermentation technology: Modeling and control of biotechnological processes*. Eds. Fish N., Fox R., Thornhill N., Elsevier, Amsterdam, Nederland. 195 – 204.
- Munack A. (1991) Optimisation of sampling. In: *Biotechnology, a Multi-volume Comprehensive Treatise*, Vol. 4. *Measuring, Modelling and Control*. Ed. Schügerl K., VCH, Weinheim, 251 – 264.
- Münch E.v. and Greenfield P.F. (1998) Estimating VFA concentrations in prefermenters by measuring pH. *Water Res.*, **32**, 2431 – 2441.
- Naidoo V., Urbain V. and Buckley C.A. (1998) Characterisation of wastewater and activated sludge from European municipal wastewater treatment plants using the NUR test. *Water Sci. Technol.*, **38**(1), 303 – 310.
- Nichols H.A., Pitman A.R. and Osborn D.W. (1985) The readily biodegradable fraction of sewage: its influence on phosphorus removal and measurement. *Water Sci. Technol.*, **17**, 73 – 87.
- Novák L., Larrea L. and Wanner J. (1994) Estimation of maximum specific growth rate of heterotrophic and autotrophic biomass: A combined technique of mathematical modelling and batch cultivations. *Water Sci. Technol.*, **30**(11), 171 – 180.
- Nowak O., Schweighofer P. and Svardal K. (1994) Nitrification inhibition - A method for the estimation of actual maximum growth rates in activated sludge systems. *Water Sci. Tech.*, **30**(6), 9 – 19.
- Nowak O., Franz A., Svardal K., Muller V. and Kuhn. (1999) Parameter estimation for activated sludge models with help of mass balances. *Water Sci. Technol.*, **39**(4), 113 – 120.
- Orhon D., Artan N. and Cimsit Y. (1989) The concept of soluble residual product formation in the modelling of activated sludge. *Water Sci. Technol.*, **21**(4-5), 339 – 350.
- Orhon D., Sözen S. and Artan N. (1996) The effect of heterotrophic yield on assessment of the correction factor for the anoxic growth. *Water Sci. Technol.*, **34** (5-6), 67 – 74.

- Payne W.J. (1991) Denitrification. Wiley-Interscience, New York.
- Pedersen J. and Sinkjær O. (1992) Test of the activated sludge models capabilities as a prognostic tool on a pilot scale wastewater treatment plant. *Water Sci. Technol.*, **25**(6), 185 – 194.
- Petersen B., Gernaey K. and Vanrolleghem P.A. (2000) Improved theoretical identifiability of model parameters by combined respirometric-titrimetric measurements. A generalisation of results. In: Proceedings IMACS 3rd Symposium on Mathematical Modelling, February 2-4, 2000, Vienna University of Technology, Austria. Vol.2, 639 – 642.
- Pohjanpalo H. (1978) System identifiability based on the power series expansion of the solution. *Mathematical Biosciences*, **41**, 21 – 33.
- Pollard P.C., Steffens M.A., Biggs C.A. and Lant P.A. (1998) Bacterial growth dynamics in activated sludge batch assays. *Water Res.*, **32**, 587 – 596.
- Posten C. and Munack A. (1989) Design of optimal dynamical experiments for parameter estimation. In: Proceedings American Control Conference 1989, 2010 – 2016.
- Raksanyi A., Lecourtier Y., Walter E. and Venot A. (1985) Identifiability and distinguishability testing via computer algebra. *Mathematical Biosciences*, **77**, 245 – 266.
- Ramadori R., Rozzi A. and Tandoi V. (1980) An automated system for monitoring the kinetics of biological oxidation of ammonia. *Water Res.*, **14**, 1555 – 1557.
- Randall E.W., Wilkinson A. and Ekama G.A. (1991) An instrument for the direct determination of oxygen uptake rate. *Water SA*, **17**, 11 – 18.
- Rao B.S. and Gaudy A.F.Jr (1966) Effect of sludge concentration on various aspects of biological activity in activated sludge. *J. Water. Pollut. Control. Fed.*, **38**, 794 – 812.
- Rickert D.A. and Hunter J.V. (1971) General nature of soluble and particulate organics in sewage and secondary effluent. *Water Res.*, **5**, 421 – 436.
- Robinson J.A. (1985) Determining microbial parameters using nonlinear regression analysis: Advantages and limitations in microbial ecology. *Adv. Microb. Ecol.*, **8**, 61 – 114.
- Robinson J.A. and Tiedje J.M. (1982) Kinetics of hydrogen consumption by rumen fluid, anaerobic digester sludge, and sediment. *Appl. Environ. Microbiol.*, **44**, 1374 – 1384.
- Robinson J.A. and Tiedje J.M. (1983) Nonlinear estimation of Monod growth kinetic parameters from a single substrate depletion curve. *Appl. Environ. Microbiol.*, **45**, 1453 – 1458.
- Ros M., Dular M. and Farkas P.A. (1988) Measurement of respiration of activated sludge. *Water Res.*, **22**, 1405 – 1411.
- Rozzi A., Massone A. and Alessandrini A. (1997) Measurement of rbCOD as biological nitrate demand using a biosensor: Preliminary results. In: Proceedings EERO/EFB International Symposium Environmental Biotechnology ISEB3. April 21-24, Ostend, Belgium.
- San K.Y. and Stephanopoulos G. (1984) Studies on on-line bioreactor identification. IV. Utilization of pH measurements for product estimation. *Biotechnol. Bioeng.*, **26**, 1209 – 1218.
- Sharma B. and Ahlert R.C. (1977) Nitrification and nitrogen removal. *Water Res.* **11**, 897 – 825.

- Siano S. (1995) On the use of pH control reagent addition rate for fermentation monitoring. *Biotechnol. Bioeng.*, **47**, 651 – 665.
- Siegrist H. and Tschui M. (1992) Interpretation of experimental data with regard to the activated sludge model no. 1 and calibration of the model for municipal wastewater treatment plants. *Water Sci. Technol.*, **25**(6), 167 – 183.
- Siegrist H., Brunner I., Koch G., Linh Con Phan and Van Chieu Le (1999) Reduction of biomass decay rate under anoxic and anaerobic conditions. *Water Sci. Technol.*, **39**(1), 129 – 137.
- Simkins S. and Alexander M. (1985) Nonlinear estimation of the parameters of Monod kinetics that best describe mineralization of several substrate concentrations by dissimilar bacterial densities. *Appl. Environ. Microbiol.*, **50**, 816 – 824.
- Smets B.F., Jobbagy A., Cowan R.M. and Grady C.P.L. Jr. (1996) Evaluation of respirometric data: Identification of features that preclude data fitting with existing kinetic expressions. *Ecotoxicology and Environmental Safety*, **33**, 88 – 99.
- Söderström T. and Stoica P. (1989) Model validation and model structure determination. *System Identification*. Prentice Hall, New York.
- Sollfrank U. and Gujer W. (1990). Simultaneous determination of oxygen uptake rate and oxygen transfer coefficient in activated sludge systems by an on-line method. *Water Res.*, **24**, 725 – 732.
- Sollfrank U. and Gujer W. (1991) Characterisation of domestic wastewater for mathematical modelling of the activated sludge process. *Water Sci. Technol.*, **23**, 1057 – 1066.
- Sollfrank U., Kappeler J. and Gujer W. (1992) Temperature effects on wastewater characterization and the release of soluble inert organic material. *Water Sci. Technol.*, **25**(6), 33 – 41.
- Sözen A., Ubay Cokgör E., Orhon D. and Henze M. (1998) Respirometric analysis of activated sludge behaviour -II. Heterotrophic growth under aerobic and anoxic conditions. *Water Sci. Technol.*, **32**(2), 476 – 488.
- Spanjers H. (1993) Respirometry in activated sludge. Ph.D. thesis, Landbouwniversiteit Wageningen, the Netherlands, 199 p.
- Spanjers H. and Olsson G. (1992) Modelling of the dissolved oxygen probe response in the improvement of the performance of a continuous respiration meter. *Water Res.*, **26**, 945 – 954.
- Spanjers H., Olsson G. and Klapwijk A. (1994) Determining influent short-term biochemical oxygen demand and respiration rate in an aeration tank by using respirometry and estimation. *Water Res.*, **28**, 1571 – 1583.
- Spanjers H. and Vanrolleghem (1995) Respirometry as a tool for rapid characterisation of wastewater and activated sludge. *Water Sci. Technol.*, **31**(2), 105 – 114.
- Spanjers H., Vanrolleghem P.A., Olsson G. and Dold P. (1998) Respirometry in control of the activated sludge process. International Association on Water Quality, London, UK.
- Spanjers H., Takacs I. and Brouwer H. (1999) Direct parameter extraction from respirograms for wastewater and biomass characterisation. *Water Sci. Technol.*, **39**(4), 137 – 145.

- Spérandio M. (1998) Développement d'une procédure de compartimentation d'une eau résiduaire urbaine et application à la modélisation dynamique de procédés boues activées. PhD thesis, Institut National des Sciences Appliquées de Toulouse, France, 221 p.
- Spérandio M. and Paul E. (2000) Estimation of wastewater biodegradable COD fractions by combining respirometric experiments in various S_0/X_0 ratios. *Water Res.*, **34**, 1233 – 1246.
- Spérandio M., Urbain V., Audic J.M. and Paul E. (1999) Use of carbon dioxide evolution rate for determining heterotrophic yield and characterising denitrifying biomass. *Water Sci. Technol.*, **39**(1), 139 – 146.
- Spriet J.A. and Vansteenkiste G.C. (1982). *Computer-aided Modelling and Simulation. Lecture Notes in Computer Science*, Academic Press, London.
- Stokes L., Takács I., Watson B. and Watts J.B. (1993) Dynamic modelling of an A.S.P. sewage works - A case study. *Water Sci. Technol.*, **28**(11-12), 151 – 161.
- STOWA (1996) Methoden voor influentkarakterisering - Inventarisatie en richtlijnen. STOWA Report 80-96. STOWA, Utrecht, The Netherlands. (in Dutch)
- Stumm W. and Morgan J.J. (1981) *Aquatic Chemistry, An introduction emphasizing chemical equilibria in natural waters*. John Wiley & Sons, New York, 780 p.
- Suschka J. and Ferreira E. (1986) Activated sludge respirometric measurements. *Water Res.*, **20**, 137 – 144.
- Takamatsu T., Shioya S., Morisaki K. and Ihara D. (1982) On-line monitoring and control of an activated sludge process for wastewater using 'MMOUR'. *Eur. J. Appl. Microbiol. Biotech.*, **14**, 187 – 192.
- Torrijos M., Cerro R.M., Capdeville B., Zeghal S., Payraudeau M. And Lesouef A. (1994) Sequencing batch reactor: A tool for wastewater characterisation for the IAWPRC model. *Water Sci. Technol.*, **29**(7), 81 – 90.
- Ubay Çokgör E., Sözen S., Orhon D. and Henze M. (1998) Respirometric analysis of activated sludge behaviour-I. Assessment of the readily biodegradable substrate. *Water Res.*, **32**, 461 – 475.
- Ubisi M.F., Jood T.W., Wentzel M.C. and Ekama G.A. 1997 Activated sludge mixed liquor heterotrophic active biomass. *Water SA*, **23**, 239 – 248.
- Urbain V., Naidoo V., Ginestet P. and Buckley C.A. (1998) Characterisation of wastewater biodegradable organic fraction : accuracy of the nitrate utilisation rate test. In *Proceedings of the Water Environmental Federation 71st Annual Conference and Exposition, October 3 - 7, Orlando, Florida (USA)* , 247 – 255.
- Vajda S., Godfrey K.R., Rabitz H. (1989) Similarity transformation approach to identifiability analysis of nonlinear compartmental models. *Mathematical Biosciences*, **93**, 217 – 248.
- Van Haandel A.C., Ekama G.A., Marais G.v.R. (1981) The activated sludge process – part 3. Single sludge denitrification. *Water Res.*, **15**, 1135 – 1152.
- Van Loosdrecht M.C.M. and Henze M. (1999) Maintenance, endogenous respiration, lysis, decay and starvation. *Water Sci. Technol.*, **39**(1), 107 – 117.

- Van Vooren L., Willems P., Ottoy J.P., Vansteenkiste G.C. and Verstraete W. (1995) Automatic buffer capacity based sensor for effluent quality monitoring. In: Proceedings IAWQ Conference on Sensors in Wastewater Technology, October 25 - 27 , Copenhagen, Denmark.
- Van Vooren L. (2000), Buffer capacity based multipurpose hard- and software sensor for environmental applications. PhD thesis, University of Gent, Belgium.
- Vandebroek R. (1986) Study and development of a microcomputer controlled sensor for the determination of the biodegradability and the toxicity of wastewaters: The RODTOX. PhD. Thesis. Faculty of Agricultural Sciences. University of Gent, Belgium. pp. 171.
- Vanderhasselt A., Aspegren H., Vanrolleghem P.A. and Verstraete W. (1999a) Settling characterisation using on-line sensors at a full-scale waste water treatment plant. *Water SA*, **25**, 453 - 458.
- Vanderhasselt A., Fuchs A., Vanrolleghem P., Staudinger G. and Verstraete W. (1999b) Monitoring of the effects of additives on sludge separation properties by using sensors. *Water Environ. Res.*, **71**, 355 – 362.
- Vanrolleghem P.A., Dries D. and Verstraete W. (1990) RODTOX: biosensor for rapid determination of the biochemical oxygen demand and the on-line monitoring of the toxicity of wastewaters. In: Proceedings 5th European Congress on Biotechnology. Copenhagen, Denmark, July 8 - 13 1990. Vol. **1**, 161 – 164.
- Vanrolleghem P.A., Van Impe J.F., Vandewalle J. and Verstraete W. (1992) Advanced monitoring and control of the activated sludge process: On-line estimation of crucial biological variables in a structured model with the RODTOX biosensor. In: Modeling and Control of Biotechnical Processes. Eds. Karim M.N. and Stephanopoulos G., Pergamon Press, Oxford. 355-358.
- Vanrolleghem P.A. and Verstraete W. (1993) Simultaneous biokinetic characterization of heterotrophic and nitrifying populations of activated sludge with an on-line respirographic biosensor. *Water Sci. Tech.*, **28**(11-12), 377 – 387.
- Vanrolleghem P.A. (1994) On-line modelling of activated sludge processes: Development of an adaptive sensor. Ph.D. thesis, University Gent, Belgium, 201 p.
- Vanrolleghem P.A. and Spanjers H. (1994) Comparison of two respirometric principles for the determination of short-term biochemical oxygen demand. In: Proceedings 49th Purdue Industrial Waste Conference. Lewis Publ., Chelsea, Michigan, 177 – 188.
- Vanrolleghem P.A., Kong Z., Rombouts G. and Verstraete W. (1994) An on-line respirographic sensor for the characterization of load and toxicity of wastewaters. *J. Chem. Tech. Biotechnol.*, **59**, 321 – 333.
- Vanrolleghem P.A. and Coen F. (1995) Optimal design of in-sensor-experiments for on-line modelling of nitrogen removal processes. *Water. Sci. Technol.*, **31**(2), 149 – 160.
- Vanrolleghem P.A., Van Daele M. and Dochain D. (1995) Practical identifiability of a biokinetic model of activated sludge respiration. *Water Res.*, **29**, 2561 – 2570.
- Vanrolleghem P.A. and Dochain D. (1998) Model Identification. In: Advanced Instrumentation, Data Interpretation and Control of Biotechnological Processes, Kluwer Academic Publishers, Dordrecht, The Netherlands, 251 – 318.

- Vanrolleghem P.A. and Spanjers H. (1998) A hybrid respirometric method for more reliable assessment of activated sludge model parameters. *Water Sci. Technol.*, **37**(12), 237 – 246.
- Vanrolleghem P.A., Gernaey K., Coen F., Petersen B., De Clercq B. & Ottoy J.-P. (1998) Limitations of short-term experiments designed for identification of activated sludge biodegradation models by fast dynamic phenomena. In: *Proceedings 7th IFAC Conference on Computer Applications in Biotechnology CAB7*. Osaka, Japan, May 31 - June 4 1998.
- Vanrolleghem P.A., Spanjers H., Petersen B., Ginestet P. and Takács I. (1999) Estimating (combinations of) Activated Sludge Model No.1 parameters and components by respirometry. *Water Sci. Technol.*, **39**(1), 195 – 215.
- Vernimmen A.P., Henken E.R. and Lamb J.C. (1967) A short-term biochemical oxygen demand test. *J. Water Pollut. Control Fed.*, **39**, 1006 – 1020.
- Versyck K.J., Claes J.E. and Van Impe J.F. (1997) Practical identification of unstructured growth kinetics by application of optimal experimental design. *Biotechnol. Prog.*, **13**, 524 – 531.
- Versyck K.J. and Van Impe J.F. (1998) Feed rate optimisation for fed-batch bioreactors: From optimal process performance to optimal parameter estimation. *Chem. Eng. Com.*, **172**, 107 – 124.
- Volskay V.T.Jr., Grady C.P.L.Jr. and Tabak H.H. (1990) Effect of selected RCRA compounds on activated sludge activity. *Res. J. Water Pollut. Control Fed.*, **62**, 654 – 664.
- Walter E. (1982) *Identifiability of state space models*. Springer, Berlin.
- Walter E. and Lecourtier Y. (1982) Global approaches to identifiability testing for linear and nonlinear state space models. *Mathematics and Computers in Simulation*, **24**, 472 – 482.
- Walter E. and Pronzato L. (1990) Qualitative and quantitative experiment design for phenomenological models - A survey. *Automatica*, **26**(2), 195 – 213.
- Walter E. and Pronzato L. (1995) On the identifiability and distinguishability of nonlinear parametric models. In: *Proc. Symp. Applications of modelling and control in agriculture and bioindustries, IMACS*, p. V.A.3-1–V.A.3.8, Brussels, Belgium.
- Walter E. and Pronzato L. (1999) *Identification of parametric models from experimental data*. Springer Verlag, Heidelberg.
- Wanner O., Kappeler J. and Gujer W. (1992) Calibration of an activated sludge model based on human expertise and on a mathematical optimization technique - A comparison. *Water Sci. Technol.*, **25**(6), 141 – 148.
- Watts J.B. and Garber W.F. (1993) On-line respirometry: A powerful tool for activated sludge plant operation and design. *Water Sci. Technol.*, **28**(11-12), 389 – 399.
- Weijers S. (1999) On BOD tests for the determination of biodegradable COD for calibrating activated sludge model No. 1. *Water Sci. Technol.*, **39**(4), 177 – 184.
- Weijers S.R., Kok J.J., Preisig H.A., Buunen A. and Wouda T.W.M. (1996) Parameter identifiability in the IAWQ model no. 1 for modelling activated sludge plants for enhanced nitrogen removal. In: *Proceedings 6th European Symposium on Computer Aided Process Engineering ESCAPE-6*, Rhodos, May 1996. pp. 6.

- Wentzel M.C., Mbewe A. and Ekama G.A. (1995) Batch test for measurement of readily biodegradable COD and active organism concentrations in municipal waste waters. *Water SA*, **21**, 117 – 124.
- Willems P. and Ottoy J.P. (1998) On-line data acquisition. In: Van Impe J., Vanrolleghem P. and Iserentant D. (eds.), *Advanced Instrumentation, Data Interpretation and Control of Biotechnological Processes*; Kluwer Academic Publishers, Dordrecht, The Netherlands, p 161 - 190.
- Witteborg A., van der Last A., Hamming R. and Hemmers I. (1996) Respirometry for determination of the influent Ss-concentration. *Water Sci. Technol.*, **33**(1), 311 – 323.
- Xu S. and Hasselblad S. (1996) A simple biological method to estimate the readily biodegradable organic matter in wastewater. *Water Res.*, **30**, 1023 – 1025.
- Xu S. and Hultman B. (1996) Experiences in wastewater characterisation and model calibration for the activated sludge process. *Water Sci. Technol.* **33**(12), 89 – 98.
- Yuan W. and Stenström M.K. (1996) The modelling of biomass decay in aerobic activated sludge systems: death-regeneration versus endogenous respiration. In: *Proceedings 69th Annual WEF Conference and Exposition*. 73 – 82.
- Yuan Z., Bogaert H. and Verstraete W. (1999) A titrimetric respirometer measuring the total nitrifiable nitrogen. In: *Proceedings 13th Forum on Applied Biotechnology*, September 23 – 24, Gent, Belgium.
- Zeng A.P. and Deckwer W.D. (1995) A kinetic model for substrate and energy consumption of microbial growth under substrate-sufficient conditions. *Biotechnol.Prog.*, **11**, .71 – 79.

Summary
-
Samenvatting

Summary

The activated sludge process is one of the most widespread biological wastewater purification technologies. Especially during the last two decades modelling of biological degradation processes in activated sludge plants has been an important research topic. This thesis deals with calibration, identifiability and optimal experimental design of activated sludge models. The aim was to define a more methodological approach for model calibration with special focus on the investigation, illustration and solution of the problems -of both theoretical and practical origin- encountered when deriving information from lab-scale experiments. The focus in this thesis is on the Activated Sludge Model No. 1 (ASM1; Henze *et al.*, 1987). However, the developed methodologies are transferable to model calibration applications in general.

Generally speaking, a good model calibration exercise can benefit from the information derived from lab-scale experiments. In such lab-scale experiments it is tried to characterise (part of) the kinetics of the biomass present in the full-scale system under study. In the frame of this thesis a conceptual methodology to carry out lab-scale experiments was defined, investigated and illustrated, with the purpose of obtaining accurate parameter estimates of activated sludge reaction kinetics and wastewater component concentrations. For the determination of the optimal experiments the theory of optimal Experimental Design (OED), based on the Fisher Information Matrix (FIM), was applied.

The literature review (chapter 2) begins with a detailed description of ASM1, and a discussion of the differences between ASM1 and the recently proposed ASM3 (Gujer *et al.*, 1999). However, the main part of the literature review is focusing on ASM1 model calibration methodology and available methods for characterisation of wastewater components and of activated sludge reaction kinetics. The different methods were discussed and evaluated thoroughly. Furthermore, the relevance of characterising the different wastewater components and kinetic parameters via lab-scale experiments was discussed and a list of the most relevant parameters and components was defined. Based on the literature review it was concluded that especially respirometry, and to a lesser extent titrimetry and nitrate uptake rate measurements, are powerful methods that allow for the characterisation of several activated sludge kinetic parameters and wastewater components.

With the literature review in mind, and to maximise the quality of the experimental data, a combined respirometric-titrimetric measurement methodology was developed and evaluated (chapter 3). It was already indicated in chapter 3, and investigated in more detail in chapter 5, that the accuracy of the parameter estimates improves significantly when combined measurements are available for the parameter estimation (respirometry and titration). For example, the accuracy of the kinetic parameters of the first nitrification step improved with 50% when combined respirometric-titrimetric measurements were available

compared to a situation where only respirometry was applied. Furthermore, it was concluded that especially parameter estimation based on titrimetric data was very accurate, with a fast convergence of the estimation algorithm towards a minimum. In general, however, it was found that the parameter accuracy based on oxygen measurements instead of oxygen uptake rates was the highest.

In chapter 4 the focus was on theoretical identifiability of the models that are applied to interpret the data resulting from the developed experimental set-up (see chapter 3). The nitrification process was used as an example to study the theoretical identifiability considering combined respirometric-titrimetric measurements. Two model structures were investigated, including presence and absence of biomass growth for interpretation of short- and long-term experiments respectively. The theoretical identifiability was studied via the Taylor and generating series methods. From this study it appeared clearly that the parameter identifiability improves significantly when combined respirometric-titrimetric measurements are available, since the autotrophic yield Y_A becomes uniquely identifiable. The most important result of the theoretical identifiability study was however that the results could be generalised. It appeared that the theoretical identifiable parameter combinations for Monod type growth models described in an ASM1-like matrix notation, could be obtained directly via a simple set of generalisation rules only based on (i) knowledge of the process under study, (ii) measured component(s) and (iii) the substrate component(s) that is degraded. Application of these generalisation rules results in a significant reduction in the often very time consuming task of assessing the theoretical identifiable parameter combinations. Furthermore, it can help the users to obtain the identifiable parameter combinations directly without the need to go too deeply into the mathematical background of theoretical identifiability.

The practical identifiability was investigated in chapter 5 for a specific nitrification example. The identifiability analysis was carried out via an evaluation of the output sensitivity functions and the corresponding FIM. Local parameter identifiability requires that the rank of FIM is full. In this study, however, it appeared that the FIM became singular when it was calculated based on the output sensitivity functions with respect to all theoretically identifiable parameters, considering combined respirometric-titrimetric measurements. The singularity was clearly related to the presence of the output sensitivity function with respect to the autotrophic biomass yield. However, when investigating the sum of squared errors based objective function as a function of the model parameters, it was clearly observed that the yield was practically identifiable. Obviously, the FIM was not able to reflect the full information of the available combined respirometric-titrimetric dataset, and therefore gave a more pessimistic picture of the identifiability properties than predicted in the theoretical study of chapter 4.

In chapter 6 another problem related to the properties of the FIM in the different OED criteria was investigated. Different OED criteria have been developed based on different scalar functions of the FIM (e.g. the eigenvalues and corresponding trace and determinant of the FIM). Originally, the analysis described in chapter 6 was undertaken to improve the numerical properties of the FIM, allowing for a

more stable matrix inversion (the inverse of FIM is the parameter estimation covariance matrix). The condition number, i.e. the ratio between the largest and the smallest eigenvalues, was used as a measure of the robustness of the inversion. It appeared that improvements in the condition number up to a factor 10^{10} could be obtained just by rescaling the time units of the parameters. In addition, it was found that by rescaling the parameter units it was possible in some cases to obtain the optimal condition number (= 1). Only the D-criterion (maximisation of the FIM and thereby minimisation of the generalised parameter covariance) appeared to be unaffected by the parameter rescaling. The rescaling was especially critical for the modE criterion, which focuses on the minimisation of the condition number. Thus, these results have some serious implications for the optimal experimental design methodology.

Finally, the focus was turned back to the conceptual methodology for optimal experimental design in chapter 7. In this chapter a step-wise procedure was defined for the FIM based OED, and using the results obtained in the previous chapter as a basis. This OED procedure was illustrated for two case studies, first for the two-step nitrification process and second for a combined nitrification and COD degradation process. In both cases it was aimed at obtaining accurate parameter estimates, and the issue of parameter transferability between the obtained lab-scale results and the full-scale WWTP under study was addressed. Furthermore, some emphasis was put on the definition of experimental conditions that would lead to the desired experimental response. In both case studies improvements in parameter accuracy of about 50% were obtained for the optimal experiments. These theoretical predictions were validated based on experiments carried out according to the optimal experimental designs resulting from the simulations. In both case studies it was found that the reproducibility of the parameter estimates was rather high for experiments carried out with the same activated sludge sample. However, differences in parameter estimates (up to a factor 2) were found for experiments with sludge collected at different days within the same week. The sensitivity of the proposed optimal experiments towards parameter changes were therefore addressed in detail for both case studies, and the critical situations that would lead to very inaccurate parameter estimates were identified. Finally, the choice was discussed between on the one hand a robust experiment with resulting lower parameter accuracy, and on the other hand a more frequent update of the optimal experiment.

In the last part of the thesis a systematic model calibration procedure was defined for ASM1, and applied on a municipal-industrial WWTP. Here it was clearly illustrated how the information obtained from different tests for hydraulic and biological characterisation can help to frame the model calibration, e.g. to choose realistic parameter values. Moreover, the calibrated model was evaluated via a sensitivity study, investigating the influence of changes of model parameters and influent component concentrations on the model output. This analysis clearly showed that the calibrated model was sensitive to changes of the parameters that were also modified during the model calibration procedure. The model calibration was finalised with a model reduction, resulting in a 50% reduction of the calculation time needed for the

simulation compared to the original calibrated model.

Samenvatting

Het actief slib proces is één van de meest populaire waterzuiveringstechnieken. Vooral tijdens de voorbije twee decennia was het modelleren van biologische afbraakprocessen in actief slib installaties een belangrijk onderzoeksgebied. Deze thesis behandelt de kalibratie, de identificeerbaarheid en optimale proefopzetten voor actief slib modellen. Daarbij wordt in deze thesis in het bijzonder aandacht besteed aan Actief Slib Model Nr. 1 (ASM1; Henze *et al.*, 1987). De methodes die ontwikkeld werden in het kader van deze thesis zijn echter overdraagbaar naar om het even welk actief slib model, of zelfs meer algemeen naar toepassingen waarin de kalibratie van een model een belangrijke rol speelt.

Algemeen wordt aangenomen dat bij de uitvoering van een modelkalibratie voordeel kan gehaald worden uit de informatie die afgeleid wordt uit experimenten op laboratoriumschaal. In dergelijke experimenten wordt getracht om (een deel van) de kinetische parameters te karakteriseren van de biomassa aanwezig in de volschalige installatie die moet gemodelleerd worden. In het kader van deze thesis werd een conceptuele methodiek om dergelijke experimenten op laboratoriumschaal uit te voeren gedefinieerd, onderzocht, en concreet toegepast, met als doel het verkrijgen van accurate parameterschattingen met betrekking tot de actief slib reactiekinetiek en de concentratie van afvalwatercomponenten. Voor de bepaling van de optimale proefopzet werd de optimale proefopzet theorie (“optimal experimental design”, OED), gebaseerd op de Fisher Informatie Matrix (FIM), toegepast.

Het literatuuroverzicht (hoofdstuk 2) start met een gedetailleerde beschrijving van ASM1, en een discussie die de verschillen behandelt tussen ASM1 en het recent voorgestelde ASM3 (Gujer *et al.*, 1999). Het belangrijkste deel van het literatuuroverzicht is echter gewijd aan de kalibratie van ASM1, en de beschikbare methodes voor het bepalen van afvalwatercomponenten en de actief slib reactiekinetiek. De verschillende methodes werden in detail besproken en geëvalueerd. Verder wordt ook de relevantie besproken van het bepalen van de verschillende afvalwatercomponenten en kinetische parameters. Op basis van het literatuuroverzicht werd besloten dat vooral respirometrie, en in mindere mate titrimetrie en metingen van de nitraatverbruikssnelheid, veelzijdige methoden zijn die toelaten om heel wat verschillende actief slib kinetische parameters en afvalwatercomponenten te bepalen.

Met de conclusies van het literatuuroverzicht in het achterhoofd, en met het oog op het maximaliseren van de kwaliteit van de experimentele data, werd een gecombineerde respirometrische-titrimetrische methode ontwikkeld en grondig geëvalueerd (hoofdstuk 3). Reeds in hoofdstuk 3, en later in meer detail uitgewerkt in hoofdstuk 5, werd erop gewezen dat de accuraatheid van de geschatte parameters significant toeneemt wanneer de gecombineerde datasets beschikbaar zijn voor het schatten van parameters (respirometrie en titrimetrie). Zo verbeterde de accuraatheid van de kinetische parameters van de eerste stap van het

nitrificatieproces met 50% wanneer gecombineerde respirometrische-titrimetrische data beschikbaar waren, dit in vergelijking met een situatie waar alleen respirometrie werd aangewend. Verder kon ook besloten worden dat vooral de schattingen gebaseerd op titratiedata heel accuraat waren, met een snelle convergentie van het gebruikte schattingsalgoritme naar een minimum in de kwadratenom. Meer algemeen werd geconcludeerd dat de accuraatheid van de parameters bekomen op basis van opgeloste zuurstofmetingen in plaats van zuurstofopnamesnelheden beter was.

In hoofdstuk 4 wordt aandacht besteed aan de theoretische identificeerbaarheid van de modellen die gebruikt worden voor de interpretatie van de data die gegenereerd werden met de ontwikkelde proefopstelling (zie hoofdstuk 3). Het nitrificatieproces werd als voorbeeld gebruikt voor het bestuderen van de theoretische identificeerbaarheid wanneer gecombineerde respirometrische-titrimetrische data beschikbaar zijn. Twee modelstructuren werden onderzocht, respectievelijk een model met en een model zonder biomassa aangroei. De theoretische identificeerbaarheid werd bestudeerd via de Taylor en de “generating series” expansiemethoden. Uit deze studie voor het nitrificatieproces bleek duidelijk dat de identificeerbaarheid van de parameters significant toeneemt wanneer gecombineerde respirometrische-titrimetrische metingen beschikbaar zijn, aangezien de autotrofe celopbrengstcoëfficiënt Y_A identificeerbaar wordt. Het belangrijkste resultaat van de theoretische identificeerbaarheidsstudie was echter dat de resultaten konden veralgemeend worden. Voor Monod groeimodellen die uitgeschreven worden in een matrixnotatie, zoals in ASM1, bleek dat de theoretisch identificeerbare parametercombinaties direct konden bekomen worden via een beperkt aantal algemene formules, louter op basis van (i) kennis van het te bestuderen proces, (ii) de gemeten component(en) en (iii) het substraat dat wordt afgebroken. Toepassing van deze algemene formules resulteert in een significante vermindering van de energie en tijd die moet geïnvesteerd worden in de vaak heel tijdrovende taak die het bepalen van de theoretisch identificeerbare parametercombinaties is.

De praktische identificeerbaarheid werd bestudeerd in hoofdstuk 5 voor een specifiek nitrificatievoorbeeld. De studie van de identificeerbaarheid werd uitgevoerd via een evaluatie van de output sensitiviteitsfuncties en de daarmee overeenkomende FIM. Lokale identificeerbaarheid van de parameters vereist dat de rang van de FIM volledig is. In deze studie bleek echter dat de FIM singulier werd wanneer de FIM werd berekend op basis van de output sensitiviteitsfuncties voor alle theoretisch identificeerbare parameters, en in de veronderstelling dat gecombineerde respirometrische-titrimetrische metingen beschikbaar zijn. Het feit dat de FIM singulier was, werd duidelijk veroorzaakt door de aanwezigheid van de output sensitiviteitsfunctie met betrekking tot de autotrofe celopbrengstcoëfficiënt Y_{A1} . Wanneer echter de op basis van de som van kwadratische fouten bekomen doelfunctie werd bestudeerd als functie van de modelparameters, bleek duidelijk dat de celopbrengstcoëfficiënt toch praktisch identificeerbaar was. De FIM was dus niet in staat om alle informatie aanwezig in de gecombineerde respirometrische-titrimetrische dataset optimaal te benutten, en gaf daarom een meer pessimistisch beeld van de identificeerbaarheid dan

werd voorspeld in de theoretische studie uitgevoerd in hoofdstuk 4.

In hoofdstuk 6 werd een ander probleem gerelateerd tot de eigenschappen van de FIM en de verschillende OED criteria onderzocht. Verschillende OED criteria werden ontwikkeld op basis van verschillende scalaire functies van de FIM (vb. de eigenwaarden en het spoor en de determinant van de FIM). De analyse in hoofdstuk 6 werd gestart met het oog op het verbeteren van de numerieke eigenschappen van de FIM, wat moest toelaten om een meer stabiele matrixinversie te bekomen (inversie van de FIM geeft de parameterschatting covariantiematrix). Verbeteringen in het conditiegetal tot een factor 10^{10} konden bekomen worden door gewoon de tijdseenheden van de parameters te herschalen. Daarenboven bleek dat het herschalen van de eenheden van de parameters in sommige gevallen toeliet om het optimaal conditiegetal (= 1) te bekomen. Verder werd ook duidelijk dat zowel het A, modA, E en modE OED criterium beïnvloed werden door het herschalen van de parameters. Alleen het D criterium bleek niet beïnvloed te worden door de parameterschaling. De parameterschaling had vooral een belangrijke invloed op het modE criterium, dat gesteund is op de minimalisatie van het conditiegetal. Deze resultaten hebben dus ernstige implicaties voor de OED methodologie.

Uiteindelijk werd in hoofdstuk 7 opnieuw ingegaan op de conceptuele methodologie voor het bekomen van optimale proefopzetten. In dit hoofdstuk werd een stapsgewijze procedure gedefinieerd voor ontwikkeling van FIM gebaseerde optimale proefopzetten, daarbij gebruik makend van de resultaten die bekomen werden in het vorige hoofdstuk. De procedure voor het bekomen van de optimale proefopzet werd concreet uitgewerkt voor twee gevalstudies. Eerst werd het tweestapsnitrificatieproces bestudeerd, daarna een gecombineerd proces bestaande uit nitrificatie en CZV afbraak. In beide gevallen werd ernaar gestreefd accurate parameterschattingen te bekomen. Tevens werd het probleem behandeld van de overdraagbaarheid van de parameters tussen de op laboratoriumschaal behaalde resultaten en de praktische situatie van de volschalige actief slib waterzuiveringsinstallatie. Verder werd aandacht besteed aan het definiëren van experimentele condities die resulteren in de gewenste experimentele respons. In beide gevalstudies werden voor het optimale experiment verbeteringen in de accuraatheid van de parameters van 50% bekomen. Deze theoretische voorspellingen werden gevalideerd op basis van experimenten die werden uitgevoerd in overeenstemming met de optimale proefopzet die eerder als resultaat van de simulaties naar voren kwam. Voor beide gevalstudies was de herhaalbaarheid van de parameterschattingen betrekkelijk hoog voor experimenten die uitgevoerd werden met hetzelfde actief slib monster. Grotere verschillen in geschatte parameters (tot een factor 2) werden echter gevonden voor actief slib monsters die op verschillende dagen binnen dezelfde week genomen werden. De gevoeligheid van de voorgestelde optimale proefopzetten voor veranderingen van de parameters werd daarom uitvoerig bestudeerd voor beide gevalstudies, en de kritische situaties die zouden resulteren in weinig accurate geschatte parameterwaarden werden geïdentificeerd. Tenslotte werd de keuze besproken tussen aan de ene kant een robuust experiment met de daarmee overeenstemmende lagere accuraatheid van de geschatte

parameter en, aan de andere kant, een meer frequente aanpassing van de optimale proefopzet.

In het laatste deel van de thesis werd een systematische modelkalibratieprocedure gedefinieerd voor ASM1, en in praktijk toegepast voor een gecombineerde huishoudelijk-industriële actief slib waterzuiveringsinstallatie. Er werd duidelijk aangetoond dat de informatie die werd bekomen uit verschillende experimenten voor de hydraulische en biologische karakterisering, een bijdrage kan leveren bij het kiezen van realistische waarden voor de modelparameters. Daarnaast werd het gekalibreerde model verder geëvalueerd via een sensitiviteitsanalyse, waarbij onderzocht werd hoe de output van het model bij invloed wordt door veranderingen van de waarden van de parameters in het model. Deze analyse toonde duidelijk aan dat het gekalibreerde model gevoelig was aan veranderingen van die parameters die ook gewijzigd waren tijdens de modelkalibratie. De modelkalibratie werd vervolledigd met een modelreductie. Deze laatste resulteerde in een reductie van de benodigde rekentijd voor de simulaties met 50%, in vergelijking met het originele gekalibreerde model.

Curriculum Vitae

Curriculum Vitae

Personal information

Name : Britta Petersen

Nationality : Danish

University diploma

1995 Master of Science in Engineering (Environmental Engineering)

Thesis : Start-up of Bio-P after low COD load and P-uptake rate as function of PHB (Supervisor: Prof. Mogens Henze). Institute of Environmental Science and Technology. Technical University of Denmark.

Post-graduate courses

1998 October 20-22 : Course in "Modelling and regulation of biochemical processes", given in the frame of the Graduate School in Systems and Control at the University of Leuven, Belgium.

1998 March 15 : 1-day course in "Modelling Terminology and Methodology for Activated Sludge Modelling", Copenhagen, Technical University of Denmark.

1997 December 8-19 : "Advanced Course on Microbial Physiology and Fermentation Technology." The Kluyver Instituut, Technologische Universiteit Delft, The Netherlands.

1995 Autumn 1995. Course Statistical Quality Control, Technical University of Denmark.

Working Experience

July 2000 – December 2000 : Employed by Ecole Polytechnique de Montreal (with Prof. Yves Comeau).

August 1999 – December 1999 : Four months stay at University Laval in Quebec City (with Prof. Paul Lessard) and Ecole Polytechnique Montreal (with Prof. Yves Comeau) in the frame of the Quebec-Flanders exchange project.

June 1997 : Four week stay at the University of Rome "La Sapienza" in the Department of Chemistry with Dr. M.Majone in the frame of a COST 682 exchange project.

April 1996 - January 2000 : Employed by EPAS NV, Technologiemark 3, B-9052 Zwijnaarde, Belgium.

August 1995 - January 1996 : Teaching assistant at The Institute for Environmental Science and Technology, Technical University of Denmark (with Prof. Mogens Henze).

February 1994 – June 1994 : Trainee-ship as part of education as Master of Science in Engineering at "The Environmental Protection Department" in Hong-Kong.

Scientific publications

Publications in journals (with review).

Temmink H., Petersen B., Isaacs S. and Henze M. (1996) Recovery of biological phosphorus removal after periods of low organic loading. *Water Sci. Technol.*, 34(1-2), 1-8.

Petersen B., Temmink H., Henze M. and Isaacs S. (1998) Phosphate uptake kinetics in relations to PHB. *Water Res.*, 32, 91-100.

Coen F., Petersen B., Vanrolleghem P.A., Vanderhaegen B. and Henze M. (1998) Model-based characterisation of hydraulic, kinetic and influent properties of an industrial WWTP. *Water Sci. Technol.*, 37(12), 317-326.

Vanrolleghem P.A., Spanjers H., Petersen B., Ginestet P. and Takács I. (1999) Estimating (combinations of) Activated Sludge Model No.1 parameters and components by respirometry. *Water Sci. Technol.*, 39(1), 195-214.

Baetens D., Hosten L.H., Petersen B., Van Volsem S. and Vanrolleghem P.A. (2000) Optimal experimental design for the calibration of models of phosphorous removal activated sludge systems. *Journal A* (in press).

Gernaey K., Petersen B., Ottoy J.P. and Vanrolleghem P.A. (2001) Activated sludge monitoring with combined respirometric - titrimetric measurements. *Water Research*, **35**, 1280-1294.

Petersen B., Gernaey K. and Vanrolleghem P.A. (2001) Practical identifiability of model parameters by combined respirometric - titrimetric measurements. *Water Science and Technology*, **43**(7), 347-356.

Gernaey K., Petersen B., Nopens I., Comeau Y. and Vanrolleghem P.A. (2002) Modelling aerobic carbon source degradation processes using titrimetric data and combined respirometric-titrimetric data: Experimental data and model structure. *Biotechnology and Bioengineering*, **79**, 741 - 753.

Gernaey K., Petersen B., Dochain D. and Vanrolleghem P.A. (2002) Modelling aerobic carbon source degradation processes using titrimetric data and combined respirometric-titrimetric data: Structural and practical identifiability. *Biotechnology and Bioengineering*, **79**, 754 - 767.

Petersen B., Gernaey K., Devisscher M., Dochain D. and Vanrolleghem P.A. (2002) A simplified method to assess structurally identifiable parameters in Monod-based activated sludge models. *Water Research* (submitted).

Petersen B., Gernaey K., Henze M. and Vanrolleghem P.A. (2002) Evaluation of an ASM1 model calibration procedure on a municipal-industrial wastewater treatment plant. *Journal of Hydroinformatics*, **4**, 15-38.

Petersen B., Gernaey K. and Vanrolleghem P.A. (2002) Anoxic activated sludge monitoring with combined nitrate and titrimetric measurements. *Water Science and Technology*, **45**(4-5), 181 – 190.

Publications in journals (without review).

Gernaey K., Petersen B., Ottoy J.P. and Vanrolleghem P. (1999) Biosensing activated sludge. *Water Quality International*, May-June 1999, p.16-22.

Publications in books or book chapters.

Petersen B., Gernaey K., Henze M. and Vanrolleghem P.A. (2000) Calibration of activated sludge models: A critical review of experimental designs. In: Agathos S. and Reineke W. (Eds.), *Biotechnology for the Environment. Focus on Biotechnology*, Vol. 3, Kluwer Academic Publishers BV.

Contribution to papers presented on congresses and seminars.

Petersen B. (1995) Recovery of Biological Phosphorus Removal after low organic loading. Control of the process In: Second Annual Network meeting of MATECH (European centre for Mathematics and Technology of Urban Water Pollution), Exeter, England, July 25 1995.

Petersen B., Temmink H., Henze M. & Isaacs S. (1996) The influence of PHB on the stability of the Bio-P process. In: Proceedings Workshop Modelling, Monitoring and Control of Wastewater Treatment Plants, 10th Forum for Applied Biotechnology, Brugge, Belgium, September 26-27 1996. Med. Fac. Landbouww. Univ. Gent, 61/4a, 1761-1767.

Petersen B. (1996) The use of respirometry for determination of wastewater and sludge characteristics. In: COST682 report, Wastewater and biomass characterisation. COST-682 Working Group Meeting. Bologna, Italy, November 18-19 1996.

Petersen B., Coen F., Henze M., Vanderhaegen B. and Vanrolleghem P.A. (1997) Design and interpretation of dedicated experiments for hydraulic and biokinetic characterisation of an industrial activated sludge system. In: Proceedings EERO/EFB International Symposium Environmental Biotechnology ISEB3. Ostend, Belgium, April 21-24 1997. Part I, 207-210.

Petersen B. (1997). Minimum effort calibration of activated sludge models. In: 1st workshop on Industrial Mathematics for Nordic Ph.D. students. Hillerød, Denmark, August 29-31, 1997.

Petersen B. (1998) Effect of experimental design, So/Xo ratio. In: COST682 report, Wastewater and biomass characterisation. COST-682 Working Group Meeting. Copenhagen, Denmark, January 12-13 1998.

Vanrolleghem P.A., Gernaey K., Coen F., Petersen B., De Clercq B. and Ottoy J.-P. (1998) Limitations

of short-term experiments designed for identification of activated sludge biodegradation models by fast dynamic phenomena. In: Proceedings 7th IFAC Conference on Computer Applications in Biotechnology CAB7. Osaka, Japan, May 31 - June 4 1998.

Gernaey K., Petersen B., Vanderhasselt A., Verstraete W., Ottoy J.P. en Vanrolleghem P. (1998) Meten van actief slib activiteit en bezinkingskarakteristieken: recente evoluties. KVIV Studiedag Waterverontreiniging. Antwerpen, Belgium, November 26 1998 (In Dutch).

Petersen B., Gernaey K. and Vanrolleghem P.A. (1999) Modelling of activated sludge process kinetics using a combination of hybrid respirometric and titrimetric data. In: Proceedings 9th European Congress on Biotechnology. Brussels, Belgium, July 11-15 1999.

Petersen B., Gernaey K., Ottoy J.P. and Vanrolleghem P.A. (1999) Application of biosensors in wastewater treatment. In: Proceedings 22nd Symposium sur les eaux usees et 11th Atelier sur l'eau potable. Quebec, Montreal, October 20-21 1999.

Petersen B., Gernaey K. and Vanrolleghem P.A. (2000) Improved theoretical identifiability of model parameters by combined respirometric-titrimetric measurements. A generalisation of results. In: Proceedings IMACS 3rd Symposium on Mathematical Modelling, Vienna, Austria, February 2-4 2000.

Janssen M.J.M, Hopkins L.N., Petersen B. and Vanrolleghem P.A. (2000) Reduction of an Activated Sludge Process Model to Facilitate Controller Tuning. In: Proceedings 14th European Simulation Multiconference (ESM2000) Gent, Belgium May 23-26, 2000.

Gernaey K., Petersen B., Parmentier G., Bogaert H., Ottoy J.P. and Vanrolleghem P. (2000) Application of dynamic models (ASM1) and simulation to minimize renovation costs of a municipal activated sludge wastewater treatment plant. In: Proceedings 1st World Congress of the International Water Association. Paris, France, July 3-7 2000. CD-ROM F-2258